THE PETROLOGY AND STRUCTURE OF THE KALKA AND EWARARA LAYERED BASIC INTRUSIONS, GILES COMPLEX, CENTRAL AUSTRALIA

Volume 1

by

Alan Douglas Tracy Goode, B.Sc. (Hons), Dip.T.

Department of Geology and Mineralogy,
The University of Adelaide,
Adelaide, South Australia.

December, 1970.

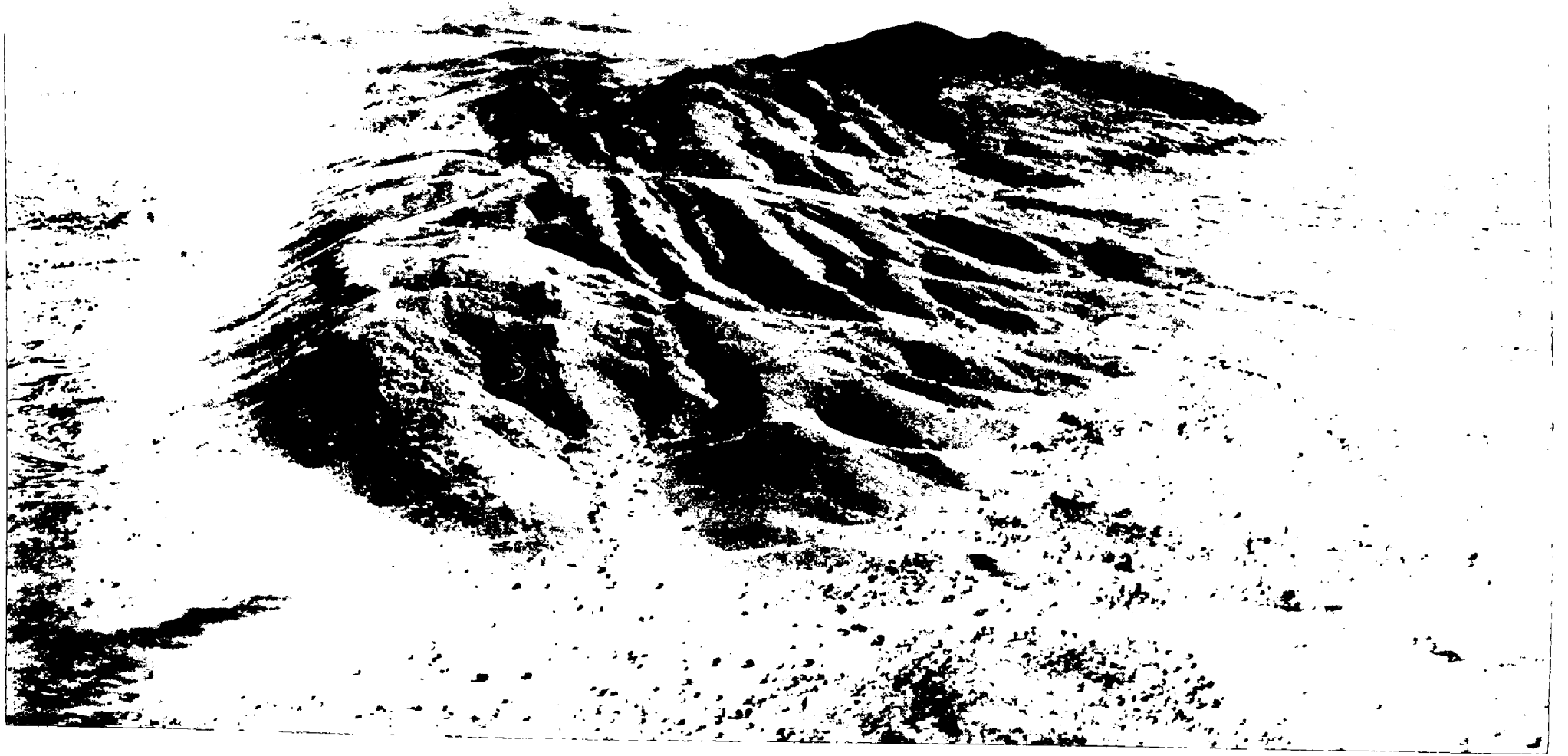

FRONTISPIECE KALKA INTRUSION

Oblique aerial view of the Kalka Intrusion looking west towards the Hinckley Intrusion (left background). Mt Kalka forms the highest point of the body with Scarface the prominent cliff to its right. The southern margin of the body is bounded by the Hinckley Fault. Igneous layering in the foreground is overturned.

CONTENTS

VOLUME 1

Page

CONTENTS

VOLUME 2

SUMMARY

Petrological, geochemical and structural studies have been carried out on Kalka and Ewarara, two of the layered basic intrusions of the Giles Complex from the eastern Tomkinson Ranges in central Australia. Studies have also been made of the granulite country rocks and the numerous younger minor intrusive suites. The local tectonic development of the area is also discussed, together with its application to the more regional development of the Musgrave Block.

The layered intrusions are remarkable for their development of high pressure characteristics, which indicate crystallization at about 10 to 12 kilobars. The fractionation of the anhydrous tholeiite magma is controlled by the early crystallization of orthopyroxene at these pressures. Consequent fractionation leads to the relatively late development of olivine in the layered sequence. The highest level cumulates in Kalka are dominated by plagioclase, revealing a genetic link between anorthosites and layered basic intrusions.

Studies on igneous layerings present in Kalka have led to the formation of models for both large scale (cyclic unit) layering and small scale layering. The cyclic units in Kalka were derived by a combination of convectional overturn and fresh injection of magma. There are indications of differences in magma composition at various stages of fresh injection. The small scale layering was derived by discontinuous nucleation followed by differential settling between pyroxene/olivine and plagioclase. Structures resulting from the action of strong, localised bottom currents

are also observed. Current velocities have been estimated at between 10^{-2} and 1 cm/sec.

Pronounced gneissic foliations were imposed on the stratiform intrusions soon after crystallization by localised minor thrusting-type movements. The resultant fabrics reveal many similarities to bodies previously considered to be "alpine" in origin.

This thesis contains no material which has been accepted for the award of any other degree or diploma in any University nor, to the best of my knowledge and belief, does it contain any material previously published or written by another person, except where due reference is made in the text.

A.D.T. Goode.

ACKNOWLEDGEMENTS

The author is indebted to Dr. R.W. Nesbitt, who instigated and supervised this project and criticized the final draft of this thesis. I am also grateful to Professor R.W.R. Rutland, Dr. J.B. Jones, Miss E.M. McBriar and Dr. T.P. Hopwood for critical discussion of the thesis text.

I would also like to express my appreciation to many other members of the Department of Geology and Mineralogy for their advice and assistance, notably Messrs A.C. Moore, P.D. Fleming and K.D. Collerson, Drs A.W. Kleeman, R.L. Oliver and G.E. Williams and Professor D.M. Boyd. Mr. W. Dowling was of great assistance in the preparation of plates. I am also grateful to many people outside this University who freely gave of their time and knowledge, viz. Messrs C.M. Gray, R.B. Major, B.P. Thomson and I.S. Rowan, Professors C.W. Burnham, J.C. Jaeger, W.D. Romey and J. Sutton, Drs J.L. Daniels, R.A. Facer and R. Vernon.

Finally my wife, Belinda, who, apart from typing this thesis and carrying out innumerable other tasks associated with its compilation, has been a constant source of encouragement. I am also deeply grateful to both our families for their support during the preparation of this thesis.

This study was carried out during the tenure of a Commonwealth Postgraduate Award. Financial assistance was also obtained from the Nuffield Foundation and the A.R.G.C. through grants to Dr. R.W. Nesbitt. Most of the electron microprobe results presented in this thesis were financed by the South Australian Department of Mines.

PART ONE

INTRODUCTION

CHAPTER 1

GENERAL INTRODUCTION

The Giles Complex of central Australia forms one of the largest groups of layered basic and ultrabasic intrusions in the world, yet, because of its remote location, has only in recent years been studied in detail. These investigations, which include this study, have revealed that the Complex can be best described as a series of deformed stratiform sheets intrusive into the high grade metamorphic terrain of the Musgrave Block. A unique feature of some of these bodies is that they contain characteristics of high pressure crystallization which have important application to many petrogenetic problems.

The present study is principally concerned with two of the Giles Complex intrusions, Kalka and Ewarara, and with a discussion of the local and regional tectonic development of the Musgrave Block. A preliminary investigation of the Ewarara Intrusion (Goode and Krieg, 1965) was most useful in this regard. Several publications prepared during the course of this thesis are enclosed in the back pocket of Volume 2 viz. Goode and Krieg (1967), Goode and Nesbitt (1969) and Nesbitt, Goode, Moore and Hopwood (1970).

In this thesis sample locations (together with thin section and polished section locations) and some relevant field stations are given in Figs 3 and 4. Samples collected from the Ewarara area are prefixed in the text by A300- or A301- while those from Kalka are indicated by A314-. Abbreviations used in the text are given in Table 1.

Methods of sample preparation and chemical analysis are described in Appendix 1. All electron microprobe results used in this thesis were obtained by Mr. P. Schultz of the Australian Mineral Development Laboratories, Adelaide.

The classification of igneous rocks developed for this thesis is given in Appendix 2, while the structural terminology used is given in Chapter 13. Descriptions of cumulate igneous textures are essentially based on Wager et al's (1960) and Jackson's (1961) suggestions. These are reviewed and modified in Appendix 3. In many of the igneous rocks described in this thesis secondary recrystallization assemblages are observed; the criteria for distinguishing these assemblages from primary igneous ones are given in Appendix 4. Jackson's (1967) nomenclature for igneous layerings and fabrics is followed in later descriptions.

1.1 Location and Access

The area studied lies immediately north of the Mt Davies ridge in the eastern Tomkinson Ranges in the remote northwest corner of South Australia (Fig. 1). It consists of two discrete areas totalling about 64 sq km in outcrop - Ewarara in the north and Kalka in the south.

Access is gained by the "Gunbarrel Highway", an unsealed road connecting the Giles Meteorological Station in W.A. to the main Adelaide-Alice Springs road. The area lies in the North West Aboriginal Reserve, the headquarters of which is at Amata (formerly Musgrave Park), about 220 km to the east. Permits are required to enter the reserve. South-western Mining Limited maintain a small mining camp about 30 km to the

west at Wingellina.

Field trips have been made to the area in May 1966, May 1967 and November 1968 and eight weeks field work was completed. A field trip of three weeks was also made to Ewarara in May 1965 as part of an Honours project.

The area is sparsely inhabited. Most of the aboriginals who belong to the Pitjantjatjara tribe at present live at Amata, the only permanent settlement in the area. However, occasional nomadic groups of aboriginals are found in the Tomkinsons, and recently small groups have begun mining chrysoprase near Mt Kalka.

1.2 Physiography

The Tomkinson Range, together with the Mann and Musgrave Ranges to the east, forms the "backbone" of the Australian continent. They consist of chains of rugged hills, ridges and inselbergs, separated by flat sandy plains which lie at an altitude of approximately 700 metres. The ranges rise up to 800 m above the plains (e.g. Mt Woodroffe 1,432 m a.s.l., Mt Davies 1,024 m a.s.l.). Away from the central chain of ranges the plains and hills are lower and more broken and lesser ranges are found (e.g. Everard, Birksgate, Barrow, Petermann, Olia and Ayers). Sand ridges and thick mulga scrub predominate to the south towards the Great Victoria Desert.

An appreciation of the local physiography can be gained from the field photographs presented in the thesis (e.g. Frontispiece, Plates 1, 2, 3, 4 and 5).

Evaporation rates greatly exceed rainfall which is capable of great seasonal variations; temperature ranges are extreme (Mirams, 1964). Creeks are restricted to the hilly zone and terminate abruptly in alluvial outwash areas on the margins of the extensive flats between the hills. Drainage patterns are shown in Figs 3 and 4. Incised conglomeratic piedmont fans are found where the larger creeks leave the ranges.

The vegetation is typical of the arid to sub-arid environment. Areas of sparse mulga scrub (Acacia sp.) with minor corkwood (Hakea sp.) and native cypress (Callitris sp.) occur on the plains and in the ranges.

Bloodwoods and river gums are found in the larger watercourses. Strong growth of spinifex (Trioda sp.) occurs on the Giles Complex rocks. Few large trees grow on the basic rocks: native cypress, ti-tree and bloodwoods are found in the rocky gorges, while stunted eucalypts (mallee) grow preferentially on certain rock types in the layered sequences (mulga is restricted to the plains and the ranges composed of granulite).

1.3 Geographical Nomenclature

In the naming of the topographic features from the area, the policy of using local aboriginal names has been followed as often as possible. In a few cases names have been taken from earlier publications, but most have been supplied by local aborigines (especially Mr. Tommy Dodd).

The name Ewarara for one of the Giles Complex intrusions (Goode and Krieg, 1965) is derived from the nearest named topographic feature, the Ewarara Creek (Thomson, Mirams and Johnson, 1962). The term is also applied by the author to the long ridge formed by the intrusion, although the name Tent Hill has also been recorded from this approximate area and may be the same feature.

The naming of the highest point of the Kalka area, which is slightly lower than the summit of Mt Davies (1,024 m a.s.l.), has been the subject of some controversy. It has previously been called Mt Parairie (Terry, 1933) and Dulgunja Hill (Thomson, 1964). However, aboriginals of the local Pitjandjatjara tribe, consistently call this feature Kalka (meaning big stone) and have not recognised or used the terms Parairie (meaning a long way - S.A. Museum, pers. comm.) or Dulgunja (a possible corruption ofgunyah meaning hut - S.A. Museum, pers. comm.), in relation to it. It was therefore decided to call the feature Mt Kalka. Since the term Kalka, as in many other cases, is applied by the aboriginals to an area rather than a specific point, the spectacular gorge to the northwest of the summit is named Kalka Gorge. The prominent black cliff to the north of the summit has been named Scarface. This term has previously been placed (probably by a draughting mistake in view of their relative topographic prominence) on a small cliff area (now named Waralkulpa - meaning rainfall) about 5 km to the south-east (Thomson, Mirams and Johnson, 1962).

Other features from the Kalka area (Fig. 3) have been named - Walter Hill (Nesbitt and Talbot, 1966), Epipinja Gorge (taken from the area name Epipinja - Thomson, Mirams and Johnson, 1962; Thomson, 1964;

local aborginals, however, do not recognise the name), Minno (named after an aboriginal folk lore character who is closely connected with the dream time story involving Kalka and the surrounding area, and who is now "represented" as a large boulder perched on top of a small knoll), Albitalbiti Creek (meaning is related to the ringneck parrot), Peepulla-turra Creek (meaning big water), Ninno Creek (meaning is related to the white tailed rat), Yultadurra (meaning hollow tree), and several other creeks.

Because of its prominence, Mt. Kalka has given its name to the Giles Complex intrusion in which it occurs (Goode and Nesbitt, 1969), although it has previously been referred to as the Walter Hill intrusion (Nesbitt and Talbot, 1966).

1.4 Previous Investigations

Collection of geological data from the Musgrave Block has been made in two distinct and widely separated periods.

Early Workers

The area was extensively explored in the late nineteenth and early twentieth centuries (e.g. see Murray, 1901; Terry, 1933, p. 272). Many of these explorers made geological observations, but few are of any present day significance.

While Gosse (1874), Giles (1874), Tietkins (1891) and Carruthers (1892) reported that the ranges consisted essentially of grey and red granites, Brown (1890), Streich (1893), Murray (1904), Wells and George (1904), Basedow (1905) and Jack (1915) also found rocks with metamorphic

characteristics. It appears that the grey granites of the early workers correspond to what is now known as the Giles Complex.

Of the early workers the most important field studies are those of Streich (1893), Basedow (1905) and Talbot and Clarke (1917, 1918). Detailed petrographic descriptions of some of the rocks were done by Streich, Basedow, Thomson (1911; from rocks collected on the Elder Expedition) and Farquharson (in Talbot and Clarke, 1917). A.W. Stelzner (in Streich, 1893) found a strong similarity between a sample from the Barrow Range in Western Australia and the granulites of Saxony, while Farquharson noted similarities between rocks from Western Australia and charnockites from India, Africa and Saxony.

Clarke (1938) gave a summary of geological knowledge prior to World War II.

Recent Workers

No further work was done until World War II when Wilson began studying the rocks in the vicinity of Ernabella in the eastern Musgrave Ranges. Interest in the more remote western parts of the Musgrave Block was aroused during the search for possible uranium deposits and the discovery instead of low-grade nickeliferous ochre bodies. The first visit to the Tomkinson Ranges by the South Australian Mines Department was made in 1953, but it was not until 1960 that they commenced a field mapping programme. Earlier mapping was carried out by Gold and Mineral Exploration N.L. in 1954 and then by South Western Mining Limited in 1955-8. The Geology Department of the University of Adelaide first began field work in the area in 1963 under the direction

of Dr. R.W. Nesbitt.

A complete bibliography of early and recent publications of research on the Musgrave Block is given in Table 2. Internal reports of the South Australian Geological Survey are not included in this list unless relevant.

1.5 Geological Setting

At the beginning of this project very little detailed work had been published on the Musgrave Block. Wilson (1954 and other papers) had described rocks from the eastern Musgrave Ranges, while the first report on the Giles Complex of any detail had been published by Nesbitt and Kleeman in 1964. However a great deal more is now known about this area and a much more balanced general appreciation of the geology can now be given than was possible several years ago. However, it should be realised that gaps remain in our knowledge, and the following summary represents an arrested view of a rapidly modifying picture. A more detailed discussion is given in Chapter 15.

The Musgrave Block was named by Hossfeld (1954) and forms a present-day stable shield area of approximately 140,000 sq. km. in Central Australia (Figs. 1,36). It is surrounded by younger sedimentary basins: the Amadeus (Proterozoic-Palaeozoic) to the north, the Officer (Proterozoic-Palaeozoic) to the south, the Canning (Palaeozoic) to the west and the Great Artesian (Mesozoic) to the east. Proterozoic sediments are also found within the Block itself i.e. in the Levenger Basin.

The Precambrian high-grade metamorphic terrain of the Musgrave Block consists of both high-amphibolite and granulite facies grade gneisses. They are generally acidic (i.e. quartz-bearing) in composition although basic interbands and other rock types are also observed. The rocks are usually well layered.

These high-grade gneisses are intruded by a considerable number of younger igneous rock suites.

Orthopyroxene-bearing adamellites (or charnockites) appear to be confined to the granulites, while the hornblende- and biotite-bearing varieties are more common in the amphibolite facies terrains. The adamellite plutons may be up to 40 km long e.g. Ernabella (Wilson, 1960) in the eastern Musgrave Ranges and Illbillie in the Everard Ranges. They are generally relatively conformable with the overall granulite structure. Several generations of granites may be present in the Musgrave Block.

The metamorphics are also intruded by a series of large layered mafic and ultramafic intrusions, known as the Giles Complex (Nesbitt and Kleeman, 1964; Nesbitt and Talbot, 1966; Daniels, 1967; Nesbitt, Goode, Moore and Hopwood, 1970). Although originally only recognised in the Tomkinson Ranges by Sprigg and Wilson (1959), Giles Complex intrusions have now also been mapped in the Musgrave Ranges (Major et al., 1967). One of these bodies, the Woodroffe intrusion, has also been mentioned by Wilson (1947). The basic feature of the Complex is that it consists of a large number of mafic layered intrusions emplaced within a large crustal area.

Several anorthositic bodies have been mapped in the eastern Tomkinson Ranges (Thomson et al., 1962) but recent work on the Teizi anorthosite by Gray (1967) has shown that at least one of these is very similar to the Giles Complex intrusions nearby.

Minor intrusions are found throughout the Musgrave Block: although acid pegmatites are observed, most of the smaller intrusives are basic in composition. Basic dykes are very numerous and several suites have been distinguished (Wilson, 1948; Goode and Nesbitt, 1969; Nesbitt et al., 1970). Olivine-bearing plug-like bodies are also common, especially in the eastern Tomkinson Ranges (Goode and Nesbitt, 1969; Nesbitt et al., 1970). Many other varieties of transgressive basic igneous rocks are observed.

In general the structural trends in the Block vary from area to area - in the central western zone (western Musgrave and Tomkinson Ranges), the granulites and layered basic bodies have a predominantly east west trend whereas the eastern Musgrave Ranges have essentially north-south trends. Three main fold styles are recognised in the eastern Tomkinson Ranges, the second of which is responsible for the overall east-west trend.

The east-west trend, which parallels the general elongation of the Block, is further accentuated by the development of large east-west mylonitic fault zones (e.g. Mann, Woodroffe, Davenport, Hinckley). Some of these faults (which may extend laterally for at least 160 km) appear to have a major control on the distribution of rock types in the Musgrave Block (Fig. 37). Regional mapping by the South Australian Geological Survey (Thomson et al., 1962; Major et al., 1967) has

shown that in the Musgrave Ranges these large faults appear to separate amphibolite and granulite facies terrains. The Giles Complex is generally confined to granulite facies terrains either south of the Mann Fault (Tomkinson group) or south of the Woodroffe Thrust (Musgrave group). One isolated body is found north of the Ayliffe Hill Thrust. The Bell Rock sheet in the Tomkinson group is probably in amphibolite facies terrain.

During the Tertiary(?), economically important nickel-rich weathering profiles developed on olivine-rich rocks in the area. These profiles, commonly preserved as silcrete cappings in the Tomkinson Ranges, have been described by Thomson (1963, 1965), Turner (1967, 1968) and Miller (1969).

PART TWO

ASSOCIATED ROCKS

CHAPTER 2

GRANULITES

2.1 Introduction

The metamorphic country rocks to the Giles Complex intrusions in the eastern Tomkinson Ranges are typical of granulite facies assemblages elsewhere.

The term granulite facies is used to indicate a certain group of mineral assemblages which are defined for rocks of all bulk compositions (e.g. Winkler, 1967; Turner, 1968). The term granulite applies to the rocks containing these assemblages and has no textural significance. Terms such as charnockite* are mentioned only in connection with previous work.

The division of the granulite facies into subfacies (e.g. de Waard, 1965), although criticised by various authors (e.g. Fyfe and Turner, 1966; Chesworth, 1967), is retained in later discussions although the rocks are firstly described in terms of their actual assemblages. The use of subfacies for groups of assemblages probably forming over wide variations in physical conditions is considered worthwhile whereas such divisions for more physically restricted assemblages, although valid, is less necessary. Winkler (1970) has recently embodied these concepts in a proposal for the abolition of "facies" and replacement by "stages".

---

* "Charnockite" has become widely used in many different contexts following Holland's (1900) original definition, and its use in this study would not act in the interests of precision.

The textural terminology used in the present description of the granulites from Ewarara and Kalka is based on that suggested by Moore (1970b). Moore's scheme is essentially an extension and modification of Katz's (1968) and Berthelsen's (1960) proposals.

Previous investigations of the granulites in the Tomkinson Ranges have been limited. McCarthy (in Mirams, 1964) has made petrographic descriptions of the major granulite types from the area, while Nesbitt and Talbot (1966) and Gray (1967) have noted the types of assemblages observed in the Mt Davies and Teizi areas. Barnes (1968) investigated rocks collected by R.L. Oliver from an area between Ewarara and Teizi. Moore (1970a) has studied the granulites in the vicinity of Gosse Pile in some detail. The granulites in the immediate vicinity of Ewarara have previously been described by Goode and Krieg (1965). The present investigation forms an extension and revision of this earlier work.

The rocks considered to be granulites in this study are the conformable* group of interlayered acid and basic gneisses forming the country rocks to the Giles Complex intrusions. The division into acid or basic granulites is made on the field recognition of the presence or absence of free quartz.

---

* Some of the conformable basic units are separated as members of various igneous suites on other evidence.

2.2 Petrography

1. Ewarara

(1) Acid granulites

The acid granulites have been divided into several groups on the basis of modal composition.

(a) Quartz + feldspar + pyroxene ± garnet granulites

These rocks form the thickest and most common lithological units at both Ewarara and Kalka (Plates 2,3,4). They can be further divided in the field into banded gneisses and augen gneisses. The augen gneisses are more massive (i.e. with a weaker foliation) and not as well layered as the banded gneisses, although they are mineralogically identical. The foliation S_1^m in the augen gneisses is mainly defined by the elongate feldspar augen. Alternating lithological units up to a kilometre thick can be mapped at Ewarara as dominantly augen or banded gneiss terrains (Fig. 2).

The bulk composition of these rocks is approximately granitic to adamellitic. They consist of quartz (about 20%), perthitic K-feldspar (about 30%) and plagioclase (about 20%; about An_{30}) with lesser amounts of ortho- and clino-pyroxene (in approximately equal proportions) and opaques (about 5% ilmenite and minor magnetite). Magnetite, which contains spinel exsolution, may or may not be directly associated with ilmenite. Apatite (stubby crystals) and zircon (rounded) are accessories in most rocks, but biotite and brown-green hornblende are rare. Garnet is present in some rocks. Details of assemblages are given in Table 3.

The potassium feldspar is usually strongly perthitic. The plagioclase lamellae and blebs are normally about 0.1 mm long giving rise to a mesoperthite but in some cases, even within the same grain, much smaller lamellae (<0.01 mm) are observed (Plate 8A). The latter are termed microperthites. The two types occur within mutually exclusive areas in any one grain. Moore (1970a) has suggested that for Gosse Pile granulites microperthite may form at a distinct and later stage than the mesoperthite, following annealing of deformed mesoperthite-bearing megacrysts. However, a coalescing origin of microperthite to form mesoperthite seems more reasonable for the Ewarara examples. Quartz and also feldspars commonly contain minute rods and blebs of opaque material.

A wide variety of textures are observed within the rocks. They are normally granoblastic (Plates 6A, 12B), but in some examples the felsic constituents exhibit a pronounced platy granoblastic or flaser fabric. Grain size variations are considerable and most commonly the grains are inequigranular. However, both equigranular and seriate grain size distributions are also observed. Grain size varies from about 0.5 to 1.5 mm. Grain boundaries are polygonal to interlobate. There is a slight tendency in the granoblastic varieties for grain elongation to be parallel to foliation S_1^m. Deformation features are common and include undulose extinction, dislocation bands, glide twinning and kinking.

The augen are much coarser-grained than the normal groundmass (Plate 12B); they are normally about 1 to 5 cm long (up to 2-3 cm wide) with individual feldspar grains up to about 5 mm long. The augen are very inequigranular, however, and grain boundaries vary from polygonal

to amoebeid. They consist dominantly of perthite with minor plagioclase and rare quartz and ferromagnesian minerals. The S_1^m foliation in the groundmass, defined by lenticular grain aggregates, is bent around the augen. Plagioclase is more common in the groundmass, and may also form an enriched zone around the augen.

An unusual "buckshot" texture is commonly found within perthitic grains in the augen (Plate 8A). The texture results from groups of rounded quartz and plagioclase inclusions which exhibit simultaneous extinction. There may be several groups within any one perthite grain. The inclusions reach a maximum grain size of about 0.5 mm and may be surrounded by a zone about 0.2 mm wide in the host feldspar where no perthite is observed. The texture is sometimes strongly developed in the groundmass marginal to the large perthite augen. In some examples there is a sympathetic size variation between inclusions and perthite lamellae.

It is believed that the augen represent segregations of K-feldspar relative to all other phases in an originally homogeneous rock. This process involved replacement of the original groundmass giving rise to the buckshot textures. Augen formation is assumed to have preceded the development of S_1^m which wraps around them (this latter argument is based on evidence presented by Rast, 1965).

"Myrmekitic" intergrowths (between feldspar/feldspar?) are observed at grain boundaries in some cases in both banded and augen gneisses (Plate 8B).

In some rocks at Ewarara, especially at Island Hill, garnet is

commonly observed as a symplectic intergrowth with probable quartz and perhaps feldspar (Plates 9A, 9B). The quartz inclusions are generally aligned approximately perpendicular to the opaque-garnet boundary or form irregular wormy intergrowths with the garnet. The garnet is directly associated with opaque phases which it generally surrounds. Commonly a thin rim of "solid" garnet without the quartz occurs at the opaque boundary, and in many cases the garnet/quartz intergrowth becomes finer grained away from the opaque phase. The rims are not observed between opaques and orthopyroxene, clinopyroxene or possibly quartz. They are therefore interpreted as representing a solid state reaction between ilmenite(?) and feldspar, although rims are not always observed between these two phases either. The reactions are in some cases only observed in restricted areas of a thin section suggesting compositional control. Banno and Green (1968) have noted that authors such as Brögger (1934), Shand (1945) and Gjelsvik (1952) have described garnet coronas around iron oxides in granulites from other areas. These probably represent similar reactions to those at Ewarara.

(b) Quartz + feldspar + garnet ± sillimanite granulites

These medium-grained gneisses form thin bands within the acid gneisses (Fig. 2) reaching a maximum thickness of about 150 metres (generally much thinner). They are well banded with alternating fine layers rich in quartz, feldspar or garnet. Mineral aggregates are aligned to give a foliation S_1^m parallel to the layering.

These rocks consist essentially of quartz and perthitic K-feldspar (together forming about 70% of the rock) with smaller quantities of

garnet (up to 20%), sillimanite (0 to 20%) and opaques (about 5%). Orthopyroxene, clinopyroxene and plagioclase are rarely observed. Red-brown biotite is found in a few layers and spinel and zircon are accessories in some rocks. Commonly perthite is more abundant than quartz but a complete modal gradation exists between these rocks and the quartz-feldspar and quartz-rich granulites. Details of the observed mineral assemblages are given in Table 3.

Antiperthitic plagioclase observed in one sample (A301-156) was found to contain 18.9% of the K-feldspar molecule (Goode and Krieg, 1965). Goode and Krieg also found that garnet from the same rock was of pyropic almandine composition (partial analysis in Table 5).

Textures within this rock type are variable. In general the texture is granoblastic, inequigranular. Grain boundary relations between quartz and feldspar are generally interlobate although some more polygonal grains are observed. The mafic minerals are usually polygonal. In some cases normal granoblastic textures are overprinted by a strong platy granoblastic or flaser texture in quartz and feldspar (Plate 7A). The ribbon-like grains tend to wrap around the garnet and sillimanite porphyroblasts (Plate 7B) which together with relic granoblastic quartz/feldspar lenses outline the earlier foliation S_1^m. Rotation of sillimanite porphyroblasts (Plate 7C) is rarely observed. Amoeboid grain boundary relations are common within the highly strained quartz/feldspar ribbons (Plate 7D). The younger foliation is commonly oblique to S_1^m and in some areas can be shown to represent S_2^m, axial plane foliation of the F_2 fold phase (see Chapter 13). All phases observed within these rocks can be shown to predate the younger

foliation, and probably also S_1^m.

Coronal textures of perthite and garnet on sillimanite, described by Moore (1969), are commonly observed in these rocks. Moore's Type 2 corona involving plagioclase rather than perthite has not been found at Ewarara.

Following a detailed examination of all available thin sections, the following progressive textural sequence was observed:

Stage 1 (e.g. A301-147): sillimanite with various inclusions commonly enclosed by perthite coronas (Plate 11A). Thin garnet rims partially enclosing sillimanite in some cases (Plate 11B; also Moore, 1969, Fig. 1).

Stage 2 (e.g. A301-15): garnet enclosing sillimanite within perthite corona (Plate 11C). Rounded inclusions of quartz, feldspar, opaques (ilmenite) and spinel are found in both garnet and sillimanite.

Stage 3 (e.g. A301-159): garnet occurs as spongy grains or idioblastic groups with occasional cores of sillimanite. Perthitic rims are absent (Plate 12A).

Stage 4 (e.g. A300-75): garnet as rounded spongy to compact grains without sillimanite cores or perthite rims (other inclusions present).

Within any one thin section different stages may be recognised in different areas suggesting a compositional control on the phase distribution (Plate 11A). No obvious geographic control on the distribution of reaction stages has been observed at Ewarara.

Moore (1969) has suggested that the garnet was produced by a dehydration reaction between biotite and sillimanite in response to increasing P,T

biotite + sillimanite + Na-rich K-feldspar + quartz ⟶
garnet + Na-bearing K-feldspar + water.

An excess of sillimanite over biotite would result in remnant cores of sillimanite in garnet (cf. Stages 2 or 3).

Such a reaction, however, cannot explain some of the features observed at Ewarara. The essential reaction does appear to be the production of garnet from sillimanite (the more garnet present, the smaller and less abundant the sillimanite), although the role of biotite is not proven in any case*. However, with increasing garnet/sillimanite ratio it has been noted in many cases that the perthite rim becomes thinner and eventually vanishes (e.g. Stages 3,4). This feature does not support the essential stability of K-feldspar as indicated by Moore (1969). From these observations, therefore, a modified reaction involving the production of garnet from sillimanite, biotite and perthitic K-feldspar may be necessary.

The primary sillimanite-perthite association may result from an earlier dehydration reaction between muscovite and quartz (after Guidotti, 1963, p. 785; Vejnar, 1966, p. 181) as a result of increasing grade of metamorphism. Guidotti (1963, p. 786) has also suggested a dehydration reaction between quartz, muscovite and sodic plagioclase

---

* In one example, biotite is directly associated with garnet with no sillimanite preserved, suggesting an excess of biotite in Moore's reaction (Plate 11D).

(e.g. An_5) to produce sillimanite, soda-rich K-feldspar and more calcic plagioclase. Following reaction between the sillimanite, K-feldspar and biotite to produce garnet, textures similar to Moore's Type 2 corona could result i.e. plagioclase (about An_{40}) around garnet with relic sillimanite cores*.

Wilson (1954) has described assemblages from the eastern Musgrave Ranges in which cordierite rims occur around sillimanite (with magnetite and spinel inclusions). Moore (1969) interprets these features as representing a lower pressure expression of the same reaction as above. It is interesting to note that Forestier and Lasnier (1969) have described rimming of corundum by spinel and zoisite (or by sapphirine) in pargasite from amphibolite facies schists in France. These rims may represent an equivalent lower pressure reaction in more undersaturated rocks.

(c) Quartz-feldspar granulites

These rock types are completely gradational from the quartz-feldspar-garnet granulites and are arbitrarily separated only on their lack of garnet. They have not been distinguished in the field from the other type (Fig. 2).

They consist of quartz and perthitic K-feldspar with minor to trace amounts of plagioclase, orthopyroxene and opaques in some rocks. Zircon and rare green-brown hornblende are accessories. Details of the assemblages are given in Table 3.

---

* Moore (1970, Fig. 2.35) has also described rims of perthite (outer) and plagioclase (inner) around garnet with a sillimanite core. This could be an arrested stage of this reaction.

Textures are similar to the quartz-feldspar-garnet granulites. They vary from granoblastic, inequigranular to granoblastic, equigranular (few small grains) to platy granoblastic. The first two groups are quite similar with interlobate to amoeboid grain boundaries for quartz and feldspar. Garnet tends to be "spongy" (i.e. filled with inclusions). It is interesting to note that quartz within garnet tends to have straight grain boundaries whereas outside the garnet its boundaries are amoeboid (Plate 9C). This would suggest that the amoeboid grain boundaries are an imposed feature, and, since they are strongly developed in the platy granoblastic textures, are related to the F_2 deformation.

Myrmekite-like intergrowths (between two feldspars?) are common in some rocks (Plates 8B,C,D). They are usually associated with the finer-grained portions of inequigranular or seriate populations (i.e. those apparently derived by recrystallization of the coarser-grained assemblages). In these areas they are commonly directly associated with perthites.

(d) Quartz-rich granulites (quartzites)

The gradation between quartz-feldspar-garnet and quartz-feldspar granulites also continues to those quartz-rich granulites with little or no feldspar.

These rocks usually consist of essentially quartz with variable, sometimes major, quantities of garnet, orthopyroxene, sillimanite or opaques (usually ilmenite exsolving haematite). Assemblage details are given in Table 3.

Textures are normally platy granoblastic with amoeboid grain boundaries. It has been noticed that the type of fabric developed in the granulites is generally controlled by the proportion of quartz present. Textures vary from granoblastic equigranular to platy granoblastic and grain boundaries from polygonal to amoeboid with increasing quartz.

A common variety of this rock type forms as blue, thin, irregular but conformable quartz-rich sheets at lithological boundaries. They are strongly lineated and foliated.

A layered iron-rich quartz granulite (A300-74) has been mapped as small thin lenses at two locations at about the same "stratigraphic" level at Ewarara (Fig. 2). The rock is highly deformed with the quartz exhibiting a platy granoblastic texture. The magnetite layers, however, while highly lenticular contain granular magnetite which is coarse-grained compared to the layer thickness. Exsolution lamellae of spinel and haematite are also undeformed and quite long. This suggests that the magnetite annealed and underwent extensive grain growth with subsequent exsolution of spinel and haematite after the deformation.

(2) Basic Granulites

Like the acid granulites, the basic granulites have also been divided into several groups on the basis of modal composition.

The basic granulites form relatively minor lithological units within the acid granulites, reaching a maximum thickness of about 50 to 100 metres (Fig. 2). Thomson (1964) has also mapped most of the

basic granulites in the eastern Tomkinson Ranges as thin bands. Several examples of thicker outcrops recorded by Thomson near Kalka and Ewarara have proved on closer examination to be partially recrystallized Giles Complex rocks.

(a) Plagioclase - orthopyroxene - clinopyroxene granulites

Assemblages of this type are commonly observed in the northwestern parts of Ewarara (Fig. 5) and not around Island Hill.

The rocks consist essentially of plagioclase (about 60%), orthopyroxene and clinopyroxene (in approximately equal proportions of 15 to 20%) and opaques (about 5%). Plagioclase is sometimes antiperthitic and has a composition of about An_{55-70}. In some cases clinopyroxene contains opaque exsolution plates which are very fine and in some instances give a dusty effect. Orthopyroxene contains minute unidentified rods oriented in several directions. The opaques consist of ilmenite and magnetite, either as granular aggregates or separate grains. Both contain some haematite exsolution. Magnetite is commonly found intergrown with hornblende at pyroxene grain boundaries (Plate 12C). Brown-green hornblende ($2V_z \simeq 80$; with rare opaque exsolution plates) and dark-brown biotite are present in some rocks, rarely in significant quantities. Rounded to lath-like apatite is a ubiquitous accessory but green spinel has not been observed*. Quartz segregations have been found in some rocks in the field. Details of the assemblages are given in Table 4.

---

* Unlike similar rocks at Gosse Pile (Moore, 1970a) where spinel is common.

The textures of these assemblages are characteristically granoblastic, equigranular (0.5 to 1 mm) with polygonal grain boundaries (Plate 6B). Grain aggregates (and biotite foliae in biotite-rich samples) are aligned parallel to layering to form a distinct S_1^m foliation. The presence of glide twinning in plagioclase and undulose extinction indicates a degree of strain imposed after the last period of annealing.

The modal compositions of these rocks are very similar to opaque-bearing clinopyroxene norites of the Giles Complex and to Type B dolerite dykes. In recrystallized assemblages it can therefore be very difficult to distinguish these rock types, especially in the field. Thick sequences of these rocks can usually be shown to be closely associated with Giles Complex rocks and commonly retain relic igneous textures. However, thin conformable bands may represent either "primary" granulites or sill-like intrusions of Type B dykes.

It is quite possible that some of the bands mapped as plagioclase - orthopyroxene - clinopyroxene granulites on Fig. 2 are in fact recrystallized younger igneous rocks. Some relic igneous textures have been observed in A300-22 and A301-123b, 132. These include lath-shaped plagioclase and pyroxene inclusions in plagioclase (cf. Appendix 4). Lath-like apatite could also indicate a primary igneous origin (Wyllie et al., 1962). Most bands, however, are probably older than the Giles Complex (some are transgressed by the Ewarara Intrusion). Other subtle differences also exist e.g. lack of spinel, deep-brown biotite rather than red-brown biotite.

(b) Garnet - clinopyroxene - plagioclase granulites

Rocks with these assemblages have so far only been observed at Island Hill and southwest of Ewarara (Figs. 2 and 5) and have not been found interbanded with plagioclase - orthopyroxene - clinopyroxene granulites.

They are generally more ultramafic than the other type of basic granulite, containing about 10 to 20% plagioclase (about An_{85} in one X.R.D. determination). Garnet commonly forms about 40 to 50% of the rock with clinopyroxene about 20 to 30%. However, in some rocks containing significant amounts of orthopyroxene, clinopyroxene is more abundant than garnet. Clinopyroxene may contain opaque exsolution plates (or fine grained dusty equivalents). In some cases garnet contains cores of opaque rods in oriented sets (probably ilmenite or rutile). A cell edge of 11.577Å was measured for garnet A300-58 suggesting an almandine-rich composition (by comparison with Table 5). The garnet is closely associated with orthopyroxene when the latter phase is present suggesting that it results from solid state reaction between orthopyroxene and plagioclase (see Green and Ringwood, 1967b). In some cases it also rims opaques as it does in some of the quartz - feldspar - pyroxene ± garnet granulites.

Brown hornblende ($2V_z \simeq 80$; with opaque exsolution plates - Plate 108) is observed in all samples, commonly associated with and probably forming at the expense of clinopyroxene. The opaque phases, dominantly ilmenite (some haematite exsolution) with rare magnetite, are commonly associated with green spinel. The ilmenite normally occurs

as granular aggregates, but may also form wormy intergrowths with pyroxene at garnet or pyroxene grain boundaries. Small (up to 0.5 mm by 0.1 mm) oriented corundum plates are commonly observed in the ilmenite (Plate 9D). Moore (in press) has interpreted similar bodies from Gosse Pile granulites as exsolution features and has suggested the existence of an earlier homogeneous Fe - hogboemite phase. It is interesting to note that whereas the corundum described by Moore occurs in ilmenite from acid garnet-bearing granulites, the Ewarara examples are in ilmenites from basic garnet-bearing granulites.

Textures in these rocks are generally granoblastic equigranular (0.5 to 2 mm) with grain boundaries varying from polygonal to interlobate (Plates 6C,D). Glide twinning in plagioclase and undulose extinction indicate that the assemblages are strained. In rocks containing remnant orthopyroxene textures tend to be inequigranular as garnet is finer grained than usual. Relic igneous textures are observed in several of the rocks. Plagioclase lath shapes are rare but clinopyroxene inclusions in plagioclase are common (cf. Appendix 4). Some of the textures could be interpreted as partially recrystallized mesocumulates. Opaques tend in many cases to be interstitial. Details of mineral assemblages are given in Table 4.

Summary

The assemblages observed in the Ewarara area can be divided into two subfacies of the granulite facies viz. the orthopyroxene - plagioclase and garnet - clinopyroxene subfacies of de Waard (1965), or the equivalent intermediate and high pressure granulites of Green and

Ringwood (1967b). The use of subfacies is thought to be justified as the assemblages are from geographically distinct areas (Fig. 5), and therefore are not considered to be only the result of chemical effects on mineral stabilities. Transitional assemblages observed in both the acid and basic granulites indicate the garnet - clinopyroxene subfacies assemblages formed from orthopyroxene - plagioclase subfacies assemblages.

The present assemblages appear to have been in equilibrium at the completion of the F_1 deformation (and possibly before), with textural overprinting occurring during F_2 folding.

2. Kalka

The Kalka granulites are similar to those at Ewarara although they tend to be finer-grained. Quartz - feldspar - pyroxene, quartz - feldspar and plagioclase - orthopyroxene - clinopyroxene (± hornblende) are the most common assemblages. Garnet has only been observed in one acid granulite specimen (A314-423). In this instance is occurs as a very fine-grained granular rim on biotite (Plate 10D), and postdates a foliation similar to S_2^m at Ewarara.

3. Minno

The acid granulites south of the Hinckley Fault are also in general similar to those at Ewarara. However, the rocks in the immediate vicinity of Minno, which have been mapped by Thomson (1964) as hypersthene adamellites, deserve further comment. Unlike other granites in the Musgrave Block which are generally massive (Wilson, 1960), the

Minno rocks are well layered and foliated.

The dominant rock type is a well foliated quartz - feldspar gneiss. The foliation, formed by quartz-rich aggregates and apparently equivalent to S_1^m as it is folded by F_2, anastymoses around large (up to 5 cm) perthitic K-feldspar porphyroblasts. These porphyroblasts are somewhat different to the feldspar augen at Ewarara in that they tend to be single crystals rather than crystal groups. Biotite is more common than orthopyroxene and commonly rims ragged orthopyroxene crystals (Plate 10C) suggesting replacement. It also exhibits pleochroic halos around unidentified high relief inclusions (biaxial negative optics). Well developed myrmekite-like intergrowths associated with and penetrating perthite grain boundaries (Plate 8C) are unusually common.

Interlayered with this rock type are thin even grained (and finer grained) quartz - feldspar bands without ferromagnesian minerals.

The rock is therefore distinct in some ways (e.g. myrmekitic intergrowths, biotite halos) from the normal granulites and could be considered as a deformed and partially retrograded porphyritic orthopyroxene granite with associated aplite veins.

2.3 Physical conditions of metamorphism

While it is generally considered by most authors that the granulite facies represents assemblages formed at high pressures and temperatures, there are quite wide variations in the suggested absolute ranges of these variables (e.g. compare Fyfe and Turner, 1966 and Green and Ringwood, 1967b).

The derivation of absolute P-T conditions for certain specific metamorphic conditions depends on experimentally determined reactions and mineral stability fields. With the assumption that the experimental data is correct (not necessarily justifiable as the variance in determined aluminosilicate stabilities demonstrates - see Fyfe, 1967), the transferance of data from laboratory to natural systems is often open to question. The possible effect of variations in bulk composition, water content, f_{O_2} and other factors must be taken into account in each instance.

It is considered that P_L was much greater than P_{H_2O} during the granulite metamorphism because of the general lack of hydrous phases such as biotite and hornblende. It is unlikely that this paucity would be due to stabilization of anhydrous phases at high temperatures (as suggested by Turner and Verhoogen, 1960) since Lambert and Wyllie (1968) have indicated that hornblende is stable under most crustal conditions. Furthermore the general lack of acid igneous rocks in the area (only rare acid pegmatites are observed) demonstrates that anatectic melting of the granulites was very limited. However, Luth et al. (1964) and Tuttle and Bowen (1958) have shown that considerable granitic melting might be expected in "wet" acid rocks for temperatures and pressures above about 700°C* and 2 kilobars. This would further indicate the anhydrous nature of the granulites during their last recorded metamorphism.

---

* The lack of muscovite in the Ewarara rocks indicates minimum country rock temperatures of about 700°C (Burnham and Shade, 1968).

It is therefore considered that P_{H_2O}, and hence P_{O_2} are both low during the granulite metamorphism. Their effect on anhydrous experimental data will therefore be ignored in the following attempt to categorise the P-T conditions of the metamorphism.

(1) Al_2SiO_5 stability

The limits of the sillimanite stability field are shown in Fig. 6, curves 1a and 1b. The data used are from Fyfe's (1967) review of the available experimental data, and from recent determinations by Richardson et al. (1969).

(2) Hornblende stability

The approximate upper stability of hornblende in basic rocks is shown in Fig. 6, curve 2. It should be remembered however, that the hornblende observed in the granulites may have formed during cooling of the assemblages (it is commonly observed rimming and apparently replacing clinopyroxene) or in some cases during intrusion of the Giles Complex as an aureole effect (see Chapter 5.2).

(3) Partial melting

Melting curves for "wet" granite, granite with 2% H_2O and "dry" granite are plotted on Fig. 6, curves 3a, b, c, d. The dry granite curve will give the approximate maximum temperatures of metamorphism since little evidence for rock melting is observed in the anhydrous granulites.

(4) Sillimanite - garnet reaction, and muscovite stability

No experimental information is available for this reaction observed in the quartz - feldspar - garnet ± sillimanite granulites, except that it appears to lie outside the stability of cordierite. The sillimanite - perthite assemblage associated with this reaction was interpreted as inferring the previous existence of quartz and muscovite. The break-down curve for muscovite - quartz determined by Burnham and Shade (1968) is shown in Fig. 6, curve 4.

(5) Cordierite stability

The upper stability limits of Mg-cordierite (Schreyer and Yoder, 1964) and cordierite in SiO_2 - saturated synthetic rocks (Hensen and Green, 1970) are shown in Fig. 6, curves 5a and 5b. These will give minimum conditions for the metamorphism since cordierite is not observed in the assemblages considered to be of suitable composition (p. 21). The strict application of these curves is open to question because of the dependence of cordierite stability on composition and P_{O_2}.

(6) Orthopyroxene - garnet reaction

It was concluded previously that the assemblages and textures observed in the Ewarara basic granulites indicated the transitional reaction of orthopyroxene with plagioclase to give garnet. The reaction lines for pure end members enstatite and anorthite to give pyrope-grossular and quartz (Kushiro and Yoder, 1966) and of orthopyroxene - plagioclase in quartz tholeiite compositions to give garnet - quartz

(Green and Ringwood, 1967b) are plotted on Fig. 6, curves 6a and 6b (other data in Fig. 29B). The lack of garnet with orthopyroxene - plagioclase in acid granulites give a lower temperature limit for the metamorphic conditions. Green and Lambert's (1965) data for this reaction in anhydrous adamellite compositions is shown in Fig. 6, curve 6c. These data indicate that orthopyroxene - plagioclase assemblages are stable to lower temperature in acid rocks than they are in basic rocks at any given pressure. This probably explains the interlayering of garnet-free* acid gneisses and garnet-bearing basic granulites in the Island Hill area of Ewarara.

(7) Opaque - garnet reaction

Following Banno and Green's (1968) review it is not considered possible at this stage to accurately categorise the conditions of this reaction observed in acid granulites at Island Hill. Chemical control may be important in this reaction.

(8) $CaCO_3$ stability

Although carbonate-bearing rocks have not been observed in the present field area, calcite has been observed in various marbles and calc-silicate rocks elsewhere in the Tomkinson Ranges (Mirams, 1964; Moore, 1970a). Boettcher and Wyllie (1968b) have reviewed the available data on the calcite-aragonite transition and their preferred curve is shown on Fig. 6, curve 7. Care in use of this data is recommended, however, as Metzger and Barnard (1968) have noted evidence for the

---

* Garnet in these rocks is associated with ilmenite, not orthopyroxene.

stability of aragonite outside the plotted field at low pressures and temperatures.

A comparison of the experimental data available and the assemblages observed has lead to the outlining of a stability field for the metamorphism of the Ewarara granulites as shown in Fig. 6. Maximum P-T conditions range from about 10 to 12 kilobars* (i.e. 35-40 km) and 900 to 1050°C. This field lies in the area of intermediate to high pressure granulites (Green and Ringwood, 1967b). In a detailed study at Gosse Pile, Moore (1970a) has also suggested pressures of about 10 kilobars and temperatures of about 1000°C. Geothermal gradients associated with such conditions would be of the order of 20°C/km to 30°C/km.

The variations in assemblages at Ewarara could either indicate that the transition from orthopyroxene - plagioclase to clinopyroxene - garnet in the Island Hill area was achieved by decrease in temperature (i.e. cooling after the peak of metamorphism) or by progressive increase in pressure during metamorphism (or a combination of both). If the two areas of different assemblages were at the same pressure, it seems unlikely that the Island Hill area would cool more than the other. It is therefore suggested that the Island Hill area represents a slightly higher pressure regime than that to the northwest of it. Its present exposure could be the result of younger F_2 folding as it forms the core to a large F_2 anticline.

---

* Pressure estimates may extend to lower values dependant on the limits of cordierite stability.

The proposed increase in pressure to the east may also be part of a more regional variation. Barnes (1968) has suggested the presence of a possible pressure gradient between Ewarara and Teizi*. At Teizi, Gray (1967) has noted only assemblages of the clinopyroxene - garnet subfacies, and indeed the Giles Complex in this area also appears to be at higher pressure than those intrusions at Ewarara and Kalka. On the other hand, granulites at Gosse Pile are dominantly of the lower pressure orthopyroxene - plagioclase subfacies (Moore, 1970a). It has been noted that in the Ewarara basic granulites, the spinel/opaque association only occurs in garnet - clinopyroxene subfacies granulites whereas at Gosse Pile spinel is found in orthopyroxene - plagioclase subfacies basic granulites. If the spinel/opaque association is an indication of similar bulk compositions**, this may also suggest higher pressure conditions for Ewarara compared to Gosse Pile.

Other indications of P-T conditions in granulites elsewhere in the Musgrave Block are limited. Wilson (1954) has described sillimanite and cordierite-bearing granulites from the eastern Musgrave Ranges. These assemblages would indicate pressures of less than 10 kilobars (from Fig. 3). Virgo (1968) has demonstrated an increase in temperature from amphibolite to granulite facies terrains in the eastern Musgrave Ranges but was unable to quantitatively estimate these temperatures. Kyanite is found in at least one locality in the Musgrave Block viz. in the Everard Ranges (G.W. Krieg, pers. comm.).

---

* Barnes (1968), however, suggests much lower absolute pressures and temperatures for the granulite metamorphism viz. about 4 to 6.5 kilobars pressure and temperature of about 600 to 700°C.

** In the Kalka layered intrusion, primary spinel is only found with opaques in olivine-bearing rocks and not in olivine-free units (Chapter 6).

The dominance of acid granulites of approximate adamellite composition (over 90% of the total outcrop) in lower crustal conditions is contrary to the widely accepted geochemical-geophysical model of a gabbroic lower crust. Ringwood and Green (1966), following experimental investigations, have also recommended that the gabbroic model be abandoned. It is far more likely that the crust contains a markedly heteregeneous mixture of lithologies in diverse structural settings, and is not a simple stratified shell on the mantle.

2.4 Origin of the granulites

The author is in agreement with the general view of other workers in this area that the granulites are mainly metasedimentary in origin. The presence of rare calc-silicate and quartzitic horizons lends support to this concept.

The dominant rock type, the quartz - feldspar - pyroxene gneisses, are therefore considered to represent original sediments approximating micaceous arkoses (and possibly greywackes or shales) in composition. The more quartz - feldspar rich bands could have originally been arkoses, while sillimanite-rich granulites indicate more pelitic compositions. Occasional iron-rich quartzites may have formed from original banded iron formations although Moore (1970a) has suggested a metamorphic origin for these rocks near Gosse Pile.

Basic granulites are not common anywhere in the Musgrave Block and in the present area some retain several features indicative of plutonic igneous crystallization. They are therefore interpreted as representing intrusive basic sills, although some may represent basic lava flows in

the original sedimentary pile.

If the present granulites were in fact originally sediments then their anhydrous state during the last recorded metamorphism would seem to indicate a probable polymetamorphic history. Ringwood and Green (1966) also believe that anhydrous lower crustal terrains indicate complex and repeated metamorphic episodes. On the other hand, if the dominant acid gneisses represent an original rhyolitic lava sequence, then the rocks may have already been essentially dry, and only one period of metamorphism may be recorded.

The degree of chemical modification of the sediments and/or volcanics cannot be accurately gauged. Heier and Adams (1965) and Lambert and Heier (1968) have shown significant depletions in U, Th and Rb in high pressure granulites elsewhere. I.B. Lambert (pers. comm.) has measured low concentrations of uranium (0.90 ppm U) and thorium 2.5 ppm Th) in an augen gneiss (A301-72) from Ewarara containing 3.60% K_2O. This suggests that similar depletions could be expected throughout this area.

The gross chemical layering now observed in the granulites is considered to represent the approximate original sedimentary variations. However, because of the several (at least three) periods of deformation which have affected the rocks no primary bedding is specifically recognised.

CHAPTER 3

MINOR INTRUSIONS

A wide variety of minor intrusive bodies, most of basic composition, have been found within the Ewarara - Kalka area (Fig. 2). Some intrusions have been described previously by Goode and Krieg (1965, 1967) but have been redescribed and regrouped during the present study.

Most of the intrusions are demonstrably younger than the Giles Complex, although several (e.g. transgressive medium-grained gabbros) are probably genetically related.

A large proportion of the bodies can be grouped into two main types viz. the dolerite dykes and the transgressive picritic suite. The other intrusions include transgressive medium-grained gabbros, transgressive magnetite - ilmenite bodies, acid pegmatites, transgressive norite, mafic pegmatites, pyroxenite lenses, anorthosite and garnet pyroxenite.

3.1 Dolerite dykes

The dolerite dykes have been divided into four major suites on the basis of their field orientation, size, mineralogy (summarised in Table 6A; detailed mineralogy in Appendix 6), special mineralogical properties (e.g. types of exsolution in pyroxene, colour of amphibole etc.), texture, early crystallizing phases, mineralogical geochemistry and relative ages (Table 7; Chapter 14).

Analyses of representative examples of the four suites also reveal differences in total rock geochemistry (Table 8). Classification by CIPW norms (Table 8) and by SiO_2 v. ($Na_2O + K_2O$) and Al_2O_3 v. ($Na_2O + K_2O$)

diagrams (Figs. 7A,B) reveal that the Type A dolerite corresponds to an olivine tholeiite whereas the Type C dolerite is an alkali olivine basalt (basalt nomenclature from Green, 1970). Types B and D plot as tholeiites in Figures 7A and 7B, but by CIPW norms correspond to alkali olivine basalts or possibly olivine basalts (they have low normative nepheline contents).

Fractionation diagrams (Fig. 7C) and the crystallization index (Table 8; after Poldervaart and Parker, 1964) show that the Type A dolerite is significantly more iron enriched than the other suites. The crystallization index also suggests that the dykes become less fractionated as they become younger.

There is therefore a general tendency for the dolerites to become more undersaturated and less fractionated as they become younger. Such a geochemical tendency requires further investigation because of its possibly important genetic implications.

The descriptions on which the petrographic distinctions between the dolerites rely are based on a study of over 40 thin sections and several polished sections from the author's field area and on thin sections kindly supplied by other workers* from throughout the Musgrave Block.

The exceptions to such a classification within the author's field area are very few, and even in these cases similarities with one of the four suites can be observed.

---

* Dolerite specimens or thin sections were obtained from A.C. Moore, C.M. Gray, R.W. Nesbitt, K.D. Collerson, G.W. Krieg, R.B. Major, P.C. Smith and the S.A. Geological Survey.

3.1.1 Type A (one pyroxene) dolerite dykes

1. Field Occurrence

These deformed medium-grained dykes are generally quite thick (up to 100m, although some are only a few metres wide) and continuous (up to 20km long, or perhaps 60km or more if isolated outcrops are joined) in the Tomkinson Ranges (Figs. 2,8,9). They maintain, in most cases, a NW trend and are generally steep dipping. The margins are often finer grained than the central portions of the dykes. The dykes have apparently intruded along a major fault system as significant lateral displacements can be observed at Teizi (Gray, 1967); later movements are apparently responsible for the common development of pseudotachylite and other features of brittle deformation at dyke margins.

Identical deformed dykes are also found near Gosse Pile, Teizi, Mt Aloysius and west Hinckley in the Tomkinson Ranges and near Amata in the western Musgrave Ranges (Fig. 9). In the Deering Hills similar dykes become much more undeformed along strike to the southeast. South of Mt Davies in the Tomkinson Ranges, north of Ernabella in the Musgrave Ranges and in the Everard Ranges undeformed Type A dolerite dykes are observed. The Deering Hills appears to constitute a transition zone between the highly deformed dykes to the northwest and the undeformed dykes to the southeast.

The dykes parallel a major continental linear magnetic anomaly pattern extending to the southeast to Eyre Peninsula (Fig. 9). These anomalies have been shown to be caused by dolerite dykes of identical mineralogy and texture to the undeformed Type A dolerites (Price, 1970; Drew, 1970).

2. Mineral Assemblage and Texture

Apart from grain size variations between dykes and at their margins, and variations in the degree of deformation they have undergone, the dykes are consistent in their mineralogy and texture.

A deformation fabric is present in all samples but the least deformed exhibit typical doleritic textures (Plate 13A). The rock consists of plagioclase (55-60%), clinopyroxene (40-45%) and magnetite/ilmenite (<5%) with accessory apatite. Blue-green pleochroic amphibole, present in varying amounts, is a characteristic mineral associated with pyroxene boundaries in these dykes. In some dykes quartz, K-feldspar(?) and biotite are also observed in the interstitial areas.

The doleritic texture, homogeneous mineral distribution, textural similarity to the finer grained margin, and random orientation of the plagioclase laths indicate that the rock texture developed by rapid cooling of the melt. In A314-701 the chilled margin differs from the central parts of the dyke in that it contains phenocrysts of clinopyroxene and plagioclase in the doleritic matrix. It therefore appears that in at least some cases the melt was already beginning to crystallize when intruded.

The dykes have all been deformed following their crystallization with grains exhibiting undulose extinction, bending or kinking. In the more strongly deformed varieties, the lenticular plagioclase grains show a strong preferred morphological and crystallographic orientation (Plate 13C), which, together with grain aggregate stringers of pyroxenes and opaques, produce a strong foliation and less well developed lineation.

The foliation is axial plane to F_2 folds observed in the granulites (Chapter 13). The plagioclase crystals retain their primary characteristics (e.g. general lath-like shape, simple twinning, zoning). They also retain their inclusion clouds which could be expected to be expelled if the grains had been recrystallized. However, there is a strong tendency for equidimensional grain development at grain boundaries. Zone and twin boundaries become diffuse and complex grain boundary and twin relationships are developed. In the most extreme cases thin lenticular ribbons of plagioclase, with equidimensional grain aggregates and no clouding, are developed parallel to the foliation at grain boundaries (Plate 13B). They have a tendency to anastomose around the primary plagioclase crystals.

The fabric suggests that the deformation in the dyke was plastic and occurred at low strain rates with the retention of many of the igneous characteristics. The lack of development of similar fabrics in the associated basic granulites is considered to indicate that the deformation occurred before the dykes cooled to the regional temperature operating in the country rocks. The rotation of the plagioclase laths was probably attained largely by recrystallization of the pyroxene matrix. The development of ribbon plagioclase probably occurred in zones of higher strain rate, with later recrystallization and some grain growth. Possible reasons for the general lack of recrystallization (as a strain release mechanism) in the dykes are discussed in Chapter 3.1.2).

3.1.2 Type B (two pyroxene) dolerite dykes

1. Field Occurrence

These medium to coarse-grained dykes are generally less than about 3 metres thick and are not as laterally persistent as the Type A dykes (Figs. 2,8). They occur in the granulites in the vicinity of Ewarara and Kalka, and have previously been called gabbroic dykes by Goode and Krieg (1967, p. 189). Their attitude is variable from area to area but is generally consistent within a small region. They are both cross-cutting and conformable to the granulite layering. Grain sizes are generally unusually coarse compared to dyke thickness, although fine-grained variants are also found. The latter are commonly associated with more well developed chill textures.

Although generally dyke-like in character, they sometimes form lensoid bodies which intertongue with the granulites. They rarely have finer grained margins. Pseudotachylite is often found at the contacts, and this, together with the parallelism of dykes in a particular area and small displacements of granulite layering indicates that the cross-cutting varieties were probably intruded along minor fault zones. In some cases, the dykes intrude along more important faults.

Similar dykes are also observed elsewhere in the Tomkinson Ranges at Teizi, Gosse Pile, west Hinckley and also to the east of Ewarara.

Despite the field relations which indicate that the dykes are younger than the Giles Complex (Gray, 1967), the Type B suite is the most similar of all the dyke suites to the nearby intrusions of the Complex. Similarities are observed in grain size, mineralogy, texture

and mineralogical properties.

Strong similarities in mineralogy and texture are also observed between the dyke suite and the basic pyroxene granulites. Completely recrystallized dyke assemblages are impossible to distinguish petrologically or chemically (i.e. plagioclase composition) from pyroxene granulites. They can only be differentiated on field evidence (e.g. on transgressive relationships), on the recognition of any relict igneous component (e.g. recrystallized plagioclase laths or pyroxenes with exsolution lamellae) or on small differences in mineralogy.

2. Mineral Assemblages and Textures

This suite of rocks show more variation in their properties than the other suites but possess common and distinctive mineralogical and textural characteristics which enable them to be grouped together and distinguished from the other dyke suites.

In general the dykes consist of plagioclase with orthopyroxene and clinopyroxene (in approximately equal amounts, although one or the other may predominate in some examples). There are quite pronounced variations in pyroxene/plagioclase ratios from about 40/60 to 80/20 within the suite. Lesser amounts of brown hornblende and/or red-brown biotite and/or magnetite/ilmenite may also be present. There is some tendency for biotite to associate more with opaque phases than hornblende which is more associated with pyroxene, and for each to form in different rocks. The biotite - opaque association is thought to result from final iron-enrichment in the melt whereas hornblende is considered to represent more of a hydration assemblage. Spinel and garnet are rarely

observed.

The texture of the rocks is characteristic (Plate 14C): 1 to 5mm megacrysts of orthopyroxene and/or clinopyroxene (both pyroxenes commonly mantled - Plate 15A, or in epitaxial relationship - Chapter 9) and/or plagioclase, forming a primary assemblage with igneous characteristics, are contained in a finer-grained (0.1 to 0.5mm) secondary assemblage with recrystallization characteristics (criteria in Appendix 4). The primary assemblages are opx - cpx - plag; opx - cpx; opx - plag; cpx - plag; opx; cpx.

The secondary assemblage consists essentially of a polygonal, equigranular mosaic of orthopyroxene, clinopyroxene and plagioclase with lesser amounts of hornblende, biotite, magnetite/ilmenite, spinel and garnet in some rocks. By comparison with other basic igneous rocks in the area it is probable that all these lesser constituents were also present in the original primary assemblage. The temperature of recrystallization must be lower than the temperature required for solid solution of the various phases observed as exsolution bodies in the primary phases as these are not present in the secondary assemblage.

The garnet, found only in A300-108 where it is associated with orthopyroxene, is probably formed by a sub-solidus cooling reaction between orthopyroxene and plagioclase prior to recrystallization as was suggested by Gray (1967) for similar Teizi dykes (see also Chapter 11). Gray has shown that garnet only forms in the more iron-rich rocks.

Both primary and secondary assemblages exhibit minor strain features such as undulose extinction.

The dolerites exhibit some evidence of having an original chill texture as in some dykes plagioclase laths, or recrystallized equivalents, are randomly oriented. Rarely finer grained rocks show strong development of chill textures (Plate 14A); plagioclase and rarely clinopyroxene laths may be in parallel or radial groups with overall random orientation.

However, especially in the coarser grained rocks there is a tendency for the plagioclase laths to exhibit a slight lamination, suggestive of a more cumulus mode of origin. This would be in accord with the tendency for the dyke suite to be more variable in composition than the other suites which have well developed chill textures.

Most of the dykes have a relatively homogeneous distribution of minerals although there is a small tendency for pyroxene-rich clumps, 5 - 10mm in diameter, to occur in many (Plate 14A). This is much more pronounced in some rocks; hornblende and biotite also tend to be concentrated in these areas. The clumping is not a cumulus feature as it is also found in rocks exhibiting good chill texture.

The development of the secondary fabric is, the result of two distinct but related processes - deformation and recrystallization.

The indication of deformation lies in the development of a foliation. The foliation tends to a fine layering (plagioclase v pyroxene) in the most deformed samples (Plate 13D) but is generally present as a morphological preferred orientation of grain aggregates and to a lesser extent individual grains. The foliation is not usually strongly developed in either hand specimen or thin section and can only

be observed on careful scrutiny. A further indication of extreme high temperature deformation is found in A300-93, which has a fine layering-type foliation, where a remnant "flow" orthopyroxene has been found (cf. Chapter 13.2). The foliation is tentatively considered to be formed by the F_3 deformation (Chapter 13.4).

In general the more deformed a rock (i.e. the better the foliation development) the greater the degree of recrystallization (i.e. higher secondary/primary grain ratio). This together with the petrographic descriptions of the secondary grains is interpreted as indicating that the secondary assemblage resulted from an annealing recrystallization of a previously deformed primary igneous fabric; the residual primary crystals representing the least strained portions of the primary assemblage.

The following assemblages are therefore observed:

(a) remnant primary pyroxene - plagioclase with secondary pyroxene - plagioclase

(b) remnant primary pyroxene with secondary pyroxene - plagioclase

(c) secondary pyroxene - plagioclase (with best development of foliation).

Although all available information is consistent with the Type B dykes being intruded in the same chronological interval, cross-cutting relations have been observed between A300-108 and A300-110 (older and larger). It is interesting to note that the smaller and younger dyke is now more recrystallized than the older. It is suggested that if both dykes were deformed at the same time while still at a high

temperature, then 108 might tend to recrystallize more than 110 as it would be at a higher temperature because of its later injection.

This could also explain why the Type A suite, while being strongly deformed, is not recrystallized to any degree. Although it has been argued that the A dykes were still "hot" relatively to the country rocks when deformed, if they were at a relatively low temperature compared to the solidus at that stage, then perhaps the strained fabric would not recrystallize by annealing processes.

This also shows that the recrystallization event in Type B dykes is not caused by regional reheating effects otherwise the Type A dykes would also be recrystallized. It is therefore concluded that the temperature of the rock at the time of deformation is of prime importance in determining whether the strained assemblage will recrystallize or not.

3.1.3 Type C olivine dolerite dykes

1. Field Occurrence

This suite of dykes is confined to the northwest corner of the Kalka layered intrusion, and has not been found in the granulites (Figs. 2,8). They are cut by Type D dolerites but as they are undeformed and not recrystallized they are considered to be younger than the Type A or Type B dykes.

They have a maximum thickness of about 5 metres and may change thickness and attitude along strike. They generally have a moderate (45^{o}) dip to the north, but vertical contacts have been recorded. A maximum lateral extent of about $1\frac{1}{2}$km has been measured. Dyke margins

are sometimes finer grained than the central parts of the dykes.

The dykes cross-cut, and sometimes slightly displace and incorporate the layered gabbros. This, together with common brittle deformation (pseudotachylite and microfaults) at the margins and the linearity of the dykes, suggest that they were intruded along a fracture system, which was reactivated at some stage after solidification. In parts the dykes are pod-like and unconnected; this may be a primary or secondary feature.

2. Mineral Assemblages and Textures

The dykes consist of irregular concentrations of plagioclase megacrysts in a homogeneous olivine dolerite matrix (Plate 16C). The megacrysts may make up to 30-40% or more of the rock, producing a coarse-grained "anorthositic" dyke with an olivine dolerite matrix or may be completely absent, producing a medium-grained olivine dolerite dyke.

The matrix exhibits a typical medium-grained doleritic texture (Plate 14D) and consists of plagioclase (60%) with lesser amounts of clinopyroxene (25%), olivine, biotite, magnetite, ilmenite, spinel, orthopyroxene and antiperthite. Rare pyrite(?) is also observed.

The texture is controlled by randomly oriented 1 to 3mm plagioclase laths with all other minerals tending to be interstitial to the laths. The rocks have been slightly deformed as minor undulose extinction is common. Subgrain growth in clinopyroxene is common but recrystallization is rare. A core of primary massive clinopyroxene is often preserved in areas of subgrain growth. The doleritic texture is still preserved in

these areas so there has been no gross redistributive deformation.

A fine-grained dolerite from one of the dyke margins is generally similar to the normal matrix although it does not contain olivine.

The aggregates of magnetite/ilmenite/spinel are commonly rimmed by red-brown biotite which may be intergrown with pyroxene or plagioclase at its outer margins and which forms at the grain boundaries of all the other phases as well. The biotite is therefore interpreted as a late stage crystallization product. It is difficult to determine whether liquid reaction was involved in the case of the "opaque" aggregates; these may simply provide favourable sites for biotite nucleation. This four-mineral association is common in other rocks in the area. Hornblende sometimes forms as a further rim on the biotite in other rocks.

The edges of many of the early formed plagioclase laths and the interstitial areas between earlier formed grains are often characterised by the presence of masses of clinopyroxene inclusions in plagioclase.

The plagioclase megacrysts have identical properties to the matrix lath feldspar. X-ray diffraction compositions of non-magnetic plagioclase fractions from megacryst-rich and megacryst-absent rocks are similar (An_{65})*. The megacrysts have an average size of about 6mm but range from about 50mm to 2mm (matrix size). The fabric varies with grain size - in rocks where the megacrysts are aligned, the matrix laths tend to be randomly oriented. At their edges the megacrysts are inter-

---

* Plagioclase composition of magnetic plagioclase fraction from megacryst-rich rock is An_{62}.

grown with matrix phases (Plate 17D). They are therefore considered to be early formed precipitates from the olivine dolerite melt and are termed phenocrysts.

The phenocrysts sometimes occur as clumps. In these cases grain boundaries are either complex welded* or planar structures (Plates 17A,B). In both cases thin selvages of matrix minerals developed between the phenocrysts are considered to represent former trapped liquid.

The large phenocrysts do not occur in the chilled margins of the dykes, and are generally found only in the thicker parts of the dykes. They are patchily distributed along strike and have a non-homogeneous distribution in a homogeneous olivine dolerite matrix. Sometimes the phenocrysts are concentrated on the northern or upper sides of the dykes.

Banding caused by variations in phenocryst abundance is sometimes observed. The layers are up to 30cm thick. The layering is approximately parallel to the dyke margins and the lath-like phenocrysts are aligned parallel to the layering (Plate 18A).

It is therefore suggested that the early formed plagioclase phenocrysts have been selectively separated from the olivine dolerite melt and concentrated as inhomogeneous patches in the dykes by processes of gravity separation at a pre-injection stage (cf. Frankel, 1969). Flow processes acting during injection of the dyke could explain the absence

---

* These structures commonly occur at lath ends where growth rates are maximum.

of large phenocrysts near the walls of the dyke (i.e. in the chilled margins and in the thinner parts of the dyke), and the separation of phenocrysts to cause banding and the alignment of phenocrysts parallel to the banding (see Bhattacharji, 1967). The alignment or lamination is not due to gravitational settling because the phenocrysts are not in contact (i.e. they are non-packing structures) and the alignment is parallel to the dyke margin which is not horizontal. The alignment of microphenocrysts in the fine-grained marginal zone (Plate 14B) shows that stable laminar flow was operating in the magma during emplacement.

Alternatively, the banding could be due to successive phases of injection and crystallization inwards from the walls of phenocryst-bearing and phenocryst-free olivine dolerite magmas. Flow processes would still be required to produce the fabrics observed.

It is also possible that the lateral variations in phenocryst concentration in the central portions of the dykes could be due to local flow instabilities and that flow processes only, with no previous gravity separation, caused the features observed in the dykes.

3.1.4 Type D porphyritic olivine dolerite dykes

1. Field Occurrence

These medium-grained dykes are found throughout the area but are most densely concentrated at the western and south-eastern ends of the Ewarara Intrusion and in the Kalka Intrusion (Figs. 2,8; not all dykes have been mapped because of difficulty in recognising them from the other basic rocks in the intrusions proper). They are usually less than 0.5 metres wide (Plate 16D).

Chilled margins are found and in some cases a crude banding may result next and parallel to the contacts. Some of the "dykes" are actually thin shear zones, but have not been differentiated on Fig. 2 because of their parallelism to the dykes and because in some cases dolerite has been traced into highly sheared rocks.

The country rocks have in many instances been displaced by the dykes and/or shears - a consistent sinistral lateral displacement is observed at both Kalka and Ewarara; the major displacement zones occur at fairly regular intervals (Fig. 2). Pseudotachylite and brecciation (Plate 18B) are also common at dyke margins, but internal deformation effects are absent.

Dyke orientation is different in the Kalka and Ewarara areas:

a) Kalka - two orthogonal sets: NE and NW trending, with vertical or steeply dipping contacts.

b) Ewarara - NE trending, dipping moderately (45-55^{o}) to the south-east.

These dykes are probably widespread over the Musgrave Block but as yet have not been widely documented. They have been observed at west Hinckley and probably also intrude the South Mt Davies Intrusion (with similar orientation to those in Kalka: see Thomson, 1964; Goode and Nesbitt, 1969, Fig. 2). Wilson (1948) has described apparently similar dykes from the eastern Musgrave Ranges.

2. Mineral Assemblages and Texture

(1) Kalka

These dykes generally contain olivine phenocrysts*, about Fo_{80} in composition and 1 to 5mm in size, which are evenly distributed and randomly oriented in the matrix (0.1 to 0.5mm average grain size). Plagioclase and rarely clinopyroxene phenocrysts are found in some dykes. In some instances up to 30% phenocrysts have been observed.

The matrix consists of 50 to 60% plagioclase laths with about 40% interstitial clinopyroxene and magnetite with associated ilmenite and green spinel. Magnetite is intergrown with some silicate phases (Plate 12D). Very dark subhedral to euhedral spinel crystals and aggregates are also observed in the matrix and as inclusions in olivine phenocrysts. Red-brown biotite, sometimes intergrown with a silicate phase, commonly rims the opaque/spinel aggregates.

The texture is a typical doleritic variety and is controlled by the disoriented plagioclase laths (Plate 16A). The matrix surrounding the olivine phenocrysts, (but not the plagioclase phenocrysts), is usually richer in ferromagnesian phases and opaques than the normal groundmass (Plate 18C). A similar textural relationship is observed around sodalite phenocrysts in sodalite trachytes from Mt. Suswa in Kenya (Nash et al., 1969). Similar depletions in certain matrix elements around phenocrysts or spherulitic growths have been noted in other basaltic rocks (e.g. Bottinga et al., 1966; Kesler and Weiblen, 1968), and appear to be related to crystal growth of the phenocrysts.

---

* Commonly surrounded by thin fibrous orthopyroxene rim considered to have formed as a result of an olivine-liquid reaction (Chapter 9).

Some olivine phenocrysts tend to be skeletal but they may also be solid euhedra with sharp or rounded edges (Fig. 10A). The skeletal form is interpreted as being a growth feature rather than representing corrosion as the embayments are deep and narrow, and limbs are parallel, often with euhedral outlines. Furthermore, core zoning, marked by fine opaque exsolution, parallels the identations (cf. convolute zoning in plagioclase which is a growth feature: Blackerby, 1968). Skeletal growth is fairly common in olivines from chilled rocks elsewhere (Drever and Johnston, 1957). The rounded terminations are thought to represent some degree of resorption by the liquid as sharp edges are common in skeletal olivines. Rounding is common in olivines from cumulate rocks in the area. The solid euhedra often have apparent internal skeletal form as outlined by the zoning (Plate 17C), although in some cases close examination reveals coarser and rarer opaque material suggestive of exsolution coalescement in the clear areas. Opaque exsolution plates as well as very fine opaque exsolution granules are also present.

The phenocrysts commonly clump together to form interlocking synneusis aggregates (Plate 16A). Growth has apparently continued after joining as grain boundaries are irregular and interpenetrant.

Olivine has not been observed in the matrix although rarely it may be intergrown with matrix plagioclase at grain boundaries.

Plagioclase phenocrysts are lath-like; some are intergrown with the matrix at their edges. They sometimes form in clumps with interpenetrant laths common (Fig. 10B). Synneusis relations appear very probable for some if not all. Simple twinning is common; multiple

twinning is more rare. Some crystals have cores or annular zones of clinopyroxene/opaque inclusions (Plate 15C). Marginal extinction zoning and rare plagioclase inclusions are also observed.

Stubby clinopyroxene phenocrysts are usually augitic ($2V_z$ = 40-50°) although one phenocryst had an irregular rim of subcalcic pyroxene ($2V_z$ < 30°). Simple twinning is sometimes observed. The phenocrysts may intergrow with the groundmass.

A marginal chilled phase from one dyke has a similar mineralogy to the normal dykes. However, the skeletal elongate olivine and ragged plagioclase phenocrysts become coarser grained inwards from the contact as does the dolerite matrix. The phenocrysts are aligned parallel to the contact, although plagioclase tends to be more disoriented away from the contact. The matrix plagioclase is also aligned parallel to the contacts near the margin but is disoriented further inwards. (Note: olivine phenocrysts have sharper terminations than usual, and have opaques associated with the fibrous orthopyroxene rims).

These features are interpreted as indicating that flow processes acted on both phenocrysts and, to a certain extent, matrix plagioclase during crystallization. The grain size variations are thought to indicate that phenocrysts as well as matrix underwent longer crystallization times further inwards from the contact (unless the phenocrysts were initially size sorted by flow processes) and that phenocrysts were intimately associated with the matrix in terms of paragenesis although they formed slightly earlier.

(2) Ewarara

These dykes contain 1 - 2mm olivine, generally pseudomorphed by orthopyroxene - opaque aggregates or serpentine, sometimes clinopyroxene and rarely orthopyroxene phenocrysts. The doleritic matrix consists of randomly oriented plagioclase laths (50-60%) and elongate subcalcic clinopyroxene. The clinopyroxene is commonly arranged in radial sheaf-like aggregates (Plate 15D). Small amounts of green spinel and associated opaques are usually rimmed by brown hornblende. Garnet is observed in some dykes.

When observed, olivine phenocrysts (or serpentinised equivalents) are encased in fibrous orthopyroxene rims which pseudomorph the primary olivine crystal. Opaques are closely associated, and sometimes vermicularly intergrown, with the orthopyroxene. In some rocks pyroxene(?)/spinel symplectites are consistently associated with the orthopyroxene/opaque rims. The symplectite is not preferentially associated with any matrix phase but incorporates, as inclusions, all the matrix phases except plagioclase, suggesting the reaction occurred in the solid state at the expense of that mineral. Similar coronas are discussed in more detail in Chapter 9. Although olivine is not common, granular aggregates of orthopyroxene and opaques are found in all dykes and probably represent primary olivine (Chapter 9). A similar association is also found in some Type D dykes at Kalka.

Clinopyroxene phenocrysts are similar to matrix clinopyroxenes and form a gradational size range. Euhedral orthopyroxene phenocrysts, containing opaque and clinopyroxene exsolution lamellae, are rarely observed.

In some dykes irregular patches, about 5mm in diameter, of granular garnet (pinkish, high relief, isotropic) are homogeneously distributed in the rock (Plate 16B). These patches also contain plagioclase, clinopyroxene and opaques but are depleted in plagioclase and hornblende relative to the matrix. The patches may form around orthopyroxene/opaque aggregates (olivine pseudomorphs) when these are present (Plate 15B) but this does not appear to be a necessary association. It does appear, however, that olivine pseudomorphs are less common in those rocks containing garnet. This could indicate a more fractionated and therefore a more iron-rich dyke, and therefore easier formation of garnet by a plagioclase - pyroxene reaction (cf. Chapter 11).

The order of appearance of the early-formed primary phases appears to be spinel - olivine - plagioclase - clinopyroxene.

3. Comparison of the Kalka and Ewarara sub-suites

The primary features of both sets of dykes are similar i.e. field occurrence, relative ages, mineralogy and texture. Therefore the dykes are considered to form a single suite. However, several major differences exist:

(a) dyke orientation is different for the two sub-suites

(b) the Ewarara sub-suite appears to develop some high pressure characters (cf. Chapter 11) not present in the Kalka sub-suite:

1) spinel exsolution in clinopyroxene

2) spinel/pyroxene(?) symplectites (associated with olivine - plagioclase reactions?)

3) development of garnet

4) spinel exsolution in plagioclase

(c) plagioclase phenocrysts have not been observed in the Ewarara sub-suite.

3.2 Transgressive Picrite Suite

1. Introduction

A group of at least sixteen bodies of olivine-bearing rocks, having intrusive relationships to both the granulites and the Giles Complex, are found in the area (Figs. 2,8) and are provisionally correlated as one suite. Age relationships to other events are consistent within the group (Table 7).

Because of rubbly outcrop great difficulty has been encountered in the Olivine Gabbro Zone of the Kalka Intrusion in distinguishing some of the transgressive olivine-rich rocks (dunitic to picritic) from those in the layered sequence. Several outcrops of still indeterminate affinities exist in Kalka and may also form part of this suite.

The suite has been sub-divided into five groups -

(a) dunitic group (five members: A314-739, A314-489, A300-501a, DDH A14, A314-441a)

(b) picrite group (seven members: A300-84, A300-710, A314-124, A314-456a, A314-738a, A300-67, A300-384)

(c) olivine mesogabbro group (two members: A300-80, A300-712)

(d) olivine leucogabbro group (one member: A301-153)

(e) leucogabbro group (two members: A300-79, A300-386).

Other plug-like bodies of similar composition are common in the Tomkinson Ranges (Thomson, 1964) but none have as yet been specifically reported from elsewhere in the Musgrave Block. Some of them have been described briefly by Moore, 1970a (olivine gabbro, picrites, and associated? serpentinites), Gray, 1967 (picrite), Barnes, 1968 (olivine gabbro), Daniels, 1967 (picrite) and R.W. Nesbitt (pers. comm.; picrites from east of Ewarara and in the Mt Davies Intrusion).

2. Shape and size of the intrusions

The bodies are generally up to a hundred metres in diameter, although some of the members of the dunitic group are much larger. In a diamond drill hole, DDH A14, put down by South Western Mining in the Scarface Silcrete Zone, dunite (and serpentinised equivalents) was intersected under the silcrete. Turner (1967) believes that the silcrete formed from the dunite - serpentinite rocks and therefore that this transgressive body could be as large as the surface outcrop of the silcrete zone viz. 10km long and 1km wide.

The bodies are usually plug-like in form, especially when intruding the granulites, and have sharp contacts. They tend to be circular to elliptical in cross-section (elongate parallel to country rock layering). Generally their contacts are steep but it is possible that A314-124 and associated bodies may have shallower-dipping boundaries. Some members of the dunitic group are more irregular and elongate in their shape e.g. DDH A14 (see above) and A314-739, which is elongate and appears to interfinger with the layered sequence of the Kalka Intrusion.

3. Description

With the exception of minor developments of chilled rocks at the margins of the intrusions, the members of the picrite suite are all cumulate in origin. The classification of the members into groups is somewhat artificial as, in general, their properties are gradational from one group to the next.

(a) Modal Variations (Fig. 11A)

In general as modal olivine decreases in abundance from the dunite to the leucogabbro groups, plagioclase increases in abundance. After an initial increase total pyroxene content remains constant at approximately 30%.

(b) Cumulus Mineralogy (Table 6B)

Olivine and spinel cumulus crystals gradually give way to cumulus pyroxene and plagioclase from the dunite to the leucogabbro groups.

(c) Interstitial Mineralogy (Table 6B)

Overgrowths of olivine were only observed in the dunite group. Plagioclase, orthopyroxene and clinopyroxene were the major interstitial phases in the other groups.

(d) Mineral Composition

Forsterite content of olivine decreases in direct relation to modal olivine (Fig. 11B). In the more iron-rich olivines, opaque exsolution blades were observed. Anorthite content of plagioclase

(An_{67-50}) is quite variable within and between groups. Cumulus spinel varies in colour from dark (almost opaque) green to more transparent green from the dunite group to the picrite group. Opaque exsolution (compared with spinel exsolution) in pyroxenes was observed in later overgrowths in the same rock, or in more plagioclase rich bodies, probably indicating an iron enrichment of pyroxenes (see Chapter 9).

(e) Cumulus Grain Sizes

In general olivine and spinel tend to become finer grained as modal olivine decreases.

(f) Interstitial Crystallization

Evidence for more extreme differentiation (e.g. biotite, iron oxides, apatite) is more apparent in the olivine-poorer members of the sequence.

There thus appears to be a continuous mineralogical and chemical series between members of the suite. The dunite group represents the most magnesian end of the fractionation sequence, and the leucogabbro group the iron-rich end. There is a possibility, however, that part of the dunite group is not related to the picrite - leucogabbro suite. Some of the dunite plugs are irregularly shaped or non-pluglike, and appear more deformed than the other members of the suite. One of the dunites (A314-739) is also cut by a dolerite dyke (A314-740) of possible Type A affinities. The Type A dykes are however older than other members of the picrite suite (Chapter 14). For the purpose of this discussion, however, it will be assumed that all groups are genetically related. All bodies exhibit some effects of minor deformation e.g. undulose extinction, kinking.

(1) Dunitic group

This group comprises rocks of dunitic and lherzolitic composition (or serpentinite equivalents). They consist of 80-90% olivine (1 - 5mm long) with accessory amounts of chrome spinel (0.05 - 0.3mm), orthopyroxene, clinopyroxene (both pyroxenes with spinel exsolution), plagioclase, hornblende and biotite. The chrome spinel is of picotite composition (Turner, 1967). Olivine varies from Fo_{90} to Fo_{87}.

The texture is controlled by olivine which forms a cumulate packing structure of rounded granular to euhedral crystals (Plate 19A). Spinel, found as inclusions in the olivine and as small euhedra packed between the olivines, is also a cumulus phase. In the more dunitic rocks, significant adcumulus olivine growth has occurred slightly obscuring the cumulate texture. The other minerals tend to be irregularly shaped and interstitial to the olivine. Plagioclase is strongly zoned marginally.

A peridotite plug (A314-441a), consisting of 50-60% olivine (Fo_{84}), 30-40% pyroxene (cpx > opx; with spinel exsolution) and minor plagioclase (strongly clouded cores of spinel exsolution), is transitional to the picrite group.

(2) Picrite group

Rocks of this group contain between 50 and 65% olivine, 10 to 30% plagioclase (An_{50-63}), clinopyroxene and/or orthopyroxene (total pyroxene 20 to 30%). Accessory amounts of red-brown biotite, brown hornblende, apatite, green spinel, ilmenite, magnetite and trace sulphides (pyrite, chalcopyrite, pyrrhotite) may also be present.

They all possess a characteristic texture (Plate 19B). A cumulate packing structure of granular to rounded euhedral olivine crystals (average grain size about 2 to 3mm, but up to 7mm) is enclosed by poikilitic plates (often 2 to 3cm in diameter) of plagioclase and pyroxene. The accessory minerals are usually concentrated in the interstitial areas between the pyroxene and plagioclase. Biotite can be a major (5-10%) interstitial phase in some rocks. Olivine and green spinel are the only definite cumulus phases yet observed, although in A300-710 orthopyroxene grains are also cumulus.

Although olivine generally occurs as convex polyhedra, some tendency to dendritic forms is observed. Compositions vary from Fo_{85} to Fo_{82}. Opaque exsolution blades are sometimes present in the olivine. As well as euhedral spinel inclusions, olivine may also rarely contain inclusions of plagioclase, hornblende and biotite. These could have crystallized from liquid trapped during fill-in growth of the dendritic olivine.

Hourglass zoning in orthopyroxene in A300-710 suggests a cumulus origin for this mineral in this rock (cf. Chapter 9). Elsewhere, however, pyroxene forms a well developed poikilitic texture. In A300-710, orthopyroxene also contains exsolution lamellae of clinopyroxene as well as spinel whereas only spinel or opaque exsolution, if any, is present in pyroxene from other rocks in this group. This further indicates its unique nature.

In some of the plugs (e.g. A300-84, 710) biotite, hornblende, ilmenite, magnetite and apatite are strongly developed in localised interstitial patches. Biotite is also found as intergrowths (? eutectic)

with pyroxene or plagioclase at their edges, suggesting that the biotite - hornblende - ilmenite - magnetite - apatite patches are the final closed system differentiates of interstitial pore crystallization. Opaque exsolution occurring at the iron enriched edge of pyroxene grains is preferentially developed adjacent to these areas (Plate 20B), supporting the concept. Anderson and Greenland (1969) further suggest that apatite only crystallizes at advanced stages of basaltic fractionation.

In these residual patches a common coronal arrangement of the phases often occurs (Plate 20A). Ilmenite/magnetite/spinel granular aggregates are commonly rimmed successively by red-brown biotite and brown hornblende. In some cases the hornblende rim is gradationally followed by a hornblende/spinel symplectite. Rarely a partial clinopyroxene/spinel symplectite rim is observed in contact with plagioclase and intergrown with either biotite or hornblende. The other rims, however, show no preferred association for plagioclase, pyroxene or olivine. Apatite euhedra are commonly found within the biotite and to a lesser extent in the hornblende. Hornblende may be in contact with the opaques when the biotite rim is incomplete, while biotite is sometimes intergrown with plagioclase when the two are in contact. Similar associations of the first one or two rims on the opaque/spinel aggregate are observed in other igneous rocks in the area e.g. more differentiated members of the picrite group, Type C and Type D dolerite dykes, and in the Anorthosite Zone of the Kalka Intrusion.

Opaques rimmed by biotite have been described by Hermes (1968) and Gjelsvik (1952) in other basic igneous rocks. Additional amphibole and

garnet rims (in contact with plagioclase) have been reported by Sutton and Watson (1950), Starmer (1969) and Glaveris (1970).

The rims (at least the inner biotite and possibly the outer hornblende) appear to have crystallized from the liquid. The eutectic(?) intergrowth between biotite and plagioclase, and the presence of apatite supports this. Whether the rim(s) formed by progressive reaction with the liquid during the final stages of fractionation, or whether they merely represent a preferred physical association is indeterminate. Possibly part or all of the hornblende rim results from sub-solidus breakdown of biotite. Starmer (1969) has suggested that both the biotite and hornblende rims result from solid state reaction between iron ores and plagioclase, with the addition of Fe and Mg from contemporaneous olivine - plagioclase reactions. Eugster and Wones (1962) have, however, shown that annite can form from magnetite and sanidine. It is therefore possible that in the final stages crystallization in the interstices, K-enriched liquids (to be expected) might react with the iron ores and crystallize iron-rich biotite as reaction rims.

Optical properties reflect the unusual chemical compositions of biotite and hornblende. The biotite has a very pronounced red-brown colour, suggesting it may be rich in either Ti or Fe^{3+} (Deer et al., 1963, vol.3). Electron microprobe examination supports a relatively high Ti content. Biotite in all other igneous rocks in the area has a similar property but mica in the granulite is a more normal dark brown colour. The Ca-amphibole has a $2V_{\gamma} \simeq 80^{\circ}$ in the basic igneous rocks and in the granulites, suggesting it is a magnesium-rich hornblende, possibly Al-rich or pargasitic (Deer et al., 1963, vol.2).

Subdivision of the picrite group

Despite a general similarity in texture, composition, relative age and mode of occurrence, several distinct differences exist between the plugs in the Ewarara area (A300-84, 710) and those in the Kalka area (A314-124, 456a, 738a).

	Ewarara	Kalka
1. olivine composition	$Fo_{81.5}$, $Fo_{82.5}$	Fo_{85}
2. cumulus phases	ol + spin (+ opx)	ol + spin
3. modal olivine	~50 - 60	~60 - 70
4. modal plagioclase	~20 - 30	~10 - 20
5. biot - hb - ilm - mag - apat rich areas	present	absent
6. exsolution in interstitial pyroxene	opaque	spinel
7. spinel exsolution in plagioclase	present	absent
8. olivine - plagioclase coronas (Chapter 9)	present	absent (or poorly developed)
9. olivine - spinel corona (Chapter 9)	present	absent

These differences indicate that the Ewarara sub-group is more iron-rich and in a more advanced stage of fractionation (some of the interstitial differences could, however, be explained by variations in the degree of adcumulus v orthocumulus growth. The Kalka sub-group are more adcumulate or heteradcumulate).

Two plugs (A300-67; A300-384 - small outcrop next to A300-386) near Ewarara are thought to be related to A300-710. They are of olivine

melanoritic to olivine orthopyroxenitic composition, and somewhat similar to the lowest part of the Ewarara layered series. However, the olivines are more iron-rich ($Fo_{81.5}$; opaque exsolution) and less abundant. Cumulus phases include olivine, orthopyroxene (hourglass zoning) and spinel.

(3) Olivine mesogabbro group

Two plugs of the olivine mesogabbro group have been recognised viz. A300-80, 712. Both are in the Ewarara area.

They consist of olivine (40-50% in A300-80, 10-20% in A300-712), plagioclase (30-40%), clinopyroxene (20-30%) and orthopyroxene (10% in A300-712). Accessory minerals include red-brown biotite, brown hornblende, green spinel, opaques and apatite. Spinel is more common in A300-80 where it is found as a granular phase associated with olivine.

The textures are somewhat different in the two rocks. A300-80 is rather similar to A300-84 of the picrite group. However, the olivine is finer grained relative to the other phases and more dendritic. Also plagioclase and clinopyroxene are not poikilitic but have a greater tendency to cumulus shapes. A300-712 is similar to A300-710 except that olivine is usually much finer grained, spinel inclusions are not observed in the olivine, and both ortho- and clino-pyroxene (and to a certain extent plagioclase) tend to cumulus morphologies. Simple twinning in clinopyroxene and plagioclase is much more common in these rocks than in the picrite group.

Cumulus minerals in A300-80 are olivine, spinel, probably plagio-

clase and perhaps clinopyroxene. In A300-712, olivine, orthopyroxene, clinopyroxene and possibly plagioclase are the cumulus phases.

Spinel exsolution in clinopyroxene is observed in A300-80, but only opaque exsolution in both pyroxenes in A300-712. Clinopyroxene exsolution in orthopyroxene, and vice-versa, is also observed.

In A300-80, olivine contains orthopyroxene - spinel intergrowths around spinel inclusions. However, in A300-712, spinel inclusions are absent and olivines are altered, sometimes completely, to granular orthopyroxene, spinel and vermicular opaque intergrowths (see Chapter 9).

Double coronas of orthopyroxene (inner) and clinopyroxene/spinel (outer) are well developed on olivine (or its pseudomorphs) in contact with plagioclase. Vermicular opaque is also sometimes associated with the rims. These are discussed fully in Chapter 9.

Thin (0.05 - 0.1mm) rims of massive orthopyroxene are sometimes observed between olivine and primary clinopyroxene. The more irregular boundary seems to be between the two pyroxenes. It appears to be a normal crystallization rimming not involving reaction. Interstitial texture and mineralogy is similar to the Ewarara picrite sub-group and is biased to orthocumulus growth.

(4) Olivine leucogabbro group

Only one of these plugs (A301-153), in the Ewarara area, has yet been recognised. It consists of plagioclase (60%), clinopyroxene (20-25%), orthopyroxene (5-10%) and olivine (10%). Biotite, hornblende, opaques, spinel and apatite are accessories.

The texture is cumulate with plagioclase laths forming a planar lamination (Plate 19C). In hand specimen a weak lineate lamination is also observed. Clinopyroxene, olivine and possibly orthopyroxene also form cumulus phases.

Plagioclase laths (An_{62}) are usually between 5 to 8mm long and 0.5 to 1.5mm wide. Carlsbad synneusis twins are common. Maximum primary length/width ratios are approximately 30:1. The laths are irregularly clouded with spinel rods.

Clinopyroxene crystals are overgrown by interstitial crystallization as are plagioclase and orthopyroxene. They exsolve orthopyroxene and spinel (at cores) or opaque (at boundaries or throughout). Orthopyroxene exsolves opaque plates, commonly at grain edges.

Olivine is surrounded by thick double coronas of orthopyroxene and clinopyroxene/spinel when in contact with plagioclase (see Chapter 9). The core olivine is sometimes partially pseudomorphed by granular orthopyroxene/vermicular opaque aggregates.

The interstitial texture and mineralogy is similar to the Ewarara examples of the picrite group, although the major interstitial phases are not poikilitic. Diffuse chemical zoning is present at the edges of overgrown cumulus phases, suggestive of orthocumulus growth. Globular plagioclase - pyroxene intergrowths are sometimes observed in the interstices.

(5) Leucogabbro group

Two plugs near Ewarara (A300-79, A300-386) have a leucogabbroic

composition. They consist of cumulus plagioclase (60%), clinopyroxene (20-30%) and orthopyroxene (15-20%). Rare and scattered pseudomorphs (granular orthopyroxene with vermicular opaque) after olivine are observed in A300-79. Double coronas consisting of orthopyroxene and clinopyroxene/spinel are well developed around these areas, further indicating the former presence of olivine. Hornblende, biotite, opaques, spinel and apatite are accessories.

The plagioclase laths show a slight lamination in both cases. In A300-386, the laths are 5 to 8mm long and exhibit simple, synneusis twinning. In A300-79, the primary crystals are smaller but poikilitic overgrowths extend their size up to 10 - 15mm. Plagioclase is lightly clouded with aligned anisotropic needles.

Orthopyroxene crystals (1 - 3mm) tend to be concentrated in synneusis(?) groups. Clinopyroxene exsolution, and opaque exsolution in the overgrowths, are observed. Clinopyroxene exhibits orthopyroxene exsolution, with spinel exsolution or opaque exsolution (most in A300-386) also present.

The interstitial products are orthocumulus similar to the other Ewarara plugs.

(6) Contact rocks

Finer grained gabbroic to noritic rocks are found as thin border phases to some of the plugs. They all consist of plagioclase (60%), clinopyroxene (20-30%) and orthopyroxene (10-20%). Minor quantities of magnetic opaques are also present. Red-brown biotite and brown

hornblende are present in some rocks.

Textures in A300-83 and A314-116a are typically those of a fast cooled dolerite: randomly oriented plagioclase laths with euhedral to subhedral pyroxenes. The ragged plagioclase laths are commonly found in radiating groups (Plate 20C). In A300-83, clinopyroxene laths also form part of these groups. The laths tend to thicken, and perhaps branch in rare cases, away from the central point. Grain sizes vary: in A300-80 plagioclase laths are 1 - 2mm long, pyroxene subhedra 0.5mm across; in A314-116a plagioclase is up to 5mm long and pyroxene $2\frac{1}{2}$ to 3mm in diameter. Globular intergrowths of pyroxene and plagioclase are observed in interstitial areas (cf. Chapter 9).

Plagioclase (An_{60-67}) is slightly clouded with minute opaque(?) particles and may also be antiperthitic. Both simple and multiple twinning has been observed. Simple twinning is not observed in well developed radial aggregates. Diffuse zoning at grain boundaries is observed. Orthopyroxene exsolves clinopyroxene and/or opaques. Clinopyroxene exsolves orthopyroxene and/or opaques.

At a sharp but irregular contact with acid granulite in A300-83, a thin selvage (about 0.4mm thick) of fine-grained granular pyroxene is intergrown with some plagioclase. A patchy plagioclase-rich selvage of equal thickness occurs inwards from the contact (Plate 20D), while further inwards radiating clumps of pyroxene and plagioclase tend to become coarser grained inwards from the contact. The irregular margin with the granulite appears to be controlled by the distribution of K-feldspar augen in the granulite. These crystals are commonly mottled marginally and myrmekitic intergrowths are developed in the groundmass.

These features may be related to proximity of the picrite plug as they are not common in the granulite elsewhere, and probably result from thermal metamorphism.

Near the margin of A300-386, a leucogabbro plug, a finer grained rock (A300-383) of similar composition to both the plug and the other contact rocks was observed. Part of it contained strongly aligned plagioclase laths (of unknown angular relation to the margin). Biotite was much rarer in the marginal rock than in the plug. It is possible that the rock represents a flow aligned chill phase of the plug.

A partially recrystallized noritic gabbro (A314-441c) associated with the peridotite plug (A314-441a) may possibly represent a chill phase but cumulate tendencies are also present. Recrystallized aggregates of orthopyroxene/spinel (very dark green, almost opaque) may represent oxidation products of primary olivine.

With reservations of Appendix 7 in mind, it is therefore assumed that the chill textures indicate the composition of the original magma in the pipes. This would then be basaltic, with probable tholeiitic tendencies. Quartz xenoliths in basaltic material near A300-80 indicate contamination in some cases (Plate 19D).

4. Discussion

By comparison with pipes and plugs elsewhere it is assumed that these plugs probably have considerable vertical extensions. In association with this geometry the plugs may also have had high magma

discharge rates. This would allow preheating of the country rock* and prevent substantial chilling, one of the observed features.

Following the formation of the plugs the magma discharge rate would probably slow or stop. In the resultant vertical standing column in relatively slow cooling conditions, gravity accumulation of crystals would have a good chance to occur. A resultant cumulate fractionation series from dunite through picrites, olivine mesogabbros, olivine leucogabbro to leucogabbros could then form from the basaltic liquid (Fig. 12). The presence of semi-dendritic olivine, and absence of layering indicative of discontinuous nucleation (Chapter 10) suggest, however, that the rock series accumulated in faster cooling conditions than the Giles Complex cumulates.

It is thought that the presently exposed series of plugs represent examples of these cumulate columns cut at different levels of erosion. Plugs containing more advanced members of the fractionation series are concentrated in the Ewarara area. This could perhaps indicate that the Kalka plugs are more deeply exposed by erosion and originated from a slightly higher pressure environment. However, it should be remembered that some of the features indicative of more advanced fractionation in the Ewarara plugs could be due to contamination by the host acid granulites after intrusion. The Kalka plugs on the other hand are found in basic rocks where contamination would be ineffective.

Since the layered rocks of the Giles Complex do not seem to contain stratiform chromite deposits (Nesbitt et al., 1970), it is believed that

---

* Contact temperatures tend towards the intrusional temperatures with prolonged preheating (Jaeger, 1968).

the only possible deposits of chromite or chrome spinel in the area would be at the base of the cumulate columns (Fig. 12). This accumulation, however, would depend on crystallization of chromite without olivine at an early stage.

3.3 Transgressive medium-grained gabbros

Medium-grained gabbroic bands have been occasionally observed in the upper parts of the N1 Subzone in the Kalka Intrusion, and become increasingly abundant in the N2 and N3 Subzones (Fig. 15). They are common in the Anorthosite Zone, where they attain up to 30 metres thickness.

The bands are lenticular and relatively conformable to the layered sequence although detailed mapping reveals their locally transgressive nature. Contacts are usually relatively sharp in the field, and in some cases are associated with unusually coarse-grained pyroxene - plagioclase borders.

Schlieren of irregular thickness are commonly developed parallel to the contacts. They consist of thin lenses of different grain size or composition (e.g. pyroxene v. plagioclase, or clinopyroxene v. orthopyroxene). A weak foliation parallel and similar to S_1^9 in the host rocks is sometimes developed.

Coarse-grained pyroxene - plagioclase clots and lenses, varying in length from a few centimetres to 5 to 10 metres and aligned parallel to contacts, are found in many bands. These inclusions have identical mineralogy and texture to the host rocks and are considered to be

xenoliths. In most cases these clots have a plagioclase-rich margin (Plate 21A). In some layers large single crystals or crystal-groups (Plate 21B) appear to have a similar origin.

In general the gabbros consist of about 50-60% plagioclase and 40-50% pyroxene. Orthopyroxene content is variable but is always subsidiary to the clinopyroxene. Olivine, opaques and spinel are accessories in some examples. Small quantities of hornblende and biotite are found in olivine-bearing and olivine-free rocks respectively. Spinel/pyroxene symplectites are associated with olivine (see Chapter 9).

Textures are typical of partially recrystallized medium-grained gabbros. A few relic plagioclase laths or large primary crystals of plagioclase or pyroxene* are contained in an annealed pyroxene - plagioclase matrix (Plate 21C). Rarely poikilitic pyroxene plates are also observed. The matrix grain size varies from 0.2 to 0.5mm and the relic plagioclase laths are usually smaller than primary plagioclases in the host rocks. The textures are very similar to those developed in partially recrystallized Type B dolerite dykes.

The composition of the bands is related to the composition of the surrounding rocks of the Kalka layered sequence e.g. magnetite-rich transgressive gabbros are found in magnetite-rich layered gabbros.

These features have lead to the conclusion that the transgressive gabbros were derived from the interstitial liquid of the host layered gabbros. If this liquid was partially crystalline on intrusion, flow

---

* Primary pyroxenes contain opaque and/or pyroxene exsolution.

processes could explain the alignment of schlieren and xenoliths parallel to the contacts.

The reason for preferential intrusion of these bodies in the upper parts of the Kalka cumulus pile may be related to the time of emplacement i.e. at a relatively late stage when interstitial liquid in the lower parts of the body had completely crystallized.

It has been noted in Chapter 13.2 that a thrusting-type deformation affected the cumulus pile soon after crystallization. This deformation was not active during cumulus sedimentation but possibly could have begun prior to complete crystallization of the interstitial liquid. By virtue of accompanying seismic shocks, such events may have caused compaction in the upper parts of the cumulus pile and, by a filter pressing action, resulted in local intrusion of the expelled interstitial liquid. Similar mechanisms have been suggested by Jackson (1961) to account for the formation of transgressive pegmatites in the Stillwater Intrusion. Continued deformation of the transgressive gabbros after crystallization could explain the weak foliation and the high degree of subsequent recrystallization observed.

3.4 Transgressive magnetite - ilmenite bodies

A body consisting of almost pure coarse-grained magnetite with lesser quantities of ilmenite has been observed in West Kalka. Although transgressive to general layering trends and to transgressive medium-grained gabbros in the surrounding magnetite-bearing layered gabbros of the Kalka Intrusion it intertongues locally with the surrounding rocks (Fig. 2).

The body, A314-240, is about 100 metres long and between 20 and 50 metres wide. The magnetite, a lodestone variety, is oxidized to martite at grain boundaries and along fractures, and contains spinel exsolution. Some silicate phases are also present as accessories.

Miller (1969) has reported V_2O_5 contents of 1.28% and TiO_2 contents of 10% for this body. These assays are comparable with V_2O_5 contents between 0.57% and 1.4% for stratiform magnetite bands in the Jameson Range Intrusion, the most westerly Giles Complex body (Daniels, 1967).

Another smaller but similar body has been mapped as a highly deformed pod in the Hinckley Fault. Other smaller lenses in West Kalka may be associated with local faulting and related to this type. Alternatively they could be related to stratiform magnetite bodies found in the layered sequence.

During studies of deformation in the Kalka layered sequence it has been noted that iron oxide phases are much more mobile than the silicates. Fractures in plagioclase or pyroxene grains related to bending are commonly filled with opaque phases (Plate 21D). This demonstrates the ability of iron oxides to deform by plastic mechanisms under conditions which cause brittle fracture in silicates. It is therefore thought that the large magnetite - ilmenite bodies are formed by related processes i.e. solid state segregation of iron oxides to sites of lower strain energy as a result of deformation of the surrounding magnetite-bearing layered gabbros. There is, however, no obvious structural reason for the observed position of the body. Structural control on the development of magnetite bodies in New York has been suggested by Hagner and Collins (1967).

3.5 Transgressive norite

Coarse-grained noritic rocks have been found associated with lherzolites and picrites of the transgressive picrite suite, mafic pegmatites and abundant magnesite in an elongate body in the Ewarara Intrusion (Fig. 2, Plate 2). The body is transgressive to nearby igneous layering in the host pyroxenites and the rocks much less deformed.

Xenoliths of partially recrystallized websterite and olivine orthopyroxenite similar to the major rock types in the Ewarara layered sequence have been observed in the norites. The norites are slightly deformed as some kinking of pyroxenes is observed. Some degree of recrystallization and development of fingerprint texture in clinopyroxene (Plate 23C) are further indications of strain. These features indicate that the rocks were intruded after the gneissic deformation producing S_1^9 in Kalka and Ewarara (Chapter 13.2) but prior to some later deformation. Similar conclusions were reached by Moore (1970a) for identical rocks at Gosse Pile.

The norites are variable in composition but in general contain about 70% pyroxene (orthopyroxene > clinopyroxene) and 30% plagioclase. Brown hornblende, red-brown biotite, brown-green spinel and rare opaques are accessories.

The texture is characterised by the development of pyroxene euhedra and subhedra up to 2 to 5mm in size. These crystals, and some plagioclase, form a cumulate packing structure while most plagioclase and the other phases are interstitial.

Orthopyroxene contains both clinopyroxene and spinel exsolution. Rounded to ragged clinopyroxene inclusions are commonly observed, some being arranged in zones around the orthopyroxene core (Plate 22A). Clinopyroxene exsolves both orthopyroxene and massed spinel, and contains orthopyroxene inclusions. Plagioclase (An_{51-55}) contains spinel and pyroxene exsolution. Spinel sometimes forms wormy crystals (Plate 22B).

3.6 Mafic pegmatites

Very coarse-grained mafic pegmatites have been observed in parts of Ewarara and West Kalka. In West Kalka they are quite commonly developed as small transgressive bodies in the Anorthosite Zone adjacent to or near a small shear (Fig. 2). At Ewarara pegmatite has been found in association with transgressive norites and other rocks in an elongate transgressive body (Fig. 2, Plate 2).

The pegmatites consist of plagioclase crystals up to 20cm long and small amounts of interstitial coarse-grained pyroxene. The plagioclase (An_{55}, An_{66}) contains spinel or magnetite exsolution as well as small pyroxene, hornblende or opaque inclusions. Sharp multiple twinning is also present in the feldspars. The crystals are commonly kinked and partially recrystallized.

Mafic pegmatites were also observed in the lower part of the Ewarara Intrusion by Goode and Krieg (1967, p. 188). These veins appear to vary between mafic pegmatites, somewhat similar to those described here, and the transgressive norites revealing a possible genetic relationship between the two rock types.

3.7 Acid pegmatites

Apart from a few rare examples in the granulites, coarse-grained acid pegmatites are limited to minor occurrences in the Kalka Intrusion.

They are usually small lenticular bodies up to several metres long and are found only in the vicinity of granulite contacts or acid xenoliths in the intrusion. Pegmatites are especially common in Norite Subzone N2b (Fig. 15).

They consist essentially of white perthitic K-feldspar (orthoclase) with lesser amounts of quartz and minor pyroxene or opaques. The opaque phases consist of magnetite exsolving haematite (Plate 24A) and haematite exsolving ilmenite (Plate 24B). Ilmenite is also a minor granular phase. A black glassy material with conchoidal fracture was observed in some pegmatites but could not be identified by X-ray techniques. J.E. Johnson (pers. comm.) has reported allanite from pegmatites in this area. Graphic intergrowths between feldspar and quartz are rare (Plate 24D).

The pegmatites are deformed and partially recrystallized* but are transgressive to the S_1^g gneissic foliation in the Giles Complex. In part of southern Kalka pegmatites are closely associated with deformed xenolithic(?) granulites. Orthoclase is found in the fine-grained granulites as small ovoidal single crystals up to about 0.5mm in size, and also as segregations in the cores of F_2 folds (Plate 24C).

---

* Exsolution in the opaque phases postdates recrystallization.

The pegmatites are therefore interpreted as having been formed by partial melting of anhydrous xenolithic acid granulites (K-feldspar rich) during F_2 folding, and subsequent injection into the surrounding norites. The association of the pegmatites with intrusional contacts is related to the prior distribution of the granulite xenoliths. The composition of the acid pegmatites as well as their younger age would prohibit them from being developed from the host norites of the Giles Complex.

3.8 Pyroxenite lenses

Several small medium-grained pyroxenite lenses have been mapped in the granulites around Ewarara (Fig. 2). They are conformable with the granulites although hybrid margins were observed in one instance by Goode and Krieg (1965). Rare layering is observed in one of the bodies.

The lenses generally consist of predominantly orthopyroxene (exsolving clinopyroxene) with lesser amounts of clinopyroxene and/or brown hornblende. Clouding of these phases by minute opaque exsolution bodies is common. Apatite is an accessory. In one float sample (A300-359) magnetite, with spinel exsolution, ilmenite and green spinel were observed, sometimes as intergrown aggregates (Plate 38D).

The textures are typical mesocumulate to adcumulate with orthopyroxene $\pm$ clinopyroxene being the cumulus phases (Plate 23D). The other phases form typical interstitial textures between the cumulus grains. Some kinking of the pyroxenes is observed but little or no recrystallization is recognised.

One sample (A301-176b) associated with pyroxenites was of a harzburgitic composition (i.e. cumulus olivine and orthopyroxene with

interstitial opaques and green spinel).

3.9 Anorthosite

A small outcrop of grey anorthosite (A300-105b) has been mapped by Goode and Krieg (1965, 1967) to the north of the Ewarara Intrusion (Fig. 2; Plate 2). It occurs as a thin dyke-like body about 0.5km in length along a major fault zone. Granulite gneisses in the fault zone have augen with extreme elongation in the fault plane.

The anorthosite consists of about 90% plagioclase (An_{60}) and about 10% pyroxene (mainly clinopyroxene with some orthopyroxene), with accessory amounts of alkali feldspar, opaques, hornblende and apatite. The rock has a cumulate texture formed by plagioclase crystals, but is strongly deformed (Plate 23B). It is probably intermediate between an anorthosite and a jotunite (terminology of de Waard and Romey, 1969) in composition.

The plagioclase laths are usually about 3 x 1mm in size, but occasional crystals up to 10 x 2mm are also observed. Magnetite(?) exsolution rods up to about 0.03mm long occur in the centre of the laths. An outer zone of antiperthite exsolution, about 0.2mm wide, occurs at the edge of the laths when they are not in contact with pyroxene. The laths are often strongly zoned near the edges. Simple and multiple twinning is present. Synneusis relations with other plagioclase grains are sometimes observed.

The pyroxenes are usually equidimensional (1 - 2mm) and contain opaque exsolution.

Apatite occurs as long needles (0.5mm) and/or as skeletal crystals (Plate 22C) with a fine-grained groundmass of intergrown plagioclase and alkali feldspar (Plate 22D). The apatites are identical to those described by Wyllie et al. (1962) from quench textures.

The rock is therefore interpreted as having formed by rapid cooling of a silicate melt carrying a high proportion of plagioclase crystals. The silicate melt was at an advanced stage of basaltic(?) fractionation prior to quenching; this is indicated by the presence of potassium feldspar, apatite (see Anderson and Greenland, 1969), and the general lack of ferromagnesian minerals.

The rock is highly deformed. Plagioclase laths are often bent and a mylonitic fabric in the groundmass extends through the rock. The foliation formed by ribbon aggregates of interstitial feldspar extends both through and around primary laths. The ribbon aggregates are in part similar to reconstituted interstitial feldspar intergrowths. Presumably the deformation was related to movements on the fault zone.

3.10 Garnet pyroxenite

An unusual garnet pyroxenite rock (A300-713) was collected from southeast of Ewarara in the granulites (Figs. 2,4). In this locality it was conformable with the surrounding acid gneisses and was originally thought to be part of the granulite sequence. However, Gray (1967) has reported a similar rock (A298-100) as a transgressive dyke at Teizi.

The pyroxenite is internally layered on a fine-scale with three basic layer types being recognised:

(a) medium-grained (1 - 2mm) clinopyroxene (spinel and magnetite? exsolution plates) and orthopyroxene (spinel and clinopyroxene exsolution) layers with about 15% interstitial green spinel (opaque exsolution), 5-10% plagioclase and rare magnetite (haematite exsolution). The texture (Plate 25A) is typical of adcumulates-mesocumulates, and an igneous origin is supported by the types of exsolution bodies in pyroxene. The spinel is characteristically rimmed by a thin (0.04mm) corona of plagioclase (Plate 25B).

(b) similar clinopyroxene-rich layers with less orthopyroxene, spinel and plagioclase

(c) layers containing large garnet porphyroblasts elongate parallel to layering. These crystals are about 1 to 2cm in diameter, and commonly contain clinopyroxene inclusions. Rare magnetite intergrowths are also observed (Plate 25C). The garnet is surrounded by finer grained sievelike intergrowths of orthopyroxene, plagioclase, green spinel and garnet. Clinopyroxene grains like those in the other layer types are scattered throughout the assemblage but appear to have no significant association with the other minerals. The spinel is usually intergrown with orthopyroxene rather than plagioclase (Plate 26A). In many cases it is rimmed by garnet at its own expense (Plates 26B,C,D) suggesting a sub-solidus reaction of the type:

spinel + orthopyroxene ⟶ garnet

Gray (1967) has observed garnet rims on spinel and also biotite in the Teizi example. The lack of reaction between orthopyroxene and spinel in the other layer types could be due to compositional differences or to the general lack of physical proximity. Garnet is occasionally

observed in these layers in association with sieve-like intergrowths of orthopyroxene, spinel and plagioclase.

Similar reactions have been described from other localities e.g. Saggerson (1968) has suggested a spinel - clinopyroxene reaction to give garnet in Kenyan eclogite nodules, while Lovering and White (1969) have noted spinel rimmed by garnet of similar MgO, FeO composition in a spinel pyroxenite nodule from the Delegate pipe, NSW. Harley (1969) has described garnet rims on spinel from high pressure mafic intrusions in the Fraser Ranges, WA. Green (1966) and Jackson and Wright (1970) have reported garnet ± olivine (or orthopyroxene) rims on spinel in contact with clinopyroxene from garnet pyroxenite inclusions in Hawaiian volcanics, while O'Hara (1961) has described complex garnet - spinel - orthopyroxene - plagioclase intergrowths in a clinopyroxene-rich rock from a high grade Scottish terrain. These observations would suggest that the reaction is a high pressure one.

A similar reaction to that described has been investigated experimentally (Macgregor, 1964, 1965; Ito and Kennedy, 1967; Green and Ringwood, 1967c). The reaction is:

pyroxene + spinel $\rightleftharpoons$ garnet + olivine

The experimental data is plotted in Fig.29A. Macgregor's data is from the MgO - Al_2O_3 - SiO_2 and MgO - CaO - Al_2O_3 - SiO_2 systems but Green and Ringwood's and Ito and Kennedy's results were obtained from natural or synthetic iron-bearing rocks. The production of garnet - pyroxene - plagioclase assemblages from spinel - pyroxene - plagioclase assemblages in olivine tholeiite compositions has been investigated by Green and Ringwood (1967a), and the experimental reaction curve is shown in Fig.29A.

While accurate comparisons probably cannot be made between the experimental results and the Ewarara reaction because of compositional dissimilarities, useful indications of possible reaction temperatures may be gained.

If a reaction pressure of about 10 kilobars is assumed (from other data on the associated rocks - Chapter 11), then unusually low reaction temperatures for an anhydrous assemblage are suggested by extrapolation of Green and Ringwood's and Macgregor's (1) curves i.e. less than about 400°C. Macgregor's curve (2) gives a temperature of about 900°C while a maximum temperature for Ito and Kennedy's data is about 1050°C. It can be readily seen that the range is considerable, but is probably of the order of 400 to 900°C. By comparison with other experimental work reaction temperatures may be higher for more iron-rich compositions such as the Ewarara example.

The reaction is assumed to occur by cooling rather than by pressure increase (by comparison with other reactions in associated rocks).

Thin garnet rims between orthopyroxene and plagioclase are also observed in parts of the rock (Plate 25D). This reaction is discussed in detail in Chapter 11 and is also considered to form by cooling at high pressures.

PART THREE

GILES COMPLEX

CHAPTER 4

INTRODUCTION

The Giles Complex was originally defined by Sprigg (1958) and Sprigg and Wilson (1959) as a dismembered "once continuous basic and ultrabasic composite(?) lopolith" confined to the Tomkinson Ranges. However, more recent work has shown that this definition is inadequate. Firstly, the Complex has been shown to consist of more than one discrete body (Nesbitt and Talbot, 1966; Nesbitt et al., 1970). The presence of large basic bodies similar to those in the Tomkinson Ranges has also been revealed by mapping in the Musgrave Ranges (Major et al., 1967), thereby increasing their geographical extent. Furthermore some of the rocks thought by Sprigg and Wilson (1959) and Thomson (1964) to be part of the Complex are significantly younger than the large layered intrusions. Many of these bodies belong to the transgressive picrite suite, described in Chapter 3.2, which is temporally separated from the Giles Complex by three deformations and the injection of at least two dolerite suites (Table 7).

It seems desirable to the author to restrict the term Giles Complex to the large layered basic bodies of the Musgrave Block but it is difficult to formally define such a restriction. At the present stage it is probably better to characterise the Complex as much as possible, rather than define it.

The Giles Complex is therefore taken as those basic igneous intrusions in the Musgrave Block which have the following properties:

(a) large size

(b) igneous layering

(c) dominantly cumulate textures (although these may have been partially overprinted by deformation and recrystallization)

(d) tholeiitic affinities

(e) intruded after F_1 folding in the granulites but before F_2 folding and the injection of Type A dykes (see Chapter 14).

Such a set of characters includes at least one of a series of anorthositic bodies in the eastern Tomkinson Ranges not included in the Giles Complex by Thomson (1964) but excludes those basic bodies described in Chapter 3. Gray (1967) has shown that at least one of the anorthositic bodies, Teizi, is petrologically very similar to parts of the Giles Complex, a conclusion supported in Chapter 12. Several other massive anorthosites in the same area may also be related to Teizi and hence the Giles Complex (Gray, 1967).

For the purposes of this study the Complex is divided into two groups. The Tomkinson Group contains the intrusions south of the Mann Fault and includes those in the Tomkinson Ranges as well as isolated bodies such as Hanging Knoll and Palpatjaranya further to the east. The Musgrave Group contains the intrusions immediately south of the Woodroffe Thrust in the Musgrave Ranges as well as isolated bodies such as Ayliffe Hill.

Ewarara and Kalka, two of the intrusions from the Tomkinson Group, are the principal subjects of this thesis. Although they are smaller in areal extent than many of the Giles Complex intrusions, they possess some special characteristics which makes their study especially valuable.

Ewarara exhibits one of the few unambiguous basal contacts observed in the Complex. The Blackstone Range Intrusion is in contact with a thin strip of contaminated granulites on its northern (basal) edge but the granulite may be part of a country rock sliver (as in Kalka). A similar situation may exist in the Michael Hills - Mt West - Bell Rock series of intrusions although the country rock slivers here are considerably thicker than they are at Kalka and probably completely separate each body (Fig. 1).

Kalka possesses one of the thickest layered sequences yet measured in the Complex (cf. Nesbitt and Talbot, 1966, Table 1; Nesbitt et al., 1970). More importantly it is the only intrusion within the Complex which exhibits a complete gradation from pyroxenitic through noritic to anorthositic rocks. The two combined features provide an excellent opportunity to study and evaluate the unique fractionation processes operative within the Complex.

CHAPTER 5

GEOLOGY OF THE EWARARA INTRUSION

The Ewarara Intrusion has been described in detail by Goode and Krieg (1965, 1967), and the following brief description of the body is based largely on that work. More recent work on the body has been mainly in connection with the igneous layering present in the intrusion.

5.1 Shape and Size

Ewarara occurs as an elongate sheet resting on, and discordant with, acid granulites (Plates 5, 27A; Fig. 2). The body extends for about 6km in an approximately east-west direction, and varies in width from 1½km in the west to about ½km in the east. It is divided into two lobes by a small but distinct break in topography associated with a fault (Fig. 2). The upper parts of the intrusion have been eroded, leaving only the basal 200 metres of ultramafic material.

Both the basal contact and igneous layering along the northern and western boundaries of the body dip gently to the south and are approximately conformable or at small angles to each other (Plate 4; also Fig. 2, Zone A in Goode and Krieg, 1967). The country rock adjacent to the contact sometimes has a sheared appearance. In the much faulted north-western area, the contacts and layering dip at anomalously higher angles up to 55°. The basal contact becomes progressivly higher at the western end of the body (Plate 5).

The southern boundary of the eastern lobe (Fig. 2, Zone C in Goode and Krieg, 1967) appears coincident in strike with a major fault, but

despite close examination at the southern end of the deep gorge cutting this lobe it could not be ascertained if they were coincident in dip or if the intrusional contact was steeper. The fault dips at a moderately steep angle to the north (approximately coincident with the granulite layering in the vicinity).

The south-eastern boundary of the western lobe (Fig. 2, Zone B in Goode and Krieg, 1967) is transgressive to but locally interpenetrant with the granulite layering. The contact is interpreted as steep dipping, since a vertically layered igneous horizon is found close to the contact in the ultramafics. The intertonguing with the granulites is more pronounced in Zone D to the south and here the contacts also appear steep.

A gravity profile carried out by the South Australian Department of Mines obliquely across the western lobe indicates that the intrusion is a sub-horizontal sheet about 120 to 200 metres thick (Goode and Krieg, 1965). This confirms surface indications from measurements of the northern contact. Insufficient gravity data are available for any further remarks to be made about the southern contact, although about 100 - 200 metres west from the contact the ultramafics are present to about 200 metres below the surface (the contact is therefore probably steeper than 45^{o}).

The body is therefore interpreted as being an erosional remnant of a previously more extensive and considerably thicker sheet (most other Giles Complex bodies are thicker, larger in areal extent, and contain a high proportion of gabbroic (mafic) rocks relative to their ultramafic content - see Nesbitt and Talbot, 1966, Table 1; Nesbitt et al., 1970).

At present the intrusion forms an elongate sheet with a "half-lens" cross-section (Fig. 3 in Goode and Krieg, 1967).

5.2 Contact and Contamination Features

At Ewarara the contact between the intrusive ultramafic rocks and the granulites is generally gradational over several feet (Goode and Krieg, 1965, 1967). However, in a few cases along the northern edge of the body, thin chilled margins are observed.

The hybrid rocks associated with the gradational contacts are usually noritic to gabbroic in composition. In thin section the contact is marked by the appearance of red biotite and an increase in the proportion of pyroxene to plagioclase. Plagioclase tends to be anhedral and commonly contains small rounded pyroxene inclusions. Large megacrysts of orthopyroxene (up to 5cm) are occasionally found in these rocks (Plate 32B).

The chilled margins are recognised by the presence of fine to medium-grained dolerite in abrupt contact with the acid granulites (Plate 27A). They consist of plagioclase laths (An_{66}) with clinopyroxene and orthopyroxene, and minor amounts of biotite, hornblende and opaques. Grain sizes increase gradationally from about 0.5mm to 2mm about 10cm from the contact.

The textures are partially recrystallized but relic primary plagioclase laths are arranged in a typical doleritic texture. Groups of ragged laths are arranged approximately perpendicular to the contact in rare cases, indicating fast growth rates (cf. Appendix 3).

Scattered orthopyroxene phenocrysts up to 2mm in size and with hour-glass zoning (see Chapter 9) are found in chilled dolerite, A301-1. Epitaxial overgrowths of clinopyroxene are common towards grain edges.

One specimen of websterite, found as float near the intertongued zone, contains strongly aligned large elongate plates of clinopyroxene over 100mm long, 20mm wide and about 2mm thick (Plate 28A). Elongation is parallel to [001], and flattening parallel to (100). The plates, sometimes interpenetrant at low angles, are slightly crenulated in cross-section as a result of small scale F_2 folding. The pyroxene contains abundant mottled orthopyroxene and spinel exsolution. Spinel exsolution is concentrated in zones and patches parallel to the elongation, and in some cases converges to produce arrowhead structures (Plate 28C). A fabric, delineated by alignment of plagioclase lenses and patchy spinel exsolution in clinopyroxene, and oriented perpendicular to the pyroxene plates in sections cut both perpendicular and parallel to elongation, is also observed but has not been interpreted (Plate 28D).

Rare lenses of felsic xenoliths up to a few centimetres long are observed near the contact of the east lobe of Ewarara, indicating at least some contamination of the magma by the country rock. This is supported by the presence of biotite and opaques in the lower parts of the layered sequence. The concentration of these minerals decreases with distance from the contact rather than with vertical height from the base of the body, which would appear to indicate a contamination origin. These minerals are rarely observed elsewhere in the layered sequences of Ewarara and Kalka (except in the more fractionated members of the Kalka succession).

An aureole surrounding the intrusion is characterized by a lack of foliation which is usually present in granulites further from the body. Hornblende replacing pyroxene is especially noticeable in the ferromagnesian-rich rocks where it increases in abundance near the intrusion. The aureole is physically visible over a width of the order of metres, but its limits are difficult to define as traces of hornblende can still be found much farther from the intrusion.

5.3 Stratigraphy and Petrography of the layered sequence

The layered sequence of Ewarara consists of two conformable major layers, an upper pyroxenite and a lower olivine bronzitite, which are separated by a distinct physical and chemical break.

5.3.1 Olivine Bronzitite Zone

This basal part of the Ewarara Intrusion has a maximum thickness of about 50 to 60 metres on the southern margin but is much thinner on the northern side. It consists of cumulus olivine (20 to 40%) and orthopyroxene (50-70%) with interstitial clinopyroxene (5-10%) and plagioclase (5%). Some spinel, apatite, hornblende, biotite and opaques (mainly ilmenite with lesser amounts of magnetite and sulphide minerals) are also present.

Cumulus modes are shown in Fig. 13. The presence of spinel inclusions in cumulus orthopyroxene may indicate the presence of some cumulus spinel, but this is uncertain.

Orthopyroxene, of bronzitic composition (En_{88})*, occurs as pleochroic euhedra or subhedra generally 1.5 to 3mm in diameter and contains olivine inclusions and various types of exsolution. Irregular patches of clinopyroxene are common, but the dominant exsolution is formed by masses of small spinel needles.

Two types of zoning are observed in the orthopyroxenes, both physically outlined by variations in spinel exsolution abundances. One is a normal (edge-parallel) zoning and the other is an hourglass variety (Plate 42 ; fully described in Chapter 9).

Olivine (Fo_{88}) occurs as rounded euhedral to subhedral grains between 1 and 4mm in diameter, and exists as both individual crystals and aggregates. It is often enclosed by bronzite, clinopyroxene or by pyroxene/spinel coronas (see Chapter 9).

Spinel occurs as green anhedra up to about 0.5mm in size in both the cumulus orthopyroxene and the groundmass. It is also observed in the central parts of some plagioclase grains (Plate 28B). Similar textures are also observed in some other rocks from the area e.g. the garnet pyroxenite dyke (Plate 25B; Chapter 3.10). Lovering and White (1969) have also observed spinel inclusions in plagioclase, while Oliver (1964) and Philpotts (1966) have reported texturally similar plagioclase rims around garnet and magnetite. The significance of such textures is not understood, although the association may be purely a physical one.

Plagioclase, which is interstitial to the olivine and orthopyroxene, contains spinel exsolution.

---

* Pyroxene compositions for Ewarara determined by optical methods which may be in error (Chapter 8).

Clinopyroxene, of diopsidic augite composition, exists as a smoky coloured interstitial phase with massed spinel exsolution in the primary assemblage.

The textures in these rocks are typically orthocumulate. Compositionally different overgrowths on orthopyroxene and the abundant presence of non-cumulus phases in the interstices testify to this.

5.3.2 Pyroxenite Zone

The Upper 130 to 150 metres of the Ewarara Intrusion lies with sharp and apparently conformable contact on the Olivine Bronzitite Zone.

It consists only of cumulus orthopyroxene at the base but cumulus clinopyroxene becomes more common towards the top (clinopyroxene is never the dominant phase). Rock types vary from bronzitites to websterites.

Interstitial phases are orthopyroxene, clinopyroxene and plagioclase. Traces of biotite and opaques are rare, and olivine has not been observed.

Orthopyroxene, of bronzitic composition (En_{83}), occurs as pleochroic euhedra to subhedra between 1 and 4mm in diameter. Clinopyroxene exsolution is common, but spinel exsolution is sparse. Clinopyroxene, of augite composition, exists as euhedral to subhedral crystals and exsolves orthopyroxene and sparse spinel. Plagioclase commonly exhibits antiperthite exsolution.

Rock textures are typical orthocumulates. In the least recrystall-

ized examples good crystal packing structures are observed.

5.4 Layering

Igneous layering in Ewarara can be divided into two types on the basis of attitude.

5.4.1 Horizontal Layering

Much of the layering in the intrusion has a low dip and is referred to as horizontal. Various scales of layering are observed.

A large scale phase layering, expressed by an abrupt change in cumulus mineral association is shown by the two major rock types (Plate 4; Fig. 2).

A prominent fine-banded horizon has been mapped in the Pyroxenite Zone about 30 to 40 metres above its base (Plates 4, 27B). Similar layering has been mapped in isolated occurrences elsewhere in both the Olivine Bronzitite and Pyroxenite Zones (Fig. 2). The banding is of a rhythmic nature and is formed by modal variations of the constituent minerals and by textural variations. Each layer has a lenticular form and a thickness of the order of centimetres.

In some parts of the Pyroxenite Zone, small coarse-grained pyroxene lenses up to 50cm long and 10cm thick are observed. Pyroxene crystals are up to several centimetres long and possess well developed igneous lineate lamination in some cases.

These layerings are considered to have formed by gravity controlled processes and are further discussed in Chapter 10.

5.4.2 Vertical Layering

Two vertical fine-banded horizons in the upper Pyroxenite Zone occur in en echelon pattern along the steep(?) southern contact of the western lobe (Fig. 2; Plates 2, 3, 27C). The horizons (referred to as the south and north horizons) were not located west of the intertongued zone. The distribution of the two horizons is controlled by major intertonguing positions of the granulite (Fig. 2). The horizons cannot be traced around these tongues.

The layering is formed by repetition of two basic layer types; Type 1 consists of coarse-grained dark coloured orthopyroxenite or olivine orthopyroxenite while Type 2 consists of medium-grained lighter coloured orthopyroxenite to websterite. It is isomodal with rare size grading(?), and layer boundaries are phase contacts.

Despite partial recrystallization, cumulate textures are reasonably well preserved. In Type 1 layers, most rocks consist of cumulus orthopyroxene (with hourglass zoning and olivine inclusions) and olivine (Fo_{88} approximately) and are very similar to rocks from the Olivine Bronzitite Zone. Some, however, lack cumulus olivine. Type 2 layers consist of cumulus orthopyroxene (less spinel exsolution and no hourglass zoning or olivine inclusions) with interstitial plagioclase, clinopyroxene and spinel. Rare Type 1 cumulus orthopyroxenes may also be present. With the exception of these exotic phenocrysts the Type 2 bands are similar to rocks from the host Pyroxenite Zone.

The lenticular layering has usually planar contacts although rarely small flexures have been observed. A small lens (about 20mm x 3mm) of

fine-grained pyroxenite found in medium-grained Type 2 pyroxenite was similar to some nearby fine-grained pyroxenite bands, and may represent a cognate xenolith.

Near the western end of the southern horizon, the horizon has a thickness of about five metres. The northernmost three metres are crudely banded while the other two metres are well layered (Plate 21C) and have been mapped in detail. Fig. 12B shows the relative thicknesses of Type 1 and Type 2 layers for this part. To the east, this horizon degenerates into one or two Type 1 bands (each about 5cm wide), and eventually thins to one layer about 1cm thick. In the northern, Type 1 layers up to about 30cm thick have been observed.

The origin of this layering is considered to result from flow processes acting along the southern margin and is discussed in Chapter 10.

CHAPTER 6

GEOLOGY OF THE KALKA INTRUSION

The Kalka Intrusion has not been described in detail previously, although brief descriptions of the body are given in Nesbitt and Talbot (1966), Goode and Nesbitt (1969) and Nesbitt et al. (1970).

6.1 Shape and size

Kalka is a much larger body than Ewarara. Kalka itself is 12km long and up to 5½km wide with several isolated outcrops existing further to the west and northwest (Fig. 2; Frontispiece; Plates 1, 29A,B). A belt of ultramafic-mafic rocks extends discontinuously eastwards from the main body for 5½km in the Scarface Silcrete Zone to Gosse Pile where more rocks of a similar nature are found (Moore, 1970a). A layered succession of mafic and ultramafic igneous rocks over 5000m thick is observed in Kalka — these layers are generally steeply dipping, and are truncated on the southern margin by the Hinckley Fault (Fig. 2; Plate 58B).

Contacts of the intrusion with the granulites are rare. One of the granulite outcrops occurs as a long thin sliver within the western part of the intrusion. The granulite bifricates on a macroscopic scale to intertongue with the mafic rocks. At least in part the sliver appears to be a normal contact although small later movements may have localised along it (Chapter 13). The steeply dipping contact is approximately parallel to the layering in both the granulites and the intrusion. (Note: those parts of the intrusion to the west of the sliver are sometimes referred to as West Kalka).

The other major granulite outcrop is much wider and does not penetrate as far into the intrusion (it does, however, have an associated long thin sliver parallel to one of its sides). The contacts are locally conformable to and intertonguing with the granulites but on a broader scale the mafic rocks are transgressive to the granulite layering. The contact is in part a small fault.

Although no detailed work has been done, the Kalka Intrusion has much less effect on the regional gravity anomaly than the South Mt Davies body (I.S. Rowan, pers. comm.). Steele (1966) has estimated from a detailed traverse that the South Mt Davies body extends to a depth of about 5000 metres. Therefore it would appear that Kalka is a shallower body than this, but still considerably thicker than Ewarara which only produces a 2.5 milligal Bouger anomaly.

Local gravity surveys on the northern boundary between the intrusion and alluvium reveal a sharp decrease in the Bouger anomaly to the north (Miller, 1969). It is therefore unlikely that the present northern margin of the intrusion lies much further to the north than the outcropping pyroxenites.

The body is interpreted as forming a thick steeply inclined (lopolithic) sheet with approximately conformable contacts to the granulites. The granulite slivers are thought to represent erosional intersections with intertongued side walls* of the intrusion which extend into the body from below and the northwest (see diagrammatic

---

* The western granulite sliver is not considered to completely separate West Kalka from the main body as mineralogical and chemical variations are continuous across the sliver.

representation in Fig. 14A). No top or bottom contacts to the intrusion are observed.

6.2 Contact and contamination features

Thin gabbroic margins, generally finer grained (0.1 to 0.5mm) than the bulk of rocks in the intrusion, are found associated with parts of the granulite contacts at Kalka. When examined in various creek sections these margins exhibit sharp contacts with the acid granulite gneisses but grade inwards over a short distance (maximum of about a metre, and generally considerably thinner) to more normal coarser grained norites.

The rocks consist of a granoblastic equigranular assemblage of plagioclase (50 to 60%), clinopyroxene and orthopyroxene (cpx > opx) with accessory apatite. Brown hornblende, red-brown biotite and opaques are also present in minor amounts in some cases. Some pyroxenes contain very fine opaque exsolution, giving a dusty appearance. The texture is believed to represent an annealed chilled margin.

In one instance basic rock (A314-472) containing small acid xenoliths was found near the contact. The crystals are slightly strained and the groundmass partially recrystallized but the general texture is well preserved. The texture is that of a typical dolerite consisting of plagioclase laths (up to 1mm) and subhedral to lath-like ortho- and clino-pyroxene with minor opaques. The matrix consists essentially of unusual felsic (feldspar - feldspar or feldspar - quartz?) intergrowths resembling myrmekites (Plate 30A). They are similar to very rapid quench textures observed in experimental investigations, suggesting that the

rock underwent fast cooling during crystallization.

This rock may represent an unrecrystallized example of the chilled margin although it may also be a significantly younger intrusion*.

Felsic blebs, lenses and veins are commonly associated with both the fine-grained margins and with normal norites near the margins, but are not observed at any distance from the granulite contact. Typical examples are shown in Plates 30C, D, E.

The marked lenticular development of these blebs in many examples is a reflection of the gneissic deformation affecting the norites (Chapter 13).

The lenses and blebs consist essentially of quartz and perthitic K-feldspar with minor antiperthite. These phases are usually coarser grained than the surrounding marginal gabbroic material. Grain boundaries tend to be amoeboid to interlobate with minor associated recrystallization. The boundaries with the gabbroic material are somewhat diffuse in contrast with the sharp contacts observed in the veins.

In the veins, pyroxene tends to be coarser grained (up to 1mm) along the margins. In general, textures are similar to those in the felsic lenses although quartz up to 2.5mm long and elongate parallel to the vein walls has been observed. Myrmekitic intergrowths are observed on the vein walls and also within the vein (Plate 30F). Networks of

---

* It is, however, dissimilar to all other suites of younger igneous rocks in the area (Chapter 3.1).

veins in norite have been observed rarely along the contact of the northeastern granulite area.

Quartzite xenoliths are commonly associated with the granulite contacts, especially on the western side of the granulite sliver (Fig. 2). These xenoliths are usually raft-like and up to about a kilometre long (although usually much less). They are generally found approximately parallel to layering in the intrusion. In one example banded quartzitic layers were found associated with "lacy network" veining of norites (Plate 34E).

Small felsic xenoliths tend to be of two types in A314-472. Quartz xenoliths maintain sharp boundaries with the host dolerite (Plate 30A) whereas feldspar-rich xenoliths have gradational contacts with the dolerite (Plate 30B). An intermediate rim of felsic dolerite rich in radial plagioclase laths separates the xenolith from the normal dolerite in this case.

In conclusion the presence of quartz-bearing material in basic rocks near intrusional contacts is considered to be indicative of magma contamination by the country rock granulites. The diffuse nature of the margins of quartz - feldspar xenoliths and lenses compared to the sharp boundaries of quartz xenoliths is thought to be related to their relative melting points. The rare presence of acid veins is interpreted as indicating melting of the country rock near the contacts with subsequent injection into the norites. The veins are probably similar in origin to rheomorphic veins from Mt Davies described by Nesbitt and Talbot (1966).

Contact Temperatures

Contact temperatures have been estimated for Ewarara and Kalka with the assumption that intrusional temperatures were about 1350°C (Chapter 11). Granulite temperatures at the time of intrusion are assumed to lie between about 400°C (assuming a geothermal gradient of about 10°C/km, characteristic of today's shield areas) and 1000°C (maximum temperature of metamorphism – Chapter 2).

From Jaeger's (1957) data, Fig. 14B has been constructed. From this, contact temperatures between about 1000°C and 1250°C can be estimated (bearing in mind the limitations of Jaeger's tables). The stability of sillimanite in one quartzite xenolith (A314-394b) at Kalka is consistent with such temperatures at about 10 kilobars (see Fig. 6 for sillimanite stability field, and Chapter 11 for pressure estimations), although it may also be due to the sluggish transformation rates characteristic of the Al_2SiO_5 polymorphs. The presence of only limited melting of the acid granulites in these areas suggests that contact temperatures were nearer 1000°C as at higher temperatures complete melting of even near-anhydrous acid granulites would occur (cf. Chapter 2). This would mean that the granulites had cooled considerably below their peak metamorphic temperature by the time the Giles Complex was intruded i.e. at least to about 400 to 600°C.

6.3 Stratigraphy and petrography of the layered sequence

Detailed investigations in the Kalka Intrusion have allowed the layered sequence to be divided into four main groups of rocks: the

Pyroxenite, Norite, Olivine Gabbro* and Anorthosite Zones (Fig. 15). Stratigraphic Sections 1 to 11, based on field mapping and petrographic examinations, have allowed the compilation of Fig. 16, which, by use of certain marker horizons, shows the lateral and vertical facies changes within the layered sequence (location of Sections in Fig. 15). Although the body is deformed, structural investigations have revealed little repetition of the layered succession by folding or faulting; the relationships in Fig. 16 are therefore taken directly (with dip corrections) from Fig. 2.

The order of deposition of the Kalka layered series can be ascertained by several methods with consistent results. The overall rock sequence varies from pyroxenites on the northern edge through norites and olivine gabbros to anorthosites at the south-west corner. The associated cumulus mineralogical sequence varies from pyroxene through pyroxene + plagioclase $\pm$ olivine to plagioclase + minor pyroxene and olivine.

Although marked internal variations occur, the average chemical fractionation sequences for plagioclase and olivine (Fig. 13) indicate that the southwestern rocks formed last as these rocks are more differentiated (i.e. lower An, Fo). Within the cyclic units (Chapter 7) the chemical and mineralogical trends indicate a gradational increase in

---

* The Olivine Gabbro Zone is not distinguished from the Norite Zone in Fig. 2 because of lack of detailed information in some areas. However, its extent is shown in Fig. 16, and also approximately in Fig. 15 (see Chapter 10 for further discussion).

fractionation towards the southwest, followed by a sharp reversal at the beginning of the overlying cyclic unit.

In the great majority of cases, mineral graded layering (plagioclase overlying pyroxene or olivine) indicates younging towards the southwest (Fig. 17). A few examples of reverse grading were recorded. Several examples of possible cross-stratification were observed in the layered sequence. Those not obviously of tectonic origin are recorded in Fig. 17. Of these, only two in the Anorthosite Zone are considered to be of definite sedimentary origin (Plates 36A,B; Chapters 6.3.4, 10). The one example in situ gives a south-west younging direction (the other possible examples are also consistent with this direction). A scour channel is also considered to be of primary erosional origin, and gives a similar younging direction (Chapters 6.3.1, 10).

A comparative study of the plagioclase and olivine fractionation trends in the Olivine Gabbro Zone shows that the former trend is relatively displaced towards the south-west (Chapter 10). By analogy with the graded layering this indicates that the sequence is younging to the south-west (a full discussion of the sedimentological aspects of the layering is given in Chapter 10).

6.3.1 Pyroxenite Zone

1. Field Relationships

The Pyroxenite Zone (P.Z.) extends for about five km along the northern margin of Kalka, but other isolated outcrops of olivine-free pyroxenitic rocks are also found throughout the Scarface Silcrete

Zone (Fig. 2). A maximum thickness of about 450m has been measured on the Mt Kalka (No. 6) Section.

Rock types vary from medium to coarse-grained orthopyroxenites to websterites. Olivine is never present.

The "base" of the zone occurs against either alluvium or silcrete. Thus the lower extent of the zone is not known, although comparisons can probably be made with the pyroxenitic zones of the Ewarara and Gosse Pile Intrusions (see Chapter 7).

The upper limit of the zone is defined at the first appearance of noritic rocks. A more precise location could be given as the first appearance of settled cumulus plagioclase but this would be more difficult to map, and in any case would occur at approximately the same position (the first large cumulus plagioclase, 3mm in size, is found in A314-155). The contact of the Pyroxenite Zone with the overlying Noritic Zone is gradational over a relatively short distance. No noritic rocks have been observed at any distance below this boundary in the main body, although some noritic rocks are observed with pyroxenites in the Scarface Silcrete Zone.

Igneous lamination due to the alignment of tabular orthopyroxene crystals is observed in some instances (e.g. Plate 34C). Deformation and recrystallization effects, however, make positive observations difficult in many cases. Igneous layering is mainly defined by ratio or form (grain size) contacts. Small variations in relative proportions of the main minerals which cause differences in weathering characteristics produce the most common layering (such layering is almost impossible

to discern on fresh surfaces). Extreme care has to be taken in using layering caused by grain size variations (especially fine grain sizes) as an igneous structural indicator. In at least some cases this layering is of a tectonic origin (Chapter 13). Possible cross-stratification and scour channels (which give satisfactory younging directions) are observed in the banded pyroxenites in some cases but in at least one of these localities the rocks are strongly deformed (lineated) and recrystallized.

2. Primary Mineral Assemblage and Texture

The pyroxenites generally contain about 55 to 90% orthopyroxene, 5 to 25% clinopyroxene and 5 to 10% (sometimes much less) plagioclase. Biotite is a rare accessory mineral. Approximate cumulus modes are orthopyroxene 100 to 50%, clinopyroxene 0 to 50%, and plagioclase 0 to 5%. Cumulus plagioclase* is only observed as inclusions in orthopyroxene. Plagioclase in these rocks is generally an interstitial mineral (sometimes as recrystallized aggregates between larger primary pyroxenes). It can be distinguished from the cumulus plagioclase inclusions by its shape, antiperthite exsolution and lack of simple twinning (Plate 31D).

Most of those orthopyroxenes with cumulus plagioclase inclusions are found in the main body of Kalka or associated with norites in the Scarface Silcrete Zone (see distribution in Fig. 17). Orthopyroxenes without inclusions are found mainly in this latter area. These pyroxenes are similar to those in the Ewarara and Gosse Pile sequences

---

* Two types of plagioclase inclusions are observed in orthopyroxene (Chapter 9.1.3). One type has a cumulus origin, the other an interstitial one.

which appear to be stratigraphically lower accumulates (Chapter 7). It is therefore suggested that much of the pyroxenite sequence in the Scarface Silcrete Zone is stratigraphically lower than the pyroxenite sequence in Kalka itself.

Grain sizes vary up to 7mm for orthopyroxene (generally 3 to 4mm), up to 5mm for clinopyroxene (average 2mm) and vary from about 0.5 to 1mm for plagioclase.

No purely primary texture has yet been observed in the Pyroxenite Zone as recrystallization assemblages are observed in all rocks. These assemblages are concentrated at grain boundaries of the cumulus crystals, often obscuring the original interstitial texture. In some rocks very few or no residual primary crystals are observed.

In the least recrystallized samples the textures are typical adcumulates (Plate 31A). Pyroxene crystals are essentially tabular to equant with strongly interlocking pyroxene - pyroxene grain boundaries. Pyroxene - plagioclase grain boundaries are usually more euhedral in favour of the pyroxene. In samples where interstitial plagioclase is more common, the cumulus shapes of the pyroxenes are more evident (Plates 31B,C). Both features indicate a more orthocumulus interstitial history.

A rough planar lamination involving an alignment of tabular pyroxene crystals is sometimes present and synneusis orthopyroxene groups (other than those described in Chapter 9.1.3) are sometimes observed.

The degree of deformation and recrystallization varies and is discussed more fully in Chapter 13. The recrystallization assemblage consists of orthopyroxene, clinopyroxene and plagioclase with minor quantities of rutile.

6.3.2 Norite Zone

1. Field Relationships

The Norite Zone (N.Z.) comprises the bulk of the Kalka Intrusion, a maximum thickness of over 3500 metres being measured in the No. 4 (Walter Hill) Section. It extends from the Pyroxenite Zone at its base to the Anorthosite Zone at the top, and also forms an envelope for the Olivine Gabbro (O.G.) Zone in its central portion.

Three main subzones have been distinguished in this zone. The two upper subzones are distinct from the lowest subzone in that they contain interstitial opaques, biotite and hornblende (distribution of these phases shown in Fig. 13). The top subzone differs from the middle subzone by the more abundant olivine-bearing rocks and less marked lateral thickness variations.

(1) N1 Subzone

This lowest subzone, approximately 1500-2000 metres thick, comprises essentially an alternating sequence of medium to coarse-grained leucocratic to melanocratic clinopyroxene norites (tending to orthopyroxene gabbros) with minor developments of pyroxenites (orthopyroxenites, websterites and rare clinopyroxenites), gabbros, anorthosites, olivine-bearing norites and olivine websterites.

In the western parts of the body (e.g. Sections 2, 3, 4) the sequence is generally relatively plagioclase-rich, with only a few relatively major developments of more melanocratic rocks. However, in the central portion (e.g. Section 6) a more alternating sequence of mela- and leuco-norites is found, as well as occasional thin websterite and orthopyroxenite bands. Similar alternations are found further to the east (e.g. Sections 7, 8, 10, 11). In the two easternmost sections, it has been possible in part of the sequence to group these units into a lower dominantly leucocratic group (A314-46 to A314-42), a middle group with approximately equal proportions of mela- and leuco- bands (A314-42 to A314-36) and an upper group of mainly melanocratic rocks (A314-36 to A314-26). The upper two groups extend into and include the O.G. Zone. In the eastern and central parts of the body the Norite Zone above the O.G. Zone is medium-grained and relatively plagioclase-rich although some melanocratic layers occur.

The bulk composition of this subzone would be that of a clino-pyroxene mesonorite.

Layering within the Norite Zone is of two distinct but often associated types. The most common layering results from a conformable alternation of pyroxene and plagioclase-rich layers. This layering occurs on two distinct scales: a large scale (tens to hundreds of metres thick normally) and a small scale (several centimetres thick). The contacts between neighbouring layers are often gradational (especially in the large scale layering) but sometimes sharp ratio contacts are observed between plagioclase-rich layers and the overlying

or underlying pyroxene-rich bands. Because of the rubbly outcrop the contact relationships are often difficult to fully ascertain in the large scale banding.

Some layering is also caused by variations in grain size. Both gradational and sharp form contacts are observed. This type of layering is more easily seen in the small scale layers. Grain size variations may or may not be associated with the modal layering — in some cases the plagioclase-rich bands in the modal layers are more fine-grained than the pyroxene-rich layers.

The more prominent and thicker large scale layers can be traced for lateral distances of up to several miles, especially in the central and eastern sections, but are overall of a lenticular nature (Plates 29B,C). The small scale layering is also lenticular.

Small scale layering within the larger scale units is uncommon and much of the sequence, especially in the western portions, is massive and unlayered.

Igneous planar lamination* is common in most of the rocks (although it can be obscured by S_1), and results from a parallel arrangement of tabular pyroxene and/or plagioclase crystals (e.g. Plate 31E). Where associated, the lamination is parallel to the layering.

Sedimentary structures are found in various parts of the body (Fig. 17). Mineral grading is found in various localities: in one

---

* Primary lamination since grains contain exsolution and simple twinning, and little deformation or recrystallization is observed (cf. Appendix 4).

case it is reverse grading (younging north) but usually it is normal grading (younging south-west with nearby cross-stratification younging in the same direction). Good continuous grading was observed on a fine scale in Rockhole Creek (Plate 34D). Cross-stratification was observed in two localities but a possible tectonic origin could not be excluded. An example of definite tectonic cross-stratification is shown in Plate 35D. The structure must have been formed after the production of the tectonic foliation S_1^9 as this is also cut-off by the plane of discordance. Other layering irregularities are sometimes observed but in many cases these could be directly related to local brittle deformation (e.g. faults).

However, a primary discordant layered structure has been observed in mesonorite about 200 metres above the base of the Norite Zone in Kalka Gorge (Plate 35C). A sequence of at least sixteen streaky plagioclase-rich bands (from 3mm to 3cm thick with sharp ratio contacts) within the mesonorite are cut-off by a plagioclase-rich band between 4 to 8cm thick. The dips of both layer sets are near vertical, and the angular discordance is about 20^o, decreasing towards the east. The eastern side of the structure is obscured by rubble. The observable height and width of the structure are approximately 1m and $2\frac{1}{2}$m respectively. The discordant plagioclase-rich band has a good planar plagioclase lamination indicating an igneous origin. The cut-off plagioclase-rich bands, while being rather streaky in some cases, also have planar igneous laminations. Thus the structure has a cumulate igneous origin rather than a tectonic one (e.g. segregation of plagioclase in joints).

If the eastern side reflects the western side of the structure, it would resemble a scour channel similar to those observed in other igneous intrusions (Table 20). If it is a scour channel, or other erosional sedimentary structure, it would give a younging direction to the south which is consistent with other evidence.

A somewhat similar feature (Fig. 10C) of apparent tectonic origin has been found in the Norite Zone about 1.6km northwest of Walter Hill (field station 729). Other examples of irregular layering are probably tectonic in origin e.g. Fig. 10D.

Minor locally transgressive veins have been observed in some areas. Near the scour channel in Kalka Gorge, irregular pyroxenite veins up to about 3cm thick cut the more regular layered and laminated sequence. In other areas, and more commonly, thin plagioclase-rich veins are observed. These are rarely observed to cut S_0, but themselves contain S_1.

Towards the top of Subzone N1 occasional medium-grained gabbros similar to the transgressive bodies in West Kalka (Chapter 3.3) are observed, but no definite transgressive relationships were found.

(2) N2 Subzone

The middle subzone contains rocks of essentially similar composition to the N1 Subzone, with one important exception. Magnetite/ilmenite and sometimes biotite are present as minor phases in most rocks. A few olivine-bearing members have been observed in this zone but they are not common.

The boundary between the two subzones is difficult to map. In the northwest part of Kalka, magnetite/ilmenite has only been observed to the west of the granulite sliver (from Sections 2, 3 and 4). However, in No. 6 Section, small quantities of magnetite/ilmenite are found in the recrystallized clinopyroxene norites immediately below the granulite sliver. The approximate boundary is shown in Fig. 15.

The upper boundary of the subzone is easier to define. A small but prominent erosional valley can be traced throughout the lateral extent of outcrop in West Kalka, and has been arbitrarily made the division with the upper N3 Subzone.

The N2 Subzone has been subdivided into three smaller units N2a, N2b and N2c. Subzone N2a contains those magnetite-bearing clinopyroxene norites below the granulite sliver in the main body of Kalka (the distribution of these rocks in Fig. 15 is based entirely on recognition of magnetite in thin sections from No. 6 Section*). Subzone N2b contains a lenticular body of similar rocks (maximum thickness 250 metres) between two divergent granulite slivers. Small but relatively common bodies of acid pegmatites, and rare lenses of acid granulite gneisses are also found in this area. Subzone N2c contains those norites above the granulite sliver and immediately below the upper subzone. Contaminated rocks are commonly found in the lower parts of this subzone immediately above the granulite sliver. Subzone N2c is very lenticular and shows a

---

* There is a possibility because of their composition and lack of preserved textures that the N2a Subzone rocks represent recrystallized marginal phases. However, the presence of rare interbanded olivine-rich rocks suggest that the subzone is part of the layered sequence.

large increase in thickness from Section 3 (250 metres) to Section 4 (about 500 metres) to Section 5 (750 metres). Somewhat anorthositic rocks are developed in parts of this subzone. Transgressive medium-grained gabbros are also found in parts of the subzone (Chapter 3.3).

Subzone N2c contains the best small scale isomodal layering of the three groups. The layering results from an alternation of pyroxene and plagioclase-rich bands. Large scale layering of the same type is not well developed but is more easily recognised in the thickest part of N2c (Section 5).

In general the composition of Subzone N2 is that of magnetite-bearing clinopyroxene mesonorite.

(3) N3 Subzone

The upper subzone, about 500 metres thick, consists of magnetite gabbros and norites, some olivine-bearing. A thin (less than 1 metre) but prominent layered peridotite occurs about 150 metres above the base of the subzone in the southern part (Fig. 2). This marker band can be traced laterally for about 2km.

This subzone is distinct from the N2 Subzone in that it contains more olivine-bearing rocks, including the peridotite band, and does not exhibit marked lateral thickness variations. Igneous layering is caused by variations in the relative concentrations of olivine and clinopyroxene, and/or pyroxene and plagioclase (Plate 35B). Some graded layering is observed.

Transgressive medium-grained gabbros are well developed in this subzone and in the overlying Anorthosite Zone (Chapter 3.3).

It should be noted that distinct differences in the subzone exist between those southern outcrops east of the road and those northern outcrops west of the Gunbarrel Highway (Fig. 15). The two parts are separated by a fault with about 100 metres lateral displacement and unknown vertical movement. The northwest section contains little (if any) olivine, the peridotite marker band also being absent. Magnetite is more common, float from a possibly conformable magnetite band being found near the base at A314-383. The transgressive medium-grained gabbros are much more common in this area and in parts make up almost half the outcrop. The rocks also appear more deformed (i.e. better developed S_1 foliation) and recrystallized. Igneous layering is also less well developed in this area.

The two areas of outcrop are, however, contained within the same rock sequences and are broadly similar. They have therefore been correlated. The overall composition of the subzone is difficult to judge but would probably be that of an olivine magnetite orthopyroxene mesogabbro.

A transgressive magnetite - ilmenite body is found in the northern area (Chapter 3.4). A similar body occurs in the Hinckley Fault approximately along strike from the N3 Subzone (Fig. 2).

2. Primary Mineral Assemblage and Texture

(1) N1 Subzone

For the purposes of description the rock types have been divided into three groups: the clinopyroxene norites (including anorthositic and pyroxenitic varieties), the olivine-bearing orthopyroxene gabbros and the olivine pyroxenites.

Clinopyroxene norites

A wide range of modal abundances* is observed depending on rock type. Orthopyroxene ranges from about 20 to 50% (occasionally about 90-100%), clinopyroxene from 0 to 30% (up to 60%) and plagioclase from 0 to 60%. Orthopyroxene is almost always present in greater abundance than clinopyroxene. Biotite**, spinel and rutile are rare accessories. Cumulus modes (Fig. 13) vary from 10 to 100% (average 40 to 50%) for orthopyroxene, 0 to 30% (average about 20%) for clinopyroxene and 0 to 80% (average 40 to 50%) for plagioclase.

Grain sizes vary considerably. Orthopyroxene is usually 1 to 6mm in diameter, clinopyroxene usually 1 to 5mm, and plagioclase usually about 1 to 3mm. The grain size for any one mineral is usually relatively

---

* These are not measured from rocks containing fine scale layering.

** Biotite has been noted in orthocumulate pyroxenites in parts of the P.Z. and N.Z. which, from the surrounding rocks, would be expected to contain antiperthitic plagioclase. However, the plagioclase is not antiperthitic and it is suggested that the potassium was used in formation of biotite instead of entering the plagioclase lattice in these cases.

constant in one rock, although occasionally outsize phenocrysts* (5 to 30mm) of pyroxene or plagioclase are found in the rock. Clinopyroxene is usually finer grained than orthopyroxene within any one specimen*.

Rock textures in the least recrystallized samples are usually adcumulate to mesocumulate. In the more pyroxene-rich varieties intergrown pyroxene - pyroxene boundaries are common, with plagioclase occurring as interstitial stringers between the pyroxene grains. The reverse texture is observed in the plagioclase-rich cumulates where small granular pyroxene grains occur between the plagioclase crystals. In the more plagioclase-rich adcumulates, overgrowths on the cumulus pyroxene crystals are less well developed with the result that the cumulus shape is retained (Plate 31F).

Some rocks have more mesocumulate to orthocumulate textures. Zoning is observed and some phases (e.g. clinopyroxene) may be relatively common as interstitial growths although they may be rare or absent as cumulus phases. Interstitial clinopyroxene commonly rims or occurs at the edges of cumulus orthopyroxene crystals. Rarely orthopyroxene may in turn rim the clinopyroxene (Fig. 22A).

In the least recrystallized samples castellate texture is commonly observed between clinopyroxene (host), orthopyroxene and plagioclase (Plate 47C; Chapter 9.2.2).

---

* In at least some cases the large orthopyroxene crystals can be shown to be synneusis aggregates (cf. Vance, 1969). A complete gradation to crystals with no obvious synneusis features make any interpretations on primary grain size dubious.

Olivine-bearing orthopyroxene gabbros

These rocks are in general similar to those of the preceding group although clinopyroxene is more abundant than orthopyroxene. However, some other differences exist. Small quantities (<10%) of olivine are found as small irregularly shaped anhedral crystals at the grain boundaries of cumulus (or in overgrowths on cumulus) pyroxenes and plagioclase. These grains are much smaller (e.g. about 0.4mm) than the cumulus crystals in the rock or cumulus olivine in the Olivine Gabbro Zone or Anorthosite Zone. They are not found as primary inclusions* with the cumulus pyroxenes or plagioclase, and hence are interpreted as interstitial phases. The rocks therefore tend to orthocumulates.

These rocks first occur in the stratigraphic succession just below the Olivine Gabbro Zone, and support the theory that, in general, any cumulus phase is first represented as an interstitial phase lower in the sequence (Appendix 3).

Both orthopyroxene/green spinel and clinopyroxene/green spinel symplectites are always observed in these rocks, but are very rarely found in rocks without olivine. These symplectites, like the olivine, are found only at grain boundaries of the cumulus grains. They preferentially occur at or near pyroxene/plagioclase boundaries but also occur at pyroxene/pyroxene boundaries. A direct relationship between the

---

* Olivine is rarely associated with opx and/or plag inclusions in cpx or cpx/plag inclusions in opx: these patches have an apparently similar origin to inclusion groups described in Chapter 9.1.3 i.e. they crystallized from liquid inclusions.

olivine and the symplectites in a thin section cannot be proved in many cases. This problem is further described and discussed in Chapter 9.3.2.

Some rocks contain more and larger olivines and are similar to the olivine gabbros of the Olivine Gabbro Zone.

Olivine websterites

Several thin apparently conformable olivine websterites have been observed in the noritic sequence (A314-145, 36, 412a). They consist of about 40% orthopyroxene, 30% clinopyroxene and 30% olivine. Rare antiperthitic plagioclase is also observed. The textures are similar to the other cumulates. Zoning at grain boundaries and presence of interstitial antiperthitic plagioclase suggest a mesocumulus rather than adcumulus formation.

The separation of this group of rocks from the other members of the Norite Zone was considered important because of their anomalous nature. They are mineralogically and chemically out of sequence with their neighbouring rocks. Cumulus olivine is first observed elsewhere in Kalka in the Olivine Gabbro Zone, and there it is considerably more iron-rich (maximum Fo_{86}, generally Fo_{70-80}, compared with Fo_{87} for A314-145). Spinel exsolution in both ortho- and clino-pyroxene is indicative of more magnesian pyroxenes than are normally encountered in Kalka (Chapter 9.1.1). The absence of plagioclase inclusions in ortho-pyroxene is characteristic of rocks normally much lower in the sequence, as are the other features. Indeed, these rocks are similar to some rocks

in the Gosse Pile ultramafic sequence (Moore, 1970a, p. 124) and are not unlike some of the Ewarara pyroxenites.

They are therefore interpreted as resulting from a short-lived return to crystallization conditions more normal in the basal parts of the layered sequence. A314-145, at the base of cyclic unit 7 (Fig. 13), is associated with a rapid alternation of cyclic units related to injections of fresh magma (Chapter 10). A314-36 is also associated with what could represent a fundamental change in crystallizing conditions (see p. 113).

(2) N2 Subzone

The general mineralogy and texture of this subzone is similar to that of the noritic group of the N1 Subzone. However, several important differences exist.

Magnetite/ilmenite are interstitial phases (<5%), especially in the N2c Subzone. Biotite is also observed in appreciable though minor quantities (up to about 5%) in some specimens. Pyroxenes exsolve opaque phases instead of rutile or spinel in this subzone. Trace amounts of chalcopyrite are observed in some rocks.

The presence of primary interstitial opaques in the N2a Subzone is difficult to establish. The rocks in this area are highly deformed and recrystallized, which means that the opaque phases could have been derived from original exsolution bodies in the pyroxenes. It is believed, however, that at least some of the opaques were originally interstitial.

(3) N3 Subzone

The norites and gabbros of this subzone contain up to 5 to 10% interstitial magnetite and ilmenite with some minor chalcopyrite (Plate 31G). Biotite (up to 5%) and hornblende are present in some samples, and may rim the opaque aggregates. Clinopyroxene is more abundant relative to orthopyroxene than in the N1 and N2 Subzones.

An important feature of this subzone is that interstitial granular green spinel is only observed in the olivine-bearing rocks, commonly with the opaque aggregates. This suggests that the interstitial melt and the parent melt of the cumulus phases were both relatively undersaturated. A similar association is observed in the O.G. and Anorthosite Zones.

Spinel is also observed in vermicular intergrowths with magnetite or ilmenite (Plate 38C), but in these instances it is not confined to olivine-bearing rocks. It is also found as thin discontinuous rims on ilmenite inclusions in magnetite (Plates 38E,G).

Plagioclase inclusions in orthopyroxene are not as apparent as lower in the sequence. Both pyroxenes exsolve opaques rather than rutile, a characteristic of the N1 Subzone.

Olivine is usually, but not always, separated from plagioclase by thick granular to massive rims of orthopyroxene or clinopyroxene. Small quantities of pyroxene/spinel symplectites are patchily developed between these rims and plagioclase. These rims are discussed further in Chapter 9.3.2.

The peridotite (A314-205) deserves some comment. This rock contains both clinopyroxene (rich in opaque exsolution) and orthopyroxene (no exsolution), and the true composition is probably lherzolitic to peridotitic. Olivine (Fo_{76}) is the major mineral, with plagioclase (about 10%), spinel, opaques, biotite and hornblende being minor phases. Olivine, clinopyroxene and perhaps plagioclase are the cumulus phases in this rock.

6.3.3 Olivine Gabbro Zone

1. Field Relationships

The Olivine Gabbro Zone (O.G. Zone) is completely enclosed by the Norite Zone in the central and eastern sections of the main part of Kalka. It reaches a maximum thickness of about 600 metres in the central parts of the body thinning to the east and west over a total outcrop length of about 6.5km.

It consists essentially of olivine gabbros (leucocratic to melanocratic), some orthopyroxene-bearing. These rocks grade to picrites and dunites, olivine clinopyroxenites and clinopyroxenites. They are interlayered with clinopyroxene norites, some olivine-bearing, similar to those in the Norite Zone. The average composition of the zone would probably be that of an orthopyroxene-bearing olivine mesogabbro.

The O.G. Zone has proved the most difficult part of the intrusion to map. The alternating presence of olivine-rich and olivine-poor rocks has resulted in the common development of extensive magnesite cover on the olivine-rich areas, and in sharp variations in topography (resulting

in rubbly outcrop and scree). Furthermore at low concentrations olivine is very difficult to observe in hand specimen and so in many cases such rock types are recorded on the map only on the basis of thin section studies (this should be kept in mind when consulting Fig. 2). Because of the rubbly outcrop great difficulty has also been encountered in distinguishing some of the olivine-rich members (e.g. dunites, picrites) of the transgressive picrite suite (Chapter 3.2) from those in the layered sequence. The problem still exists but certain criteria for distinction can be used in many cases (these criteria are drawn up from observations on definite transgressive and layered sequence rocks):

i) the transgressive rocks are very rarely layered (although they may possess an igneous lamination).

ii) cumulus plagioclase and clinopyroxene are only found in a few of the transgressive group of this composition, and these types are readily distinguishable by other methods.

iii) the transgressive group may be chemically and mineralogically out of sequence (however marked chemical variations are also characteristic of the Olivine Gabbro Zone layered sequence).

iv) transgressive rocks have generally suffered little or no deformation, and certainly do not exhibit the S_1 foliation characterisitic of most of the layered sequance.

The limits of the zone are particularly difficult to define, as they grade into the Norite Zone both laterally and vertically, and laterally continuous horizons are difficult to find over the whole zone. The base of the Olivine Gabbro Zone has been defined as the base of the

lowest major olivine gabbro unit (thin bands* or bands with low olivine concentration occur up to 200 to 500 metres below this level in the Norite Zone).

The top of the O.G. Zone has been defined in east Kalka as the top of the Johnson layered unit, a spectacular rhythmic horizon. Once again thin olivine-bearing bands sometimes occur higher in the sequence, but this is uncommon.

With these two definitions problems immediately arise. In Section 5b the base of the Zone is about 250 metres below the base in Section 6 (see stratigraphic correlations in Fig. 16; and Fig. 2). Similarly, further to the east in Sections 8 and 9, the base is again higher, this time by another 200 metres. The major band defining the base in the second case becomes less distinct towards the east and eventually inter-tongues with the Norite Zone while another band higher in the sequence becomes the lowest major olivine gabbro band (see Fig. 2). There is no evidence that the sequence is faulted at this stage (a minor fault laterally displaces the Johnson Horizon by about 50 metres in this area but this would not be sufficient to explain the stratigraphic relation-ships). A continuous stratigraphic sequence seems certain. The position is less clear between Sections 5b and 6 as faulting may play some part at the eastern end of the olivine melagabbro outcrop (east of field station 808). This, however, would probably not affect the overall result.

---

* Also bands of green clinopyroxenite which are characteristic of the O.G. Zone are found below this level at times.

At the top of the Zone similar problems arise. The Johnson Horizon is not observed in Section 10 and is abruptly cut-off by a fault near A314-320. However, a prominent mela-leuco boundary about 40 to 50 metres below the Johnson Horizon at A314-320 is observed to the east of the fault and is there used as the top of the Zone. A similar procedure is followed west of the Johnson Horizon. The top is here defined at the top of the highest major olivine gabbro unit. Once again, as at the base, this causes marked fluctuations in the upper stratigraphic level although the absence of good marker bands makes correlation more difficult. Special mention should be made of the area around Drum Hill. In Section 6, a relatively thick but laterally confined area of olivine-rich rocks (dunites) is found around A314-406. Towards the west this area grades to norites and towards the east possibly intertongues over a short distance with norites. These layered norites appear to also intertongue sharply(?) with more olivine melagabbros and clinopyroxenites further to the east around A314-402 in Peepullaturra Creek. The lateral facies changes appear primary as no evidence for faulting could be found in these areas, but there remains an unresolved possibility that the rocks around A314-406 are transgressive. Stratigraphic correlation over the Albitalbiti Fault (Fig. 2) is also difficult in detail although it is believed the rocks represent the same general stratigraphic interval (note: the rocks on both sides of the fault possess primary fine scale layering S_0^g, tectonic foliation S_1^g, and are interbanded with norites i.e. they are not transgressive olivine-rich rocks).

The lateral limits of the O.G. Zone, however, are probably the most difficult of all to define. Both field mapping and thin section studies

indicate a definite gradational decrease in olivine content of rocks to the east and west. In Section 4 major olivine bands are relatively thin (cf. Sections 5b and 6) and about 500 metres or more further to the west no olivine has been observed in traverses or thin sections. To the east between Sections 9 and 10, the major olivine-rich bands thin and lens out. Therefore the O.G. Zone - Norite Zone boundary in this area has been drawn schematically as an intertongued facies change (it has been drawn to include an olivine melagabbro at A314-26 which is probably part of the layered sequence and not transgressive). Minor quantities of olivine are observed in thin sections from Section 10 but further to the east no olivine is observed. Because of the difficulty of recognising small quantities of olivine in the rocks in the field it has been decided to place all Section 10 into the Norite Zone although in the upper part (A314-39 to A314-26) the rocks are gradational from the O.G. Zone.

A small lens of olivine melagabbro is also observed to the east at A314-14, but is not separated from the Norite Zone.

Igneous layering in the Kalka Intrusion is well developed in the O.G. Zone. The large scale layering can be best observed in Fig. 2 and Plate 33A. The contacts between the layers are usually relatively sharp. The layering is caused by variations in the concentrations of olivine, clinopyroxene and plagioclase giving rise to the alternation of rock types previously described. These layers are lenticular, especially in the east, and may in one instance laterally give way from dunitic and picritic rocks to thin clinopyroxenites. A marked thickening in the

lowest olivine melagabbro - picrite band at field station 92 in east Kalka may be associated with magmatic erosion as apparently transgressive trends are observed (Fig. 2). However, no direct evidence was obtained on this problem.

Fine scale layering is well developed, especially in the eastern part. Generally the conformable layering is caused by variations in the concentration of plagioclase relative to pyroxene and olivine. Both sharp and gradational ratio contacts between the layers are observed. Gradational contacts have only been observed between a lower pyroxene - olivine-rich layer and an upper plagioclase-rich layer (i.e. normal grading). Sometimes the layering is also accompanied by variations in grain size (Plate 35F).

A spectacular development of this isomodal and graded layering is observed in the Johnson Horizon at the top of the O.G. Zone in the eastern section (Fig. 2). Up to two horizons may be present, but the uppermost one displays the best layering (Plate 33B). This top horizon is about 5 metres thick (maximum) and contains a rhythmic succession of isomodal and graded (Plates 34A, 35F) layers of olivine melagabbroic and leucogabbroic composition. The double layers (ol - cpx and plag) usually have a combined thickness of about 2 to 30cm. Little lensing is observed within any outcrop and the layering is very regular. The horizon has been mapped over a lateral extent of almost 3km. Limited horizons of similarly strongly layered rocks have been observed at field station 526 and field station 509 (Plate 34B). However, these rocks are much further to the west and apparently(?) higher in the stratigraphic succession. The lateral extent of the Johnson Horizon, although considerable for its

thickness, is not unusual. Worst (1960) and Jackson (1963) report thin chromitite bands up to 70 and 30 miles long respectively, while Cameron (1963) has traced layers in Bushveld up to 45 miles along strike. Jackson (1967) reports a minimum range of lateral continuity to thickness of 10^4 or 10^5 to 1 (cf. about 10^3 to 1 for the Johnson Horizon).

Fine scale layering in the ultramafic rocks is also developed as a result of variations in the proportions of olivine and clinopyroxene (Plate 35A). The contacts are normally fairly sharp. Complete separation of cumulus olivine and clinopyroxene has not been observed (grain sizes are comparable).

An irregularly layered structure in olivine(?) mesonorite (Plate 35E), found as a float block in Johnson Creek, probably originated in the Olivine Gabbro Zone further to the north. The structure consists of a double layer of leuconorite and melanorite with sharp ratio contacts. The leuconorite band maintains a regular thickness of about 2cm, whereas the melanorite has an irregular contact with the mesonorite and varies in thickness from 2cm to 5cm. The structure must predate the S_1 deformation since S_1 forms a planar streaky foliation throughout the layering. It is therefore considered to have an igneous origin and resembles load casts in aqueous sedimentation. Ferguson and Pulvertaft (1963) and Hess (1960) have described similar structures in other igneous intrusions.

Thomson (1964) has previously mapped the Olivine Gabbro Zone as intrusive to the surrounding norites but this conclusion is believed unfounded. The field relationships, including the presence of conformable interlayered norites, and the recognition of cyclic units (Chapter

7) demonstrate that the Olivine Gabbro Zone is part of the Kalka layered sequence.

2. Primary Mineral Assemblage and Texture

The O.G. Zone contains a wide variety of rocks. These can be grouped for the purposes of description into four related groups viz. clinopyroxene norites (including pyroxenitic and anorthositic varieties); olivine-bearing orthopyroxene gabbros; olivine melagabbros (including olivine clinopyroxenites, clinopyroxenites and peridotites); and dunites (including troctolites).

The clinopyroxene norites and olivine-bearing orthopyroxene gabbros are very similar to those rocks of similar composition in the N1 Subzone.

The olivine gabbros are usually melanocratic but grade to more leucocratic varieties. They consist of approximately equal amounts of olivine and clinopyroxene with smaller quantities of plagioclase. Spinel and sometimes orthopyroxene are present in small amounts. The clinopyroxenes are unusually green in colour and are probably chrome-bearing.

Grain sizes vary from about 0.5 to 3mm for primary olivine, and 1 to 5mm for clinopyroxene. Primary textures are difficult to interpret because of the common development of secondary recrystallized aggregates at grain boundaries, although there is little doubt that they are cumulates. The cumulus phases would be clinopyroxene, olivine and possibly plagioclase. Occasional phenocrysts of orthopyroxene up to 6mm in size are observed. Apart from containing rounded olivine inclusions these crystals are similar to those in the Norite Zone.

Brown-green spinel is thought not to be a cumulus phase as it is not observed as inclusions in any of the other cumulus phases and is found associated with grain boundaries in recrystallized aggregates.

Both clinopyroxene/green spinel and orthopyroxene/green spinel symplectites are commonly found associated with olivine and plagioclase grain boundaries (see Chapter 9.3.2).

The dunites consist almost entirely of olivine, although 10 to 20% plagioclase is found in some varieties. In the least recrystallized rocks, primary grain boundaries are interlocking (Plate 31H) and textures tend to mesocumulate and adcumulate. Small amounts of interstitial orthopyroxene and clinopyroxene, and rare biotite are found in the rocks.

The presence of up to 5% anhedral to subhedral green to dark green spinel, mostly at grain boundaries, is a feature of the dunites and olivine mesogabbros (most opaque in the dunites). Its derivation is an enigma. In a deformed and recrystallized assemblage, anhedral spinel at grain boundaries could have originally been a primary cumulus and/or interstitial phase or may represent recrystallized spinel exsolution in pyroxene (coalesced at grain boundaries) or recrystallized pyroxene/spinel symplectite. Although it is very probable that the two latter explanations partly explain its presence (note: rarely distinct colour differences in spinel are observed in the one rock) spinel is also found as rare rounded or euhedral inclusions in and between* olivine in

---

* Not an olivine - plagioclase reaction product in dunites as no plagioclase reactant or pyroxene product are directly associated with spinel, nor from coalescing of spinel exsolution from pyroxene as pyroxene is rare in these rocks.

relatively unrecrystallized areas. The spinel therefore appears to be partly cumulus in origin (its abundance is proportional to the abundance of olivine). More irregularly shaped grains are probably at least partly interstitial.

6.3.4 Anorthosite Zone

1. Field Relationships

The Anorthosite Zone (A.Z.) forms the uppermost part of the observed layered sequence. The highest units are in contact with alluvium, and there is a marked structural discontinuity with the layered rocks of the Hinckley Range. A maximum thickness of about 800 metres has been measured in the Walter Hill Section (No. 4).

The A.Z. consists essentially of leucogabbroic and anorthositic rocks, commonly magnetite- and olivine-bearing, and sometimes grading to leucotroctolites and olivine leucogabbros. Occasional limited occurrences of conformable* magnetite/ilmenite-rich layers are observed. Other occurrences of melanocratic rocks are rare.

The boundary between the Anorthosite Zone and the underlying Norite Zone is defined as occurring at an erosional valley which can be traced throughout the entire length of outcrop. In the northern part of West Kalka this valley contains subdued outcrop at the top of the Norite Zone. On its western side in this area a characteristic olivine - magnetite

---

* Some bands are definitely conformable. Others, outlined by concentrations of magnetite/ilmenite float, may be related to the transgressive type of magnetite body (Chapter 3.4) although they appear to parallel the layered sequence.

marker band is observed. The base of this band is taken as the base of the A.Z. in this area. The marker band cannot be traced over the fault separating the two different parts of the N3 Subzone, possibly because of the fault or because of the increased zone of no outcrop. The latter reason is more likely as the overlying sequences in both areas are similar. It should be realised, however, that the marker band is lenticular and may not extend very far to the south of observable outcrop.

Although there is no particular evidence to suggest that the A.Z. itself is lenticular, individual units within the Zone commonly lens out. It is interesting to note that a possible correlation exists between A314-418 (Section 1), an olivine gabbro, and parts of the A.Z. (e.g. A314-388 in Section 3). This means that the underlying N3 Subzone, which in itself is generally of a uniform thickness, could lens out very quickly to the northwest between Section 3 and Section 1 (unless unseen faults are present).

Clinopyroxene mesonorites, interlayered with mesogabbros, olivine-bearing gabbros and troctolites, are found in an isolated outcrop to the west of West Kalka viz. A314-447, 448, 449 and 450. Their structural position appears to place them stratigraphically above the rocks of West Kalka. (Possible cross-stratification in the rocks indicates that they young to the west).

Transgressive mafic pegmatites as well as transgressive medium-grained gabbros are found in the Anorthosite Zone (Chapter 3).

It has been difficult to recognise large scale layering in the field in West Kalka although the geochemistry and petrography suggests a

large scale variation exists (Chapter 7). However, fine scale layering and planar igneous lamination are very well developed in the Anorthosite Zone. The layering is caused by variations in pyroxene - olivine/ plagioclase content (Plate 36C). Graded layering is sometimes observed (facing west). The layering is often markedly lenticular. The olivine - magnetite marker band thickens from about $\frac{1}{2}$ metre at its extremities to about 3 metres in the centre (and may sometimes itself be internally layered).

In one locality in the A.Z. of West Kalka, within a limited vertical section of several metres (maximum) and lateral extent of 10 to 20 metres, markedly lenticular layering with associated sedimentary-type structures has been observed.

One of the most prominent anorthositic lenses is shown in Plate 36E. The lens, about 25cm thick (maximum) and at least 2 metres long, occurs within an alternating anorthositic and leucogabbroic layered sequence. It is overlain by a leucogabbroic band with a basal concentration of clinopyroxene. The lens is well sorted — the lower centimetre consisting of dominantly clinopyroxene while the rest of the lens is composed of anorthosite (grain size of these rocks is about 3 to 5mm generally).

It has a possibly erosional lower surface, and its upper surface is marked by two (possibly three) asymmetric humps. The crests of these humps are associated with thinning in the overlying leucogabbroic band. They, therefore, do not appear to have formed by folding, and an origin by slumping is not supported by other evidence in the surrounding rocks. However, they appear to be very similar to asymmetric current ripples in

aqueous sedimentation (e.g. Allen, 1963, 1968b; Harms, 1969) and are interpreted in a similar manner (Chapter 10). Ripples or possible ripples have been rarely reported from other intrusions (Table 20).

The angular relationships of the ripple marks are as follows: ϕ, angle of lee face (to layering) $\sim 5^{o}$; θ, angle of slip face (to layering) $\sim 35^{o}$ (max.). Because the measurements are made on only a two dimensional outcrop, lateral distances could be excessive. With these limitations in mind, several ripple mark indices (Tanner, 1967) can be calculated:

$$\text{Ripple index (RI)} = \frac{\text{wavelength}}{\text{height}} \simeq 10 \text{ to } 20$$

$$\text{Ripple symmetry index} = \frac{\tan \theta}{\tan \phi} \simeq 3 \text{ to } 5$$

Slightly to the north, marked erosional truncation of a thin clinopyroxene band by a similar layer was observed within anorthositic rocks (Plate 36A). The older band also appeared to be developed on an erosional surface as marked thinning of the underlying anorthosite band occurred beneath it. An angular discordance of about 30^{o} was measured between the two bands. A similar structure, but with smaller angular discordance, was observed in a nearby float boulder (Plate 36B).

The relative lack of recrystallization and absence of foliation and folding within this area mitigates against any tectonic origin for these structures (compare with tectonic cross-stratification in Plate 35D).

They appear similar to cross-stratification in normal sediments and are classified on similar principles (see McKee and Weir, 1953; Allen, 1963). The above examples have planar to slightly curved surfaces of

erosion, and hence are examples of planar cross-stratification.

Other similar structures have been observed in many other igneous intrusions (Table 20).

Marked lenticular banding is observed commonly within the anorthositic layers in this locality, although the more gabbroic bands also may show marked thickening along strike (Plate 36D). Lateral facies changes are also observed with gradational changes in pyroxene/plagioclase ratios.

Throughout the Anorthosite Zone but best developed about 250 to 500 metres above its base, distinctive "clump" textures are developed in certain layers. There are two distinct varieties which consist of pyroxene - plagioclase (rarely magnetite - plagioclase) and plagioclase (Plates 32E,F). They are sometimes spherical in shape and between 2 and 10cm in diameter, but their usual morphology is plate-like with irregular boundaries. Plate groupings often give a planar structure parallel to layering in surrounding rocks (Plate 32G).

The dark clumps can consist of plagioclase with either orthopyroxene, clinopyroxene or orthopyroxene/clinopyroxene (in mutually exclusive bands). In each clump (unless recrystallized) the pyroxene usually forms one or few plate-like or poikilitic crystal(s) containing many smaller (up to 5mm) plagioclase euhedra (Plate 36H) i.e. an ophitic texture.

The light clumps are usually partially recrystallized, with some residual larger elongate crystals of plagioclase being present.

Several general observations have been made about these bands:

1) orthopyroxene-bearing clumps are usually coarser than clinopyroxene-bearing clumps

2) coarser euhedral plagioclase within the dark clumps are sometimes associated with larger clumps

3) in many instances clinopyroxene clump horizons immediately overlie orthopyroxene clump horizons.

Identical textures have been reported as "mottled" anorthosites from the Bushveld Complex and from anorthositic rocks in Labrador by Emslie (1970) and Phinney (1969). Rather similar textures have also been observed as clots or nodules in chromitites (Macdonald, 1967; Cameron, 1969; Mukherjee, 1969) and other rocks elsewhere. The textures are interpreted as heteradcumulates.

Although the primary texture is partially overprinted by recrystallization, it is interesting to note that cumulus plagioclase grain sizes appear to be approximately the same in both pyroxene and plagioclase clumps. This suggests that little postcumulus enlargement occurred in these rocks. Cameron (1969) reported enlargements of up to 300% in some Bushveld Complex rocks.

2. Primary Mineral Assemblage and Texture

Modal abundances vary depending on rock type; in the anorthosites up to about 95% plagioclase is present whereas in the other rock types between about 60 to 90% is present. The bulk of the rocks are leucocratic. About 10 to 30% clinopyroxene is present in many rocks, but primary orthopyroxene is rarely present in the A.Z. The leucotroctolites

contain up to about 20% olivine. Up to about 5 to 10% magnetite/ilmenite is commonly found in the A.Z. Minor quantities of hornblende and red-brown biotite are found in some rocks; primary granular spinel associated with opaques is found only in olivine-bearing units. Minor amounts of chalcopyrite and pyrrhotite are observed in some rocks (Plate 38B); sulphide phases appear more common than in the underlying Norite Zone. Apatite is a very rare and minor constituent.

Cumulus modes are shown in Fig. 13. Plagioclase is the dominant cumulus phase, but clinopyroxene and/or olivine are also present in appreciable amounts. Orthopyroxene is only found as a cumulus phase in the uppermost strata west of the main body (i.e. A314-447 to 450).

The rocks are generally coarse-grained; grain sizes vary from about 2 to 8mm. Primary rock textures are partially obscured by secondary annealing at grain boundaries, but excellent residual cumulate textures are observed in many cases. Planar lamination parallel to layering is well developed for plagioclase laths in these rocks. Textures vary from adcumulate to orthocumulate.

The troctolites and olivine gabbros have a characteristic texture. Large elongate olivine crystals commonly have irregular shapes because of interstitial overgrowths. These overgrowths frequently outline cumulus plagioclase laths (Plate 32A). Olivine is rarely intergrown with green spinel near grain boundaries (Plate 37A). Clinopyroxene and plagioclase are also elongate, and may be partially overgrown. Brown granular to massive hornblende is commonly found only in olivine-bearing rocks in the A.Z.; it either rims clinopyroxene (Plate 37E) or opaque

phases (Plate 37C). A greenish fibrous amphibole(?) is found associated with fibrous orthopyroxene rims on olivine in some rocks. In some cases plagioclase contains common pyroxene inclusions comparable to those in plagioclase in other rocks (see Chapter 9.4.3). Pyroxene and/or pyroxene/spinel symplectites are commonly observed between olivine and plagioclase (further descriptions in Chapter 9.3.2).

In the olivine-bearing gabbros, olivines tend to be small and rounded, or may be represented by a granular aggregate of pleochroic orthopyroxene and opaques (see olivine oxidation reaction in Chapter 9.3.4).

The anorthosites are adcumulates: minor amounts of pyroxene or opaques developed at plagioclase grain boundaries tend to outline the original cumulus plagioclase crystals (Plate 32C). The anorthosites are probably directly related to the heteradcumulate "clump" rocks described previously. Both consist solely of cumulus plagioclase; the present differences are related to the type of interstitial crystallization (compare Plates 32C and 32D).

Cumulus orthopyroxene in the noritic rocks is similar to pyroxene in the Norite Zone in that it contains inclusions of cumulus plagioclase. In one grain, exsolution lamellae of clinopyroxene were in optical continuity with a clinopyroxene rim surrounding the orthopyroxene (Plate 37D). It is thought that the rim clinopyroxene represents an epitaxial overgrowth on the orthopyroxene, thereby giving it the same optical orientation as the exsolution.

Biotite is usually found associated with and commonly rimming opaques in these rocks (cf. Chapter 3.2). It is also rarely observed intergrown

with pyroxene in interstices (Plate 37B). It is not commonly found in the same rocks as hornblende.

Spinel-iron oxide associations and textures are identical to those described in the N3 Subzone.

28001

The olivine - magnetite rock at the base of the Anorthosite Zone contains rounded cumulus olivine crystals with about 40% interstitial opaques. The opaques consist of magnetite, ilmenite and minor green spinel. These are sometimes intergrown with silicate phases (probably pyroxene) at olivine grain boundaries in the more restricted interstices (Plate 38A). Magnetite tends to be larger and more abundant in the larger interstices and may perhaps also be a cumulus phase.

6.4 Primary mineralogy of the Kalka layered sequence

The following brief descriptions are a summary of detailed observations made throughout the layered sequence. Details of individual characteristics such as exsolution features are given in Chapter 9.

1. Orthopyroxene

Orthopyroxene contains clinopyroxene exsolution lamellae in varying quantities throughout the entire layered sequence (usually Bushveld type; rarely Stillwater type in the Anorthosite Zone). Variations in lamellae abundance sometimes give rise to edge parallel zoning near grain boundaries in the Pyroxenite and lower Norite Zones (Plate 41G).

Rutile exsolution rods are found throughout the Pyroxenite Zone,

where they are rarely associated with minor spinel exsolution, and the N1 Subzone. Rutile exsolution is also observed in norites from the Olivine Gabbro Zone. Spinel is only observed as an independent exsolution body in the olivine websterites of the N1 Subzone.

Opaque exsolution plates are rarely noted in the N1 Subzone but are commonly observed in the N2 and N3 Subzones and the Anorthosite Zone. Both opaque and rutile exsolution are observed in rare orthopyroxenes from the upper N1 Subzone.

Plagioclase inclusions, sometimes associated with clinopyroxene (or olivine in olivine-bearing rocks), form two distinct types within orthopyroxene from most of the layered sequence (see Chapter 9.1.3). Both groups appear to be more common in the lower parts of the intrusion, with Type 1 being more abundant than Type 2 in the upper parts of Kalka.

2. Clinopyroxene

Clinopyroxene contains orthopyroxene exsolution lamellae in varying quantities throughout Kalka. Rutile exsolution is observed in parts of the Pyroxenite Zone and N1 Subzone, but is not a dominant feature. It is sometimes observed with rare spinel exsolution in the Pyroxenite Zone. Spinel exsolution is a major exsolution product in the olivine melagabbros of the O.G. Zone but is rarely observed in other rocks in this area. Opaque exsolution plates are found throughout the N2 and N3 Subzones and the Anorthosite Zone.

Plagioclase - orthopyroxene inclusions found in clinopyroxene in parts of the Pyroxenite Zone and N1 Subzone are described more fully in

Chapter 9.2.2. Simple and multiple twinning in the clinopyroxene are commonly observed.

3. Olivine

Olivine contains opaque exsolution bodies, especially at grain boundaries, in parts of the Olivine Gabbro and Anorthosite Zones. The exsolution appears to be more common in the latter.

4. Plagioclase

Antiperthite has been observed in plagioclase in the Pyroxenite, Olivine Gabbro and Norite Zones. It generally forms in an interstitial environment although cumulus antiperthites are rarely observed.

Magnetite exsolution is found throughout the layered sequence. It appears to give plagioclases a pinkish-grey colour in the N1 Subzone, especially. Plagioclase from olivine-rich rocks in the O.G. Zone contain no magnetite and are characteristically very white.

Pyroxene inclusions similar to those described in Chapter 9.4.3 are found in parts of the Anorthosite Zone. These inclusions are in some cases concentrated on simple twin planes in plagioclase. Both simple and multiple twins are observed in plagioclase in Kalka (Chapter 9.4.2).

5. Iron Oxides

Iron oxides are confined to the upper Norite Zone and the Anorthosite Zone.

Magnetite commonly contains spinel exsolution lamellae (Plates 38C, E,G) and in many cases is partially oxidized to martite around grain boundaries and along fractures (Plate 38H).

Ilmenite sometimes contains haematite and/or spinel exsolution lamellae (Plate 38F). Unusual bireflectance variations are rarely observed in ilmenite and probably represent twinning (Plate 38H).

CHAPTER 7

CYCLIC UNITS IN THE LAYERED SEQUENCES

Within many layered intrusions examples of repeated sequences of rock units showing similar trends in mineralogy and composition are observed (e.g. Wadsworth, 1961; Jackson, 1967, 1970; Irvine and Smith, 1967; Sorensen, 1969). These sequences are termed cyclic units. The complete units are not always present — sometimes they may be either debased or beheaded (Jackson, 1970).

Cyclic units are not as obvious or as well developed within the Kalka layered sequence as they are in some other bodies. However, a study of the various stratigraphic columns (Fig. 16) shows many instances of plagioclase enrichment cycles (e.g. pyroxenite → melanorite → mesonorite → leuconorite).

A small scale example of this type of cycle from the Johnson Horizon at Waralkulpa is shown in Plate 33B. An analysis of the relative thickness of the mafic layers and immediately overlying felsic layers reveals the presence of two broad groups of layer sets, X and Y (Fig. 18B). These groups correspond to two main cycles in the sequence, the X group occurring higher in the sequence (Fig. 18C). X group has a higher ratio of felsic to mafic rocks than Y group which reflects the overall fractionation trend toward plagioclase enrichment in the whole intrusion.

Indications of chemical fractionation for olivine and plagioclase within cycles are also found. In Fig. 13, suggested cyclic units in the Mt Kalka (No. 6) and upper part of the Walter Hill (No. 4) Sections have been recognised on the basis of cumulus pyroxene/olivine/plagioclase

modal variations, and olivine and plagioclase chemical trends (where available chemical analyses of pyroxenes support the suggested cyclic divisions).

Twenty one cyclic units have thus been established for the Kalka Intrusion at this stage although further detailed sampling may reveal more. The various methods of recognising these units are generally in agreement, although some problems still exist in the Olivine Gabbro Zone and in a few other areas. Units distinguished by one method (e.g. plagioclase composition) may not be confirmed by another method (e.g. relative proportions of cumulus phases). Furthermore, because of differential settling between co-crystallizing phases (see Chapter 10), it is difficult in some cases to interpret which cumulus phases belong to which cyclic unit. This is especially true for plagioclase relative to pyroxene/olivine.

Between the Pyroxenite Zone and the top of the Olivine Gabbro Zone (i.e. Cycles 1 to 14) the following generalised progressive sequence of cycles is found:

(1) opx $\longrightarrow$ opx + cpx

(2) opx $\longrightarrow$ opx + cpx $\longrightarrow$ opx + cpx + plag

(3) opx $\longrightarrow$ opx + cpx $\longrightarrow$ opx + cpx + plag $\longrightarrow$ cpx + ol + plag

(4) opx $\longrightarrow$ opx + cpx $\longrightarrow$ opx + cpx + plag $\longrightarrow$ cpx + ol + plag

($\longrightarrow$ ol + plag ?)

The upper part of the Norite Zone from Cycles 15 to 18 is not well understood but it appears that orthopyroxene may succeed olivine as a

cumulus phase in some cycles i.e. in reverse to the order in the earlier cycles.

Cycles 19 to 21 in the Anorthosite Zone reveal more definite examples of cyclic units i.e.

(5) ol + plag $\longrightarrow$ ol + cpx + plag $\longrightarrow$ cpx + plag $\longrightarrow$ plag

This form of cycle appears gradational from (4) above.

Because of its limited thickness only two cyclic units have been recognised from the Ewarara layered sequence. The two cycles, represented by the Olivine Bronzitite and Pyroxenite Zones, are considered beheaded and debased respectively*. The sharp physical and chemical break between the units testifies to this suggestion viz. disappearance of cumulus olivine, sharp decrease in magnesium content of orthopyroxene and in cumulus grain size.

Cumulus phase variations are:

Cycle 1 : ol + opx

Cycle 2 : opx $\longrightarrow$ opx + cpx

Moore (1970a) has reported four cyclic units from the nearby ultramafic Gosse Pile Intrusion. These units show the following progressive changes in cumulus mineralogy.

ol + opx $\longrightarrow$ opx $\longrightarrow$ opx + cpx $\longrightarrow$ opx + cpx + plag

It can therefore be seen that the Gosse Pile cycles support a connection between the Ewarara and Kalka cyclic units and allow the

---

* Alternatively only one cyclic unit which has been "de-middled" is represented. There is also some indication of a third cycle represented by A300-126 between Cycles 1 and 2 (Fig. 13).

preparation of an idealised master cycle of cumulus phases for bodies of this type viz.

ol + opx ⟶ opx ⟶ opx + cpx ⟶ opx + cpx + plag ⟶ cpx + ol + plag ⟶ ol + plag ⟶ ol + cpx + plag ⟶ cpx + plag ⟶ plag

Within these phase groupings gradational modal variations will probably occur preceding the formation of each new cumulus phase. The master cycle indicates the overall enrichment of plagioclase observed for the Kalka Intrusion. This trend can also be shown by thickness analysis of adjacent pyroxene-rich and plagioclase-rich small scale layers. The thickness ratio of felsic to mafic bands in central Kalka is about 0.5 to 2 whereas towards the top of Kalka it can be up to 20 to 25.

CHAPTER 8

GEOCHEMISTRY AND MINERALOGICAL VARIATIONS IN THE LAYERED SEQUENCES

The general geochemistry of Ewarara has previously been reported by Goode and Krieg (1965, 1967). The pyroxenes and olivines are particularly magnesium-rich although they exhibit minor iron-enrichment upwards in the sequence (Chapter 5). Total rock analyses of some of the cumulates also show their magnesian character; on an FMA diagram they plot in a similar position to the least fractionated rocks of South Mt Davies (compare Nesbitt and Kleeman, 1964, Fig. 2; Nesbitt et al., 1970, Fig. 9).

Rocks from the Kalka layered series have not been analysed for this thesis. In Appendix 7 the geochemical significance of such analyses, especially for cumulates, is discussed and it is considered that valid geochemical variations in igneous rocks are best obtained from individual minerals.

Studies of both mineral compositions and modes reveal an overall tendency for increased fractionation with height in the Kalka sequence. As shown in Chapter 7, the presence of cyclic units tends to obscure or reverse this trend in places.

The anorthite content of plagioclase and the forsterite content of olivine best demonstrate this trend towards increased fractionation with height (Fig. 13). Plagioclases in the lower half of the sequence are generally between An_{80} and An_{70} while those above the Olivine Gabbro Zone are usually between An_{70} and An_{60}. Olivines vary from Fo_{85-70} in the Olivine Gabbro Zone (Fo_{87} in the lower Norite Zone) to Fo_{75-60} in the

Anorthosite Zone. With corrections for differential settling (Appendix 7), $\Delta An/\Delta Fo$ ratios for co-crystallizing plagioclase and olivine remain constant at about 0.9 to 1.0 throughout the layered sequence (Fig. 40C). Similar ratios from limited data* are observed in the Blackstone and Bell Rock Intrusions but higher ratios of about 3.0 are obtained for South Mt Davies (Fig. 40C). It is interesting to note that the olivine - plagioclase curve for the Anorthosite Zone of Kalka is displaced from the curve for the Olivine Gabbro Zone (Fig. 40C) i.e. the O.G. Zone olivines are less fractionated relative to plagioclase. The curves of Bell Rock and Blackstone pairs are also not coincident although they have parallel slopes. Such features may be indicative of significant variations in melt compositions not related to fractionation (note: the O.G. Zone olivines and the A.Z. olivines in Kalka are both associated with major fresh injections of magma — Chapter 10).

Because of difficulties in mineral separation only a few cumulus pyroxenes have been analysed from Kalka. However, allowing for local variations in the cyclic units, both ortho- and clino-pyroxenes tend to become more iron-rich upwards in the sequence viz. orthopyroxene A314-70 is more magnesian than A314-153 and A314-157; clinopyroxene A314-418, from near the top of Kalka, is more iron-rich than pyroxenes lower in the sequence (Fig. 18A; Table 9). The most magnesian pyroxenes are similar to those from Ewarara and Gosse Pile (Fig. 18A) which supports the comparison between the bodies made in Chapter 7.

---

* Data from Nesbitt and Talbot (1966); olivine - plagioclase pairs not necessarily co-crystallizing phases.

It can be seen from Fig. 18A that although the Kalka cumulates become more fractionated with increased crystallization they remain clustered at the magnesian end of typical basaltic fractionation trends. The occurrence of rare Stillwater-type pyroxenes in the upper-most parts of Kalka (Chapters 6 and 9) suggest that the most iron-rich orthopyroxenes are hypersthenes (about En_{60-70}). Uranium determinations for various minerals (Table 11B) reveal a general increase in uranium for clino-pyroxene* which is consistent with fractionation (Kleeman, 1969).

The trends in mineral chemistry are also accompanied by modal variations. As well as the overall cumulus phase changes described in the cyclic units (domination of orthopyroxene in the lowest cumulates giving way to marked plagioclase enrichment; olivine forming as a cumulus phase in the upper parts of the body — Fig. 13), other modal variations are also observed.

Towards the top of the sequence, interstitial phases such as iron oxides, biotite, hornblende and sulphides occur and become increasingly common although they are generally present in accessory to minor amounts (Fig. 13). These features are considered to support the other evidence for increased fractionation towards the top of Kalka. The very rare occurrence of apatite in the uppermost parts of the sequence also indicates increased fractionation (Anderson and Greenland, 1969).

The most interesting feature of the mineral chemistry is probably the high Al_2O_3 contents of the pyroxenes. Both ortho- and clino-pyroxenes

---

* The only reversal, A251-177D, has a mineralogy consistent with a relatively low position in a cyclic unit compared with the other samples.

contain between 2 and 5% Al_2O_3 (Table 9). Similar contents were measured from Gosse Pile and South Mt Davies pyroxenes by Moore (1970a) and Miller (1966) respectively. Moore has also reported high chromium concentrations e.g. 0.3 - 1.0% for orthopyroxene, 0.4 - 1.1% for clinopyroxene (these ranges are supported by Miller (1969) for two pairs of Kalka pyroxenes). The high alumina contents are reflected in the structural formulae of the pyroxenes (Table 9). %Al in the Z position varies from 3 to 5.5% for orthopyroxene and from 5.5 to 7% for clinopyroxene, while %Al in the WXY positions reaches 5% in some orthopyroxenes and 3.5% in some clinopyroxenes. Such values are significantly higher than for normal igneous pyroxenes (cf. Atkins, 1969, p. 234).

Aluminous pyroxenes are considered to result from a variety of crystallization conditions. Howie (1965) has indicated that pyroxenes formed in a peraluminous environment could be expected to have high Al_2O_3 contents but the Giles magma does not appear to have been excessively aluminous. Le Bas (1962), Kochkin *et al.* (1967) and Bence *et al.* (1970) have also noted that the Al_2O_3 content of pyroxenes increases with increasing undersaturation with respect to SiO_2 of the melt. However, the tholeiitic nature of the Giles magma does not support such an origin for the pyroxenes under consideration.

Under high crystallization pressures abnormal quantities of aluminium are also considered able to enter the pyroxene lattice in octahedral co-ordination (Hess, 1952; Boyd and England, 1960; Green, 1963, 1964). This condition is the most likely cause of the Al_2O_3-rich Giles pyroxenes in view of the supporting evidence presented in Chapter

11. The high proportions of Al^{VI} in Kalka, Ewarara, South Mt Davies and Gosse Pile clinopyroxenes are more characteristic of high pressure assemblages than normal igneous rocks and support such an argument (Fig. 19A; Aoki and Kushiro, 1968).

The aluminous nature of the pyroxenes prohibits the effective use of optical methods for compositional determinations because of its effect on cell parameters (Howie, 1963; Winchell and Leake, 1965; Leake, 1968). Similarly limited measurements of Kalka pyroxenes suggest that X-ray determinative curves cannot be applied to these orthopyroxenes (e.g. Himmelberg and Jackson, 1967).

Partial analyses of several plagioclases from Kalka and some minor intrusions are presented in Table 10.

Partial analyses by Simkin and Smith (1970) for several olivines are given in Table 11A. The olivines contain negligible Ca which is typical of plutonic environments (Simkin and Smith, 1970). Manganese contents are appropriate to the forsterite content, and nickel values reported by Miller (1969) for some Kalka olivines are also consistent with the range in forsterite contents observed in Kalka.

Prior to the petrogenetic discussions of Chapter 12 it is important at this stage to deduce the nature of the magma which produced the Giles Complex.

There is little doubt that the primary melt was basaltic in character. Although tectonic remnants of some bodies are almost entirely ultramafic (e.g. Gosse Pile) the bulk composition of the total Complex is

gabbroic with plagioclase being the most common mineral (Nesbitt, 1966; Nesbitt and Talbot, 1966).

The chilled contact at Ewarara contains orthopyroxene phenocrysts and is contaminated but, like the chilled margin at South Mt Davies and Kalka, is doleritic in character (Chapter 5). The bulk composition* of the Davies chill is basaltic (Nesbitt, 1966).

Chemical data reported by Nesbitt and Talbot (1966) indicate that the Mt Davies magma had tholeiitic affinities. This is supported by the chemical characteristics of clinopyroxenes from Kalka and Ewarara (Figs. 19B,C,D) which generally plot in the tholeiitic fields. The alkaline tendencies in some cases may be related to the high pressure environment which results in unusually high Al_2O_3 values. Similar tholeiitic affinities were obtained by Miller (1966) and Moore (1970a) for South Mt Davies and Gosse Pile.

Because of the dominance of orthopyroxene as an early crystallizing phase, the Ewarara - Kalka magma may have been an olivine tholeiite (see Chapter 11).

It is considered that the magma was essentially dry. The only hydrous phases, hornblende and biotite, are found in minor quantities only towards the top of Kalka and at the base of Ewarara (Fig. 13) and would contribute negligible water to the overall bulk composition. Similar abundances for these minerals are observed throughout the

---

* Bulk compositions of chilled rocks are considered to give the original melt composition (with the reservations of Appendix 7 in mind).

Complex. Minor local developments of hornblende are found around parts of the Ewarara Intrusion (Chapter 5) but would be insignificant on an overall scale. Furthermore the bulk of the granulites are essentially dry (hornblende is only developed to any extent in the minor basic interbands — Chapter 2) and could not contribute significant water to the intrusions.

Contamination of the melt at both Ewarara and Kalka after intrusion is considered to have been caused by assimilation of acid granulites from the contacts and by stoping. The physical evidence for such events is generally limited to contact phenomena (Chapters 5,6). Recent strontium isotope measurements by C.M. Gray of the Australian National University reveal extremely large variations of $^{87}Sr/^{86}Sr$ in Ewarara and especially Kalka cumulates (Table 12A). Such large scale variable chemical "contamination" may be the result of several processes (C.M. Gray, pers. comm.):

(a) variable contamination by country rocks as $^{87}Sr/^{86}Sr$ ratios appear to generally decrease with increasing crystallization*.

(b) variable contamination by crustal rock during magma transit between source and chamber.

(c) variable $^{87}Sr/^{86}Sr$ ratios in magma source rocks allied with several intrusional pulses (these do occur — Chapter 10).

(d) dispersion by addition of radiogenic strontium since crystallization

---

* Measurements from some Gosse Pile rocks considered to be stratigraphically equivalent to the Norite Zone of Kalka are also consistent with this variation (Table 12A).

(normally in these rocks Rb/Sr ratios are very low and this mechanism is not likely).

Of these possibilities the physical evidence of contamination favours (a), although (b) may also be a contributory factor.

CHAPTER 9

MINERALOGICAL PROBLEMS

During the course of this study a number of unusual mineralogical problems arose which were considered to have important bearings on the overall petrological investigations. The features giving rise to these problems were observed in both the Giles Complex rocks and in the minor intrusions but, for convenience, were brought together in this one section.

9.1 Orthopyroxene

9.1.1 Exsolution

(1) Clinopyroxene

Most of the igneous orthopyroxenes observed in this study contain very fine clinopyroxene exsolution lamellae of the Bushveld type aligned in (100) (Plate 41A). Their recognition as Ca-rich clinopyroxenes has been made from optical and electron microprobe investigations (e.g. Plate 39C) confirming Boyd and Brown's (1967) results. Their composition had previously been a source of some dispute (see Hess, 1960, p.29).

In most examples irregular, coarse patches of clinopyroxene with surrounding zones poor in lamellae are scattered throughout the crystals (Plate 41A). These features are considered to have formed by coalescing of lamellae. In some rock types unusual coarse branching lamellae are found (Plate 41B) while in others the lamellae are concentrated in zones parallel to the crystal faces (Plate 41G). The lack of lamellae at grain boundaries in many cases is characteristic of exsolution bodies

in all minerals found in the area. Concentration of lamellae and patches sometimes also occurs at planes of bending or kinking (Plate 41A) and presumably results from migration of lamellae to zones of lower free energy. Kinking of orthopyroxenes also produces structures identical to those suggested by Brown (1967) to be "inverted pigeonites" (compare Plate 41C with Brown, 1967, Plate 1B; also see Plates 51A and 51C).

The exsolution is assumed to result from instability and removal of calcium from the lattice on cooling (Hess, 1952, 1960). Hess (1952, p. 181) has reported that a maximum of about 1.65% CaO can initially enter the lattice on crystallization from the melt. Some of the analyses in Table 9 contain significantly more calcium than 1.65%, but this may be due to analytical error and/or contamination by clinopyroxene.

In A314-449, a gabbro from near the top of Kalka, examples of exsolution lamellae of the Stillwater type were observed in hypersthene ($2V_x \simeq 60$) (Plates 41D,E; compare Brown, 1967, Plate 1C). These are the first examples of this type of exsolution recorded from the Giles Complex. One set of lamellae is assumed to have exsolved from an original pigeonite host which later inverted to hypersthene on cooling and continued to exsolve the second set of lime-rich pyroxene lamellae (Hess, 1960). The general lack of such bodies in the Giles Complex is probably related to its magnesian character.

(2) Spinel

Spinel exsolution has previously been reported from Ewarara orthopyroxenes by Goode and Krieg (1967), and has since also been found in

some of the associated minor intrusions and rarely in ultramafic parts of the Kalka layered sequence (Chapter 6).

It occurs as small green plates and rods generally about 5-10μ long (Plate 43A), and has been identified by electron probe examination and its optical properties (it grades to coarser green isotropic anhedra). Moore (1970a) has shown that similar bodies in Gosse Pile orthopyroxenes are of picotite composition. The plates and rods are elongate parallel to [001], or sometimes [100], within (010)*.

Within the Giles Complex intrusions spinel exsolution is found only in the basal parts of the sequences. This, together with the abundance of exsolution in some specimens, is presumed to indicate the magnesian and aluminous nature of the original pyroxene (one sample, A300-121, with rare spinel exsolution contains about 4% Al_2O_3 but other pyroxenes without exsolution contain between 2 and 5% - Table 9).

Similar properties are observed for spinel plates and rods in clinopyroxene (Chapter 9.2.1). Both examples are considered to form by exsolution processes as their physical properties are consistent with exsolution criteria developed in this study (p. 208).

It is suggested that cooling of aluminous pyroxenes above a certain critical high pressure and a critical Al_2O_3 (or R_2O_3) concentration (<5% for these pyroxenes) would result in the exsolution of the Al_2O_3 as spinel**. At lower pressures for the same Al_2O_3 concentrations (or

---

* All optical orientations for exsolution bodies measured by univeral stage.

** A similar mode of origin has also been proposed by Green and Ringwood (1967a, p. 183) for spinel exsolution in pyroxene.

vice versa) the small Al^{3+} ions would remain stable in the lattice and exsolution would not occur. This may explain why some other workers have reported higher Al_2O_3 contents but not spinel exsolution (e.g. Aoki and Kushiro, 1968; Sakhno et al., 1968), although perhaps the Mg/Fe ratios of the pyroxenes are also important.

An extensive survey of the literature has revealed several other reports of spinel exsolution in pyroxene (Table 13). The host rocks in all cases are basic or ultrabasic nodules or intrusive rocks, and usually contain other features indicative of high pressure crystallization (cf. Chapter 11).

(3) Rutile

Rutile exsolution in orthopyroxene has been observed in the lower half of the Kalka layered intrusion (Goode and Nesbitt, 1969; Chapter 6) and rarely in some minor intrusions (Plate 43B). It has been previously identified and described by Moore (1968) for Gosse Pile orthopyroxenes which have similar physical properties to those in the author's field area. Gray (1967) also observed the exsolution in Teizi orthopyroxenes.

Rutile occurs as rods in (010) of the orthopyroxene, elongate in three directions: (601), ($\bar{6}01$) and (001) (Moore, 1968). The physical properties of the rods indicate that they formed by exsolution rather than by inclusion (p. 208). The rutile rods are generally found in pyroxenes higher in the Kalka layered sequence than those containing spinel exsolution i.e. in presumably more fractionated pyroxenes with

lower Mg/Fe ratios.

Similar rutile bodies have been observed in clinopyroxene in this study (Chapter 9.2.1). In both cases they are considered to be indicative of high pressure environments as suggested by Moore (1968). Moore found that the Gosse Pile orthopyroxenes contained average TiO_2, a feature supported by this study (maximum 0.16% TiO_2 for orthopyroxenes, maximum 0.30% TiO_2 for clinopyroxenes - Table 9), and concluded that the exsolution resulted from the instability of titanium in the pyroxene lattice on cooling at high pressure.

The rare and confined occurrence of rutile exsolution in other areas to rocks containing high pressure features lends support to such an argument e.g. Dallwitz (1968), Starmer (1969) and Macgregor and Carter (1970).

(4) Opaques

Opaque exsolution in orthopyroxene is found in the upper parts of the Kalka Intrusion (Chapter 6) and in several of the minor intrusions.

The thin opaque plates, generally about 50 to 500μ long, are usually oriented in several directions e.g. in (100) elongate parallel to [010] and [001] (Plate 43C). Similar bodies are observed in clinopyroxene (Chapter 9.2.1); both occurrences are physically consistent with an exsolution origin (p. 208).

Mineragraphic investigations have revealed that both magnetite and ilmenite form the plates, but limited electron microprobe examinations

have found only magnetite. In both these cases the magnetite had significant chrome content (about 5 to 10% in orthopyroxene; about 1% in clinopyroxene — Plates 39J,K,L,B); little or no magnesium, aluminium, titanium or vanadium was observed in the plates.

A limited literature survey has revealed the relatively common occurrence of ilmenite as well as magnetite bodies in pyroxene (Table 14). Miller (1966), in a study of South Mt Davies pyroxenes, reported unusually high Ti contents of those pyroxenes containing opaque "inclusions" suggesting that ilmenite may have also been the exsolution phase in that case.

The occurrence of the opaque exsolution bodies in the most fractionated (iron-rich) parts of the Giles Complex intrusions* suggests that the exsolution results from instability of excess iron in the pyroxene on cooling. By analogy with rutile and spinel exsolution the effect of high pressure may be important. A limited literature survey has revealed the common occurrence of these bodies in pyroxenes from such environments (Table 14).

The general control of exsolution type by stratigraphic position in both the Kalka and Ewarara layered sequences suggest a chemical control on the type of body exsolved. With decreasing Mg/Fe ratio spinel exsolution gives way to rutile exsolution which gives way to opaque exsolution. Such a chemical zonation is to an extent exemplified in Plate 41F where opaque exsolution rims spinel exsolution in orthopyroxene from one of

---

* Opaque exsolution is also associated with the most fractionated interstitial crystallization in some picrite plugs (Chapter 3.2).

the picrite plugs. Insufficient data is at present available to define the pyroxene compositional limits for each type of exsolution.

(5) Discussion

Ringwood and Seabrook (1962, 1963), while investigating high pressure phase transformations in germanate pyroxenes, found that with increasing pressure and constant temperature pyroxene structures for $Mg(GeSi)O_3$ convert firstly to spinel and rutile structures then to ilmenite structures. In some other compounds (e.g. $CaMgGe_2O_6$) diopside structure converts to ilmenite and garnet structures at higher pressures.

Assuming that $\Delta P/\Delta T$ for the transformations are positive, then the transformations could also be theoretically produced by decreasing temperature at constant pressure.

It seems more than coincidental that both ortho- and clino-pyroxene in the Kalka - Ewarara area exsolve spinel, rutile, magnetite and ilmenite with decreasing temperature at a constant pressure* of approximately 10 kilobars (Chapter 11). Garnet exsolution in pyroxenes in other areas (e.g. Green, 1966; Saggerson, 1968; Peters, 1968; Kornprobst, 1969; Lovering and White, 1969; Irving and Green, 1970; Macgregor and Carter, 1970; Beeson and Jackson, 1970) probably occurred by similar processes although possibly at higher pressure (about 15 kilobars: Irving and Green, 1970).

---

* No evidence of vertical movements prior to exsolution (from structural and mineral reaction studies).

The exsolution is a lattice stabilization phenomenon and may be simply a preliminary expression of the complete transformation in the pure substance. Moore (1968) has suggested that the "foreign" elements would be the first to move from the pyroxene lattice to form the denser transformation products. The transformations of the pure pyroxene would take place at much higher pressures (Ringwood and Major, 1966).

In the case of rutile exsolution, TiO_2 is the equivalent of SiO_2 (stishovite) in the pure pyroxene transformation. Ti^{4+} has a much larger ionic radius than Si^{4+} (0.68Å v 0.41Å) and hence would tend to exsolve at much lower pressures. In similar fashion the exsolution of magnetite (or chromite) from olivine in some of the Kalka - Ewarara rocks (Chapter 9.4.1) may represent the preliminary expression of the olivine - spinel transition (Akimoto and Fugisawa, 1965).

9.1.2 Hourglass Zoning

Hourglass structures have been recorded in many varieties of minerals, notably augite and chloritoid (Johannsen, 1931). However, the author is unaware of any previous description of hourglass structure in orthopyroxene, excepting that of Goode and Krieg (1965, 1967) on the samples described below.

These orthopyroxenes occur as cumulus bronzite crystals in the lower olivine bronzitite layer at the base of the Ewarara Intrusion. They are also found in several of the younger transgressive picrite suite plugs nearby.

The hourglass structures which occur in the cumulus orthopyroxene are physically outlined by the massing of pale green spinel exsolution rods. They are massed in what is known as sector A and are rare in sector B (Plate 42). The light coloured sector B does contain some spinel needles which are arranged in symmetrical (in both upper and lower sectors) oscillatory zones parallel to the present crystal faces (Plate 42). Complementary and parallel zones in this sector are formed by massed clinopyroxene lamellae. The clinopyroxene exsolution is rarely observed in sector A, and thus forms a crude complementary hourglass structure. Clinopyroxene exsolution lamellae sometimes occur in overgrowths around the complete periphery of the hourglass grains. Both the light and dark sectors are in optical and physical continuity.

The 3-dimensional shape of the hourglass structure has been determined. The dark spinel-rich sector A has a prismatic "hopper" shape (Fig. 21A). Because of the inherent properties of thin sectioning, it is difficult to determine whether the two "hoppers" meet at a central point or not. Usual sections give structures as in Plates 42B,C,D but rarely structures as in Plate 42A are observed. The light sector B has a complementary shape to the "hoppers", merely filling them in and completing the normal orthopyroxene crystal morphology.

Closer examination of the hourglass structures shows that small (0.4mm) rounded olivine inclusions are found predominantly in sector A, and only occasionally in sector B. They are not necessarily confined to central portions of the crystal, and generally show no systematic crystallographic relationship to the pyroxene host. Olivine (1 - 4mm)

occurs as a cumulus phase in the same rocks, and the small olivine inclusions in the orthopyroxene are probably cumulus olivine crystals captured early in their growth cycles. Small spinel anhedra, although found in sector B, are more common in sector A. As no definite cumulus spinel has been observed in the intrusion, and as coalescing of spinel exsolution as a result of deformational strain effects is common in these rocks, their origin is most probably that of exsolution coalescement. The occasional presence of clinopyroxene patches in sector A, and the irregular boundaries between the two sectors in some cases, may be due to the same cause.

Rarely dual hourglass pyroxenes are observed (Figs. 20A,C). In these cases two hourglass crystals have been joined on either mutual (100) or (010) faces so that the grains have parallel c-axes. Growth appears to have continued after joining to form spinel-poor overgrowths. In one case the hourglass pattern in one crystal was almost obscured because of massed spinel exsolution in sector B as well as sector A. Preferential attachment of freely suspended like crystals (synneusis) has been described in porphyritic rocks by Vance and Gilreath (1967) and Vance (1969) while union of olivine grains during settling has been suggested by Brothers (1964) to explain features in Rhum cumulates. However, Cameron (1969) believes "chain structure" in chromite is a packing feature.

Rare hourglasses of a different nature have been observed in the Gosse Pile Intrusion (Moore, 1970a). Clinopyroxene exsolution is concentrated in sector A relative to sector B (Plate 41H). Spinel exsolution

is absent. Moore has only observed the hourglasses on (010) faces but a more detailed search may show that sector A has a "hopper" shape similar to the Ewarara examples. In the Kalka Intrusion oscillatory zones rich in clinopyroxene exsolution are found on all faces (i.e. in sectors A and B) but no hourglasses were observed (Plate 41G).

Origin of the zoning

It was concluded in Chapter 9.1.1 that spinel exsolves from an aluminous host as a result of cooling at high pressures. The clinopyroxene exsolution in sector B results from instability of Ca in the orthopyroxene lattice on cooling. It can therefore be seen that, prior to exsolution, sector A was rich in Al, and probably also Cr (spinel exsolution in orthopyroxene from Gosse Pile is rich in Cr – Moore, 1968), while sector B was apparently enriched in Ca relative to sector A (although some zones rich in Al and poorer in Ca are observed in sector B).

From the preceding descriptions and the deduced chemical variations within the crystals, it is apparent that an hypothesis involving some form of crystal growth provides the most satisfactory explanation for the hourglass structures (a review of crystal growth mechanisms is given in Appendix 3).

(1) Selective Adsorption Theory

It is well known that, because of different structural and electrostatic aspects of different faces of many crystals, it is possible to have preferential adsorption of particles on to certain faces during

growth (see Buckley, 1951). These particles may be incorporated into the lattice on the atomic scale by substitution or as Frenkel defects. At lower temperatures the crystal structure may become unstable causing exsolution of these "impurities".

In the case of the Ewarara examples it would appear that Al^{3+}, and to a lesser extent possibly also Cr^{3+}, have been preferentially adsorbed on to the (010), (100) and (110) faces during growth. Progressive growth results in the Al-rich area forming an hourglass structure (Fig. 21C). Later exsolution of these "impurities" as spinel would account for the observed massing of spinel rods in sector A. The occasional spinel-rich zones observed in sector B (parallel to the present crystal edges) could be the result of Al adsorption on all faces following an increase in Al concentration in the melt above a critical value (Fig. 21C(3)). (Note: Al and Ca are probably distributed throughout the crystal, but not in sufficient concentrations in some cases to be exsolved as spinel and clinopyroxene bodies).

When spinel exsolution is absent, clinopyroxene exsolution in the orthopyroxene is either preferentially arranged on the prismatic faces (e.g. Gosse Pile hourglasses) or is distributed evenly on all faces (e.g. oscillatory zoning in Kalka orthopyroxenes). Exsolution on all faces may result from excess Ca in the melt (above a critical value) being adsorbed on to all faces instead of only the prismatic ones (cf. behaviour of Al). However, in the Ewarara pyroxenes where spinel exsolution is present, the clinopyroxene is found almost exclusively on the pyramidal faces in an antipathetic relationship to the spinel (for discussion see later).

The reasons for the preferential adsorption of Al (and Ca in the Gosse Pile hourglasses) on to the prismatic faces are obscure. However, these faces contain the planes of closest oxygen packing which may be a significant factor. Gregg and Sing (1967) state that in an ionic lattice the anions tend to predominate relative to cations at the exterior. Hence over short distances the electrostatic attractions of the packed oxygen anions may be sufficient to attract the small, highly charged Al cations to the prismatic faces where they are admitted in both tetrahedral and octahedral sites. Similar forces may explain the preferential adsorption of Ca cations on the prismatic faces.

The apparent competition between Al and Ca in the Ewarara orthopyroxenes is difficult to explain as they are not competing for the same sites. Ca would enter the M_2 site whereas Al, being a small ion, would probably enter the M_1 site (little data on this is available, however e.g. Smith et al., 1969). The only explanation which would appear plausible at this stage is that the competition between the two is only apparent. It may be that the Ca was adsorbed over the whole growth surface but was not required to exsolve in sector A due to a stabilization of the lattice in this area because of the exsolution of spinel. This would overcome the otherwise anomalous observation that Ca is adsorbed preferentially on to the prismatic faces in the Gosse Pile hourglasses.

If the suggested variations in Al and Ca in the melts are correct, then they may represent a subtle chemical stratification in the magma chamber through which the crystals were settling during growth.

Detailed work on the oscillatory zoning throughout the accumulated crystal pile may allow these zones to be mapped for areal and temporal distribution.

Oblique or off-centre sections of the orthopyroxenes commonly give an hourglass in which the sectors are separated by slopes of varying gradients (Fig. 20). Usually up to four distinct slopes are present in any one crystal (Fig. 21B):

Slope 1: horizontal (i.e. perpendicular to c)

Slope 2: low gradient

Slope 3: usually steep gradient

Slope 4: usually low gradient

These slopes result from intersection of the various internal "hopper" faces, and depend on the relative growth rates of the prismatic and pyramidal faces i.e. the boundary faces between sectors A and B are crystallographically irrational. The change in orientation between Slopes 3 and 4 is sometimes repeated (e.g. Fig. 20L) and indicates a change in the boundary slope for one of the "hopper" faces.

Since faster crystal growth in the a direction relative to the c direction results in flatter slopes of the sector boundary interface relative to c (Fig. 21D), the generally sharp decrease in gradient between Slopes 3 and 4 is interpreted as indicating a sudden increase in the growth rates of the prismatic relative to the pyramidal faces. The resultant elongation in the a and b directions is unusual for orthopyroxenes, as these crystals are generally elongate in the c direction. Further changes in slope, sometimes observed, could indicate further

changes in relative growth rates of the prismatic and pyramidal faces. The reason for the change in relative growth rates is unknown. It is possibly due to a change in the chemical environment as Buckley (1951) and others have shown that impurities often cause changes of habit (see Appendix 3). In this case a change in Al concentration may be the cause. It has been noted in several (but not all) crystals that the change in slope is associated with spinel exsolution zones in sector B i.e. a proposed increase in Al concentration in the melt.

The preferential arrangement of the olivine inclusions on the prism faces (i.e. in sector A), if a statistically valid observation, is possibly caused by stronger attractive forces on these faces. Similar forces may have caused the aggregation of two hourglass grains on mutual (010) and (100) faces to form dual grains.

(2) Dendritic Growth Theory

It was first thought that the hourglass structures were produced by primary dendritic growth of an Al-rich hopper crystal (sector A) followed by a secondary fill-in growth stage (sector B). Such a mechanism is favoured by Strong (1969) to explain hourglass structures in augite phenocrysts in volcanics from the Comores Islands. He considers, however, that the hourglass skeleton was developed by impeded growth of some faces due to preferential adsorption of some unknown impurities on to these faces. This is in contrast to Preston's (1966) concept that augite hourglasses develop as a result of possible Ca - Fe ordering on the different faces.

The dendrite hypothesis is, however, no longer considered viable. The concept developed because of the early observation that olivine inclusions predominated in sector A suggesting that this section grew first. However, a great many difficulties are involved in using this growth mechanism to form the hourglasses. The major ones are summarised below:

(i) Dendritic growth is favoured by fast growth rates and static conditions neither of which could be expected in cumulate rocks showing many features of crystal settling during growth.

(ii) Very special growth conditions would be required: sector B has not been observed to undergrow the so-called hopper, and rarely to overgrow it; a radical and complete change in relative growth rates of faces would be required to grow A first and then sector B.

(iii) It would be unusual in a fast growth rate environment that cumulus hopper crystals would all grow to approximately the same size before fill-in occurred.

Conclusions

It is concluded that the Ewarara hourglass orthopyroxenes result from spinel exsolution following selective adsorption of Al on the prismatic faces during growth. The concentration of adsorbed particles must be above a certain level such that exsolution of spinel occurs, but below a critical value in the melt so that the particles are not adsorbed on to all faces.

A similar situation is envisaged for the Gosse Pile hourglass orthopyroxenes, except that in this case clinopyroxene exsolution followed Ca being preferentially adsorbed to the prismatic faces.

Hourglass pyroxenes of this type are considered to form only in unrestricted or cumulus igneous crystallization environments.

9.1.3 Plagioclase inclusions

Throughout most of the Pyroxenite, Norite and Olivine Gabbro Zones and part of the Anorthosite Zone of the Kalka Intrusion, cumulus pyroxene crystals, especially orthopyroxene, have been observed to contain plagioclase inclusions. These inclusions vary between two extremes:

Type 1: stubby, rounded lath-like crystals, either singly or in groups (Plate 43F; Figs. 22A,C); about 0.2 - 0.5mm long for individual crystals, about 1mm across for clumps; sometimes lightly clouded with magnetite; with simple twins; arranged parallel to crystal faces (Plate 43F).

Type 2: irregular shapes, sometimes bounded in part by orthopyroxene crystallographic faces (Plate 43D; Figs. 22D,E,F); often antiperthitic; close association of irregular clinopyroxene patches.

Between these two extremes lies a complete gradation. It can therefore be extremely difficult in the intermediate types to classify them as one of the two types e.g. Figure 22G shows Type 1 and Type 2 plagioclases with clinopyroxene as an irregular inclusion in orthopyroxene.

Nevertheless it is believed that two distinct forms of origin are involved.

The Type 1 plagioclases, because of their shape, parallelism to faces in some cases, simple twinning (Chapter 9.4) are interpreted as having grown in an unrestricted environment and incorporated on to growing cumulus orthopyroxene* faces as solid inclusions. Because of their relatively small size compared to cumulus plagioclase in the layered sequence it is assumed that inclusion took place at an early stage in the plagioclase growth cycle. The plagioclase cluster groups are interpreted as forming by synneusis prior to inclusion (cf. Fig. 10B). In some cases (e.g. Fig. 22C) the pyroxene is so crowded with plagioclase crystals and/or clusters that it takes on a pseudo-dendritic appearance. In these cases it is likely that the whole association is a synneusis one between several orthopyroxene crystals as well as the plagioclases. The association of unlike crystal groups is unusual (Vance, 1969). Synneusis orthopyroxene groups have also been observed in some of the picritic plugs (Chapter 3.2). In some of these cases (e.g. Fig. 22B) plagioclase, clinopyroxene and biotite inclusions are found in specific zones throughout optically continuous crystals. Opaque exsolution, closely associated with interstices elsewhere in these rocks and representing iron-enrichment in the last formed orthopyroxene, is also found associated with these zones in the crystal. The "single"

---

* The orthopyroxene is not believed to have grown either as a poikilitic interstitial crystal or in the solid state from smaller cumulus crystals. The straight grain boundaries, edge parallel zoning. and its abundance in some rocks would not satisfy such models.

orthopyroxene crystals are therefore interpreted as synneusis aggregates in which trapped interstitial liquid crystallized after settling.

The Type 2 plagioclases because of their morphology, antiperthitic nature (Chapter 9.4.1) and their association with clinopyroxene are interpreted as having crystallized from melt (basaltic composition) inclusions within the orthopyroxene*. These liquid inclusions could have been derived in the same way as described immediately above i.e. interstitial to synneusis orthopyroxene groups.

Liquid could still be trapped if Type 1 plagioclases formed part of the synneusis groupings. This could explain the gradation between the Type 1 and Type 2 plagioclase inclusions. Trapping of liquid by orthopyroxene overgrowth during interstitial crystallization may explain some but not all of the Type 2 inclusions. Equivalent liquid inclusions in clinopyroxene are described in Chapter 9.2.2.

The association of clinopyroxene may in part be due to exsolution coalescement (a feature commonly observed in these rocks) and in part due to primary clinopyroxene inclusions, but in the bulk of cases these explanations do not hold. Volume relations as well as the fact that the clinopyroxene may exsolve other phases such as rutile (a feature never observed in normal clinopyroxene exsolution) do not support an exsolution origin, while clinopyroxene morphologies mitigate against an inclusion origin.

---

* Any orthopyroxene crystallizing from this melt would precipitate on the host orthopyroxene and hence be physically undetectable.

Similarly volume relations, antiperthitic exsolution, and morphologies would not support an exsolution origin for the Type 2 plagioclase inclusions. Philpotts (1966) suggested that some features of plagioclase plates in clinopyroxene favoured exsolution but concluded that overall the properties were more in accordance with eutectic crystallization of the two phases.

Plate 43E shows an example from the Hinckley Intrusion in which an orthopyroxene crystal contains sharp, non-rounded plagioclase laths (Type 1) and diffuse plagioclase inclusions with boundary zones of globular pyroxene - plagioclase intergrowths (Type 2). These intergrowths are very similar to eutectic intergrowths developed in interstices in many other rocks in the area (see Chapter 9.4.3).

In conclusion, then, the plagioclase inclusions in orthopyroxene are interpreted as forming by two distinct mechanisms: (1) by inclusion as solid crystals at a cumulus stage and (2) by crystallization of trapped liquid. The occurrence of the Type 1 inclusions in orthopyroxene in the Pyroxenite Zone has important implications since it indicates that plagioclase was crystallizing as a cumulus phase throughout the entire Kalka layered sequence (except in parts of the Scarface Silcrete Zone). Further, since plagioclase was not accumulating with orthopyroxene and clinopyroxene in the basal Pyroxenite Zone, the melt density at that time must have been greater than about 2.72. The settling of plagioclase in the Norite Zone indicates a decrease in melt density with differentiation.

It is therefore pertinent to consider what happened to the floating or rising plagioclase. The absence of a thick, unique anorthositic layer immediately above the Pyroxenite Zone indicates that the accumulated floating plagioclase had become otherwise fixed or removed from the overlying melt before the critical density was reached. The possibility that the plagioclase became fixed as a cumulate phase at the roof of the body cannot be directly tested since this part of the sequence is missing. However, no anorthosite accumulations are observed immediately underneath the granulite slivers. It is more likely that as the small plagioclase crystals floated upwards into overlying undersaturated melt they were resorbed; the rounded corners of most of the Type 1 inclusions could represent the initial stages of this process (however, rounded corners are also characteristic of plagioclase when it was a settling phase in the later layered sequence). The resorption of plagioclase would cause complications in the geochemical development of the intrusion: the formation of a Ca, Al, Si-rich layer would occur above the crystallization zone at the base of the body.

9.1.4 Epitaxial relations between pyroxenes

In some members of the Type B dolerite dyke suite at Ewarara, and in other rock types, oriented overgrowths of clinopyroxene on orthopyroxene and vice versa are observed (Plate 43H). Each phase usually exsolves the other pyroxene as well, and spinel exsolution is preferentially observed in the orthopyroxene.

Overgrowth orientations are such that (100) planes, b- and c-axes of both host and overgrowth coincide. Reversals of overgrowth-host

layers may be observed, giving rise to a repetitive zoning. In many cases orthopyroxene forms the initial host material, overgrowths of clinopyroxene occurring on the (110) faces. The faster rate of growth on these faces, however, leads to the progressive prominence of the (100) and (010) faces. In this respect the epitaxial relations are slightly different to those described by Tarney (1969) who found the initial nucleation of the overgrowth phase to occur on the (100) face of the host, and who did not find evidence of repeated epitaxy in the one crystal.

9.2 Clinopyroxene

9.2.1 Exsolution

Many igneous clinopyroxenes observed in this study contain lamellar structures similar in appearance to polysynthetic twinning (Plate 47D) although in some cases they are more irregular (Plate 43G). Electron microprobe (Plates 39A,B) and optical examinations of some of these bodies allow their identification as orthopyroxene. The lamellae are found in (100) of the host lime-rich pyroxenes, and are assumed to represent exsolution of orthopyroxene from an original augitic pyroxene (Hess, 1960).

Spinel exsolution in clinopyroxene was originally described in the Ewarara Intrusion by Goode and Krieg (1967). It has since also been observed in the Kalka layered intrusion (especially in olivine mela-gabbros from the Olivine Gabbro Zone) and in some of the minor intrusions.

It occurs as small green plates and rods in (010), elongate either parallel or perpendicular to [001] (Plate 44A). The plates, generally about 20 to 200μ long, have been identified by optical and electron microprobe examination. Turner (1967) has reported that the plates in Kalka were of picotite composition, a feature verified in this investigation (Plates 39D,E). Within any one rock specimen spinel is commonly, more plentiful in clinopyroxene than orthopyroxene. One clinopyroxene, A314-411, containing spinel exsolution, was more aluminous than other pyroxenes without the exsolution (Table 9).

The origin of the exsolution is discussed in Chapter 9.1.1. It is interesting to note that in the garnet pyroxenite minor intrusion (Chapter 3.10) spinel plates in clinopyroxene contain minute oriented rods and blebs of magnetite(?) (Plate 44A). This demonstrates an unusual occurrence of two stage exsolution.

Rutile exsolution in clinopyroxene was first reported by Goode and Nesbitt (1969) from rocks in the lower and central parts of the Kalka Intrusion (Chapter 6). Starmer (1969) and Macgregor and Carter (1970) have since noted similar bodies in clinopyroxene from other areas.

The small rutile rods, arranged in the characteristic tri-orientation in (010) (one direction approximately perpendicular to [001]), are only sparsely developed both in the rocks as a whole and in any single grain (Plate 44B). The rutile was identified by optical and electron microprobe examination (Plate 39F) and is considered to result from exsolution processes (Chapter 9.1.1).

Opaque exsolution in clinopyroxene is observed in the upper parts of the Kalka Intrusion (Chapter 6) and in several of the minor intrusions. The opaque plates and rods are usually about 20 to 200μ long. They are oriented in several different directions (Plate 44C) e.g. parallel to [100] and [001] in (010), and parallel to [010] in (100). Further descriptions and discussion on their exsolution origin are given in Chapter 9.1.1.

9.2.2 Plagioclase inclusions and intergrowths

At the boundary of clinopyroxenes in undeformed rocks from the Morgan Range and Hinckley Intrusions (thin sections courtesy R.W. Nesbitt) delicate intergrowth structures between orthopyroxene, clinopyroxene and plagioclase were observed. Rectangular orthopyroxene and clinopyroxene crystals (opx as epitaxial overgrowths, cpx optically continuous with the host) project into the plagioclase in a castellate texture. Orthopyroxene also penetrates the clinopyroxene host. The intergrowths are in some cases associated with extinction zoning in the plagioclase (Plates 47A,B) and preferentially occur in interstices. They are interpreted as representing eutectic crystallization of the three phases late in the crystallization of the interstitial liquid.

Similar structures have been observed at clinopyroxene/plagioclase grain boundaries both within and at the edge of cumulus clinopyroxene crystals in Kalka (Plates 47C,D). The castellate textures developed internally in the clinopyroxene are interpreted as indicating the former presence of liquid or partially liquid inclusions* (cf. Chapter

* Some of these plagioclase inclusions, have a rounded lath-like shape similar to the Type 1 inclusions in orthopyroxene. Castellate textures and opx rims indicate at least partial liquid inclusion, however.

9.1.3).

Castellate textures are usually not well preserved in the more deformed and recrystallized parts of the Kalka sequence. This is presumably because of their location at grain boundaries i.e. areas where strain would be most concentrated.

The castellate projections are best developed on the maximum growth rate faces (i.e. the [001] direction). The orthopyroxene projections are sometimes continuous with orthopyroxene exsolution lamellae, suggesting that they may provide a nucleation site for exsolution.

The mechanism of liquid inclusion is unknown but it may be a result of synneusis groupings or post-cumulus overgrowth.

9.3 Olivine

9.3.1 Opaque exsolution

Opaque plates are sometimes observed in the more iron-rich olivines from the Kalka Intrusion and from some of the minor intrusions. These plates are elongate parallel to [010] or [001] in (100) of the olivine (Plate 37F).

Electron microprobe examination of one example revealed that the plates were chrome-bearing magnetites (Plates 40K,L). Turner (1967) has also reported chromite plates from olivine in this area.

The plates are physically typical of exsolution bodies (p. 208) and are considered to result from exsolution of excess iron (and chromium) from the olivine lattice on cooling. Whether the iron and perhaps the

chromium were originally incorporated in the olivine lattice as Fe^{3+} and Cr^{3+} or whether they were formed by oxidation of bivalent ions in the lattice is unknown.

9.3.2 Coronas between olivine and plagioclase

One of the most common features in olivine-bearing rocks of all suites in the Kalka - Ewarara area is the presence of coronas or rims on olivine. These coronas vary in type and composition and provide a most complex and difficult problem.

The most prevalent coronas around olivine are those in contact with plagioclase, which were originally described by Goode and Krieg (1967). In the best developed coronas of this type a double rim of orthopyroxene* (inner) and clinopyroxene/spinel* (outer) is observed (Plate 37H). These rims are developed only when olivine is in contact with plagioclase and never between olivine and other primary phases whether these are cumulus or interstitial in origin. The inner rim tends to be scalloped towards the olivine and the outer rim tends to fan into the plagioclase. This results in preservation of the original olivine - plagioclase boundary between the rims, enabling the original textural relationship to be observed.

The inner rim is usually continuous, of relatively constant thickness (about 0.02 to 0.4mm), and composed of fibrous plates of orthopyroxene aligned perpendicular to the olivine. These fibres are usually elongate parallel to [001].

---

* Identified by optical and electron microprobe examination.

The outer rim is more discontinuous and of variable thickness. It consists of a symplectic intergrowth between fibrous clinopyroxene and wormy green spinel. The "worms" in the symplectite tend to fan into the plagioclase. In some cases spinel worms tend to grade into larger anhedral spinels indicative of coalescing.

In coronas of this type in the Kalka Intrusion the orthopyroxene rim is commonly granular* or platy granular rather than fibrous, and markedly pleochroic. In rare instances a gradational sequence from fibrous to granular rims around olivine perimeters is observed. It appears as though the granular rims may form from an initial fibrous aggregate by thermal annealing processes**.

The textures observed are consistent with solid state reaction between olivine and plagioclase and lead to the following proposed reaction:

Olivine + Ca-rich plagioclase $\longrightarrow$ orthopyroxene + clinopyroxene + spinel + Ca-poor plagioclase.

---

* Rim terminologies have been defined as follows:

(a) fibrous: rim consists of fibrous crystals, commonly oriented perpendicular to the interface

(b) granular: rim consists of equidimensional granular aggregates. Platy granular rims contain granular aggregates elongate parallel to the interface

(c) massive: rim retains optical continuity over large lateral distances (compared to rim thickness) in contact with varying crystallographic orientations of host.

** The replacement of a fibrous aggregate by coarse-grained granular phases would result in a decrease in free energy associated with grain boundaries and is thus a thermodynamically favoured process.

The reaction essentially involves the breakdown of olivine to orthopyroxene, and the anorthite component of plagioclase to clinopyroxene and spinel. Redistribution of certain elements such as Mg, Fe into the outer rim and Si into the inner rim are also required. Electron microprobe studies also indicate enrichment of Ca in the clinopyroxene/spinel rim relative to plagioclase and dilution of both Mg and Fe in both rims relative to olivine (Plates 39G,H,I). Both pyroxenes contain some Al. Mg/Fe ratios remain approximately constant in the pyroxenes and the olivine. Small increases in Mg/Fe ratios from olivine to the coronas were obtained by Murthy (1958) and Mason (1967) on related coronas in India and Norway, whereas Griffin and Heier (1969) measured slight decreases in the ratio from olivine to orthopyroxene.

The preferential removal of Ca relative to Na in plagioclase is not normally recognised. However, in some examples where olivine is much more abundant than plagioclase or coronas are very thick, abnormally low anorthite contents of plagioclase have been measured (about An_{30}). Sodium enrichment of plagioclase has also been observed by Griffin and Heier (1969).

A general compositional control on the development of the double coronas has been recorded* (Fig. 24A). Spinel/pyroxene symplectites are found only on the less magnesian olivines with a possible enlargement of the coronas field for more albitic plagioclases.

---

* It should be remembered, however, that these data were collected from various stratigraphic positions and therefore physical conditions (e.g. pressure, water content) may vary from sample to sample although examination of the results reveals no consistent deviations.

The incomplete nature of the reaction in most cases suggests an armouring effect by the rims such that solid state diffusion of the essential ions through the pyroxene lattices was prohibited. For this particular reaction under any given conditions there will be a particular temperature below which ionic diffusion for at least one of the essential elements through the pyroxene lattices will be insignificant. The reaction will then cease leaving the relic olivine and plagioclase in a metastable state. As this reaction has a positive $\Delta P/\Delta T$, this diffusional cut-off temperature, termed T_{dc}, will also have a slight positive $\Delta P/\Delta T$*.

The general limitations of the rims to a thickness of much less than 0.5mm suggest that diffusion processes through the lattices were difficult although the time available for reaction may have been important. This is probably in part related tc the general anhydrous nature of the rocks since little water was available to help in transport. Even in more hydrous assemblages diffusion processes appear to be limited. Blackburn (1968) has noted that the attainment of chemical equilibrium in some Grenville gneisses was limited to only a few cubic centimetres. Jensen (1965) and Mueller (1967) have also suggested the limited lattice mobility of ions such as Ca, Mg and Fe to a maximum distance of a few centimetres.

In some finer grained rocks reaction rims have been observed between olivine phenocrysts and primary pyroxene as well as plagioclase. It

---

* The higher the pressure, the higher the temperature of reaction. This will mean that complete armouring will occur at higher temperatures than for reactions at lower pressures (even allowing for increased particle mobility at higher temperatures for the higher pressure reaction).

therefore appears that the protective encasement of olivine by primary pyroxene is only effective when the length of the protected boundary is greater than the maximum distance of diffusion along the boundary by the relevant ions.

Initial nucleation of the coronal phases would have occurred along the original olivine - plagioclase boundary. For orthopyroxene, forming essentially from olivine, growth competition between nuclei in such a semi-restricted environment would mean that the fastest growing nuclei would be favoured to survive (Correns, 1969, p. 165). This would explain why the orthopyroxene fibres are aligned with [001] perpendicular to the boundary regardless of the olivine orientation, as this is its fastest growth direction. The scalloped nature of the olivine - orthopyroxene boundary probably results from some areas growing faster or for longer periods than others. The granular nature of the Kalka rims are possibly favoured by slower cooling in such a large intrusion which would allow a more ordered growth or alternatively more time at high temperatures for grain boundary adjustment of pre-existing fibrous rims.

The clinopyroxene/spinel rims are much less continuous indicating that less nuclei were developed along the interface. This would result in less lateral competition and hence a fanning of the wormy intergrowths away from the interface.

Variations on the above coronal relationships are quite common and intimately associated with the described coronas. In some of the rocks of the picritic suite, double coronas of fibrous orthopyroxene and symplectic brown hornblende/spinel are observed. These rims are found

in the same rocks as the orthopyroxene - clinopyroxene/spinel coronas and apparently are their hydrous equivalents.

In the Kalka Intrusion both clinopyroxene/spinel and orthopyroxene/spinel* symplectites are associated with granular orthopyroxene aggregates or rims on olivine (Fig. 23C). In rare examples the symplectites fan into the olivine rather than the plagioclase. The symplectites maintain a constant association with olivine and only occur in olivine-bearing rocks. However, in some cases the association is not direct e.g. pyroxene/spinel symplectites are occasionally found on primary pyroxenes (Plate 37G). Such features make generalised comments on the textures difficult.

In some cases the pre-existence of olivine can only be recognised from the presence of granular orthopyroxene and symplectite. Normally, however, some relic olivine is preserved.

The most common variation, however, is the development of a single granular to platy granular orthopyroxene rim between olivine and plagioclase i.e. the symplectite rim is completely absent (Fig. 23D). This raises the question as to whether the clinopyroxene/spinel symplectite is developed as an independent reaction to the olivine $\longrightarrow$ orthopyroxene transition. The consistent association of the two rims elsewhere, however, does not support this. It may be that kinetic factors associated with nucleation are important in the apparent independent development of the rims.

---

* Mooro (1970a) has also observed similar intergrowths near olivine at Gosse Pile.

On the other hand there is evidence of other types of orthopyroxene rims on olivine. In some rocks orthopyroxene surrounds olivine such that the original olivine euhedral shape is not destroyed or replaced in any way. In these cases the rim is of the massive type, and the orthopyroxene may contain exsolution lamellae of clinopyroxene (a feature never observed in symplectite associations) i.e. they are distinct from the single granular rims described above. These massive rims are interpreted as non-reaction textures and are related in development to poikilitic textures.

Fibrous orthopyroxene rims replacing olivine are described in Chapter 9.3.3. In these examples the fibrous rims are developed in contact with all phases (not only plagioclase) and are considered to represent olivine-liquid disequilibria. They are therefore also distinct from the single granular orthopyroxene rims in Kalka.

In Figs. 23A,B and E, thick massive to platy granular orthopyroxene surrounds both olivine and clinopyroxene cumulus grains*. In areas where olivine and plagioclase are not separated by this orthopyroxene, narrow fibrous to platy granular orthopyroxene rims are observed (see also Fig. 23D). These may be partially accompanied by clinopyroxene(?) rims and/or fibrous green amphibole. Similar textures are observed in other rocks in the upper parts of the Kalka Intrusion. In some cases, clinopyroxene/spinel symplectites are associated with the fibrous orthopyroxene and amphibole. It therefore appears that the single

---

* The orthopyroxene is commonly in epitaxial relationship with the clinopyroxene.

thick rims of orthopyroxene in at least some cases crystallized from the interstitial liquid, possibly at the expense of or in competition with earlier formed phases. The thin fibrous rims appear to be equivalents of the solid state double coronas. In some samples the fibrous rims only occur between olivine and plagioclase inclusions, whereas the massive rims are present on the outside parts of the olivine i.e. those parts which were in contact with the interstitial liquid (Fig. 23D). Therefore in some textures it appears as though the single granular orthopyroxene rims are not related to the symplectite-bearing double coronas.

There is also evidence that pyroxene/spinel symplectites develop in different ways. In rare cases intergrowths of spinel with primary olivine (Plate 37A) or pyroxene have been observed, and are interpreted as resulting from eutectic crystallization from the original melt (spinel is a primary interstitial phase in the upper parts of the Kalka sequence and in some of the minor intrusions). In other instances oxidation of primary olivine has also lead to the development of pyroxene/spinel intergrowths (Chapter 9.3.4). However, in these cases various criteria can be developed to distinguish them from those produced by the olivine - plagioclase reaction.

In conclusion it is considered that there is good textural evidence for the recognition of various types of coronas on olivine, but that their convergent properties makes it difficult in some cases to distinguish them.

Coronas between olivine and plagioclase similar to the double

coronas described here have been widely reported in the literature (Table 15). These have been grouped according to the presence of clinopyroxene/spinel or amphibole/spinel symplectites in the outer corona. Some examples of possibly related coronas without spinel are also listed.

A common property of the coronas is that they are all found in igneous rocks from high grade metamorphic terrains (or rarely as upper mantle(?) inclusions in basalt). These observations are in accord with experimentally determined conditions for similar reactions. The reaction curves of Kushiro and Yoder (1966) for pure end members anorthite and forsterite are plotted on Fig. 29C. These are at significantly lower pressures than reaction points determined by Green and Ringwood (1967a) for anhydrous olivine tholeiite and alkali olivine basalt compositions. The data of Green and Ringwood is probably more applicable to the natural coronas because of a closer similarity in composition. Ito and Kennedy (1968) have also noted experimental evidence for similar reactions in picrite and olivine-rich tholeiite compositions at higher pressures i.e. approximately 13kb at 1100 to 1200°C. Bultitude and Green (1970) have produced clinopyroxene - spinel from olivine and plagioclase at pressures of 9 to 13.5kb at 1100°C for olivine nephelinite compositions. Yoder and Tilley (1962, p. 493) have also suggested the presence of this reaction at high pressures.

Using the $\Delta P/\Delta T$ for the reaction from Kushiro and Yoder's data, it would therefore seem reasonable to suggest reaction pressures above 8 kilobars for temperatures greater than 800°C allowing for compositional

variations. It should be realised, however, that O'Hara and Biggar (1969) have demonstrated the stability of diopside - spinel assemblages at atmospheric pressures at high temperatures for original anorthite - forsterite-bearing compositions.

The production of the observed natural coronas could therefore be produced by several reaction paths e.g. by lowering of temperature (Fig. 29D) or by increase of pressure. Since the coronas are all found in igneous rocks it would seem reasonable to assume that the simplest method of producing them would be during the cooling of the intrusions at constant pressure (e.g. Goode and Krieg, 1967; Mason, 1967).

It should be noted that the reaction curves would be displaced to lower temperatures and/or higher pressures for more magnesian compositions (by comparison with Green and Ringwood's, 1967b, data). This could explain the lack of reaction between relatively magnesian olivine and plagioclase reported in the present study (i.e. reaction temperatures are below T_{dc}, the critical diffusion cut-off temperature).

Furthermore for any one composition the reaction would occur at lower temperatures for lower pressures. This could explain the lack of reaction coronas in the more fractionated (i.e. higher level) parts of the Giles Complex (e.g. Nesbitt et al., 1970) as well as the spasmodic development of coronas in the upper parts of the Kalka Intrusion* (Fig. 29D). It should be realised, however, that since the higher level olivines are in general less magnesian there will be an opposing tendency

---

* A load pressure differential of 1.5 kilobars would have existed across the Kalka layered sequence prior to folding.

for them to react at higher temperatures.

The olivine - plagioclase reaction is typical of the transition from low to intermediate pressure granulite (Green and Ringwood, 1967b). The presence of amphibole rather than clinopyroxene in some coronas is considered to be the equivalent hydrous reaction. Some of the amphibole-bearing coronas described in the literature may, however, be more representative of the upper amphibolite facies than the granulite facies. In these cases perhaps the nature and colour of the amphibole may be different from the higher grade types (cf. Binns, 1964).

In some of the coronas reported elsewhere garnet is also present (e.g. Shand, 1945; Herz, 1951; Gjelsvik, 1952; Murthy, 1958; Starmer, 1969; Griffin and Heier, 1969; Glaveris, 1970). The production of garnet is probably the result of a later reaction between the coronal products (e.g. opx + cpx + spin $\longrightarrow$ garnet) as suggested by Griffin and Heier (1969). This would result from further cooling (Fig. 29D) or pressure increases (experimental data for this reaction is shown in Fig. 29A, and discussed in Chapter 3.10).

Kuno and Aoki (1970) have described a coronal sequence of orthopyroxene/clinopyroxene/spinel symplectite (inner) and olivine/plagioclase (outer) around garnet in a lherzolite nodule. Such a sequence would result from decreasing pressure, possibly during nodule transport towards the surface.

9.3.3 Olivine-liquid reactions

Fibrous orthopyroxene rims are commonly observed on olivine in Type C and D dolerite dykes at Kalka. The rims are about 0.05mm wide, of uniform thickness, and maintain straight edges. However, in some cases the olivine-rim boundary is scalloped (convex towards the olivine) or irregular while the outer boundary pseudomorphs the primary olivine crystal. The pyroxene fibres are elongate parallel to [001] and arranged perpendicular to the grain boundaries.

In the Type C dykes the rims only occur on some edges and are not associated with any particular phase. In the Type D dykes the rims usually occur between olivine phenocrysts and matrix but may or may not be present between clumped intergrown olivine phenocrysts. They are also found on olivine phenocrysts which have been included in plagioclase phenocrysts (Plate 44E).

The rim morphologies are consistent with solid state replacement of olivine by orthopyroxene (cf. Chapter 9.3.2), and the mineral associations are interpreted as demonstrating that the reaction occurred in response to olivine-liquid disequilibrium i.e.

olivine + liquid $\longrightarrow$ orthopyroxene.

In the case of the Type C dykes the reaction developed late in the crystallization cycle while in the Type D dolerites it occurred prior to groundmass crystallization, and in some cases before olivine aggregation or growth of plagioclase phenocrysts.

Fibrous orthopyroxene rims are also observed on olivine in some

members of the layered sequence in Kalka. In some cases these rims are separated from plagioclase by biotite (Plate 44F). The biotite appears to have a normal late stage interstitial origin as it is often found between cumulus phases eutectically(?) intergrown with the major silicate phases (e.g. Plate 37B). The rims are therefore distinct from those formed by olivine - plagioclase solid state reactions and are considered to represent olivine-liquid reactions prior to the crystallization of the biotite.

There have been previous suggestions that olivine-liquid reactions to give orthopyroxene are indicative of relatively low pressures of less than 5 kilobars (e.g. Boyd et al., 1964; Weedon, 1965; Nesbitt, 1966) but these have been criticised by O'Hara and Stewart (1966) (see Chapter 11). However, their occurrence in the Kalka Intrusion and in associated rocks indicates higher reaction pressures of about 8 to 10 kilobars in these cases (Chapter 11). It is considered that reactions between olivine and liquid to give orthopyroxene probably result from chemical disequilibria brought about by fractionation and are not necessarily indicative of low pressures.

9.3.4 Oxidation of olivine

In members of the transgressive picrite suite at Ewarara, primary spinel inclusions in olivine are surrounded by thin (0.01 to 0.2mm) rims of fibrous to granular orthopyroxene. Small quantities of vermicular to granular dark green spinel are commonly intergrown with the orthopyroxene (Plates 44H, 40G-J). The spinel core is largest when associated

with the thickest rims, suggesting that the primary spinel has grown by addition of reaction product spinel. Both spinel types are of similar picotite composition (Table 58). Spinel inclusions in other phases are not rimmed. Olivine compositions vary from Fo_{75} to Fo_{84}.

In more differentiated members of the transgressive picrite suite at Ewarara and in parts of the Anorthosite Zone in the Kalka Intrusion, olivine has partially or completely altered to granular orthopyroxene-vermicular opaque aggregates (Plate 44G). Primary spinel inclusions are absent. Olivine compositions are more fayalitic than Fo_{75} in the picrite suite and in Kalka, aggregates were observed in olivines of Fo_{63} but not Fo_{76} composition. Similar intergrowths are found in some Type C and Type D dolerite dykes. Other olivines appear stable in the same rocks.

For more forsteritic olivines (Fo_{85} to Fo_{89}) in the transgressive picrite suite, no signs of alteration were observed even though euhedral green spinel inclusions were present. No intergrowths are observed around primary spinel inclusions in olivine phenocrysts (c. Fo_{80}) in a chilled Type D olivine dolerite dyke.

It is believed that the orthopyroxene - opaque intergrowths result from subsolidus oxidation of primary iron-rich olivine. A reaction for olivine of composition Fo_{50} could be envisaged as two part reactions:

$$3Fe_2SiO_4 + O_2 \rightleftharpoons 2Fe_3O_4 + 3SiO_2 \quad \text{(Eugster and Wones, 1962)}$$

$$3Mg_2SiO_4 + 3SiO_2 \rightleftharpoons 6MgSiO_3$$

i.e. $3Mg_2SiO_4 + 3Fe_2SiO_4 + O_2 \rightleftharpoons 2Fe_3O_4 + 6MgSiO_3$

forsterite fayalite magnetite enstatite

olivine Fo_{50}

Such a reaction involves a volume decrease of about 3%. Relative volumes of 1 magnetite to 3 enstatite would be produced i.e. approximately what is observed. The orthopyroxene produced would be much more Mg-rich than the primary olivine due to the oxidation of the fayalite molecule. Both optical and electron microprobe examinations support such a prediction.

Griffin and Heier (1969) have reported the presence of granular orthopyroxene and opaques, apparently pseudomorphous after olivine, in rocks apparently penetrated by a transient oxidizing fluid phase. Taylor (1968) has shown that very large areas of the Adirondacks granulite-facies terrain have undergone oxygen-isotope exchange with some pervasive fluid. However, the origin of the oxidation in the Ewarara - Kalka rocks is unknown. The oxidation may be related to the development of hydrous fluids as olivines of composition Fo_{63} in Kalka are only oxidized in rocks containing biotite. Alternatively reheating, a possibility during F_2 folding (p. 317), may increase oxygen fugacity (Carmichael and Nicholls, 1967). The oxidation is relatively late stage. Coronas typical of the solid state olivine - plagioclase reaction are observed around some orthopyroxene - opaque aggregates indicating that oxidation occurred after the olivine - plagioclase reaction.

The possible association of the reactions with high grade terrains may also be significant. Other similar textures have been reported by Hermes (1968), Frodesen (1968a,b), Griffin and Heier (1969) and Glaveris (1970) from such environments.

The orthopyroxene - spinel intergrowths presumably formed by similar oxidation of more magnesian olivines in the presence of spinel:

olivine $\longrightarrow$ orthopyroxene + spinel.

The spinel is picotite, (Fe, Mg) (Al, Fe, $Cr)_2O_4$, corresponding to magnetite, $FeFe_2O_4$, in the more iron-rich oxidation reaction. The presence of chromium in at least some olivine lattices is indicated by the presence of chromite exsolution plates in some olivines from the area (Turner, 1967). The chromium was probably originally incorporated in olivine as Cr^{2+} in isomorphous substitution with Mg^{2+} and Fe^{2+}. Therefore part of the equivalent oxidation reaction for more magnesian olivines could be:

$$Fe_2SiO_4 + 2Cr_2SiO_4 + O_2 \rightleftharpoons 2FeCr_2O_4 + 3SiO_2$$

i.e. the spinel phase would contain some chromite component.

The origin of the aluminium in the spinel is more difficult to explain. It may have been derived from the associated primary spinel inclusions (as could the chromium) which subsequently were homogenised with respect to the vermicular spinel. Its alternative source from Al-bearing phases (e.g. plagioclase) outside the olivine involves diffusion problems as movement would need to be through the olivine lattice. However, it is interesting to note that Muir and Tilley (1957) propose movement of Mg, Fe and Si through olivine lattices during similar oxidative processes in some Kilauean picrite - basalts.

9.4 Plagioclase

9.4.1 Exsolution

(1) Potassium Feldspar

Antiperthite has been observed in plagioclases from both the Ewarara and Kalka Intrusions and also in some minor intrusions (Plates 46A,B). It is most prominent in the ultramafic parts of the Giles Complex bodies as an interstitial phase. Its distribution is less common and more irregular in the upper parts of Kalka; its occurrence as a cumulus phase is extremely rare.

The antiperthite is generally similar to that described from other areas, the potassium feldspar blebs and rods being oriented approximately parallel to the c-axis (cf. Carstens, 1967). It is, however, unusual in that it occurs in plagioclases of labradoritic to bytownitic composition i.e. abnormally calcic feldspars (cf. Deer et al., 1963, vol.4, p. 121). The occurrence of antiperthite in layered basic intrusions is also unusual (Wager and Brown, 1968) although it is commonly observed in anorthositic bodies which appear genetically related to the more mafic intrusions (Chapter 12).

Gray (1967) has shown that antiperthitic plagioclases from the Teizi Intrusion are enriched in potassium and plot in the antiperthite field (Fig. 24B). Similarly the only antiperthite analysed in this study plots in the antiperthite field whereas the other plagioclases plot in the normal field (Fig. 24B).

The antiperthite is assumed to result from exsolution of excess

potassium from the plagioclase lattice on cooling (Sen, 1959). In the ultramafic rocks interstitial crystallization, especially the orthocumulate type, would result in early pyroxene crystallization and potassium enrichment in the final liquid fractions. Late stage crystallizing plagioclase would therefore be enriched in potassium and eventually give rise to antiperthites. However, in the overlying gabbroic rocks plagioclase would probably precipitate from the beginning of interstitial crystallization and thus prevent or reduce any significant build up of potassium in the final liquid. The significance of the common occurrence of cumulus antiperthitic plagioclase in the Teizi Intrusion is discussed in Chapter 12.

(2) Spinel, magnetite and clinopyroxene

Many plagioclases observed in this study contain numerous minute particles which, in some examples, are so massed that they cause near opacity in the feldspars (Plate 45A). In many cases, however, the inclusions are only sparsely developed. The particles are generally much finer than the normal sized inclusions found in some feldspars (e.g. Chapter 9.4.3) but it can be difficult to distinguish them at intermediate grain sizes. This phenomenon has been termed clouding (Poldervaart and Gilkey, 1954) and is almost entirely confined to plagioclases from basic igneous rocks (Table 16).

Clouding is present in both cumulus grains and interstitial material within the igneous rocks but with few exceptions has not been observed in recrystallized plagioclase aggregates. Small granular particles of

the same type, clouding the associated primary plagioclase, are commonly observed at grain boundaries in the recrystallized mosaics. This strongly suggests that clouding preceded recrystallization.

Several different types of particles have been identified as clouding the plagioclase grains. Similar materials usually form the particles in clouded feldspars described from other areas (Table 16).

Magnetite* particles vary in size and shape from minute specks to slender rods (generally 5μ - 50μ x 0.5μ). The coarsest particles are often arranged in trains (50μ - 500μ x 5μ). In these trains the particle axis may be parallel, perpendicular or oblique (en echelon) to the train axis. The rods generally show a strong crystallographic orientation. Alignment of rods may be in one, two or sometimes up to four directions (Plate 45C). The main direction is parallel to simple and multiple twin planes (i.e. //Z in (010)) with a subsidiary set //Y in (001). The globular trains may be curved or straight on rational or irrational crystallographic directions (Plate 45D).

---

* Identification based on opacity; black and magnetic host plagioclase when strongly clouded (others are pinkish-grey when finely clouded); elimination of ilmenite and haematite by X-ray powder photographs (magnetite is indeterminable in small quantities in plagioclase). Electron microprobe examination of A314-418 revealed presence of titaniferous magnetite with Fe: Ti $\simeq$ 5:1 (Plates 40A-C).

Spinel* commonly occurs as rods and sometimes plates between 10μ and 100μ long and about 1μ wide (Plate 45B). The rods normally have rounded ends but in the coarser varieties sharp terminations are observed (see Goode and Krieg, 1967, Plate 9.3). The spinel rods are usually aligned parallel to Z in (010) with a subsidiary set parallel to Y in (001). In some cases other sets are also present.

Clinopyroxene (and/or hornblende)** particles are generally found as fine specks (<1μ) grading up to small rods (20μ x 4μ) generally stubbier than the magnetite rods (Plates 46C,D). The rods are normally aligned parallel to a multiple twin plane set.

Magnetite clouding is probably the most widely distributed in the area but is rarely abundant (<<5%) in any one specimen. Spinel is also found in many rocks and is usually much more abundant than magnetite (<20%). Because of the fineness of the particles relative to the thickness of the thin section, about 20% clouding can cause near opacity for the sample. The finer the particle size the greater the apparent degree of clouding. Burns (1966) has estimated that the particles make

---

* Identification is based on the following properties: transparent, green in thicker grains (host plagioclase is bright green in strongly clouded samples); high relief; isotropic; an X-ray powder photograph of A300-1 plagioclase revealed a subsidiary spinel pattern (probably Mg-rich as a comparison of ASTM cards of pure spinel and pure hercynite revealed a line d = 2.33Å lacking in the hercynite pattern); electron microprobe examination of A300-84 revealed presence of (Mg,Fe) spinel rods (Plates 40D-F).

** Identification is based on the following properties: transparent, colourless (or brown, pleochroic); high relief; anisotropic; inclined extinction.

up about 25 volume percent of the feldspar in strongly clouded plagioclases from Scotland. Chemical analyses of two strongly clouded samples in this study are consistent with 10 to 20% clouding by spinel. Clinopyroxene is not found in many rocks and is about as abundant as magnetite.

In most cases plagioclase is clouded by only one type of particle but in some cases two types may be present (Plate 46C).

Clouding has been observed almost entirely from the basic igneous rocks of the area. Within this group, however, no particularly significant association has been observed. Magnetite has been observed in plagioclase from Type A, B and C dykes, the picrite plug suite, transgressive anorthosite, mafic pegmatites and the Kalka Intrusion; spinel in Type B and D dykes, the picrite plug suite, mafic pegmatites and the Ewarara Intrusion; and clinopyroxene in Type A, C and D dykes, mafic pegmatites and the picrite plug suite.

Rutile(?) clouding has only been observed in the Minno acid granulites which have some igneous affinities (Chapter 2; note also that Poldervaart, 1966, has observed rutile in plagioclase in charnockitic adamellites from South Africa). Clouding has not been observed in other granulite plagioclases.

Commonly clouded plagioclase grains have clear edges where few or no clouding particles occur (e.g. Plate 46A). These clear edges can be either primary or secondary.

Towards the primary clear edges the clouding particles usually decrease in abundance, gradationally but sharply, sometimes with an

associated decrease in grain size. The clear edges are optically continuous with the clouded plagioclase. In many cases the clear edges are associated with products indicative of advanced or late stage fractionation e.g. biotite, apatite, iron-rich pyroxene, green amphibole or castellate texture between orthopyroxene, clinopyroxene and plagioclase. In some cases the edges were also zoned probably indicating a more albitic plagioclase than in the core; in others antiperthitic margins were observed (Plate 46B); in others no compositional change was apparent (at least by extinction methods).

These observations are in accord with those of other workers. Poldervaart and Gilkey (1954) and Williamson (1936) found that the clear edges were in some cases more albitic than the clouded sections. Shand (1945) observed no compositional change but Macgregor (1931), Bentor (1951), Weedon (1961) and Starmer (1969) have found more albitic margins.

Secondary clear edges are associated with recrystallization (Plates 48C,D). The equidimensional aggregates are normally associated with grain boundaries. Recrystallization is accompanied by coalescing* of the clouding particles into coarser globular inclusions.

Clouding particle distributions may also be inhomogeneous within grains. In some cases the change in particle concentration may only be

---

* The criteria for coalescing are taken as an increase in size and a decrease in numerical abundance (but constant volume abundance). It is usually accompanied by a decrease in preferred orientation and a decrease in degree of elongation of the primary particles.

apparent. An irregular coarsening and fining is observed in many cases - these may be primary changes in size or due to coalescing (Plates 45E,F) or recrystallization.

In many grains quite sharp concentration variations are observed within the grains. These variations may be patchy but in general they are parallel to major crystallographic directions. These zones are commonly parallel and coincident with multiple twin lamellae (Plates 48A,B); where no twins are observed there are no changes in extinction or any associated boundary enrichment zones (which would be suggestive of coalescing). In other examples there are extinction differences associated with primary changes in concentration. Along other twin planes either boundary enrichment or concentration of coarser particles (coalescing?) occurs (Plate 45H). In one example, concentrated magnetite droplet trails were observed extending along from twin planes into untwinned feldspar. In some cases clouding is not observed in the vicinity of inclusions.

Special mention should be made of particle distribution in A300-501c. The plagioclase is divided into areas of fine-grained ($<1\mu$) specks of magnetite(?), and areas of spinel rods (10 to $40\mu \times 3\mu$) and fine magnetite (?) specks grading to rods (slightly smaller than the spinel rods). The areas are generally defined by rational crystallographic directions (Plate 45B). The magnetite is possibly slightly less abundant in the second area but this is difficult to judge accurately. Regularly spaced density zones (perpendicular to (010)) extend through both areas as continuous thin clear bands with associated central trains of magnetite

specks (Plates 45B,F). Spinel rods are not found in these areas. These zones may represent coalescing of magnetite rods but conclusive evidence is lacking.

The relationship between types of clouding and all analysed plagioclases has been investigated. For magnetite clouding, compositions vary from An_{60} to An_{77} without any well defined peak (Fig. 24C). Although limited data are available, spinel clouding has been observed in plagioclase from An_{50} to An_{62} (Fig. 24C). Lack of clouding in 23 unrecrystallized samples is often, but not always, associated with olivine-bearing rocks (14 samples; composition range An_{65} to An_{83}) or antiperthitic exsolution (4 samples).

Analyses for MgO and total iron (as Fe_2O_3) in eleven plagioclases are summarised in Table 17. These results reveal two distinct chemical groups viz. those with spinel clouding and those with magnetite or no clouding. The spinel clouded plagioclases are high in MgO and total iron relative to the other group.

However, even the unclouded plagioclases (pure white, no hint of internal particles of any size even under the electron microprobe) have considerably higher concentrations of total iron and magnesium* than plagioclases normally described in the literature. Deer et al. (1963, vol. 4) report maximum Fe_2O_3 contents up to about 1% (normally much less) and MgO up to about 0.7%. Ribbe and Smith (1966) have reported total

---

* Even allowing for possible maximum MgO and Fe_2O_3 contents of 0.3% and 0.2% for 1% pyroxene impurity.

iron values up to 0.53% and MgO values less than 0.02% for inclusion-free portions of plagioclase.

Origin of clouding in plagioclase

Varying hypotheses have been put forward to explain clouding of plagioclase — their applicability in relation to clouded feldspars from this area and in general will now be discussed.

(a) Solid state inclusions

An origin of clouding by inclusion of solid particles during plagioclase growth is not considered viable because the particles are not always found as separate mineral phases outside the feldspar, the morphologies of the particles are different in the groundmass and in the plagioclase, and inequidimensional particles are not necessarily aligned parallel to growth faces of the plagioclase*.

However, particles of definite inclusion origin are also commonly found in the described clouded feldspars. In some cases great difficulty may be experienced in distinguishing inclusion particles from clouding particles. This is especially so in the case of clinopyroxene. Complete gradations in inclusion morphology, orientation etc. from normal inclusions to particles with the characteristic properties of clouding particles are found e.g. in Type C olivine dolerite dykes such gradations are observed, but in this case it has been interpreted that the pyroxene

---

* These are the criteria of exsolution.

particles in plagioclase result from eutectic crystallization of the two materials (see Chapter 9.4.3). Clouding described by Joplin (1935, Fig. 1a,b) has many similarities to some feldspars described here which are thought to have an inclusion origin. Some of these granular inclusions were arranged in zones apparently parallel to feldspar growth faces.

Bottinga et al. (1966) have suggested that concentration of Fe and Mg at the boundary of the growing plagioclase due to depletion of other elements may cause precipitation of Fe, Mg-rich phases which would then be incorporated into the feldspar. Density zoning of the clouding particles may be expected in such circumstances. Bentor (1951) has described clouded zones in plagioclase fitting this prediction but the clouding often appears to follow resorption rather than growth.

(b) Effect of H_2O

Burns (1966) and Bridgwater (1966) have found that clouded plagioclase contained more water than associated unclouded feldspar. Bridgwater suggested that the water controlled the state of the iron present which caused structural defects in the clouded samples. This opposes Wilcox and Poldervaart's (1958) hypothesis that anhydrous conditions favoured clouding. Although no data are available, the described plagioclases in this thesis crystallized in anhydrous conditions and probably contain little water.

(c) Metamorphism

Following MacGregor's (1931) work, many authors (e.g. Sutton and

Watson, 1950, 1951; Pichamuthu, 1959; Dearnley, 1962) have used clouding of feldspar to indicate exsolution resulting from thermal or regional metamorphism. However, it is difficult to imagine why the igneous feldspar should breakdown on reheating when it was apparently originally stable at higher temperatures. In the described examples such an origin is highly unlikely because clouding is not present in recrystallized plagioclase older than clouded primary plagioclase in other rocks (e.g. clouded plagioclase in Type C dykes is younger than recrystallized unclouded feldspars in Kalka which were originally clouded). Furthermore the granulite plagioclases are unclouded. Inclusions within some clouded plagioclases are also unclouded (Plate 45G).

Shand (1945) and Murthy (1958) have observed a strong association between clouded feldspar and corona formation, although Murthy noted that clouding appeared before the coronas formed. Wilson and Middleton (1968) believe the clouding of plagioclase by spinel is due to solid state growth of spinel because of the development of an unstable plagioclase lattice during metamorphic reaction with olivine. However, in the Kalka - Ewarara rocks clouding is not always associated with corona formation or vice versa and it is believed the association is an indirect one related to environment.

(d) Exsolution

Other authors have suggested that clouding results from exsolution of iron-bearing phases from the plagioclase lattice on cooling and all the physical features of clouding observed in this study are consistent with an exsolution origin (p. 208). Andersen (1915) suggested haematite

plates in plagioclase resulted from exsolution of Fe_2O_3 held in solid solution at higher temperatures as he recorded that the red clouding disappeared on heating. Similar results and explanations were given by Frankel (1969) for red-brown clouding in plagioclase. Ernst (1960) has suggested the presence of minute haematite exsolution particles to explain red clouding in potassium feldspar. Poldervaart and Gilkey (1954) and Wilcox and Poldervaart (1958) have accepted an exsolution origin for light clouding but believe another origin is required for heavy clouding. They propose the introduction of Fe into the lattice from external iron-rich fluids. Such a mechanism is considered extremely unlikely for the samples described here. The repeated production of a series of iron-rich fluids from almost anhydrous magnesian-rich rocks does not seem feasible.

The magnetite clouded samples have a high but not abnormal iron content also consistent with exsolution. At high temperatures during feldspar growth, some Fe^{3+} may substitute for Al^{3+} and, on cooling, may exsolve because of its considerably greater size (0.64Å for Fe^{3+}, 0.50Å for Al^{3+}). The general restriction of magnetite and other forms of clouding to igneous plagioclases (this study, and Table 16) could indicate that the original substitution is only feasible at magmatic temperatures ($>1000 - 1100^{\circ}C$). The common occurrence of the exsolution in plutonic environments, often but not necessarily high pressure (Table 16; and Poldervaart and Gilkey, 1954), may also indicate that the exsolution process is favoured by slow cooling. The implied difficulty in nucleation may also explain some of the primary patchy developments of clouding (abundance and grain size) as well as the very fine grain size

(relative to particle density) observed in this study and elsewhere (e.g. Poldervaart and Gilkey, 1954). The clinopyroxene clouded samples may be similarly formed but an inclusion origin is also possible for some examples.

The spinel clouded samples are the most difficult to explain. They have all the physical features of exsolution but have an abnormal chemistry. Their high Mg and Fe concentrations are unique in this regard, although this may only be apparent because of sampling discrimination by other workers. Even the unclouded samples have high Mg contents outside possible ranges of contamination suggesting that perhaps the environment of crystallization may be important. A review of the literature is difficult because many authors have not identified the nature of the clouding particles. However, some remarks can be made about those reviewed in Table 16. Spinel is the clouding particle in at least four cases (Shand, 1945; Frodesen, 1968; Wilson and Middleton, 1968; Starmer, 1969), and possibly others (e.g. Bowes et al., 1964). These cases occur in gabbros or troctolites from amphibolite to granulite facies terrains, and are closely associated with high pressure olivine - plagioclase reaction coronas (see Chapter 11). This possible association with high pressure igneous rocks may be important in the development of spinel exsolution and warrants further consideration. The most pressing need, however, involves a detailed examination of these plagioclases from a crystal chemistry viewpoint.

9.4.2 Twinning

Simple Carlsbad twins (twin plane (010)) are developed almost exclusively in crystals grown in an unrestricted environment. They are found both in cumulates (slow cooling) and in both phenocrysts and matrix laths from chill dolerites. Simple twinning in an interstitial or restricted environment is only rarely observed, and even then may have developed on original cumulus grains. Simple twins have not been observed in plagioclase from the granulites or in recrystallized igneous plagioclases. In some of the twinned plagioclases trails of concentrated pyroxene (and also hornblende, biotite and others) inclusions are aligned in (010), commonly along the twin plane (Plate 46f).

The twins are interpreted as having formed by mutual attachment of plagioclase crystals freely suspended in the melt i.e. synneusis (Vance, 1969). Vance notes that synneusis usually occurs between like crystals, and that the two crystals combine in a preferred orientation. He has suggested that the crystals joined initially in the preferred position, as this best explains features observed by him. Such an hypothesis involves some form of long range force of attraction. Synneusis relations have also been observed in olivine and orthopyroxene in this study. The common presence of simple twinning in clinopyroxene, with (100) as twin plane, in cumulus but not interstitial phases in some of the transgressive picrite suite may also be due to synneusis.

Although Vance believes that a parallel or untwinned combination is the most common synneusis relation for plagioclase, the Carlsbad twin orientation appears by far the most common in these rocks. However, the

occasional aligned pyroxene inclusion concentrations within primary untwinned crystals may indicate former planes of attachment for untwinned combination (Plate 46E). It is believed that the inclusion trails result from crystallization of liquid trapped between the faces.

It may seem unusual that, in at least some cases, other individuals did not join the twin pair to give groups of three, four or even more crystals. It could be important that permanent mutual attachment would probably require conditions of small relative velocities between grains. These conditions would be upset by a twinned crystal which would settle at twice the velocity of an individual crystal. Furthermore the twinned crystal would be in the growth zone (a necessity for permanent attachment) for only half the time of an individual crystal, further decreasing the chances of attachment. The velocity variations would not affect joining by two sets of twinned crystals but the low incidence probability would lessen the chances of this happening.

Multiple twinning is commonly developed in primary plagioclase crystals but is less widely found in secondary recrystallization assemblages (Plates 46G,H). The twinning, both albite and pericline, corresponds to glide twinning by the criteria developed by Vance (1961). Twin properties tend to vary with degree of deformation (demonstrated by bending, undulose extinction). With increasing deformation the twin boundaries become more diffuse, more lenticular and more curved. The general absence of multiple twins in recrystallized grains indicates the early development of twins in the strained assemblages and their subsequent obliteration on annealing. The development of multiple twins in

recrystallized grains is usually associated with undulose extinction and is probably caused by later deformation.

9.4.3 Pyroxene inclusions

Pyroxene inclusions in plagioclase are a common textural feature of many of the igneous rocks of the area, especially the minor intrusions.

The pyroxenes are usually rounded and stubby to elongate in appearance. In some instances they are aligned parallel to (010); in others they form complex globular intergrowths with plagioclase (compare Plates 47H and 47E).

The inclusions commonly occur near grain boundaries of lath-like plagioclase (Plate 47G) or in restricted interstitial areas between euhedral crystals (Plates 47E,F). In rare cases where they occur throughout the crystal, the host plagioclase is not lath-like (Plate 47H). In some cases the inclusions grade to more massive pyroxene in the centres of the interstices (Plate 47F).

The textures are interpreted as indicating eutectic crystallization of pyroxene and plagioclase in the last areas of melt crystallization. It is considered that such intergrowths are favoured by restricted environments and fairly fast crystallization rates (otherwise more ordered crystallization would occur). This could explain their common occurrence in the dolerite dykes and rarity in Giles Complex cumulates. It should be realised, however, that similar textures are also rarely

observed in plagioclase phenocrysts in dolerites (Plate 15C) and in some cumulus plagioclases near the top of the Kalka layered sequence. Such intergrowths would have occurred in unrestricted crystallization environments, but may have still been favoured by relatively fast growth rates. Similar interpretations on the same texture have been made by Philpotts (1966).

PART FOUR

PETROGENESIS OF THE GILES COMPLEX

CHAPTER 10

THE DEVELOPMENT OF IGNEOUS LAYERING

10.1 Introduction

The writer believes that most of the igneous layering described from the Kalka and Ewarara layered sequences can be explained by gravitational settling of crystals from their host melt, and by various processes subsequently acting on the pile of accumulated crystals (the exceptions are discussed in Chapter 10.3). Such interpretations are widely accepted by igneous petrologists but minor controversies still exist on various aspects of such mechanisms.

The following discussions deal with a theoretical treatment of crystallization in a large basic igneous body and the processes most likely to produce igneous layering, followed by their interpreted application to the layerings observed in this study and those reported in the literature.

A model of crystallization developed by Jackson (1961, p. 93-99) for the Stillwater Intrusion has been used as a theoretical basis for this study. The Giles Complex intrusions are, in general, similar to Stillwater in that they are large, thick, sheet-like igneous bodies, originally horizontal in attitude. Jackson's model involved crystallization at the base of the sheet. Convectional overturn above this zone allowed it to be replenished with magma from the roof of the intrusion which become supersaturated at the higher pressures found at the base. Thus crystallization at the base was able to continue allowing a build up of settled cumulus phases on the floor of the intrusion.

The occurrence of bottom crystallization in the Kalka Intrusion is supported by the presence of density graded layering (in contrast to features of extreme sorting) in widely separated parts of the sequence. Basal supersaturation is further indicated by the presence of adcumulus interstitial growth in parts of the sequence. If crystallization had occurred at the roof rather than the base at least some of the early formed phases would have accumulated immediately above the granulite slivers, a feature which is not observed. The general similarity in cumulus type, grain size, shape and composition, together with the preceding facts, indicates that all crystallization took place in the basal parts of the body. Occasional larger or exotic crystals (e.g. opx in ol - cpx - plag cumulates) suggest that some crystals were suspended in the crystallization zone for longer periods by some mechanism (e.g. local upcurrents).

On the general basis of Jackson's model, an attempt will now be made to devise mechanisms to produce the layering types observed. To this end, the layering is divided into various groups. Those layerings and related structures caused by variations in the properties of the cumulus phases are divided into primary (formed by crystal settling and chemical fractionation) and secondary (formed by post-depositional processes). The primary group of layerings has been subdivided for convenience into small scale and large scale. Another small group of layerings is directly caused by variations in the properties of the interstitial minerals and is discussed separately.

10.2 Cumulus Igneous Layering

10.2.1 Primary Small Scale Layering

The rock textures indicate an accumulation mechanism for the formation of the rocks of the Kalka and Ewarara layered sequences. That this concentration mechanism was controlled by gravity settling is supported by the fact that the layering is perpendicular to the general rock, mineral and chemical fractionation sequences. These sequences grade overall from the highest to the lowest temperature mineral types. Furthermore, the layering is generally parallel to the basal contacts (where exposed) but at high angles to the side contacts, and tabular crystals tend to lie within the layering. The presence of density graded layering also supports such a mechanism.

1. Mechanics of crystal settling

Since most of the common phases which can crystallize from basaltic melts are denser than those melts, gravitational settling of crystals is inevitable during crystallization in a static liquid. Plagioclase, of approximate basalt melt density, is the only phase with the potential capacity to float or rise in the liquid.

The behaviour of settling (or rising) particles can be described by Stokes Law:

$$v = \frac{2gr^2\Delta\rho}{9\eta}$$

where v = terminal velocity, g = gravitational acceleration, r = particle radius, $\Delta\rho$ = density contrast between particle and melt, η = melt viscosity. McNown and Malaika (1950) have found that this

law is obeyed by particles of all shapes when $R_e < 0.05$ (R_e is the Reynolds Number).

$$R_e = \frac{2\rho_m r v}{\eta}$$

where ρ_m is density of the melt. Since particle shape is not important, the particle radius for an inequidimensional particle is taken as the radius of the sphere of equivalent volume*. The condition $R_e < 0.05$ is obeyed by all particles encountered in this study (at least for pyroxene crystals up to 10mm in diameter).

The presence of other particles can affect the settling velocity for $R_e < 10$ (Lewis et al., 1949):

$$v_s = v_o (1 - \phi)^{4.65}$$

where v_s = sedimentation rate, v_o = velocity at infinite dilution, ϕ = volume fraction of particles. Hence for 30% crystals, the settling rate will be theoretically decreased to 10% of the free settling velocity. Bhattacharji (1965) found in scaled experimental work that the velocity was decreased to 20%. Particle concentration should be low for slow cooling intrusions (cumulate environment) but settling velocity corrections would be necessary for higher concentrations (e.g. in chill environments; crystal mushes). In aqueous environments, Briggs and Middleton (1965) have found that settling is hindered for concentrations greater than 1%.

---

* Care should be taken as Bhattacharji (1965) has reported that in scaled experimental studies the settling rate decreased inversely with the unequal axial ratio of the crystals.

Settling curves for basaltic and granitic minerals have previously been given by Hess (1960) and Shaw (1965). In Table 18, settling velocities for pyroxene/olivine (pyroxol) and plagioclase at infinite dilution for different melt densities and viscosities have been tabulated*. These are the only phases considered in this study.

From the discussion and documentation presented so far, it is easy to compare the processes acting in the magmatic case to those in aqueous sedimentation. Wager and Deer (1939) and Turner and Verhoogen (1960) have made comparisons in terms of detrital sedimentation while Brown (1956) and Jackson (1961) have found analogies with chemical sediments. It will become more apparent with later discussion of the structures described in Chapter 6, that both comparisons are probably valid.

One of the most obvious consequences of the calculations in Table 18 is that differential settling between phases will occur in crystallizing basaltic melts. This will be most noticeable with phases of greatly differing grain sizes or density contrasts. For example pyroxol grains will settle 200 metres in a shorter time than plagioclase of equal size will settle 2 metres. The distance of settling will accentuate any differences.

The degree of separation of co-crystallizing phases within the cumulate sequence will depend on the settling distance, the relative

---

* The physical data used in this study are derived in Appendix 8.

settling velocities, and the concentration of crystals or the thickness of the crystallization zone (which control the rate of crystal accumulation).

Upward currents in the melt will tend to increase any tendency for crystal separation by effectively increasing the distance of fall (by reducing the settling velocity). Downward currents will act in the opposite manner.

Calculations have been made for settling pyroxol and plagioclase assuming various lateral current velocities up to $\frac{1}{2} v_{px}$ (v_{px}, v_{pl} are the settling velocities for pyroxol, plagioclase respectively). At this velocity extreme lateral winnowing of plagioclase results unless the settling distance is very small. At much lower velocities (e.g. $\frac{1}{2} v_{pl}$) in a simple convection model winnowing results in variations in layering thickness for plagioclase only at the ends of the lateral part of the convection cell.

2. Comparison of settling times and solidification times

For a sheet-like body like Kalka, the melt would cool mainly by conduction of heat from its upper and lower contacts. Although theoretical data are lacking for melts with intrusional and solidus temperatures of 1350 and 1200°C respectively, the results would be similar to those in which the temperatures were 1100 and 800°C, or 1000 and 800°C (Jaeger, 1957). Jaeger gives cooling curves for these cases and finds that the time for complete solidification is about $0.014\ D^2$ (where D is body thickness in metres). Hence if D is taken at

6000 metres (maximum thickness for any Giles Complex body), the solidification time is less than a million years*. Convection in the melt will serve to decrease the time by up to one half (Jaeger, 1964).

Settling times for various conditions thought to be average for crystals observed in this study are given in Table 19A**. Since these are very much less than the cooling time, complete separation of crystals from melt by gravity settling seems inevitable for Kalka.

3. Mechanics of crystallization

1) Continuous Nucleation

If crystallization is continuous above the floor of the intrusion, differential settling between co-crystallizing pyroxol and plagioclase will still occur. However, isomodal layering cannot be produced as a result of the settling since the faster settling pyroxol will merely catch up to previous crystallized plagioclase. Hence only a homogeneous and unlayered massive sequence will be produced.

Wager and Deer (1939), Wager (1953) and Hess (1960) have postulated that variable currents can cause variable differential winnowing of settling crystals thereby giving rise to rhythmic isomodal type layering.

---

* These calculations are based on country rock temperatures of zero. For granulites at 30 to 40km, these temperatures could be between 400 and 800°C, thereby decreasing the rate of heat loss and increasing the time of solidification.

** In reality grain growth will usually be slow and hence cumulus grain sizes will gradually increase during settling. However, for convenience the grain sizes used in the calculations in this chapter are the final size on accumulation (with the reservations of p. 121).

However, it was shown on p. 222 that only vertical currents could produce variations in relative settling rates. Since these would have limited areal extent such a mechanism does not seem to provide an adequate explanation for the widely distributed isomodal layering observed in many intrusions. The variable current mechanism has since been abandoned by Wager (1963).

If there are gradational chemical changes occurring in the nucleation zone due to fractionation processes, then pyroxol can accumulate with plagioclase of different composition to that with which it crystallized (or vice versa). If the fractionation also results in a gradational change in the proportion of each mineral crystallizing, then mineral-graded (but not isomodal) layering can result. Similarly, size-graded layering can result if, for physical reasons, cumulus grain size changes during crystallization.

2) Discontinuous Nucleation

If crystallization occurred in discontinuous bursts, differential settling between pyroxol and plagioclase would cause the partial or complete separation of these phases on accumulation. Complete separation would result in the formation of a pair (set) of isomodal layers with an internal phase contact, while partial separation would result in mineral-graded layering (density grading).

Discontinuous nucleation would be quite feasible in slow cooling intrusions. Supersaturation values would usually be small, and consequently on crystallization the melt temperature might be raised (due to

the release of the heat of crystallization) sufficiently for saturation values to be too low for growth. Further cooling would result in further crystallization at a later stage when the heat of crystallization was dissipated.

This may explain why isomodal layering is not observed in small bodies of cumulate origin in the vicinity of Kalka and Ewarara, although igneous planar lamination is well developed. In small bodies with presumably faster cooling rates, conditions for discontinuous nucleation would be harder to achieve.

It is also worthwhile noting that Hoffer (1965) has suggested that intermittent seismic tremors could cause discontinuous crystallization in igneous plutons.

Let us take our previously developed model involving a zone of nucleation and consider the results of differential settling from this zone under conditions of discontinuous crystallization (Fig. 25A).

In this model the two most important crystal groups for our purpose are the pyroxol crystals from the top of the nucleation zone, and the plagioclase crystals from the bottom of the zone.

If t = time for complete separation between these two groups, d the thickness of the crystallization zone, and L_c the critical distance, then

$$t = \frac{L_c + d}{V_{px}} = \frac{L_c}{V_{pl}}$$

$$\therefore \quad \frac{2(L_c + d)gr^2\Delta\rho_{pl}}{9\eta} = \frac{2L_c gr^2 \Delta\rho_{px}}{9\eta}$$

Therefore for plagioclase and pyroxol of same grain size,

$$d >> L_c$$

i.e. $L_c + d \simeq d$

Hence complete separation of pyroxol and plagioclase would occur just below the nucleation zone. For mineral graded layering to be produced therefore, the crystallization must extend to virtually the floor of the intrusion (unless the nucleation zone is exceptionally thick, since L_c is dependent on d).

Examples: For 2mm crystals,

a) if nucleation zone is 1000m thick, L_c = 75m

b) if nucleation zone is 500m thick, L_c = 40m

The production of isomodal layering means that the nucleation zone did not extend completely to the top of accumulated crystal pile.

These results have important implications. Mineral graded horizons would probably accumulate within a supersaturated environment, and hence there may be an increase in the degree of adcumulus growth within the interstices towards the top of each layer (assuming sufficient time before the accumulation of the next burst). Campbell (1968) has reported a change from heteradcumulus to adcumulus growth within layers in the Jimberlana norite, Western Australia.

Furthermore, for the condition $L > L_c$ there will be a zone below the crystallization zone where the melt is not supersaturated with

respect to the phases crystallizing above. The development of such an undersaturated zone constitutes one of the most important problems encountered in this study. It is possible that crystals settling through this zone continue to grow and thus prevent fresh nucleation from occurring there i.e. the zone is only apparently undersaturated.

We will now consider the results of a build up of repeated bursts of nucleation.

(a) $L > L_c$ (i.e. complete separation).

In this case, a rhythmic series of melanocratic and leucocratic rocks will usually result, with neighbouring layers being separated parts of the same crystallization burst (Fig. 26A). The thickness of each layer pair for any one melt composition would be proportional to the time of crystallization, concentration of crystals in the crystallization zone and the thickness of the zone.

However, if the crystallization bursts were so close together that the previous set(s) had not yet completely settled, then overlap of sets could occur with pyroxol of one set catching up with or overtaking plagioclase formed one or more bursts previously (Fig. 26B).

That such overlap can occur is convincingly shown in the Olivine Gabbro Zone in Kalka. Within this zone compositional trends for olivine and plagioclase show irregular but sympathetic variations in their compositions (Fig. 40A). The maxima of the plagioclase curve are displaced towards the top of the layered sequence relative to the maxima of the olivine trend. This strongly indicates separation of the two

phases during settling. Furthermore, co-crystallizing phases (obtained by matching the curves) are sometimes separated in the cumulate series by another pair of isomodal layers and are not from neighbouring isomodal layers. Hence settling overlap must have occurred.

The settling overlap between cycles of crystallization is an excellent mechanism for the production of reverse grading (Fig. 26C), and even normal grading. Mukherjee (1968) has also suggested such a mechanism for reverse grading in ultramafic rocks in India. The predominance of normal mineral grading over reverse mineral grading in Kalka is, however, an indication that overlap did not occur very often. From observations based on size grading Bishop and Force (1969) have shown that normal grading is common in "deep" marine sediments but about 30% reverse grading is found in non-marine and shallow marine environments. They also found that reverse graded beds tended to occur in groups. Similar groupings might be expected in the igneous cases described above since reverse grading can result from a condition which might be expected to persist for some time.

(b) $L < L_c$ (i.e. incomplete separation).

As discussed previously this condition will result in the development of a mineral graded sequence. Complete settling of both pyroxol and plagioclase between crystallization bursts will result in sharp phase or ratio contacts between each set of graded layers (Fig. 26D).

The effect of overlapping (Fig. 26E) or overtaking (Fig. 26F) cycles of settling could result in the formation of an continuous

alternating sequence of normal and reverse graded layers with few or no ratio contacts.

It can be readily seen that almost any combination of layer types of this kind can be formed by variations in the crystallization conditions. It is interesting to note that if the base of the nucleation zone was oblique to the top of the accumulating crystal pile then it would be possible in some cases to grade laterally from conditions where L was greater than L_c to areas where L was less than L_c.

4. Effect of pressure variations

Crystallization at different levels (and therefore pressures) of the intrusion may produce chemically and possibly mineralogically different precipitates, which on settling could give rise to mixed or alternating layers.

Pressure variations with time could produce similar effects. No evidence has been collected to support such a layering mechanism in Kalka, however. Small pressure increases following fresh injections of magma could be expected at times in Kalka but these would be unlikely to be of sufficient magnitude or duration to cause any appreciable effect.

Magma release to higher levels as suggested for parts of the Giles Complex by Nesbitt et al. (1970) might cause short term pressure reductions but no effects on the precipitates has been observed.

5. Effect of staggered and simultaneous crystallization

It has been assumed, for simplicity, that when two or more cumulus phases are precipitating from a melt they begin crystallizing at the same time in any one crystallization burst i.e. simultaneous nucleation.

That the nucleation fields are at least partly overlapping for Kalka and Ewarara is proved by presence of inclusions of one phase within the other at various levels in the intrusions.

However, Wager (1959) and Hawkes (1967) have suggested that different phases have differing orders of nucleation depending on their atomic structural complexity. In such cases staggered nucleation would result. While Wager's and Hawkes' evidence could be interpreted as resulting from a combination of differential settling and fractionation instead of staggered nucleation, the possibility should still be kept in mind. Fluctuating nucleation of olivine and orthopyroxene has been suggested as a cause of layering in the Losberg Intrusion (Abbott and Ferguson, 1965).

6. Application to Kalka layering

Much of the layering described from the Kalka sequence can be directly interpreted from the preceding models based on continuous and discontinuous crystallization. The relatively massive unlayered sequences found over much of the Norite Zone, for example, are probably the result of continuous crystallization.

The small scale isomodal layering involving separation of pyroxol

and plagioclase (e.g. Plates 33B, 35F, 36C) is in accord with the predictions for repeated bursts of discontinuous crystallization when $L > L_c$. The density graded layering observed (e.g. Plate 34A) satisfies the predictions for $L < L_c$.

The density graded layering is distinct from turbidite-type graded layering in some other igneous intrusions (e.g. Irvine, 1963, 1965, 1967) in that they are not size graded, have no uppermost finely banded layers, show no evidence for deposition during current action, and lack a source of material (only one scour channel has been found in the body so far, and no slumping is observed).

Density grading similar to the Kalka type has been observed in many other igneous intrusions (e.g. Table 20). It should be realised, however, that graded layering can also develop in non-sedimentary environments e.g. Peterson (1968), Wilshire (1969).

The spectacular repetitive layering of the Johnson Horizon probably resulted from repeated fluctuations of the melt supersaturation about a critical value giving rise to pronounced conditions of discontinuous crystallization over a considerable area.

10.2.2 Primary Large Scale Layering (Cyclic Units)

Large scale repetitive vertical variations in cumulus properties have been described for Kalka and Ewarara in Chapter 7. These cyclic units contain numerous examples of internal small scale layering and therefore could not have originated solely by differential gravity settling processes.

The units described in Chapter 7 are usually accompanied by chemical variations associated with the overall fractionation trends and are similar to cyclic units described elsewhere (e.g. Wadsworth, 1961; Jackson, 1967, 1970; Irvine and Smith, 1967; Sorensen, 1969).

The author is in agreement with other writers on the interpretation of these cycles. It is believed that the repetition of the crystallization cycles indicates repeated replenishment of fresh magma into the crystallization zone. The replenishment of magma could be due to two causes viz. convectional half-overturn where magma from the top of the chamber replaces "used" magma at the base or fresh injection of magma into the chamber, particularly at the base.

It should be chemically possible to distinguish cyclic deposits formed under ideal conditions by these two mechanisms. The lowermost member (unless the cycle has been debased) for progressively younger cyclic units should show evidence of increased fractionation for deposits formed from convectional overturn (Fig. 27A). A series of fresh injections from a "developing" source (i.e. one where increasing percentages of mantle material was being melted) would give rise to a sequence showing reverse fractionation (Fig. 27B). Fresh injections of the same composition from a "stable" source would give rise to deposits of constant composition (Fig. 27C). The effect of dilution of the fresh injection by old "used" magma is shown in Fig. 27D; the envelope slope of the fractionation trend resembles that for convectional half-overturn but is not so pronounced.

Total iron content of chromites from the base of the Stillwater Intrusion decrease upwards at first, then begin to increase (Jackson, 1963). These variations are compatible with a dual model involving an initial series of fresh injections from a "developing" source, followed by convectional overturn in a static chamber when injection was completed. The Rhum Intrusion appears to be an example of fresh injection from a "stable" source as olivine compositions remain constant at the base of each of the cyclic units (Wager and Brown, 1968, p. 253).

The convectional type may be more indicative of closed magma chambers, while the fresh injection type would be more common in open* or developing magma chambers.

Cyclic units in the Kalka layered sequence are described in Chapter 7.

From the overall variation in cumulus mineralogy and composition with stratigraphic height it can be inferred that the changes are of a progressive nature consistent with normal fractionation (see Chapter 8). The cycles can therefore be interpreted as forming by repeated convectional half-overturn with associated progressive differentiation both within and between cycles.

A study of the chemical cycles, however, shows several reversals of the expected trends viz. Cycles 3 → 7 via transitional cycles 4, 5 and 6; Cycles 8 → 9; Cycles 10 → 11; Cycles 15 → 16 and Cycles

---

* Those which act as staging points for volcanic sources.

18 → 19. Such reversals probably result from injection of fresh magma into the chamber although internal melt inhomogeneities could also be the cause. The fact that the types of cumulus phases at these reversals do not necessarily return to those of the oldest cycles is probably due to dilution of the fresh magma by the host melt to a less basic composition (Fig. 27D). Mixing (for either fresh injection or convectional half-overturn) accompanied by continuous crystallization is indicated by the sharp (but still gradational) increase in plagioclase composition between cycles in some cases (e.g. Cycles 9 to 10).

It is considered that the best explanation for the cyclic units in Kalka is one of convectional half-overturn combined with occasional fresh injections of magma following Cycles 3, 8, 10, 15 and 18. The most important periods of injection occurred after Cycles 8, 10 and 18.

An indication of the relative volumes of fresh magma introduced to the crystallization zone can be gained by comparing the stratigraphic thickness of each cyclic unit and its degree of chemical fractionation. For example, Cycle 4 is 100 metres thick with plagioclase variation $An_{73} \rightarrow An_{67}$ (i.e. $\Delta An/\Delta T = 0.06$), whereas Cycle 7 is 450 metres thick with plagioclase variation $An_{76} \rightarrow An_{71}$ (i.e. $\Delta An/\Delta T = 0.011$). This would indicate that Cycle 7 was derived from about six times the volume of fresh magma than Cycle 4.

It can be seen in Fig. 13 that while olivine chemical cycles are synchronous with the modal cycles as might be expected, the plagioclase chemical cycles are in many cases consistently displaced upwards in the Kalka layered sequence. This is suggestive of differential settling,

and means that plagioclase cycles tend to overlap into the next younger cycle (e.g. Cycles 9 and 10). Such overlap can also result in "felsification" of the lower members of each cycle. For instance Cycle 14 consists of mesonorite, olivine melagabbro, dunite and olivine mesogabbro.

Convectional half-overturn with associated beheading of Cycle 1 and debasing of Cycle 2 in the Ewarara Intrusion is considered to be adequately explained by convectional half-overturn (Goode and Krieg, 1967).

1. Comparison between large scale cyclic units and small scale layering

Much of the layering described is visible by virtue of the separation of plagioclase from pyroxol. Since this separation can be caused by both differential settling (i.e. small scale layering) and by fractionation (i.e. large scale cyclic units), it is important to be able to differentiate them when the cyclic units are not internally layered (i.e. the cyclic unit has crystallized by continuous nucleation). This can be extremely difficult as both differential settling and fractionation are active in both cases. However, as a general rule differential settling is more pronounced, and chemical fractionation less pronounced in the small scale layering. The cyclic units are also usually much thicker.

It can be seen, however, that any division between the two is somewhat arbitrary.

2. Lateral Facies Changes

The base of the Olivine Gabbro Zone was previously defined as occurring at the base of the first major olivine gabbro unit. By comparing Stratigraphic Columns No. 6 and 8 (Fig. 16), it can be seen that the base of the O.G. Zone in No. 8 Section lies stratigraphically about 250 metres above the base of the O.G. Zone in No. 6 Section.

Furthermore it can be observed from Fig. 16 that the O.G. Zone reaches its maximum thickness of about 600 metres in the central parts of the intrusion (e.g. Sections No. 5 and 6), thinning to the east and west. In fact olivine has not been observed in No. 3 Section (below the granulite sliver) and is only a minor mineral in No. 4 Section.

There is no evidence and little likelihood that lateral current winnowing could have caused the distribution of olivine in such a manner.

The disappearance of olivine to the west is associated with a lack of development of cyclic units (e.g. see lower part of Stratigraphic Section No. 4, and Stratigraphic Sections 2 and 3).

Since olivine appears to develop as an advanced fractionation product in the cyclic units (Chapter 12), its distribution would appear to indicate the following:

1) fractionation was most intense in No. 5 and 6 Sections as the O.G. Zone is thickest there

2) fractionation advanced to the olivine-bearing stage first in No. 5

Section, then No. 6 Section and finally Nos. 8, 9 (and 10 and 11?) Sections i.e. the area of olivine crystallization gradually enlarged with time towards the east.

3) the lack of olivine (an indicator of fractionation) and cyclic units (indicators of repeated fractionation cycles) in the west could be related to the proximity of the intrusion wall (indicated by the northeastern granulite outcrop). In this area more vertical current activity might be expected. This would result in more continuous mixing, preventing extreme fractionation and causing the formation of a uniform rock series.

10.2.3 Secondary Sedimentation Structures

Some of the features described in the Kalka layered sequence have morphological similarities to structures in normal sedimentary rocks, and have been described and named on the same basis. Similar features have been observed in many igneous intrusions and it seems reasonable to assume that processes similar to those operating in aqueous or aeolian environments were responsible for the formation of at least some of these structures.

They have been termed secondary sedimentation structures as they are interpreted as having been formed by post-depositional redistribution or removal of cumulus sediments before complete consolidation.

Secondary structures have been further subdivided into two groups:

(a) reworked — involving interaction of sediment and melt at the bed

surface during or after deposition, with the formation of either erosional or non-erosional interfaces (e.g. cross-stratification, ripples). Some of these structures are known as bed forms* in aqueous sedimentation. Examples of bed forms include large and small scale ripples. From the definition it can be seen that cross-stratification is not a bed form. However, it is widely considered that many forms of cross-stratification result from the migration of "avalanche faces" of sand such as occur on the slipface in advancing ripples (Allen, 1963, 1965; McKee, 1966).

(b) modified — involving redistribution of sediments as a result of internal instabilities (e.g. slumps, load casts). Although slumps are widely reported in layered intrusions (Table 20), none have been recognised in Kalka or Ewarara.

1. Reworked Structures

The existence of erosional surfaces in parts of the Kalka layered sequence indicates that at least at certain times currents were active in the intrusion, and more particularly at the depositional surface. It would be useful to know the nature of these currents and their velocities in the magma.

---

* "A bed form is any deviation from a flat bed that depends on its origin on an interaction between a bed material and a fluid flow such that there occurs a spatially non-uniform transfer of material from bed to flow or between bed and flow. The occurrence of bed forms is independent of the precise nature of the fluid and also of the nature of the bed material" (Allen, 1968a).

The currents would of necessity have to be approximately parallel to the depositional surface, at least in the cases being considered. Their existence would probably arise during periods of mass instability in the melt. Three causes will be considered viz. convection (due to temperature differentials in the chamber), fresh magma injection or turbidity currents (mass instability due to load of suspended crystals).

It has previously been shown that the deposits typical of turbidity currents are not present in Kalka (cf. Kuenen, 1953; Irvine, 1965). It has also been shown that there is evidence for only a few restricted fresh injections of magma into the system. On the other hand it would be quite reasonable to assume that convection was active in a body the size of Kalka both from Jackson's (1961, p. 96) intuitive reasoning and from Bartlett's (1969) theoretical approach. From a study of the Raleigh Number, Ra_h, Bartlett has shown that the condition $Ra_h^* > 1700$, necessary for convection to occur, is obeyed by all igneous intrusions greater than 15 metres thick for viscosities up to 10^8 poise.

Convection currents have previously been postulated to have occurred in many intrusions e.g. Daniels (1967), following a study of cross-stratification in the western Giles Complex, suggests that the inferred current directions are consistent with a number of convection cells in the bodies.

---

* $$Ra_h = \frac{L^4 \alpha_T g \beta \rho m}{r_L K}$$

where L is thickness (in cm); α_T is thermal expansion coefficient; β is vertical temperature gradient (in $^{o}Kcm^{-1}$); K is melt thermal diffusivity.

Two types of currents will now be considered viz. broad, gentle currents and localised, vigorous currents. The former have previously been invoked in the discussion of cyclic units and probably are the most common. However they are probably neither strong enough or limited enough in areal extent to account for the localised erosional and depositional features described in Chapter 6. The close association of markedly lenticular layering, cross-stratification, asymmetric ripples, strong sorting and lateral facies changes in part of West Kalka (Chapter 6.3.4), together with the possible scour channel in Kalka Gorge (Chapter 6.3.2), suggest the presence of occasional strong, localised channel-type currents. These probably have a convection origin, but the deposits resulting from their actions are similar to those of alluvial origin. A similar classification of currents has also been made by Hess (1960) and Wager (1963).

(1) Formation of reworked sedimentary structures

The most important factor in determining the mode of sediment transport is the mobility of detrital material. In the igneous case, the mobility of the settled crystals will depend on their size, density and shape (i.e. their fall velocity), the degree of interstitial crystallization (i.e. the degree of cohesion) and the properties of the melt (e.g. viscosity, density, flow type and velocity). Sedimentary transport will be as bed load (comprising contact and saltation loads) and as suspended load.

Flow in a straight, open channel can be characterised by the

Reynolds and Froude Numbers, R_e^* and F^* (Allen, 1965; Briggs and Middleton, 1965). A combination of the critical R_e and F values (Fig. 28A) gives rise to four flow regimes, only two of which are important in aqueous channels. These are rapid turbulent and tranquil turbulent. The flow regime can also be divided into upper and lower flow regimes on the basis of surface roughness (Allen, 1965). Simons and Richardson (1961) have shown that the effective Froude Number seems to decrease with an increase in the scale of the system.

Allen (1965), Harms and Fahnestock (1965) and others have shown that the type of bed form developed in open channels is dependent on the flow regime or more directly, the Froude Number (Fig. 28B). Because of the obvious distinctions between aqueous and basalt systems, it is likely that absolute comparisons between the two would not be justified. This is supported by an arbitrary examination of the effects of certain parameters on particle mobility (and hence F) in basalt/pyroxol - plagioclase and water/quartz systems (Table 19B) which demonstrates that in the basalt system particle mobility will be significantly greater than in the aqueous system. Hence Froude Numbers associated with any particular bed form will be effectively decreased in the basalt system. However, relative comparisons would still seem to be reasonable for the relationship between F and the development of bed forms.

---

* $R_e = \frac{v r_h \rho}{\eta}$ $\qquad$ $F = \frac{v}{\sqrt{gd}}$

where v is flow velocity, d is depth, r_h is hydraulic radius (area of cross-section divided by wetted perimeter for channel flow).

It may be important that in the aqueous case, the upper flow surface is a definite hydraulic interface (i.e. water-air) whereas in the basalt case this interface is not so marked. However, Allen (1968b) has recorded ripples forming within a closed water pipe suggesting that the nature of the upper interface is not of prime importance.

(2) Interpretation of Kalka and Ewarara structures

(a) Ripple marks

The ripples observed in West Kalka are thought to result from current action on a granular bed of cumulus plagioclase crystals. In terms of bed forms, they belong to the lower flow regime. Their interpretation as small or large scale ripples cannot be made, however, as not enough comparative data is available, and direct comparisons cannot be made with aqueous and aeolian examples. The ripple parameters which were measured cannot be directly compared with Tanner's (1967) data for similar reasons although they would be consistent with a current origin.

It is worthwhile noting that angles of up to 35^{o} (relative to layering) have been measured for the slip faces of the asymmetric ripples in West Kalka. Ferguson and Pulvertaft (1963) have reported that 45^{o} appears to be the maximum angle of rest in the Nunarssuit Intrusion, Greenland. Upton (1960) gives 40 to 50^{o} as the angle of rest for Kûngnât syenites, while in the Rhum Intrusion 15^{o} appears to be the maximum angle of rest for ultrabasic cumulates (Brown, 1956). The maximum angle of repose for sand in aqueous sediments has been recorded as 34 to 36^{o} by Potter and Pettijohn (1963), whereas McKee (1966) found that in aeolian sand dunes the repose angle varied from

30 to 34°.

(b) Cross-stratification

As stated previously, cross-strata are thought to develop by migration of "avalanche faces" of granular material. Conditions such as these exist in advancing ripples or deltaic fronts. In the Kalka examples their formation was preceded by erosion of pre-existing layering and their relationship to migrating "avalanche faces" is not proved.

It is also very important to note that erosion followed by deposition to form cross-strata can occur in vertical pipes by non-sedimentary processes (Philpotts, 1968; Peterson, 1968; Wilshire, 1969).

Irrespective of their mode of formation, cross-strata with erosional boundaries give an indication of the depth of consolidation of the cumulus sediment. Ferguson and Pulvertaft (1963) indicate that this depth was at least 2 metres for parts of the Nunarssuit Intrusion. In West Kalka the depth was at least 25cm. This has very important implications. It indicates that interstitial crystallization was probably far from complete at depths of 25cm. However, since the rock types at this depth are anorthositic and are required to form by adcumulus processes, the interstices at this depth must have been in diffusional contact with the overlying melt. This therefore indicates that melt diffusion can occur through at least 25cm of cumulus aggregate.

(c) Scour Channel

The scour channel in Kalka Gorge (Chapter 6.3.2) is developed in

a rhythmic succession of small scale mesonorite and anorthositic bands, suggestive of repeated crystallization bursts. However, the lowermost unit in the channel is of anorthositic composition, and the associated preceding mesonorite layer is apparently missing. The following sequence of events is therefore postulated:

i) discontinuous nucleation cycles giving rise to mesonorite (cumulus pyroxene, plagioclase) and anorthosite (cumulus plagioclase) layers on differential settling (Fig. 25B1)

ii) development of fresh cycle, with settling of pyroxene and plagioclase with some plagioclase still in suspension (Fig. 25B2)

iii) channel erosion by strong, localised bottom current (Fig. 25B3). Depth of unconsolidated sediment was at least 1 metre.

iv) continued settling of plagioclase in static conditions to form basal anorthosite band (Fig. 25B4)

v) development of continuous crystallization to fill remainder of scour with unlayered mesonorite (Fig. 25B5).

Scour channels (and related trough banding) are also found in other intrusions (Table 20), including vertical pipes (Philpotts,1968).

(d) Pyroxene lenses

The small lenticular pockets of pyroxene crystals in Ewarara (Chapter 5.4.1) are thought to result from current concentration into depressions in the cumulus pile. The igneous lineation present in some pockets further supports this hypothesis.

(3) Calculation of current velocities

Williams (1969) has used the relationship between F and bed forms to calculate floodwater velocities in central Australia, and an attempt was made to apply this method to the localised Kalka currents. However, the lack of hydrodynamic equivalence between basalt and water systems made this impossible.

However, another sedimentological method for determining current velocities was possible. It was assumed that for erosion and movement of bed material in lower flow regime conditions current velocities would approximate settling velocities of the bed material.

The relationship between sediment transport, flow velocity and grain size for aqueous sedimentation is shown in Fig. 28C. From this data the minimum transport velocity should be of the order of $\frac{1}{2}$ magnitude higher than the particle settling velocity. For currents producing the lower flow regime structures in West Kalka, the maximum current velocity would be less than one magnitude higher than the minimum transport velocity (by comparison with Allen's, 1965, data).

From these calculations, for melt currents producing lower flow regime structures in pyroxol/plagioclase (2 - 5mm grain size) cumulates, lateral current velocities would be of the order of 10^{-3} to 5cm/sec (more probably 10^{-2} to 1cm/sec). The velocity of the current producing the scour channel would be greater than about 10^{-1}cm/sec. Similar velocities would be required to concentrate the coarse pyroxene lenses in Ewarara.

The lack of lower and upper flow regime bed forms in most of the remainder of the Kalka layered sequence suggests that current activity in the vicinity of the floor (if at all present) was not great.

Shimazu (1959), from theoretical calculations based on convection in the Skaergaard Intrusion, suggested vertical flow rates of the order of 10^{-2}cm/sec. Shaw (1965) suggested vertical convection velocities of the order of 3×10^{-4}cm/sec to allow heat transfer to occur in a large ($1km^3$) granitic body. Larger velocities could occur for smaller convection cells.

In the western Giles Complex, Daniels (1967) has suggested that convection currents could cause accumulation of economic minerals such as chromite or magnetite in the centres of the bodies. For the current velocities calculated for Kalka, transport of chromite and magnetite grains up to about 3mm in diameter could be accomplished. However, the general lack of cumulus chromite in basal Giles Complex sequences (e.g. Ewarara) suggest that such accumulations of chromitite would be lacking.

2. Modified Structures

(1) Production of load casts

In aqueous sedimentation load casts are produced when a more massive layer (e.g. sand) overlying a less dense layer (e.g. clay) becomes unstable and parts of it sink into the underlying layer. Generally the upper surface of the more massive layer remains relatively smooth.

In the Johnson Creek example (Chapter 6.3.3), the denser melanorite layer appears to have settled into the mesonorite layer in a similar fashion. The structure gives a younging direction consistent with other criteria.

No other modified structures have been observed in Kalka although disturbed layering is found in some areas, especially in the Norite Zone (Chapter 6.3.2). However, these may have tectonic origins rather than sedimentary ones.

10.2.4 Cumulate Fabrics

The cumulate fabric of any rock is assumed to result primarily from the cumulus morphology. Three morphologies will be considered: equidimensional, tabular and elongate. Pyroxols are usually equidimensional to tabular, although sometimes elongate pyroxenes are observed. Plagioclase is usually tabular to elongate.

The cumulate fabric results from the morphological orientation at five stages.

1. At nucleation: nucleation orientation is assumed to be random. Petrofabric data from Brothers (1964, p. 259) for tabular plagioclase tend to support this. Tabular monoclinic crystals have two possible positions of rest — both are equally represented in Rhum cumulate fabrics, suggesting initial random orientation of nuclei.

2. During settling: in a static melt, initial particle orientation is stable for symmetric particles (McNown and Malaika, 1950). However,

in laminar flow tabular crystals will align themselves within the flow planes and rod-like crystals parallel to the flow direction (Goldsmith and Mason, 1962).

3. On settling: the moment of settling is usually accompanied by a physical reorientation of the crystal as it comes to a stable rest position. Tabular and elongate crystals will tend to form a planar lamination (assuming a relatively smooth horizontal floor).

4. After settling (at cumulus-melt interface): current activity at the interface may reorientate elongate crystals into a lineate lamination.

5. After burial (below cumulus-melt interface): post-depositional consolidation will tend to increase planar lamination for tabular and elongate crystals.

The contribution of each of these stages in static and laminar current flow conditions to the overall cumulate fabric is shown in Table 21. Of course, minerals with different morphologies may have different fabrics within the same rock.

The cumulate fabrics from Kalka and Ewarara vary from isotropic to planar laminate for pyroxol. Rare lineate lamination is observed for pyroxene in Ewarara. Plagioclase fabrics are planar laminate to varying degrees. A slight lineate lamination has been observed in an olivine gabbro plug near Ewarara (A301-153). The fabrics are directly related to cumulus morphologies, and are interpreted as forming by the processes described above.

The degree of development of a lamination can depend on several variables:

1. crystal shape: the greater the degree of tabularity (or elongateness), the better the lamination
2. proportion of equidimensional to tabular/elongate crystals
3. current activity during or after settling. The development of a lineate lamination after settling would require much greater current velocities than those required during settling. Currents may also aid the development of a planar lamination by helping compaction.
4. consolidation effects, e.g. load compaction, seismic compaction.

Although little petrofabric work has been done on cumulates (Brothers, 1964), it would appear from the literature that lineate laminations are rare. This is probably due primarily to the general lack of lineate cumulus minerals, although lack of current activity may be a further reason. Moore (1970a) has reported lineate lamination in pyroxenites from Gosse Pile, while Brothers (1964) has observed it in Rhum and Skaergaard cumulates. Jackson (1961) has observed a lineate lamination for bronzite in Stillwater, and Ferguson (1969) has described similar fabrics in the Bushveld Complex.

In the Rhum rocks, Brothers has suggested that a lineate lamination in plagioclase-rich rocks, and a planar lamination in olivine-rich rocks, indicated current activity during plagioclase deposition but not during olivine deposition. However, the lack of lineation in the olivine rocks could simply be due to the tabular habit of olivine.

The relationship of elongate grain orientation to current direction is interesting. Brothers reports in Skaergaard that plagioclase is elongate parallel to the current (as would be expected), but interprets both plagioclase shape and current direction in Rhum to show that plagioclase is elongate perpendicular to the current.

Many authors have considered the alignment of tabular or rod-like minerals to indicate melt flow during crystallization. However, it should be remembered that similar fabrics can be formed by gravity settling as shown. It is unfortunate that Brothers (1959) and others have apparently overlooked the latter mechanism in interpreting planar laminate fabrics in layered basic rocks.

There are means of discriminating the two mechanisms, however. Flow controlled laminations are usually parallel to a bounding surface (e.g. a contact) and may be of any attitude. On the other hand, gravity controlled lamination, may have variable angular relationships to contacts but approaches a horizontal attitude. In cumulate fabrics, cumulus grains are in contact whereas in flow textures aligned phenocrysts are usually separated by the groundmass. A typical flow texture for potassium feldspar in the Taratap adamellite near Kingston, South Australia is shown in Plate 27D.

10.2.5 Ewarara vertical layered horizons

The vertical layered horizons at Ewarara are a major problem in interpretation as they are perpendicular to the fine scale layering and the major rock-type distribution elsewhere in the intrusion (Chapter

5.4.2). Several mechanisms for their formation have been considered by Goode and Krieg (1967) but are more fully discussed here.

1. Tectonic layering

The production of the layering by tectonic movements associated with the nearby contact is not supported by the presence of igneous textures and compositional layering.

2. Multiple injection

The lack of cross-cutting relationships does not support the hypothesis of multiple injection of Type 1 bands into the Type 2 host.

3. Wall crystallization

With variation in physico-chemical conditions during crystallization it might be possible to build up a compositionally layered sequence on the contact wall. However, the presence of cumulate textures and hourglass orthopyroxenes (which require complete freedom of growth on all faces to form — Chapter 9.1.2) constitute evidence against such an hypothesis. Also it is hard to imagine local and repetitive changes in crystallizing conditions that would produce neighbouring layers of differing mineralogy when only one such change occurs in the gravity-formed part of the intrusion.

4. Folding of gravity-settled layering

It is also possible that originally horizontal layering formed by gravity-settling processes (as occurs elsewhere in the body) was folded

into a vertical position together with the originally horizontal contact. Mesoscopic F_2 folds have been observed both in the pyroxenites and in the granulites in the intertongued zone near the southern horizon.

However, a wide variety of evidence does not support such an hypothesis.

(1) The contact associated with the vertical layering is characteristically intertongued with the granulite in direct contrast to planar transgressive contacts associated with horizontal layering elsewhere in Ewarara. The intertonguing appears primary (i.e. not formed by F_2 fold culminations). South of the southern vertical horizon intertonguing is in close proximity with horizontal layering in the body. The granulites maintain a constant macroscopic attitude throughout this area (Plates 2, 3). Furthermore about 1½ kilometres to the southwest of the intertongued zone, along strike from the vertical horizons (and the proposed F_2 culminations), horizontal layering is undisturbed (Plates 3, 4). The granulites themselves show no evidence of major fold closures (note: granulite layering is not coincident with F_2 axial planes, and would not remain planar on folding).

(2) The fact that the layering cannot be traced around the tongues of granulite penetrating the body, but is closely associated with them, seems to indicate further that the tongues do not constitute F_2 culminations but have some control on the formation of the layering.

(3) The lack of olivine orthopyroxenite (the basal unit in the horizontal sequence) at the contact near the vertical layering provides further evidence against the folding hypothesis. Of course, folding may

have preferentially occurred where this layer was thin or non-existent, but this is not probable as the Olivine Bronzitite Zone has a wide lateral extent in the rest of the body.

(4) The layering has no counterpart in any of the horizontally layered sequence. Phase contacts associated with fine scale layering have only been observed in the vertical horizons.

(5) In the Ewarara area, in general, macroscopic F_2 folds are observed to have an average wavelength of about two miles (Thomson, 1964). However, the vertically layered horizons are only about one mile from a major F_2 antiform.

It is therefore concluded that the evidence does not support an hypothesis of rotation of horizontal layering to a vertical position by F_2 folding.

5. Flow differentiation

The mechanisms and applications of flow differentiation processes are reviewed in Appendix 5. If a mechanism of the flow differentiation (axial migration?) type caused the vertical layering in Ewarara, the solid phase may have been derived by flowing magma from a fresh injection stirring up the settled but unconsolidated olivine and bronzite of the lower Olivine Bronzitite Zone. The olivine in the Type 1 bands has the same composition as olivine from the Olivine Bronzitite Zone, and hour-glass zoning of the type found in orthopyroxenes from the Type 1 bands and the Olivine Bronzitite Zone has not been observed anywhere else in

the Giles Complex. The imperfect segregation of cumulus phases in the banding could be expected in such a mechanism.

Goode and Krieg (1967) postulated that magma flow occurred along the steep southern contact on the basis that this was the most structurally favourable position for injection to occur. Later mapping by the author has revealed the presence of transgressive norite, harzburgite and mafic pegmatite near this contact. In fact this transgressive body continues the en echelon pattern (related to intertonguing) established by the two vertical layered horizons (Fig. 2).

This mechanism, however, has difficulty in explaining the formation of such a large number of bands (over 20 in part of the horizons), and the lack of olivine in some Type 1 bands.

Furthermore, if Type 2 bands represent the separated liquid it is difficult to explain their ultramafic composition (identical to the surrounding gravity settled pyroxenite) and their cumulate textures. Also the mechanism requires the presence of a confining north wall although this may have been formed by Pyroxenite Zone gravity-settled cumulates. The preservation (or freezing) of Type 1 bands during crystallization of Type 2 is also difficult to understand.

6. Mush flow

The layering may have also been produced by differential viscous flow of a crystal mush along the steep southern contact. Wilshire (1961) has invoked such a mechanism for the production of layering in diatremes.

The mechanism would probably require an initial compositional inhomogeneity, but this would already exist in the horizontal layered sequence providing the material. Some form of disruptive mechanism may be indicated by the presence of the possible cognate xenolith. Alper and Poldervaart (1957) have suggested a similar mechanism to produce banding in a porphyritic quartz monzonite stock in New Mexico. The formation of vertical banding in the Troodos massif has also been ascribed to the same mechanism (Gass and Masson-Smith, 1963).

Such a mechanism would overcome the difficulties of the number of bands, and the texture and composition of the Type 2 bands (i.e. most of the objections to the flow differentiation hypothesis). It would still, however, not be able to explain the lack of olivine in some Type 1 bands, unless pure orthopyroxene (hourglass zoning type) cumulates exist within or below the Olivine Bronzitite Zone. Orthopyroxene phenocrysts (without olivine) have been observed in the chilled margin to the body.

Of the mechanisms considered the mush flow hypothesis, and possibly the flow differentiation hypothesis, are preferred.

10.3 Interstitial Igneous Layering

It might be suspected that variations in intercumulus crystallization would be controlled by two surfaces — the cumulus-melt interface (normally parallel to cumulus banding) and the melt-country rock interface — since this controls the distribution of isotherms. In sheet-like intrusions the two are often parallel. The cumulus-melt interface

is probably the most important since this controls the composition of the trapped liquid and diffusional processes between this liquid and the free melt.

The banding associated with clump textures in the Anorthosite Zone of Kalka (Chapter 6.3.4) is a compositional as well as a textural one, and presumably is related to the composition of the trapped melt. The reason for the elongation of clump plates parallel to the gross layering is not understood, but is probably also controlled by the cumulus plagioclase fabric.

The only other example of interstitial layering is found at Ewarara where variations in modal interstitial plagioclase are observed (Goode and Krieg, 1965).

Dunham (1965) has described a form of interstitial layering at Rhum, which he associates with cooling variations and hence is parallel to the intrusion contacts. Robins (1969) has also recorded matrix layering in the Melkvann Complex of northern Norway.

CHAPTER 11

CHARACTERISTICS OF HIGH PRESSURE CRYSTALLIZATION

An important aspect of the present study has been the recognition and description of the high pressure environment of crystallization of the Ewarara and Kalka layered intrusions. The high pressure criteria first reported by Goode and Krieg (1967) for Ewarara have been expanded and revised during this investigation. The Giles Complex intrusions in both the Tomkinson and Musgrave groups which possess high pressure characteristics are unique amongst other layered intrusions, and possess significantly different fractionation trends as a result of the high pressures of crystallization (see Chapter 12). Many of the minor intrusions in the study area also possess high pressure characteristics.

The features on which the evidence for high pressure crystallization of Ewarara and Kalka is based are as follows*.

1. Olivine - plagioclase subsolidus reaction

The occurrence of double coronas of orthopyroxene and clinopyroxene/spinel between olivine and plagioclase is described in Chapter 9.3.2, and interpreted as a subsolidus reaction:

olivine + plagioclase $\longrightarrow$ orthopyroxene + clinopyroxene + spinel.

These coronas have been observed in the Kalka Intrusion, in the transgressive medium-grained gabbros and in the Type D dolerite dykes (at

---

* Throughout this thesis, the use of experimental data is subject to the normal problems of applying such results to geological phenomena (e.g. water content, rock composition etc.), and also to internal errors related to experimental precision (see also discussion by Richardson, 1970, p. 66).

Ewarara).

The reaction has been interpreted as resulting from cooling at constant pressure after crystallization. The experimental data for the reaction is reviewed in Chapter 9, and given in Fig. 29C. It was concluded that, for reaction temperatures in excess of 800°C, reaction pressures would be greater than 8 kilobars (Note: $\Delta P/\Delta T \simeq 1$ kilobar/200°C).

2. Orthopyroxene - plagioclase subsolidus reaction

Gray (1967) has reported garnet coronas between orthopyroxene and plagioclase in parts of the Teizi Intrusion and in some Type B dolerite dykes. Garnet is also rarely observed with similar associations in one Type B dyke at Ewarara (Chapter 3.1.2) and in a small garnet pyroxenite intrusion (Chapter 3.10).

The reaction is probably very similar to the olivine - plagioclase reaction, occurring during cooling at constant pressure as an auto-metamorphic process. The general lack of reaction in the Ewarara - Kalka area could be due either to the regional decrease in pressure to the west (suggested in Chapter 2) or to compositional differences.

Experimental data for the reaction is plotted on Fig. 29B. The most useful experimental work is that based on natural rock compositions and this appears in the present case to give more realistic P-T estimates than Kushiro and Yoder's (1966) data for pure anorthite and enstatite. It can, however, be easily seen that the conditions for the formation of garnet from pyroxene and plagioclase vary considerably with rock

composition e.g. compare T.H. Green's (1970) gabbroic anorthosite curve with Green and Ringwood's (1967b) quartz tholeiite curve. It appears that with increasing SiO_2 content, garnet appears at higher pressures or lower temperatures. Higher $^{MgO}/_{MgO + FeO}$ ratios also produce the same effect e.g. Green and Ringwood (1967b).

It is therefore considered impossible at this stage to accurately assess the P-T conditions of the observed reaction at Teizi and Ewarara although it would be consistent with high pressures. A high pressure origin would also be consistent with other similar reactions reported in the literature. Garnet rims on orthopyroxene in contact with plagioclase in basic igneous rocks have been observed by Sutton and Watson (1950), Dearnley (1962), Engels and Vogel (1966) and Griffin and Heier (1969) in high grade metamorphic terrains.

3. High Al_2O_3 content of pyroxenes

Both ortho- and clino-pyroxenes from Ewarara and Kalka have high Al_2O_3 and R_2O_3 contents, which, in Chapter 8, were interpreted as being indicative of crystallization in a high pressure environment.

4. Spinel exsolution in pyroxenes

Spinel exsolution in both ortho- and clino-pyroxene has been observed in the Ewarara and Kalka Intrusions as well as some of the minor intrusions e.g. transgressive picrite suite, transgressive norites, garnet pyroxenite, Type B dolerites and Type D dolerites (at Ewarara only). Such exsolution is considered indicative of high pressure environments

(Goode and Krieg, 1967; also Chapter 9).

5. Rutile exsolution in pyroxenes

Rutile exsolution in both ortho- and clino-pyroxene has been observed in the Kalka Intrusion and in some members of the Type B dolerites. Moore (1968) suggested that rutile exsolution in ortho-pyroxene was a result of cooling at high pressure, and this conclusion is also considered valid for clinopyroxene (Chapter 9).

6. Early crystallization of orthopyroxene

Evidence for the early crystallization of orthopyroxene at Ewarara is provided by the presence of orthopyroxene phenocrysts in the chilled margin of that body (Chapter 5). Furthermore, the base of the layered sequence* at Ewarara consists of orthopyroxene (containing olivine inclusions)** and olivine as cumulus phases. Similar cumulates have been recognised in the lower parts of Gosse Pile by Moore (1970a) although no basal contact has been observed there. The overlying parts of Ewarara and Gosse Pile, and the ultramafic sequence of Kalka are all dominated by the presence of cumulus orthopyroxene and, to a lesser extent, clinopyroxene. All major ultramafic sequences elsewhere in the Giles Complex are dominated by orthopyroxene e.g. North Hinckley, Murray Range (Nesbitt et al., 1970).

---

* The layered sequence at Ewarara overlies a basal contact and therefore represents the first phases deposited from the magma.

** Olivine inclusions are not observed in orthopyroxene phenocrysts in the chilled margin.

These features are rare in layered basic intrusions. Most layered sequences elsewhere begin with olivine (± chromite) crystallization.

Experimental work by Green and Ringwood (1964, 1967a) and Cohen et al. (1967) demonstrates the absence of olivine as a liquidus phase above 9 to 12 kilobars for olivine tholeiite compositions* (Fig. 30). The experimental work on the wide range of basalt compositions so far studied (see Fig. 30; also T.H. Green et al., 1967; T.H. Green and Ringwood, 1968; Ito and Kennedy, 1968) also indicates that orthopyroxene is only stable as a liquidus phase for some olivine tholeiite to alkali olivine basalt compositions at high pressure (Green and Ringwood, 1967a). In no basalt composition was orthopyroxene stable on the liquidus at low pressures. Evidence in Chapter 8 suggests that the Giles magma was tholeiitic; for these P-T calculations Green and Ringwood's (1967a) olivine tholeiite has therefore been chosen as an experimental equivalent composition as it best fits the observed features.

At 13 kilobars this liquid begins to crystallize orthopyroxene, while at 9 kilobars olivine is the first phase to form (Fig. 30A). At 11 kilobars olivine and orthopyroxene both form on the liquidus.

Thus crystallization at 10 to 12 kilobars would produce the initial cumulus precipitates observed at Ewarara while crystallization during magma ascent (say 13 kilobars) could explain the orthopyroxene phenocrysts

---

* The stability of olivine as a liquidus phase is extended to higher pressure for more undersaturated compositions e.g. picrite, olivine nephelinite (Green and Ringwood, 1967a; Bultitude and Green, 1967; Ito and Kennedy, 1968) whereas it is decreased for more saturated magmas e.g. high alumina quartz tholeiite (T.H. Green et al., 1967).

in the chilled margin. Pressure buildup in the magma chamber during intrusion because of an increasing head of basaltic liquid may explain the disappearance of olivine above the base of the ultramafic series and the continued sole precipitation of orthopyroxene, although fractionation or fresh injections of different compositions may also be important.

Liquidus and solidus temperatures for olivine tholeiite are 1350°C and 1200°C respectively for these pressures. However, small compositional changes (e.g. alkali content) can result in significant changes in the liquidus temperatures (Seifert and Schreyer, 1968; Green and Ringwood, 1967a).

The effect of water on the basalt liquidus is not considered important in the Giles situation because of the extremely anhydrous nature of the rocks (Chapter 8). If the small amount of water present was significant, however, orthopyroxene may be a stable liquidus phase at lower pressures. The importance of water on the stability of orthopyroxene in undersaturated melts has been discussed by Bultitude and Green (1967).

7. Distribution coefficients of co-existing pyroxenes

Moore (1970a) has shown that coefficients for the distribution of Mg and Fe^{2+} between orthopyroxene and clinopyroxene (K_D*) are

---

* $K_D = \left(\frac{Mg}{Fe^{2+}}\right)_{opx} / \left(\frac{Mg}{Fe^{2+}}\right)_{cpx} = \frac{1}{K_T}$ (Barthomelé, 1961).

significantly higher for Gosse Pile pyroxenes than normal igneous pyroxenes. Moore measured an average K_D value of 0.83 for 12 pyroxene pairs while the author has measured a distribution coefficient of 0.78 for one pyroxene pair (A300-121) from Ewarara. Saxena (1968) has reported a range from 0.501 to 0.647 (average 0.556) for metamorphic pyroxenes and from 0.536 to 0.857 (average 0.717) for igneous pyroxenes while Kretz (1961) reported average metamorphic and igneous K_D values of 0.54 and 0.73 respectively for pyroxene pairs.

Although it is apparent that K_D is dependent on composition and perhaps other factors, it is generally considered that its values are primarily controlled by temperature (e.g. Davidson, 1968; Zussman, 1968). Moore (1970a) therefore interpreted the Gosse Pile results to indicate unusually high crystallization temperatures for that intrusion viz. about 1400°C. Such crystallization temperatures are only found in basalts at high pressures (cf. Fig. 30, and previous liquidus estimation of 1350°C at 10 kilobars for olivine tholeiite (this Chapter)).

8. Thin chilled margins

Chilled margins to the layered intrusions are rare in the Complex, and are thin when present (order of centimetres at Ewarara and South Mt Davies). These features could indicate high country rock temperatures, which would in turn be compatible with intrusion at depth. However, it must be remembered that at best the temperature difference between the intruding magma (about 1350°C) and the granulite (400 to 1000°C — see Chapter 6) is considerable, and one might expect a larger chill. The

relatively large thermal conductivities of the granulites* would also tend to give larger chills.

Nesbitt (1966) has suggested that the lack of thick chilled margins may be due to high rates of heat transfer in the magma. An alternative suggestion which takes account of the actual injection and chill processes may have some application. It is thought that in the case of Ewarara, magma was accommodated by brittle fracture and uplift of a granulite block caused by forcible magmatic injection (Goode and Krieg, 1967). If so, magma would be chilled during injection along the initial fractures and, on subsequent movement of the block during its uplift, the chills could be mechanically destroyed. Further chills would not be formed because sufficient time would have elapsed for a thermal equilibrium to have been established between the magma and the country rock. Partial resorption of the chills by the magma may also have some application in explaining the lack of thick chilled margins.

9. Other features

The formation of garnet by reaction of spinel and orthopyroxene in a small garnet pyroxenite lens was described in Chapter 3.10. Although experimental data is variable the reaction is consistent with high pressure conditions, as indeed its occurrence in other areas would suggest (see Chapter 3.10).

The presence of spinel exsolution in plagioclase, and perhaps

---

* By analogy with conductivities for gneisses and granites (Clark, 1966).

opaque exsolution in pyroxene, may also be consistent with high pressure conditions (Chapter 9).

Discussion

Experimental data available for the observed phenomena, combined with the occurrence of comparable features in supposed high pressure natural rocks elsewhere, strongly suggest high pressures of crystallization for the Ewarara and Kalka Intrusions, and for many if not all of the younger minor intrusions.

Based essentially on the dominance of orthopyroxene as a liquidus phase in the Ewarara Intrusion but consistent with all the other data, these pressures are considered to be of the order of 10 to 12 kilobars. These pressures are equivalent to depths of crystallization of about 35 to 40km i.e. at the base of a normal crust.

These estimations are compatible with those calculated for the granulite country rocks (Chapter 2), supporting the structural data which indicates that no important crustal movements took place in the period between the two events. The profusion of basic intrusives in the area is also compatible with such a deep seated setting i.e. with proximity to the mantle.

It should be noted, however, that Nesbitt (1966), on the basis of orthopyroxene rimming olivine in the South Mt Davies Intrusion, has suggested relatively shallow (< 9km) depths of intrusion for the Complex. This estimate is based on experimental work in the system $MgO - SiO_2$ by

Boyd et al. (1964). These workers have suggested that olivine-liquid reactions to give orthopyroxene would occur at less than 5.4 kilobars or 20km (on thermodynamic grounds they would probably occur at less than 2.3 kilobars or 9km). Weedon (1965) has postulated such shallow depths of intrusion for some Scottish gabbros by applying this experimental evidence to coronal textures observed on olivine. This argument has been rejected by O'Hara and Stewart (1966) on the grounds that no evidence was presented to demonstrate that the reaction was an olivine-liquid reaction, and that results from the MgO - SiO_2 system have limited direct application to the crystallization of basaltic liquids. It appears that similar arguments could be used in rejection of Nesbitt's (1966) hypothesis.

Because of the areal extent of the Giles Complex it would be unwise, however, without specific local evidence, to assume that all the intrusions are high pressure varieties. Daniels (1967) has suggested that the intrusions become structurally shallower towards the west, a conclusion supported by Nesbitt et al. (1970) and in Chapter 15. In this context Nesbitt's (1966) hypothesis may still be to some extent valid as the high pressure features of Kalka and Ewarara are absent in South Mt Davies (apart from high R_2O_3 contents of pyroxenes).

High pressure characteristics have been observed in several other Giles Complex bodies and adjacent minor intrusions e.g. Gosse Pile (Moore, 1968, 1970a), Teizi (Gray, 1967). Several other intrusions from the Tomkinson group also display some features indicative of high pressure crystallization e.g. Claude Hills, North Hinckley, Morgan Range and Murray Range. Few data are available for intrusions from the Musgrave

group although some high pressure features have been observed in the Woodroffe Intrusion (R.B. Major, pers. comm.).

It is interesting to compare the Ewarara and Kalka Intrusions with the Stjernoy Intrusion of northern Norway (Oosterom, 1963). While Stjernoy displays many of the high pressure characteristics of the two Giles Complex bodies (e.g. olivine - plagioclase reactions, high Al_2O_3 content of pyroxenes, spinel exsolution in pyroxenes), its earliest precipitates are dominated by olivine and not orthopyroxene. This could be the result of slight pressure or composition differences.

CHAPTER 12

PETROGENESIS OF THE KALKA AND EWARARA INTRUSIONS

In common with other interpretations of layered basic intrusions elsewhere, the author considers that the differentiation of the Ewarara and Kalka Intrusions occurred by fractional crystallization on cooling. This process is linked with continuous removal of cumulus phases from the melt by gravity processes (full discussion in Chapters 8, 10). As shown in Chapter 8 progressive crystallization resulted in normal iron and sodium enrichment in ferromagnesian minerals and plagioclase respectively, although evidence of extreme fractionation is lacking.

However, the Ewarara and Kalka Intrusions are unusual in their development of high pressure characteristics (Chapter 11). These features invite their comparison with the classical low pressure tholeiitic suites such as Stillwater, Bushveld and Skaergaard. Normal low pressure crystallization of tholeiites leads to the early precipitation of olivine and chromite. Subsequent melt enrichment in SiO_2 results in the formation of late stage silicic residues e.g. granophyres. However, the early precipitation of orthopyroxene, the most important and unique consequence of the high pressure regime at Kalka and Ewarara, could be expected to give radically different trends*.

In these conditions SiO_2 depletion or undersaturation of the magma could be expected as orthopyroxene (and clinopyroxene) crystallization

---

* SiO_2 contents vary orthopyroxene > olivine tholeiite > olivine

proceeded. Furthermore the entrance of Cr_2O_3 into the pyroxene structure at high pressures (Chapter 8) could prevent the early formation of chromite, a mineral notably lacking in the Giles Complex (Nesbitt et al., 1970).

The increasing undersaturation of the melt with progressive crystallization could cause the precipitation of olivine instead of orthopyroxene. This could explain the presence of olivine (and spinel) high in the Kalka layered sequence i.e. the Olivine Gabbro and Anorthosite Zones (Chapter 6). Such a result is in direct contrast with processes active in the Stillwater Intrusion where Jackson (1961) believes that the early precipitation and settling of olivine and chromite caused the subsequent crystallization of orthopyroxene.

There are, however, several alternative explanations for the appearance of olivine midway through the Kalka sequence which should be considered.

Firstly decreasing pressure* with stratigraphic height could result in the formation of liquidus olivine. However, the interbanding of orthopyroxene cumulates with the olivine cumulates and the lack of olivine at the same stratigraphic level to the northwest of Walter Hill (Fig. 2) does not support such an origin.

Secondly the occurrence of cumulus olivine in the Kalka sequence is commonly associated with periods of fresh magma injection. The injection

---

* A pressure differential of 0.5 kilobars would have existed between the base of the Pyroxenite Zone and the base of the Olivine Gabbro Zone. Furthermore, olivine is stable to higher pressures in more undersaturated liquids.

of liquid of original composition (or more olivine normative), even allowing for dilution on mixing, may result in the liquidus precipitation of olivine because of the lower load pressure. However, the presence of interstitial olivine lower in the sequence than the "first" cumulus olivine in the Olivine Gabbro Zone* does not confirm that this is the sole reason for the appearance of cumulus olivine at that stage.

The formation of cumulus olivine midway through the Kalka layered sequence is therefore considered to result from increased melt undersaturation because of the early precipitation of orthopyroxene. Decreasing load pressure and fresh magma injections may have contributed to its occurrence (further discussion on the distribution of olivine in the Olivine Gabbro Zone is given in Chapter 10.2.2).

The suggested early depletion of SiO_2 in the melt could also prevent the development of classical late stage siliceous differentiates. The lack of acidic rocks is a characteristic and hitherto puzzling feature of the Giles Complex (Nesbitt, 1966). Small amounts of quartz have been observed in part of the Jameson Range Intrusion (Daniels, 1967) while Blight (1969) has reported that the uppermost unit of the Bell Rock Intrusion contains small quantities of interstitial quartz and K-feldspar. However, these occurrences are insigificant in view of the enormous volumes of basic rocks observed in the Complex. Nesbitt (1966) has suggested that the "unseen" acidic portions of the differentiated magma were extruded as the rhyolitic Tollu Volcanics (Fig. 1). However, the

---

* Cumulus olivine below the O.G. Zone in A314-145 is considered to be related in formation to the cumulus olivine at the base of Ewarara (see Chapters 6, 11).

author considers that these lavas are younger than and unrelated to the Giles Complex and that significant quantities of acidic differentiates were not formed from the Giles Complex by fractionation.

One of the most important features of the Kalka Intrusion is that it is the only Giles Complex body in which the complete rock series from pyroxenites through norites and olivine gabbros to anorthosites is observed. For this reason the rock sequences of almost every other Giles Complex body can be "correlated" in a broad manner with part of the Kalka layered series (Fig. 31). The pyroxenitic sequences of Murray Range, North Hinckley and Claude Hills are similar to Kalka's Pyroxenite Zone while Michael Hills is equivalent to the Norite Zone. Morgan Range contains rocks apparently transitional between Norite and Olivine Gabbro Zone type rocks, and South Mt Davies and Mt West sequences are similar to rocks from the Olivine Gabbro Zone. Hinckley Range is transitional from Norite to Anorthosite Zone equivalents while Bell Rock and Blackstone are very similar to the Anorthosite Zone. The bodies equivalent to the highest parts of the Kalka sequence are in general more chemically fractionated than those equivalent to the lower portions (Nesbitt et al., 1970).

It can therefore be seen that the major fractionation trend of tholeiitic magma in Kalka (i.e. enrichment in plagioclase relative to pyroxene, with eventual sole production of cumulus plagioclase) is a feature characteristic of the whole Complex. Such a trend is of obvious

importance in the problems associated with anorthosite genesis* (e.g. Isachsen, 1969).

Anorthosites are of two major types in the Giles Complex viz. the Bell Rock - Blackstone troctolitic or olivine-bearing type and the Teizi noritic or orthopyroxene-bearing type. Both of these types are observed in Kalka e.g. the troctolitic anorthosites of the Anorthosite Zone and the leuconoritic rocks of parts of the Norite and Anorthosite Zones (Chapter 6). Such a division seems applicable to most major anorthosite bodies of the world —

(1) olivine-bearing e.g. Michikamau (Emslie, 1969, 1970); Kiglapait (Morse, 1969)

(2) orthopyroxene-bearing e.g. Adirondacks (Buddington, 1969; de Waard and Romey, 1969); South Rogaland (Michot and Michot, 1969).

The latter type is commonly associated with more acidic rocks such as mangerites and charnockites, revealing a further affinity with the Teizi Intrusion which contains abundant antiperthitic feldspar. Such an enrichment in potassium feldspar is perhaps foreshadowed in the Kalka and Ewarara Intrusions where antiperthite is abundant as an orthocumulus product in the ultramafic rocks (see p. 201).

Such a modal division of anorthosites is also supported by chemical data, with the orthopyroxene-type tending to be more fractionated (e.g. Blackstone An_{70-60}, Teizi An_{60-45}; see also Anderson and Morin, 1969).

---

* Only thick anorthositic sequences with few associated ultramafic rocks are considered as anorthosites in this discussion.

In an alternative attempt at anorthosite classification, Berrangé (1965) has suggested that anorthosites form by two main processes: (1) crystallization of anorthositic magma derived from within the crust to produce "orogenic - plutonic anorthosites", (2) fractional crystallization of basaltic magma to produce "gravity stratified anorthosites". These two types differ in their environment, age, form, internal structures, textures, composition and associated rocks.

From the preceding descriptions of field relations, textures and geochemistry it cannot be doubted that the Kalka anorthosites are cumulate in origin and represent the late fractionation products of tholeiitic magma. However, they also display features of Berrangé's orogenic - plutonic association e.g. deformation, recrystallization and presence of antiperthite. Many of the orogenic - plutonic characteristics could be produced by deformation with complete or partial recrystallization of high pressure cumulate anorthosites under granulite-facies conditions. Such a process has already been envisaged by Windley (1967) and Gray (1967).

Indeed, Berrangé's classification has been criticised widely (e.g. Windley, 1967; Romey, 1968) on the grounds that in actual fact a complete continuum of anorthosites is observed. Many anorthosites display properties typical of both of Berrangé's types.

This is not meant to indicate that the differences recognised by Berrangé are not important. They are significant, but only in the sense that they indicate the presence or absence of modifying processes having acted on the original cumulate anorthosite.

Considerable speculation on the composition of the melt crystallizing the anorthosite is present in the literature*. Many writers consider the magma to have been originally anorthositic (e.g. Michot, 1964, 1969) because of the large volume of anorthositic rocks and apparent lack of associated ultramafic and mafic rocks. However, isotopic studies point to a genetic relationship with basaltic magma (Heath and Fairbairn, 1969; Taylor, 1969). The presence of major anorthositic sequences in differentiated tholeiitic magmas has long been known (e.g. Stillwater – Hess, 1960) and their formation as a result of basalt fractionation is well demonstrated in the Kalka Intrusion.

Nesbitt et al. (1970) have shown that, in general, the higher level Giles Complex intrusions are more fractionated than the lower level high pressure bodies. The higher level bodies are also dominantly anorthositic whereas many of the deeper intrusions are more mafic and ultramafic. Such a depth stratification of intrusions appears to indicate that the higher level bodies were derived from partially fractionated tholeiitic liquids at lower levels. Thus an original tholeiitic magma, by tapping of fractionating systems, can give rise to derivative liquids capable of crystallizing anorthosite sequences without associated mafic and ultramafic rocks. This conclusion removes many of the difficulties previously envisaged in the derivation of anorthosites from basalts and could well

---

* For the remainder of this discussion, anorthosites will be considered as cumulates formed by gravity settling of plagioclase. The formation of anorthosites by flotation of plagioclase has been previously suggested by some authors (e.g. Morse, 1969; Emslie, 1969, 1970) but has only been satisfactorily demonstrated for Flastadøy in Norway (W.D. Romey, pers. comm.).

apply to the large anorthosite provinces in the Adirondacks, Norway and eastern Canada.

Green (1969c) has concluded from experimental studies that a quartz diorite (andesitic) magma could also give rise to anorthosites, and it may be that anorthosites are derived from a range of magma compositions (although difficulty in distinguishing primitive from derivative liquids makes such conclusions difficult to make). Green also suggested that hydrous fractional crystallization of a basaltic liquid could not give rise to significant quantities of plagioclase-rich rocks, but did not consider the results of anhydrous crystallization of basalts. The common association of anorthosites with high grade metamorphic terrains may be significant. However, differentiation of basaltic liquids at low pressures also leads to plagioclase enrichment e.g. the Anorthosite Zone of the Stillwater Intrusion (Hess, 1960).

PART FIVE

STRUCTURE AND TECTONIC DEVELOPMENT OF PART OF THE EASTERN TOMKINSON RANGES

CHAPTER 13

STRUCTURE AND DEFORMATION OF THE IGNEOUS AND METAMORPHIC ROCKS

A wide variety of structures and fabrics have been recognised within both the granulite and igneous tectonites of the area. To facilitate their discussion it is perhaps best to define some of the descriptive terms to be used.

The term S-surface is used to denote penetrative planar (including curviplanar) structures (Turner and Weiss, 1963). S-surfaces of metamorphic or deformational origin are called foliations*. These are distinct from other structures in these rocks, often parallel to a foliation, which are defined by compositional differences and have significant thickness. These are termed layerings or bandings, and may grade into foliations as thickness decreases. Any fold phase is termed F and any lineation L.

The structures observed in this study** will now be described in order of decreasing age (evidence for relative age is given in Chapter 14). It should be stated here that the different deformations are recognised essentially on their different geometries (e.g. fold style) as well as their relative ages to other events and each other.

---

* Foliations denoted by S_y^x where x refers to rock type (m = metamorphics, granulites; g = Giles Complex; d = dolerite), y = 1,2,3 .... (refers to deformation episode). S_o refers to lithological layering.

** All structural data measured in this study are plotted on Fig. 2. Faults associated with the various dolerite dyke suites (Chapter 3.1) are not discussed in this section.

13.1 F_1 Folding

Macroscopic folds of this generation have not been observed as yet within the present field area. However, examples of this fold style have been previously found immediately south of the South Mt Davies Intrusion in the granulites (Nesbitt et al., 1970), and more recently near Gosse Pile (Moore, 1970a). Axial plane traces vary from NE trending in the Mt Davies area to NNW trending near Gosse Pile, and may result from an original difference in orientation of layering or from later rotation.

On a mesoscopic scale, the F_1 folds are intrafolial, commonly appressed (Nesbitt et al., 1970, Figs. 2a and 2b), with a fairly well developed axial plane foliation, S_1^m (parallel to S_o^m in fold limbs). This foliation is defined by a preferred orientation of flat, lensoid aggregates of quartz, feldspar and pyroxene (Plates 6A,B and 12B). Within some fold hinges thin quartz-rich lenses appear to have been deformed into many small rootless folds, producing a rodded linear structure containing remnant fold hinges or hooks (Nesbitt et al., 1970, Figs. 2c and 2d).

S_1^m is observed within the granulites at Ewarara and Kalka as lensoid aggregates of pyroxene, garnet or quartz/feldspar. It is developed parallel to the lithological layering S_o^m. Pseudo-cross-stratification ("hockey stick") structures are observed in parts of the acid granulites where apparent axial plane slip has caused the juxtaposition of limb and hinge areas of the fold. Rare mesoscopic intrafolial F_1 folds* are

---

* Distinguished from F_2 mesoscopic folds by parallelism of S_o^m and S_1^m, moderately steep plunge of fold axis, and isoclinal nature.

observed in this area (Fig. 32A).

13.2 Gneissic Foliation

A streaky foliation, S_1^g, is well developed in parts of the Kalka Intrusion (Plate 49A). It is defined by alternating parallel lenticular aggregates or single crystals of pyroxenes and plagioclase, and is therefore, more difficult to observe in hand specimen in mono-mineralic rocks (e.g. pyroxenites, anorthosites). It is usually accompanied by a strongly developed lineation, L_1^g, also related to the alignment of mineral aggregates of single crystals (Plate 56E). In some olivine - clinopyroxene rocks a localised ribbon foliation defined by lenticular grains is observed (Plate 53C). In some cases it is associated with brittle fractures and it is not certain if this foliation is related to S_1^g or to a later event.

Although generally parallel to the primary igneous layering, S_o^g, the foliation is also observed at low angles (up to 30^o) relative to S_o (Plate 49B), and can therefore be shown to post-date the crystallization of the Giles Complex.

In all the foliated rocks, the texture consists of large (generally 1 to 5mm long) porphyroblasts of pyroxene (and sometimes olivine) and plagioclase within a finer grained recrystallized matrix of the same minerals (Plate 53A). In the most deformed rocks, the texture resembles that of an augen gneiss (Plates 49A, 56D).

The porphyroblasts represent the deformed equivalents of the primary cumulus crystals — they are often subhedral tending to euhedral, and

contain exsolution and inclusion bodies characteristic of cumulus crystals in less deformed rocks. They are usually strained to varying degrees. Descriptions of the more extreme forms of single crystal deformation follow.

Although kinking of orthopyroxene is also found in rocks much younger than the gabbro gneiss, there is a definite association between the amount of kinking and the degree of deformation (represented by the development of the S_1^g foliation) in many of the Giles Complex rocks. The degree of kinking appears greater in the plagioclase-poor rocks. Examples of both simple and conjugate kink banding are shown in Plates 51A,B (terminology of Paterson and Weiss, 1966). The kink geometry is identical to that described elsewhere by many other authors. Adjacent kink planes are slightly oblique to each other, both approximately normal to [001]. Kink spacing varies in different specimens (compare Plates 51A,B). In many examples exsolution bodies (e.g. clinopyroxene, spinel) are massed along the kink plane (Plate 53E). It is thought these features formed by exsolution coalescence on straining of the lattice (since exsolution preceded recrystallization — Appendix 4) because of the lower free energies associated with the more strain-free areas near the kink planes. Kinking is thought to be formed by slip on the system (100), [001] (Carter and Raleigh, 1969). Recrystallization mosaics in some cases occur preferentially along certain kink bands (Plate 51C), and in extreme cases give rise to a parallel series of elongate (approximately perpendicular to [001]) optically continuous discrete crystals (Plate 51D).

Trommsdorf and Wenk (1968) have reported clinoenstatite within kink bands in similar rocks from Wingellina, about 50 kilometres to the west. Unlike the occurrences reported by Dallwitz et al. (1966) and Binns et al. (1963), this example is not the result of inversion from protoenstatite but is closely associated with the primary "orthoenstatite" and represents a unique terrestrial example of this polymorph. However, despite an intensive search, clinoenstatite has not been observed in the area under discussion.

Metamorphic clinoenstatite has long been observed in "squeezer" experiments and in meteorites and has been suggested to represent one of the few examples of a stress mineral i.e. one stabilised by shearing stress (e.g. Turner et al., 1960; Reiker and Rooney, 1967; Munoz, 1967). The experimentally determined polymorphic stability relations of enstatite are shown in Fig. 12C, although recent work by Schwab (1969) and Smyth (1969) suggest that these relations may be incorrect. It can therefore be seen that, although it is extremely rare in nature, clinoenstatite is stable at low temperatures and pressures. Borg and Handin (1966) and others have noted the appearance of clinoenstatite at high strain rates, while Raleigh (1967) has suggested that it may only be formed by deformation at strain rates which are fast by comparison with natural deformations. This has been recently supported by Coe (1970). Schwab (1969) has also noticed the increased stability of orthoenstatite with increasing Fe content.

The most extreme form of crystal deformation of orthopyroxene is only observed in a few specimens. Tenuous single crystal ribbons up to 17mm long and $\frac{1}{2}$ to 1mm wide (Plate 53A), and parallel to L_1^9, are rarely

observed in some rocks (general grain shape and size is stubby to equant, 2½ to 5mm long). Plagioclase inclusions commonly observed in less deformed orthopyroxene (Fig. 22A) are represented as thin recrystallized elongate ribbons (Plate 53A). Other crystals are also attenuated in a more inhomogeneous manner (Plate 53B).

These crystals are interpreted as having undergone extreme ductile elongation approximately parallel to [001] with associated flattening on the prismatic faces. Simple shear acting on the (100) glide planes in the [001] direction (Raleigh, 1965a; Carter and Raleigh, 1969) would result in "rectangular" crystals being deformed into "parallelogram" shapes (Figs. 32C,D). In these cases crystal elongation, originally parallel to [001], would become oblique to (100) and [001]. It has been noted in every example of extreme elongation that the clinopyroxene exsolution lamellae, parallel to (100), are at a slight angle to the elongation direction (Plates 53A,B) supporting this hypothesis. This form of deformation of single orthopyroxene crystals, to the author's knowledge, has not been described before from natural rocks.

It is perhaps appropriate at this point to distinguish various types of elongate orthopyroxene crystals. In undeformed single crystals, the pyroxene is normally elongate parallel to [001] (Fig. 32C). In the examples of "flow" orthopyroxenes the direction of elongation is slightly oblique to [001] (Fig. 32D), while orthopyroxenes representing relic kink bands (Plate 51D) are elongate approximately normal to [001] (Fig. 32E).

Kinking in clinopyroxene is observed in some instances (Plate 52A), with the kink plane approximately normal to [001]. By comparison with

orthopyroxene the kinking probably occurred by slip on (100), [001], the dominant translation glide mechanism (Carter and Raleigh, 1969). The development of multiple twinning in clinopyroxene may also result from glide on this system (Raleigh and Talbot, 1967) but no detailed work has been attempted on this problem.

A fingerprint texture in clinopyroxene from Ewarara (Plate 23C) is formed by trails of globular spinel inclusions (apparently coalesced exsolution rods) aligned approximately in (100). These textures are closely associated with recrystallized areas, and may represent an initial ordering of spinel exsolution in response to plastic flow on (100) glide planes prior to recrystallization of the strained lattices.

Kink bands or undulose extinction bands have also been commonly observed in olivine from deformed rocks throughout the area, particularly those affected by the gneissic deformation (Plate 52B). Similar bands have been described frequently elsewhere (e.g. Raleigh, 1965b; Challis, 1967). Raleigh (1968) has pointed out the dependence of slip mechanism on temperature and strain rate for olivine, but it has not been determined which mechanism was dominant in the present cases.

Plagioclase is not commonly found as relic crystals in the most deformed rocks. However, when observed it is highly strained. Extreme and abnormal elongation (measured maximum 35mm x $\frac{1}{2}$ - 1mm), parallel to L_1^g, is observed with accompanying strong development of undulose extinction zones and glide twinning (Fig. 32F). The two latter properties, along with rare kinking (Plate 52C), are observed in deformed rocks throughout the area of all ages but extreme elongation is only observed

in rocks containing the gneissic foliation. The elongation, like that in orthopyroxene, is assumed to occur by glide on (010), [001]* (Carter and Raleigh, 1969), and to the author's knowledge has not been described before from natural rocks. The kinking, with kink bands normal to (010), is also rare in nature (Carter and Raleigh, 1969), and is assumed to occur by the same mechanism. Recrystallization trains (Plate 52D) have been observed in the kinked plagioclase parallel to the kink planes and is thought to represent recrystallization of thin individual kink bands (cf. orthopyroxene). Unlike the natural kinks in plagioclase described by Seifert (1965), the density of albite glide twins changes over the kink planes (Plate 52D).

The finer grained (about 0.05 to 0.3mm) matrix surrounding and in some cases penetrating the porphyroblasts consists of pyroxene (and olivine where olivine is present as porphyroblasts) and plagioclase. Minor quantities of biotite and/or spinel and/or rutile and/or magnetite are observed in some rocks. They form a granoblastic mosaic of polygonal, equidimensional grains (Plates 53A,B). Triple point boundaries between grains are common in the coarser varieties with intergranular angles of about 120° being commonly measured on the flat stage. Grain boundary relations appear to be more complex in the finer grained varieties. Exsolution bodies and twinning are usually absent from the grains. They rarely exhibit undulose extinction, and the strain features commonly

---

* From a limited optical study of twin plane and magnetite exsolution orientation, the elongation direction appeared to be approximately (010), [001]. Like the orthopyroxene "flow" crystals, the elongation direction was sometimes at a low angle to (010) conforming to the model of simple shear.

present in the porphyroblasts (e.g. kinking) are not found. Glide twinning is rarely observed in plagioclase. These textures are more fully described and interpreted in Appendix 4. It was concluded there that the grains represent an annealed recrystallization assemblage from primary strained material similar to the porphyroblasts. The small quantities of spinel, rutile and magnetite represent the former exsolution bodies in pyroxene and plagioclase.

The fabric of the gneisses gives much information important in the interpretation of these rocks. As already stated the lenticular aggregates of recrystallized and porphyroblastic grains are aligned parallel to S_1^g and L_1^g.

The types of deformation experienced by the porphyroblasts are related to their orientation. Those orthopyroxene with [001] approximately parallel to S_1^g are highly elongate ("flow" crystals) and are interpreted as indicating that the principal elongation direction was parallel to L_1^g. Orthopyroxene with [001] approximately normal to S_1^g are either stable (with only marginal recrystallization) or are kinked. This is interpreted as indicating that S_1^g was perpendicular to the principal compressional direction. A strong preferred orientation of kink planes parallel to S_1^g is observed throughout Kalka (e.g. Plate 53D) and Ewarara (Goode and Krieg, 1965, Fig. 21). In some rocks kink planes in olivine also lie approximately parallel to S_1^g.

The texture of the matrix is interpreted as resulting from annealing recrystallization at high temperature. This process preferentially took place in the most strained grains and at grain boundaries. It appears

from a study of the porphyroblastic assemblages that the stability to recrystallization of primary crystals for a given deformation decreases from orthopyroxene to plagioclase to clinopyroxene. A strong crystallographic preferred orientation of recrystallized plagioclase was observed with the aid of a gypsum plate in sections normal to S_1^9 and L_1^9, but was not so conspicious in sections normal to S_1^9 and parallel to L_1^9. The annealing process therefore appears to have been syntectonic, a conclusion also reached by Moore (1970a) for similar rocks at Gosse Pile.

Pseudofolds have been observed in the foliation in some specimens. However on close examination the cores of these pseudofolds have always been found to contain porphyroblasts of either plagioclase (Plate 50D) or pyroxene. It therefore appears that the folds represent wrapping of a plagioclase layer around a plagioclase porphyroblast or pyroxene layer around a pyroxene porphyroblast. The relationship between unlike layers and porphyroblasts is shown in Plate 50C. The similarity between the two cases is easily appreciated. The development of "tails" of recrystallized grains on porphyroblasts (Plate 57C) produces a similar geometry. The presence therefore of lenticular recrystallized aggregates oblique to and bridging the normal S_1^9 lenses (Plate 57D) presents a difficult problem. Does this geometry represent a true monoclinic fabric in the rock or does it result from warping of the foliation around pre-existing porphyroblasts? In view of the previous descriptions it does not appear possible at present to distinguish the two cases.

In conclusion, the foliation is interpreted as representing a deformation fabric resulting from plastic flow elongation of primary

cumulus and interstitial crystals or crystal aggregates parallel to L_1^9, with contemporaneous annealing recrystallization of the most strained areas. The most deformed rocks conform to the definition of blastomylonite (Christie, 1960).

The deformation of the orthopyroxene and plagioclase porphyroblasts indicate principal elongation and compressional directions parallel to L_1^9 and normal to S_1^9 respectively. The presence of clinoenstatite in similar rocks at Wingellina (Trommsdorf and Wenk, 1968) may indicate unusually high strain rates for the deformation. In this case the unique plastic flow deformations observed in orthopyroxene and plagioclase would indicate extremely high temperatures of deformation (T_d). The lack of slump structures and turbidite deposits in the layered sequences suggest that the deformation was not active during crystallization (i.e. $T_d < 1200^oC$). Similarly the lack of exsolution bodies in recrystallization products indicates the syntectonic annealing occurred below the solvus temperatures for these minerals. However, the preservation of delicate pyroxene/spinel symplectite textures in foliated and partially recrystallized rocks (Chapter 6) indicate that the deformation occurred at temperatures above that for the olivine - plagioclase subsolidus reaction described in Chapter 9.3.2. This temperature has been estimated at approximately 800 to 1000^oC for load pressures of 8 to 10 kilobars (i.e. $T_d > 800 - 1000^oC$). There is some indication that deformation was active prior to complete interstitial crystallization of the upper parts of Kalka (Chapter 3.3).

Although considered previously as only a foliation, it is obvious

in some specimens (e.g. Plates 50A,B) that S_1^g is more accurately described as a layering. Indeed in most cases the lenticular aggregates delineating the foliation constitute a layering sensu stricto. In most cases the thin lenses can be adequately explained as recrystallized "flow" single crystals or groups of crystals.

It should be noted that the layers in all cases are monomineralic with regard to both porphyroblasts and recrystallized matrix. This form of layering is quite distinct from normal igneous layering affected by the deformation (e.g. Plates 49B, 34A) which is polymineralic.

The most gneissic or blastomylonitic rocks are found within two distinct belts in the Kalka Intrusion (Fig. 33). The northernmost belt extends via isolated outcrops in the Scarface Silcrete Zone to a belt of very similar rocks in the Numbunja Pass on the southern side of Gosse Pile (Moore, 1970a). It is proposed to call these rocks the Numbunja Gneissic Belt. The second belt, the West Kalka Gneissic Belt, occurs along the granulite sliver separating the two major parts of the Kalka Intrusion. These belts, especially the Numbunja Gneissic Belt, are the site for younger undeformed dunitic and picritic intrusions of the picritic suite (Chapter 3.2).

Away from the gneissic belts S_1^g is less well developed (e.g. Plate 34A) and a measurable lineation, L_1^g, is only found within the most deformed parts of the gneissic belts. It should be realised that Fig. 33 only depicts the approximate area of the most deformed parts of the gneissic belts, and observable foliations are often found outside them.

The degree of recrystallization (i.e. proportion of recrystallized to primary grains) also decreases away from the gneissic belts to a point where between the two belts completely or dominantly primary textures are observed. Moore (1970a) has delineated the limit of annealing recrystallization in Gosse Pile, but such a limit is more difficult to draw in Kalka because of possible overprinting recrystallization of the F_2 or F_3 deformations. The approximate southern limit for annealing recrystallization associated with the Numbunja Gneissic Belt in the No. 6 Section is shown in Fig. 33 (to the east F_3 overprinting occurs).

The inhomogeneity of the deformation on a macroscopic scale is also demonstrated on a local scale. Plate 56G shows an example of highly deformed zones adjacent to or grading to areas showing less intense foliations. Generally, however, any hand specimen exhibits a homogeneous fabric which is similar to those described from shear belts (Ramsay and Graham, 1970).

Refolding of S_1^g by the earliest fold phase recognised after the intrusion of the Giles Complex (Chapter 14) means that the foliation was originally almost horizontal since it is parallel or at very low angles to S_o^g. The present orientations of L_1^g, shown on Fig. 2, can therefore be approximately unfolded from the effects of F_2 and F_3. At present they plunge from about vertical to almost horizontal, always with an easterly component, with an average plunge of about 50 to 60°E. When unfolded these plunges become approximately horizontal with a trend direction varying from 090° to 180° (an average at about 140° to 150°).

The original orientation of these belts is shown on a generalised vertical E-W cross-section in Fig. 34. The effects of the younger F_2 and F_3 folding and several major cross-faults have been removed.

The Numbunja Gneissic Belt (NGB) passes from norites (above pyroxenites) in Gosse Pile (Moore, 1970a) through pyroxenites and norites in the Scarface Silcrete Zone to pyroxenites in Kalka. The effects of the deformation are limited to kinking and recrystallization in lower Kalka implying that the main zone of deformation lies below (to the north) the present outcrops. Similarly in Gosse Pile the main zone of deformation may lie above (to the south) of the outcropping rocks as L_1^g is not present in this area (Moore, 1970a). The belt therefore appears to have a regional low dip to the west relative to the igneous layering.

The West Kalka Gneissic Belt (WKGB) is best developed adjacent to the thin granulite sliver (Fig. 33), especially on the bottom or northern side. The degree of deformation, represented by S_1^g and L_1^g, decreases away from this area, as does the degree of annealing.

Several other observations should be presented at this stage. Primary features such as contact contamination and fine-grained margins are preserved along both sides of the granulite sliver in the WKGB. The boundary between the Pyroxenite Zone and Norite Zone in Kalka and Gosse Pile is at the same level on both sides of the NGB* (Fig. 34). Also primary igneous layering, although foliated, is still intact and apparently undisturbed in these belts.

---

* This is assuming the boundaries on both sides are the same, and not cyclic repetitions of the same boundary at different levels.

It is therefore concluded that, although the deformation fabrics are very similar to those expected in high temperature thrust zones, and probably do represent a similar type of deformation, the degree of lateral movement was small. Because of this, and since the rare presence of clinoenstatite may indicate high strain rates the activity of these belts was probably limited in time. From Jaeger's (1957) data it is possible to estimate very approximately that a maximum of 10 million years after crystallization were available for deformation to occur while the rocks cooled to 800°C.

The areal extent of this deformation was considerable as similar rocks are observed over a 130 km zone from Teizi (Gray, 1967), Gosse Pile, Kalka, North Mt Davies, Ewarara, Murray Range, North Hinckley (Nesbitt et al., 1970) and West Hinckley (Smith, 1970). With the possible exception of North Davies and West Hinckley these intrusions are all high pressure bodies, and it therefore appears that this deformation was restricted to the lower crust.

This deformation has not yet been observed within the granulites, possibly for a variety of reasons. Granulites have only been mapped in detail near Ewarara, Kalka and Gosse Pile, and hence the localised zones may not occur within these areas although some flaser gneisses may perhaps represent the deformation. Furthermore, the different rock types and temperatures (about 400 to 800°C maximum) may either not reflect the deformation or may reflect it in an entirely different fashion. The granulite gneisses within the sliver associated with the West Kalka Gneissic Belt contain a foliation similar to S_1^m. This

foliation is parallel to S_1^g in the norites, S_o^g, and also S_o^m (granulite layering). If the foliation is S_1^m, then the gneissic deformation affecting the norites would only serve to accentuate the structure and would not produce an easily recognisable overprinted fabric. In one creek section S_1^m in the granulites became more pronounced towards the norite contact.

Foliations similar to S_1^g have been quite widely reported from other igneous bodies although they have excited little comment. Oosterom (1963), Battey (1965), Bilgrami (1968), Harley (1969) and Ghisler (1970) have reported gneissic structures from basic intrusions. Ayrton (1968) has reported similar structures axial plane to isoclinal folds and approximately parallel to primary layering in the Vourinos massif.

These reports, together with the descriptions by Moore (1970a) and in this thesis, cast some doubt on the validity of Thayer's (1960, 1963, 1967) use of "flow layering". Thayer has proposed the concept of solid or semi-solid intrusion of alpine-type bodies into their present observed positions and considers these bodies to be quite distinct from stratiform intrusions. A vital part of his argument has been the recognition of so-called flow layers which are considered to reflect the movement of the masses during their emplacement. The descriptions of these layers by Thayer reveal an almost identical geometry and fabric to the gneissic foliation, S_1^g, or S_o^g layers containing S_1^g, described in this thesis (cf. Thayer, 1963, Figs. 2-5). It seems quite conceivable to the writer that, in at least some cases, Thayer's structures could be explained by in situ deformation of normal stratiform bodies, and therefore the distinction

between alpine and stratiform bodies, if at all valid, would need to be redefined with different criteria. Nesbitt and Kleeman (1964) have noted that the Giles Complex, while undoubtedly stratiform, contains features characteristic of alpine origin by Thayer's (1960) criteria while Nesbitt et al. (1970) have remarked on the chemical similarities between stratiform and alpine type intrusions. Furthermore Bowes and Skinner (1970) have also noted chemical similarities between the stratiform Stillwater Complex and nearby alpine-type ultrabasic bodies in the Beartooth Mountains.

A further comment on the pre-F_2 reconstruction of Kalka and Gosse Pile in Fig. 34 is perhaps worth making. The bodies are shown essentially in their initial relationship. It is possible to construct a large primary sheet-like body incorporating both Gosse Pile and Kalka (Fig. 34). The proto-body is about 7000m thick (minimum - no base* or top to the sequences have been observed in either Kalka or Gosse Pile) and at least 27km long. The presence of intertongued granulites at the western end of Kalka suggests that the sheet did not extend much further to the west. However, the body could have extended an unknown distance to the east. This proto-body would compare with the Blackstone - Bell Rock supersheet (about 65km long and at least 6000m thick) to the west.

The proto-body is now dissected by large faults, the Hinckley Fault and the hypothetical Scarface Lineament. A large block of granulite immediately to the west of Gosse Pile interrupts the continuity of the

---

* The lowest cumulates in Gosse Pile (Moore, 1970a) are similar to those in Ewarara, which does exhibit a basal contact. In fact, Ewarara could have originally been part of the proto-body.

Pyroxenite Zones between that body and Kalka. It has a faulted and in part concealed (later noritic intrusive) contact with Gosse Pile (Moore, 1970a) suggesting it may have been introduced to its present position some time after the crystallization of the proto-body.

13.3 F_2 Folding

On a mesoscopic scale F_2 folds are moderately open to fairly tight symmetrical folds with (generally) a steep dipping east-west axial plane*. Folding of S_o^m, S_1^m, S_o^g and S_1^g has been observed in various parts of the area (e.g. Plates 54A,C and 55A,C) and refolding of F_1 has been found south of Mt Davies (Nesbitt et al., 1970, Fig. 2). Crenulation of the folded S-surface (especially S_1 surfaces) in the hinge zones is common (Plates 54A, 55A), although crenulations have also been observed in limb zones. Thickening of S_o layering in the crest is sometimes observed (Plate 54C). Mesoscopic folds are sometimes dismembered in the limbs along displacement zones parallel to the axial plane, with associated development of pseudotachylite.

An axial plane foliation, S_2^m, outlined by quartz/feldspar lenses in the granulites (Plate 54B), is best developed in or near hinge zones at Ewarara. In thin section this fabric (in some specimens resembling the F_1 quartz hook fabric; compare Plate 54B with Nesbitt et al., 1970, Fig. 2) consists of platy granoblastic quartz lenses which anastomose

---

* Recumbent to inclined sinistral folds with shorter steep limbs are sometimes found in the granulites near Ewarara, but generally in both granulites and Giles Complex the folds are upright and symmetrical. Axial plane variations are sometimes due to refolding by F_3.

around the feldspar, garnet and sillimanite porphyroblasts (Plates 7A,B, C). The quartz exhibits a strong crystallographic preferred orientation. The texture is discussed further in Chapter 2.2. (Note: this fabric is very similar to that developed in mylonites from the Grenville Front in Canada — Dalziel and Bailey, 1968).

A rodding-type L_2^m lineation, formed by the intersection of S_o^m and S_2^m, is commonly found in the major F_2 hinge zones in the granulites (Plate 54D).

Within the Giles Complex rocks an axial plane foliation, S_2^g, is rarely observed. However, in a few examples small recrystallized and relatively unstrained pyroxene or plagioclase lenses are observed parallel to the axial plane (Plate 55C) or at high angles to S_o^g and S_1^g (Plate 55B). In the contaminated zone of Kalka, felsic segregations are rarely observed along the short limb zones of asymmetrical folds (i.e. parallel to the axial plane).

In one fold (see Plate 54A) a layering has been observed parallel to the axial plane and transgressive to S_1^g. The layering is monomineralic with a core of plagioclase (or rarely pyroxene) about 1 to 2mm thick enclosed on both sides by thin (0.3mm) rims of pyroxene. The outer bands are always recrystallized (0.1 - 0.2mm grain size) but the central band is variable, sometimes having a typical annealed texture similar to the host rock and sometimes containing alternating single crystals (up to 5mm long) of plagioclase and pyroxene elongate in the layering (Plates 57A,B).

The layering has been interpreted as forming by metamorphic differentiation in the axial plane during the formation of the fold. The large single crystals in the layering do not appear to contain exsolution bodies but otherwise are similar to the deformed cumulus crystals described in Chapter 13.2. They are interpreted as having grown by secondary processes from a recrystallized aggregate (with secondary plagioclase nuclei alternating with pyroxene nuclei along the banding). Large primary deformed cumulus crystals are not common elsewhere in the specimen.

A strong crystallographic preferred orientation of plagioclase parallel to the fold axis in some folds indicates syntectonic annealing and delineates a lineation, L_2^g. This lineation is not observed in hand specimen as a morphological feature.

A well developed foliation in some of the Type A dolerite dykes (Plate 13C; see also Chapter 3.1.1) is in some cases approximately parallel to the dyke margins, but generally it is oblique. In two areas, the foliation is parallel to a well developed axial plane foliation, S_2^m, in adjacent quartz-bearing granulites, and is assumed to represent the same deformation in the dykes. The foliation in the dykes is termed S_2^d. It is interesting to note that an undeformed Type A dyke is found south of Mt Davies in an area dominated by macroscopic F_1 folds (pre-Type A dolerite). The general linearity of Type A dykes across major F_2 folds in the Tomkinson Ranges is presumably related to their steep orientation and the steep axial plane of the F_2 folds.

No major F_2 folds have been observed within the Kalka layered

sequence, and this, together with consistent sedimentary younging evidence and chemical variations, has led to the conclusion that only a very small proportion of the stratigraphic thickness of Kalka results from repetition by folding. The Kalka Intrusion is therefore lying on the southern limb of a major anticlinal structure. Axial planes are steep dipping and vary in strike from E-W to NW-SE (due to F_3 refolding). Fold axes are shallow plunging (see Fig. 2).

A major anticlinal F_2 fold (steep axial plane, shallow axis) has been mapped in the granulites to the south-east of Ewarara (Figs. 2, 5B). Large mesoscopic folds are found in the nose of the structure. Although the Ewarara Intrusion lies on the northern limb of the fold, it maintains a relatively shallow dip (some vertical layering in the body is considered primary — see Chapter 10.2.5). Such a geometry indicates that the pre-Ciles Complex granulite layering orientation in the immediate vicinity of Ewarara was much as it is today i.e. 40 to 50°N. Stereographic plots of poles to S_o^m and S_o^g in the Ewarara area (Figs. 35D,E) form a girdle with a pole consistent with measured L_2^m lineations and a mesoscopic fold axis in the granulites (i.e. about 070°, 15°E).

Although not mapped in detail a major hinged(?) fault on the southern side of the Ewarara anticline near the picrite plug A300-386 is associated with a major discordance in S_o^m layering and is apparently related to the F_2 structure (FA in Fig. 5B). A similar structure (FB in Fig. 5B) associated with a major discordance has been mapped south of picrite plug A300-79 but has not been traced to the east (the lineation within this fault parallels the F_2 fold axis and the fault zone is partly intruded by a less deformed Type B dyke which postdates the F_2 folding).

It is also possible that the fault separating the two lobes of the Ewarara Intrusion (FC in Fig. 5B) is related. A mylonite foliation in acid granulites adjacent and parallel to this fault is identical to what is considered to be S_2^m elsewhere in the area (cf. Plate 7A). In a tentative interpretation the author believes that these structures represent macroscopic equivalents of the limb displacement zones found in mesoscopic folds.

In Fig. 5B it will be noticed that the westward extension of the anticlinal axis is curved into the FB fault. This curvature is based only on measurements of S_o^m to the north and south of this hypothetical axis immediately south of the FB fault (see Fig. 2) which suggest such an anticlinal relationship.

Major F_2 folding is developed throughout the Tomkinson Ranges. Two other major F_2 closures are found to the southeast of Ewarara. One, a synformal structure, contains a "granitic" core (Thomson, 1964), while the second, an anticlinal feature, occurs within the Teizi Intrusion (Gray, 1967). Another synformal structure is found to the north of Ewarara (Thomson, 1964). Spacing between the major fold axes varies from 3 to 10km.

Although only mesoscopic folds are found in many of the Giles Complex bodies, it is believed the major rotation of the Giles Complex, as evidenced by their present general east-west strike and high angle dips is the result of macroscopic F_2 folding (Nesbitt et al., 1970). Apart from the Teizi and possibly Michael Hills Intrusions, all the presently outcropping bodies are preserved on limb zones of these folds.

The absence of the S_2^d foliation in Type A dolerite dykes from the southern Deering Hills, the Everard Ranges and Ernabella may indicate that the F_2 deformation was only active in the Tomkinson and southern Musgrave Ranges (Chapter 15).

13.4 F_3 Folding

In the contaminated rocks associated with the granulite sliver of West Kalka simple, open mesoscopic folds have been observed in one outcrop (Fig. 32B). These folds warp both the lithological layering and the axial plane of F_2 folds around the noses of the F_3 folds, and thus postdate them. Brittle fracture and irregular pseudotachylite veining is sometimes associated with the folds. It has been impossible to measure the axial plane to the F_3 folds accurately. It appears to trend approximately south-west and may have a variable dip.

In one specimen (A314-712c) from this locality, a moderate morphological preferred orientation for feldspar but not biotite has been observed, axial plane to a small warp in a limb of a larger F_2 fold (Plate 56F). The fabric, which is at a high angle to the S_2 axial plane and not folded by it, has been interpreted as an S_3 axial plane foliation.

The sigmoidal shape of Kalka is considered to be a macroscopic reflection of the small F_3 folds. S_2^g axial planes within Kalka are bent with the layering and hence pre-date the warping.

The Ochre Fault, a hinged structure, is intimately associated with the F_3 warping in east Kalka (Fig. 2). The S_0^g layering is continuous around its western extension but further to the east a major structural

discontinuity in the body occurs. At the eastern extension of the fault, associated recrystallized pyroxenites are often unusually fine-grained and are sometimes finely banded (Plate 56H). The banding does not appear compositional and is apparently caused by grain size variations in the recrystallized matrix. Some relic exsolution-bearing primary orthopyroxene crystals are still preserved, and of these a proportion are unusually elongate, parallel to the layering. Unlike the elongate "flow" orthopyroxenes in S_1^g, clinopyroxene exsolution lamellae are usually parallel to the elongation. The fabric also differs from the gneissic foliation in that kink planes, although rare, are at high angles to the layering. The layering is therefore considered to be directly related to the F_3 deformation, and is termed Sl_3^g. Its attitude is 250^o, 50^oN. The elongate orthopyroxenes are lineate 040^o, 50^o in the layering. Other irregular layerings in the Pyroxenite Zone may also be related to this deformation, or possibly to S_1^g (Plate 58C).

The F_3 warping in Kalka is reflected in stereographic plots of S_o^g, S_1^g and L_1^g (Figs. 35A,B,C) where secondary girdles tend to develop, especially in L_1^g, indicating refolding (possible F_2 contributions are ignored since Kalka is on only one limb of a major F_2 fold). The girdles give an approximate pole at about 315^o, 40^o which is taken as the F_3 fold axis for the eastern F_3 fold associated with the Ochre Fault (the western F_3 warping does not contribute as many measurements to the diagrams). The F_3 folding is responsible for the strong overturning relationships observed in east Kalka.

F_3 folding has not been directly recognised in the Ewarara area.

However, the possible curvature of the major F_2 anticlinal axis at Ewarara (Fig. 58) may result from F_3 warping.

There is also a possibility that the weak foliation described from Type B dolerite dykes (Chapter 3.1.2) may also be related to the F_3 deformation. Field measurements in the Ewarara - Kalka area have not been made, but some measurements made by B. Fehlberg (R.W. Nesbitt, pers. comm.) in the Teizi area indicate that the foliation is not parallel to S_2 as for Type A dykes (although possible foliation refraction cannot be ignored). This supports the field observation (Gray, 1967) that the dykes (strike 300°, dip 50°N) maintain linearity across the macroscopic F_2 fold (axial plane strike 250°, dip 60-70°S). The foliation is not necessarily parallel to the dyke margins, and is therefore interpreted as being a regionally penetrative fabric related to F_3.

Furthermore, the hinged FB fault associated with the F_2 deformation (Fig. 58) is displaced by a bifricating fault FD. The dextral sense of apparent lateral displacement is supported by the curvature of the layered granulites next to the fault. A basic dyke, A300-93, (almost completely recrystallized but of the Type B suite) which is intruded into this younger fault zone, exhibits a strong foliation (in fact a fine layering) parallel to the fault strike. The younger fault is approximately parallel to the Ochre Fault in east Kalka which is associated with the F_3 deformation, and may be related to it. The foliation in the dyke is approximately parallel to the banding $S1_3^g$ found in pyroxenites in close proximity to the Ochre Fault (295°, 60°N in dyke; 250°, 50°N in pyroxenite).

It may be significant that dykes containing primary plagioclase laths are in general found in the northern and southern parts of the area whereas only recrystallized laths are found in rocks from the central area (Fig. 58). This may suggest that the F_3 deformation was most severe in the latter area, as implied in the previous discussion.

On a regional scale, it is possible that the apparent broad warping of the South Mt Davies Intrusion and the Bell Rock - Blackstone sheet is the result of the F_3 deformation. Similarly the complex structural patterns observed in the Michael Hills Intrusion (see Nesbitt and Talbot, 1966, Figs. 1 and 3) can probably be explained by F_3 folds overprinting F_2 folds.

13.5 S_4 Fracture Cleavage

Within many of the rock types in the field area, a prominent fracture cleavage is observed. This cleavage has a consistent orientation within any one specimen and is independent of the crystallographic orientation of the individual grains although slight refraction can occur (Plates 53A, 23A). In partially recrystallized rocks the cleavage is present in both primary and secondary grains. The cleavage is possibly observed in the field as a weathering feature in some rocks (Plate 58D). It has been designated S_4.

No deformation, recrystallization or other structures are associated with the cleavage. It has been observed in both primary and secondary grains in the Giles Complex, Type A and Type B dolerite dykes, and in members of the transgressive picrite plug suite, suggesting that it is

at least younger than the F_3 deformation (Table 7). This is supported to some extent by the presence of aligned fractures at high angles to the axial plane in both hinge and limb areas of an F_2 fold in Kalka.

Although the fabric was not directly measured in the field, a study of oriented thin sections reveals that the cleavage has an approximately horizontal attitude in the Kalka area.

It is tentatively interpreted as a relaxation feature resulting from uplift of the high pressure rocks with an associated relief of load pressure.

13.6 Hinckley Fault

The southern edge of the Kalka Intrusion is bounded by the transgressive, mylonitic Hinckley Fault (Goode and Nesbitt, 1969) which separates the intrusion from both the Minno acid granulites and the North and South Davies Intrusions and which is associated with a major break in structure and rock types (Frontispiece, Plate 58B; Figs. 2, 37). A probable continuation of the fault zone has been mapped by Moore (1970a) as separating the Gosse Pile and South Davies Intrusions to the east. To the west, the structure continues into Western Australia as a wide mylonite zone along the southern boundary of the Hinckley Intrusion (Thomson, 1964; Smith, 1970). Bowden (1969) has suggested it continues westward south of the Blackstone Range.

The mylonite is up to about a kilometre wide at Kalka but is much thinner to the east at Gosse Pile. At Kalka the mylonite layering or foliation dips moderately steeply to the north (Fig. 2). A strong

mineral streaking found within the foliation plane dips to the northwest.

The rocks within the mylonite zone consist of a heterogeneous mixture of acid granulites and basic rocks. They are highly deformed and usually very fine-grained (flinty in some cases). The layering is extremely lenticular, and is commonly folded into tight, isoclinal intrafolial folds (Plate 57G). These fold axes are not necessarily parallel to the lineation. In quartz-bearing mylonites, a very strong crystallographic preferred orientation of quartz was observed in sections perpendicular to S and L. In many cases it is difficult to determine whether the layering is due to compositional or grain size variations, or both. In A314-332 the layering consists of alternating dark and light quartz-rich layers. The light layers consist mainly of fine-grained (0.02 to 0.05mm) equigranular, interlobate grains, while the darker layers are much finer grained. The darker layers also contain abundant small (0.01mm) garnet euhedra suggesting the layering results from compositional as well as grain size variations (Plate 57E).

Coarser grained (0.1 to 0.5mm) relic crystals of feldspar, pyroxene(?) and garnet(?) are observed as strained, rounded single crystals, elongate in S (Plate 57F). In other examples the deformation is less homogeneous and the mylonitic foliation occurs as localised zones around strained "primary" mineral aggregates.

The rock textures conform to the definition of mylonite (Christie, 1960) and have been so termed in this study. It is difficult to estimate the degree of recrystallization in these rocks. The strong preferred orientation of quartz grains indicate syntectonic annealing in some

examples. In these cases the quartz grains are also quite coarse-grained and in light coloured layers. In neighbouring darker coloured layers the quartz grain size is very much less. It is possible that the original grain size in both layers was very fine, and subsequent coarsening associated with the syntectonic annealing* occurred only in the light coloured layers (small quantities of impurities in the darker coloured layers may have inhibited grain boundary adjustment processes in those layers). The small euhedral garnets (rather than lenticular crystals or aggregates) in some rocks may also indicate a certain amount of post-tectonic neomineralization (assuming garnet was not originally present in the very fine matrix). It is therefore probable that in at least some cases the rocks could be better described as partial blastomylonites.

Between the most deformed parts of the mylonite zone and the undeformed (by this deformation) rocks of the Kalka Intrusion a thin transition zone is found. In this zone irregular pseudotachylite veining and other features of more brittle deformation are found (cf. Plate 57H). Pseudotachylite veins, approximately parallel to S, are most common within the mylonite zone itself.

Other mylonitic rocks are found in various parts of the Kalka and Ewarara areas (e.g. Plates 56A,B,C) but cannot be related with confidence to any specific deformational episode.

Deformations younger than the Hinckley Fault are generally small scale features. The mylonite zone is strongly jointed and small cross-

* The interlobate grain boundaries indicate that the coarsening was not post-tectonic.

faults (lateral displacements of several centimetres) and kinks are observed. These cross-faults trend approximately north-south, and parallel a pronounced geomorphological lineament over a kilometre long in Tertiary(?) calcrete south of West Kalka.

East of the main Kalka Intrusion, the Hinckley Fault is considerably displaced laterally by about a kilometre in a dextral sense (Fig. 2). The Scarface Silcrete Zone and the Pyroxenite - Norite Zone boundary are also displaced in the same manner. A similar displacement of the Hinckley Fault is also observed about 2 kilometres further east near Yultadurra.

In the first case the displacement can be associated with a Type A dolerite dyke (A314-760) separating Kalka norites from silcrete. However, this produces grave problems as the Type A dolerite from other evidence is much older than the Hinckley Fault. However, it is perhaps important that dextral lateral movements parallel to Type A dolerites at Gosse Pile have displaced a fault which is younger than several of the dolerites (Moore, 1970a). The movement is certainly older than the development of the undeformed Tertiary(?) silcretes.

13.7 Scarface Lineament

It has been previously noted that small but significant differences exist between the Kalka and Ewarara field areas.

The Type D dolerite dykes display both structural and petrological discontinuities between the two areas (Chapter 3.1.4), while members of the picrite plug suite also show petrological differences in the two

areas (Chapter 3.2). Type B dykes also appear to be much more common in the north (Fig. 8).

This discontinuity coincides with a major geomorphological lineament of no outcrop trending at about 110° between Kalka and Ewarara. This zone extends into desert to the west and continues as a marked break of outcrop south of the Deering Hills and Mt Kintore to the east (Fig. 37) i.e. over a total distance of more than 160km.

It has been termed the Scarface Lineament. Granulite trends and fold axes in the Ewarara - Teizi block appear to be truncated by those in the Kalka block (Thomson, 1964; see also Nesbitt et al., 1970, Fig. 3). Similarly the outcrop ratio of Giles Complex/granulite is much less in the Ewarara - Teizi block than to the west (Fig. 37), and in Chapter 2.3 it was shown that granulites from the Ewarara - Teizi belt are higher pressure than those from the Kalka - Gosse Pile belt.

The Scarface Lineament may therefore represent a significant structural discontinuity between these two areas, and may be related to the Hinckley Fault, Mann Fault and similar structures.

13.8 HK Lineament

The HK lineament represents another hypothetical structure trending approximately in a NNW direction between the Hinckley and Kalka Intrusions. A high angle discontinuity in the igneous layering in both bodies (Plate 58A; Nesbitt et al., 1970, Fig. 3) indicates that a major structural break, probably a fault, exists between the two areas.

Furthermore, while the Kalka layered sequence youngs to the southwest, sedimentary structures and rock sequences indicate that the layered succession in the Hinckley Intrusion youngs to the north.

The structure may be related in origin to the younger Hinckley Fault, which is transgressive to it.

CHAPTER 14

AGE RELATIONSHIPS IN THE MUSGRAVE BLOCK

14.1 Age Relationships in the eastern Tomkinson Ranges

The relative age relationships of the major events in the eastern Tomkinson Ranges are illustrated in Table 7 (other relationships for minor events are given in the general thesis text).

The layered granulites are the oldest rocks recognised in the area; they are transgressed by all other igneous rocks in the area including the Giles Complex. Both the South Mt Davies and Ewarara Intrusions cut the granulite layering although other bodies are more concordant (Thomson, 1964).

The oldest deformation recognised in the area, the F_1 fold phase, is also older than the Giles Complex as macroscopic folds of this generation are transgressed by the South Mt Davies Intrusion (Nesbitt et al., 1970). The granulite facies metamorphism is also apparently older than the Giles Complex as the assemblages, although overprinted, appear to have been in textural equilibrium at the completion of the F_1 deformation (Chapter 2.2).

The Giles Complex intrusions are the oldest basic igneous rocks* in the area. Many of the bodies in the eastern Tomkinson Ranges were deformed by a localised "thrust-type" mechanism soon after crystallization producing a gneissic foliation, S_1^g, in some of the cumulates

---

* Ignoring some of the basic interbands with igneous characteristics in the granulites (Chapter 2.2).

(Chapter 13.2).

The Type A suite of dolerite dykes cuts both the Giles Complex primary layering (S_0^9) and their imposed foliation (S_1^9) at Kalka, Gosse Pile (Moore, 1970a) and Teizi (Gray, 1967), as well as the granulite layering.

Folds of the F_2 generation have been shown to postdate the Giles Complex and the Type A dolerites at Kalka and Ewarara (Chapter 13.3). Facer (1967, 1970) considers that the present magnetic properties of the Giles Complex were imprinted on the rocks after the completion of F_2 folding*.

The Type B dolerite dyke suite at Ewarara cuts and displaces Type A dykes, and at Teizi intrudes Giles Complex rocks (Gray, 1967). It also postdates F_2 folding at Teizi (Chapter 13.4).

Apart from being younger than the F_2 fold phase and older than the Type D dolerite suite, F_3 folds cannot be accurately dated relative to other events. It has been argued in Chapter 13.4 that the F_3 deformation postdates the Type B dolerite suite at Ewarara. The general lack of deformation in the transgressive picrite suite suggests the folds are older than that event.

The transgressive picrite suite has been mapped as intrusive into the Giles Complex at Kalka and Ewarara, and into a Type B dolerite dyke at Teizi (Gray, 1967).

---

* Note: Curie temperature for magnetite is about 575°C decreasing to about 400°C for titanium-rich magnetite.

Type D dolerites are intrusive into most rocks in the area including the Giles Complex and the transgressive picrite suite. They also post-date the F_3 fold phase at Kalka as they maintain parallelism over widely separated parts of the fold.

The Hinckley Fault is transgressive to the Type D dolerites and to older rocks (Fig. 2). Along with possibly the Scarface and HK Lineaments, it represents the youngest large scale event in the area. Several minor cross-faults are observed at Kalka indicating even younger movements (Chapter 13.6).

14.2 Comparison with other parts of the Musgrave Block

In general little is known in detail about many other parts of the Musgrave Block. Table 7 has been constructed from all the evidence available and the general sequence of events recorded in the eastern Tomkinson Ranges appears consistent with relationships observed elsewhere.

The western Tomkinson Ranges are in general gradational from the area described in this thesis and contain a similar sequence of events (Nesbitt et al., 1970). Daniels (1967) has, however, reported two deformations in the granulites prior to intrusion of the Giles Complex although the evidence for these events has not been recorded.

Data from the eastern Musgrave Block is limited. Investigations by K.D. Collerson and R.B. Major in the western Musgrave Ranges will provide much needed information from this area. Preliminary observations on the granulites, Giles Complex bodies and Type A dolerite dykes in particular are in accord with those in the Tomkinson Ranges, and allow

equivalent structures to be recognised e.g. F_2 folds of this study are similar in geometry and relative age to Collerson's F_3 folds at Amata; F_3 folds of this study are possibly equivalent to F_5 folds at Amata. Although it is realised that correlation of structural events is unwise over long distances (Park, 1969), it does appear that the equivalence of fold style in these instances provides reasonable grounds for correlation because of similar corresponding relationships to certain basic intrusive events (e.g. Type A dolerites). Collerson (pers. comm.) has also recognised a fold phase older than a structure apparently equivalent to F_1 in the Tomkinson Ranges. The presence of such structures was suggested by Nesbitt et al. (1970). Observations by Collerson will also be important in possible correlation of events between granulite facies, amphibolite facies and retrograde granulite facies terrains at Amata.

14.3 Absolute age determinations

Only limited studies of absolute ages have so far been made of the Musgrave Block (Table 22). Most of these are confined to the eastern parts of the region although current investigations by C.M. Gray of the western parts of the Block should provide valuable information.

Selected results from granulite and amphibolite facies rocks from the eastern Musgrave Ranges give approximately the same ages i.e. about 1400 ± 150 m.y. (Table 22). By further subjective data selection Arriens and Lambert (1969) have recognised two composite groups of ages from the two terrains viz. a high age group (1655 ± 110 with initial ratio of

0.7079 ± 0.0008) and a low age group (1410 ± 60 with initial ratio of 0.7047 ± 0.0013).

The significance of the bulk age of about 1400 m.y. or the two composite ages of about 1400 m.y. and 1650 m.y. is not yet fully understood. The "old" age, if present, may represent an early event subsequently largely overprinted by a younger event at about 1400 m.y. ago. The most pressing problem, however, involves the interpretation of the 1400 m.y. event i.e. what caused the last homogenisation of the system relative to radiogenic strontium at that time? The most obvious answer is that the last recorded metamorphism terminated at 1400 m.y. as suggested by Arriens and Lambert (1969).

Other datings from the Musgrave Block are limited. Acid veins cutting the Giles Complex at Blackstone give an age of about 1100 m.y. thereby fixing a minimum age on the Giles Complex (Nesbitt et al., 1970). Although the acid veins may be rheomorphic in origin (cf. veins at Mt Davies — Nesbitt and Talbot, 1966), it is also possible that they are similar to the acid pegmatites at Kalka which are younger than the Giles Complex and related to F_2 folding* (Chapter 3.7). C.M. Gray (pers. comm.) has obtained an age of 1140 ± 17 m.y. on a biotite from the Jameson Range Intrusion which would appear to place a minimum age limit on the Giles Complex.

---

* Various granites from the eastern and northern parts of the Musgrave Block also generally give absolute ages of about 1100 m.y. (Table 22), suggesting a possible major widespread episode of acid igneous activity at about this time. The rhyolitic Tollu Volcanics are also about 1060 ± 140 m.y. old (Compston and Nesbitt, 1967). However Type A dolerites, older than F_2 folding in the Tomkinsons, cut several of these granitic bodies.

Type A dolerite dykes cut both the Ernabella and Illbillie adamellites thus fixing a maximum age of 1120 ± 100 m.y. for the dykes (Arriens and Lambert, 1969). The dykes do not intrude sediments of the Officer Basin near Mt Illbillie in the Everard Ranges. These sediments include glacial beds probably equivalent to Proterozoic glacials in the Kimberleys which have been dated at about 650 to 750 m.y. old (Compston and Arriens, 1968). Dykes equivalent to the Type A dolerites (see Chapter 3.1) cut the Gawler Range Volcanics (1535 ± 25 m.y.) and the Roopena Volcanics (1345 ± 30 m.y.) in the Gawler Block supporting the maximum age relationships in the Musgrave Block (Price, 1970).

Because of their retention of radiogenic strontium below about 250 to 300^{o}C, mica ages are commonly considered to indicate times of uplift of high grade metamorphic terrains (e.g. Jager et al., 1967). Granitic biotites in the northern Musgrave Block give ages of about 600 m.y. overprinting much older rocks, while metamorphic muscovite near Gosse Pile gives an age of about 900 m.y. (Table 22). Biotite from a transgressive picrite plug near Ewarara gives an age of about 800 m.y. depending on the assumed initial ratio (Table 128). Hence uplift of the Musgrave Block appears to have been active in various parts from about 900 to about 600 m.y. ago.

CHAPTER 15

TECTONIC DEVELOPMENT OF THE EASTERN TOMKINSON RANGES AND ITS RELATIONSHIP TO THE MUSGRAVE BLOCK

In the final remarks of this thesis it is intended to integrate the results and inferences of this local study into a more regional interpretation of the tectonic development of the Musgrave Block. It should be noted that the lineaments and related tectonic activity of the Musgrave Block are currently the subject of research by other workers so that the conclusions reached here must be regarded as proliminary.

The oldest rocks preserved in the Musgrave Block are considered to have been originally sediments, probably siliceous to argillaceous clastics (Chapter 2.4). There is no particular evidence to suggest that these rocks were deposited in a geosynclinal environment as has been suggested by some other workers (e.g. Sprigg and Wilson, 1959; Arriens and Lambert, 1969). The nature of the original sediments and the lack of basic volcanics are not typical of more modern geosynclines. Furthermore the general north-easterly trends of the oldest observed fold phase (Chapter 13.1) does not support the concept of an east-west geosyncline as inferred by Sprigg and Wilson (1959).

It is, however, apparent that most of the sediments of the eastern Tomkinson Ranges at least were buried to approximately 30 to 40kms (Chapter 2.3) prior to the last recorded regional metamorphism at about 1400 m.y. B.P.

At a later stage (but prior to about 1100 m.y. B.P.) and without

any uplift subsequent to the metamorphism the Giles Complex was intruded into the lower crust as a stratified series of basaltic sheets*. Initial intrusion probably occurred in the lowest sheets via dykes and/or plugs as suggested by Goode and Krieg (1967), with the higher level bodies being fed by similar means from the lower bodies after fractionation in those staging chambers (Nesbitt et al., 1970). In most cases the sheets are concordant with the country rocks and were probably accommodated by local interfingering with the granulite layering. In some cases (e.g. Ewarara) the magma may have been accommodated by actual relative uplift of a granulite block as a result of intrusion along older zones of structural weakness (Goode and Krieg, 1967).

There is no evidence to suggest that the intrusion of the Giles Complex was associated with any significant structural event in the crust. The general absence of slumping indicates a tectonically quiescent period of crystallization. There is evidence, however, that minor "thrusting"-type movements occurred along localised zones in the lowest sheets soon after crystallization. These produced the gneissic zones observed in parts of the Kalka Intrusion.

Thomson (in Parkin, 1969) has suggested that the intrusion of the Giles Complex was controlled by large scale faults such as the Woodroffe

---

* The general character of the Giles Complex (i.e. a large number of layered basic intrusions emplaced within a large crustal area) reveals its similarity to many other basic igneous provinces e.g. Somalia (Daniels et al., 1965), Bay of Islands, Newfoundland (Smith, 1958), Nain Province, Labrador (Emslie, 1970), northeastern Scotland (Wager and Brown, 1968), Stjernoy, northern Norway (Oosterom, 1963).

Thrust. However, present evidence suggests that, although such faults probably have long histories, they are certainly younger than the Giles Complex (Chapter 14). In the few areas where flat-lying Giles Complex bodies are preserved no preferred elongation direction is observed as would be expected with such a tectonic control on intrusion e.g. Cavenagh Range is approximately circular in plan (Fig. 1); the basal contact at Ewarara, one of the few observed in the Giles Complex, also does not appear to be controlled by any major fault.

The development of F_2 folds in the Tomkinson Ranges appears to mark a major change in the tectonic history of the region. Lithological trends throughout the central Musgrave Block (i.e. Tomkinson Ranges and western Musgrave Ranges) are dominantly east-west (Nesbitt et al., 1970; Major et al., 1967). However, trends in other parts of the Musgrave Block are generally northerly to north-easterly e.g. northwestern and eastern Musgrave Ranges, and the southern parts of the Block (Thomson, in Parkin, 1969). In the Tomkinson Ranges the east-west trends are controlled by major development of F_2 folding with minor modifications by F_3 warping, whereas the more northerly trending structures occur in terrains dominated by older F_1 folds (Chapter 13.1, 13.3; also Nesbitt et al., 1970).

Such relationships are interpreted to indicate the development of an F_2 fold belt in the central Musgrave Block which overprinted an older folded terrain. That this later fold belt is essentially confined to the central parts of the Block is also supported by the distribution in Type A dolerites of foliations equivalent to the axial plane schistosity of

F_2 folds (Chapter 13.3). These foliations are found in dolerites at Kalka, Ewarara, Gosse Pile, Teizi, Mt Aloysius, Hinckley and Amata* but not in equivalent rocks at Mt Davies, Ernabella and the Everard Ranges (Fig. 37; Chapter 3.1.1). In the Deering Hills the foliation is absent in the southeast but is increasingly well developed to the northwest.

There is also some evidence for a regional increase in heat flow in the Tomkinson Ranges at the time of F_2 folding. Acid pegmatites were formed in essentially anhydrous rocks at Kalka (Chapter 3.7), and Type B dykes, intruded after F_2 folding, are unusually coarse-grained for their thickness, possibly indicating higher country rock temperatures**. Such features are typical of those observed in reactivated basement complexes elsewhere (Watson, 1967; Wynne-Edwards and Hasan, 1970).

The uplift of the eastern Tomkinson Ranges must have occurred at some stage after the intrusion of the Type D dolerite suite since these rocks are the youngest to contain features characteristic of high pressure (Chapter 3.1.4). The only major structural elements younger than these dykes in this area are the Hinckley and Scarface lineaments. These structures, as well as similar lineaments elsewhere in the Musgrave Block, appear to separate strips of different petrological characteristics in the Block (Fig. 37).

---

* K.D. Collerson, pers. comm.

** Acid igneous activity was widespread in much of the Musgrave Block at about 1100 m.y. (Chapter 14; Table 22). Giles Complex temperatures were at least 400 -575°C after the completion of F_2 folding (p.309).

The extension of studies like those in this thesis on the physical conditions of crystallization of basic rocks will be most valuable in testing this apparent relationship and thus in evaluating the significance of these lineaments in the tectonics of the Musgrave Block. Other work is in progress and a general account of the tectonics of the block will be presented elsewhere. It will only be remarked here that present evidence suggests to the writer that the metamorphic facies and Giles Complex distributions may be largely controlled by movements on the east-west trending lineaments. Specifically the writer believes that the Hinckley lineament on the whole, separates lower pressure rocks on the south from higher pressure rocks on the north (Fig. 37). However, it should be stated at this point that definite exceptions to this overall tendency exist e.g. a high pressure picrite plug south of the Hinckley Fault in W.A. (Daniels, 1967); the South Mt Davies Intrusion which contains aluminous pyroxenes (but no other high pressure features). Furthermore lateral pressure variations within slices may complicate the structure e.g. in what appears to be a single tectonic unit (IIb in Fig. 37) between Ewarara and Teizi*, granulite assemblages indicate a decrease in pressure towards the west (Chapter 2.3).

The lineaments are therefore considered to represent movement zones whereby tectonic slices of a previously stratified crust were faulted against each other during uplift of the Block**. In broad terms the

---

* A large mylonite zone recorded by Thomson (1964) to the east of Ewarara through this belt was not observed during field mapping by the author.

** The association of a pronounced positive gravity anomaly with the uplifted Giles Complex rocks and the Mann Fault is discussed in Appendix 9.

original stratified crust is considered to have consisted of granulite facies metasediments and associated Giles Complex intrusions (themselves showing a depth stratification - Nesbitt et al., 1970), which graded upwards into amphibolite facies metasediments, possibly via a zone of partially retrograded granulites.

From the limited data available on mica ages (Chapter 14) it would appear that uplift was active about 800 m.y. ago in the eastern Tomkinson Ranges. Since the basal sediments in the adjoining Officer and Amadeus Basins are of this approximate age*, it would seem reasonable to suggest that the uplift of the Musgrave Block was accompanied or followed by flanking subsidence of and sedimentation in the adjoining areas.

The Type A dolerites have not been considered in the tectonic evaluation of the Musgrave Block so far presented because they appear to belong to an unrelated continental event. It has been previously shown that the dykes extend in a narrow belt from the Gawler Block to the Musgrave Block (Chapter 3.1.1). Their persistence to the northwest and southeast is probable although actual data are lacking. It is believed that the distribution and orientation of the dykes delineates a major continental fracture pattern.

---

* The Bitter Springs Formation is considered to have a maximum age of about 950 m.y. (Glaessner et al., 1969) while two tillites in both the Amadeus and Officer Basins (Wells et al., 1967; Wilson, 1952b)can possibly be correlated with tillites in the Kimberley region which are between 650 and 750 m.y. old (Compston and Arriens, 1968).

CHAPTER 16

CONCLUSIONS

The Giles Complex of central Australia, one of the largest groups of layered basic intrusions in the world, is important because of its potential in answering or providing clues to many critical problems of petrology. Although stratiform in origin, many of the bodies display features typical of "alpine"-type intrusions, and the association of anorthositic intrusions with more mafic and ultramafic bodies is also significant. High pressure characteristics found in some of the intrusions provide a unique chance to test experimental studies on basaltic magmas and to examine the resultant fractionation trends.

Kalka and Ewarara, the subjects of this thesis, are excellent intrusions to study in these regards. Ewarara is one of the few bodies in the Complex to exhibit a true basal contact with associated chilled basaltic marginal phases and thus allows an opportunity to examine the initial cumulus phases of crystallization of the (olivine?) tholeiite magma. The Kalka Intrusion contains over 5000 metres of layered cumulates and provides a rare chance in the Complex to study a complete rock sequence from pyroxenites through norites and olivine gabbros to anorthosites.

The dominance of orthopyroxene as an early liquidus phase at Ewarara and Kalka results from high pressures of crystallization (considered to be about 10 to 12 kilobars). Mineral reactions in the rocks (e.g. olivine + plagioclase $\longrightarrow$ orthopyroxene + clinopyroxene + spinel), exsolution of spinel and rutile in pyroxenes, high alumina contents of the pyroxenes and unusually high distribution coefficients for co-existing

pyroxenes support such pressure estimations. Similar and additional features (e.g. orthopyroxene + plagioclase ⟶ garnet; orthopyroxene + spinel ⟶ garnet) are also observed in many of the younger minor intrusions found near or in the major bodies. Maximum pressures of about 10 to 12 kilobars have also been estimated for the earlier metamorphism of the granulite country rocks.

The early crystallization of orthopyroxene referred to earlier is considered to cause progressive depletion of SiO_2 in the melt which results in the appearance of olivine at a relatively late stage in the fractionation sequence. Such a feature is opposite to that observed in classical low pressure suites such as Stillwater (e.g. Jackson, 1961).

General chemical trends for olivine, pyroxenes and plagioclase show moderate enrichment of iron and sodium upwards in the layered sequences, but indications of extreme fractionation are lacking. The overall enrichment and sole production of cumulus settled plagioclase in the upper parts of Kalka is relevant in discussions on the origin of anorthosites. The Kalka Anorthosite Zone demonstrates that anhydrous fractionation of tholeiitic magmas can lead to the derivation of such rocks. Such a mechanism has been largely rejected on negative evidence in many recent publications (see Isachsen, 1969).

Twenty one cyclic units have been recognised from the Kalka layered sequence, and two from the much thinner Ewarara Intrusion. A combination of these cyclic units show the progressive changes in cumulus mineralogy resulting from fractionation viz.

opx + ol (1) ⟶ opx (2) ⟶ opx + cpx (3) ⟶ opx + cpx + plag (4) ⟶ cpx + ol + plag (5) ⟶ ol + plag (6) ⟶ ol + cpx + plag (7) ⟶ cpx + plag (8) ⟶ plag (9).

Cycles (1) ⟶ (2) ⟶ (3) are typical of the ultramafic Ewarara Intrusion, while the Pyroxenite Zone at the base of Kalka exhibits (2) ⟶ (3). Upwards into the Norite Zone of Kalka the cycles progressively change from (2) ⟶ (3) ⟶ (4) to (4) ⟶ (5) in the Olivine Gabbro Zone. The Anorthosite Zone at the top of the sequence shows repeated examples of the (7) ⟶ (8) ⟶ (9) cycle. The recognition of cyclic units in gabbroic zones of stratiform intrusions has not, to the author's knowledge, been previously attempted and several problems not apparent in ultramafic cycles are encountered. For example differential settling between plagioclase and pyroxene/olivine is common and in fact settling overlap of phases from different cycles has been recorded in Kalka. Cycles indicative of increased fractionation are only found in the central parts of Kalka and not near intrusional walls indicating more complete mixing and current activity in these latter areas. Furthermore more advanced stages of fractionation in Kalka are found progressively further eastwards with time in Kalka. By comparison with various models developed for cyclic units, it is considered that the Kalka units were derived by a combination of convectional overturn and fresh injection of magma. Slight compositional differences for early and late injections of fresh magma have been suggested for parts of the sequence on the basis of co-crystallizing olivine - plagioclase compositions.

Models have also been developed for the production of small scale primary igneous layering. For gabbroic sequences continuous nucleation

of crystals results in a massive unlayered series of rocks, whereas only discontinuous nucleation followed by differential settling can give rise to small scale layering. Complete separation of these phases on settling gives isomodal layering; incomplete separation gives mineral graded layering. Graded layering is indicative of bottom crystallization. Settling overlap between phases formed in different bursts of crystallization can result in the formation of reverse mineral grading. The occurrence of secondary structures in small scale layering in Kalka (e.g. cross-stratification, scour channels) is considered to result from action by strong, localised bottom currents. Current velocities have been estimated at between 10^{-2} and 1 cm/sec.

Pronounced gneissic foliations imposed on the igneous layering in Kalka produce many effects previously considered indicative of "alpine"-type intrusions (Thayer, 1960, 1963). However, the deformation in Kalka is shown to be caused by minor thrusting-type movements acting in localised zones on the cumulates soon after crystallization (or possibly prior to final interstitial crystallization). The gneissic foliations and associated lineations are interpreted as resulting from plastic flow elongation of primary crystals parallel to the lineation with contemporaneous recrystallization of the most strained areas. Porphyroblast studies indicate principal elongation and compressional directions parallel to the lineation and normal to the foliation respectively.

Minor intrusions, most if not all younger than the Giles Complex, are common throughout the area. Four major suites of dolerite dykes have been distinguished on the basis of their mineral assemblages,

textures, chemistry and orientation. They provide a valuable chronological tool in separating the various events in the area. The oldest suite is found to be part of a major continental dyke swarm.

A wide variety of olivine-bearing cumulate plugs varying from dunites and picrites to leucogabbros and with gradational properties have been found to represent members of a single suite. It is thought that the presently exposed series of plugs represent different erosional levels of vertical cumulate columns formed by crystallization of basaltic magma.

As well as the gneissic deformation affecting the Giles Complex intrusions, several other deformations are also recognised. An F_1 fold phase represented by tight, isoclinal folds in the acid granulites predates the emplacement of the Giles Complex. These folds are overprinted by moderately open major east-west F_2 folds (and minor F_3 folds) which control the present distribution of lithological layering in the area. The second fold phase is considered to form an east-west fold belt confined to the central parts of the Musgrave Block.

Uplift at about 800 m.y. B.P. postdates all igneous activity as most of the igneous rocks, including the youngest, display features characteristic of high pressure crystallization. The only structural elements younger than the last igneous event are a large east-west mylonite zone (the Hinckley Fault) and an apparently similar feature, the Scarface Lineament. These structures are similar to others in the Musgrave Block which also control the distribution of rock types and are therefore interpreted as being responsible for the uplift.

APPENDICES

APPENDIX 1

METHODS OF CHEMICAL ANALYSIS

1. Sample Preparation

1) Total Rocks

Fresh clean blocks of about 250 gms (160gm for A300-361) of the samples were cut from the hand specimen and crushed, firstly to about 5mm grain size using a fly-press (with stainless steel crusher and plate), and then by repeated crushings to less than 120 mesh* in a 200ml chrome steel vessel in a Siebteknik mill. The final coarse fraction was hand ground in an agate mortar (with loss tolerance of less than 1%).

2) Minerals

Fresh blocks of the total rocks were crushed firstly to about 5mm in a fly-press, and then in a rotating steel plate grinder. Highly magnetic portions of the 120 to 224 mesh fraction were initially removed by hand magnet. Mineral separates were obtained from the remaining sample by use of a Frantz isodynamic separator. Hand picking was usually required to remove impurities of clinopyroxene from orthopyroxene concentrates, limiting the number of samples analysed.

3) Contamination

Contamination derived from crushing in the total rock samples is probably negligible because of the methods used. The chrome steel

---

* As recommended by Kleeman (1967) for statistical rock powder homogeneity.

vessels of the Siebteknik mill have the following composition: 1.7% C, 0.3% Si, 0.35% Mn, 12.0% Cr, 0.12% V, 85.53% Fe.

Contamination in the mineral separates is small. Sample purities (and types of impurities) are given below:

a) Plagioclase: Impurities (<< 1%) are usually of ferromagnesian silicates or rarely iron oxide coatings.

b) Orthopyroxene: Impurities (always < 2%) are generally confined to some iron oxide coated grains, and clinopyroxene. In the latter case only Ca will be measurably affected (2% impurities can lead to a relative error of up to 15% in Ca).

c) Clinopyroxene: Impurities (other than some iron oxide coatings) are less common in clinopyroxene than orthopyroxene. Orthopyroxene is more easily removed from clinopyroxene than vice versa, consequently clinopyroxene samples are usually more than 99% pure (minimum purity 98%).

2. Chemical Analysis

All major elements, except FeO, MgO and alkalies, were analysed using X-ray fluorescence (X.R.F.) operating under the conditions listed in Fig. 41. Rock and mineral samples were fused with a lithium borate - lanthanum oxide mixture to produce a glass and analysed against an artificial standard FS11. The analytical technique is that devised by Norrish and Hutton (1969). As a check on accuracy, standard rocks were also analysed.

Alkalies (Na_2O and K_2O) were determined using an EEL flame photometer. The samples were dissolved with hydrofluoric and perchloric acids in platinum crucibles according to the scheme of Riley and Williams (1959). Standard solutions of Na_2O and K_2O were used to calibrate the flame photometer and a blank was run with each batch of samples.

MgO was determined by TECHTRON atomic absorption spectrophotometer (A.A.S.), as well as by X.R.F., using the same solutions as for the alkali determinations. The scheme used was that of Nesbitt (1966b). Conditions were as follows:

Slit width: 100μ

Lamp filament current: 6mA

Wavelength: 2852Å

Flame: rich N_2O/C_2H_2

FeO was determined by titration against a standard $KMnO_4$ solution. The total iron determined by X.R.F. spectrography was corrected for the FeO content and the difference regarded as Fe_2O_3. Triplicate analyses for FeO were made on each sample resulting in good precision (maximum variation of 3% from mean value). Accuracy was also checked by analysis of standard rock BCR-1. FeO was determined at 8.94% which compares well with the recommended values (Flanagan, 1969).

3. Mineral Compositions

Mineral compositions for plagioclase and olivine were measured by X-ray diffractometry. Powdered samples were mounted as powder-acetone smears on oriented quartz plates.

Plagioclase compositions were determined by the method of Kleeman (1965) and Kleeman and Nesbitt (1967) by comparing τ values with the calibrated curve. Ca values for eleven analysed plagioclases (Table 10) were generally consistent with the determined An values, suggesting that structural states of the Kalka - Ewarara plagioclases are essentially the same as those of Mt Davies plagioclases.

Olivine compositions were measured by the method of Yoder and Sahama (1957) with the modification that zinc oxide instead of silicon was used as an internal standard (Nesbitt and Kleeman, 1964). Where measured, Mg contents of the olivines are generally consistent with determined Fo contents (see Table 11A analyses by Simkin and Smith, 1970).

Cell edges of garnets were determined from X-ray powder photographs using an 11.46cm diameter camera (after Sriramadas, 1957).

APPENDIX 2

A MODAL CLASSIFICATION FOR COARSE TO MEDIUM GRAINED BASIC IGNEOUS ROCKS CONSISTING OF OLIVINE, ORTHOPYROXENE, CLINOPYROXENE AND PLAGIOCLASE

Introduction

Streckeisen (1967), in classifying igneous rocks consisting essentially of quartz, alkali feldspar, plagioclase and feldspathoids, commented on the importance of unified nomenclature in scientific discussions of petrological problems. The classification of coarse to medium grained igneous rocks consisting of olivine (ol), orthopyroxene (opx), clinopyroxene (cpx) and plagioclase (pl) is at present only partially unified and considerable diversity in terminology exists in the literature.

Principles of classification

The aim of this classification is to devise a non-genetical scheme which can be readily and easily used both in the field and laboratory. To this purpose a scheme based on modal abundances of the minerals ol, opx, cpx and pl in the rock has been established.

Apart from the identification of the rock as igneous, the scheme does not require any genetic interpretation of the texture and origin of the rock or any knowledge of the actual chemistry of the phases. The latter has caused both difficulty in usage and proliferation in names in many other schemes e.g. the rocks troctolite and allivalite are essentially distinguished on their plagioclase composition by

many authors (e.g. Holmes, 1928). Such schemes are clearly impossible to use easily both in the field and in the laboratory. However, the modal scheme is of wide and easy application, and can be supplemented by chemical data if necessary. Although such a method is used in most previous schemes (e.g. Holmes, 1928; Johannsen, 1931; Peterson, 1961; Wedepohl, 1969), it was felt necessary to develop a more unified, simple and consistent nomenclature for this important group of rocks.

Indeed the stipulation that the rock must even be igneous is open to debate. De Waard (1969), in defining the term charnockite, applies it to both igneous and metamorphic rocks, and suggests using the term norite (and others) for more basic igneous and metamorphic rocks of the charnockitic association.

Method of classification

The ol-opx-cpx-pl tetrahedron has been divided by use of several critical modes. These modes serve to formally define the various rock types but it must be emphasised that these boundaries should not be rigidly enforced otherwise the use of the scheme in the field (and in the laboratory - unless point counting methods are used) is made more difficult.

Critical modes have been defined at

(a) 10% plagioclase, 30% plagioclase, 70% plagioclase and 90% plagioclase,

(b) 10% olivine, 50% olivine and 90% olivine,

(c) orthopyroxene : clinopyroxene = 1 : 1,

(d) 10% orthopyroxene,

(e) 10% clinopyroxene,

(f) 10% total pyroxene (i.e. orthopyroxene + clinopyroxene).

The resultant classification scheme is shown diagrammatically in Fig.42 and 43, and is formally defined (Table 25) on the basis of firstly, plagioclase content, then olivine content and finally pyroxene content.

For rocks in which clinopyroxene cannot be distinguished from orthopyroxene, a suggested classification is shown in Fig.43E. Also when dealing with rocks of somewhat indeterminate modal composition an indication of their composition can be given by use of terms such as gabbroic (instead of gabbro), noritic (instead of norite) etc. Furthermore it may be found impossible to use some of the critical modes effectively in the field. The 10% orthopyroxene and 10% clinopyroxene modes are the most difficult in this regard - if these are abolished by the worker then terms such as olivine clinopyroxene melanorite become defunct and other fields such as olivine melanorite are enlarged to take their place (see Table 25). These terms are, however, useful when both pyroxenes are present in major amounts (cf. Peterson's (1961) use of the term eucrite).

In rocks of this general composition other minerals can sometimes be important components of the rock e.g. chromite, spinel, magnetite. In these cases these minerals can be attached to the rock name as a prefix (e.g. spinel bearing dunite) if it is considered necessary. Classifications for some rock types of this kind, where other minerals are present in more than accessory amounts (i.e. greater than 10%), are shown in Fig. 43F,G,H (similar principles to the Fig.43A-D

classification are used).

Rocks which have a degree of metamorphic character can be prefixed by the term "meta-" (e.g. metagabbro) if considered necessary.

Discussion

The names used in this classification have been taken from previous schemes (e.g. Holmes, 1928; Johannsen, 1931; Hatch, Wells and Wells, 1961), and in most cases have been applied to rocks of similar modal composition*. However, in some cases some alterations have been made e.g. peridotite was defined by Rosenbusch (1877) as containing no feldspar, but in this scheme, to preserve consistency, it is defined as tolerating up to 10% plagioclase. Also picrite is allowed to contain more plagioclase than originally envisaged (cf. Holmes, 1928). As previously stated this nomenclature is not based on mineral chemistry and so rocks like norite consist of plagioclase of all compositions (and not only labradorite as defined by Holmes, 1928 and Joplin, 1964). However, in some cases where mineral composition is known, more precise names can be used e.g. orthopyroxenite consisting of enstatite, bronzite or hypersthene becomes enstatolite (Joplin, 1964), bronzitite or hypersthenite respectively.

No critical grain size has been used in this scheme, although it is thought that it would be applied only to rocks of medium or coarse

---

* Several names previously used by some authors have been rejected in favour of more widely used names e.g. wehrlite and saxonite are covered by olivine clinopyroxenite and olivine orthopyroxenite respectively; allivalite becomes troctolite; olivinite (as used by Hatch et al., 1961) is replaced by dunite, a much more widely used term; eucrite (of leucogabbroic composition) is rejected as it was originally applied only to meteoritic rocks.

grain sizes. Similarly no textural limitations have been placed on the terminology - this of course leads to some problems e.g. dolerite which usually exhibits a characteristic chill texture would be synonymous with medium-grained gabbro in this scheme. However in the bulk of rocks these problems would not arise.

One of the major problems encountered in deriving this scheme was in the selection of critical plagioclase modes. In this study modes of 30% plagioclase and 70% plagioclase were used to separate rocks of melanocratic, mesocratic (or intermediate) and leucocratic composition. These modes have been slightly modified from Shand's (1947) usage (viz. 30% and 60%) to make the division more standardised. Holmes (1928) and Hatch et al. (1961) favoured such a general division e.g. Holmes defined leucocratic rocks as being "abnormally poor in mafic minerals relative to the normal or average rock type of the mass or series". (Note: strict application of Holmes' definitions would not be of any benefit in comparative studies between different masses and hence a more formal division is necessary). Such a division has proved most useful in mapping the layered and massive gabbroic rocks of the Kalka Intrusion.

The distinction between mafic and felsic rocks is taken at 50% plagioclase. Ultramafic and ultrafelsic rocks are defined as containing over 90% mafic and felsic minerals respectively.

Jackson (1967) has proposed a classification scheme for igneous rocks formed by crystal settling processes (i.e. cumulates) viz.

1) semiquantitative - based on cumulus crystals only; cumulus minerals are listed in order of decreasing abundance e.g.

olivine-orthopyroxene cumulate.

2) quantitative - based on cumulus crystals only; the measured volume proportions of cumulus minerals are listed by subscript e.g. the proportions of cumulus minerals in the cumulate are ol_{75} opx_{25}.

While this is an excellent scheme it can be difficult to use in some cases in the field (and even in the laboratory) if cumulus minerals cannot be easily distinguished from intercumulus ones. This scheme also requires the rocks to be cumulates, and so, as well as being partly limited in application, requires genetic interpretations of the textures.

Cameron (1969) has also proposed a nomenclature scheme for cumulates in which the rock name indicates the cumulus phases present e.g. norite contains cumulus orthopyroxene and plagioclase.

In such schemes as Jackson's and Cameron's, the classification presented in this paper can still be applicable. The critical modes will in this case only be applied to the cumulus phases, instead of the total mineral assemblage.

APPENDIX 3

TEXTURES IN BASIC IGNEOUS ROCKS

1. Crystal Growth

Before discussing any interpretations of textures in igneous rocks, theories of nucleation and growth of crystals are reviewed. This resume draws on observations made on crystal growth in solutions and vapours as well as melts but all the conclusions drawn are believed to hold for growth in rock melts. General accounts of the crystal growth theories presented here can be found in Buckley (1951), Bunn (1964), Gilman (1963), van Hook (1961) and Jackson (1967). It should be noted that although observational data on crystal growth are good, a completely satisfactory theoretical treatment of growth is lacking (Jackson et al., 1967).

This summary will concern itself with two main problems, viz. nucleation and growth.

(1) Nucleation

There is an initial energy barrier which must be overcome before crystals can grow — this process is known as nucleation. Defay and Prigogine (1966) consider that bulk melts are in equilibrium with populations of nuclei of various sizes. The dependence of both the rate of formation and the rate of growth of nuclei on supersaturation* is shown in Fig. 39D (after Zhdanov, 1965). They both increase initially

---

* Supersaturation $\sigma = \alpha - 1$ where saturation ratio $\alpha = n/n_o$ (n = actual concentration; n_o = saturation concentration). Supersaturation is often controlled by degree of supercooling.

because of the increase in free energy differences between melt and crystal, but at large degrees of supersaturation viscosity increases inhibit diffusion and hence growth. The coincidence of the two curves will lead to strong crystallization tendencies but the lack of superposition will lead to amorphous solidification.

For a given degree of supersaturation, there is a critical nucleus size which is such that all crystals of larger size tend to grow and all smaller crystals (embryos) tend to disintegrate (by thermal activity). At a critical supersaturation the largest embryos reach the critical nucleus size and because of random fluctuations some of them continue to grow as crystallite phases. As supersaturation increases, the critical nucleus size decreases. The constant removal of critical nuclei will not affect the equilibrium concentration of embryos (which is very large compared to the number being removed). Defay and Prigogine (1966) recognise two forms of nucleation:

(a) thermal nucleation (nucleation by proliferation of embryos) where an increase in supersaturation increases the number of embryos and decreases the critical nucleus size (hence the number of embryos of required size is increased).
As well as the degree of supersaturation, the concentration of nuclei can depend on the degree of agitation in the melt.

(b) athermal nucleation (nucleation by pre-existing embryos) where existing embryos become critical nuclei due to a decrease in critical size with increasing supersaturation.

Fisher et al. (1948) show that these two processes, often operating

simultaneously, can lead to two extremes of behaviour. For a slow or moderate drop in temperature, thermal nucleation preceded by an induction period occurs. For rapid cooling, athermal nucleation occurs (rapid and of short duration).

The ease of nucleation varies for different compounds.

(2) Crystal Growth

(a) Slow rates of growth

At slow or moderate growth rates, crystals are commonly observed to grow by building up layers of material on the individual faces. These layers often begin in the centre and spread out across the faces. Layer growth usually takes place on low index faces and the resultant crystals are usually convex polygonal euhedra (morphological terminology after Correns, 1969, p. 174).

In classical theory each layer begins by fresh nucleation and is propagated across the face by advancing stepped layers (Kossel model). The step heights are equal to or multiples of the unit cell. Nucleation in the advancing layers is easier owing to the presence of steps, kinks and imperfections in the surface. These imperfections are sometimes referred to as active centres, and control what is known as the roughness of the surface (Jackson et al., 1967).

The number of kinks in each step is controlled by temperature (Verma and Krishna, 1966). Increases in supersaturation decrease step widths and increase frequency of step formation (Distler and Zvyagin, 1966).

However, while supersaturation values of 20 to 25% were required for growth to occur according to theory, growth was actually observed at supersaturations of less than 1% (Burgers and Burgers, 1956; Grisdale, 1963; Zhdanov, 1965). This feature has been explained by recently discovered physical dislocations in the crystals, notably the screw dislocation which allows continuous spiral growth of the face to occur with no initial nucleation problems for each layer (e.g. Sunagawa, 1963; Verma and Krishna, 1966). Grisdale (1963) has also suggested that the supersaturation problem could also be explained by the accretion of intermediate droplets which have fluid properties and a structural organisation intermediate between the liquid and solid states. Such growth would be controlled by forces of attraction rather than diffusion. In this case the crystal surface becomes a zone over which the degree of ordering changes. Distler and Zvyagin (1966) consider the supersaturation problem may also be solved by long range effects of local active centres (such as aggregates of point defects) on or below the crystal surface which cause crystallization to be made easier. They note that layer growth can occur at very low supersaturations even when screw dislocations do not appear to be present. Whereas dislocations are thermodynamically unstable, point defects are stable and present in all crystals.

The rate of growth is determined by several factors:

(i) supersaturation, which is generally controlled by the degree of supercooling. Local variations can occur due to release of heat of crystallization — this is especially important at faster growth rates

when heat dissipation is more difficult, and can cause discontinuous growth and hence zoning.

(ii) supply of material. A major control on the rate of growth of the crystal surface is the rate at which the material can be supplied to the surface. Two major supply mechanisms are microconcentration currents, and diffusion transport (these mechanisms also help to dissipate the heat of crystallization). At high supersaturations, viscosity increases prohibit movement of microcurrents and supply is by diffusion alone (rate of diffusion depends on many factors including the size of the ions diffusing).

(iii) rate of surface migration. Surface diffusion to step faces is very active compared to bulk diffusion as the activation energy is much less (Zhdanov, 1965). Mason (1963) has suggested that particles arriving on basal surfaces of ice were not being assimilated but were migrating over the surface to be built on to prism faces.

(iv) concentration of active centres, e.g. screw dislocations. At very slow rates of growth the production of smooth crystal surfaces with few active centres can lead to almost complete lack of growth.

(v) impurities. Adsorption of impurities (these do not include ions involved in isomorphous substitution) may tend to either "poison" the active centres or produce more of them, thus altering the growth rate (Buckley, 1951; Cabrera and Coleman, 1963). Impurities may also crystallize on the crystal face as epitaxial overgrowths (as long as the melt is supersaturated with regard to the impurity as well). Impurities can also radically change growth shapes, e.g. PO_4^{-3} anions

alter the habit of $KMnO_4$ (Buckley, 1951). Such habit changes can also be caused by other factors e.g. ice changes its habit up to five times in the temperature interval 0 to $-25^{o}C$ (Mason, 1963; Bunn, 1964). Jackson (1967) records the change from planar interface growth to dendritic growth in several compounds with additions of impurities.

The rate of growth for each face may vary depending on the atomic properties of the faces. Growth is most difficult on smooth surfaces and hence growth rates would be expected to be slowest on closest packed faces. Jackson et al. (1967) have shown that anisotropic growth rates would be expected for silicates as these possess faces with varying degrees of roughness (rough surfaces are characterized by small entropies of fusion (Jackson, 1967)). Paradoxically the fastest growing faces tend to become smaller in relative area as growth proceeds – in fact an equilibrium crystal is usually bounded by its slowest growing faces and hence may not indicate the initial crystal shape (e.g. in Chapter 9.1.4, (110) faces on orthopyroxene are shown to be progressively overshadowed by the slower growing (010) and (100) faces). Once a crystal has reached its equilibrium end form it will continue to grow but will not change its shape (assuming equilibrium conditions). The Wulff Theorem states that the habit faces of the equilibrium end form lie at distances from the centre of the crystal that are proportional to the surface energy values for the respective faces. Igneous crystals might seem to have more chances than most of growing in approximately equilibrium conditions and of achieving their end forms. However, because static crystallization in a rock melt is probably rare and since crystals are often readily

removed from the growth area (e.g. by crystal settling) it is hard to evaluate these processes in igneous crystallization. Forbes (1969) believes that variations in morphological characteristics of zircons from the Belknap Mountain Complex are due to length of the crystallization period, and thus it would be dangerous in this case, and probably many others, to attempt to infer the equilibrium form from these shapes. Furthermore, Jackson (1967) states that equilibrium shape is never observed in macroscopic crystals (larger than a fraction of a millimetre) since the shape will be determined by diffusive processes or by the kinetics of the growth process.

(b) Fast rates of growth

Fast rates of growth are usually caused by sudden and large decreases in temperature which induce a highly supersaturated state. The resultant mode of growth appears to be of a pile-on nature rather than the more ordered layer growth. It is probable that at such fast growth rates, surface migration to layer fronts cannot cope with the avalanche of crystallizing particles. In these conditions corners and edges are more favoured than faces for growth and once any irregular shapes such as cusps or hoppers are developed further growth tends to preferentially favour them.

Dendritic or skeletal forms are common. Rounded corners and edges are commonly observed (e.g. in magnetite), possibly due to the lack of steps (Cabrera and Coleman, 1963). It can be difficult to distinguish rounded edges caused by growth and rounded edges due to resorption. However some minerals with dendritic habits still commonly maintain

sharp edges e.g. olivine (Drever and Johnston, 1957). It is worthwhile noting that dendritic growth is a product of large differences in relative growth rates between faces as well as large absolute growth rates.

Cahn (1967) has shown on theoretical grounds that dendrites are the result of diffusion control processes, whereas large, non-facetted, non-dendritic morphologies indicate interface control of growth.

The growth of needle-like forms is a good example of one face receiving the bulk of the material. Growth parallel to a large thermal gradient is probably an important factor in this form of growth. It can be difficult to distinguish these forms from whisker growths (a form of slow layer growth) in which the active centres on one set of faces are poisoned allowing growth only in one direction on one face, or from growth in semi-restricted conditions.

When growth slows down, as usually happens (due to impoverishment of supply and decrease in supersaturation), dendritic forms tend to fill in and approach a more equilibrium form. Dendritic growth is not favoured by agitated conditions.

Chemical inhomogeneities in the melt are more common at fast growth rates due to local impoverishment, and consequently chemical zoning is more common than at slower growth rates.

(c) Variation of crystal habit with rate of growth

The principal types of igneous minerals commonly develop different

habits according to their environment of crystallization. These environments appear to be related to varying rates of cooling and hence probably rates of growth and nucleation. Fast rates of cooling are usually found at the contacts between the rock melt and colder country rock. If the intrusion is small these conditions may hold throughout the body (although the centres will usually cool more slowly), but in larger bodies slow cooling conditions are found away from the contacts. Slow cooling conditions will also be found in smaller bodies if the country rock has been preheated.

Typical grain shapes for extreme rates of growth in unrestricted growth environments are given below.

(i) plagioclase tends to become more lath-like at faster growth rates (it is characteristically more lath-like in dyke rocks than in the layered intrusions).

(ii) olivine is commonly dendritic in dyke rocks (Drever and Johnston, 1957), with extreme elongation in some instances; in most of the layered rocks, olivine tends to be polygonal euhedral and forms stubby crystals (in some, however, dendritic tendencies are observed). Parallel growth structures seem characteristic of intermediate growth rates, but may in part be related to synneusis processes (Vance, 1969).

(iii) pyroxene: in some of the dyke rocks, clinopyroxene tends to form lath-like aggregates (extreme elongation is observed in clinopyroxene in some marginal rocks at Ewarara - Plate 28A); in the layered sequences pyroxenes are generally stubby to slightly elongate, although rarely at Ewarara more elongate forms are observed.

(iv) spinel group: in layered intrusions generally, spinel and chromite tend to form equidimensional polygonal euhedra; magnetite and spinel form dendritic growths in many dyke rocks.

2. Environments of Igneous Crystallization

Most igneous minerals crystallize in two distinct environments, and therefore before discussing the textures resulting from this crystallization, these environments will be reviewed.

(1) Spatially Unrestricted

In this environment crystals are free to grow with only limited interference and competition from other phases i.e. concentrations of nuclei are relatively low and crystals are unattached and free floating in the melt (i.e. they have something of a planktonic existence). In such circumstances the grain shapes are characteristic - crystals tend to be

(a) euhedral i.e. with well developed crystal faces and few interference boundaries (occasionally clumping and mutual growth of crystals will occur).

(b) symmetrical i.e. equal amounts of growth have occurred on opposite faces (although more irregular growth patterns might occur at high growth rates).

Fixed crystallization on the roof, wall or base of an intrusion would be partially restricted, but the growing ends of the crystals would be essentially in an unrestricted environment.

(2) Spatially Restricted

The essential characteristic of this environment is that interference and competition between growing crystals is common, and the unrestricted growth of each face is stopped in many cases. This leads to crystals without their characteristic shape (or else with a modified version of it) or symmetrical growth development i.e. formation of anhedral to subhedral crystals. Unrestricted crystals transferred to this environment are modified, and freshly nucleated crystals suffer interference growth through their later growth period.

The division between these two environments is arbitrary.

Using subdivisions based on growth rate and degree of spatial restriction for growth, four main environments of igneous crystallization are envisaged; these are unrestricted slow, unrestricted fast, restricted slow and restricted fast.

	Growth Rate	
	Slow (S)	Fast (F)
Unrestricted (U)	U.S.	U.F.
Restricted (R)	R.S.	R.F.

There is a natural progression in most igneous crystallizations* from the unrestricted (or relatively unrestricted) to the restricted type of environment, due to the increasing proportion of crystals to

---

* The exceptions are those in which crystallization is virtually instantaneous (i.e. formation of glasses) or in which the restricted environment is occupied at least partially by a gas phase (vughs will result in this type which is confined to low pressure regimes)

liquid. The progression would be gradational — approximate critical ratios of crystals/liquid would depend on crystal shapes but would be approximately 40:60 to 60:40. As the environment becomes more restricted there are increasing tendencies for chemical sub-systems to develop as diffusion mechanisms are restricted, although the resultant inhomogeneities are only minor. This restricted environment is also more static which in turn leads to material impoverishment and heat dissipation problems as microcurrents are restricted. There is also no possibility of relative movement between the growing crystal and associated melt which could cause "flushing" of the growth zone.

The progression from the unrestricted to the restricted environment can be the result of various processes:

(a) by concentration or accumulation of early phases (formed in an unrestricted environment) as crystal packing structures. The interstitial melt trapped between the euhedral crystals will then crystallize on further cooling in environment R. The most important concentration mechanism is that of gravity separation, whereby crystals are accumulated at either the floor or roof of an intrusion. A fuller discussion of gravity separation is found in Chapter 10.

Other means of concentrating early formed crystals include flowage differentiation (Bhattacharji, 1967) and synneusis (Vance and Gilreath, 1967; Vance, 1969).

There will be, in general, a chemical discontinuity between materials initially formed in U and those formed in R, and the geochemical

significance of analyses of the resultant rock types is discussed in Appendix 7.

(b) by progressive in situ crystallization: if the rate of crystallization is fast or there is little tendency for gravity separation to occur (e.g. in granitic bodies) the environment will become progressively restricted and the resultant rock remains a single chemical entity.

3. Development of Igneous Rock Textures

Only generalised comments about the development of igneous rock textures observed in this study will be made in this section. More detailed comments about individual textures will be found elsewhere in the text.

(1) Grain Size

The most obvious component of any texture is the grain size. The grain size of any igneous mineral is usually controlled by the size it reached during growth in the unrestricted environment U. During further growth in the restricted environment R, enlargement may take place but this is usually of a limited nature. However, modifications of the absolute grain size may take place after crystallization by several mechanisms, e.g. Cameron (1969) has shown that post-cumulus (i.e. post-environment U) growth has resulted in grain size increases of over 300% in rocks of the Bushveld Complex. Hence any measured grain size should be carefully checked before being interpreted as indicating a primary grain size of the mineral.

However, assuming that the mineral grew only in environments U and R, then the resultant grain size will principally depend on the degree and rate of nucleation, and the rate and time of growth.

The largest grain sizes will be favoured by slow rates of nucleation and fast rates of growth over long periods.

It can be seen that the degree of supersaturation (i.e. degree of supercooling) is of critical importance in controlling grain size since it controls nucleation and growth rate. Low degrees of supersaturation decrease the degree and rate of nucleation (favouring larger grain sizes) but also decrease rate of growth (favouring smaller grain sizes). It will also allow greater time for growth, thereby increasing the grain size, but will also give greater opportunity for crystals to be removed from the growth zone (e.g. by crystal settling), to a restricted environment or to a non-supersaturated one.

Despite these opposing factors, it is generally considered that grains in the faster cooling environments (i.e. with greatest degrees of supersaturation) tend to be smaller than those in slower cooling environments. This is because at high rates of nucleation, the number of nuclei per unit volume is so large that potential grain size is limited (dispersion of nuclei usually cannot occur since high nucleation rates are usually associated with high growth rates and hence short times of crystallization). Therefore nucleation and hence degree of supersaturation are of prime importance in controlling grain size.

(2) Cumulate Textures

The discussions of cumulate textures are based on previous papers by other petrologists (notably Wager et al., 1960; Jackson, 1961; Wager, 1963; and Cameron, 1969) and on the author's own work.

It is now widely accepted amongst igneous petrologists that many igneous rocks are formed by the accumulation or sedimentation of crystals from a melt by gravity settling with subsequent crystallization of the interstitial liquid. Wager et al. (1960) proposed the term cumulate for any rock formed in this way. It is, however, becoming increasingly apparent that crystals can accumulate by flotation as well as by settling under the influence of gravity (e.g. sodalite in syenites — Ferguson and Pulvertaft, 1963; plagioclase in anorthosites — W.D. Romey, pers. comm.). Furthermore, accumulation of crystals from environment U can occur by other processes than gravity and yet have identical textures. A definition based partly on Jackson's (1967) definition of a cumulus crystal (although meant for gravity accumulation) is probably best for a cumulate rock viz. a rock formed by accumulation of crystals that came into existence outside of, and previously to, the concentration of which it nows forms part.

The accumulating crystals are known as cumulus (Wager et al., 1960) or primary (Jackson, 1961) crystals. The products of crystallization in environment R are known as interstitial phases, although the terms intercumulus or postcumulus material have been used by Wager et al. (1960) and Jackson (1961) respectively.

Because the great majority of cumulate rocks are formed by gravity separation and accumulation the textures will be discussed from this point of view.

There will be a critical time (dependent on the rate of crystal separation v the rate of crystallization) below which significant settling or flotation is not possible. This form of accumulation is therefore very effective in slow cooling basaltic magmas. The slow cooling environments are usually found in large, thick plutonic bodies or smaller bodies in "hot" or pre-heated country rock.

Accumulation stage

The resultant rock texture therefore is a combined result of crystallization in environments U.S. and R.S., and will be controlled by the mode of packing of the cumulus crystals and the resultant porosity (see Table 26). The mode of packing will depend on:

(a) grain shape (Figs.38A and 38C). In general cumulus grain shapes are typical of the slow growth environment but in some cases tendencies to faster growth rate forms (e.g. dendritic olivine) have been observed in this study.

(b) relative grain sizes. Cumulus silicate grains are usually of approximately similar sizes, but oxide grains (e.g. chromite, spinel) are often considerably smaller than the "critical ratio of occupation" (Fraser, 1935, p. 919) and tend to fill in the interstices between the larger silicate grains (e.g. Jackson, 1961, Fig. 53) thus decreasing porosity (Fig.38D). The smaller the grain size variation in the rock,

the greater the degree of porosity which will result (Jackson, 1961).

(c) proportion of different grain morphologies (e.g. Fig. 38E).

(d) accumulation conditions during settling and also afterwards which may effect the relative orientation of grains and the degree of packing (Fig. 38B). Post-settling processes (e.g. compaction by the overlying crystal load, seismic disturbances or slumping) can also cause expulsion of interstitial liquid and modify the original packing structure. In fact, Jackson (1961) considers that the porosities of rocks from the Ultramafic Zone of the Stillwater Intrusion are smaller than those of comparable sedimentary rocks because of consolidation effects after settling.

Transition stage

As discussed previously, the transition between environment U.S. and R.S. will often be a sharp one especially if the cumulus phases have separated from their growth zone into an area in which the melt is undersaturated with respect to them. However, if growth continues into the accumulation stage the original cumulus phases may continue to grow on their upper surface while they form the top layer of the crystal pile if their orientation is favourable (see Wager and Brown, 1968, p. 122). The amount of growth of this kind will depend on post-accumulation growth rate and rate of accumulation of crystals. Extreme forms of upward growth are represented in the harrisitic olivine horizons of Rhum (Wadsworth, 1961). In these horizons tabular olivine crystals (tabular // (010)) are oriented perpendicular to the layering and commonly show

parallel growth structures suggestive of relatively fast rates of growth. Such rocks have been termed harrisitic cumulates (Wager et al., 1960) and more recently crescumulates (Wager, 1968), but in actual fact they are not cumulates at all (although they may have grown from original cumulus seeds). Similar growth features are observed in clinopyroxene in some intrusions from Ontario (MacRae, 1969). Crystals with strongly anisotropic growth rates (e.g. plagioclase) during cumulus growth would tend to settle with the minimum growth rate faces in the horizontal plane (Fig. 38A) and hence without radically changing relative growth rates would not tend to have any marked upward extension. Hence Wager et al's. (1960) assertion that the perpendicular feldspar rock of Skaergaard (described by Wager and Deer, 1939) grew by extension of cumulus plagioclase does not seem valid since a considerable proportion of the laths would have to have been initially vertical. Furthermore the perpendicular feldspar rock is developed on steep contacts not conducive to cumulus accumulations. However, crystals with more isotropic growth rates (e.g. olivine) are more able to adopt an anisotropic growth character when conditions of restricted supply demand it (further discussion of selectivity of nuclei in semi-restricted environments is given by Correns, 1969, p. 165).

Interstitial stage

In general growth on the top surface of the pile appears limited and the most important stage of post-accumulation growth is that in the interstitial or restricted environment R. Because of the more restricted conditions, growth processes can be quite complicated. Wager et al.

(1960) were the first to attempt to classify these processes on the basis of whether the interstices were open or closed systems relative to the associated bulk melt.

(a) open systems

Open systems are usually only effective near the top of the crystal pile because of the limited range of effective material diffusion. Hence they are only important in conditions of slow crystal accumulation and relatively high rates of interstitial crystallization (Wager, 1963). With progressive interstitial crystallization, open systems will automatically progress to more closed systems as permeability decreases.

1. melt supersaturated with respect to cumulus phases

If the surrounding melt is supersaturated with respect to the cumulus phases then overgrowths of constant composition will form on the cumulus phases. If the interstitial melt is also open relative to the bulk melt, then free diffusional exchange will allow constant replenishment of the interstitial melt. This will allow constant compositional overgrowths to form until decreasing permeability of the system gradually changes the system from an open to a closed one. Possible grain size enlargements of up to 29% have been calculated by Jackson (1961).

This form of growth is known as <u>adcumulus growth</u> (Wager <u>et al</u>., 1960). It is thought to provide an explanation for the occurrence of essentially monomineralic igneous rock types (> 90% one mineral) since crystal accumulation alone cannot readily produce rocks of more than

80-85% of one phase (e.g. Cameron, 1969, p. 757).

2. melt undersaturated with respect to cumulus phases

If the growth zone is not directly in contact with the accumulation zone, then the interstitial melt will probably be undersaturated (or only saturated) with respect to the cumulus phases. In these cases either no overgrowths will occur or else the cumulus grains may be modified by reaction. In an open system, reaction may proceed further than usual because of potential chemical "flushing" of the system.

If rare nuclei of phases other than the cumulus phases are developed in the trapped liquid, then adcumulus processes could cause these to grow as unzoned crystals. Rocks formed in this way are termed heter-adcumulates (Wager et al., 1960, p. 81). Wager et al. consider these nuclei may develop because of supersaturation of these phases in the trapped liquid due to continued interstitial growth of the cumulus phases.

3. effect of decreasing temperature

Decreasing temperature will result (for both cases 1 and 2) in over-growths of lower temperature compositions on the cumulus phases. The thickness of these zones will depend on the rate of cooling v the rate of diffusional exchange with the bulk melt. Hence in a more closed system (i.e. where diffusional exchange is decreased in effectiveness) the zoning should be more pronounced for the same cooling rate.

(b) closed systems

In a closed system the interstitial melt is trapped by the cumulus crystals with no diffusional interchange occurring with the bulk magma. With lowering of temperature, progressively lower melting point phases crystallize and there is a progressive change in composition of the interstitial melt. Rocks formed by this type of growth are termed orthocumulates by Wager et al. (1960).

Such crystallization usually results in the formation of lower temperature zones or overgrowths on the cumulus grains, and nucleation of new phases as the interstitial melt composition changes. The interstitial phase chemistry will depend on whether the trapped liquid is supersaturated or undersaturated with respect to the cumulus phases.

The interstices therefore act in many ways as micro-magma chambers and often indicate the differentiation trends to be observed in the later formed rocks. The composition of the trapped melt will be that of the contemporary associated magma, but is not necessarily the same as that of the melt from which the cumulus phases grew. Consequently changes in the composition of the contemporary magma can be recognised by studying the variations in interstitial phase chemistry and mineralogy with height in the cumulate sequence. Thus indications of both bulk chemical changes in the melt, and possible later cumulus phases to crystallize can be obtained by studying the crystallization of any interstitial closed system (assuming no phase boundaries are crossed during subsequent differentiation of the bulk melt). This can be very important when

indications of later rock types are sought when parts of the overlying layered sequence are missing. The application of such methods is supported by studies of both the Kalka and Ewarara layered intrusions, and the transgressive picrite group of minor intrusions. Cameron (1969, p. 776) has also argued that changes in the bulk and mineralogical composition of interstitial phases in the Bushveld Complex is the result of progressive differentiation of the melt. Campbell (1968) considers that, due to continued supercooling of the melt, heterad minerals indicate the cumulus phases to form in adcumulate layers immediately following.

(c) mixed systems

Wager et al. (1960) consider that closed systems (sensu stricto) are rare in actual igneous cumulates, and furthermore no purely open system exists since any open system naturally progresses to a closed system. Hence most interstitial crystallization will take place in mixed systems. Hence the resultant rocks are midway between ortho- and ad-cumulates. Wager et al. (1960) term these rocks mesocumulates. They usually consist of cumulus crystals with overgrowths of the same composition (i.e. adcumulus), and remnant interstitial (pore) material consisting of new phases and zoned overgrowths on the adcumulus phases (i.e. orthocumulus).

Fabric of cumulates

The fabric of cumulates is composed of both the cumulus and the interstitial subfabrics.

The cumulus subfabric will depend on the processes of accumulation and the cumulus grain shapes. The latter vary from equidimensional to tabular to rod-like, and hence both morphological and crystallographic fabrics can be quite varied (see fuller discussion in Chapter 10).

In a restricted or interstitial environment the relationship between morphology and crystallography of any crystal is usually limited, as the morphology is controlled largely by the shape of the interstices which in turn is controlled by the cumulus morphology and fabric. Hence any pronounced preferred morphological interstitial subfabric is usually absent, although in part of the Anorthosite Zone of Kalka (Chapter 6.3) such a fabric may be represented. Although from a faster cooling environment, Wager and Brown (1968, p. 111) have described a preferred morphological elongation of interstitial pyroxene sheets perpendicular to the margin of Skaergaard Intrusion. Such elongation is probably controlled by material supply from the crystallization interface. The crystallographic orientation of grains is controlled by two factors:

i) orientation of cumulus grains. This only applies for overgrowths (or epitaxial overgrowths) on cumulus grains. However, these overgrowths are usually included with the cumulus subfabric.

ii) thermal gradient. In a population of randomly oriented nuclei which have anisotropic growth rates those with their fastest growth rate faces perpendicular to a steep thermal (and hence supersaturation) gradient, will dominate the texture in terms of size. Hence a morphological preferred orientation may result in such circumstances. The general absence of a preferred orientation in interstitial subfabrics

for minerals with anisotropic growth rates suggests that thermal gradients are small, as could be expected in slow cooling cumulate environments.

In conclusion, therefore, the total fabric will be controlled by the cumulus subfabric.

Cumulus and interstitial grain size variations

Assuming that the cumulus and interstitial phases have approximately equigranular populations, then three combinations of grain sizes can exist:

1) cumulus much coarser than interstitial (porphyritic texture). Such textures can be caused by extreme adcumulus interstitial growth, or by accumulation of outsize cumulus crystals. Such crystals can grow by unusually prolonged contact with supersaturated melt.

2) cumulus and interstitial of similar grain size.

3) interstitial much coarser than cumulus (poikilitic texture).

Poikilitic textures can be formed if:

i) some of the interstitial phases are not present as major cumulus phases (otherwise the interstitial phases form as cumulus overgrowths and become not readily distinguishable from cumulus phases).

ii) concentration of interstitial nuclei is low. This will be favoured by low degrees of supersaturation and environments of slow cooling.

In such circumstances large plates of the interstitial phases can enclose the cumulus phases. It may be difficult to distinguish between heteradcumulus and coarse-grained orthocumulus growth. However, in the orthocumulus textures, more phases (including those indicative of fractionation e.g. biotite) will tend to form and zoning will be present.

(3) Chill Textures

If the rates of crystallization are sufficiently fast in basaltic magmas, separation of early formed phases completely or partially from the host melt will not occur, especially as settling is inhibited at high particle concentrations. Textures resulting from such crystallization in environments U.F. and R.F. can be termed chill (or quench) textures since they often result from fast rates of cooling.

With high concentrations of nuclei and fast growth rates, interference/interpenetration growth types and fast growth rate morphologies are typical of these textures. In any one locality grain size is often related to the size of the igneous body — hence it appears that the grain size is controlled primarily by the rate of cooling.

Since fast cooling environments occur typically near intrusion walls, crystallization proceeding inwards from the wall may cause preferential growth of crystals perpendicular to the wall i.e. towards a more unrestricted environment. Such growth would be favoured by crystals with more anisotropic growth rates.

In the Willow Lake Intrusion in Oregon, plagioclase and ferro-

magnesian crystals are elongate perpendicular to the contacts (Poldervaart and Taubeneck, 1959; Taubeneck and Poldervaart, 1960), and have been interpreted as growing in a fast cooling environment. Similarly, the perpendicular feldspar rock of the Skaergaard Intrusion (Wager and Deer, 1939) appears to have been formed by a combination of relatively fast rates of growth and semirestricted environment rather than as extensions of cumulate grains as suggested by Wager et al. (1960). Crystals perpendicular to layering are also found in other intrusions (e.g. Pulvertaft, 1965; Loomis, 1963). Platten and Watterson (1969) have described a preferred elongation of plagioclase, pyroxene and dendritic olivine perpendicular to dyke margins in some Skye dolerites. Crystal morphology is indicative of a fast growth environment, which in turn indicates high degrees of supersaturation. This is not consistent with Platten and Watterson's interpretation of growth at implied small degrees of supersaturation.

Such fabrics are easy to distinguish from cumulate and flow fabrics. In the chill textures, crystals are elongate perpendicular to the contact or layering, whereas in gravity cumulates they are parallel to the layering, and in the flow case are parallel to the margin or bounding flow surface.

Normally, however, the fabric is an isotropic one with the crystals neither morphologically nor crystallographically aligned in any marked way (e.g. Plate 14D). In rocks of basaltic composition this texture is known as a doleritic texture in medium to coarse-grained rocks. These fabrics would result from growth of a population of homogeneously

distributed nuclei in a fast growth rate environment with no marked supersaturation gradient (otherwise preferential growth parallel to the gradient might occur). Crystallization would probably proceed inwards from the wall but would not occur on an advancing solid interface which would cause semirestricted growth. It should be noted that McNown and Malaika (1950) have shown that initial crystal orientation is stable on settling (except for asymmetric particles) for all basaltic conditions. Hence crystal orientations will not be altered early in the crystallization cycle when some degree of settling is possible.

In some textures observed in this study, radial aggregates of crystals (e.g. plagioclase, clinopyroxene) are found within the typical chill texture (e.g. Plate 20D). These aggregates are homogeneously distributed and are thought to have developed in an unrestricted environment. In a highly supersaturated melt in which a few isolated nuclei had developed, further nucleation may take place at these points rather than at fresh sites. Thus radial aggregates could be developed from these point sites. Such conditions could be found at an early unrestricted stage in a static fast cooling melt. Leray (1970) has noted the formation of such structures under conditions of large, sudden increases in the degree of undercooling.

Essentially the processes of progressive crystallization are similar to those in cumulate rocks, except that in chill rocks the processes are usually continuous and the early formed crystals do not separate from their host melt. Crystallization in environment R is usually of the closed system type comparable with orthocumulus growth. Diffusion

rates relative to crystallization rates are usually too low to allow any form of open system to develop (an exception could be in the growth of the perpendicular feldspar rock of Skaergaard (Wager and Deer, 1939, p. 148) and in other semirestricted environments at intermediate growth rates).

(4) Porphyritic Chill Textures

Many rocks with abundant chill features also contain coarser grained euhedral crystals in a non-packed porphyritic texture. The phenocrysts usually appear to have crystallized in an unrestricted environment and may exhibit features of either fast or slow growth. The resultant rock may be summarised as having crystallized in component environments U.S., U.F. and R.F. (slow growth phenocrysts) or U!F., U!!F. and R.F. (fast growth phenocrysts).

Such textures are commonly found in dyke rocks generally thought to have crystallized during ascent of the magma. In ascending basalt magmas melting points decrease with decreasing pressure, and magma temperature may increase (Harris, 1962). Consequently any phenocrysts present at lower levels may well be partially or completely resorbed during the ascent. The rounded skeletal olivines in the Type D dolerite dykes, and partially resorbed high pressure quartz phenocrysts in Victorian rhyodacites (Green and Ringwood, 1968b) and high pressure pyroxene phenocrysts in a New Zealand olivine basalt (Green and Hibberson, 1970b) may represent examples of this phenomenon.

APPENDIX 4

THE DEVELOPMENT OF SECONDARY RECRYSTALLIZATION ASSEMBLAGES IN EWARARA AND KALKA ROCKS

In many of the Giles Complex rocks studied in this investigation, as well as in some other suites of rocks (especially the Type B dolerites and also the basic granulites), two mineral assemblages have been recognised. The primary assemblage, discussed in detail in each section, is characterised by igneous features e.g. cumulate textures, euhedral grain shapes, exsolution bodies in pyroxene etc. The secondary assemblage, similar to those normally observed in the basic granulites, is characterised by very different properties, and is distinguished from the primary assemblage by the following empirical criteria: grain size and shape, grain distribution, grain boundary relations, the shape and distribution of exsolution bodies and inclusions, types of twinning and mineralogical zoning.

Grains are smaller and more equigranular in the secondary assemblages than in the primary crystals (e.g. Plates 53A, 53F). The anhedral, equidimensional secondary grains also contrast with the primary crystals which tend to be euhedral to anhedral and stubby to lath-like (e.g. Plate 53G). The distinction is also brought out by grain distribution since the secondary grains form polygonal aggregates, commonly monomineralic, with the preservation in some cases of ghost primary morphologies e.g. plagioclase laths. They commonly mantle primary crystals (e.g. Plates 18D, 53F).

Secondary grains commonly exhibit simple (straight or curved) grain boundaries with triple point terminations (e.g. Plate 53H). Interfacial angles for similar minerals approximate 120°, but may vary for dissimilar grains (cf. Vernon, 1968).

Coarse exsolution bodies or primary inclusions are not observed in secondary pyroxene or plagioclase. However, rounded inclusions (disoriented and coarser than primary exsolution) of the pre-existing exsolution bodies are found both in the secondary grains or at secondary grain boundaries (e.g. Plate 23A). Opaque exsolution blades are occasionally observed in secondary hornblende. Coalescing of orthopyroxene exsolution in clinopyroxene is commonly observed and appears to precede the formation of the secondary assemblage. It produces the characteristic mottling effect seen in many rock types. Very fine dusty exsolution(?) bodies are found in some secondary grains. Plagioclase laths in pyroxene, as well as plagioclase - pyroxene intergrowths (Chapter 9.4.3), are characteristic of the igneous or primary assemblages.

Simple twinning has not been observed in secondary plagioclase, although multiple twinning is occasionally observed (see Chapter 9.4.2). Twinning is not observed in secondary clinopyroxene.

Chemical zoning is not observed in secondary grains. Marginal diffuse extinction zoning in secondary plagioclase (e.g. Plate 44D) may resemble chemical zoning but in those cases investigated by electron microprobe the zoning represents strain effects at grain boundaries.

The secondary assemblages generally are better developed in the more

deformed rocks, and although primary crystals in the deformed rocks commonly exhibit the effects of the strain (e.g. kinking, bending, marked undulose extinction), the secondary grains are usually unstrained or exhibit only minor undulose extinction*.

It is generally considered that the secondary assemblages have very similar properties to aggregates recrystallized from strained metals (e.g. Beck, 1954; McLean, 1965) and they are therefore interpreted in a similar manner.

The term recrystallization has been used in many different contexts but in this study it means the replacement of strained grains by unstrained ones at a lower free energy (Voll, 1960). Annealing is used as a synonomous term in this thesis as suggested by Read (1965). The annealing temperature is that temperature above which the processes of physical adjustment are able to occur.

Beck (1954) has shown that annealing takes place in five stages for metals: recovery, subgrain growth or polygonisation, primary recrystallization, gradual grain growth and secondary recrystallization or coarsening. It is very likely that similar processes occur for geological materials e.g. Carter et al. (1964); Hobbs (1968).

The earliest stage observed in geological materials, polygonisation, results from internal migration and accumulation of dislocations to form strain free substructures with low angle boundaries i.e. less than 10^{o}

---

* This is probably due to overprinting by a younger deformation(s) after the formation of the secondary assemblage.

difference in adjoining lattice orientations (Voll, 1960). Primary recrystallization involves the growth of new, strain-free grains by migration of high angle boundaries at the expense of the strained matrix (Beck, 1954). Gradual grain growth occurs by boundary migration under the influence of interfacial tension to give an increase in average grain size with little change in size distribution. Migration of selected boundaries* in secondary recrystallization may result in the production of marked grain size contrasts and produce "duplex structures" (Beck, 1954, p. 291).

The most common texture in the annealed assemblages in this study are those characteristic of primary recrystallization. Grain relationships are typical of those developed in high grade metamorphic assemblages (cf. Kretz, 1966; Vernon, 1968). Similar textures have been observed widely in other deformed basic igneous rocks and basic granulites, and interpreted in a similar manner e.g. Elsdon (1969), Ragan (1969), Sturt (1969), Hermes (1970) and Moore (1970a).

Hornblende aggregates in this study are usually coarser grained and have straighter grain boundaries and better developed triple point junctions than either pyroxene or plagioclase (Plate 47G). Coarser grained orthopyroxene aggregates with straighter grain boundaries are also developed within the secondary assemblages in some instances (Plate 53H). In both cases, however, the aggregates maintain the same size distributions.

---

* Immobilisation of some grain boundaries may occur as a result of inhibition by a dispersed foreign phase or by similarity in lattice orientation between grains (Beck, 1954, p. 291; Aust and Rutten, 1963).

Plagioclase aggregates in some rocks also exhibit unusually straight grain boundaries and well developed 120° interfacial angles. These features probably form from primary recrystallization assemblages by grain boundary migration and represent examples of gradual grain growth and a closer approach to textural equilibrium.

In most cases observed the annealing processes took place at temperatures lower than those required for solid solution of the various phases seen as exsolution bodies in the primary grains. On recrystallization, exsolution phases such as spinel, rutile or magnetite appear to accumulate as small rounded grains on the secondary grain boundaries (Plate 23A). These bodies, common in most igneous rocks in the area, could be expected to inhibit grain boundary migration and may be a contributory reason why gradual grain growth processes appear to have been limited in these rocks.

No changes in actual mineralogical assemblages following recrystallization have been observed in the Ewarara - Kalka rocks. All phases present in the secondary aggregates can also be observed in the primary assemblages* in the same or equivalent rocks. In view of the general anhydrous nature of the rocks such a feature is not surprising.

In most cases a marked association of secondary and primary phases of the same type is observed, and in some instances ghost primary morphologies are preserved. These features indicate that recrystall-

---

* Primary assemblages in these instances include phases formed by subsolidus reactions between the igneous constituents prior to recrystallization.

ization occurred as an essentially non-redistributive process, and compares with the homogeneous textures described by Kretz (1969) and Flinn (1969). The fact that nucleation of the secondary phases is controlled by the previous distribution of the deformed primary crystals does not comply with Flinn's (1969) thesis that insertion of grains of one phase between pairs of like phases under the influence of interfacial energies produces ordered homogeneous textures. It is, however, more in line with Kretz's (1969) belief that nucleation was a random process not controlled by neighbouring phases.

APPENDIX 5

REVIEW OF FLOW DIFFERENTIATION

Many hydrodynamicists have experimented with the principle of flow differentiation because of its importance in the flow of solid-liquid mixtures, and in the separation of solids from liquid (see Poole and Doyle, 1966; Bhattacharji, 1967; Simkin, 1967). It has been known for some time that red cells can separate from plasma during blood flow (Vejlens, 1938). Similar effects have been observed during the flow of wood pulp, coal slurries and polymers (e.g. Busse, 1962; Schrieber and Storey, 1965).

During laminar viscous or Poiseuille* flow in capillaries, it has been noticed that solid particles (both rigid and deformable) have migrated away from the tube walls leaving a particle free zone near the wall (Goldsmith and Mason, 1961, 1962). At very low Reynolds Numbers ($Re_p < 10^{-3}$) the effect has not been observed with rigid particles although deformable particles such as liquid droplets can migrate at Re_p of 10^{-6} (Karnis et al., 1963). At very high Reynolds Number, flow becomes turbulent and no effect is observed.

For a given particle shape, the rate of migration increases with increased flow rate, particle size and displacement from the equilibrium position to which the particles are moving, but decreases with increased particle concentration (Starkey, 1956; Karnis et al., 1963; Bhattacharji and Smith, 1964; Brandt and Bugliarello, 1965). The

---

* velocity profile is parabolic.

equilibrium position varies with the type of flow differentiation, which in turn is controlled by apparently critical flow conditions. Viscosity and velocity will control whether differentiation will occur or not, but it appears that particle concentrations and relative density of particle and fluid will determine the type of differentiation to occur. However, it must be said that there is not yet enough experimental evidence to either place limiting conditions on any of the four following types or to state, beyond hypothesis, what the causes are.

Axial migration occurs when particles migrate to the central parts of the tube. The concentration of particles in the core is non-uniform at first; marked concentration peaks form at the margins but disappear on further transportation as the core narrows (Brandt and Bugliarello, 1965).

However, in some cases for neutrally bouyant particles the equilibrium or collecting position is at about 0.5 to 0.6 of the tube radius. The collected particles thus form an annulus or ring, with particles in the central part of the tube moving outwards and particles near the wall moving inwards (Segre and Silberberg, 1961, 1962; Oliver, 1962; Karnis et al., 1963; Jeffrey and Pearson, 1965). This form of collection is known as the tubular pinch effect. Little is known about this effect or its limiting conditions. Detailed studies by Jeffrey and Pearson (1965) and Oliver (1962) have shown that for upward flow particles denser than fluid migrate towards the tube axis, and those less dense towards the tube wall. For downward flow the reverse occurs.

Maude and Yearn (1967) have reported a high concentration of particles near the wall in particle flow. This has been termed a "wall peak" effect. Gotoh (1970), in a theoretical treatment, has suggested that for small particles and high Reynolds Number (as in Maude and Yearn's experiments) only particles near the wall will migrate and thus produce a wall peak. He believes it is similar to the tubular pinch effect.

At higher particle concentrations plug flow is obtained with a broad central core of immobilized solid-fluid and a lubricating casing of crystal-free liquid (Oldroyd, 1956). The change from axial migration is gradational. It may be that particle interactions become more important at higher concentrations as suggested by Oliver (1962). Segre and Silberberg (1962) have observed "necklace" formation and particle capture at high concentrations while studying the tubular pinch effect.

Modifications to these effects can be obtained by various means such as pulsating flow which may break up the patterns. Changes in other conditions such as viscosity and particle concentration can be important. Bhattacharji (1967) has shown the importance of gravity on these effects in non-vertical flow. Below a critical flow rate significant particle settling may occur. He notes, however, that a broad size distribution of particles tends to hinder settling. Bhattacharji also notes that, in changing from vertical to horizontal flow, the horizontal particle distribution is largely controlled by the initial vertical flow distribution.

The causes of the effects are not well understood, especially for the tubular pinch effect. However, at least two mechanisms appear to operate.

A "wall effect" involving mechanical interaction between particles and the wall appears to be locally effective (Vand, 1948). Oliver (1962) has found that the thickness of the boundary layer appears to be dependent only on particle size. Maude and Whitmore (1956) have suggested that the wall effect may be due to an initial redistribution of particles on entering the tube.

The more important Magnus effect (Pao, 1961, p. 424) is related to the parabolic velocity profile of Poiseuille flow. A particle within this velocity profile will be subjected to a differential flow velocity gradient across itself and will subsequently be rotated. The resultant combination of translatory and rotary motions will cause the particle to migrate inward towards a lower velocity gradient. It is significant that in Couette* flow no migration occurs across planes of shear (Goldsmith and Mason, 1962). Karnis et al. (1963) have reported an accumulation of particles where the velocity profile was blunted for Poiseuille flow. Obviously the two way migration required for the tubular pinch effect is more difficult to explain.

Schrieber and Storey (1965) have suggested the presence of thermodynamic driving forces in the migration of long chains relative to short chains in the flow of molten polymers. It has also been suggested that there is a deformational mechanism operative during the migration of liquid droplets (Chaffey et al., 1965).

---

* linear velocity gradient

Geological applications

Bhattacharji (1964, 1966, 1967) and Bhattacharji and Smith (1964) have demonstrated the possibility of axial migration in crystal-carrying magmas during geologically scaled experimentation. Such differentiation during laminar flow in a dyke or pipe could produce layering (with lateral facies changes if melt was crystallizing during flow), chemical fractionation with lower temperature minerals mantling a core of high temperature minerals, size sorting (and density sorting?) and phenocryst accumulations in dyke centres. An analysis of the chilled margin to any flow differentiated body would not give a correct indication of the bulk melt composition.

The preservation of any particle distribution would probably require rather fast cooling of the liquid, a feature fortunately commonly found in dykes or pipes.

Geological examples

The concentration of olivine in the centre of the Muskox feeder dyke has been interpreted as forming by axial migration (Smith and Kapp, 1963; Bhattacharji and Smith, 1964). Bhattacharji (1964) and Bhattacharji and Nehru (1970) have also suggested that the Mount Johnson stock in Canada formed by flow differentiation, but recent work by Philpotts (1968, 1970) has disproved this hypothesis. Bhattacharji (1967) gave many examples of possible differentiation. The leopard rock sills of Labrador (Baragar, 1960) are one of these. However, Frarey (1967) gives an alternative explanation for leopard rocks in Quebec and Newfoundland. Similarly the role of flow differentiation in the formation of bostonite anorthosite dykes in southern Greenland

has been questioned by Bridgwater (1968).

Mikheyenko (1968) has invoked similar concepts in the plastic flow of serpophyte-serpentine cement to explain a banded texture in kimberlite from the Aeromagnitnaya pipe in the USSR.

Simkin (1967) has suggested plug flow to explain olivine phenocryst distribution in northern Skye sills. Axial migration and possibly plug flow olivine phenocryst distributions have been recognised by Gibb (1968) in southwestern Skye dykes. Similar phenocryst distributions (and one suggestive of the tubular pinch effect) in Coire Lagan dykes have been described by Drever and Johnston (1958). Brandt and Bugliarello (1965) have shown that patterns similar to the tubular pinch effect are found as an early development of axial migration.

Banding in porphyritic diabase dykes in Russia (Kazaryan and Ananyan, 1967) and medial distribution of olivine nodules in a New Zealand phonolite flow (Wright, 1966) may be other examples of axial migration.

Wright et al. (1968) have reported the separation of pyroxene from plagioclase by an unknown mechanism during lava flow in the 1965 Kilauea eruption.

APPENDIX 6

MINERALOGY OF THE DOLERITE DYKE SUITES

1. Type A dolerite dykes

Plagioclase: lath-like (length: width $\simeq$ 8:1 max.); An_{58-60}; twinned (usually simple but lesser polysynthetic); zoned at grain boundaries; irregularly clouded with minute transparent anisotropic colourless needles (pyroxene?) or rarely opaque specks; rare inclusions of rounded plagioclase grains.

Clinopyroxene forms as two varieties:

1) "clear": stubby to equidimensional; sub-calcic augite ($2V_z \simeq 30$), titaniferous in some samples; rare hourglass zoning; exsolution of pyroxene lamellae and thin brown elongate to stubby plates of ilmenite or haematite; inclusions of plagioclase laths (wedge-shaped in some dykes), rarely olive-green amphibole (in rockswhere blue-green amphibole is the interstitial phase), and blebs and lenses of magnetite (exsolution of haematite) and ilmenite; faintly to strongly pleochroic (green-pink); rare simple twinning with multiple twinning common in one dolerite.

2) "mottled": granular, "mottled" pyroxene commonly mantles "clear" pyroxene with gradational or irregular boundaries. Exsolution of pyroxene in "clear" clinopyroxene core may increase in abundance towards and appears continuous with the "mottled" material. The"mottled"pyroxene is therefore thought to be an intergrowth between the two pyroxene phases. It forms optically continuous areas around the core clinopyroxene and is believed

in some cases to pseudomorph the original clinopyroxene. The "mottled" pyroxene is interpreted as resulting from recrystallization processes as it is better developed in the more deformed dykes. In an undeformed dyke from south of Mt. Davies "mottled" pyroxene is absent.

Magnetite/ilmenite: granular aggregates; intergrown with or interstitial to silicates; haematite oxidation(?) lamellae in magnetite; inclusions of plagioclase and clinopyroxene.

2. Type B dolerite dykes

Plagioclase:

1) primary - generally lathlike; simple and multiple twinning; clinopyroxene inclusions; spinel and opaque exsolution (clouding).

2) secondary - anhedral; occasional multiple twinning; rare inclusions.

Composition An_{61-63} (8 determinations on different dykes).

Orthopyroxene:

1) primary - stubby to elongate, euhedral tendency; pleochroic; clinopyroxene, and spinel, opaque or rarely rutile exsolution (opaque and dark spinel exsolution are difficult to differentiate; when very fine they give pyroxene a smoky appearance); may be zoned by cores or rims of clinopyroxene, spinel or opaque exsolution.

2) secondary - anhedral, equidimensional.

Clinopyroxene:

1) primary - subcalcic augite ($2V_z$ low); stubby; simple

twinning; blebby orthopyroxene exsolution lamellae (//100), spinel exsolution; zoned.

2) secondary - anhedral, equidimenstional.

Hornblende: anhedral; brown, pleochroic; long opaque exsolution plates rarely (when very fine grained these give smoky appearance to hornblende).

Biotite: red-brown.

Magnetite/ilmenite:

1) magnetite (slightly anisotropic?, and with haematite lamellae) with associated ilmenite rim and spinel.

2) magnetite (?) as needles and globules in silicate (pyroxene?).

Spinel: Green (very dark at times); as exsolution rods and plates in pyroxenes and plagioclase, or coalesced exsolution, or associated with opaques.

Garnet: rare; anhedral; associated with orthopyroxene.

3. Type C olivine dolerite dykes

Plagioclase: lath-like (length: width $\simeq$ 20:1 max.); simple and multiple twinning; pyroxene, biotite etc. inclusions and rare plagioclase inclusions; clouded with small particles of magnetite (?) and pyroxene (?); marginal diffuse extinction zoning; rare marginal oscillatory zoning (in some cases outer rim of untwinned feldspar with $2V_x \simeq$ 55-60: anorthoclase?).

Clinopyroxene: equidimensional to interstitial; subcalcic augite ($2V_z$ low); magnetite exsolution (may become sparse to absent towards primary grain boundaries). Subgrain growth with coalescing of magnetite exsolution with scattered equidimensional granules in the subgrains is common, producing "mottled" pyroxene (cf. Type A dolerites - this appendix).

Olivine: rounded, irregular shaped or interstitial grains; may or may not be rimmed by prismatic orthopyroxene.

Orthopyroxene: as fibrous rims on olivine, or as granular aggregates of vermicular intergrowths with magnetite.

Magnetite/ilmenite/spinel: commonly associated granular (0.2 mm) aggregates. Magnetite contains spinel exsolution. Spinel may form small granules along magnetite grain boundaries (exsolution coalescement?) as well as large grains.

Biotite: red-brown.

4. Type D porphyritic olivine dolerite dykes

Plagioclase (matrix): An_{71-73}; simple and multiple twinning; zoned; spinel exsolution in Ewarara dykes.

Clinopyroxene (matrix): subcalcic augite to augite (low $2V_z$); rare twinning; spinel and pyroxene exsolution in Ewarara dykes.

APPENDIX 7

THE SIGNIFICANCE OF THE GEOCHEMICAL ANALYSIS OF TOTAL IGNEOUS ROCK SAMPLES

In the geochemical analysis of rocks, the analyst is usually concerned with determining the composition of a single chemical system. In the case of metamorphic rocks this is done so that the compositions of the component mineral phases may be discussed in relation to their conditions of formation with due regard to the bulk composition of the rock. However, in the case of igneous rocks, a different situation may be encountered.

1. Non-chilled rocks

In the crystallization of all rock melts there is a finite temperature interval between the liquidus and the solidus which means that a finite time must elapse before crystallization is complete (except in the formation of glasses). When this time interval reaches magnitudes comparable to those required for significant separation of crystalline phases to occur from the melt in which they are crystallizing then the single chemical system concept may become untenable.

The separation and accumulation of early formed (cumulus) crystals from their "host" melt can occur by several different processes e.g. by gravitational settling or flotation (both in flowing and stagnant melts) or by flow separation processes (see Bhattacharji, 1967). Settling of crystals will occur easily in basaltic rocks (even when quite rapidly cooled — see Blake, 1968) because of relatively low melt viscosities

and high density contrasts between crystal and melt). The dynamics of settling are discussed more fully in Chapter 10. The process is more unlikely in granitic melts as melt viscosities are high and density contrasts are small (Shaw, 1965). This in part explains why layering is common in large basic intrusions, but not in granite bodies (when present in granites it is often formed by the accumulation of ferromagnesian minerals which have large density contrasts). Further complications will arise if differential settling occurs between two or more crystallizing phases*, or if the accumulated crystals are disturbed (e.g. reworking of settled crystals by currents or slumps as in the Duke Island Intrusion — Irvine, 1963).

For example differential settling can be well demonstrated in the Olivine Gabbro Zone of the layered Kalka Intrusion. This zone contains rhythmically interlayered clinopyroxene norites and olivine gabbros. The ratio layering in the olivine gabbros is caused by modal variations in plagioclase and ferromagnesian silicates (olivine, clinopyroxene) suggestive of differential settling. Mineral graded layering is also observed. Composition trends for olivine and plagioclase in this layered sequence show irregular but sympathetic variations in their compositions (Fig. 40A). However, the plagioclase curve is displaced towards the top of the sequence relative to the olivine trend which strongly indicates separation of the two phases during settling. As well as making any analysis of such resultant composite rocks meaningless, it is observed

---

* This will occur readily for hydraulically inequivalent particles such as pyroxene and plagioclase, but not for olivine and pyroxene; or for similar particles of different sizes.

that plots of the composition of olivine/plagioclase pairs from any one rock give a scattered distribution (Fig. 40B) whereas compositions of co-existing* (on crystallization and before differential settling) pairs give a much more linear variation which is probably more significant (Fig. 40C). It might be expected that in such cases neighbouring plagioclase-rich and plagioclase-poor layers would contain initially co-crystallizing phases but in the above example this is not necessarily the case. Co-crystallizing phases are sometimes separated by another "pair" of rhythmic layers. Such overlap is discussed further in Chapter 10.

With lowering of temperature the melt contained between the separated crystals will crystallize as interstitial phases — this process may in itself be varied. Wager, Brown and Wadsworth (1960) consider these processes in detail e.g. the trapped liquid may crystallize "in toto" or may continually change its composition by diffusional exchange with the external melt.

In these cases involving separation of mineral precipitates and subsequent interstitial crystallization a rock consisting of two distinct chemical systems will be formed — the relative contribution of each will depend on the concentration of the separated crystals. It can be easily recognised that the analysis of such a series of rocks containing both cumulate and interstitial components can only give at best approximate indications of trends in either. Thus the widespread use of

---

* Obtained by matching peaks and lows in the two trends.

analyses from layered rock sequences in basic intrusions, while giving useful data on general differentiation trends of basic melts, are unsatisfactory in any detailed study of this subject. Similar conclusions have been reached by Upton (1961).

An olivine tholeiite composition studied by Green and Ringwood (1967a) at 9 kilobars pressure has also been considered in the crystallization interval 1350 (liquidus) to 1310°C. Olivine is the only crystal phase reported in this interval. The variation in MgO/FeO ratio with temperature has been plotted for both liquids and co-existing olivines at these temperatures. Composition curves for mixtures of crystals and co-existing liquids in the ratios 80:20, 70:30, 60:40 and 50:50 have also been plotted (Fig. 39A; Table 24).

Using these basic curves, possible rock differentiation trends have been plotted for the temperature interval 1350 to 1310°C assuming orthocumulus crystallization of the interstitial liquid. Four theoretical curves are shown:

1) gradual decrease of ratio of crystals to liquid with decreasing temperature (Fig. 39B)

2) gradual increase of ratio of crystals to liquid with decreasing temperature (Fig. 39B)

3) irregular variations in degree of packing of crystals with decreasing temperature (Fig. 39B)

4) irregular packing concentrations at constant temperature (and hence constant liquid and crystal composition) (Fig. 39C).

It can be seen that the use of studying the compositions of such sequences where the degree of packing varies is of little use in determining the variation in MgO/FeO ratio for either the liquid or the crystal extract and may be grossly misleading (also see Brooks, 1968; Berlin and Henderson, 1968). Further complications would be introduced if more than one phase was crystallizing from the melt or if interstitial crystallization varied irregularly from orthocumulus to adcumulus.

Analyses on separated individual cumulus mineral components are usually much more valuable in determining meaningful chemical trends in the rocks. However, these themselves can be misleading for the following physical reasons:

1) later overgrowths of different composition (formed during interstitial crystallization)

2) zoned growth or inclusion of earlier-formed grains prior to accumulation

3) removal of various chemical components by solid state diffusion during subsolidus reactions with other phases

4) later partial recrystallization producing a possible further chemical variant of the cumulus mineral

5) production of another chemical variant of the mineral during subsolidus metamorphic reactions between other phases

6) movement of exsolution bodies to grain boundaries or other lower energy areas thereby becoming lost to the analysed system.

2. Chilled rocks

Many authors have used the composition of chilled rocks (i.e. rocks where significant crystal-melt separation has apparently not occurred) to give the composition of the melt. This has been especially used in the study of layered differentiation sequences by the analysis of chilled margins. There are several reasons why these analyses may not give a correct indication of the initial magma composition.

1) Contamination by wall rocks is commonly observed in igneous bodies - the degree and type of contamination may be difficult to determine. Contamination may be by either partial or complete assimilation of xenoliths or by partial removal of certain components from the wall rock (see Green and Ringwood, 1967a, p. 175). Dasch (1969) has shown that contamination may produce anomalous results in isotope studies.

2) The magma composition may alter during intrusion (especially if it was derived from a fractionated or developing source).

3) Earlier formed crystals are sometimes found as megacrysts in chilled rocks - these are susceptible to concentration or dilution by various mechanisms. Murata and Richter (1966) have reported the uneven distribution in time and space of olivine phenocrysts in Hawaiian magmas. Type C dolerite dykes from the Tomkinson Ranges also have irregular concentrations of early formed plagioclase phenocrysts in an olivine dolerite matrix which exhibits a typical chill texture (Chapter 3.1). In parts of the dykes the phenocrysts are absent - an analysis of this apparently homogeneous chilled dolerite would only give an approximate indication of the original melt composition.

Further problems may be encountered if the crystals are xenocrystal rather than phenocrystal.

4) Even in rocks with classical chill textures, it is apparent that definite crystallization orders are followed. This makes the system open to possible removal or addition of the early formed phases or residual liquids. Ragland et al. (1968) have shown that North Carolina dyke suites exhibiting "chill" textures show chemical variations within and between individual dykes — such variations could only be achieved (if the magma was initially homogeneous) by separation mechanisms of some type.

The lack of correspondence between chilled margin and bulk compositions for several intrusions have been recognised by a number of authors e.g. Smith and Kapp (1963), Nesbitt (1966a) and Upton and Wadsworth (1967).

It is therefore concluded that in a geochemical study of igneous rocks care should be taken before any petrologic implications are drawn from total rock analyses.

APPENDIX 8

DERIVATION OF PHYSICAL DATA FOR SETTLING VELOCITY CALCULATIONS

The calculation of settling velocities was made for conditions of about 10 kbars pressure and melt temperatures from about 1350°C to 1200°C (see Chapter 11). At these pressures, g = 985 cm/sec^2 (Jacobs et al., 1959).

Measured viscosities of basaltic magmas are summarised in Table 29. It is assumed in a slow cooling body such as Kalka or Ewarara the concentration of crystallizing particles remains too low to affect the viscosity. With increasing SiO_2 content, viscosity will decrease (Shaw, 1965). Similarly decreasing temperature will increase viscosity since $\eta = \eta_o^{exp}\ (B/T)$
where B is a constant (Gray and Crain, 1969). With differentiation in Kalka, both SiO_2 and temperature decrease (see Chapter 12), and hence will have opposing effects on the viscosity. It is expected overall, however, that decreasing temperature will be the controlling factor.

From the data in Table 23, the melt viscosity used in these calculations is taken as 100 poises (at the liquidus). It should be realised that near the completion of crystallization melt viscosity would probably be of the order of 500 poises.

The effect of pressure on viscosity is important to assess since Bridgman (1931) and Steele and Webb (1963) have shown that viscosity increases greatly with pressure. However, their experimental measurements were made largely on organic compounds which might be expected

to undergo structural modifications at high pressures. For silicate liquids Shaw (1965) has reported that pressure has little effect on viscosity up to 7.4 kbars. Similar results were obtained by Burnham (1967).

Basaltic melt densities have been reported at between 2.65 (at 1125°C) by Hess (1960) and 2.73 (at 1200°C) by Macdonald (1963). A decrease in density with differentiation would be expected in Kalka (cf. Hess, 1960), and some evidence for this is presented in Chapter 9.1.3. For these calculations melt densities of 2.6 to 2.7 have been used.

APPENDIX 9

RELATIONSHIPS BETWEEN THE ANKETELL GRAVITY RIDGE AND THE STRUCTURE OF THE MUSGRAVE BLOCK

One of the major crustal features of the Australian continent is delineated by the Anketell gravity ridge (Fig. 368) which extends east from the Pilbara Block to the Musgrave Block. In this latter area it is closely related to the Giles Complex intrusions of the Tomkinson group* and to the Mann Fault which appears to constitute the northern boundary of the anomaly (Rowan, 1967). Rowan has shown that the anomaly in the South Australian sector is composed of three elements:

(a) a broad regional gradient effect,

(b) local highs (about 30-50 milligals) associated with outcropping Giles Complex intrusions and

(c) a residual gravity ridge (about 60-70 milligals).

On the basis of his observations, Rowan has postulated the presence of a very large concealed basic intrusion related to the outcropping Giles Complex to account for element (c).

Estimations of the depth of this high density material from the surface depend on several variables and will remain uncertain until more detailed work is carried out. Rowan has suggested a depth of 1500 to 5000m in the Hanging Knoll area, but this depth would be increased by assuming larger density contrasts and by using different structural models as a basis for interpretation.

---

* Local highs are also associated with members of the Musgrave group.

The nature of the concealed high density material is unknown. It is of course possible that the residual ridge results entirely from a high proportion of Giles Complex intrusions at depth as suggested by Rowan. On the other hand the extent and linear nature of the ridge, its association with a major lineament and the Giles Complex intrusions (at least some of which originally crystallized in the lower crust) could be interpreted as being consistent with an hypothesis involving uplift of mantle material to a relatively shallow depth underneath the Giles Complex and the granulites. The terrain immediately south of the Mann Fault in the Tomkinson Ranges contains the highest pressure assemblages observed in the Musgrave Block (Chapter 15), and there is little doubt that faults of the magnitude of the Mann type could easily extend to the mantle. Woollard (1968) has also noted in the continental United States that "areas of geologic uplift are characterised by mantle uplift".

Although the crustal structure beneath the Musgrave Block is undoubtedly very complex, it is interesting to note that a simple model based on this hypothesis and the geological information available would result in a very similar gravity profile to that observed.

Such a region is therefore potentially important in relation to mantle research and investigations concerning the nature of the continental crust-mantle discontinuity, and warrants further examination in this regard. Several authors have suggested the outcrop occurrence of tectonically emplaced sections of oceanic mantle within geosynclinal sediments (e.g. Gass and Masson-Smith (1963) for the Troodos plutonic complex in Cyprus; Dow and Davies (1964) for the Papuan ultrabasic belt in New

Guinea; Burch (1968) for the Burro Mountain body in California) but outcropping or near surface expressions of continental mantle have, to the author's knowledge, not been proposed for other areas.

REFERENCES

ABBOTT, D. & FERGUSON, J., 1965. The Losberg Intrusion, Fochville, Transvaal. Trans. geol. Soc. S. Afr., 68, 31-52.

AKIMOTO, S. & FUJISAWA, H., 1965. Olivine-Spinel Transition in Fe_2SiO_4 and Ni_2SiO_4. J. geophys. Res., 70, 1969-1977.

ALLEN, J.R.L., 1963. Asymmetrical ripple marks and the origin of water-laid cosets of cross-strata. Lpool Manch. geol. J., 3, 187-236.

ALLEN, J.R.L., 1965. A review of the origin and characteristics of Recent alluvial sediments. Sedimentology, 5, 89-191.

ALLEN, J.R.L., 1968a. On the character and classification of bed forms. Geologie Mijnb., 47, 173-185.

ALLEN, J.R.L., 1968b. Current ripples: their relation to patterns of water and sediment motion. Nth Holland Publ. Co., 433p.

ALPER, A.M. & POLDERVAART, A., 1957. Zircons from the Animas stock and associated rocks, New Mexico. Econ. Geol., 52, 952-971.

ANDERSEN, O., 1915. An adventurine feldspar. Am. J. Sci., 4th Series, 40, 351-399.

ANDERSON, A.T. & GREENLAND, L.P., 1969. Phosphorus fractionation diagram as a quantitative indicator of crystallization differentiation of basaltic liquids. Geochim. cosmochim. Acta, 33, 493-505.

ANDERSON, A.T. & MORIN, M., 1969. Two types of massif anorthosites and their implications regarding the thermal history of the crust, in Origin of anorthosite and related rocks (Isachsen, Y.W., Ed.), N.Y. State Museum & Science Service Memoir 18.

AOKI, K., 1968. Petrogenesis of ultrabasic and basic inclusions in alkali basalts, Iki Island, Japan. Am. Miner., 53, 241-256.

AOKI, K., 1970. Petrology of kaersutite-bearing ultramafic and mafic inclusions in Iki Island, Japan. Contr. Miner. Petrology, 25, 270-283.

AOKI, K. & KUSHIRO, I., 1968. Some clinopyroxenes from ultramafic inclusions in Dreiser Weiher, Eifel. Contr. Miner. Petrology, 18, 326-337.

ARRIENS, P.A. & LAMBERT, I.B., 1969. On the age and strontium isotopic geochemistry of granulite-facies rocks from the Fraser Range, Western Australia, and the Musgrave Ranges, central Australia. Spec. Publs geol. Soc. Aust., 2, 377-388.

ATKINS, F.B., 1969. Pyroxenes of the Bushveld Intrusion, South Africa. J. Petrology, 10, 222-249.

AUST, K.T. & RUTTER, J.W., 1963. Grain boundary migration, in Recovery and recrystallization of metals (Himmel, L., Ed.), Gordon & Breach.

AYRTON, S., 1968. Structures isoclinales dans les péridotites du Mont Vourinos (Macédoine grecque) - un example de déformation de roches ultrabasiques. Schweiz. miner. petrogr. Mitt., 48, 733-750.

BANNO, S. & GREEN, D.H., 1968. Experimental studies on eclogites: the roles of magnetite and acmite in eclogitic assemblages. Chem. Geol., 3, 21-32.

BARAGAR, W.R., 1960. Petrology of basaltic rocks in part of the Labrador trough. Bull. geol. Soc. Am., 71, 1589-1644.

BARNES, L., 1968. The petrography and geochemistry of some high grade metamorphic rocks from the Mt. Davies - Giles region, central Australia. Unpublished Honours thesis, University of Adelaide.

BARTHOMELÉ, P., 1961. Coexisting pyroxenes in igneous and metamorphic rocks. Geol. Mag., 98, 346-348.

BARTLETT, R.W., 1969. Magma convection, temperature distribution, and differentiation. Am. J. Sci., 267, 1067-1082.

BASEDOW, H., 1905. Geological report on the country traversed by the S.A. Government Prospecting Expedition, 1903. Trans. R. Soc. S. Aust., 29, 57-102.

BATTEY, M.H., 1965. Layered structure in rocks of the Jotunheim Complex, Norway. Mineralog. Mag., 34, 35-51.

BECK, P.A., 1954. Annealing of cold worked metals. Adv. Phys., 3, 245-324.

BEESON, M.H. & JACKSON, E.D., 1970. Origin of the garnet pyroxenite xenoliths at Salt Lake Crater, Oahu. Spec. Pap. Miner. Soc. Am., 3, 95-112.

BENCE, A.E., PAPIKE, J.J. & PREWITT, C.T., 1970. Apollo 12 clinopyroxenes: chemical trends. Earth Plan. Sci. Letters, 8, 393-399.

BENTOR, Y.K., 1951. On the formation of cloudy zones in plagioclases. Schweiz. miner. petrogr. Mitt., 31, 535-552.

BERLIN, R. & HENDERSON, C.M.B., 1968. A reinterpretation of Sr and Ca fractionation trends in plagioclases from basic rocks. Earth Plan. Sci. Letters, 4, 79-83.

BERRANGÉ, J.P., 1965. Some critical differences between orogenic-plutonic and gravity-stratified anorthosites. Geol. Rdsch., 55, 617-642.

BERTHELSEN, A., 1960. Structural studies in the Precambrian of West Greenland, geology of Tovqussap Nuna. Meddr Grønland, 123 (1), 223p.

BHATTACHARJEE, S.C., 1963. Note on the 'corona'-bearing olivine metadolerites near Kalma, Purulia district, West Bengal. Rec. geol. Surv. India, 93, 265-266.

BHATTACHARJI, S., 1964. Fluid-mechanics model for the mechanics of differentiation of basaltic magma during flowage. Spec. Pap. geol. Soc. Am., 76, 14-15.

BHATTACHARJI, S., 1965. Crystal settling in basaltic magma (Abstract). Spec. Pap. geol. Soc. Am., 82, 11-12.

BHATTACHARJI, S., 1966. Experimental scale model studies on flowage differentiation in sills. Spec. Pap. geol. Soc. Am., 87, 11-12.

BHATTACHARJI, S., 1967. Mechanics of flow differentiation in ultramafic and mafic sills. J. Geol., 75, 101-112.

BHATTACHARJI, S. & NEHRU, C.E., 1970. Igneous structures and mechanism of emplacement of Mount Johnson, a Monteregian intrusion, Quebec: Discussion. Can. J. Earth Sci., 7, 191-194.

BHATTACHARJI, S. & SMITH, C.H., 1964. Flowage differentiation. Science, 145, 150-153.

BILGRAMI, S.A., 1969. Geology and chemical mineralogy of the Zhob Valley chromite deposits, West Pakistan. Am. Miner., 54, 134-148.

BINNS, R.A., 1964. Zones of progressive regional metamorphism in the Willyama Complex, Broken Hill district, NSW. J. geol. Soc. Aust., 11, 283-330

BINNS, R.A., LONG, J.V.P. & REED, S.J.B., 1963. Some naturally occurring members of the clinoenstatite-clinoferrosilite mineral series. Nature, 198, 777-778.

BISHOP, D.G. & FORCE, E.R., 1969. The reliability of graded bedding as an indicator of the order of superposition. J. Geol., 77, 346-352.

BLACKBURN, W.H., 1968. The spatial extent of chemical equilibrium in some high-grade metamorphic rocks from the Grenville of southeastern Ontario. Contr. Miner. Petrology, 19, 72-92.

BLACKERBY, B.A., 1968. Convolute zoning of plagioclase phenocrysts in Miocene volcanics from the Western Santa Monica Mountains, California. Am. Miner., 53, 954-962.

BLAKE, D.H., 1968. Gravitational sorting of phenocrysts in some Icelandic intrusive sheets. Geol. Mag., 105, 140-148.

BLIGHT, D.F., 1969. The geology, petrology and geochemistry of an area south of Tollu, Western Australia. Unpublished Honours thesis, University of Adelaide.

BOETTCHER, A.L. & WYLLIE, P.J., 1968a. Melting of granite with excess water to 30 kilobars pressure. J. Geol., 76, 235-244.

BOETTCHER, A.L. & WYLLIE, P.J., 1968b. The calcite-aragonite transition measured in the system CaO - CO_2 - H_2O. J. Geol., 76, 314-330.

BORG, I. & HANDIN, J., 1966. Experimental deformation of crystalline rocks. Tectonophysics, 3, 249-367.

BORISENKO, L.F., 1967. Correlation among iron, vanadium and titanium in pyroxenes. Geoch. Int., 4, 263-269.

BOTTINGA, Y., KUDO, A. & WEILL, D., 1966. Some observations on oscillatory zoning and crystallization of magmatic plagioclase. Am. Miner., 51, 792-806.

BOWDEN, P.R., 1969. Geology of the Tollu area, Western Australia. Unpublished Honours thesis, University of Adelaide.

BOWES, D.R. & SKINNER, W.R., 1970. Geochemical comparison of the Stillwater complex and alpine-type ultrabasic complexes, Beartooth Mountains, Montana and Wyoming. Geol. Mag., 106, 477-484.

BOWES, D.R., WRIGHT, A.E. & PARK, R.G., 1964. Layered intrusive rocks in the Lewisian of the North-West Highlands of Scotland. Q. Jl geol. Soc. Lond., 120, 153-192.

BOYD, F.R. & BROWN, G.M., 1967. Electron-probe study of exsolution in pyroxenes. Annu. Rep. Director Geophys. Lab., Carnegie Inst. Washington, Yearbook 66, 353-359.

BOYD, F.R. & ENGLAND, J.L., 1960. Minerals of the mantle. Annu. Rep. Director Geophys. Lab., Carnegie Inst. Washington, Yearbook 59, 47-52.

BOYD, F.R., ENGLAND, J.L. & DAVIS, B.T.C., 1964. Effects of pressure on the melting and polymorphism of enstatite, $MgSiO_3$. J. geophys. Res., 69, 2101-2109.

BRANDT, A. & BUGLIARELLO, G., 1965. Concentration redistribution phenomena in the shear flow of monolayers of suspended particles. 36th Soc. Rheol. Meeting, Cleveland.

BRIDGMAN, P.W., 1931. The physics of high pressure. G. Bell (London), 398p.

BRIDGWATER, D., 1966. Clouded felspar. Geol. Mag., 103, 284-285.

BRIDGWATER, D., 1968. Mechanics of flow differentiation in ultramafic and mafic sills: a discussion. J. Geol., 76, 596-599.

BRIGGS, L.I. & MIDDLETON, G.V., 1965. Hydromechanical principles of sediment structure formation. Spec. Pap. Soc. Econ. Pal. Mineral., 12, 5-16.

BRÖGGER, W.C., 1934. The south Norwegian hyperites and their metamorphism. Skr. norske vidensk-Akad. I: Mat. Naturv. K1, 1-421.

BROOKS, C.K., 1968. On the interpretation of trends in element ratios in differentiated igneous rocks, with particular reference to strontium and calcium. Chem. Geol., 3, 15-20.

BROTHERS, R.N., 1959. Flow orientation of olivine. Am. J. Sci., 257, 574-584.

BROTHERS, R.N., 1964. Petrofabric analyses of Rhum and Skaergaard layered rocks. J. Petrology, 5, 255-274.

BROWN, G.M., 1956. Layered ultrabasic rocks of Rhum, Inner Hebrides. Phil. Trans. R. Soc., 240, 1-53.

BROWN, G.M., 1967. Experimental studies on inversion relations in natural pigeonitic pyroxenes. Annu. Rep. Director Geophys. Lab., Carnegie Inst. Washington, Yearbook 66, 347-353.

BROWN, G.M. & VINCENT, E.A., 1963. Pyroxenes from the late stages of fractionation of the Skaergaard Intrusion, East Greenland. J. Petrology, 4, 175-197.

BROWN, H.Y.L., 1890. Report on journey from Warrina to Musgrave Ranges. S. Aust. Parl. Paper, 45.

BROWN, H.Y.L., 1893. Catalogue of South Australian minerals. Govt. Printer, Adelaide.

BUCKLEY, H.E., 1951. Crystal Growth. John Wiley & Sons, Inc., N.Y. 571p.

BUDDINGTON, A.F., 1939. Adirondacks igneous rocks and their metamorphism. Mem. geol. Soc. Am., 7.

BUDDINGTON, A.F., 1969. Adirondack anorthositic series, in Origin of anorthosite and related rocks (Isachsen, Y.W., Ed.), N.Y. State Museum & Science Service Memoir 18.

BULTITUDE, R.J. & GREEN, D.H., 1967. Experimental study at high pressures on the origin of olivine nephelinite and olivine melilite nephelinite magmas. Earth Plan. Sci. Letters, 3, 325-337.

BULTITUDE, R.J. & GREEN, D.H., 1970. Highly undersaturated rocks in upper mantle conditions. Nature, 226, 748-749.

BUNN, C., 1964. Crystals - their role in nature and in science. Academic Press, 176p.

BURCH, S.H., 1968. Tectonic emplacement of the Burro Mountain Ultramafic Body, Santa Lucia Range, California. Bull. geol. Soc. Am., 79, 527-544.

BURGERS, J.M. & BURGERS, W.G., 1956. Dislocations in crystal lattices, in Rheology, vol.I (Eirich, F.R., Ed.), Academic Press.

BURNHAM, C.W., 1967. Hydrothermal fluids at the magmatic stage, in Geochemistry of hydrothermal ore deposits (Barnes, H.L., Ed.), Holt, Rinehart & Winston, Inc., 670p.

BURNHAM, C.W. & SHADE, J.W., 1968. Hydrolysis equilibria in the system K_2O - Al_2O_3 - SiO_2 - H_2O. Spec. Pap. geol. Soc. Am., 101, 32-33.

BURNS, D.J., 1966. Chemical and mineralogical changes associated with the Laxford metamorphism of dolerite dykes in the Scourie - Loch Laxform area, Sutherland, Scotland. Geol. Mag., 103, 19-35.

BUSSE, W.F., 1964. Two decades of high polymer physics. Physics today, 17, 32-41.

CABRERA, N. & COLEMAN, R.V., 1963. Theory of crystal growth from the vapour, in The art and science of growing crystals (Gilman, J.J., Ed.), John Wiley & Sons, Inc., N.Y., 493p.

CAHN, J.W., 1967. On the morphological stability of growing crystals. Physics Chem. Solids Suppl. 1, 681-690.

CAMERON, E.N., 1963. Structure and rock sequences of the Critical Zone of the eastern Bushveld Complex. Spec. Pap. Miner. Soc. Am., 1, 93-107.

CAMERON, E.N., 1969. Postcumulus changes in the eastern Bushveld Complex. Am. Miner., 54, 754-779.

CAMPBELL, I.H., 1968. The origin of heteradcumulate and adcumulate textures in the Jimberlana Norite. Geol. Mag., 105, 378-383.

CARMICHAEL, I.S.E. & NICHOLLS, J., 1967. Iron-titanium oxides and oxygen fugacities in volcanic rocks. J. geophys. Res., 72, 4665-4687.

CARRUTHERS, J., 1892. Triangulation of northwest portion of South Australia. S. Aust. Parl. Paper, 179.

CARSTENS, H., 1967. Exsolution in ternary felspars. I. On the formation of antiperthites. Contr. Miner. Petrology, 14, 27-35.

CARTER, N.L., CHRISTIE, J.M. & GRIGGS, D.T., 1964. Experimental deformation and recrystallization of quartz. J. Geol., 72, 687-733.

CARTER, N.L. & RALEIGH, C.B., 1969. Principal stress directions from plastic flow in crystals. Bull. geol. Soc. Am., 80, 1231-1264.

CHAFFEY, C.E., BRENNER, H. & MASON, S.G., 1965. Particle motions in sheared suspensions: XVII. Deformation and migration of liquid drops. Rheol. Acta, 4, 56-63.

CHALLIS, G.A., 1965. The Origin of N.Z. Ultramafic Intrusions. J. Petrology, 6, 322-364.

CHALLIS, G.A., 1967. X-ray study of deformation lamellae in olivines of ultramafic rocks. Mineralog. Mag., 36, 195-203.

CHESWORTH, W., 1967. The biotite-cordierite-almandite subfacies of the hornblende-granulite facies: a discussion. Can. Mineralogist, 9, 263-268.

CHRISTIE, J.M., 1960. Mylonitic rocks of the Moine Thrust-zone in the Assynt region, north-west Scotland. Trans. geol. Soc. Edinb., 18, 79-93.

CLARK, S.P.Jr., 1966. Handbook of Physical Constants. Mem. geol. Soc. Am., 97.

CLARKE, E. de C., 1938. Middle and West Australia, in Regionale Geologie der Erde (Andrée, K., Brouwer, H.A. & Bucher, W.H., Eds), Vol. 1 Die alten Kerne, Akademische Verlagsgesellschaft M.B.H., Leipzig.

COATS, R.P., 1963. The geology of the Alberga 4-mile military sheet. Rep. Invest. Dept. Mines S.Aust., 22.

COE, R.S., 1970. The thermodynamic effect of shear stress on the ortho-clino inversion in enstatite and other coherent phase transitions characterized by a finite simple shear. Contr. Miner. Petrology, 26, 247-264.

COHEN, L.H., ITO, K. & KENNEDY, G.C., 1967. Melting and phase relations in an anhydrous basalt to 40 kilobars. Am. J. Sci., 265, 475-518.

COIN, C.D.A., 1970. A study of the granulite facies terrain near Amata. Unpublished Honours thesis, University of Adelaide.

COMPSTON, W. & ARRIENS, P.A., 1968. The Precambrian geochronology of Australia. Can. J. Earth Sci., 5, 561-583.

COMPSTON, W. & NESBITT, R.W., 1967. Isotopic age of the Tollu Volcanics, WA. J. geol. Soc. Aust., 14, 235-238.

CORRENS, C.W., 1969. Introduction to mineralogy. Springer-Verlag, 484p.

DALLWITZ, W.B., 1968. Coexisting sapphirine and quartz in granulite from Enderby Land, Antarctica. Nature, 219, 476-477.

DALLWITZ, W.B., GREEN, D.H. & THOMSON, J.E., 1966. Clinoenstatite in a volcanic rock from the Cape Vogel area, Papua. J. Petrology, 7, 375-403.

DALZIEL, I.W.D. & BAILEY, S.W., 1968. Deformed garnets in a mylonitic rock from the Grenville Front and their tectonic significance. Am. J. Sci., 266, 542-562.

DANIELS, J.L., 1967. Subdivision of the Giles Complex, Central Australia. Annu. Rep. geol. Surv. West. Aust. for 1966, 58-62.

DANIELS, J.L., 1969. Explanatory notes on the Talbot 1:250,000 Geological Sheet, WA. Rec. geol. Surv. West. Aust., 1969/14.

DANIELS, J.L., SKIBA, W.J. & SUTTON, J., 1965. The deformation of some banded gabbros in the northern Somalia fold belt. Q. Jl geol. Soc. Lond., 121, 111-142.

DASCH, E.J., 1969. Strontium isotope disequilibrium in a porphyritic alkali basalt and its bearing on magmatic processes. J. geophys. Res., 74, 560-565.

DAVIDSON, L.R., 1968. Variation in ferrous iron-magnesium distribution coefficients of metamorphic pyroxenes from Quairading, Western Australia. Contr. Miner. Petrology, 19, 239-259.

DEARNLEY, R., 1962. An outline of the Lewisian Complex of the Outer Hebrides in relation to that of the Scottish mainland. Q. Jl geol. Soc. Lond., 118, 143-176.

DEER, W.A., HOWIE, R.A. & ZUSSMAN, J., 1963. Rock-forming minerals. Longmans.

DEFAY, R. & PRIGOGINE, I., 1966. Surface Tension and Adsorption. Longmans, 432p.

DE WAARD, D., 1965. A proposed subdivision of the granulite facies. Am. J. Sci., 263, 455-461.

DE WAARD, D., 1969. The occurrence of charnockite in the Adirondacks: a note on the origin and definition of charnockite. Am. J. Sci., 267, 983-987.

DE WAARD, D. & ROMEY, W.D., 1969. Chemical and petrologic trends in the anorthosite - charnockite series of the Snowy Mountain massif, Adirondack Highlands. Am. Miner., 54, 529-538.

DISTLER, G.I. & ZVYAGIN, B.B., 1966. A dislocation-free mechanism of growth of real crystals. Nature, 212, 807-808.

DOW, D.B. & DAVIES, H.L., 1964. Geology of Bowutu Mountains, New Guinea. Rep. Bur. Miner. Resour., Geol. Geophys. Aust., 75.

DREVER, H.I. & JOHNSTON, R., 1957. Crystal growth of forsteritic olivine in magmas and melts. Trans. R. Soc. Edinb., 63, 289-315.

DREVER, H.I. & JOHNSTON, R., 1958. The petrology of picritic rocks in minor intrusions - a Hebridean group. Trans. R. Soc. Edinb., 63, 459-499.

DREW, G.J., 1970. Geophysical investigations of the southern Middleback Range area. Unpublished Honours thesis, University of Adelaide.

DUNHAM, A.C., 1965. A new type of banding in ultrabasic rocks from central Rhum, Inverness-shire, Scotland. Am. Miner., 50, 1410-1420.

ELDERS, W.A. & RUCKLIDGE, J.C., 1969. Layering and net veining in hornblende lamprophyre intrusions from the coast of Labrador. J. Geol., 77, 721-729.

ELSDON, R., 1969. The structure and intrusive mechanism of the Kap Edvard Holm layered gabbro complex, East Greenland. Geol. Mag., 106, 46-56.

EMELEUS, C.H., 1963. Structural and petrographic observations on layered granites from southern Greenland. Spec. Pap. Miner. Soc. Am., 1, 22-29.

EMSLIE, R.F., 1969. Crystallization and differentiation of the Michikamau Intrusion, in Origin of anorthosite and related rocks (Isachsen, Y.W., Ed.), N.Y. State Museum & Science Service Memoir 18.

EMSLIE, R.F., 1970. The geology of the Michikamau Intrusion, Labrador. Geol. Surv. Pap. Can., 68/57.

ENGELS, J.P. & VOGEL, D.E., 1966. Garnet reaction-rims between plagioclase and hypersthene in a metanorite from Cabo Ortegal (northwestern Spain). Neues Jb. Miner. Mh., 13-19.

ERNST, W.G., 1960. Granophyre-diabase relations, Endion Sill, Duluth, Minnesota. J. Petrology, 1 (3), 286-303.

EUGSTER, H.P. & WONES, D.R., 1962. Stability relations of the ferruginous biotite, annite. J. Petrology, 3, 82-125.

FACER, R.A., 1967. A preliminary study of the magnetic properties of rocks from the Giles Complex, Central Australia. Aust. J. Sci., 30, 237-238.

FACER, R.A., 1970. Magnetic properties of the Giles Complex, central Australia. Search, 1, 76-77.

FERGUSON, J., 1969. Compositional variation in minerals from mafic rocks of the Bushveld Complex. Trans. geol. Soc. S. Afr., 72, 61-78.

FERGUSON, J. & BOTHA, E., 1963. Some aspects of igneous layering in the basic zones of the Bushveld Complex. Trans. geol. Soc. S. Afr., 66, 259-282.

FERGUSON, J. & PULVERTAFT, T.C.R., 1963. Contrasted styles of igneous layering in the Gardar Province of south Greenland. Spec. Pap. Miner. Soc. Am., 1, 10-21.

FISHER, J.C., HOLLOMON, J.H. & TURNBULL, D., 1948. Nucleation. J. appl. Phys., 19, 775-784.

FLANAGAN, F.J., 1969. U.S. Geological Survey standards. II. First compilation of data for the new U.S.G.S. rocks. Geochim. cosmochim. Acta, 33, 81-120.

FLAVELLE, A.J. & GOODSPEED, M.J., 1962. Fitzroy and Canning Basins reconnaissance gravity surveys, Western Australia 1952-60. Rec. Bur. Miner. Resour., Geol. Geophys. Aust., 1962/105.

FLINN, D., 1969. Grain contacts in crystalline rocks. Lithos, 3, 361-370.

FORESTIER, F.H. & LASNIER, B., 1969. De'couverte de niveaux d'amphibolites à pargasite, anorthite, corindon et saphirine dans les schistes cristallins de la vallée du Haut-Allier. Contr. Miner. Petrology, 23, 194-235.

FORMAN, D.J., 1966. Regional geology of the southern margin of the Amadeus Basin, Central Australia. Rep. Bur. Miner. Resour., Geol. Geophys. Aust., 87.

FRANKEL, J.J., 1969. A megaporphyritic dolerite on Long Island, Seychelles Archipelago. Geol. Mag., 106, 260-269.

FRAREY, M.J., 1967. Willbob Lake and Thompson Lake map-areas, Quebec and Newfoundland. Mem. geol. Surv. Can., 348.

FRASER, H.J., 1935. Experimental study of the porosity and permeability of clastic sediments. J. Geol., 43, 910-1010.

FRODESEN, S., 1968a. Coronas around olivine in a small gabbro intrusion, Bamble area, South Norway. Norsk geol. Tidssk., 48, 201-206.

FRODESEN, S., 1968b. Petrographical and chemical investigations of a Precambrian gabbro intrusion, Hiasen, Bamble area, South Norway. Norsk geol. Tidssk., 48, 281-306.

FYFE, W.S., 1967. Stability of Al_2SiO_5 polymorphs. Chem. Geol., 2, 67-76.

FYFE, W.S., & TURNER, F.J., 1966. Reappraisal of the metamorphic facies concept. Contr. Miner. Petrology, 12, 354-364.

GASS, I.G. & MASSON-SMITH, D., 1963. The geology and gravity anomalies of the Troodos massif, Cyprus. Phil. Trans. R. Soc. Series A, 255, 417-467.

GHISLER, M., 1970. Pre-metamorphic folded chromite deposits of stratiform type in the early Precambrian of west Greenland. Min. Deposita, 5, 223-236.

GIBB, F.G.F., 1968. Flow differentiation in the xenolithic ultrabasic dykes of the Cuillins and the Strathaird Peninsula, Isle of Skye, Scotland. J. Petrology, 9, 411-443.

GILES, E., 1874. Mr. E. Giles's explorations, 1873-4. S. Aust. Parl. Paper, 215.

GILMAN, J.J. (Ed.), 1963. The art and science of growing crystals. John Wiley & Sons, Inc., N.Y., 493p.

GJELSVIK, T., 1952. Metamorphosed dolerites in the gneiss area of Sunnmøre on the West Coast of southern Norway. Norsk geol. Tidssk., 30, 31-134.

GLAESSNER, M.F., PREISS, W.V. & WALTER, M.R., 1969. Precambrian columnar stromatolites in Australia: morphological and stratigraphic analysis. Science, 164, 1056-1058.

GLAVERIS, M., 1970. The occurrence of olivine hyperite at Ødegårdens Verk, Bamble, South Norway. Norsk geol. Tidssk., 50, 15-17.

GOLDSMITH, H.L. & MASON, S.G., 1961. Axial migration of particles in Poiseuille flow. Nature, 190, 1095-1096.

GOLDSMITH, H.L. & MASON, S.G., 1962. The flow of suspensions through tubes. 1. Single spheres, rods and discs. J. Colloid Sci., 17, 448-476.

GOODE, A.D.T. & KRIEG, G.W., 1965. The geology of Ewarara Intrusion, Giles Complex, central Australia. Unpublished Honours thesis, University of Adelaide.

GOODE, A.D.T. & KRIEG, G.W., 1967. The geology of Ewarara Intrusion, Giles Complex, central Australia. J. geol. Soc. Aust., 14, 185-194.

GOODE, A.D.T. & NESBITT, R.W., 1969. Granulites and basic intrusions of part of the eastern Tomkinson Ranges, central Australia. J. geol. Soc. Aust., Spec. Publ. 2, 279-281.

GOSSE, W.C., 1874. W.C. Gosse's explorations, 1873. S. Aust. Parl. Paper 48.

GOTOH, K., 1970. Migration of a neutrally bouyant particle in Poiseuille flow: a possible explanation. Nature, 225, 848-850.

GRAY, C.M., 1967. The geology, petrology and geochemistry of the Teizi metanorthosite. Unpublished Honours thesis, University of Adelaide.

GRAY, N.H. & CRAIN, I.K., 1966. Crystal settling in thin sills - a model. Can. Mineralogist, 8, p.666.

GRAY, N.H. & CRAIN, I.K., 1969. Crystal settling in sills: a model for suspension settling. Can. J. Earth Sci., 6, 1211-1216.

GREEN, D.H., 1963. Alumina content of enstatite in a Venezuelan high-temperature peridotite. Bull. geol. Soc. Am., 74, 1397-1402.

GREEN, D.H., 1964. The petrogenesis of the high-temperature peridotite intrusion in the Lizard Area, Cornwall. J. Petrology, 5, 134-188.

GREEN, D.H., 1966. The origin of the "eclogites" from Salt Lake Crater, Hawaii. Earth Plan. Sci. Letters, 1, 414-420.

GREEN, D.H., 1970. A review of experimental evidence on the origin of basaltic and nephelinitic magmas. Phys. Earth Planet. Interiors, 3, 221-235.

GREEN, D.H. & HIBBERSON, W., 1970a. The instability of plagioclase in peridotite at high pressure. Lithos, 3, 209-221.

GREEN, D.H. & HIBBERSON, W., 1970b. Experimental duplication of conditions of precipitation of high-pressure phenocrysts in a basaltic magma. Phys. Earth Planet. Interiors, 3, 247-254.

GREEN, D.H. & LAMBERT, I.B., 1965. Experimental crystallization of anhydrous granite at high pressures and temperatures. J. geophys. Res., 70, 5259-5268.

GREEN, D.H. & RINGWOOD, A.E., 1964. Fractionation of basalt magmas at high pressures. Nature, 201, 1276-1279.

GREEN, D.H. & RINGWOOD, A.E., 1967a. The genesis of basaltic magmas. Contr. Miner. Petrology, 15, 104-190.

GREEN, D.H. & RINGWOOD, A.E., 1967b. An experimental investigation of the gabbro to eclogite transformation and its petrological applications. Geochim. cosmochim. Acta, 31, 767-834.

GREEN, D.H. & RINGWOOD, A.E., 1967c. The stability fields of aluminous pyroxene peridotite and garnet peridotite and their relevance in upper mantle structure. Earth Plan. Sci. Letters, 3, 151-160.

GREEN, T.H., 1967. An experimental investigation of sub-solidus assemblages formed at high pressure in high-alumina basalt, kyanite eclogite and grosspydite compositions. Contr. Miner. Petrology, 16, 84-114.

GREEN, T.H., 1969a. High pressure experimental studies on the origin of anorthosite. Can. J. Earth Sci., 6, 427-440.

GREEN, T.H., 1969b. The diopside-kyanite join at high pressures and temperatures. Lithos, 2, 333-341.

GREEN, T.H., 1969c. Experimental fractional crystallization of quartz diorite and its application to the problem of anorthosite origin, in Origin of anorthosite and related rocks (Isachsen, Y.W., Ed.), N.Y. State Museum & Science Service Memoir 18.

GREEN, T.H., 1970. High pressure experimental studies on the mineralogical constitution of the lower crust. Phys. Earth Planet. Interiors, 3, 441-450.

GREEN, T.H., GREEN, D.H. & RINGWOOD, A.E., 1967. The origin of high-alumina basalts and their relationship to quartz tholeiites and alkali basalts. Earth Plan. Sci. Letters, 2, 41-51.

GREEN, T.H. & RINGWOOD, A.E., 1968a. Crystallization of basalt and andesite under high pressure hydrous conditions. Earth Plan. Sci. Letters, 3, 481-489.

GREEN, T.H. & RINGWOOD, A.E., 1968b. Origin of garnet phenocrysts in calc-alkaline rocks. Contr. Miner. Petrology, 18, 163-174.

GREGG, S.J. & SING, K.S.W., 1967. Adsorption, surface area and porosity. Academic Press, 371p.

GRIFFIN, W.L. & HEIER, K.S., 1969. Parageneses of garnet in granulite-facies rocks, Lofoten-Vesteraalen, Norway. Contr. Miner. Petrology, 23, 89-116.

GRISDALE, R.O., 1963. Growth from molecular complexes, in The art and science of growing crystals (Gilman, J.J., Ed.), John Wiley & Sons, Inc., N.Y. 493p.

GUIDOTTI, C.V., 1963. Metamorphism of the pelitic schists in the Bryant Pond Quadrangle, Maine. Am. Miner., 48, 772-791.

HAGNER, A.F. & COLLINS, L.G., 1967. Magnetite ore formed during regional metamorphism, Ausable magnetite district, New York. Econ. Geol., 62, 1034-1071.

HARDING, R.R., 1966. The major ultrabasic and basic intrusions of St. Kilda, Outer Hebrides. Trans. R. Soc. Edinb., 66, 419-444.

HARLEY, D.N., 1969. The mafic and ultramafic intrusives of the Fraser Range, Western Australia. Unpublished Honours thesis, University of Adelaide.

HARMS, J.C., 1969. Hydraulic significance of some sand ripples. Bull. geol. Soc. Am., 80, 363-396.

HARMS, J.C. & FAHNESTOCK, R.K., 1965. Stratification, bed forms and flow phenomena (with an example from the Rio Grande). Spec. Pap. Soc. Econ. Pal. Mineral., 12, 84-115.

HARRIS, P.G., 1962. Increase in temperature in ascending basalt magma. Am. J. Sci., 260, 783-786.

HATCH, F.H., WELLS, A.K. & WELLS, M.K., 1961. Petrology of the igneous rocks. Murby & Co., 515p.

HAWKES, D.D., 1967. Order of abundant crystal nucleation in a natural magma. Geol. Mag., 104, 473-486.

HEATH, S.A. & FAIRBAIRN, H.W., 1969. Sr^{87}/Sr^{86} ratios in anorthosites and some associated rocks, in Origin of anorthosite and related rocks (Isachsen, Y.W., Ed.), N.Y. State Museum & Science Service Memoir 18.

HEIR, K.S. & ADAMS, J.A.S., 1965. Concentration of radioactive elements in deep crustal material. Geochim. cosmochim. Acta, 29, 53-67.

HENSEN, B.J. & GREEN, D.H., 1970. Experimental data on coexisting cordierite and garnet under high grade metamorphic conditions. Phys. Earth Planet. Interiors, 3, 431-440.

HERMES, O.D., 1968. Petrology of the Mecklenburg gabbro-metagabbro complex, North Carolina. Contr. Miner. Petrology, 18, 270-294.

HERMES, O.D., 1970. Petrochemistry of coexistent mafic silicates from the Mecklenburg gabbro-metagabbro complex, North Carolina. Bull. geol. Soc. Am., 81, 137-164.

HERZ, N., 1951. Petrology of the Baltimore gabbro, Maryland. Bull. geol. Soc. Am., 62, 979-1016.

HESS, H.H., 1952. Orthopyroxenes of the Bushveld type, ion substitutions, and changes in unit cell dimensions. Am. J. Sci. (Bowen Vol.), 173-178.

HESS, H.H., 1960. Stillwater Igneous Complex. Mem. geol. Soc. Am., 80.

HIMMELBERG, G.R. & JACKSON, E.D., 1967. X-ray determinative curve for some orthopyroxenes of composition Mg_{48-85} from the Stillwater Complex, Montana. Prof. Pap. U.S. geol. Surv., 575-B, B101-102.

HISS, W.L. & HUNTER, H.E., 1966. Primary orthopyroxene-spinel intergrowths in Cambrian cumulates, Wichita Mountains, Oklahoma. Okla. Geol. Notes, 26, 231-235.

HOBBS, B.E., 1968. Recrystallization of single crystals of quartz. Tectonophysics, 6, 353-401.

HOFFER, A., 1965. Seismic control of layering in intrusions. Am. Miner., 50, 1125-1128.

HOLLAND, T.H., 1900. The charnockite series, a group of Archaean hypersthene rocks in Peninsula India. Mem. geol. Surv. India, 28, 119-249.

HOLMES, A., 1928. The nomenclature of petrology. 2nd Ed., Murby & Co., 284p.

HORWITZ, R.C., DANIELS, J.L. & KRIEWALDT, M.J.B., 1967. Structural layering in the Precambrian of the Musgrave Block, Western Australia. Annu. Rep. geol. Surv. West. Aust. for 1966, 56-58.

HOSSFELD, P.S., 1954. Stratigraphy and structure of the Northern Territory of Australia. Trans. R. Soc. S. Aust., 77, 103-161.

HOWIE, R.A., 1963. Cell parameter of orthopyroxenes. Spec. Pap. Miner. Soc. Am., 1, 213-222.

HOWIE, R.A., 1965. The pyroxenes of metamorphic rocks, in Controls of Metamorphism (Pitcher, W.S. & Flinn, G.W., Eds), Oliver & Boyd, 368p.

HUANG, W.T. & MERRITT, C.A., 1954. Petrography of the troctolite of the Wichita Mountains, Oklahoma. Am. Miner., 39, 549-565.

HUDSON, D.R., WILSON, A.F. & THREADGOLD, I.M., 1967. A new polytype of taffeite - a rare beryllium mineral from the granulites of central Australia. Mineralog. Mag., 36, 305-310.

IRVINE, T.N., 1963. Origin of the ultramafic complex at Duke Island, southeastern Alaska. Spec. Pap. Miner. Soc. Am., 1, 36-45.

IRVINE, T.N., 1965. Sedimentary structures in igneous intrusions with particular reference to the Duke Island Ultramafic Complex. Spec. Pap. Soc. Econ. Pal. Mineral., 12, 220-232.

IRVINE, T.N., 1967. The Duke Island Ultramafic Complex, southeastern Alaska, in Ultramafic and related rocks (Wyllie, P.J., Ed.), John Wiley & Sons, Inc., N.Y., 464p.

IRVINE, T.N. & SMITH, C.H., 1967. The ultramafic rocks of the Muskox Intrusion, Northwest Territories, Canada, in Ultramafic and related rocks (Wyllie, P.J., Ed.), John Wiley & Sons, Inc., N.Y., 464p.

IRVING, A.J. & GREEN, D.H., 1970. Experimental duplication of mineral assemblages in basic inclusions of the Delegate breccia pipes. Phys. Earth Planet. Interiors, 3, 385-389.

ISACHSEN, Y.W., 1969. Origin of anorthosite and related rocks. Mem. N.Y. State Museum & Science Service, 18.

ITO, K. & KENNEDY, G.C., 1967. Melting and phase relations in a natural peridotite to 40 kilobars. Am. J. Sci., 265, 519-538.

ITO,K. & KENNEDY, G.C., 1968. Melting and phase relations in the plane tholeiite - lherzolite - nepheline basanite to 40 kilobars with geological implications. Contr. Miner. Petrology, 19, 177-211.

JACK, R.L., 1915. The geology and prospects of the region to the south of the Musgrave Ranges, and the geology of the western portion of the Great Australian Artesian Basin. Bull. geol. Surv. S. Aust., 5.

JACKSON, E.D., 1961. Primary textures and mineral associations in the Ultramafic zone of Stillwater Complex, Montana. Prof. Pap. U.S. geol. Surv., 358.

JACKSON, E.D., 1963. Stratigraphic and lateral variation of chromite composition in the Stillwater Complex. Spec. Pap. Miner. Soc. Am., 1, 46-54.

JACKSON, E.D., 1967. Ultramafic cumulates in the Stillwater, Great Dyke, and Bushveld Intrusions, in Ultramafic and related rocks (Wyllie, P.J., Ed.), John Wiley & Sons, Inc., N.Y., 464p.

JACKSON, E.D., 1970. The cyclic unit in layered intrusions - a comparison of repetitive stratigraphy in the ultramafic parts of the Stillwater, Muskox, Great Dyke, and Bushveld Complexes. Spec. Publ. geol. Soc. S. Afr., 1, 391-423.

JACKSON, E.D. & WRIGHT, T.L., 1970. Xenoliths in the Honolulu Volcanic Series, Hawaii. J. Petrology, 11, 405-430.

JACKSON, K.A., 1967. A review of the fundamental aspects of crystal growth. Physics Chem. Solids Suppl. 1, 17-24.

JACKSON, K.A., UHLMANN, D.R. & HUNT, J.D., 1967. On the nature of crystal growth from the melt. J. Cryst. Growth., 1, 1-36.

JACOBS, J.A., RUSSELL, R.D. & WILSON, J.T., 1959. Physics and geology. McGraw-Hill, 424p.

JAEGER, J.C., 1957. The temperature in the neighbourhood of a cooling intrusive sheet. Am. J. Sci., 255, 306-318.

JAEGER, J.C., 1964. Thermal effects of intrusions. Rev. Geophys., 2 (3), 443-466.

JAEGER, J.C., 1968. Cooling and solidification of igneous rocks, in Basalts, vol.2 (Hess, H.H. & Poldervaart, A., Eds), Interscience.

JÄGER, E., NIGGLI, E & WENK, E., 1967. Rb-Sr altersbestimmungen an glimmern der zentralalpen. Beitr. z. Geol. Karte d. Schweiz. N.F., 134.

JEFFREY, R.C. & PEARSON, J.R.A., 1965. Particle motion in laminar vertical tube flow. J. Fluid Mech., 22, 721-735.

JENSEN, M.L., 1965. The rational and geological aspects of solid diffusion. Can. Mineralogist, 8, 271-290.

JOHANNSEN, A., 1931. A descriptive petrography of the igneous rocks. Univ. Chicago Press.

JOHNSON, J.E., 1962. Geological Atlas of South Australia, Sheet Mann 1:63,360 series.

JONES, W.R., PEOPLES, J.W. & HOWLAND, A.L., 1960. Igneous and tectonic structures of the Stillwater Complex, Montana. Bull. U.S. geol. Surv., 1071H, 281-340.

JOPLIN, G.A., 1935. A note on the origin of basic xenoliths in plutonic rocks, with special reference to their grain size. Geol. Mag., 72, 227-234.

JOPLIN, G.A., 1964. A petrography of Australian igneous rocks. Angus & Robertson, 210p.

KARNIS, A., GOLDSMITH, H.L. & MASON, S.G., 1963. Axial migration of particles in Poiseuille flow. Nature, 200, 159-160.

KATZ, M., 1968. The fabric of the granulites of Mont Tremblant Park, Quebec. Can. J. Earth Sci., 5, 801-812.

KAZARYAN, A.G. & ANANYAN, E.V., 1967. Banding in dykes of diabase porphyry. Dokl.(Proc.) Acad. Sci. USSR, 169, 167-170.

KESLER, S.E. & WEIBLEN, P.W., 1968. Distribution of elements in a spherulitic andesite. Am. Miner., 53, 2025-2035.

KLEEMAN, A.W., 1967. Sampling error in the chemical analysis of rocks. J. geol. Soc. Aust., 14, 43-48.

KLEEMAN, J.D., 1965. Studies on the X-ray diffraction, analysis and geochemistry of plagioclase from the Mount Davies Intrusion. Unpublished Honours thesis, University of Adelaide.

KLEEMAN, J.D., 1969. Fission track studies and the geochemistry of uranium in rocks from the crust and upper mantle. Unpublished Ph.D. thesis, Aust. Nat. Univ.

KLEEMAN, J.D. & NESBITT, R.W., 1967. X-ray measurements on some plagioclases from the Mt Davies Intrusion, South Australia. J. geol. Soc. Aust., 14, 39-42.

KOCHKIN, Yu.N., KRIVENKO, A.P., KUTOLIN, V.A. & FROLOVA, V.M., 1967. Composition of monoclinic pyroxenes from igneous rocks of different types of associations. Dokl. Akad. Nauk. SSSR, 176, 139-142.

KORNPROBST, J., 1969. Le massif ultrabasique des Beni Bouchera (Rif Interne, Maroc): Etude des péridotites de haute température et de haute pression, et des pyroxénolites, à grenat ou sans grenat, qui leur sont associees. Contr. Miner. Petrology, 23, 283-322.

KRETZ, R., 1961. Some applications of thermodynamics to coexisting minerals of variable composition. Examples: orthopyroxene - clinopyroxene and orthopyroxene - garnet. J. Geol., 69, 361-387.

KRETZ, R., 1966. Interpretation of the shape of mineral grains in metamorphic rocks. J. Petrology, 7, 68-94.

KRETZ, R., 1969. On the spatial distribution of crystals in rocks. Lithos, 2, 39-66.

KUENEN, Ph.H., 1953. Significant features of graded bedding. Bull. Am. Assoc. Petrol. Geol., 37, 1044-1066.

KUNO, H., 1950. Petrology of Hakone volcano and the adjacent areas, Japan. Bull. geol. Soc. Am., 61, 957-1020.

KUNO, H., 1960. High-alumina basalt. J. Petrology, 1, 121-145.

KUNO, H. & AOKI, K., 1970. Chemistry of ultramafic nodules and their bearing on the origin of basaltic magmas. Phys. Earth Planet. Interiors, 3, 273-301.

KUSHIRO, I. & YODER, H.S.Jr., 1966. Anorthite-forsterite and anorthite-enstatite reactions and their bearing on the basalt-eclogite transformation. J. Petrology, 7, 337-362.

LAMBERT, I.B. & HEIER, K.S., 1968. Geochemical investigations of deep-seated rocks in the Australian shield. Lithos, 1, 30-53.

LAMBERT, I.B. & WYLLIE, P.J., 1968. Stability of hornblende and a model for the low velocity zone. Nature, 219, 1240-1241.

LEAKE, B.E., 1968. Optical properties and composition in the ortho-pyroxene series. Min. Mag., 36, 745-747.

LE BAS, M.J., 1962. The role of aluminium in igneous clinopyroxenes with relation to their parentage. Am. J. Sci., 260, 267-288.

LE MAITRE, R.W., 1965. The significance of the gabbroic xenoliths from Gough Island, South Atlantic. Mineralog. Mag. (Tilley Vol.), 34, 303-317.

LERAY, J.L., 1970. Some physical-chemical processes involved in the generation of vacancies during crystal growth. Schweiz. miner. petrogr. Mitt., 50, 21-24.

LEWIS, W.K., GILLILAND, E.R. & BAUER, W.C., 1949. Characteristics of fluidized particles. Ind. Engng. Chem., 41, 1104-1117.

LONSDALE, G.F. & FLAVELLE, A.J., 1963. Amadeus and South Canning Basins reconnaissance gravity survey using helicopters, NT and WA 1962. Rec. Bur. Miner. Resour., Geol. Geophys. Aust., 1963/152.

LONSDALE, G.F. & FLAVELLE, A.J., 1968. Amadeus and South Canning Basins gravity survey, Northern Territory and Western Australia 1962. Rep. Bur. Miner. Resour., Geol. Geophys. Aust., 133.

LOOMIS, A.A., 1963. Noritic anorthosite bodies in the Sierra Nevada batholith. Spec. Pap. Miner. Soc. Am., 1, 62-68.

LOVERING, J.F. & WHITE, A.J.R., 1969. Granulitic and eclogitic inclusions from basic pipes at Delegate, Australia. Contr. Miner. Petrology, 21, 9-52.

LUTH, W.C., JAHNS, R.H. & TUTTLE, O.F., 1964. The granite system at pressures of 4 to 10 kilobars. J. geophys. Res., 69, 759-773.

MACDONALD, G.A., 1963. Physical properties of erupting Hawaiian magmas. Bull. geol. Soc. Am., 74, 1071-1078.

MACDONALD, G.A. & KATSURA, T., 1964. Chemical composition of Hawaiian lavas. J. Petrology, 5, 82-133.

MACGREGOR, A.G., 1931. Clouded felspars and thermal metamorphism. Mineralog. Mag., 22, 524-538.

MACGREGOR, I.D., 1964. The reaction 4 enstatite + spinel $\rightleftharpoons$ forsterite + pyrope. Annu. Rep. Director Geophys. Lab., Carnegie Inst. Washington, Yearbook 63, 157.

MACGREGOR, I.D., 1965. Stability fields of spinel and garnet peridotites in the synthetic system MgO - CaO - Al_2O_3 - SiO_2. Annu. Rep. Director Geophys. Lab., Carnegie Inst. Washington, Yearbook 64, 126-134.

MACGREGOR, I.D. & CARTER, J.L., 1970. The chemistry of clinopyroxenes and garnets of eclogite and peridotite xenoliths from the Roberts Victor Mine, South Africa. Phys. Earth Planet. Interiors, 3, 391-397.

MACRAE, N.D., 1969. Ultramafic intrusions of the Abitibi area, Ontario. Can. J. Earth Sci., 6, 281-303.

MAJOR, R.B., 1966. Preliminary notes on geology of Woodroffe 1:250,000 Sheet area. Rep. Dept. Mines S. Aust., 639/66.

MAJOR, R.B., JOHNSON, J.E., LEESON, B. & MIRAMS, R.C., 1967. Geological Atlas of South Australia, Sheet Woodroffe 1:250,000 series.

MASON, B.J., 1963. Ice, in The art and science of growing crystals (Gilman, J.J., Ed.), John Wiley & Sons, Inc., N.Y., 493p.

MASON, R., 1967. Electron probe microanalysis of coronas in a troctolite from Sulitjelma, Norway. Mineralog. Mag., 36, 504-514.

MAUDE, A.D. & WHITMORE, R.L., 1956. The wall effect and the viscometry of suspensions. Br. J. appl. Phys., 7, 98-102.

MAUDE, A.D. & YEARN, J.A., 1967. Particle migrations in suspension flows. J. Fluid Mech., 30, 601-621.

McDONALD, J.A., 1967. Evolution of part of the lower critical zone, Farm Ringhoek, Western Bushveld. J. Petrology, 8, 165-209.

McKEE, E.D., 1966. Structures of dunes at White Sands National Monument, New Mexico (and a comparison with structures of dunes from other selected areas). Sedimentology, 7, 1-69.

McKEE, E.D. & WEIR, G.W., 1953. Terminology for stratification and cross-stratification in sedimentary rocks. Bull. geol. Soc. Am., 64, 381-390.

McLEAN, D., 1965. The science of metamorphism in metals, in Controls of Metamorphism (Pitcher, W.S. & Flinn, G.W. Eds), Oliver & Boyd, 368p.

McNOWN, J.S. & MALAIKA, J., 1950. Effects of particle shape on settling velocity at low Reyolds Numbers. Trans. Am. geophys. Un., 31, 74-82.

METZGER, W.J. & BARNARD, W.M., 1968. Transformation of aragonite to calcite under hydrothermal conditions. Am. Miner., 53, 295-300.

MICHOT, P., 1964. Le magma plagioclasique. Geol. Rdsch., 54, 956-976.

MICHOT, P., 1969. Geological environments of the anorthosites of South Rogaland, Norway, in Origin of anorthosite and related rocks (Isachsen, Y.W., Ed.), N.Y. State Museum & Science Service Memoir 18.

MICHOT, J. & MICHOT, P., 1969. The problem of anorthosites: the South-Rogaland igneous complex, southwestern Norway, in Origin of anorthosite and related rocks (Isachsen, Y.W., Ed.), N.Y. State Museum & Science Service Memoir 18.

MIKHEYENKO, V.I., 1968. Mode of origin of the banded flow texture in kimberlite. Dokl. Akad. Nauk. SSSR, 179, 145-148.

MILLER, C., 1966. A geochemical study of clinopyroxenes from the igneous intrusion, South Davies, NW South Australia. Unpublished Honours thesis, University of Adelaide.

MILLER, P.G., 1969. Final report on nickel investigation, Northwest Province 1953-1967. (3 vols). Rep. Dept. Mines S. Aust., 68/95.

MILLER, R., 1953. The Webster-Addie ultramafic ring, Jackson County, North Carolina, and secondary alteration of its chromite. Am. Miner., 38, 1134-1147.

MIRAMS, R.C., 1962. Geological Atlas of South Australia, Sheet Tomkinson 1:63,360 series.

MIRAMS, R.C., 1964. The geology of the Mann 4-mile sheet. Rep. Invest. Dept. Mines S. Aust., 25.

MOORE, A.C., 1968. Rutile exsolution in orthopyroxene. Contr. Miner. Petrology, 17, 233-236.

MOORE, A.C., 1969. Corona textures in granulites from the Tomkinson Ranges, central Australia. Spec. Publs geol. Soc. Aust., 2, 361-366.

MOORE, A.C., 1970a. The geology of the Gosse Pile ultramafic intrusion and of the surrounding granulites, Tomkinson Ranges, central Australia. Unpublished Ph.D. thesis, University of Adelaide.

MOORE, A.C., 1970b. Descriptive terminology for the textures of rocks in granulite facies terrains. Lithos, 3, 123-127.

MOORE, A.C. (in press). Spinel-corundum and ilmenite-corundum relationships in granulite facies rocks from central Australia. J. geol. Soc. Aust.

MORSE, S.A., 1969. Layered intrusions and anorthosite genesis, in Origin of anorthosite and related rocks (Isachsen, Y.W. Ed.), N.Y. State Museum & Science Service Memoir 18.

MUELLER, R.F., 1967. Mobility of the elements in metamorphism. J. Geol., 75, 565-582.

MUIR, I.D. & TILLEY, C.E., 1957. Contributions to the petrology of Hawaiian basalts I. The picrite-basalts of Kilauea. Am. J. Sci., 255, 241-253.

MUKHERJEE, S., 1968. Preliminary report on the sedimentary structures in the ultramafic rocks of Nausahi, Keonjhar District, Orissa. Q. Jl geol. Min. metall. Soc. India, 40, 189-190.

MUKHERJEE, S., 1969. Clot textures developed in the chromitites of Nausahi, Keonjhar District, Orissa, India. Econ. Geol., 64, 329-337.

MUNOZ, J.L., 1968. Effect of shearing on enstatite polymorphism. Ann. Rep. Director Geophys. Lab., Carnegie Inst. Washington, Yearbook 66, 369-370.

MURATA, K.J. & RICHTER, D.H., 1966. The settling of olivine in Kilauean magma as shown by lavas of the 1959 eruption. Am. J. Sci., 264, 194-203.

MURRAY, W.R., 1901. Report, etc., re exploration trip of R.T. Maurice. S. Aust. Parl. Paper, 148.

MURRAY, W.R., 1904. In, Maurice, R.T., Fowlers Bay to Rawlinson Ranges and Fowlers Bay to Cambridge Gulf. S. Aust. Parl. Paper, 43.

MURTHY, M.V.N., 1958. Coronites from India and their bearing on the origin of coronas. Bull. geol. Soc. Am., 69, 23-38.

NALDRETT, A.J. & MASON, G.D., 1968. Contrasting Archaean ultramafic igneous bodies in Dundonald and Clergue Townships, Ontario. Can. J. Earth Sci., 5, 111-143.

NASH, W.P., CARMICHAEL, I.S.E. & JOHNSON, R.W., 1969. The mineralogy and petrology of Mount Suswa, Kenya. J. Petrology, 10, 409-439.

NESBITT, R.W., 1966a. The Giles igneous province, Central Australia. An example of an eroded volcanic zone. Bull. volcan., 29, 271-282.

NESBITT, R.W., 1966b. The determination of magnesium in silicates by atomic absorption spectroscopy. Analytica chim. Acta, 35, 413-420.

NESBITT, R.W., GOODE, A.D.T., MOORE, A.C. & HOPWOOD, T.P., 1970. The Giles Complex, central Australia: a stratified sequence of mafic and ultramafic intrusions. Spec. Publ. geol. Soc. S. Afr., 1, 547-564.

NESBITT, R.W. & KLEEMAN, A.W., 1964. Layered Intrusions of the Giles Complex, central Australia. Nature, 203, 391-393.

NESBITT, R.W. & TALBOT, J.L., 1966. The layered basic and ultrabasic intrusives of the Giles Complex, central Australia. Contr. Miner. Petrology, 13, 1-11.

NORRISH, K. & HUTTON, J.T., 1969. An accurate X-ray spectrographic method for the analysis of a wide range of geological samples. Geochim. cosmochim. Acta, 33, 431-453.

O'HARA, M.J., 1961. Zoned ultrabasic and basic gneiss masses in the Early Lewisian metamorphic complex at Scourie, Sutherland. J. Petrology, 2, 248-276.

O'HARA, M.J. & BIGGAR, G.M., 1969. Diopside + spinel equilibria, anorthite and forsterite reaction relationships in silica-poor liquids in the system CaO - MgO - Al_2O_3 - SiO_2 at atmospheric pressure and their bearing on the genesis of melililites and nephelinites. Am. J. Sci., 267A, 364-390.

O'HARA, M.J. & STEWART, F.H., 1966. Olivine-liquid reaction and the depth of crystallization of the East Aberdeenshire gabbros. Nature, 210, 830-831.

OLDROYD, J.G., 1956. Non-newtonian flow of liquids and solids, in Rheology, vol.1 (Eirich, F.R., Ed.), Academic Press.

OLIVER, D.R., 1962. Influence of particle rotation on radial migration in the Poiseuille flow of suspensions. Nature, 194, 1269-1271.

OLIVER, R.L., 1964. Note on some garnetiferous rocks from Ceylon. 22nd Int. geol. Cong., Pt. 13, 59-78.

OOSTEROOM, M.G., 1963. The ultramafites and layered gabbro sequences in the granulite facies rocks on Stjernoy. Leid. geol. Meded., 28, 177-296.

OSBORNE, E.F., 1949. Coronite, labradorite anorthosite, and dykes of andesine anorthosite, New Glasgow, P.Q. Trans. R. Soc. Can., 43, Series 3, 85-112.

PAO, R., 1961. Fluid mechanics. John Wiley & Sons, Inc., N.Y., 502p.

PARK, R.G., 1969. Structural correlation in metamorphic belts. Tectonophysics, 7, 323-338.

PARKIN, L.W. (Ed.)., 1969. Handbook of South Australian geology. Geol. Surv. S. Aust., 268p.

PATERSON, M.S. & WEISS, L.E., 1966. Experimental deformation and folding in phyllite. Bull. geol. Soc. Am., 77, 343-374.

PETERS, Tj., 1968. Distribution of Mg, Fe, Al, Ca and Na in coexisting olivine, orthopyroxene and clinopyroxene in the Totalp Serpentinite (Davos, Switzerland) and in the Alpine metamorphosed Malenco Serpentinite (N. Italy). Contr. Miner. Petrology, 18, 65-75.

PETERSON, D.W., 1961. Descriptive modal classification of igneous rocks. Geotimes, 5 (6), 30-36.

PETERSON, G.L., 1968. Flow structures in sandstone dikes. Sed. Geol., 2, 177-190.

PHILPOTTS, A.R., 1966. Origin of the anorthosite-mangerite rocks in southern Quebec. J. Petrology, 7, 1-64.

PHILPOTTS, A.R., 1968. Igneous structures and mechanism of emplacement of Mount Johnson, a Monteregian intrusion, Quebec. Can. J. Earth Sci., 5, 1131-1137.

PHILPOTTS, A.R., 1970. Igneous structures and mechanism of emplacement of Mount Johnson, a Monteregian intrusion, Quebec: Reply. Can. J. Earth Sci., 7, 195-197.

PHINNEY, W.C., 1969. Anorthosite occurrences in Keweenawan rocks of northeastern Minnesota, in Origin of anorthosite and related rocks (Isachsen, Y.W., Ed.), N.Y. State Museum & Science Service Memoir 18.

PICHAMUTHU, C.S., 1959. The significance of clouded plagioclase in the basic dykes of Mysore State, India. Journ. geol. Soc. India, 1, 68-79.

PLATTEN, I.M. & WATTERSON, J.S., 1969. Oriented crystal growth in some Tertiary dykes. Nature, 223, 286-287.

POLDERVAART, A., 1952. Karoo dolerites and basalts of the eastern Bechuanaland Protectorate. Trans. geol. Soc. S. Afr., 55, 125-130.

POLDERVAART, A., 1966. Archaean charnockitic adamellite phacoliths in the Keimoes-Kakamas region, Cape Province, South Africa. Trans. geol. Soc. S. Afr., 69, 139-154.

POLDERVAART, A. & GILKEY, A.K., 1954. On clouded plagioclase. Am. Miner., 39, 75-91.

POLDERVAART, A. & PARKER, A.B., 1964. The crystallization index as a parameter of igneous differentiation in binary differentiation diagrams. Am. J. Sci., 262, 281-289.

POLDERVAART, A. & TAUBENECK, W.H., 1959. Layered Intrusions of Willow Lake Type. Bull. geol. Soc. Am., 70, 1395-1398.

POOLE, J.B. & DOYLE, D., 1966. Solid-liquid separation. H.M.S.O., Ministry of Technology, (G.B.).

POTTER, P.E. & PETTIJOHN, F.J., 1963. Paleocurrents and basin analysis. Springer-Verlag, 296p.

PRESTON, J., 1966. An unusual hourglass structure in augite. Am. Miner., 51, 1227-1233.

PRICE, D.G., 1970. Geophysical investigations of the northern Middleback Range area. Unpublished Honours thesis, University of Adelaide.

PULVERTAFT, T.C.R., 1965. The Eqaloquarfia layered dyke, Nunarssuit, South Greenland. Bull. geol. Unders. Grønland, 55.

QUENSEL, P., 1951. The charnockite series of the Varberg district on the southwestern coast of Sweden. Ark. Miner. Geol., 1, 227-332.

RAGAN, D.M., 1969. Olivine recrystallization textures. Mineralog. Mag., 37, 238-240.

RAGLAND, P.C., ROGERS, J.J.W. & JUSTUS, Ph.S., 1968. Origin and differentiation of Triassic dolerite magmas, North Carolina, USA. Contr. Miner. Petrology, 20, 57-80.

RALEIGH, C.B., 1965a. Glide mechanisms in experimentally deformed minerals. Science, 150, 739-741.

RALEIGH, C.B., 1965b. Structure and petrology of an alpine peridotite on Cypress Island, Washington, USA. Contr. Miner. Petrology, 11, 719-741.

RALEIGH, C.B., 1967. Plastic deformation of upper mantle silicate minerals. Geophys. J. R. Astron. Soc., 14, 45-49.

RALEIGH, C.B., 1968. Mechanisms of plastic deformation of olivine. J. geophys. Res., 73, 5391-5406.

RALEIGH, C.B. & TALBOT, J.L., 1967. Mechanical twinning in naturally and experimentally deformed diopside. Am. J. Sci., 265, 151-165.

RAMSAY, J.G. & GRAHAM, R.H., 1970. Strain variation in shear belts. Can. J. Earth Sci., 7, 786-813.

RAST, N., 1965. Nucleation and growth of metamorphic minerals, in Controls of metamorphism (Pitcher, W.S. & Flinn, G.W., Eds), Oliver & Boyd, 368p.

READ, R.A., 1965. The interpretation of deformation and annealing textures in metamorphic rocks. Unpublished M.Sc. thesis, University of Sydney.

RIBBE, P.H. & SMITH, J.V., 1966. X-ray emission microanalysis of rock forming minerals IV. Plagioclase feldspars. J. Geol., 74, 217-233.

RICHARDSON, S.W., 1970. The relation between a petrogenetic grid, facies series', and the geothermal gradient in metamorphism. Fortschr. Miner., 47, 65-76.

RICHARDSON, S.W., GILBERT, M.C. & BELL, P.M., 1969. Experimental determination of kyanite-andalusite and andalusite-sillimanite equilibria; the aluminium silicate triple point. Am. J. Sci., 267, 259-272.

RIECKER, R.E. & ROONEY, T.R., 1967. Deformation and polymorphism of enstatite under shear stress. Bull. geol. Soc. Am., 78, 1045-1054.

RILEY, J.P. & WILLIAMS, H.P., 1959. The microanalysis of silicate and carbonate minerals, III. Mikrochim. Acta, 6, 804-824.

RINGWOOD, A.E. & GREEN, D.H., 1966. Petrological nature of the stable continental crust. Monograph Am. geophys. Un., 10, 611-619.

RINGWOOD, A.E. & LOVERING, J.F., 1970. Significance of pyroxene-ilmenite intergrowths among kimberlite xenoliths. Earth Plan. Sci. Letters., 7, 371-375.

RINGWOOD, A.E. & MAJOR, A., 1966. High pressure transformations in pyroxenes. Earth Plan. Sci. Letters, 1, 351-357.

RINGWOOD, A.E. & SEABROOK, M., 1962. Some high pressure transformations in pyroxenes. Nature, 196, 883-884.

RINGWOOD, A.E. & SEABROOK, M., 1963. High-pressure phase transformations in germanate pyroxenes and related compounds. J. geophys. Res., 68, 4601-4609.

ROBINSON, E.G., 1949. The petrological nature of some rocks from the Mann, Tomkinson and Ayers Ranges of Central Australia. Trans. R. Soc. S. Aust., 73, 29-39.

ROMEY, W.D., 1968. An evaluation of some 'differences' between anorthosite in massifs and in layered complexes. Lithos, 1, 230-241.

ROSENBUSCH, H., 1877. Mikroskopische physiographie der mineralien und gesteine II. Massige gesteine. Stuttgart.

ROWAN, I.S., 1967. Regional gravity survey of Mann and Woodroffe 1:250,000 sheet areas. Rep. Dept. Mines S. Aust., 64/33.

SADASHIVAIAH, M.S., 1954. The form of the eastern end of the Insch igneous mass, Aberdeenshire. Geol. Mag., 91, 137-143.

SAGGERSON, E.P., 1968. Eclogite nodules associated with alkaline olivine basalts, Kenya. Geol. Rdsch., 57, 890-903.

SAKHNO, V.G., SHCHEKA, S.A., KURENTSOVA, N.A. & MAKAROVA, Zh.A., 1968. Spinel peridotite inclusions in the basalt of Oahu Volcano (Hawaiian Islands). Dokl. (Proc.) Acad. Sci. USSR, 180, 162-164.

SAXENA, S.K., 1968. Crystal-chemical aspects of distribution of elements among certain coexisting rock-forming silicates. Neues Jb. Miner. Abh., 108, 292-323.

SCHREIBER, H.P. & STOREY, S.H., 1965. Molecular fractionation in capillary flow of polymer fluids. Polymer Letters, 3, 723-727.

SCHREYER, W. & YODER, H.S.JR., 1964. The system Mg-cordierite-H_2O and related rocks. Neues Jb. Miner. Abh., 101, 271-342.

SCHWAB, R.G., 1969. Die phasenbeziehungen der pyroxene im system $CaMgSi_2O_6$ - $CaFeSi_2O_6$ - $MgSiO_3$ - $FeSiO_3$. Fortschr. Miner., 46, 188-273.

SEGRÉ, G. & SILBERBERG, A., 1961. Radial particle displacements in Poiseuille flow of suspensions. Nature, 189, 209-210.

SEGRÉ, G. & SILBERBERG, A., 1962. Behaviour of macroscopic rigid spheres in Poiseuille flow. Pt. 1: Determination of local concentration by statistical analysis of particle passages through crossed light beams. Pt. 2: Experimental results and interpretation. J. Fluid Mech., 14, Pt.1, 115-135, Pt.2, 136-157.

SEIFERT, K.E., 1965. Deformation bands in albite. Am. Miner., 50, 1469-1479.

SEIFERT, von F. & SCHREYER, W., 1968. Die möglichkeit der entstehung ultrabasischer magmen bei gegenwart geringer alkalimengen. Geol. Rdsch., 57, 349-362.

SEN, S.K., 1959. Potassium content of natural plagioclases and the origin of antiperthites. J. Geol., 67, 479-495.

SHAND, S.J., 1945. Coronas and coronites. Bull. geol. Soc. Am., 56, 247-266.

SHAND, S.J., 1947. Eruptive rocks. John Wiley & Sons, Inc., N.Y.

SHAW, H.R., 1965. Comments on viscosity, crystal settling, and convection in granitic magmas. Am. J. Sci., 263, 120-152.

SHAW, H.R., 1969. Rheology of basalt in the melting range. J. Petrology, 10, 510-535.

SHAW, H.R., WRIGHT, T.L., PECK, D.L. & OKAMURA, R., 1968. The viscosity of basaltic magma: an analysis of field measurements in Makaopuhi Lava Lake, Hawaii. Am. J. Sci., 266, 225-264.

SHIMAZU, Y., 1959. A physical interpretation of crystallization differentiation of the Skaergaard intrusion. J. Earth Sci., Nagoya Univ., 7, 35-48.

SIMKIN, T., 1967. Flow differentiation in the picritic sills of North Skye, in Ultramafic and related rocks (Wyllie, P.J., Ed.), John Wiley & Sons, Inc., N.Y., 464p.

SIMKIN, T. & SMITH, J.V., 1970. Minor element distribution in olivine. J. Geol., 78, 304-325.

SIMONS, D.B. & RICHARDSON, E.V., 1961. Forms of bed roughness in alluvial channels. Proc. Am. Assoc. Civil Engrs, J. Hyd. Div., 87, 87-105.

SMITH, C.H., 1958. Bay of Islands Igneous Complex, western Newfoundland. Mem. geol. Surv. Can., 290, 1-132.

SMITH, C.H. & KAPP, H.E., 1963. The Muskox Intrusion, a newly discovered layered intrusion in the Coppermine River area, Northwest Territories, Canada. Spec. Pap. Miner. Soc. Am., 1, 30-35.

SMITH, J.V., STEPHENSON, D.A., HOWIE, R.A. & HEY, M.H., 1969. Relations between cell dimensions, chemical composition, and site preference of orthopyroxene. Mineralog. Mag., 37, 90-114.

SMITH, P.C., 1970. Geology of the Hinckley Range, Western Australia. Unpublished Honours thesis, University of Adelaide.

SMYTH, J.R., 1969. Orthopyroxene - high - low clinopyroxene inversions. Earth Plan. Sci. Letters, 6, 406-407.

SØRENSEN, H., 1969. Rhythmic igneous layering in peralkaline intrusions. Lithos, 2, 261-283.

SPRIGG, R.C., 1958. The North-West Province, in The geology of South Australia (Glaessner, M.F. & Parkin, L.W., Eds), J. geol. Soc. Aust., 5, 1-163.

SPRIGG, R.C. & WILSON, R.B., 1959. The Musgrave Mountain Belt in South Australia. Geol. Rdsch., 47, 531-542.

SPRIGG, R.C., WILSON, R.B. & COATS, R.P., 1955a. Geological Atlas of South Australia, Sheet Ernabella, 1:63,360 series.

SPRIGG, R.C., WILSON, R.B. & COATS, R.P., 1955b. Geological Atlas of South Australia, Sheet Giles, 1:63,360 series.

SPRIGG, R.C., WILSON R.B. & COATS, R.P., 1955c. Geological Atlas of South Australia, Sheet Indulkana, 1:63,360 series.

SPRIGG, R.C., WILSON, R.B. & COATS, R.P., 1956. Geological Atlas of South Australia, Sheet Chandler, 1:63,360 series.

SPRIGG, R.C., WILSON, R.B. & COATS, R.P., 1959. Geological Atlas of South Australia, Sheet Alberga, 1:250,000 series.

SRIRAMADAS, A., 1957. Diagrams for the correlation of unit cell edge and refractive indices with the chemical composition of garnets. Am. Miner., 42, 294-298.

STARKEY, T.V., 1956. The laminar flow of streams of suspended particles. Br. J. appl. Phys., 7, 52-55.

STARMER, I.C., 1969. Basic plutonic intrusions of the Risör-Söndeled area, South Norway: the original lithologies and their metamorphism. Norsk geol. Tidssk., 49, 403-431.

STEELE, R.J., 1966. Gravimetric investigations of the Mt. Davies and Gosse Pile intrusions of the Giles Complex. Unpublished Honours thesis, University of Adelaide.

STEELE, W.A. & WEBB, W., 1963. Transport properties of liquids, in High pressure physics and chemistry (Bradley, R.S., Ed.), Academic Press.

STEWART, F.H., 1947. The gabbroic complex of Belhelvie in Aberdeenshire. Q. Jl geol. Soc. Lond., 102, 465-498.

STRAND, T., 1944. A method of counting out petrofabric diagrams. Norsk geol. Tidssk., 24, 112-115.

STRECKEISEN, A.L., 1967. Classification and nomenclature of igneous rocks. Neues Jb. Miner. Abh., 107, 144-240.

STREICH, V., 1893. Scientific Reports of Elder Exploration Expedition, 1891-2, Geology. Trans. R. Soc. S. Aust., 16, 74-115.

STRONG, D.F., 1969. The formation of hourglass structure in augite. Mineralog. Mag., 37, 472-479.

STURT, B.A., 1969. Wrench fault deformation and annealing recrystallization during almandine amphibolite facies regional metamorphism. J. Geol., 77, 319-332.

SUNAGAWA, I., 1963. Studies of crystal surfaces. Spec. Pap. Miner. Soc. Am., 1, 258-266.

SUTTON, J. & WATSON, J., 1950. The pre-Torridonian metamorphic history of the Loch Torridon and Scourie areas in the North-West Highlands, and its bearing on the chronological classification of the Lewisian. Q. Jl geol. Soc. Lond., 106, 241-307.

SUTTON, J. & WATSON, J., 1951. Varying trends in the metamorphism of dolerites. Geol. Mag., 88, 25-35.

TALBOT, H.W.B. & CLARKE, E.deC., 1917. A geological reconnaissance of the country between Laverton and the South Australian Border (near South Latitude 26°), including part of the Mt Margaret Goldfield. Bull. geol. Surv. West. Aust., 75.

TALBOT, H.W.B. & CLARKE, E.deC., 1918. The geological results of an expedition to the South Australian Border, and some comparisons between Central and Western Australian geology suggested thereby. J. Proc. R. Soc. West. Aust., 3, 70-98.

TALBOT, J.L., HOBBS, B.E., WILSHIRE, H.G. & SWEATMAN, T.R., 1963. Xenoliths and xenocrysts from lavas of the Kerguelen Archipelago. Am. Miner., 48, 159-179.

TANNER, W.F., 1967. Ripple mark indices and their uses. Sedimentology, 9, 89-104.

TARNEY, J., 1969. Epitaxic relations between coexisting pyroxenes. Mineralog. Mag., 37, 115-122.

TAUBENECK, W.H. & POLDERVAART, A., 1960. Geology of the Elkorn Mountains, north-eastern Oregon. 2. Willow Lake intrusion. Bull geol. Soc. Am., 71, 1295-1332.

TAYLOR, H.P.Jr., 1967. The zoned ultramafic complexes of southeastern Alaska, in Ultramafic and related rocks (Wyllie, P.J., Ed.), John Wiley & Sons, Inc., N.Y., 464p.

TAYLOR, H.P.Jr., 1968. The oxygen isotope geochemistry of igneous rocks. Contr. Miner. Petrology, 19, 1-71.

TAYLOR, H.P.Jr., 1969. Oxygen isotope studies of anorthosites, with particular reference to the origin of bodies in the Adirondack Mountains, New York, in Origin of anorthosite and related rocks (Isachsen, Y.W., Ed.), N.Y. State Museum & Science Service Memoir 18.

TEALL, J.J.H., 1888. British petrography. London.

TEITKINS, W.H., 1891. Journal central Australian Exploration Expedition, 1889. S. Aust. Govt. Printer.

TERRY, M., 1933. Untold Miles. Selwyn & Blount, 288p.

THAYER, T.P., 1960. Some critical differences between alpine-type and stratiform peridotite-gabbro complexes. 21st Int. geol. Congr., Pt. 13, 247-259.

THAYER, T.P., 1963. Flow layering in alpine peridotite-gabbro complexes. Spec. Pap. Miner. Soc. Am., 1, 55-61.

THAYER, T.P., 1967. Chemical and structural relations of ultramafic and feldspathic rocks in alpine intrusive complexes, in Ultramafic and related rocks (Wyllie, P.J., Ed.), John Wiley & Sons, Inc. N.Y., 464p.

THOMPSON, R.N. & PATRICK, D.J., 1968. Folding and slumping in a layered gabbro. Geol. J., 6, 139-146.

THOMSON, B.P., 1963. Nickel mineralization and the Giles Complex in the Tomkinson Ranges, South Australia. Q. Geol. Notes geol. Surv. S. Aust., 8.

THOMSON, B.P., 1964. Geological Atlas of South Australia, Sheet Davies, 1:63,360 series.

THOMSON, B.P., 1965. Weathering and related nickel mineralization Mt Davies area. Q. Geol. Notes geol. Surv. S.Aust., 16.

THOMSON, B.P., MIRAMS, R.C. & JOHNSON, J.E., 1962. Geological Atlas of South Australia, Sheet Mann, 1:250,000 series.

THOMSON, J.A., 1911. On rock specimens from Central and Western Australia. J. Proc. R. Soc. N.S.W., 45, 292-317.

TILLEY, C.E., 1921. The granite gneisses of southern Eyre Peninsula (South Australia) and their associated amphibolites. Q. Jl geol. Soc. Lond., 77, 75-134.

TROMMSDORF, V. & WENK, H., 1968. Terrestrial metamorphic clinoenstatite in kinks of bronzite crystals. Contr. Miner. Petrology, 19, 158-168.

TURNER, A.R., 1967. Mount Davies nickel deposits. Unpublished AMDEL Rep., 556.

TURNER, A.R., 1968. The distribution and association of nickel in the ferruginous zones of the laterites of the Giles Complex. Bull. AMDEL, 5, 76-93.

TURNER, F.J., 1968. Metamorphic Petrology. McGraw-Hill, 403p.

TURNER, F.J., HEARD, H. & GRIGGS, D.T., 1960. Experimental deformation of enstatite and accompanying inversion to clinoenstatite. 21st Int. geol. Congr., Pt. 18, 399-408.

TURNER, F.J. & VERHOOGEN, J., 1960. Igneous and metamorphic petrology. (2nd Ed.), McGraw-Hill, 694p.

TURNER, F.J. & WEISS, L.E., 1963. Structural analysis of metamorphic tectonites. McGraw-Hill, 545p.

TUTTLE, O.F. & BOWEN, N.L., 1958. Origin of granite in light of experimental studies in the system $NaAlSi_3O_8$ - $KAlSi_3O_8$ - SiO_2 - H_2O. Mem. geol. Soc. Am., 74, 5-98.

TYRELL, G.W., 1916. A contribution to the petrography of Benguella, based on a rock collection made by Professor J.W. Gregory. Trans. R. Soc. Edinb., 51, 537-559.

UPTON, B.G.J., 1960. The alkaline igneous complex of Kûngnât Fjeld, southwest Greenland. Meddr. Grønland, 123 (4), 1-145.

UPTON, B.G.J., 1961. Textural features of some contrasted igneous cumulates from South Greenland. Meddr. Grønland, 123 (6), 1-31.

UPTON, B.J. & WADSWORTH, W.J., 1967. A complex basalt-mugearite sill in Piton des Neiges volcano, Reunion. Am. Miner., 52, 1475-1492.

VANCE, J.A., 1961. Polysynthetic twinning in plagioclase. Am. Miner., 46, 1097-1119.

VANCE, J.A., 1969. On synneusis. Contr. Miner. Petrology, 24, 7-29.

VANCE, J.A. & GILREATH, J.P., 1967. The effect of synneusis on phenocryst distribution patterns in some porphyritic igneous rocks. Am. Miner., 52, 529-536.

VAND, V., 1948. Viscosity of solutions and suspensions. J. phys. Colloid Chem., 52, 277-314.

VANHOOK, A., 1961. Crystallization (theory and practice). Monograph Ser. Am. chem. Soc., 152.

VEJLENS, G., 1938. The distribution of leucocytes in the vascular system. Acta path. microbiol. scand. Suppl., 33.

VEJNAR, Z., 1966. The petrogenetic interpretation of kyanite, sillimanite and andalusite in the south-western Bohemian crystalline complexes. Neues Jb. Miner. Abh., 104, 172-189.

VERMA, A.R. & KRISHNA, P., 1966. Polymorphism and polytypism in crystals. John Wiley & Sons, Inc., N.Y., 341p.

VERNON, R.H., 1968. Microstructures of high-grade metamorphic rocks at Broken Hill, Australia. J. Petrology, 9, 1-22.

VIRGO, D., 1966. Some elemental distributions between coexisting feldspars in metamorphic rocks. Unpublished Ph.D. thesis, University of Adelaide.

VIRGO, D., 1968. Partition of strontium between coexisting K-feldspar and plagioclase in some metamorphic rocks. J. Geol., 76, 331-346.

VIRGO, D., 1969. Partitioning of sodium between coexisting K-feldspar and plagioclase from some metamorphic rocks. J. Geol., 77, 173-182.

VOLL, G., 1960. New work on petrofabrics. L'pool Manchr geol. Journ., 2, 503-567.

WADSWORTH, W.J., 1961. The ultrabasic rocks of southwest Rhum. Phil. Trans. R. Soc., Ser. B, 244, 21-64.

WADSWORTH, W.J., 1963. The Kapalagulu layered intrusion of western Tanganyika. Spec. Pap. Miner. Soc. Am., 1, 108-115.

WAGER, L.R., 1953. Layered intrusions. Meddr. dansk. geol. Foren., 12,(3), 335-349.

WAGER, L.R., 1959. Differing powers of crystal nucleation as a factor producing diversity in layered igneous intrusions. Geol. Mag., 96, 75-80.

WAGER, L.R., 1963. The mechanism of adcumulus growth in the layered series of the Skaergaard intrusion. Spec. Pep. Miner. Soc. Am., 1, 1-9.

WAGER, L.R., 1968. Rhythmic and cryptic layering in mafic and ultramafic plutons, in Basalts (Hess, H.H. & Poldervaart, A., Ed.), vol. 2, Interscience.

WAGER, L.R. & BROWN, G.M., 1968. Layered igneous rocks. Oliver & Boyd., 588p.

WAGER, L.R., BROWN, G.M. & WADSWORTH, W.J., 1960. Types of igneous cumulates. J. Petrology, 1, 73-85.

WAGER, L.R. & DEER, W.A., 1939. Geological investigations in East Greenland. 3. The petrology of the Skaergaard intrusion, Kangerdlugssuaq, East Greenland. Meddr. Grønland, 105 (4), 1-352.

WALLER, D.R., 1968. Musgrave Block airborne magnetic and radiometric survey, South Australia 1967. Rec. Bur. Miner. Resour., Geol. Geophys. Aust., 1968/51.

WATSON, J., 1967. Evidence of mobility in reactivated basement complexes. Proc. Geol. Ass., 78, 211-235.

WEDEPOHL, K.H. (Ed.)., 1969. Handbook of Geochemistry. Springer-Verlag.

WEEDON, D.S., 1961. Basic igneous rocks of the Southern Cuillin, Isle of Skye. Trans. geol. Soc. Glasg., 24, 190-212.

WEEDON, D.S., 1965a. The layered ultrabasic rocks of Sgurr Dubh, Isle of Skye. Scott. J. Geol., 1, 41-68.

WEEDON, D.S., 1965b. Corona structures in the basic igneous masses of East Aberdeenshire. Nature, 208, p. 885.

WELLS, A.T., FORMAN, D.J. & RANFORD, L.C., 1964. Geological reconnaissance of the Rawlinson and Macdonald 1:250,000 sheet areas, Western Australia. Rep. Bur. Miner. Resour., Geol. Geophys. Aust., 65.

WELLS, A.T., RANFORD, L.C., COOK, P.J. & FORMAN, D.J., 1967. The geology of the Amadeus Basin. Rec. Bur. Miner. Resour., Geol. Geophys. Aust., 1967/92.

WELLS, A.T., STEWART, A.J. & SKWARKO, S.K., 1966. Geology of the south-eastern part of the Amadeus Basin, Northern Territory. Rep. Bur. Miner. Resour., Geol. Geophys. Aust., 88.

WELLS, L.A. & GEORGE, F.R., 1904. Reports on prospecting operations in the Musgrave, Mann and Tomkinson Ranges. S. Aust. Parl. Paper, 54.

WHITE, R.W., 1966. Ultramafic inclusions in basaltic rocks from Hawaii. Contr. Miner. Petrology, 12, 245-314.

WILCOX, R.E. & POLDERVAART, A., 1958. Metadolerite dike swarm in Bakersville - Roan Mountain area, North Carolina. Bull. geol. Soc. Am., 69, 1323-1368.

WILLIAMS, G.E., 1969. Flow conditions and estimated velocities of some central Australian stream floods. Aust. J. Sci., 31, 367-368.

WILLIAMS, G.H., 1886. The gabbros and associated hornblende rocks occurring in the neighbourhood of Baltimore, Maryland. Bull. U.S. geol. Surv., 28.

WILLIAMSON, W.O., 1936. Some minor intrusions of Glen Shee, Perthshire. Geol. Mag., 73, 145-157.

WILSHIRE, H.G., 1961. Layered diatremes near Sydney, NSW. J. Geol., 69 (4), 473-484.

WILSHIRE, H.G., 1969. Mineral layering in the Twin Lakes granodiorite, Colorado. Mem. geol. Soc. Am., 115, 235-261.

WILSON, A.F., 1947. The charnockitic and associated rocks of North-western South Australia. I. The Musgrave Ranges - an introductory account. Trans. R. Soc. S. Aust., 71, 195-211.

WILSON, A.F., 1948. The charnockitic and associated rocks of North-western South Australia. II. Dolerites from the Musgrave and Everard Ranges. Trans. R. Soc. S. Aust., 72, 178-200.

WILSON, A.F., 1950. Some unusual alkali-feldspars in the Central Australian charnockitic rocks. Mineralog. Mag., 29, 215-224.

WILSON, A.F., 1952a. The charnockite problem in Australia. Sir D. Mawson Anniv. Vol., University of Adelaide, 203-224.

WILSON, A.F., 1952b. Precambrian tillites east of the Everard Ranges, North-western South Australia. Trans. R. Soc. S. Aust, 75, 160-163.

WILSON, A.F., 1954. Studies on Australian charnockitic rocks and associated problems. Unpublished D.Sc. thesis, University of Western Australia.

WILSON, A.F., 1958. The charnockitic rocks of Australia. Geol. Rdsch., 47, 491-510.

WILSON, A.F., 1959. Notes on the fabric of some charnockitic rocks from Central Australia. J. Proc. R. Soc. West. Aust., 42, 56-64.

WILSON, A.F., 1960. The charnockitic granites and associated granites of Central Australia. Trans. R. Soc. S. Aust., 83, 37-76.

WILSON, A.F., 1969. Granulite terrains and their tectonic setting and relationship to associated metamorphic rocks in Australia. Spec. Publs geol. Soc. Aust., 2, 243-258.

WILSON, A.F., COMPSTON, W., JEFFERY, P.M. & RILEY, G.H., 1960. Radio-active ages from the Precambrian rocks in Australia. J. Geol. Soc. Aust., 6, 179-195.

WILSON, A.F., GREEN, D.C. & DAVIDSON, L.R., 1970. The use of oxygen isotope geothermometry on the granulites and related intrusives, Musgrave Ranges, central Australia. Contr. Miner. Petrology, 27, 166-178.

WILSON, A.F. & HUDSON, D.R., 1967. The discovery of beryllium-bearing sapphirine in the granulites of the Musgrave Ranges (Central Australia). Chem. Geol., 2, 209-215.

WILSON, A.F. & MIDDLETON, D.D., 1968. Some petrological features of a spinel-bearing metagabbro in the pyroxene granulites of the Fraser Range, Western Australia. J. Proc. R. Soc. West. Aust., 51, 89-96.

WINCHELL, H. & LEAKE, B.E., 1965. Regressions of refractive indices, density, and lattice constants on the composition of orthopyroxenes. Am. Miner., 50, p.294.

WINDLEY, B.F., 1967. On the classification of the West Greenland anorthosites. Geol. Rdsch., 56, 1020-1026.

WINKLER, H.G.F., 1967. Petrogenesis of metamorphic rocks. Springer-Verlag, (2nd Ed.), 237p.

WINKLER, H.G.F., 1970. Abolition of metamorphic facies, introduction of the four divisions of metamorphic stage, and a classification based on isograds in common rocks. Neues Jb. Miner. Mh., 189-248.

WOOLLARD, G.P., 1968. The interrelationship of the crust, the upper mantle, and isostatic gravity anomalies in the United States. Monograph Am. geophys. Un., 12, 312-341.

WORST, B.G., 1960. The Great Dyke of Southern Rhodesia. Geol. Surv. S. Rhodesia Bull., 47, 239p.

WRIGHT, J.B., 1966. Olivine nodules in a phonolite of the East Otago Alkaline Province, New Zealand. Nature, 210, p. 519.

WRIGHT, T.L., KINOSHITA, W.T. & PECK, D.L., 1968. March 1965 eruption of Kilauea Volcano and the formation of Makaopuhi lava lake. J. geophys. Res., 73, 3181-3205.

WYLLIE, P.J., COX, K.G. & BIGGAR, G.M., 1962. The habit of apatite in synthetic systems and igneous rocks. J. Petrology, 3, 238-243.

WYNNE-EDWARDS, H.R. & HASAN, Z., 1970. Intersecting fold belts across the North Atlantic. Am. J. Sci., 268, 289-308.

YODER, H.S.Jr. & SAHAMA, T.G., 1957. Olivine X-ray determinative curve. Am. Miner., 42, 475-491.

YODER, H.S.Jr. & TILLEY, C.E., 1962. Origin of basalt magmas: An experimental study of natural and synthetic rock systems. J. Petrology, 3, 342-532.

YONG, S.K., 1964. The distribution of trace elements Ni, Cu, Sr, Cr and Mn in the Mt. Davies basic intrusion of South Australia. Unpublished Honours thesis, University of Adelaide.

ZHDANOV, G.S., 1965. Crystal physics, (translated by A.F. Brown), Oliver & Boyd, 500p.

ZUSSMAN, J., 1968. The crystal chemistry of pyroxenes and amphiboles. I. Pyroxenes. Earth Sci. Rev., 4, 39-67.

THE PETROLOGY AND STRUCTURE OF THE KALKA AND EWARARA LAYERED BASIC INTRUSIONS, GILES COMPLEX, CENTRAL AUSTRALIA

Volume 2

by

Alan Douglas Tracy Goode, B.Sc. (Hons), Dip.T.

Department of Geology and Mineralogy,
The University of Adelaide,
Adelaide, South Australia.

December, 1970.

CONTENTS

VOLUME 2

TABLES

TABLE 1

Abbreviations commonly used in this thesis.

ol, oliv	olivine
opx	orthopyroxene
cpx	clinopyroxene
px	pyroxene
pyroxol	pyroxene/olivine
pl, plag	plagioclase
chrom	chromite
spin	spinel
mag	magnetite
ilm	ilmenite
haem	haematite
K feldsp	potassium feldspar
qtz	quartz
garn	garnet
apat	apatite
biot	biotite
hb	hornblende
sill	sillimanite

P_L	load pressure
P_{O_2}	partial pressure of oxygen
P_{H_2O}	partial pressure of water
m.y.	million years
ppm	parts per million

PPL	plane polarised light
CP	crossed polars
XRD	X-ray diffraction
XRF	X-ray fluorescence
AAS	atomic absorption spectroscopy

TABLE 2

Bibliography of geological observations on the Musgrave Block (* Tomkinson Ranges, + Giles Complex).

EARLY WORKERS

1874 Giles*
Gosse*

1890 Brown

1891 Teitkins

1892 Carruthers*

1893 Brown*
Streich*

1904 Murray*
Wells & George*

1905 Basedow*

1911 Thomson*

1915 Jack

1917 Talbot & Clarke*

1918 Talbot & Clarke*

1933 Terry*

1938 Clarke*

RECENT WORKERS

1947 Wilson+

1948 Wilson

1949 Robinson*+

1950 Wilson

1952 Wilson

1954 Hossfeld
Wilson

1955 Sprigg et al.

1956 Sprigg et al.

1958 Sprigg*+
Wilson*

1959 Sprigg & Wilson*+
Sprigg et al.
Wilson

1960 Wilson
Wilson et al.

1962 Johnson*+
Mirams*+
Thomson et al.*+

1963 Coats
Lonsdale & Flavelle*
Thomson*+

1964 Mirams*+
Nesbitt & Kleeman*+
Thomson*+
Wells et al.
Yong*+

1965 Goode & Krieg*+
Kleeman*+
Thomson*+

1966 Forman
Major+
Miller*+
Nesbitt*+
Nesbitt & Talbot*+
Steele*+
Virgo
Wells et al.

(continued)

TABLE 2 (continued)

RECENT WORKERS

1967 Compston & Nesbitt*
Daniels*+
Facer*+
Goode & Krieg*+
Gray*+
Horwitz et al.*+
Hudson et al.
Kleeman & Nesbitt*+
Major et al.+
Rowan*+
Turner*+
Wilson & Hudson

1968 Barnes*
Compston & Arriens
Lonsdale & Flavelle*
Moore*+
Trommsdorf & Wenk*+
Turner*
Virgo
Waller

1969 Arriens & Lambert
Blight*
Bowden*
Daniels
Goode & Nesbitt*+
Kleeman*+
Miller*+
Moore*
Parkin*+
Virgo
Wilson

1970 Coin
Facer*+
Moore (a,b) *+
Nesbitt et al.*+
Smith*+
Wilson et al.

TABLE 3

Mineral assemblages for acid granulites: (1) quartz + feldspar + pyroxene ± garnet granulites, (2) quartz + feldspar + garnet granulites, (3) quartz + feldspar granulites, (4) quartz-rich granulites. Symbols used are: xx major constituent, x minor constituent, o accessory, P perthite, A apatite, H hornblende, Z zircon, I ilmenite, M magnetite, AP antiperthite, C corundum.

Sample	Quartz	K-felsp	Plag	Garn	Opx	Cpx	Sill	Opaques	Spin	Biot	Hornblende, Apatite, Zircon
(1)											
A300-64	xx	xx P	x	x	x	x		x			o A
A300-57	xx	xx P	xx	x	x	x		x I,M			o H,A
A301-72	xx	xx P	xx	x	x	x		x			o A
A301-166a	xx	xx P	xx	x	x	x		x			
A301-166b	xx	xx P	xx		x	x		x			
A301-123a	xx	xx P	xx		x	x		x			o A
A301-174b	xx	xx P	xx		x	x		x			o A?,Z
(2)											
A300-75	xx	xx P		xx		o		x	o		o Z
A301-26a	xx	xx P		xx				x	o		o Z
A301-154a	xx	xx P		xx				x			o Z
A301-133	xx	xx P		xx				x		o	
A301-151	xx	x P		xx	o			x			
A301-159	xx	xx P	x	xx			x	x	o	o	
A301-156	xx	xx P	xx	xx			x	x		x	
A301-15	xx	xx P		xx			x	x	o	o	o Z
A301-177	xx	x P		x			xx	x	o		
A301-178	xx	xx P		xx			xx	x			
A301-112	xx	xx P		xx			x	x			o Z
A301-147	xx	xx P		x			xx	x			?
A301-171	xx	xx P		x			x	x	o		
A300-702	xx	xx P		xx			xx	x	o		

Cont.

TABLE 3 (cont.)

Sample	Quartz	K-felsp	Plag	Garn	Opx	Cpx	Sill	Opaques	Spin	Biot	Hornblende, Apatite, Zircon
(3)											
A301-16b	xx	xx P	o		o			x			o H,Z
A301-128	xx	x P	x		x			x			
A301-122	xx	xx P			o			x			o Z
A300-69	xx	xx P			o			o			
A300-706	xx	xx P						o			o Z
A301-17	xx	xx P			o			x			
(4)											
A301-21	xx			xx				o			
A301-108	xx			o			xx	xx I			
A301-172	xx			x				o			o Z
A300-74	xx				x			xx M			o A

TABLE 4

Mineral assemblages for basic granulites: (1) plagioclase + orthopyroxene + clinopyroxene granulites, (2) garnet + clinopyroxene + plagioclase granulites (Symbols used as in Table 3).

Sample	Plag	Garn	Opx	Cpx	Hb	Opaques	Spin	Biot	Apatite, Corundum
(1)									
A300-7	xx		xx	xx		x I,M			o A
A300-22	xx		xx	xx	xx	x			o A
A300-94	xx		xx	xx	o	x		o	o A
A300-351	xx		xx	xx	x	x			o A
A300-360	xx		xx	xx		x			o A
A301-4	xx		xx	xx		x			o A
A301-18	xx AP		xx	xx		x			
A301-115	xx AP		xx	xx		x		x	o A
A301-123b	xx		xx	xx	x	x		o	o A
A301-129	xx		xx	xx		x			o A
A301-132	xx AP		xx	xx		x			o A
A301-137	xx		xx	xx	o	x		o	o A
A301-141a	xx AP		xx	xx	o	x		x	o A
A301-141b	xx		xx	xx		x		o	o A
A301-142	xx AP		xx	xx		x			o A
A301-174	xx		xx	xx	x	x		x	o A
(2)									
A300-58	xx	xx		xx	x	x I(M)	x		o C,A
A300-63	x	xx		x	xx	x	x		
A300-362	xx	xx	x	xx	x	x	x		o C
A300-363	x	xx		xx	x	x	x		o C

TABLE 5A

Partial analysis of garnet from acid granulite, A301-156 (after Goode and Krieg, 1965). Measured garnet cell edge 11.517Å.

Al_2O_3	19.9
ΣFe	23.8
MgO	7.07
CaO	0.65
MnO	0.55

TABLE 5B

Point analysis of spinel inclusion in olivine from picrite, A300-84. Analysis by Mr. P. Schultz, Australian Mineral Development Laboratories, Adelaide, using JEOL electron microprobe analyser (model JXA3) and element standards.

Al_2O_3	40.25
Cr_2O_3	14.14
FeO	25.53
MgO	11.53
TOTAL	91.45*

* Low total probably due to low MgO, Al_2O_3.

TABLE 6A

Comparative mineralogical composition of the dolerite suites

Suite	Major Phases				Accessory Phases
	Plag	Cpx	Opx	Ol	
A	x	x			Magnetite, ilmenite, hornblende, apatite ± biotite, orthopyroxene, quartz, K-feldspar
B	x	x	x		Hornblende ± biotite, magnetite, ilmenite, spinel, garnet
C	x	x		x	Biotite, magnetite, ilmenite, spinel, orthopyroxene, anti-perthite ± pyrite
D	x	x		x	Opaques, spinel ± biotite, horn-blende, orthopyroxene, garnet

TABLE 6B

Comparative cumulus and interstitial mineralogy of the member groups of the transgressive picrite suite.

		Dunite	Picrite	Olivine Mesogabbro	Olivine Leucogabbro	Leucogabbro
CUMULUS	spinel	x	x	(x)		
	olivine	x	x	x	x	(x)?
	orthopyroxene		(x)	(x)	(x)?	x
	clinopyroxene			x	x	x
	plagioclase			(x)?	x	x
MAJOR INTERSTITIAL	olivine	x				
	orthopyroxene		x	x	x	x
	clinopyroxene		x	x	x	x
	plagioclase		x	x	x	x

TABLE 7

Age relationships for major events in the eastern Tomkinson Ranges and correlation with other events in other parts of the Musgrave Block. Data from this thesis and from acknowledged sources.

<table>
<tr><th colspan="2">WESTERN MUSGRAVE BLOCK</th><th colspan="2">EASTERN MUSGRAVE BLOCK</th></tr>
<tr><th>Western Tomkinson Ranges</th><th>Eastern Tomkinson Ranges</th><th>Western Musgrave Ranges</th><th>Eastern Musgrave and Everard Ranges</th></tr>
<tr><td colspan="4">Major E–W mylonite zones[1,2,3]
e.g. Hinckley, Mann, Woodroffe.
(uplift at approximately 800m.y.?)</td></tr>
<tr><td rowspan="2"></td><td>Type D dolerite dykes</td><td rowspan="2"></td><td>Type D dolerite dykes[4]</td></tr>
<tr><td>Transgressive picrite suite</td><td rowspan="4"></td></tr>
<tr><td colspan="2">F_3 folding[5,6]</td></tr>
<tr><td></td><td>Type B dolerite dykes</td></tr>
<tr><td colspan="2">F_2 folding[5,6]</td></tr>
<tr><td colspan="4">Type A dolerite dykes[6,7]</td></tr>
<tr><td colspan="2">Localised high temperature deformation of parts of Giles Complex[3,5]</td><td rowspan="2"></td><td rowspan="2">Orthopyroxene adamellite intrusions[8] (1120 ± 100 m.y.[9])</td></tr>
<tr><td colspan="2">Giles Complex layered intrusions[5,10,11] (minimum age 1140 ± 17 m.y.[7])</td></tr>
<tr><td>Granulite facies metamorphism[11]. Two deformations recognised[12].</td><td>Granulite facies metamorphism[1]. One deformation recognised[5].</td><td>Granulite and amphibolite facies metamorphism[2,6]. Two deformations recognised[6].</td><td>Granulite and amphibolite facies metamorphism (1380 ± 120m.y.[9]). One deformation recognised[13].</td></tr>
</table>

References

1. Thomson et al., 1962
2. Major et al., 1967
3. Goode and Nesbitt, 1969
4. Wilson, 1948
5. Nesbitt et al., 1970
6. K.D. Collerson, pers. comm.
7. C.M. Gray, pers. comm.
8. Wilson, 1960
9. Arriens and Lambert, 1969
10. Nesbitt and Talbot, 1966
11. Daniels, 1967
12. Horwitz et al., 1967
13. Wilson, 1958

TABLE 8 Chemical analyses of representative samples of the four dolerite dyke suites, Tomkinson Ranges.

	Type A A300-514	Type B A300-361	Type C A314-389	Type D A314-717
SiO_2	49.32	48.26	45.65	46.47
TiO_2	1.40	0.57	1.52	0.99
Al_2O_3	14.19	10.74	15.15	15.49
Fe_2O_3	1.96	0.85	1.32	1.49
FeO	9.89	10.50	10.18	9.35
MnO	0.19	0.19	0.19	0.19
MgO	8.33	15.07	12.29	12.06
CaO	12.13	10.37	10.48	10.80
Na_2O	2.24	2.54	2.51	2.21
K_2O	0.22	0.16	0.27	0.30
P_2O_5	0.05	0.08	0.29	0.10
TOTAL	99.92	99.33	99.85	99.45
$\frac{100Mg}{Mg+Fe}$	60.01	71.89	68.27	69.68
Crystallization Index	53.5	56.6	58.6	60.7
CIPW Norms				
Or	1.3	1.0	1.6	1.8
Ab	19.0	19.7	16.8	17.8
An	28.0	17.4	29.3	31.5
Ne	-	1.0	2.4	0.5
Di Wo	13.3	13.9	8.7	9.0
Di En	7.5	8.9	5.4	5.7
Di Fs	5.3	4.3	2.7	2.8
Di	26.1	27.1	16.8	16.5
Hy En	7.6	-	-	-
Hy Fs	5.4	-	-	-
Hy	13.0	-	-	-
Ol Fo	4.0	20.1	17.6	17.1
Ol Fa	3.1	10.6	9.8	9.2
Ol	7.1	30.7	27.4	26.3
Mt	2.8	1.2	1.9	2.2
Il	2.7	1.1	2.9	1.9
Ap	0.1	0.2	0.7	0.2
Normative Plagioclase (%An)	60	47	64	64

TABLE 9

Chemical analyses of orthopyroxenes and clinopyroxenes from the Kalka and Ewarara Intrusions.

(Located in back pocket of Volume 2).

TABLE 9 Chemical analyses and structural formulae of orthopyroxenes and clinopyroxenes from the Kalka and Ewarara Intrusions.

	ORTHOPYROXENES				CLINOPYROXENES				
Sample	A300-121	A314-70	A314-153	A314-157	A300-121	A314-135	A314-154	A314-411	A314-418
Exsolution bodies	cpx, (spinel)	cpx, rutile	cpx, rutile	cpx, rutile	opx, spinel	opx	opx	opx, spinel	opx, magnetite
SiO_2	53.30	55.09	53.40	53.20	50.85	51.32	51.69	50.53	50.40
TiO_2	0.09	0.10	0.16	0.16	0.28	0.29	0.28	0.30	0.48
Al_2O_3	4.26	1.62	5.00	2.04	4.85	4.17	3.20	5.02	3.52
Fe_2O_3	1.30	1.32	1.28	1.20	1.80	1.11	1.79	0.44	0.87
FeO	9.43	7.76	9.92	13.03	4.82	6.38	4.85	4.97	10.20
MnO	0.25	0.20	0.17	0.28	0.18	0.25	0.16	0.16	0.21
MgO	28.14	32.32	26.39	28.07	18.45	15.61	17.81	16.74	16.36
CaO	3.18	1.23	3.61	2.23	17.18	20.09	19.72	19.53	17.03
Na_2O	0.40	0.25	0.30	0.23	0.75	0.79	0.60	1.04	0.65
K_2O	0.02	0.02	0.03	0.02	0.02	0.01	0.02	0.02	0.01
P_2O_5	0.01	0.00	0.04	0.00	0.00	0.00	0.00	0.00	0.02
TOTAL	100.38	99.91	100.30	100.46	99.18*	100.02	100.12	98.77*	99.75

Structural formulae (on basis of 6 oxygens).

Si	1.924	1.932	1.892	1.912	1.856	1.891	1.892	1.857	1.878
Al^{IV}	0.076	0.067	0.108	0.086	0.144	0.109	0.108	0.143	0.122
Al^{VI}	0.105	-	0.101	-	0.065	0.072	0.030	0.074	0.033
Fe^{3+}	0.035	0.035	0.034	0.032	0.049	0.039	0.049	0.012	0.024
Fe^{2+}	0.285	0.228	0.294	0.392	0.147	0.197	0.149	0.153	0.318
Mn	0.008	0.006	0.005	0.008	0.006	0.001	0.005	0.005	0.007
Mg	1.514	1.689	1.394	1.494	1.004	0.857	0.971	0.917	0.909
Ca	0.123	0.046	0.136	0.086	0.672	0.793	0.773	0.769	0.680
Na	0.028	0.017	0.020	0.016	0.053	0.056	0.043	0.074	0.067
K	0.001	0.001	0.001	0.001	0.001	-	0.001	0.001	-
Ti	0.003	0.003	0.004	0.004	0.008	0.008	0.008	0.008	0.013
P	-	-	0.001	-	-	-	-	-	0.001
Z	2.000	1.999	2.000	1.998	2.000	2.000	2.000	2.000	2.000
WXY	2.103	2.025	1.990	2.033	2.027	2.023	1.999	2.042	2.052
En	74.89	83.75	72.93	73.91	52.08	44.36	48.94	47.73	45.60
Fs	17.90	13.13	19.20	21.05	11.66	13.65	10.73	10.26	17.89
Wo	7.21	3.12	7.86	5.04	36.27	41.99	40.34	42.00	36.51
Mg	77.36	84.53	75.03	74.55	53.63	45.44	50.00	49.54	47.07
Σ Fe	16.35	13.16	17.65	21.16	10.47	12.51	10.20	8.91	17.71
Ca	6.29	2.30	7.32	4.29	35.90	42.05	39.80	41.55	35.21
Σ Fe as FeO	10.60	8.95	11.07	14.11	6.44	7.38	6.46	5.37	10.98
MgO/Σ FeO	2.65	3.61	2.38	1.99	2.86	2.12	2.76	3.12	1.49
mg	82.2	86.3	80.7	77.6	83.3	78.3	82.7	84.4	72.3
%Al in Z	3.80	3.35	5.40	4.30	7.20	5.45	5.40	7.15	6.10
%Al in WXY	4.99	-	5.08	-	3.21	3.56	1.50	3.62	1.61

* Totals do not include Cr_2O_3 contents, probably high for samples containing spinel exsolution (i.e. high Al_2O_3 contents) e.g. possibly about 0.7 - 1.0% Cr_2O_3 for A300-121, A314-411 by comparison with Moore's, 1970a, analyses.

Z: The trivalent and quadrivalent cations in tetrahedral co-ordination (Si^{4+}, Al^{3+}).

WXY: The bi-, tri-, and quadri-valent cations in octahedral co-ordination (Al^{3+}, Fe^{3+}, Ti^{4+}?, Mg^{2+}, Mn^{2+}, Fe^{2+}) and mono-, and bi-valent cations in hexahedral co-ordination (K^+, Na^+ and Ca^+).

En: Molecular % enstatite = $Mg + \frac{1}{2}Al^{IV} + \frac{1}{2}Ti$; Fs = molecular % ferrosilite = $Fe^{2+} + Fe^{3+} + \frac{1}{2}Al^{IV} + \frac{1}{2}Ti$; Wo = molecular % wollastonite = Ca + Na.

Mg: Molecular % Mg^{2+}. Σ Fe: molecular % ($Fe^{2+} + Fe^{3+}$). Ca = molecular % Ca^{2+},

mg: $100Mg/Mg + Fe^{2+} + Fe^{3+} + Mn$.

TABLE 10

Partial analyses of plagioclases (sodium values rejected because of abnormally high values by comparison with Ca, Al and Si). An values obtained from measured τ (after Kleeman and Nesbitt, 1967). Recrystallized samples and exsolution types given in Table 17.

	A300-84	A314-128	A314-133	A314-150	A314-157
SiO_2			50.75	49.55	51.35
TiO_2	0.11	0.00	0.00	0.01	0.01
Al_2O_3	28.04	31.30	30.19		30.92
Fe_2O_3	2.64	0.13	0.47	0.48	0.16
MnO	0.03	0.01	0.01	0.01	0.01
MgO	3.42	0.09	0.65	0.00	0.15
CaO	6.87	13.90	13.63	15.27	13.83
K_2O	0.28	0.34	0.13	0.17	0.56
P_2O_5	0.06	0.01	0.04	0.00	0.00
τ	0.58	0.96	1.01	1.11	1.03
%An	c.52	67	69	73	70

	A314-197	A314-198	A314-411	A314-418	A314-705	A314-755
SiO_2		50.28	49.17		52.09	
TiO_2	0.01	0.00	0.00	0.25	0.01	0.04
Al_2O_3	32.16	31.42	32.13		29.85	28.69
Fe_2O_3	0.14	0.19	0.28	0.53	0.32	1.39
MnO	0.01	0.00	0.00	0.06	0.01	0.02
MgO	0.22	0.05	0.62	0.37	0.56	0.67
CaO	15.43	14.08	15.19	14.17	13.05	10.32
K_2O	0.10	0.13	0.14	0.12	0.22	0.13
P_2O_5	0.00	0.00	0.06	0.12	0.07	0.22
τ	1.19	1.01	1.20	1.08	0.87	0.82
%An	76	69	76	72	64	62

TABLE 11A

Partial analyses of olivine (after Simkin and Smith, 1970); Fo composition in brackets measured by X-ray diffraction techniques (Appendix 1).

Sample	Rock Type	Fo (Mol%)	Mg (wt%)	Ca (wt%)	Mn (wt%)
A300-84	Picrite, picrite plug suite	82 (82)	26.4	0.00	0.20
A314-101	Troctolite, Kalka	78 (80)	24.6	0.01	0.20
A314-145	Olivine websterite, Kalka	83 (88)	26.8	0.00	0.19
A314-233	Olivine - magnetite band, Kalka	63 (63)	18.5	0.01	0.44

TABLE 11B

Uranium contents (in ppm U) of minerals from the Kalka layered sequence (after Kleeman, 1969)

Rock types are: A314-411 - olivine melagabbro
A251-177D - clinopyroxene norite
A251-185B - olivine mesogabbro
A314-449 - leucogabbro

Sample	Approximate height above base (metres)	Oliv	Opx	Cpx	Plag	Biot	Mag	Apat
A314-411	1950	$\leq$.0003		.013	$\leq$.0001			
A251-177D	2600	$\leq$.0001	$\leq$.001	.001	$\leq$.0002			
A251-185B	3750	$\leq$.0002		.052	$\leq$.0001	$\leq$.001	$\leq$.001	
A314-449	5200	$\leq$.001	.0034	.065	$\leq$.0002	$\leq$.001		$\sim$.25

TABLE 12A

Strontium isotopic ratios for Ewarara, Kalka and Gosse Pile rocks measured by Mr. C.M. Gray, Australian National University, Canberra.

Sample	Rock Type	Approximate height above "base" (metres)	$^{87}Sr/^{86}Sr$
EWARARA			
A300-128	olivine bronzitite	20	0.7092 ± 0.0003
A300-116	pyroxenite	100	0.7072 ± 0.0003
A300-122	websterite	200	0.7076 ± 0.0003
KALKA			
A314-156	websterite	200	0.7148 ± 0.0001
A314-209	norite	3,600	0.7095 ± 0.0005
A314-193	anorthosite	5,500	0.7056 ± 0.0002
GOSSE PILE			
A313-218	norite		0.7075 ± 0.0005
A313-41	norite		0.7078 ± 0.0005

TABLE 12B

Isotopic data from biotite from transgressive picrite plug A300-84. Measurements by Mr. C.M. Gray, Australian National University, Canberra.

Rb = 194 ppm Sr = 57 ppm

$^{87}Sr/^{86}Sr = 0.8173 \pm 0.0004$ $^{87}Rb/^{86}Sr = 9.926$

Absolute ages for various assumed initial ratios:

$^{87}Sr/^{86}Sr_{initial}$	0.700	0.703	0.705	0.710
Age (m.y.)	845	823	809	773

TABLE 13

Natural occurrences of spinel exsolution in pyroxene.

Reference	Pyroxene	Locality	Rock Type
Herz, 1951	opx, cpx ?	Maryland	gabbro
Miller, 1953	?	North Carolina	pyroxenite
Green, 1963	opx	Venezuela	peridotite
Oosterom, 1963	cpx	Norway	peridotite
Le Maitre, 1965	opx	Gough Island	basic nodules
White, 1966	opx, cpx	Hawaii	basic nodules
Peters, 1968	cpx	Switzerland	serpentinite
Harley, 1969	opx	Western Australia	gabbros, pyroxenites
Lovering & White, 1969	cpx	New South Wales	basic nodules
Irving & Green, 1970	cpx	New South Wales	basic nodules
Moore, 1970a	opx, cpx	South Australia	pyroxenites

TABLE 14

Natural occurrences of opaque exsolution in pyroxene.

Reference	Pyroxene	Exsolution Type	Locality	Rock Type
Quensel, 1951	clinopyroxene	?	Sweden	basic rocks
Gjelsvik, 1952	clinopyroxene	?	Norway	basic rocks
Philpotts, 1966	clinopyroxene	ilmenite	Canada	anorthosites
Borisenko, 1967	clinopyroxene	ilmenite		
Gray, 1967	clinopyroxene	ilmenite, haematite	South Australia	anorthosites
Hermes, 1968	clinopyroxene	?	North Carolina	basic rocks
Starmer, 1969	orthopyroxene, clinopyroxene	magnetite, haematite	Norway	basic rocks
Aoki, 1970	hornblende	ilmenite	Japan	basic nodules
Ringwood and Lovering, 1970	clinopyroxene	ilmenite	South Africa	kimberlite

TABLE 15

Natural occurrences of double coronas between olivine and plagioclase

A. Olivine - orthopyroxene - clinopyroxene/spinel - plagioclase type

Reference	Locality
Osborne, 1949	Quebec
Huang & Merritt, 1954	Oklahoma
Oosterom, 1963	Norway
Gray, 1967	South Australia
Aoki, 1968	Japan
Griffin & Heier, 1969	Norway
Harley, 1969	Western Australia
Talbot et al., 1963*	Kerguelen Island
Hiss & Hunter, 1966*	Oklahoma
Sakhno et al., 1968*	Hawaii
Wilson & Middleton, 1968*	Western Australia
Aoki, 1970*	Japan

B. Olivine - orthopyroxene - amphibole/spinel - plagioclase type

Reference	Locality
Buddington, 1939	U.S.A.
Shand, 1945	Quebec
Stewart, 1947	Scotland
Herz, 1951	Maryland
Murthy, 1958	India
Mason, 1967	Norway
Frodesen, 1968	Norway
Starmer, 1969	Norway
Bowes et al., 1964*	Scotland

C. Olivine - orthopyroxene - amphibole - plagioclase type

Reference	Locality
Sadashivaiah, 1954	Scotland
Wilcox & Poldervaart, 1958	U.S.A.
Bhattacharjee, 1963	India
Weedon, 1965	Scotland
Hermes, 1968	U.S.A.

* Possible coronas based on reported presence of pyroxene and/or amphibole symplectites with spinel.

TABLE 16

Natural occurrences of clouding in plagioclase (o opaques, p pyroxene, m magnetite, t transparent, s spinel, g glass, ol olivine, Fe iron-bearing, opx orthopyroxene, cpx clinopyroxene, cz clinozoisite, r rutile, ms mafic silicate, h haematite, amph. f. amphibolite facies, gran. f. granulite facies, gran.gn. granite gneiss).

Reference	Type	Rock Type	Environment	Locality
Williams, 1886	o	gabbro	amph.f.	Maryland
Teall, 1888		dolerite	amph.f.	Scotland
Tyrell, 1916		acid porphyries	amph-gran.f.	Angola
Tilley, 1921	p?,m	metadolerite	amph-gran.f.	South Australia
MacGregor, 1931	o	dolerite	amph.f.	Scotland
Joplin, 1935	t?	xenoliths	?	
Williamson, 1936	o	porphyry	?	Scotland
Shand, 1945*	s	troctolite	amph.f.?	Quebec
Kuno, 1950	p,o±g	andesite	volcanics	Japan
Sutton & Watson, 1950*		dolerite	amph-gran.f.	Scotland
Bentor, 1951	p,ol,o(g)	phenocrysts in basalt	volcanics	France
Herz, 1951*	Fe	gabbro	gneisses	Maryland
Sutton & Watson, 1951*		dolerite	amph-gran.f.	Scotland
Gjelsvik, 1952*		metadolerite	gneisses	Norway
Poldervaart, 1952		dolerite	sediments	Bechuanaland
Huang & Merritt, 1954*	m	troctolite	gran.f.	Oklahoma
Wilcox & Poldervaart,1958*	opx? o	metadolerite	amph.f.	North Carolina
Pichamuthu, 1959		dolerite	gran.f.	Mysore
Weedon, 1961		gabbro	?	Scotland
Dearnley, 1962*		metadolerite	gran.f.	Scotland
Bhattacharjee, 1963*	cpx?	metadolerite	gran.gn.	Bengal
Bowes et al., 1964*		picrite, gabbro	amph.f.	Scotland

continuod

TABLE 16 (continued)

Reference	Type	Rock Type	Environment	Locality
Bridgwater, 1966	Fe	gabbro dykes	?	Greenland
Burns, 1966	(H_2O rich)	dolerite	amph-gran.f.	Scotland
Harding, 1966	o(+cz?)	basic, ultrabasics	?	Scotland
Poldervaart, 1966	r?	charnockitic adamellite	gran.f.	South Africa
Goode & Krieg, 1967*	cpx?	pyroxenite, picrite	gran.f.	South Africa
Frodesen, 1968*	s	gabbro	amph.f.	Norway
Hermes, 1968*	o,ms?	gabbro	amph.f.	North Carolina
Wilson & Middleton, 1968*	s	metagabbro	gran.f.	Western Australia
Frankel, 1969	Fe	phenocrysts in dolerite	?	Seychelles
Harley, 1969*	o	norite	gran.f.	Western Australia
Starmer, 1969*	m,h,s	troctolite	amph-gran.f.	Norway

* indicates presence of high pressure olivine - plagioclase reaction coronas in same rock (Chapter 9.3.2).

TABLE 17

Variation of minor element content of plagioclase with clouding particle type (s spinel, m magnetite, - no particles, r largely recrystallized and a antiperthite).

%An	Sample	Clouding Particles	MgO	Total iron as Fe_2O_3
c.52	A300-84	s	3.42	2.64
62	A314-755	s	0.67	1.39
73	A314-150	m	0.00	0.48
76	A314-197	m	0.22	0.14
69	A314-198	m	0.05	0.19
72	A314-418	m	0.37	0.53
69	A314-133	-	0.65	0.47
76	A314-411	-	0.62	0.28
67	A314-128	- (r)	0.09	0.13
64	A314-705	- (r)	0.56	0.32
70	A314-157	- (a)	0.15	0.16

TABLE 18

Settling velocities of pyroxene/olivine and plagioclase in basalt magma.

Pyroxene/olivine $\Delta\rho = 0.7$, $\rho_m = 2.7$

$\eta = 100$ poise

diam (mm)	Velocity (cm/sec)	Velocity (metres/year)
1	3.83×10^{-3}	1.21×10^{2}
2	1.53×10^{-2}	4.83×10^{2}
3	3.45×10^{-2}	1.09×10^{3}
4	6.13×10^{-2}	1.93×10^{3}
5	9.57×10^{-2}	3.02×10^{3}
10	3.83×10^{-1}	1.21×10^{4}

$\eta = 1000$ poise

diam (mm)	Velocity (cm/sec)	Velocity (metres/year)
1	3.83×10^{-4}	1.21×10^{1}
2	1.53×10^{-3}	4.83×10^{1}
3	3.45×10^{-3}	1.09×10^{2}
4	6.13×10^{-3}	1.93×10^{2}
5	9.57×10^{-3}	3.02×10^{2}
10	3.83×10^{-2}	1.21×10^{3}

Plagioclase $\Delta\rho = 0.05$, $\rho_m = 2.65$

$\eta = 100$ poise

diam (mm)	Velocity (cm/sec)	Velocity (metres/year)
1	2.74×10^{-4}	8.64×10^{0}
2	1.10×10^{-3}	3.47×10^{1}
3	2.47×10^{-3}	7.79×10^{1}
4	4.38×10^{-3}	1.38×10^{2}
5	6.85×10^{-3}	2.16×10^{2}
10	2.74×10^{-2}	8.64×10^{2}

$\eta = 1000$ poise

diam (mm)	Velocity (cm/sec)	Velocity (metres/year)
1	2.74×10^{-5}	8.64×10^{-1}
2	1.10×10^{-4}	3.47×10^{0}
3	2.47×10^{-4}	7.79×10^{0}
4	4.38×10^{-4}	1.38×10^{1}
5	6.85×10^{-4}	2.16×10^{1}
10	2.74×10^{-3}	8.64×10^{1}

Plagioclase $\Delta\rho = 0.10$, $\rho_m = 2.6$

$\eta = 100$ poise

diam (mm)	Velocity (cm/sec)	Velocity (metres/year)
1	5.48×10^{-4}	1.73×10^{1}
2	2.20×10^{-3}	6.94×10^{1}
3	4.94×10^{-3}	1.56×10^{2}
4	8.76×10^{-3}	2.76×10^{2}
5	1.37×10^{-2}	4.32×10^{2}
10	5.48×10^{-2}	1.73×10^{3}

$\eta = 1000$ poise

diam (mm)	Velocity (cm/sec)	Velocity (metres/year)
1	5.48×10^{-5}	1.73×10^{0}
2	2.20×10^{-4}	6.94×10^{0}
3	4.94×10^{-4}	1.56×10^{1}
4	8.76×10^{-4}	2.76×10^{1}
5	1.37×10^{-3}	4.32×10^{1}
10	5.48×10^{-3}	1.73×10^{2}

TABLE 19A

Settling times for pyroxene/olivine and plagioclase; grain size 2mm, basalt viscosity 100 poise.

Distance (metres)	Settling Time (years)	
	pyroxene, olivine	plagioclase
200	.41	5.71
400	.83	11.42
600	1.24	17.13
800	1.66	22.84
1000	2.07	28.55

TABLE 19B

Comparison of particle mobility and Froude Number (F) in basalt/pyroxol - plagioclase and water/quartz systems. Arrows indicate either increases or decreases in mobility and F for basalt relative to water. (ρ_f = density of fluid, $\Delta\rho$ = density contrast between particle and fluid, v_p = fall velocity for pyroxol/plagioclase, v_q = fall velocity for quartz).

Parameter	Basalt	Water	Particle Mobility	F
ρ_f	2.7	1		
$\Delta\rho$	0 - 0.6	1.65		
size	2 - 5mm	0.5mm		
shape	equant-tabular	round		
particle fall velocity	v_p	$v_q \simeq 3 \times 10^2 v_p$	↑	↓
viscosity	10^2 - 10^3	10^{-2}	↑	↓

TABLE 20 Examples of igneous sedimentary structures.

1. Density - grading

Intrusion	Locality	Source
Skaergaard	Greenland	Wager & Deer, 1939
Tiqssaluk Complex	Greenland	Emeleus, 1963
Bushveld	South Africa	Ferguson & Botha, 1963
Stillwater	Montana, U.S.A.	Hess, 1960
Union Bay	Alaska, U.S.A.	Taylor, 1967
	Iceland	Blake, 1968
Nausahi	India	Mukherjee, 1968
	Canada	Elders & Rucklidge, 1969
Michikamau	Canada	Emslie, 1970

2. Cross-stratification

Intrusion	Locality	Source
Skaergaard	Greenland	Wager & Deer, 1939
Tiqssaluk Complex	Greenland	Emeleus, 1963
Nunarssuit	Greenland	Ferguson & Pulvertaft, 1963
Duke Island	Alaska, U.S.A.	Irvine, 1963
Sierra Nevada Batholith	California, U.S.A.	Loomis, 1963
Kapalagulu	Tanjanyika	Wadsworth, 1963
	Scotland	Bowes et al., 1964
Sgurr Dubh	Scotland	Weedon, 1965
St. Kilda	Scotland	Harding, 1966
Nausahi	India	Mukherjee, 1968
Dundonald	Canada	Naldrett & Mason, 1968
Abitibi	Canada	MacRae, 1969
Giles Complex	Australia	Daniels, 1967
Giles Complex	Australia	Nesbitt et al., 1970

continued

TABLE 20 (continued)

3. Trough banding (T) and Scour channels (S)

Intrusion	Locality	Source
Skaergaard (T)	Greenland	Wager & Deer, 1939
Stillwater	Montana, U.S.A.	Jones et al., 1960
Kungnàt (T)	Greenland	Upton, 1960
Tiqssaluk Complex (T)	Greenland	Emeleus, 1963
Nunarssuit (S?)	Greenland	Ferguson & Pulvertaft, 1963
Bushveld (S)	South Africa	Ferguson & Botha, 1963
Duke Island (S)	Alaska, U.S.A.	Irvine, 1965
St Kilda	Scotland	Harding, 1966
Giles Complex (S)	Australia	Nesbitt & Talbot, 1966
Nausahi (S)	India	Mukherjee, 1968
Fiskenaesset (T)	Greenland	Ghisler, 1970

4. Ripples

Intrusion	Locality	Source
Giles Complex (?)	Australia	Nesbitt & Talbot, 1966
Nausahi	India	Mukherjee, 1968

5. Slumps

Intrusion	Locality	Source
Stillwater	Montana, U.S.A.	Hess, 1960
Rhum	Scotland	Wadsworth, 1961
Bushveld	South Africa	Cameron, 1963
Tiqssaluk Complex	Greenland	Emeleus, 1963
Nunarssuit	Greenland	Ferguson & Pulvertaft, 1963
St Kilda	Scotland	Harding, 1966
Giles Complex	Australia	Nesbitt & Talbot, 1966
Duke Island	Alaska, U.S.A.	Irvine, 1967
Nausahi	India	Mukherjee, 1968
Sarqata qaqa	Greenland	Thompson & Patrick, 1968
Fiskenaesset	Greenland	Ghisler, 1970

TABLE 21

Variations in component cumulate subfabrics with particle shape and melt conditions. I = isotropic, P.L. = planar lamination, L.L. = lineate lamination.

Particle Shape	Equidimensional		Tabular		Elongate	
Melt condition	Static	Laminar Current Flow	Static	Laminar Current Flow	Static	Laminar Current Flow
1. Nucleation	I	I	I	I	I	I
2. During settling	I	I	I	P.L.	I	L.L.
3. On settling	I	I	P.L.	P.L.	P.L.	L.L.
4. After settling (at surface)	-	I	-	P.L.	-	L.L.
5. After settling (below surface)	I	-	P.L.	-	P.L.	-

TABLE 22

Absolute age datings of rocks and minerals from the Musgrave Block (w.r. = whole rock, musc = muscovite, biot = biotite, hb = hornblende, opx = orthopyroxene).

Rock Type	Locality	Method	Age	$^{87}Sr/^{86}Sr$ initial ratio	Reference
granulites	Ernabella	Rb-Sr w.r.	1390±130	0.706	Compston and Arriens, 1968
granulites	Ernabella	Rb-Sr w.r.	1380±120	0.7072± 0.0025	Arriens and Lambert, 1969
amphibolite facies	Kenmore Park, Kulgera	Rb-Sr w.r.	1450±160	0.7034± 0.0026	Arriens and Lambert, 1969
opx granite	Ernabella	Rb-Sr w.r.	1120±100	0.7106± 0.0014	Arriens and Lambert, 1969
hb-biot granite	Mount Illbillie	Rb-Sr w.r.	c. 1300??		Parkin, 1969
hb-biot granites	Abminga 4-mile sheet	K-A hb, biot	~1000-1100 ±110		B.P. Thomson (pers. comm.)
pegmatite	Kulgera	Rb-Sr musc	1070		Wilson et al., 1960
granite	Pottoyu Hills, Petermann Ranges	Rb-Sr w.r. Rb-Sr biot	1190,1150* 600,570		Forman, 1966
granulite	Gosse Pile	K-A musc	877		R. Armstrong, (pers. comm.)
picrite	Ewarara	Rb-Sr biot	c. 800		C.M. Gray (pers. comm) (see Table 12B)

* Calculated assuming low $^{87}Sr/^{86}Sr$ initial ratios.

TABLE 23

Compilation of viscosity data for basaltic melts.

Source	Material	Viscosity	Temperature (°C)
Macdonald (1963)	Hawaiian lavas	$2 - 4 \times 10^3$	1000 - 1100
	Hawaiian lavas	10^4	900
Clark (1966)	Hawaiian tachylite	76 → 150	1314 → 1248
	Japanese olivine basalt	296 → 3180	1300 → 1200
	Japanese andesite basalt	260 → 31200	1300 → 1200
	Japanese nepheline basalt	97 → 190	1300 → 1200
Shaw et al. (1968)	Hawaiian tholeiite	500?	1200
	Hawaiian tholeiite	4000	1130
	Hawaiian tholeiite	8000 (25% crystals)	1130
Shaw (1969)	Hawaiian tholeiite	100* → 2000 (with increasing crystal content)	1300 → 1150

* denotes data used in text.

TABLE 24

Compositions of olivine tholeiite melts, co-existing olivine crystals, and various olivine/melt mixtures. Melt and olivine compositions taken from Green and Ringwood (1967a).

Analysis	1*	2*	3**	4*	5	6
FeO	10.07	8.9	10.0	10.3	9.49	9.13
MgO	14.6	49.9	10.9	48.7	32.2	35.8
$\frac{MgO}{FeO}$	1.44	(5.61)	1.09	(4.73)	3.40	3.82

Analysis	7	8	9	10	11	12
FeO	9.25	9.13	10.2	10.2	10.2	10.2
MgO	39.3	43.8	29.8	33.6	37.4	41.1
$\frac{MgO}{FeO}$	4.25	4.80	2.94	3.30	3.66	4.02

1. Olivine tholeiite (initial composition).
2. Olivine at 1350°C, 9kb - liquidus composition.
3. Olivine tholeiite melt at 1310°C, 9kb (10% crystal extraction of olivine).
4. Olivine at 1310°C, 9kb.
5. Mixture+ of 50% 1350°C olivine (anal. 2) and 50% olivine tholeiite melt (anal. 1).
6. Mixture of 60% 1350°C olivine (anal. 2) and 40% olivine tholeiite melt (anal. 1).
7. Mixture of 70% 1350°C olivine (anal. 2) and 30% olivine tholeiite melt (anal. 1).
8. Mixture of 80% 1350°C olivine (anal. 2) and 20% olivine tholeiite melt (anal. 1).
9. Mixture of 50% 1310°C olivine (anal. 4) and 50% 1310°C olivine tholeiite melt (anal. 3).
10. Mixture of 60% 1310°C olivine (anal. 4) and 40% 1310°C olivine tholeiite melt (anal. 3).
11. Mixture of 70% 1310°C olivine (anal. 4) and 30% 1310°C olivine tholeiite melt (anal. 3).
12. Mixture of 80% 1310°C olivine (anal. 4) and 20% 1310°C olivine tholeiite melt (anal. 3).

Continued

TABLE 24 (continued)

* compositions from Green and Ringwood (1967) for experimental runs on olivine tholeiite at 9kb.

** calculated by Green and Ringwood's method –

$$\frac{[MgO]}{[FeO]\,liq} = \frac{14.55 - (m/100 \times 48.7)}{10.07 - (m/100 \times 10.3)}$$ where m = degree of crystallization

$$= 1.07$$

$$\therefore\ m = 10\%$$

$$\therefore\ m + (100-m)y = z$$ where x = olivine composition,
y = composition of residual liquid,
z = composition of initial liquid.

$$\therefore\ y = \frac{z - 10x}{90}\ .$$

∴ Analysis 3 is calculated.

\+ packing concentrations for olivine from Jackson (1961) – may vary from 50 to 80% for ultramafic zone of Stillwater Intrusion, Montana (see also Table 26). Orthocumulus crystallization of the interstitial liquid is assumed.

TABLE 25: Modal classification for igneous rocks consisting of olivine (ol), orthopyroxene (opx), clinopyroxene (cpx) and plagioclase (pl).

	m < 10 pl		30 pl ⩾ m ⩾ 10 pl		70 pl ⩾ m > 30 pl		90 pl ⩾ m > 70 pl		m > 90 pl
	opx > cpx	cpx > opx	opx > cpx	cpx > opx	opx > cpx	cpx > opx	opx > cpx	cpx > opx	
m > 90 ol	**DUNITE GROUP** Dunite								
90 ol ⩾ m ⩾ 50 ol	**LHERZOLITE GROUP** Harzburgite (m < 10 cpx) | Peridotite (m < 10 cpx) Lherzolite (10 cpx ⩽ m ⩾ 10 cpx)		**PICRITE GROUP A** Melatroctolite (m < 10 total px) Picrite (m ⩾ 10 total px)		**PICRITE GROUP B** Mesotroctolite (m < 10 total px) Picrite (m ⩾ 10 total px)				
50 ol > m ⩾ 10 ol	**OLIVINE PYROXENITE GROUP** Olivine Orthopyroxenite (m < 10 cpx) | Olivine Clinopyroxenite (m < 10 cpx) Olivine Websterite (10 cpx ⩽ m ⩾ 10 cpx)		**OLIVINE MELAGABBRO GROUP** Olivine Melanorite (m < 10 cpx) | Olivine Melagabbro (m < 10 cpx) Olivine Clinopyroxene Melanorite* (m ⩾ 10 cpx) | Olivine Orthopyroxene Melagabbro* (m ⩾ 10 cpx)		**OLIVINE MESOGABBRO GROUP** 1. m < 10 total px Mesotroctolite 2. m ⩾ 10 total px Olivine Mesonorite (m < 10 cpx) | Olivine Mesogabbro (m < 10 cpx) Olivine Clinopyroxene Mesonorite* (m ⩾ 10 cpx) | Olivine Orthopyroxene Mesogabbro* (m ⩾ 10 cpx)		**OLIVINE LEUCOGABBRO GROUP** 1. m < 10 total px Leucotroctolite 2. m ⩾ 10 total px Olivine Leuconorite | Olivine Leucogabbro	
m < 10 ol	**PYROXENITE GROUP** Orthopyroxenite (m > 90 opx) | Clinopyroxenite (m > 90 cpx) Websterite (90 opx ⩾ m ⩽ 90 cpx)		**MELAGABBRO GROUP** Melanorite (m < 10 opx) | Melagabbro (m < 10 opx) Clinopyroxene Melanorite* (m ⩾ 10 opx) | Orthopyroxene Melagabbro* (m ⩾ 10 opx)		**MESOGABBRO GROUP** Mesonorite (m < 10 opx) | Mesogabbro (m < 10 opx) Clinopyroxene Mesonorite* (m ⩾ 10 opx) | Orthopyroxene Mesogabbro* (m ⩾ 10 opx)		**LEUCOGABBRO GROUP** Leuconorite | Leucogabbro		**ANORTHOSITE GROUP** Anorthosite

* Terms become defunct if 10% cpx and 10% opx modes not used.

TABLE 26

Porosities of various igneous sediments.

Porosity (%)	Material	Reference
20	pyroxene + plagioclase	Wager & Deer (1939)
30 - 50	pyroxene + olivine	Brown (1956)
35 - 45	plagioclase (experimental)	Wager, Brown & Wadsworth (1960)
26 - 29	pyroxene + olivine + plagioclase	Hess (1960)
~35 (± 5)	orthopyroxene (equidimensional)	Jackson (1961)
~30	orthopyroxene (inequidimensional)	
~35	olivine	
~40 (± 10)	chromite	
~35	orthopyroxene + olivine (same size)	
~30	orthopyroxene + olivine (different size)	
~25 - 40*	olivine + chromite	
28 - 45	orthopyroxene (experimental)	Cameron (1969)

* Variable porosity dependent on relative grain size and proportional abundance.

FIGURES

FIGURE 1

Generalised map of Musgrave Block, showing distribution of Giles Complex intrusions and other geographical features. (Compiled from Sprigg et al., 1959; Thomson et al., 1962; Forman, 1966; Wells et al., 1966; Major et al., 1967 and Daniels, 1967). Location of the Kalka - Ewarara field area is also shown.

(Located in back pocket of Volume 2).

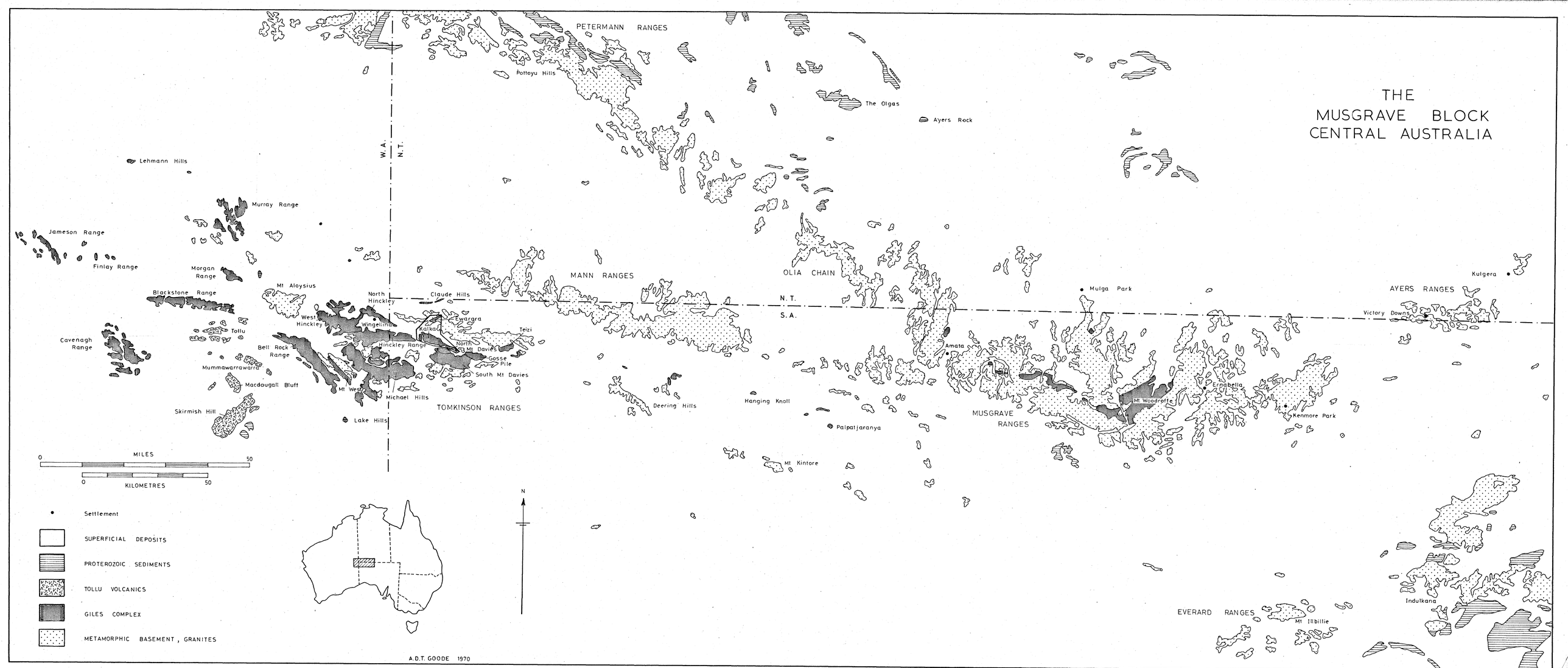
THE
MUSGRAVE BLOCK
CENTRAL AUSTRALIA
PETERMANN RANGES
Pottoyu Hills
The Olgas
Ayers Rock
W.A.
N.T.
Lehmann Hills
Murray Range
Jameson Range
Finlay Range
Morgan Range
Blackstone Range
Mt Aloysius
North Hinckley
Claude Hills
West Hinckley
Wingellina
Ewarara
Kalka
Tollu
Cavenagh Range
Bell Rock Range
Hinckley Range
North Mt Davies
Gosse Pile
South Mt Davies
Mummawarrawarra
Macdougall Bluff
Mt West
Michael Hills
Skirmish Hill
Lake Hills
TOMKINSON RANGES
MANN RANGES
OLIA CHAIN
Deering Hills
Hanging Knoll
Palpatjaranya
Mt Kintore
N.T.
S.A.
Mulga Park
Amata
Kulgera
AYERS RANGES
Victory Downs
Ernabella
Mt Woodroffe
Kenmore Park
MUSGRAVE RANGES
EVERARD RANGES
Mt Illbillie
Indulkana
0 MILES 50
0 KILOMETRES 50
N
Settlement
SUPERFICIAL DEPOSITS
PROTEROZOIC SEDIMENTS
TOLLU VOLCANICS
GILES COMPLEX
METAMORPHIC BASEMENT, GRANITES
A.D.T. GOODE 1970

FIGURE 2

Geological map of the Kalka - Ewarara area, eastern Tomkinson Ranges (location shown in Fig. 1).

(Located in back pocket of Volume 2).

GEOLOGY
OF
KALKA AND EWARARA

EWARARA

KALKA

WEST KALKA

WALTER HILL

Transgressive Picrites

MT KALKA

DRUM HILL

Genre Fault

Abialbit Fault

Hinckley Fault

SCARFACE SILCRETE ZONE

MINNO

MT DAVIES BORE

GUNBARREL HIGHWAY

M.N.

Superficial deposits

Ferruginous ochres (Tertiary?)

Silcretes, with minor magnesite (Tertiary?)

MINOR INTRUSIONS

Type D dolerite dykes, associated faults and undifferentiated dolerites

Type C dolerite dykes

Type B dolerite dykes

Type A dolerite dykes

Trangressive picrite suite (D dunite group, P picrite group, OG olivine gabbro group, G gabbro group)

Anorthosite

Matic pegmatite

Pyroxenite lens

Garnet pyroxenite

Transgressive magnetite-ilmenite bodies

GILES COMPLEX

Gabbros, olivine gabbros, troctolites and minor norites; dominantly leucocratic to anorthositic

Dominantly norites

Olivine-bearing rocks, dominantly gabbros and norites (light dots - olivine-poor, heavy dots - olivine-rich)

Pyroxenites

Olivine pyroxenites

Olivine magnetite band

Peridotite band

Johnson Horizon

Vertical layered horizon (Ewarara)

Contaminated norites, acid granulite xenoliths

GRANULITES

Undifferentiated granulites, dominantly acidic

Quartz + feldspar + pyroxene ± garnet granulites (circles - dominantly augen gneisses, b - dominantly banded gneisses)

Quartz + feldspar ± garnet granulites

Iron-rich quartz granulites

Quartz + feldspar + pyroxene granulites with granitic tendencies

Plagioclase + orthopyroxene + clinopyroxene granulites

Garnet + clinopyroxene + plagioclase granulites

Mylonite, pseudotachylite (Hinckley Fault)

Magnesite

Serpentinite

Fault

Lithological layering

S_1 foliation

S_2 foliation

Igneous contact

Mylonite foliation

L_1 lineation

L_2 lineation

Lineation, unknown type

F_2 fold axis

F_2 anticline

Trend lines

MILES

KILOMETRES

A.D.T. GOODE, 1970
(Geology of Ewarara largely from Goode & Krieg, 1965)

FIGURE 3

Location of samples, thin sections, polished sections and some field stations from Kalka. Drainage patterns and other features are also shown. Same scale as Fig. 2.

(Located in back pocket of Volume 2).

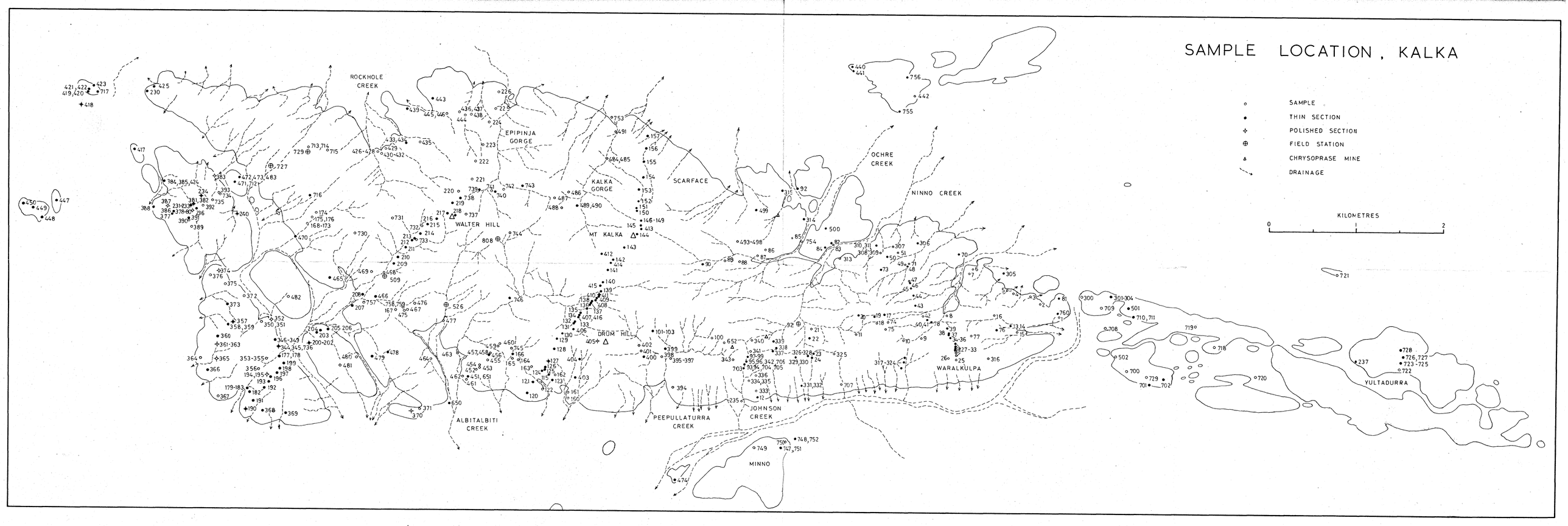
SAMPLE LOCATION, KALKA
SAMPLE
THIN SECTION
POLISHED SECTION
FIELD STATION
CHRYSOPRASE MINE
DRAINAGE
KILOMETRES
0
2
ROCKHOLE CREEK
EPIPINJA GORGE
KALKA GORGE
SCARFACE
OCHRE CREEK
NINNO CREEK
WALTER HILL
MT KALKA
DROM HILL
ALBITALBITI CREEK
PEEPULLATURRA CREEK
JOHNSON CREEK
WARALKULPA
YULTADURRA
MINNO

FIGURE 4

Location of samples, thin sections and polished sections from Ewarara. Drainage patterns are also shown. Same scale as Fig. 2.

(Located in back pocket of Volume 2).

SAMPLE LOCATION, EWARARA

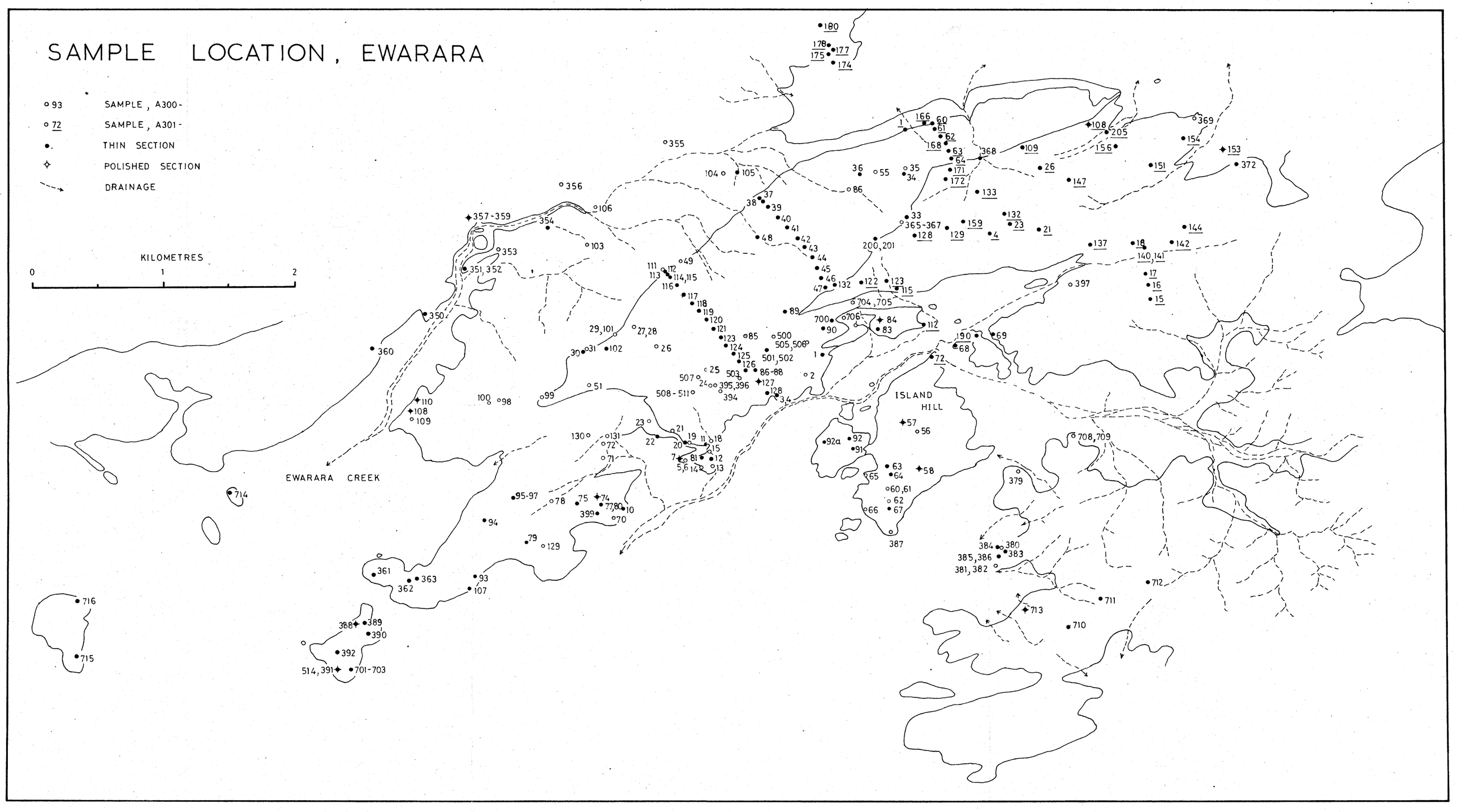

FIGURE 5

A. Granulite facies assemblages in the vicinity of Ewarara. Triangles represent basic granulites: open - orthopyroxene-bearing (no garnet); closed - garnet-bearing (no ortho-pyroxene). Circles represent quartz - K feldspar - pyroxene ± garnet granulites: open - without garnet, orthopyroxene-bearing; half closed - garnet associated with opaques, orthopyroxene-bearing.

B. Generalised structural map of the Ewarara area (modified from Fig. 2). FA, FB, FC and FD represent faults. A major anti-clinal axis is also shown; note its possible curvature towards the south. Circles represent presence of plagioclase laths in Type B dolerite dykes: open - some unrecrystallized; closed - all recrystallized.

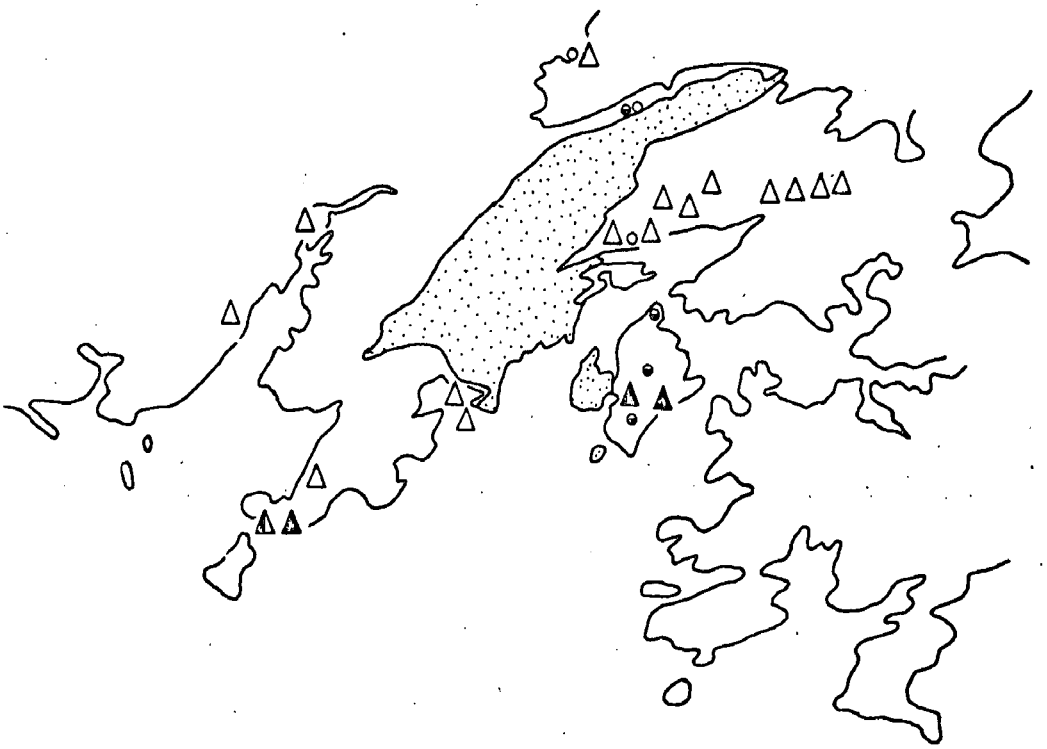

A.

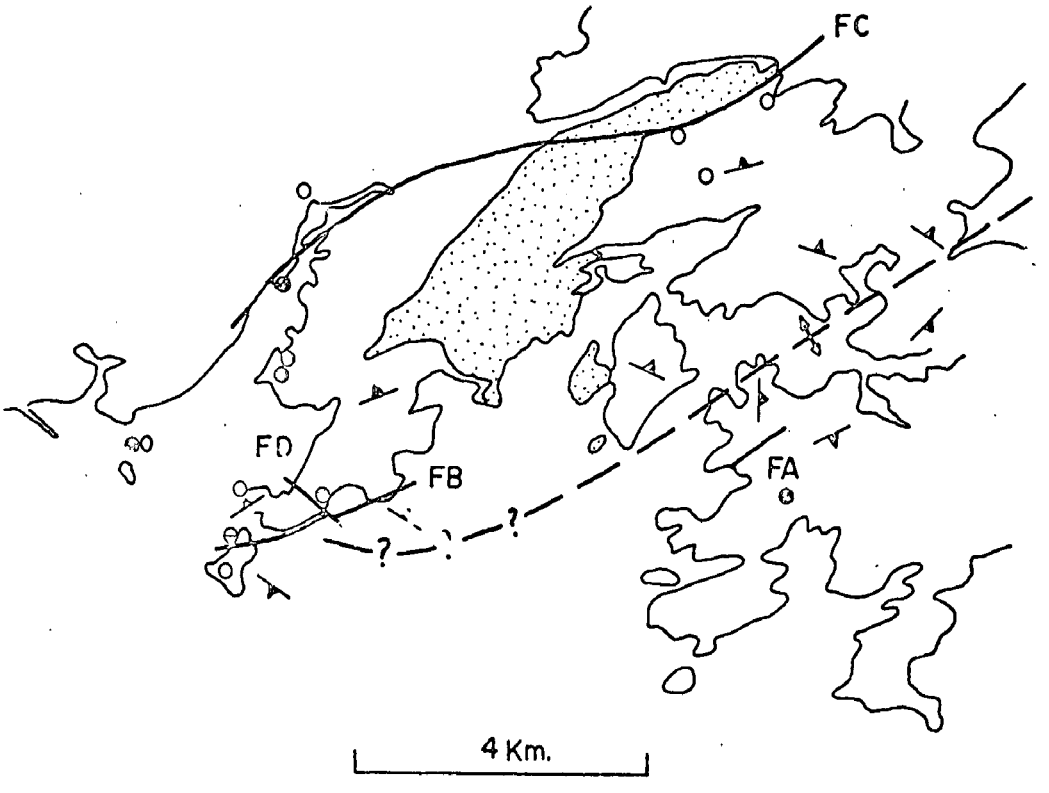

B

FIGURE 6

P-T diagram showing stability ranges of mineral assemblages in relation to granulite facies metamorphism.

1. Stability of Al_2SiO_5 polymorphs (sillimanite forms the high temperature, high pressure field):
   a. after Fyfe, 1967
   b. after Richardson *et al.*, 1969.
2. Upper stability limit of hornblende (after Lambert and Wyllie, 1968).
3. a. Solidus for "wet" granite (after Luth *et al.*, 1964).
   b. Liquidus for "wet" granite (after Boettcher and Wyllie, 1968a).
   c. Liquidus for granite with 2% H_2O (after Tuttle and Bowen, 1958).
   d. Liquidus for anhydrous granite (after C.W. Burnham, pers. comm.).
4. Quartz + muscovite $\rightleftharpoons$ K-feldspar + sillimanite + H_2O (after Burnham and Shade, 1968).
5. a. Upper stability of Mg-cordierite (after Schreyer and Yoder, 1964).
   b. Upper stability of cordierite in natural rock compositions (after Hensen and Green, 1970).
6. a. Enstatite + anorthite $\rightleftharpoons$ garnet + quartz (after Kushiro and Yoder, 1966).
   b. orthopyroxene + plagioclase $\rightleftharpoons$ garnet + quartz in quartz tholeiite compositions (after Green and Ringwood, 1967b). Stippling gives range of P-T conditions for first appearance of garnet for variable Mg/Mg+Fe ratios.
   c. orthopyroxene + plagioclase $\rightleftharpoons$ garnet + quartz in anhydrous adamellite compositions (after Green and Lambert, 1965).
7. Stability of $CaCO_3$ polymorphs (calcite forms high temperature field) (after Boettcher and Wyllie, 1968b).

Coloured region indicates the range of metamorphic conditions for the granulites described in this study.

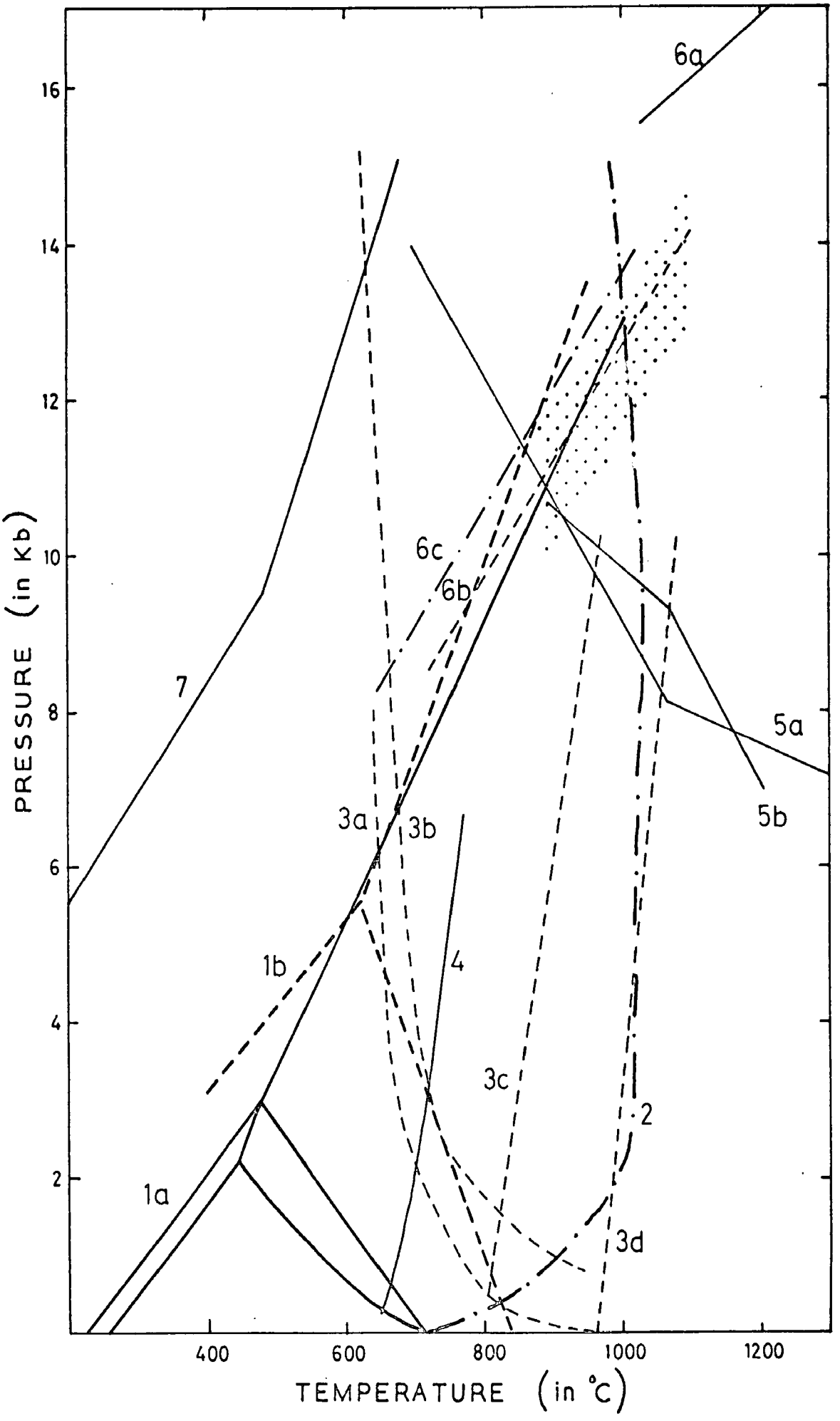
PRESSURE (in Kb)
TEMPERATURE (in °C)
16
14
12
10
8
6
4
2
400
600
800
1000
1200
6a
6c
6b
7
5a
5b
3a
3b
4
1b
3c
2
1a
3d

FIGURE 7

Chemical relationships and affinities of the four dolerite suites, Tomkinson Ranges (basalt fields after Macdonald and Katsura, 1964, and Kuno, 1960).

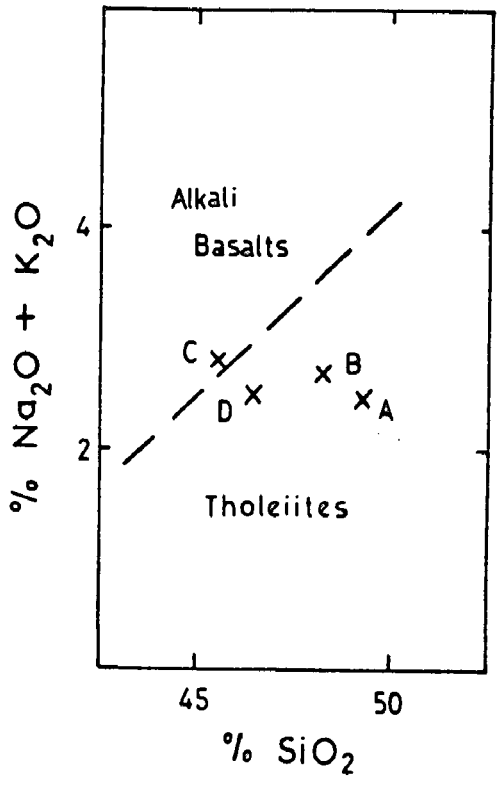
Alkali
Basalts
Tholeiites
C
D
B
A
4
2
45
50
% $Na_2O + K_2O$
% SiO_2

A

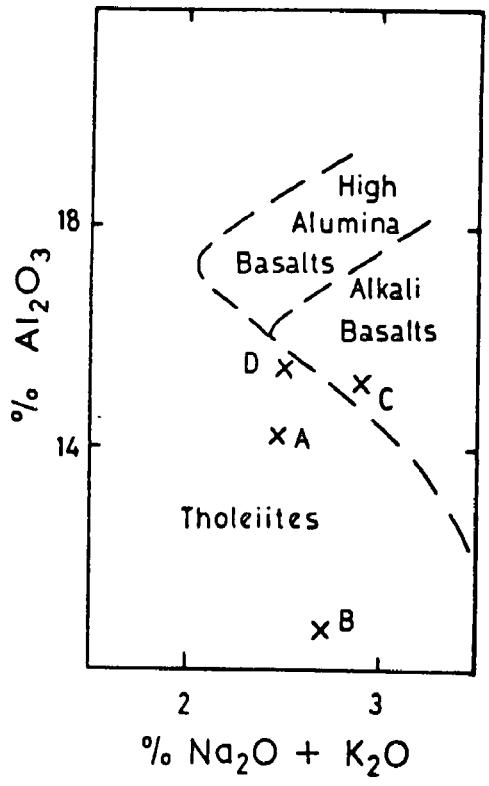
High
Alumina
Basalts
Alkali
Basalts
Tholeiites
D
C
A
B
18
14
2
3
% Al_2O_3
% $Na_2O + K_2O$

B

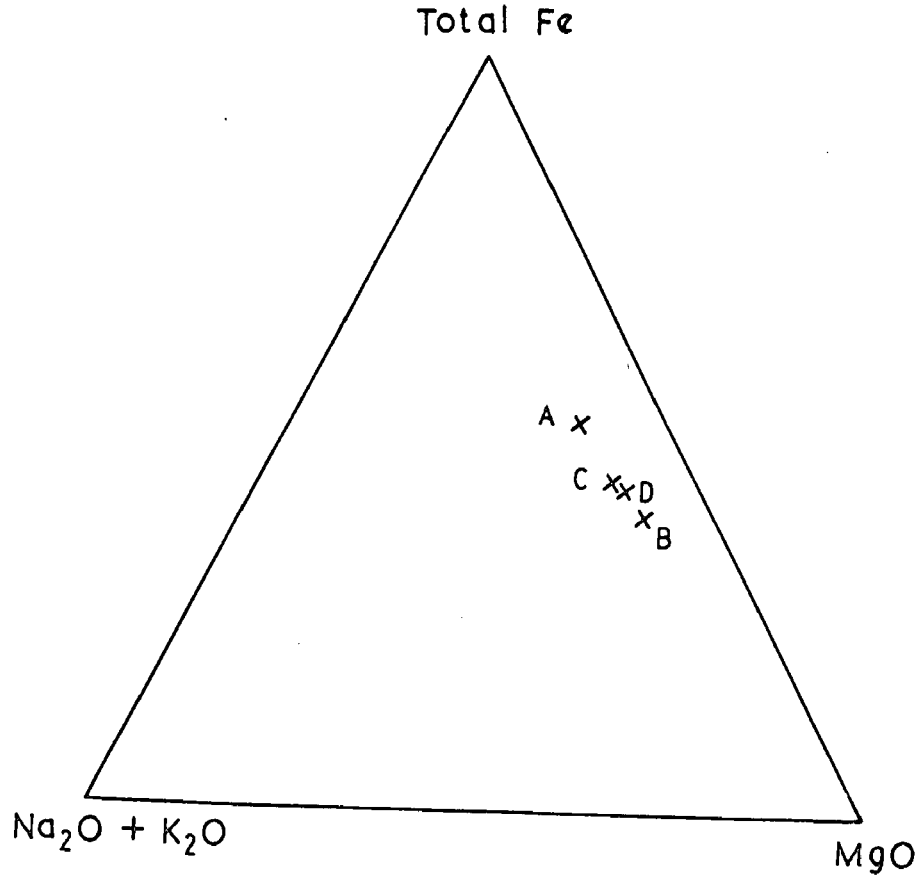
Total Fe
A
C
D
B
$Na_2O + K_2O$
MgO

C

FIGURE 8

Distribution of minor intrusions in the Ewarara - Kalka area, Tomkinson Ranges (granulites shown as light stipple).

Dolerites: Type A - blue
Type B - heavy lines
Type C - dotted lines
Type D - fine lines

Transgressive picrite suites: red, numbered as in text (stippled red areas represent silcrete supposedly overlying dunite in Scarface Silcrete Zone).

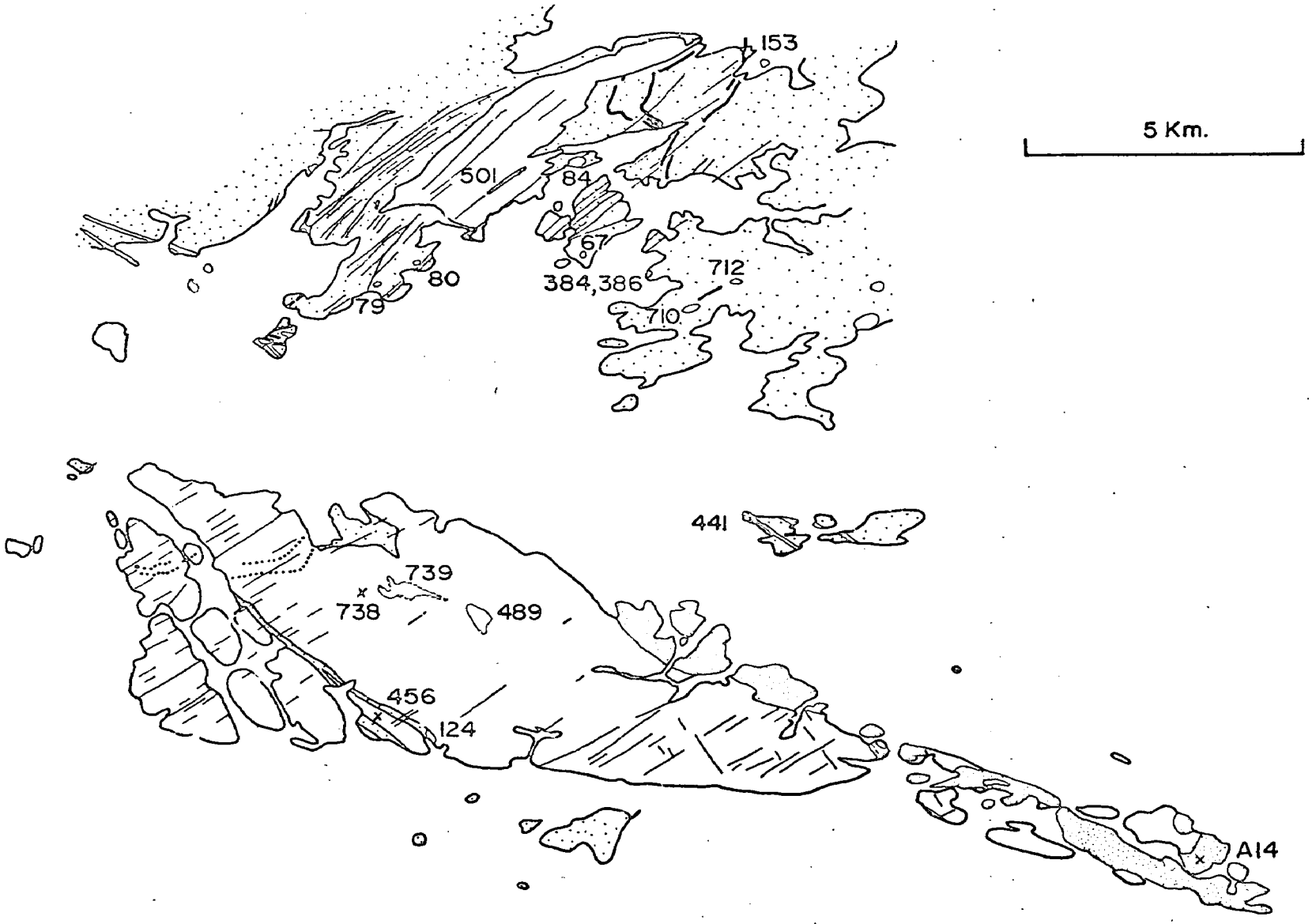
153
5 Km.
501
84
67
80
79
384,386
712
710
441
739
738
489
456
124
A14

FIGURE 9

Distribution of Gairdner dolerite dyke swarm in South Australia (Precambrian basement areas stippled).

Musgrave Block: only confirmed examples of Gairdner (or Type A) dolerites shown (many other northwest trending dykes may also be members of the same suite).

Gawler Block: Linear magnetic anomalies indicating probable distribution of Gairdner dolerites (compiled by Professor D.M. Boyd, University of Adelaide).

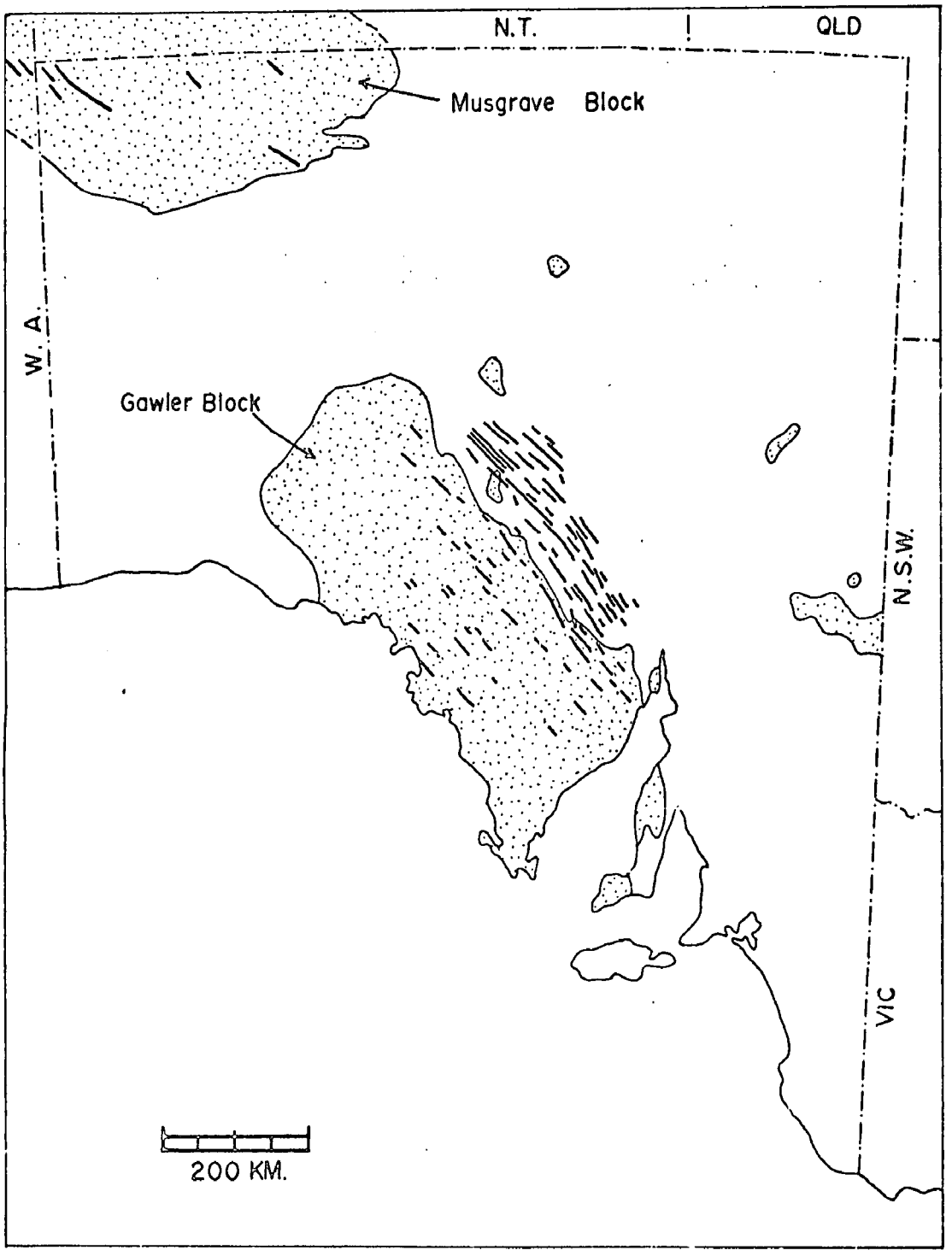
N.T.
QLD
Musgrave Block
W. A.
Gawler Block
N.S.W.
VIC
200 KM.

FIGURE 10

A. Olivine phenocryst shapes, Type D dolerite dykes. From A314-417, A314-717, A251-N1898. 1mm scales.

Note: All textural diagrams in this thesis are drawn from photographs.

B. Phenocryst group of plagioclase (stippled) and olivine (black) in Type D dolerite, A314-717. 1mm scale.

C. Leuconorite bands (stippled) in mesonorite outlining pseudo-scour channel, field station 729. Solid line is fault plane. Scale 20cm.

D. Irregular leuconorite bands (stippled) in mesonorite, field station 727, possibly outlining refolded fold structures. Scale 20cm.

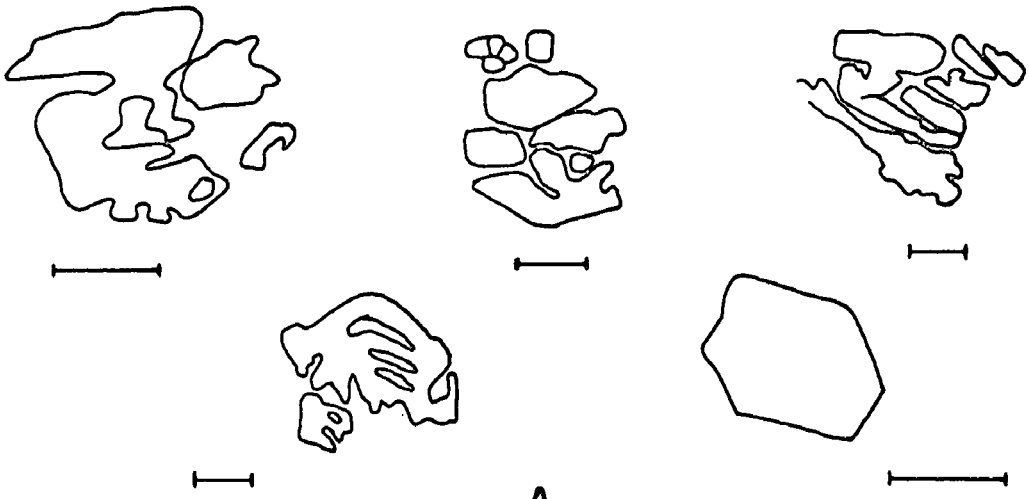

A

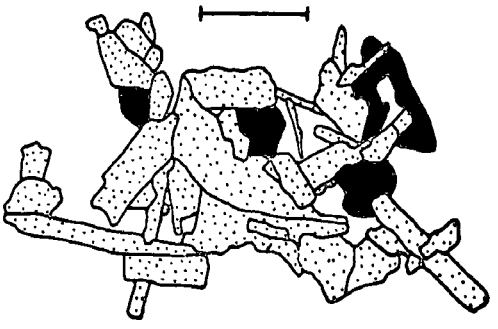

B

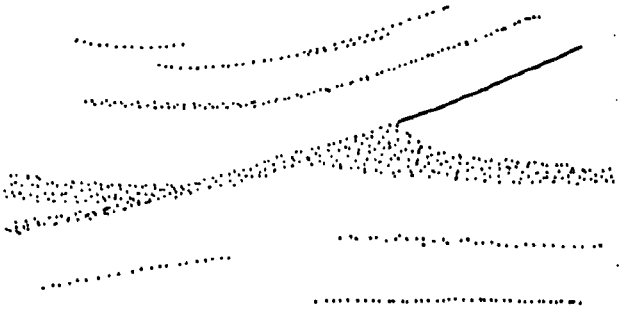

C

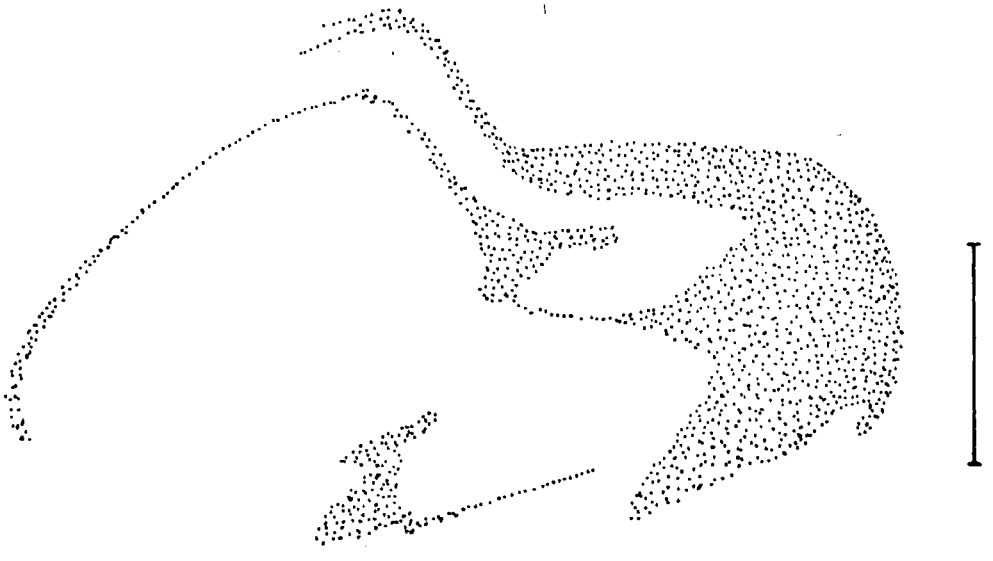

D

FIGURE 11

A. Modal fractionation trend of transgressive picrite suite, Tomkinson Ranges.

B. Variation of olivine composition with modal content of olivine, transgressive picrite suite, Tomkinson Ranges. (Crosses - dunite group; closed circles - picrite group; open circles - olivine mesogabbro group).

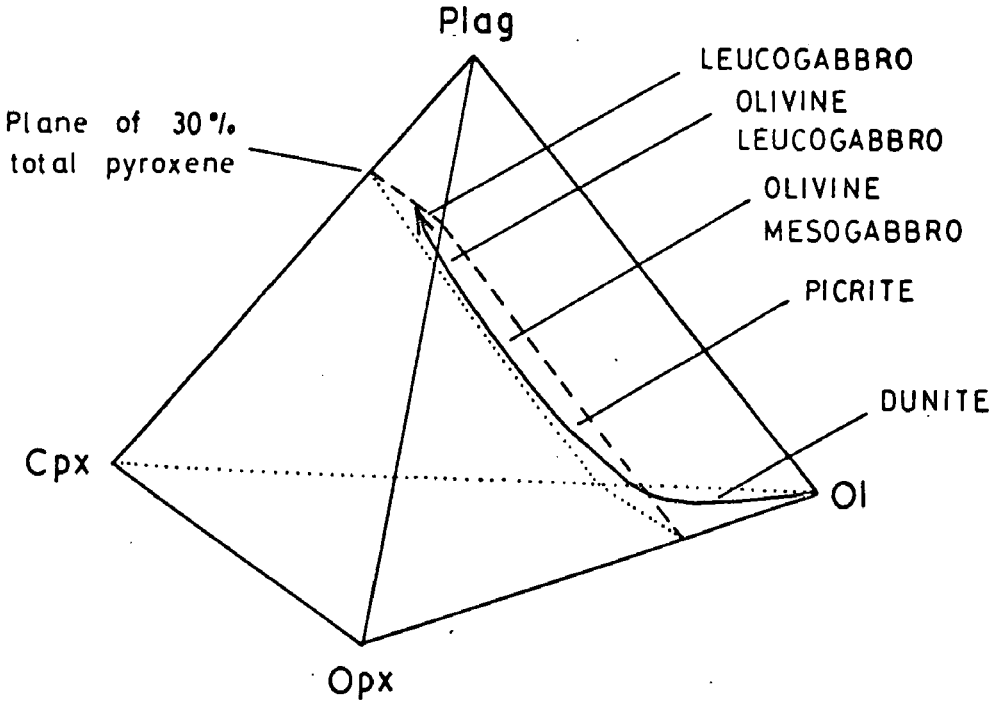
Plag
LEUCOGABBRO
OLIVINE
LEUCOGABBRO
Plane of 30 %
total pyroxene
OLIVINE
MESOGABBRO
PICRITE
DUNITE
Cpx
Ol
Opx

A

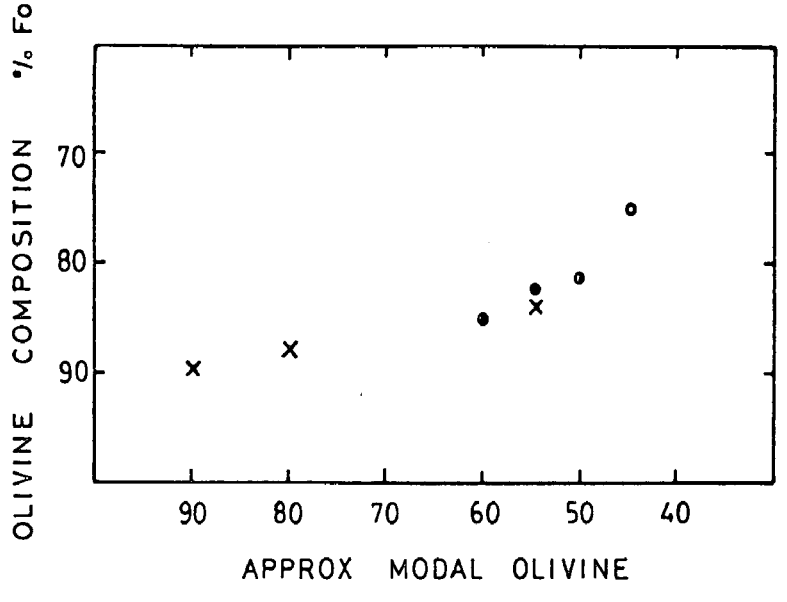
OLIVINE COMPOSITION % Fo
70
80
90
90
80
70
60
50
40
APPROX MODAL OLIVINE

B

FIGURE 12

A. Hypothetical fractionation column for transgressive picrite suite showing cumulus crystal variations with height. Symbols used are: solid circles - spinel (or chromite); open hexagonal laths - olivine; stippled hexagonal laths - pyroxene; open rectangular laths - plagioclase.

B. Stratigraphic section across the southern part of the southern vertical layered horizon, Ewarara, showing distribution of Type 1 bands (stippled) in Type 2 bands.

C. Stability fields of enstatite polymorphs. PE - protoenstatite; OE - orthoenstatite; CE - clinoenstatite (after Coe, 1970).

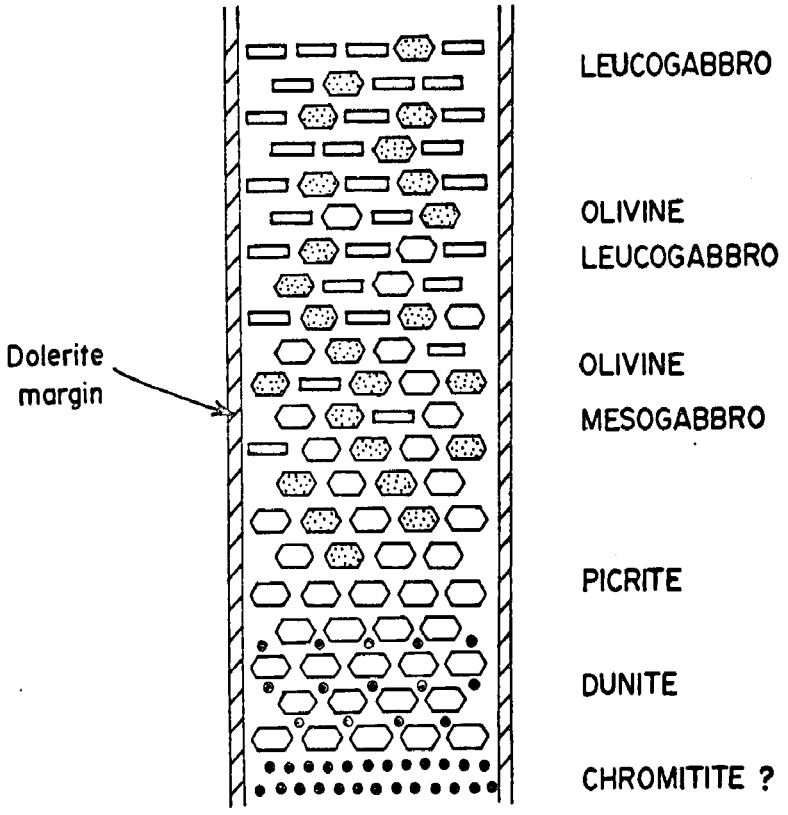
LEUCOGABBRO
OLIVINE
LEUCOGABBRO
Dolerite
margin
OLIVINE
MESOGABBRO
PICRITE
DUNITE
CHROMITITE ?

A

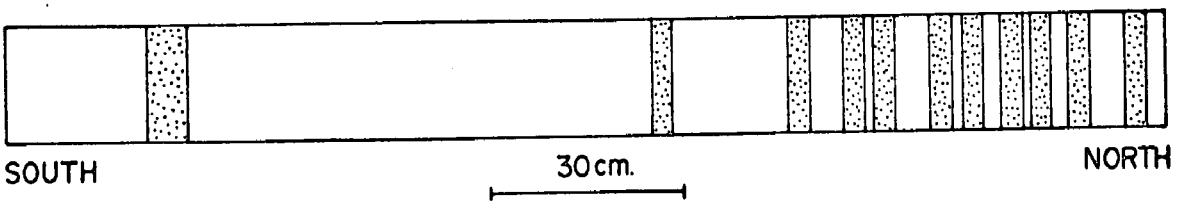
SOUTH
30 cm.
NORTH

B

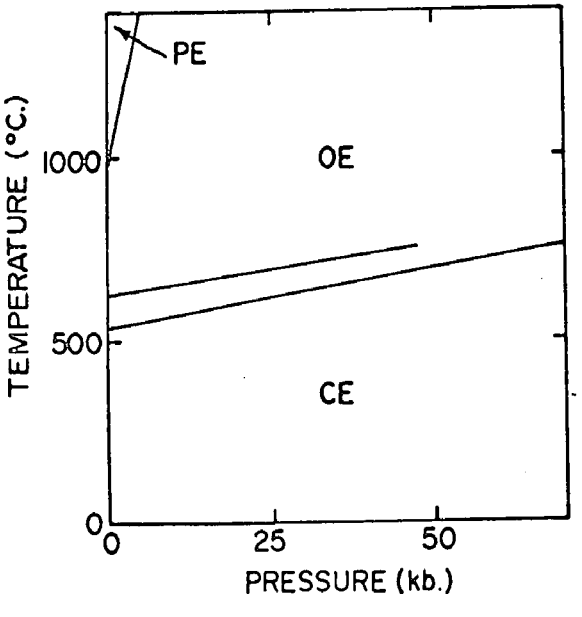
PE
OE
CE
1000
500
0
TEMPERATURE (°C.)
0
25
50
PRESSURE (kb.)

C

FIGURE 13

Vertical mineralogical and chemical variations, and cyclic unit divisions for the Ewarara and Kalka layered sequences.

1. Mineral chemistry: open circles - plagioclase (An%); solid circles - olivine (Fo%); + orthopyroxene; x clinopyroxene (mg values of pyroxenes from Table 9).

2. Cyclic units: divisions based on plagioclase composition, olivine composition and relative proportions of cumulus phases.

3. Modes (1) Interstitial: distribution of opaques (O), hornblende (H) and biotite (B).

   (2) Cumulus (approximate): orthopyroxene (black), clinopyroxene (lines), olivine (stippled), plagioclase (blank).

Traverses used for the Kalka Intrusion are No. 6 (Mt Kalka) Section for samples 157 to 126, and No. 4 (Walter Hill) Section for samples 208 to 190.

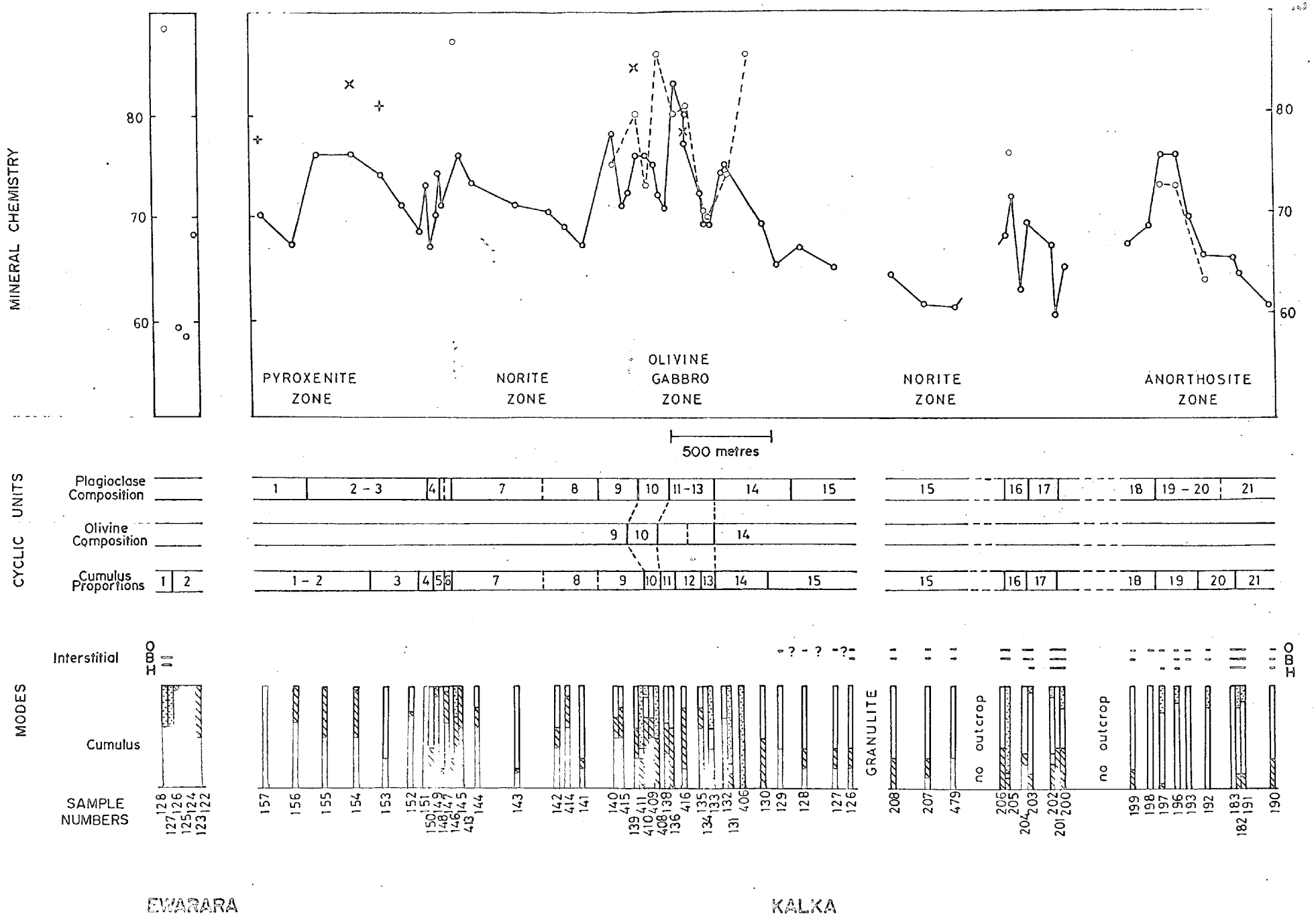
MINERAL CHEMISTRY
80
70
60
PYROXENITE ZONE
NORITE ZONE
OLIVINE GABBRO ZONE
NORITE ZONE
ANORTHOSITE ZONE
500 metres
CYCLIC UNITS
Plagioclase Composition
Olivine Composition
Cumulus Proportions
MODES
Interstitial
Cumulus
SAMPLE NUMBERS
GRANULITE
no outcrop
EWARARA
KALKA

FIGURE 14

A. Schematic representation showing interpreted relationships between Kalka Intrusion and the granulites. Arrow indicates direction of younging in Kalka layered rocks. Intertonguing of granulite from side contacts results in the granulite slivers observed in the intrusion.

B. Variations in contact temperature (T_c) with basalt intrusional temperature (T_1) for range of crystallization of 150°C and latent heat of solidification of 100 cal/gm (curve 1) and 0 cal/gm (curve 2). Both T_1 and T_c are temperatures <u>above</u> country rock temperature. After Jaeger, 1957.

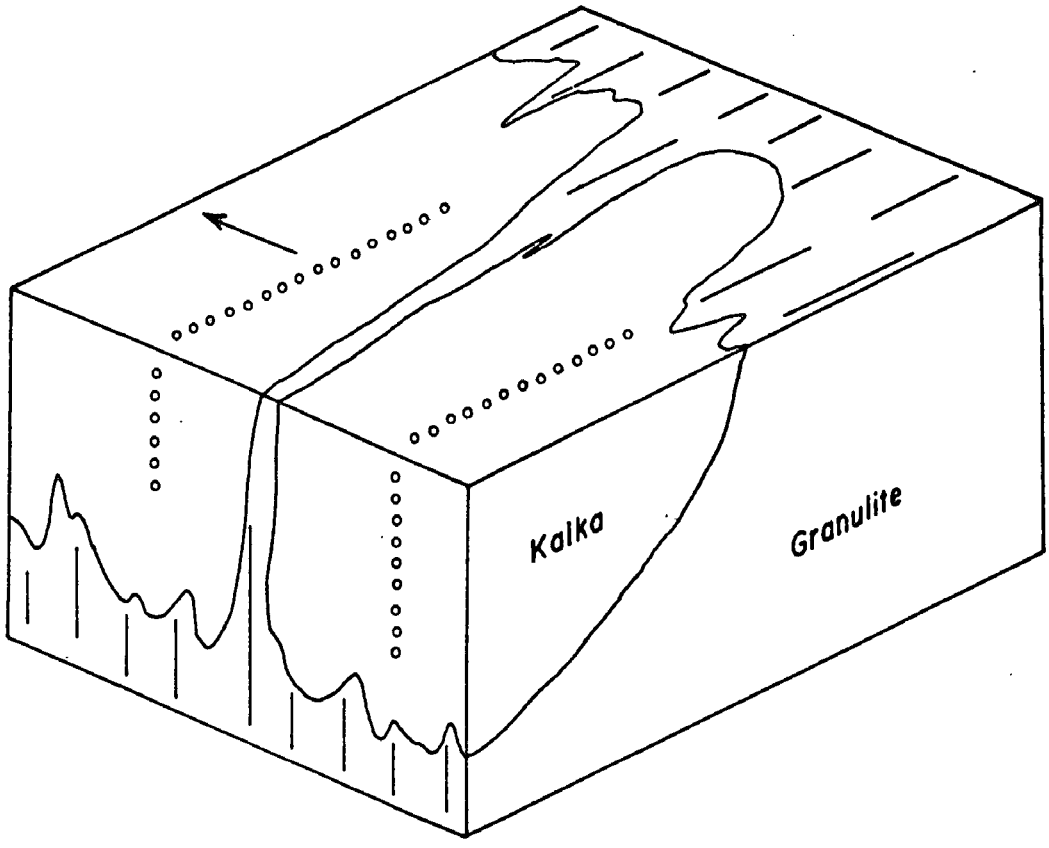

A

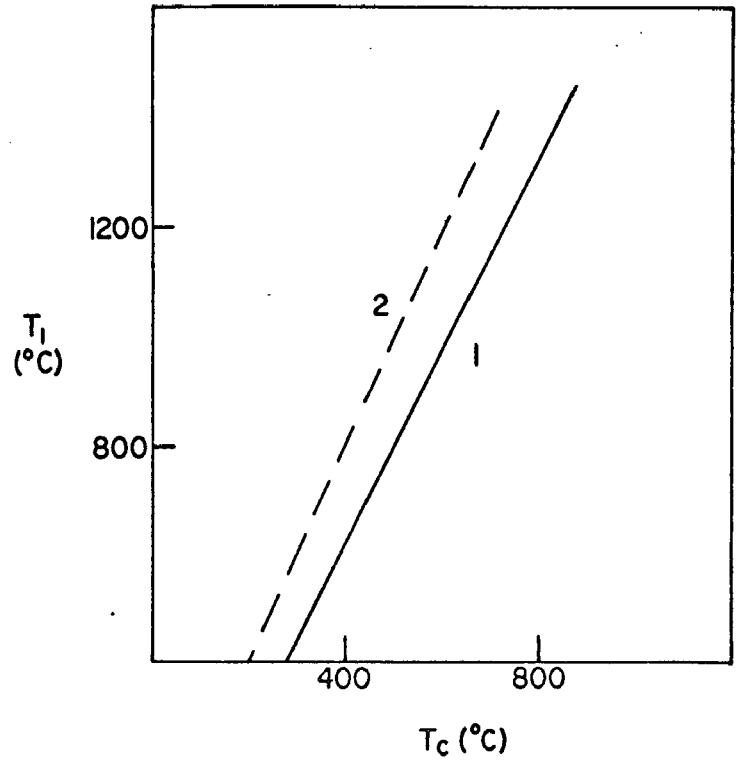

B

FIGURE 15

Distribution of lithological zones in the Kalka Intrusion (granulite shown as lines, silcrete as stipple).

Pyroxenite Zone: green
Norite Zone: blank (Subzones are numbered N1, N2 and N3)
Olivine Gabbro Zone: blue
Anorthosite Zone: circles

Location of stratigraphic sections (Nos. 1-11) are shown as dotted lines.

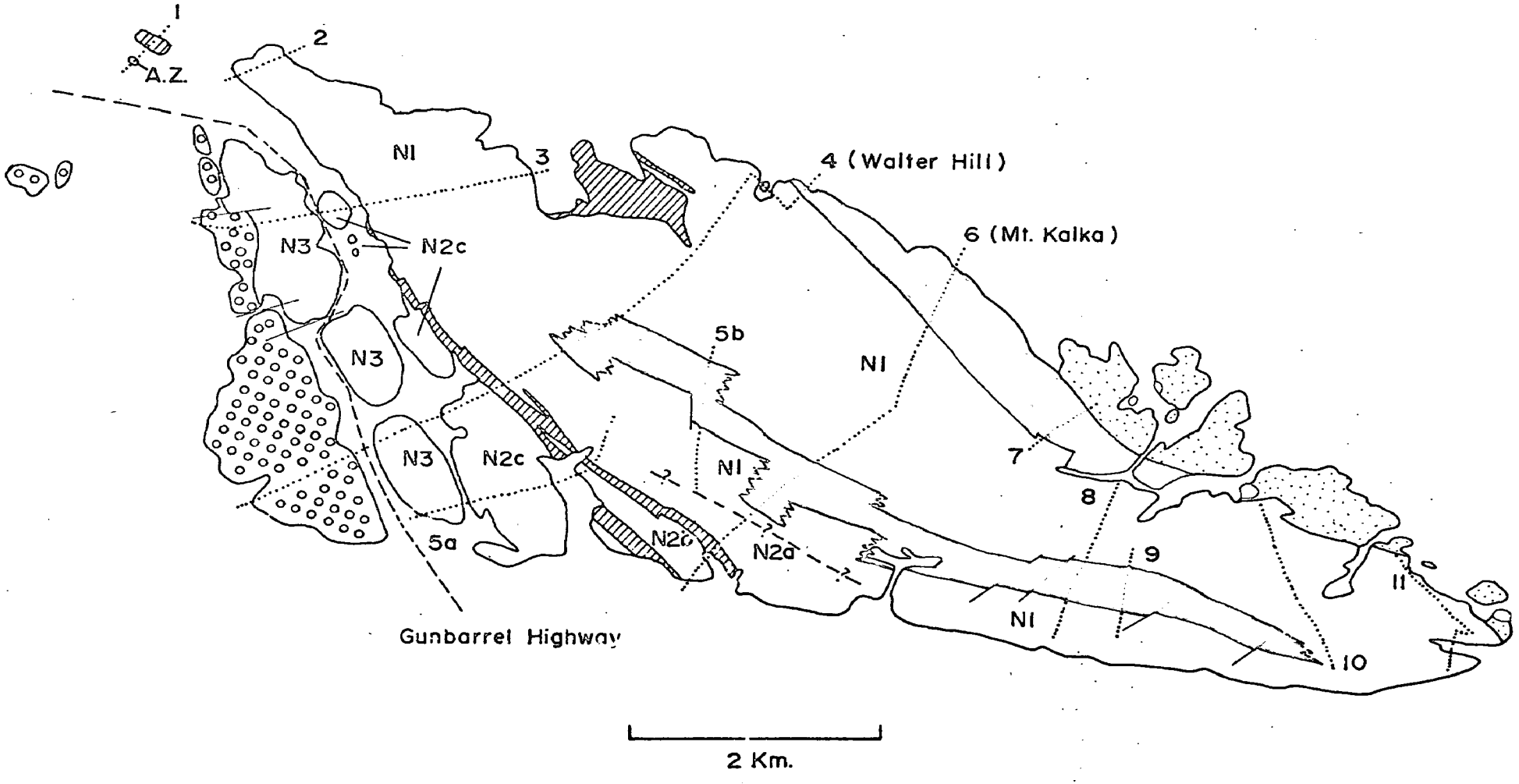
1
A.Z.
2
N1
3
4 (Walter Hill)
6 (Mt. Kalka)
N3
N2c
5b
N1
N3
7
N3
N2c
N1
8
5a
N2b
N2a
9
11
N1
10
Gunbarrel Highway
2 Km.

FIGURE 16

Vertical lithological variations in Stratigraphic Sections 1 to 11 in the Kalka Intrusion (localities of sections given in Fig. 15), with lateral correlation between sections. Position of collected samples given on side of columns. Symbols used: l leucocratic, i mesocratic, m melanocratic, p pyroxenite (op orthopyroxenite, cp clinopyroxenite, w websterite), d dunite, a anorthosite, n norite, g gabbro, t troctolite, om olivine magnetitite; granulite shown as vertical lines, contaminated basic rocks as crosses, olivine-bearing rocks as light stipple (heavy stipple for olivine-rich rocks), pyroxenites in green, Johnson Horizon as solid circles.

(Located in the back pocket of Volume 2).

STRATIGRAPHIC RELATIONSHIPS, KALKA INTRUSION

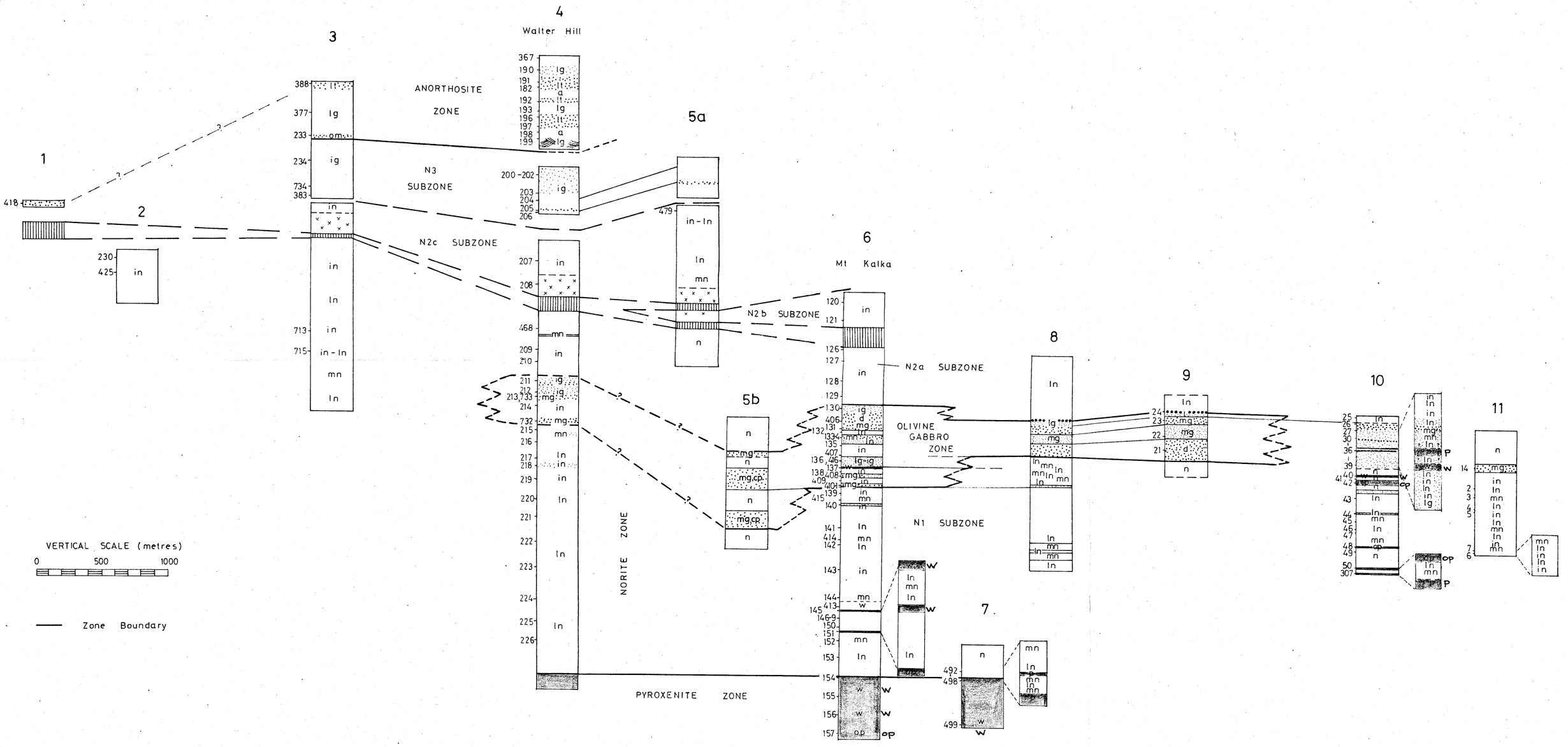

A.D.T. GOODE

FIGURE 17

Younging directions from igneous sedimentary structures in the Kalka Intrusion. Arrows represent mineral grading, arrows on open circles represent cross-stratification or scour channels (open arrows indicate uncertainty in recognising structures as definitely igneous).

Distribution of plagioclase inclusions in orthopyroxene in the Pyroxenite Zone is also shown. Closed circles indicate presence of inclusions (half open circles indicate few inclusions), crosses indicate no inclusions. Inclusions are found in all orthopyroxenes in the overlying lower Norite Zone. (Pyroxenite Zone shown as stippled area).

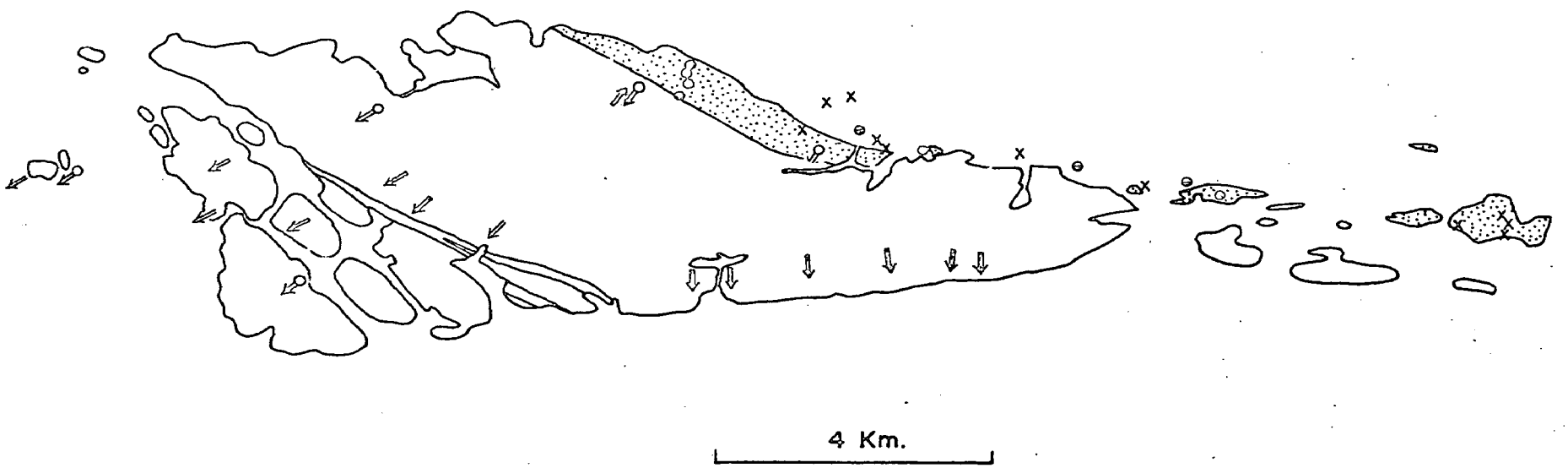
4 Km.

FIGURE 18

A. Pyroxene quadrilateral En - Fs - Di - Hd showing compositions of pyroxenes from Kalka Intrusion (solid circles) and Ewarara Intrusion (open circles, tie line joining co-existing pair). Analyses from Table 9. Compositions of Gosse Pile pyroxenes (enclosed by solid lines, after Moore, 1970a) and South Mt Davies clinopyroxenes (enclosed by dashed line, after Miller, 1966) are also shown. Solid lines (B) and dashed lines (S) represent differentiation trends for Bushveld and Skaergaard pyroxenes respectively (after Atkins, 1969, Brown and Vincent, 1963).

B. Variation in thickness ratio (F/M) with mafic band thickness for adjacent felsic (F) and mafic (M) bands in isomodal layering, Johnson Horizon, Kalka (see Plate 33B). Note two groups of layers - X group (open circles), Y group (closed circles).

C. Variation in thickness ratio (F/M) with vertical distance. Symbols as for B.

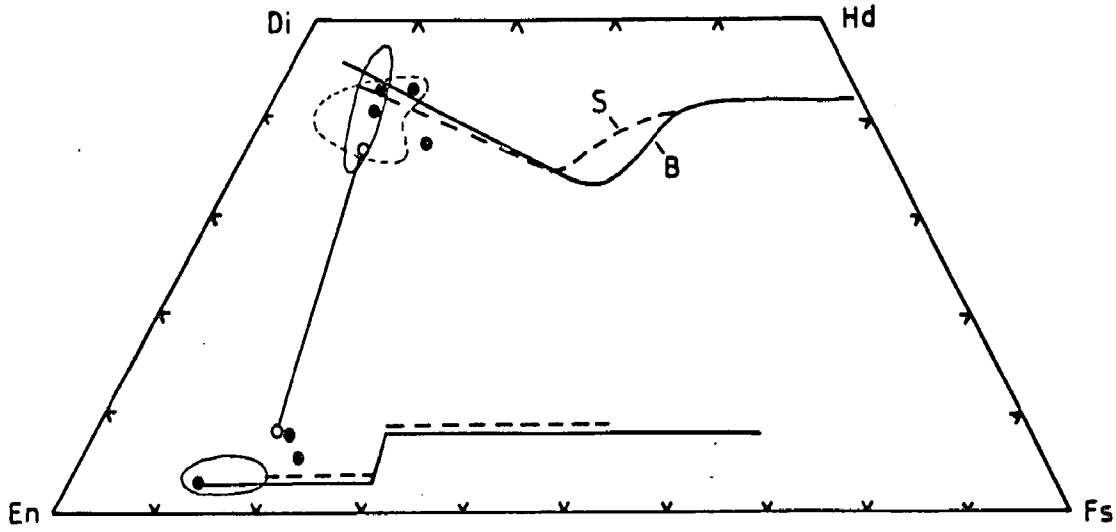

A

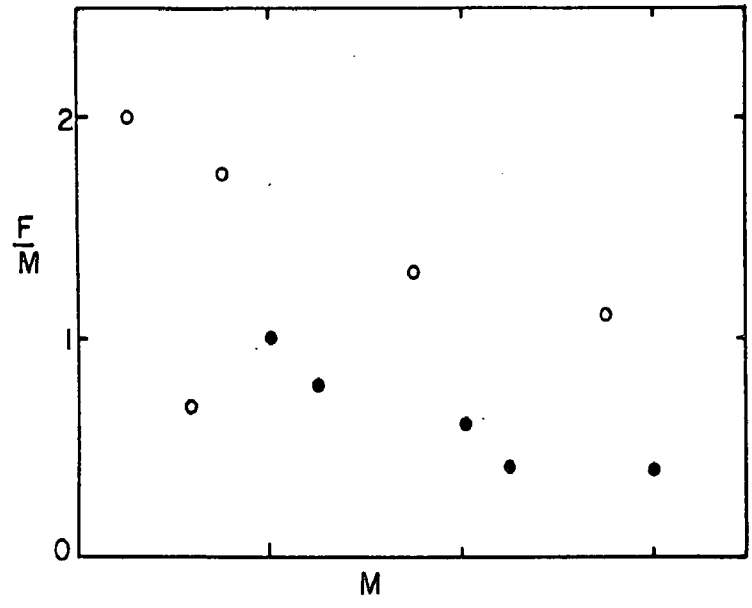

B

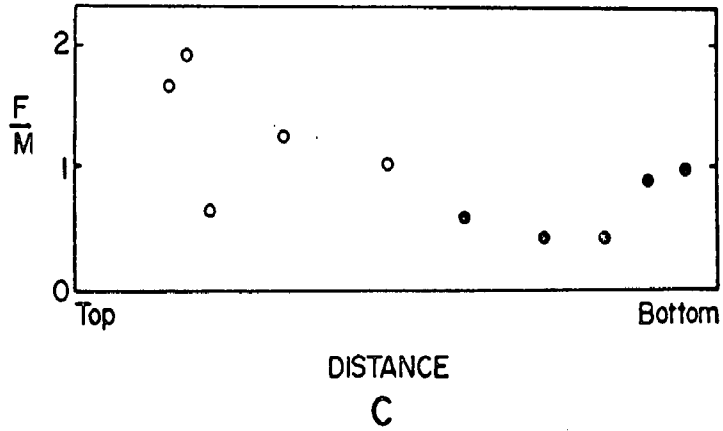

C

FIGURE 19

Chemical affinities of Kalka and Ewarara igneous clinopyroxenes (solid circles). Analyses from Table 9.

A. Al^{VI} v Al^{IV} (after Aoki and Kushiro, 1968) showing similarities to pyroxenes in granulites and inclusions but not to normal igneous pyroxenes. Gosse Pile pyroxenes shown as dashed enclosures (after Moore, 1970a), South Mt Davies pyroxenes shown as solid enclosure (after Miller, 1966).

B. Al^{IV} v Si (after Challis, 1965).

C. SiO_2 v Al_2O_3 (after Le Bas, 1962).

D. $\%Al_Z$ v TiO_2 (after Le Bas, 1962).

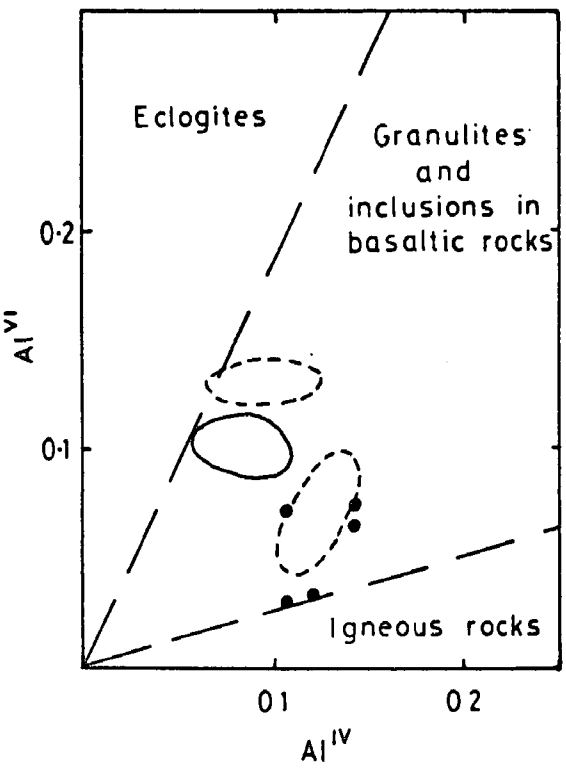
Eclogites
Granulites and inclusions in basaltic rocks
Igneous rocks
0·2
0·1
0 1
0 2
Al^{VI}
Al^{IV}

A

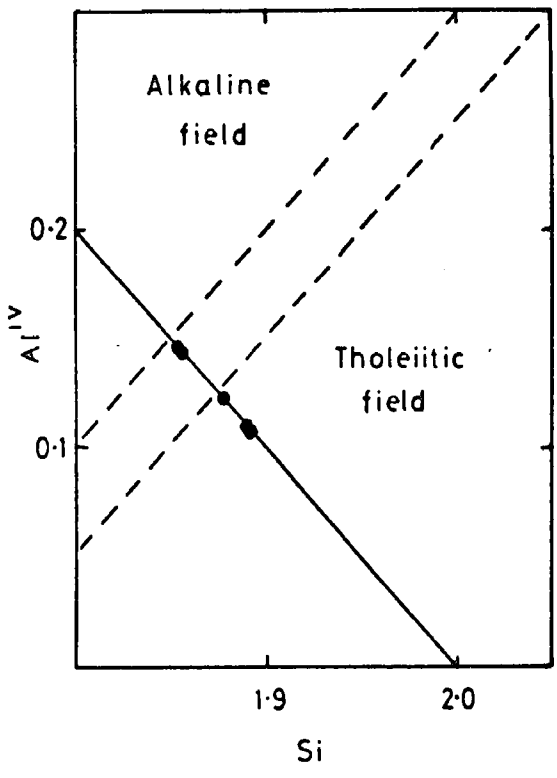
Alkaline field
Tholeiitic field
0·2
0·1
1·9
2·0
Al^{IV}
Si

B

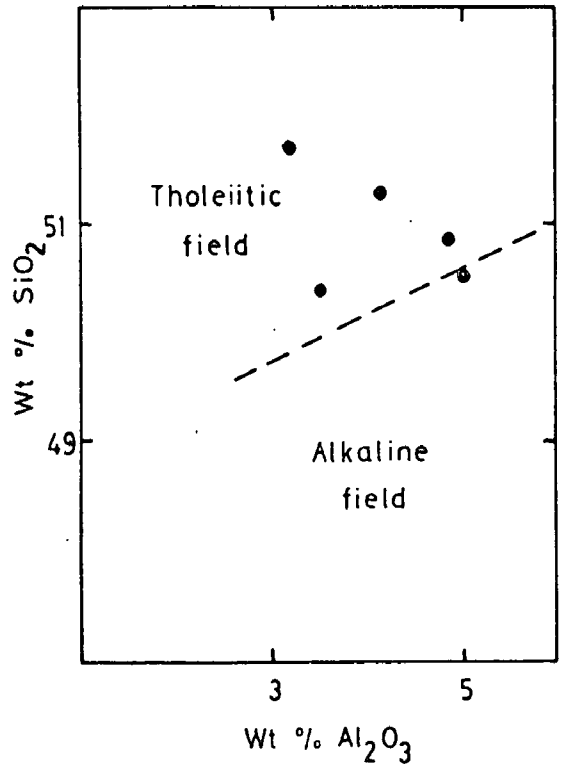
Tholeiitic field
Alkaline field
51
49
3
5
Wt % SiO_2
Wt % Al_2O_3

C

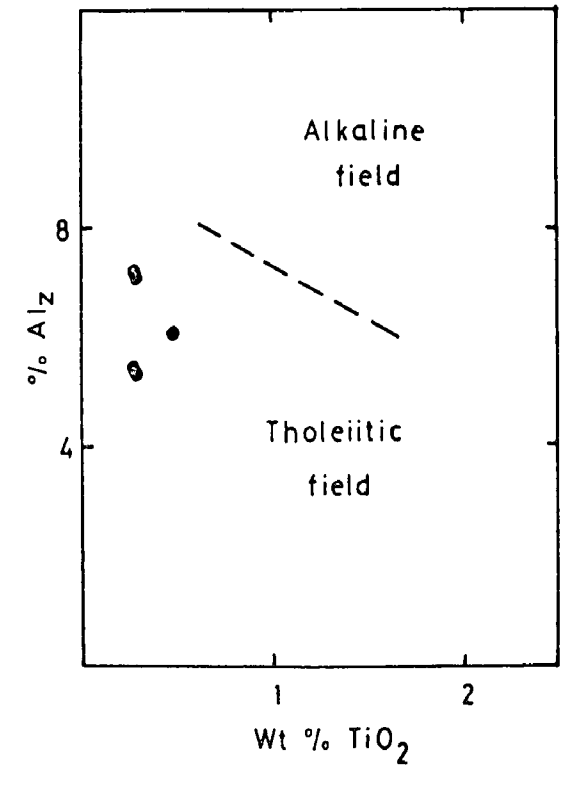
Alkaline field
Tholeiitic field
8
4
1
2
% Al_Z
Wt % TiO_2

D

FIGURE 20

Hourglass structures in orthopyroxene, Ewarara. Stippled areas represent areas of intense spinel exsolution (e.g. Sector A).

A, B, D, I	A300-201
C	A251-N246d
E,F	A300-132
G	A300-384
H, K, L	A300-113
J	A251-N248

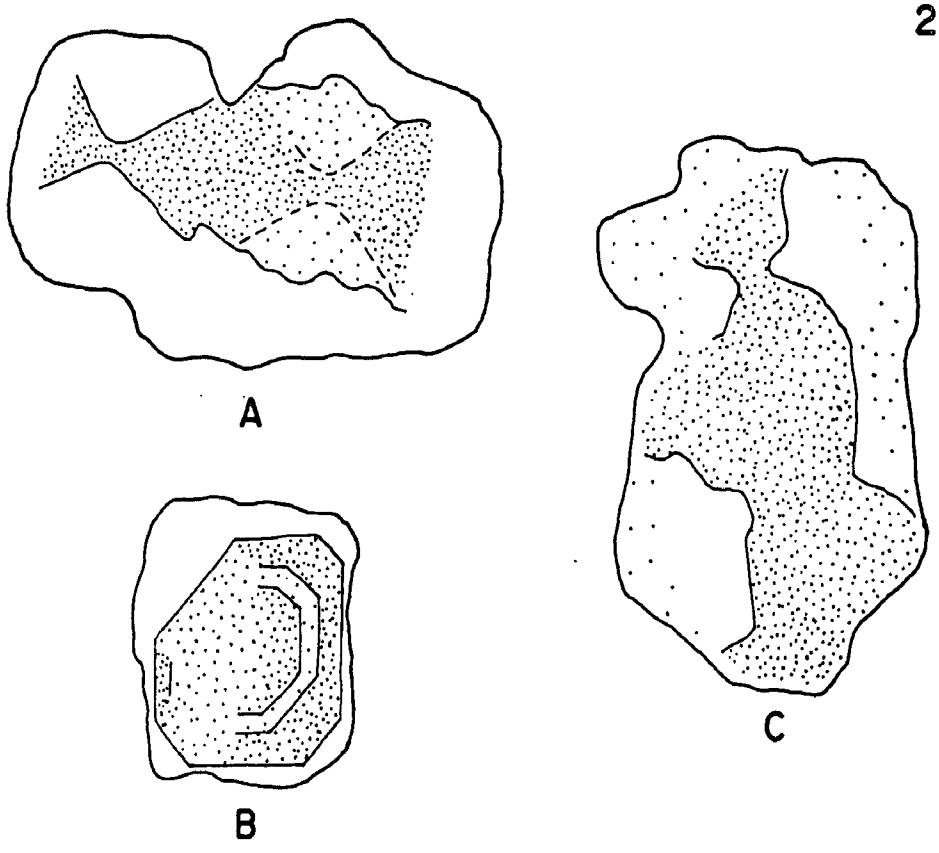

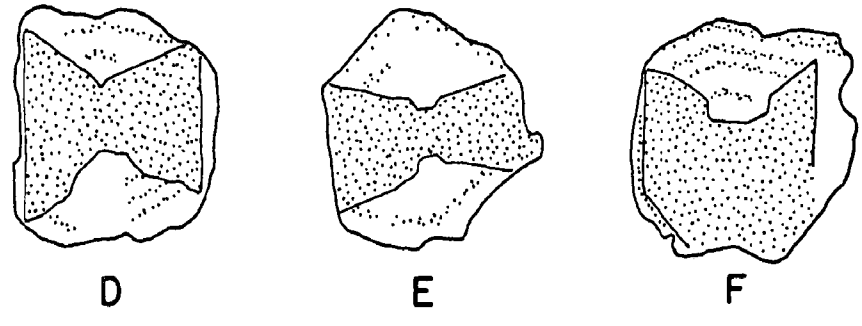

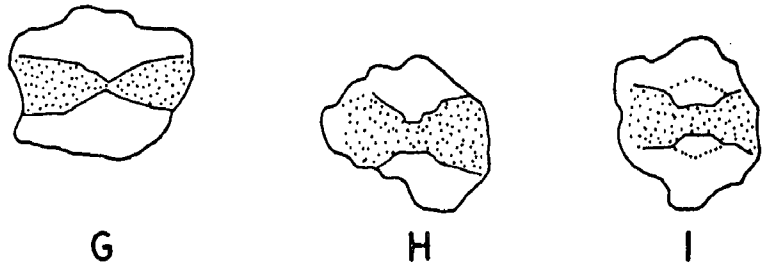

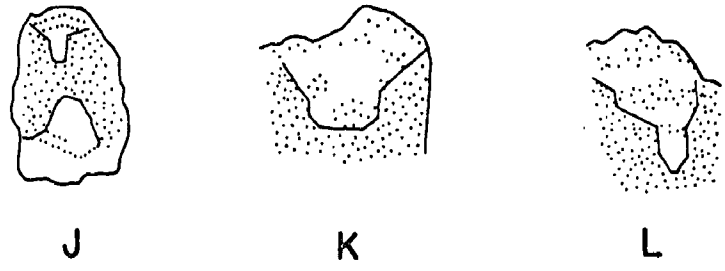

2·5 m.m.

FIGURE 21

A. Diagrammatic representation of sector A of hourglass orthopyroxenes showing hopper shape (left). Plan view of "hopper" showing distribution of (011), (101) and (111) type faces (right).

B. Variations in slope of boundary between sectors A and B, hourglass zoning in orthopyroxene.

C. Progressive growth stages of orthopyroxene showing preferential adsorption of aluminium (arrows) and consequent variations in aluminium concentration in grown crystal (stippled for high concentration).

D. Growth stages in hourglass orthopyroxene. Variations in rate of growth of prismatic faces relative to pyramidal faces result in slope changes in sector boundaries.

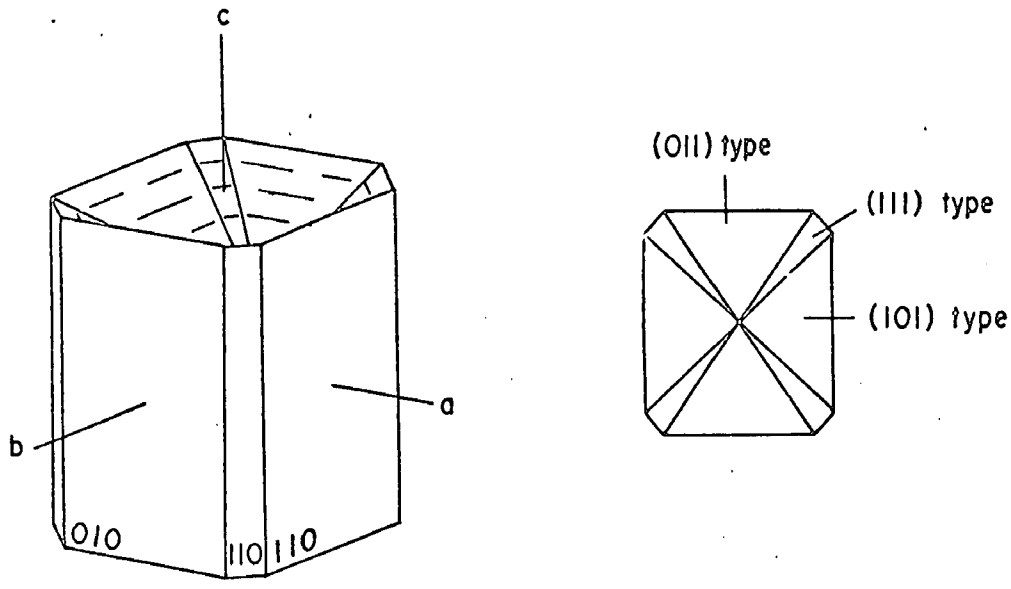

A

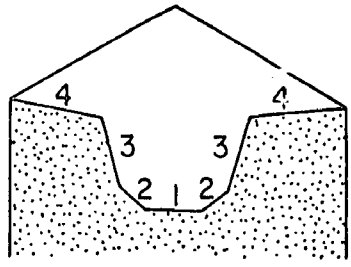

B

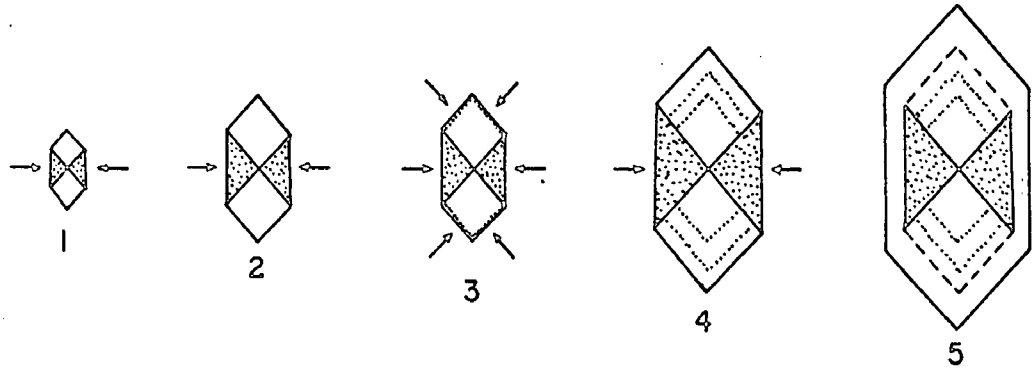

C

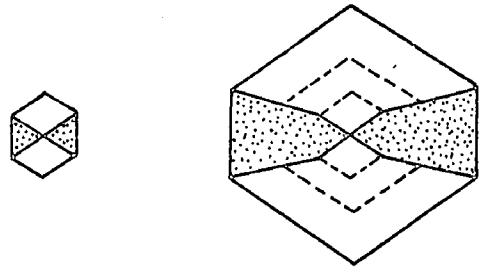

D

FIGURE 22

A. Plagioclase inclusions in orthopyroxene (stippled areas represent clinopyroxene). A314-150.

B. Orthopyroxene crystal showing distribution of inclusions of plagioclase, clinopyroxene and biotite (blank) and exsolution of opaques (stippled). A300-712.

C. Plagioclase inclusions in orthopyroxene crystal (stippled areas represent clinopyroxene). A314-154.

D. Plagioclase (blank) - clinopyroxene (stippled) composite inclusions in core of orthopyroxene crystal. A314-135.

E,F As for D. A314-412c.

G. Composite plagioclase (blank) - clinopyroxene (stippled) inclusion in orthopyroxene. A314-155. Plagioclase of two types: (1) - lath-like with simple twinning.
(2) - irregular, antiperthitic.

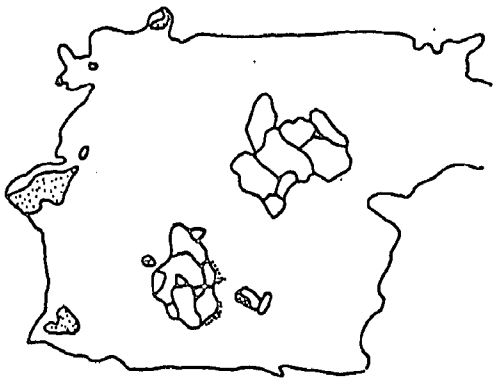

1 m.m.

A

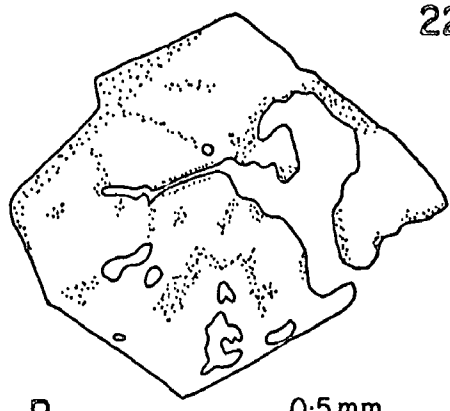

B

0·5 m.m.

1 m.m.

C

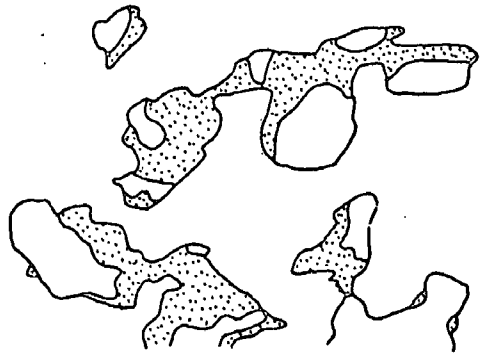

D

0·5 m.m.

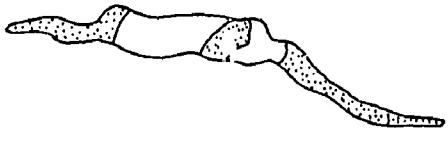

0·5 m.m.

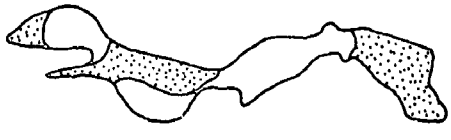

0·5 m.m.

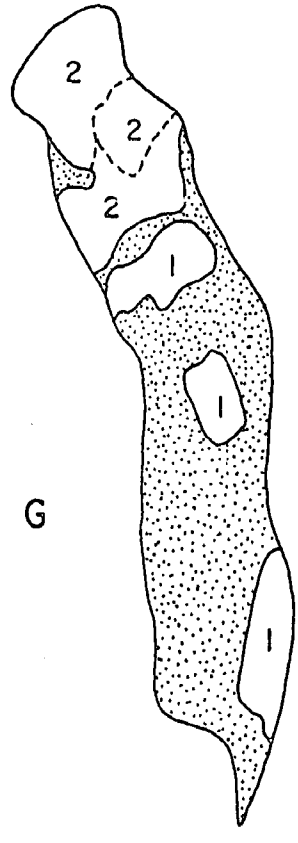

G

0·5 m.m.

FIGURE 23

A. Texture, A307-6. Olivine (stippled boundaries), clinopyroxene (cross-hatched), plagioclase (blank), massive orthopyroxene (dashed lines), fibrous orthopyroxene (black), fibrous amphibole (solid lines). Hinckley Intrusion.

B. Enlargement of part of A, showing development of fibrous rims in detail.

C. Platy granular orthopyroxene rim surrounding olivine (stippled). Note gradation from orthopyroxene to orthopyroxene - spinel symplectite (finer grained towards plagioclase), and association of orthopyroxene boundaries with cusps on olivine. A314-357.

D. Fibrous orthopyroxene (black) and fibrous amphibole (solid lines) rims between olivine (stippled) and plagioclase lath inclusion (blank). Note development of platy granular orthopyroxene rims on external boundaries of olivine with plagioclase (also note association of boundaries with olivine cusps and gradation to fibrous orthopyroxene). A314-418.

E. Massive orthopyroxene in epitaxial relationship with clino-pyroxene partially rimming olivine. Note fibrous amphibole rim at olivine - plagioclase boundary. Symbols as for A. A251-N105. South Mt Davies Intrusion.

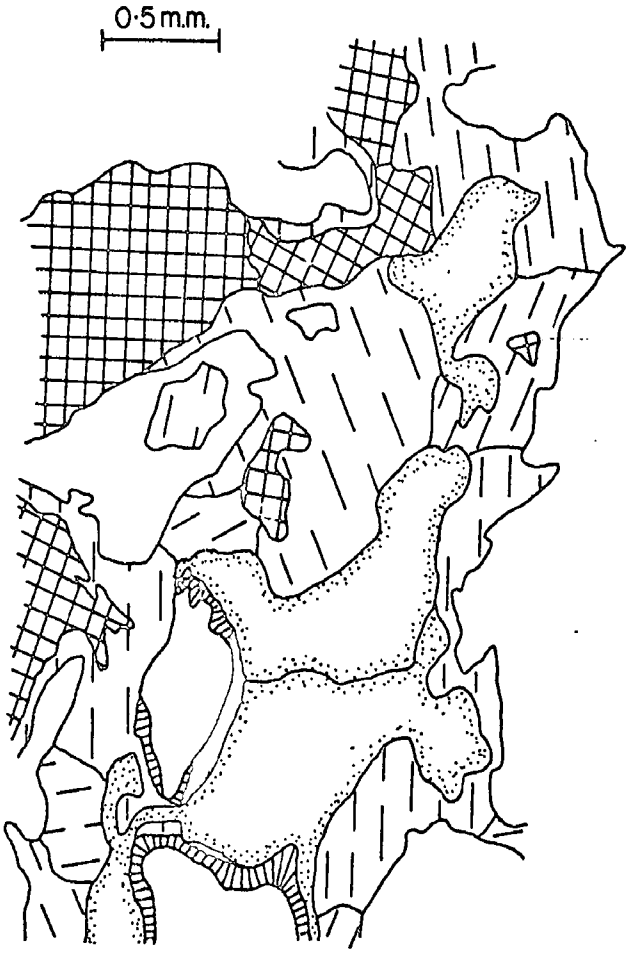
0·5m.m.

A

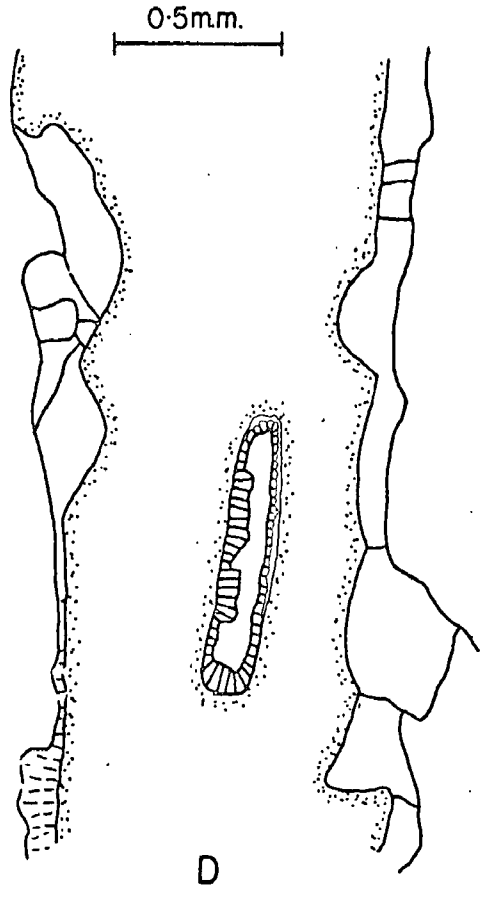
0·5m.m.

D

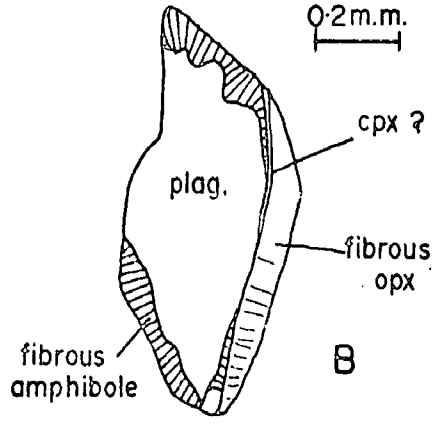
0·2m.m.
cpx ?
plag.
fibrous opx
fibrous amphibole

B

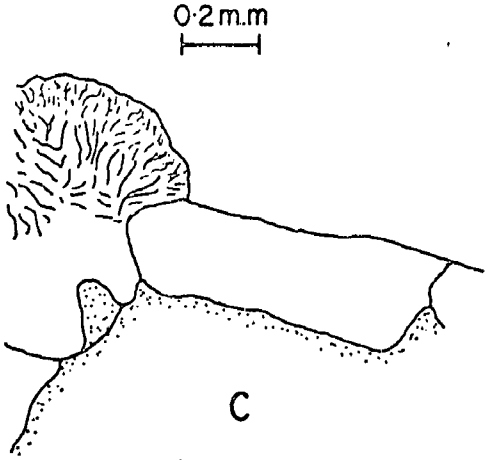
0·2m.m

C

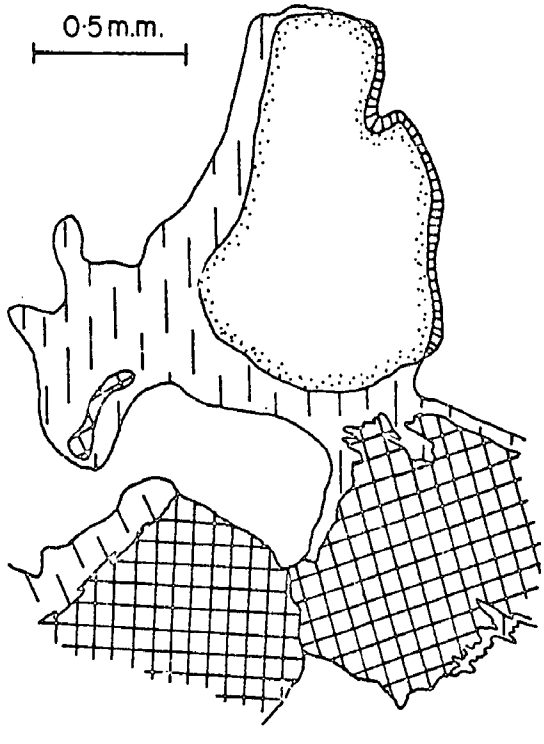
0·5m.m.

E

FIGURE 24

A. Bulk grain compositions for olivine - plagioclase pairs. Solid circles indicate presence of pyroxene/spinel symplectite near olivine - plagioclase boundaries, open circles indicate little or no symplectite.

B. Relationship between plagioclase composition and presence of antiperthite for Kalka plagioclases. Solid circles represent normal plagioclases, open circles - antiperthitic plagioclases. Dashed lines represent Teizi (T) plagioclases (Gray, 1967) and South Mt Davies (SMD) plagioclases (Kleeman, 1965). Solid line A represents approximate limit of normal plagioclase field (from compilation of data by A.W. Kleeman, pers. comm.). Approximate Or% obtained from K_2O contents (Table 10) by comparison with Deer et al., 1963, Vol.4. An% taken from XRD determinations.

C. Histogram showing variation in type of clouding particle with composition of plagioclase. Stippled fields represent spinel clouding (4 samples), blank fields represent magnetite clouding (35 samples, averaged every An_2).

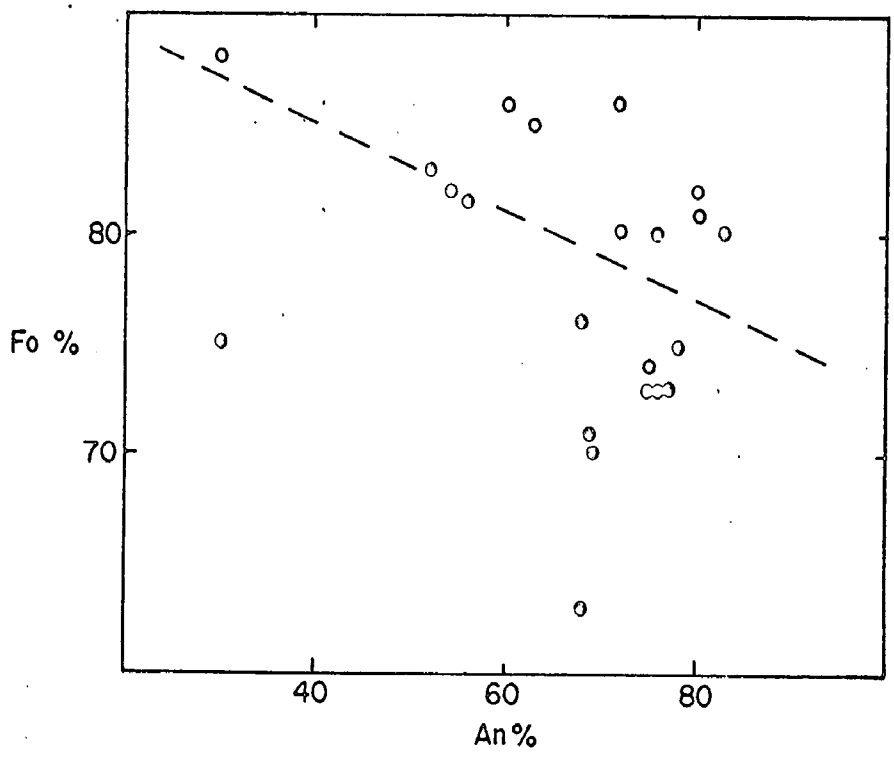
Fo %
80
70
40
60
80
An %

A

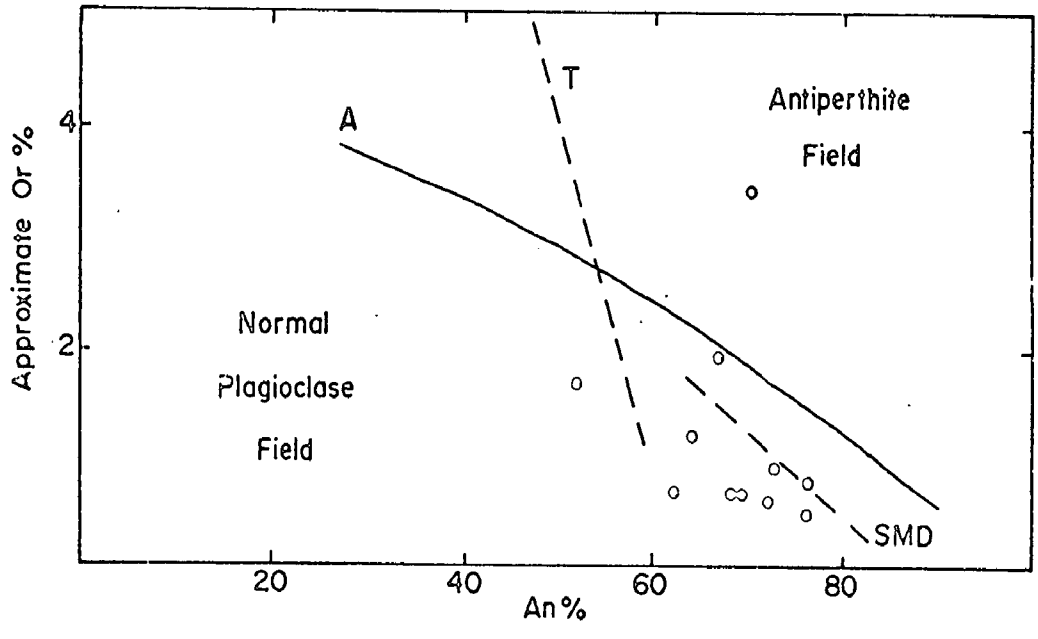
Approximate Or %
4
2
T
A
Antiperthite
Field
Normal
Plagioclase
Field
SMD
20
40
60
80
An %

B

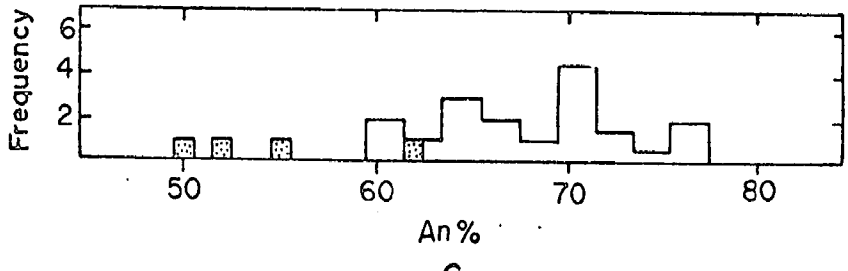
Frequency
6
4
2
50
60
70
80
An %

C

FIGURE 25

A. Crystallization model, showing development of crystallization or nucleation zone (stippled) of thickness d at distance L above top of crystal pile. L_c represents critical distance below nucleation zone at which complete separation of pyroxene/olivine and plagioclase occurs.

B. Hypothetical development of scour channel.

1. Production of rhythmic layered sequence of mesonorites (cumulus pyroxene + plagioclase, stippled) and anorthosites (cumulus plagioclase, blank).

2. Development of fresh cycle of crystallization with development of new mesonorite layer with some plagioclase still in suspension.

3. Erosion of part of layered sequence by strong, localised bottom current.

4. Continued settling of plagioclase in static conditions to give anorthosite layer.

5. Infilling of channel by mesonorite during next cycle of crystallization.

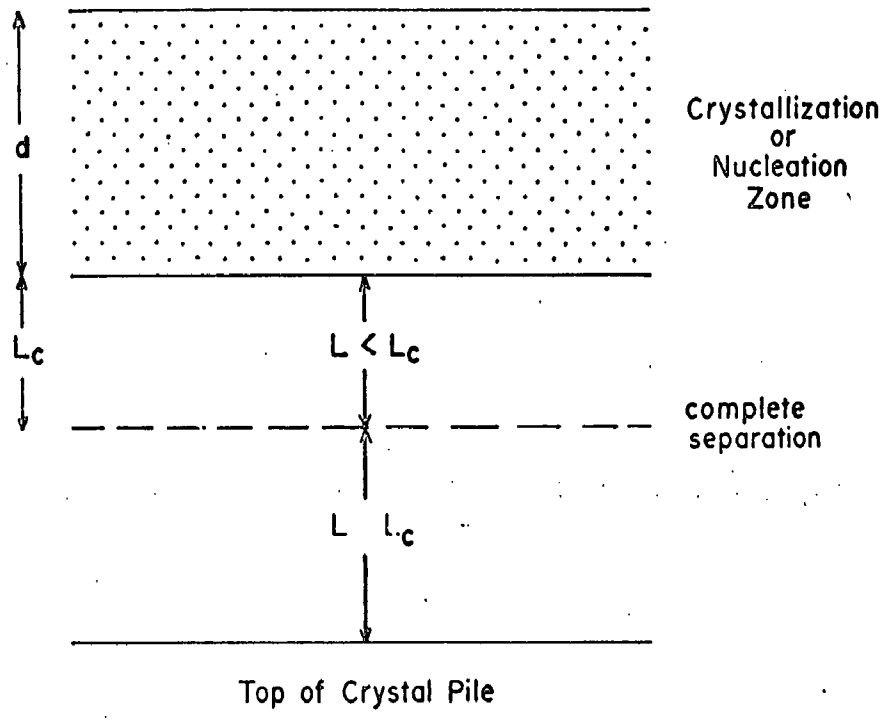
d
Lc
Crystallization
or
Nucleation
Zone
L < Lc
complete
separation
L Lc
Top of Crystal Pile

A

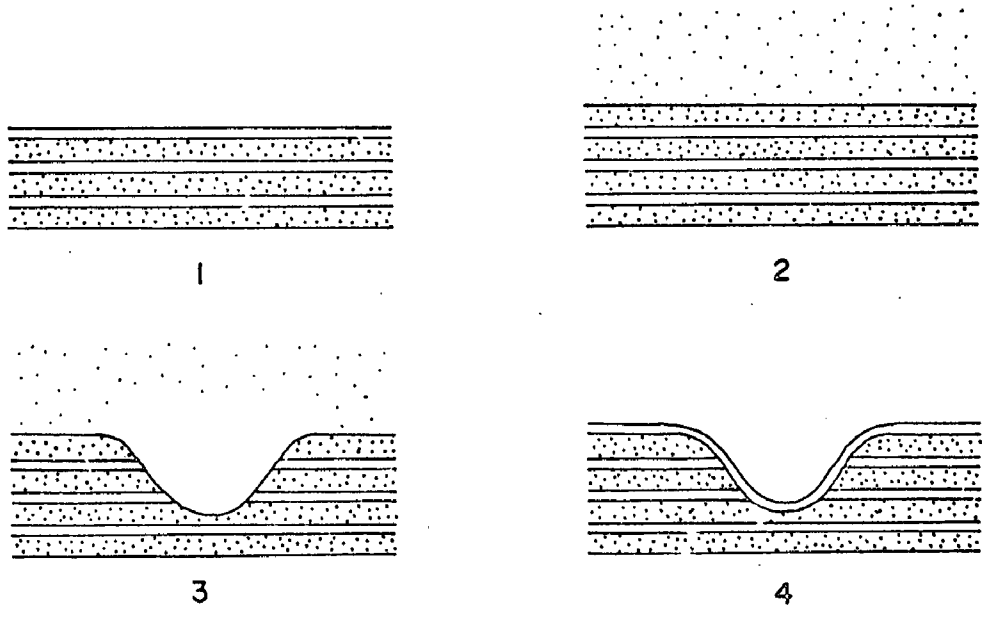
1
2
3
4

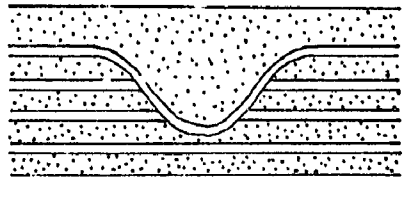
5

B

FIGURE 26

Theoretical layer groups, small scale igneous layering. Discontinuous nucleation model with varying degrees of differential settling between pyroxene/olivine (Px) and plagioclase (Pl). Subscripts indicate co-crystallizing pyroxene/olivine and plagioclase groups. Solid lines indicate ratio contacts, dots indicate pyroxene concentrations.

A. Isomodal

B. Isomodal, with overlap

C. Reverse grading

D. Normal grading

E. Continuous grading, with overlap

F. Continuous grading, without overlap.

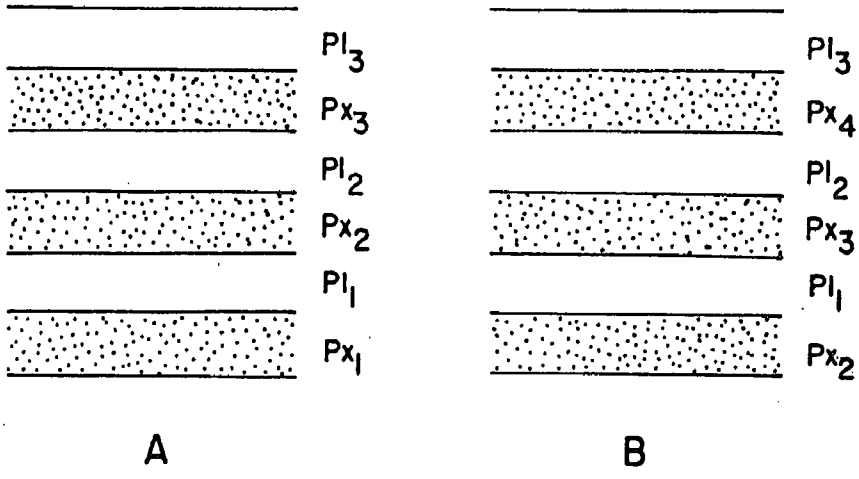
Pl3
Px3
Pl2
Px2
Pl1
Px1
A
Pl3
Px4
Pl2
Px3
Pl1
Px2
B
Px4
Pl3
Px3
Pl2
Px2
Pl1
C
Pl3
Px3
Pl2
Px2
Pl1
Px1
D
Px5
Pl3
Px4
Pl2
Px3
Pl1
Px2
E
Px4
Pl3
Px3
Pl2
Px2
Pl1
Px1
F

FIGURE 27

Types of cyclic units, showing idealised behaviour with progressive crystallization (vertical axis represents fractionation - down for increasing degree of fractionation).

A. Convectional overturn model. Note progressive increase in overall degree of fractionation - represented by negative envelope slope S_1.

B. Fresh injection model (developing source). Note decreasing degree of fractionation i.e. positive envelope slope S_2.

C. Fresh injection model (stable source). Note constant degree of fractionation i.e. envelope slope S_3 is zero.

D. As for C, but with dilution of fresh magma by the more fractionated host melt. Note slight negative envelope slope, S_4. Dilution has same effect for A and B.

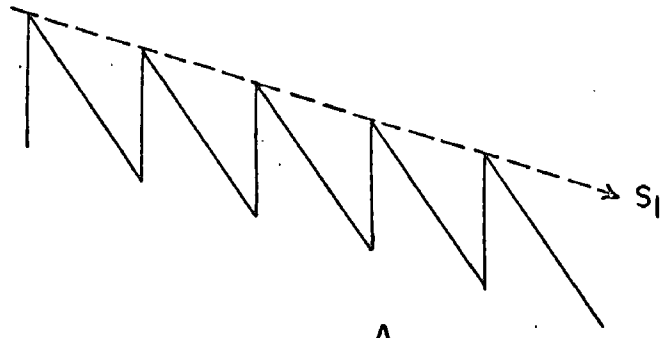

A

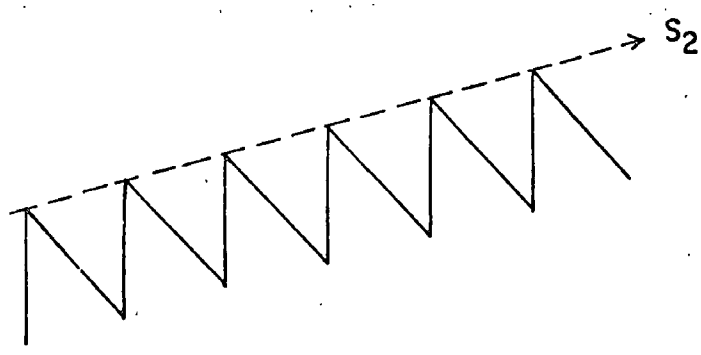

B

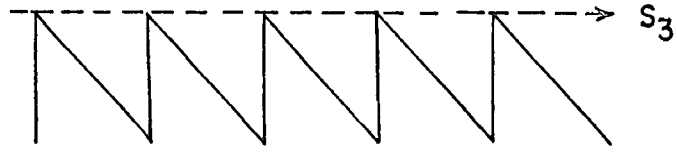

C

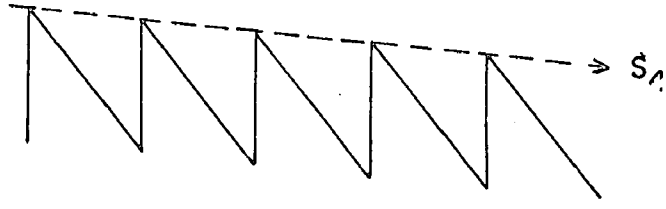

D

CRYSTALLIZATION ⟶

FIGURE 28

A. Regimes of flow in a broad, open channel (after Allen, 1965).

B. Variations in bed forms with Froude Number (and flow regimes). Bed forms are: 1 - plane bed with no sediment movement; 2 - small ripples; 3 - large ripples; 4 - transition; 5 - plane bed with movement; 6 - antidunes (after Allen, 1965).

C. Relation between flow velocity, grain size, and state of sediment. 1 - critical erosion velocity; 2 - cessation of movement; 3 - settling velocity (after Allen, 1965).

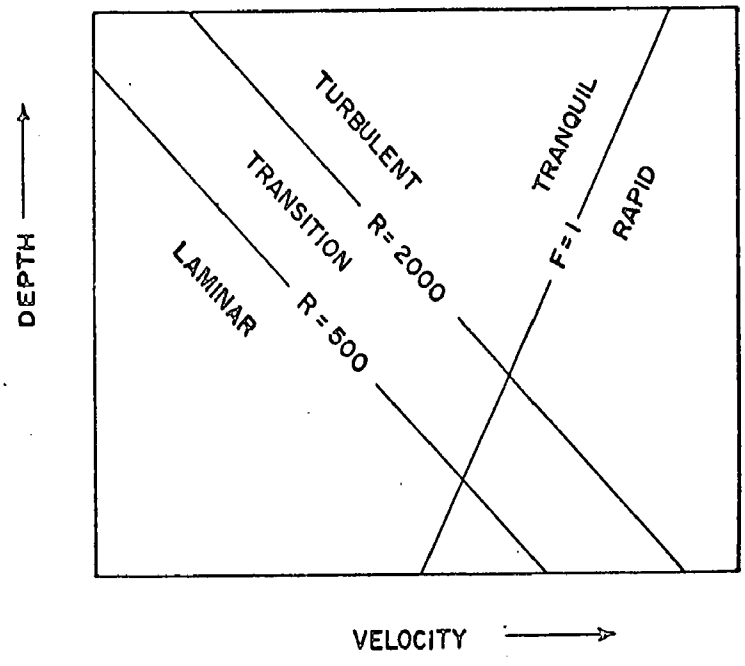
DEPTH
TURBULENT
TRANSITION
LAMINAR
R = 2000
R = 500
TRANQUIL
F = 1
RAPID
VELOCITY

A

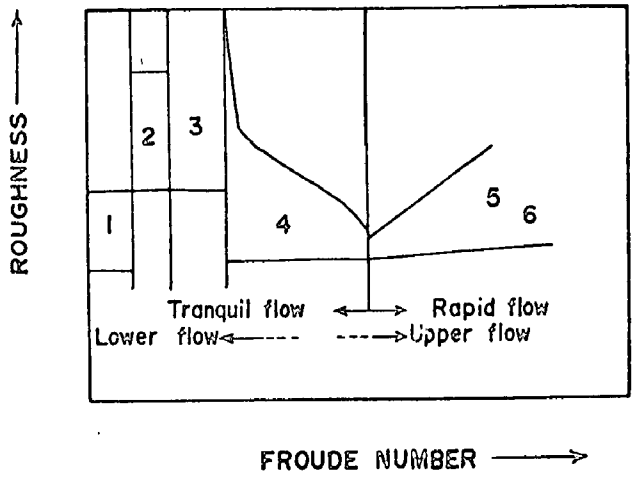
ROUGHNESS
1
2
3
4
5
6
Tranquil flow
Rapid flow
Lower flow
Upper flow
FROUDE NUMBER

B

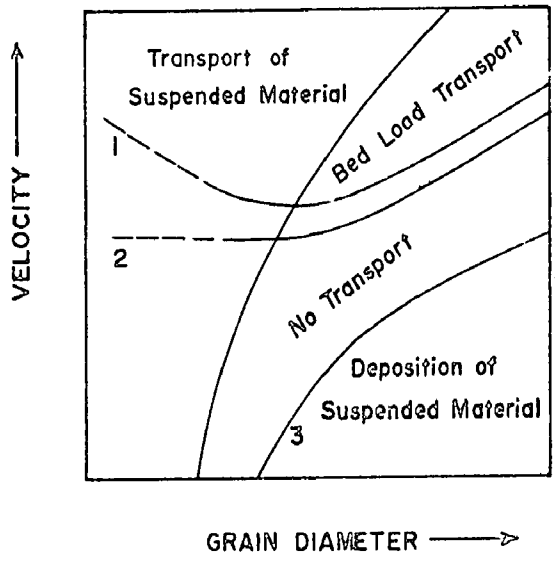
VELOCITY
Transport of
Suspended Material
Bed Load Transport
1
2
No Transport
Deposition of
Suspended Material
3
GRAIN DIAMETER

C

FIGURE 29

Experimentally determined stability fields for various mineral assemblages and rock compositions. Vertical axis for pressure (in kilobars), horizontal axis for temperature (in ^{o}C).

A. Spinel + pyroxene (bottom right) $\rightleftharpoons$ garnet + olivine (top left).

1. Macgregor, 1964 (4 enstatite + spinel composition).
2. Macgregor, 1965 (Al enstatite + Al diopside + spinel + forsterite).
3. Ito and Kennedy, 1967, p. 519 - maximum slope (garnet peridotite).
4. Green and Ringwood, 1967c (pyrolite).
5. Green and Ringwood, 1967a (olivine tholeiite).

B. Orthopyroxene + plagioclase (bottom right) $\rightleftharpoons$ garnet + quartz (top left).

1. Kushiro and Yoder, 1966 (enstatite + anorthite).
2. Green and Ringwood, 1967a (olivine tholeiite).
3. Green and Ringwood, 1967a (alkali olivine basalt).
4. Green and Lambert, 1965 (anhydrous adamellite).
5. Green and Ringwood, 1967b (quartz tholeiite).
6. T.H. Green, 1970 (diorite).
7. T.H. Green, 1970 (gabbroic anorthosite).
   Note: for high alumina basalt composition, curve is similar to 7 (T.H. Green, 1967, 1969a). For 2 anorthite + 2 enstatite + diopside composition, reaction occurs between 13.5 and 18 kilobars at 1200^{o}C (T.H. Green, 1969b).

C. Olivine + plagioclase (bottom right) $\rightleftharpoons$ orthopyroxene + clinopyroxene + spinel (top left).

1. Kushiro and Yoder, 1966 (anorthite + forsterite).
2. Kushiro and Yoder, 1966 (anorthite + 2 forsterite).
3. Green and Ringwood, 1967a (olivine tholeiite, alkali olivine basalt -using reaction slope from 1,2).
4. Green and Hibberson, 1970 (anorthite + forsterite).

D. Reaction paths on cooling at various constant pressures for olivine + plagioclase assemblages. No reaction below T_{dc}, the diffusional cut-off temperature.

Curve 1: opx + spin $\rightleftharpoons$ garnet (see Fig. 29A).
Curve 2: ol + plag $\rightleftharpoons$ opx + cpx + spin (see Fig. 29C).
Reaction A: ol + plag $\longrightarrow$ opx + cpx + spin $\longrightarrow$ cpx + garnet.
Reaction B: ol + plag $\longrightarrow$ opx + cpx + spin.
Reaction C: ol + plag stable.

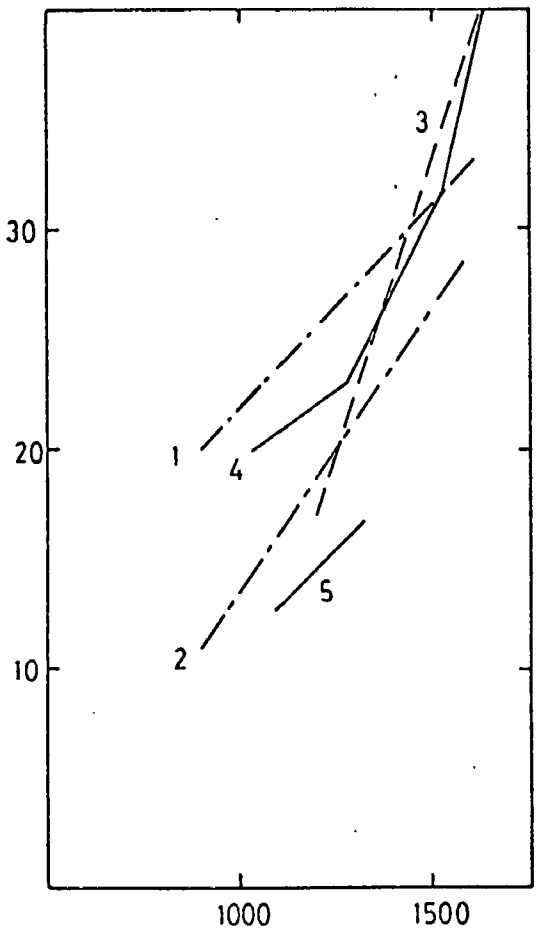
30
20
10
1000
1500
1
2
3
4
5

A

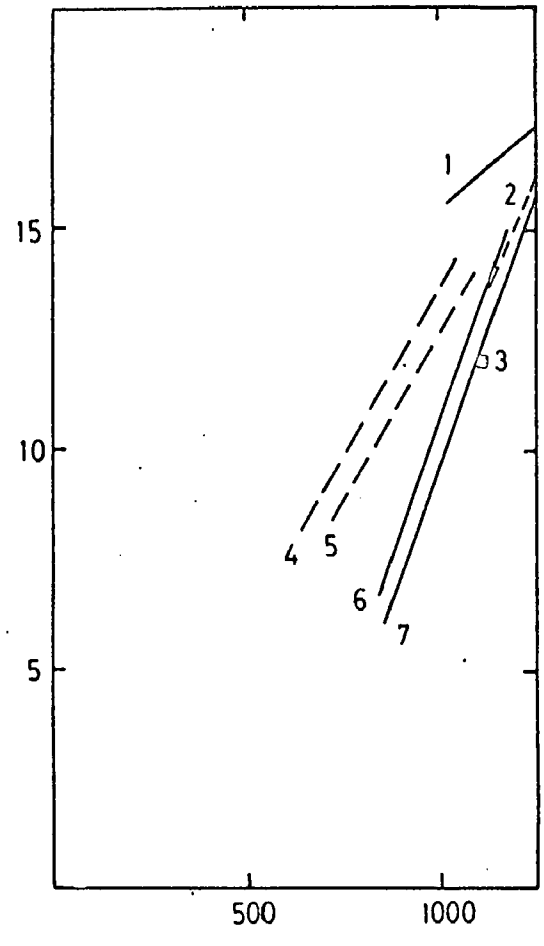
15
10
5
500
1000
1
2
3
4
5
6
7

B

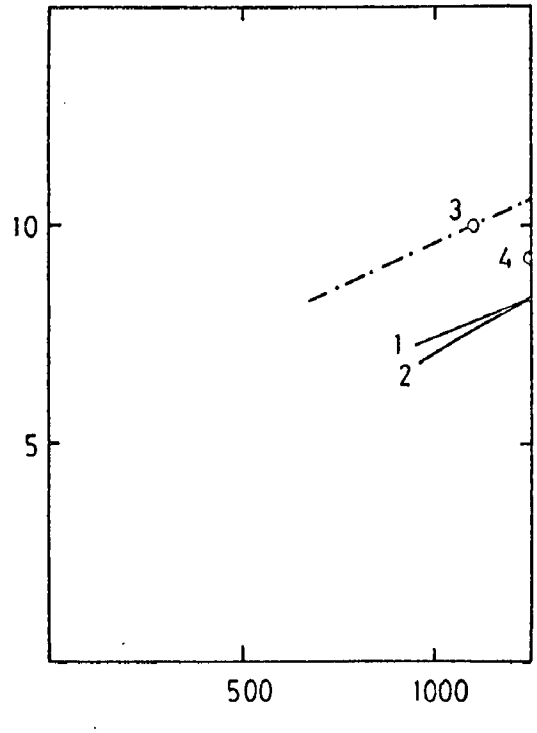
10
5
500
1000
1
2
3
4

C

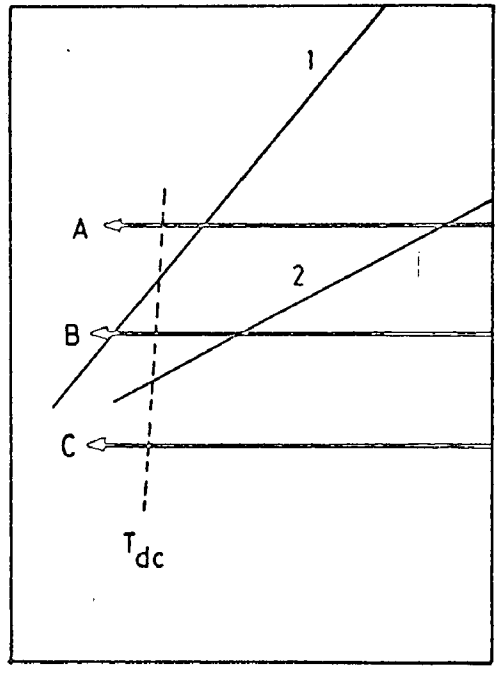
1
2
A
B
C
T_{dc}

D

FIGURE 30

Liquidus phases for various basaltic melts as determined in experimental studies for different pressure-temperature conditions (liquidus shown as dashed line, orthopyroxene as +, olivine as x, clinopyroxene as o and plagioclase as 0).

A. Olivine tholeiite (Green and Ringwood, 1967a).

B. Olivine basalt (Green and Ringwood, 1967a).

C. Alkali olivine basalt (Green and Ringwood, 1967a).

D. High alumina olivine tholeiite (Cohen et al., 1967).

E. High alumina basalt (T.H. Green, 1969a).

F. Picrite (Green and Ringwood, 1967a).

G. Olivine nephelinite (Bultitude and Green, 1967).

H. Picritic nephelinite (Bultitude and Green, 1967).

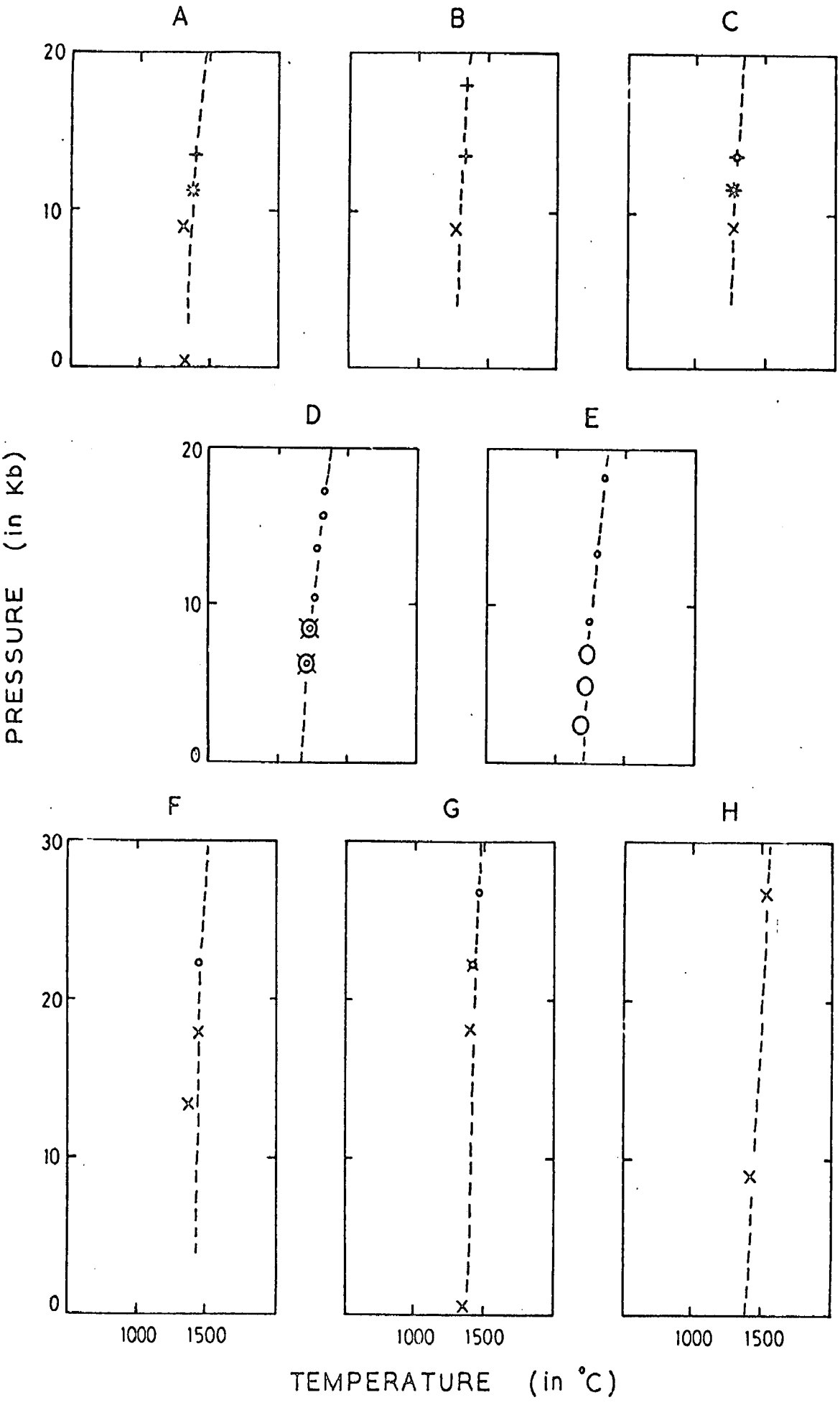
A
B
C
D
E
F
G
H
20
10
0
30
PRESSURE (in Kb)
1000
1500
TEMPERATURE (in °C)

FIGURE 31

"Correlation" of rock sequences in other Giles Complex intrusions (data from Nesbitt *et al.*, 1970) with the four major zones in the Kalka Intrusion.

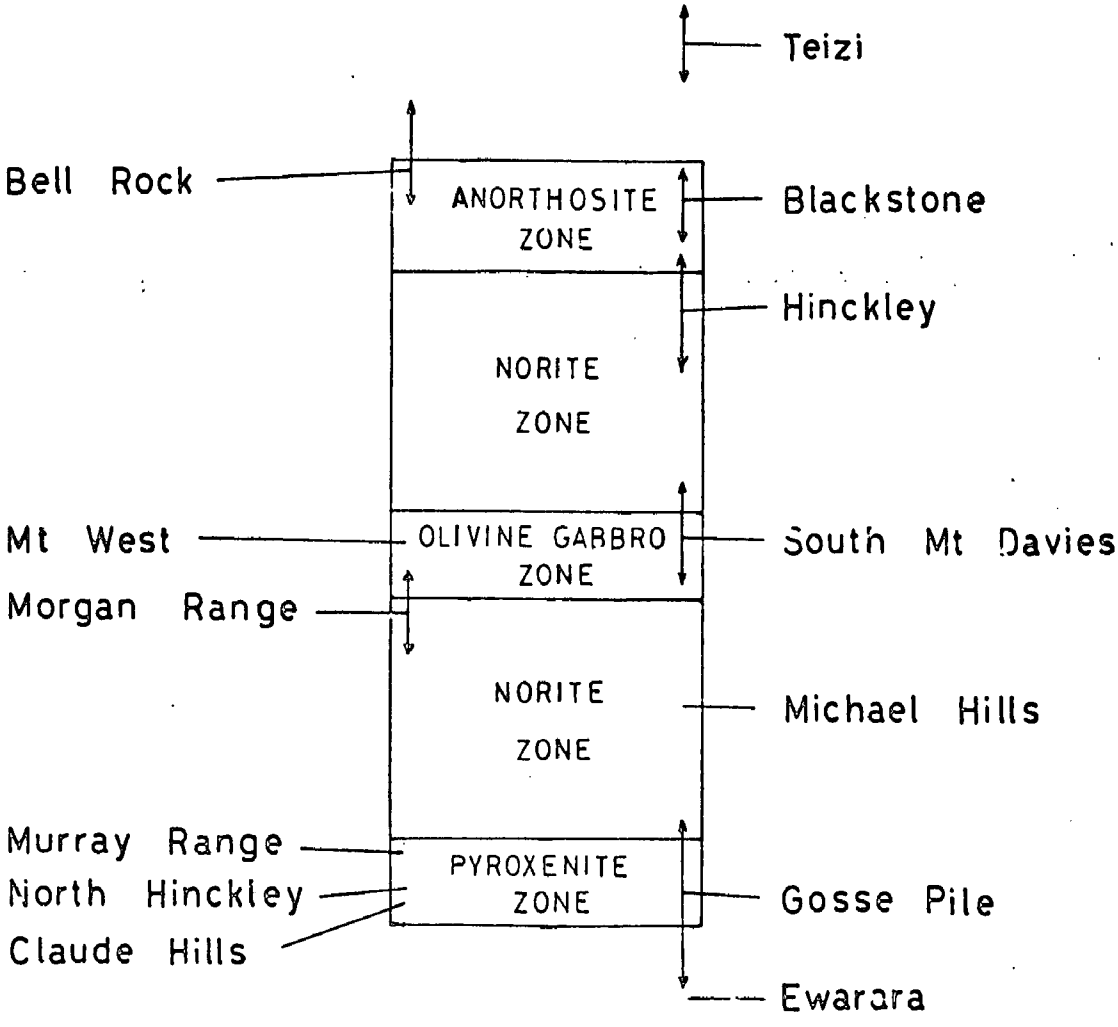
Teizi
Bell Rock
ANORTHOSITE ZONE
Blackstone
Hinckley
NORITE ZONE
Mt West
OLIVINE GABBRO ZONE
South Mt Davies
Morgan Range
NORITE ZONE
Michael Hills
Murray Range
North Hinckley
Claude Hills
PYROXENITE ZONE
Gosse Pile
Ewarara

FIGURE 32

A. Tight mesoscopic intrafolial fold, F_1 generation, in acid granulites, Ewarara. (Drawn from photograph).

Scale 20cm

B. Open mesoscopic F_3 fold, acid granulite, Kalka (near A314-712c). Note warping of axial plane (dotted) of small scale F_2 folds. (Drawn from photograph).

Scale 10cm

C. (010) sections of orthopyroxene showing orientation of (100) glide planes (upper) and (100) clinopyroxene exsolution lamellae (lower). Arrows indicate direction of elongation parallel to [001].

D. (010) sections of orthopyroxene showing result of simple shear deformation on (100), [001] glide system. Note that elongation direction is oblique and at a low angle to [001].

E. Relic kink bands in orthopyroxene (intervening kinks recrystallized). Note elongate direction at high angle to [001].

F. Extreme elongation of single plagioclase crystal, norite gneiss, A314-711. (Drawn from photomicrograph).

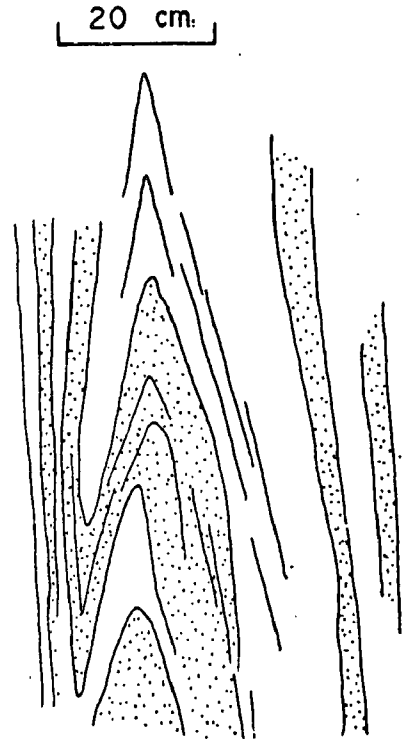

A

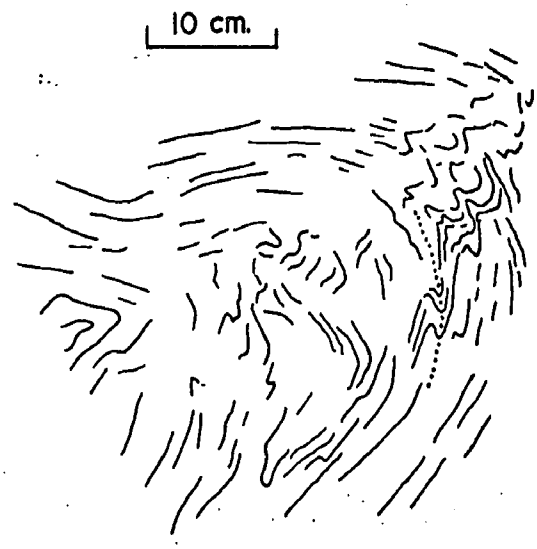

B

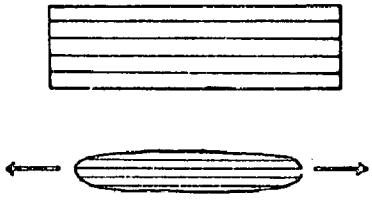

C

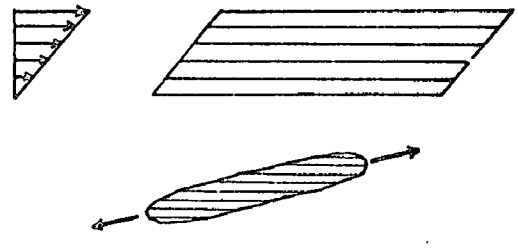

D

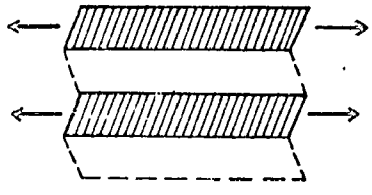

E

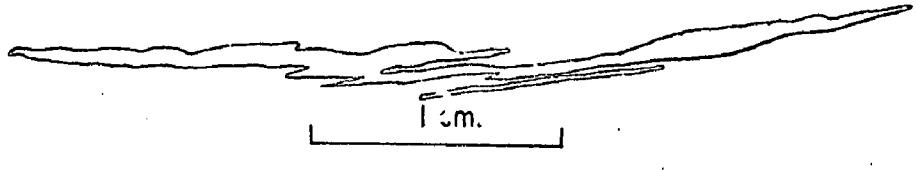

F

FIGURE 33

Location of West Kalka and Numbunja Gneissic Belts (shown as heavy dashes) in the Kalka Intrusion. The approximate southern limit for annealing recrystallization associated with the Numbunja Gneissic Belt in the Mt Kalka Section is shown as RL. Pyroxenite Zone shown in green, granulites as lines, major faults as wavy lines.

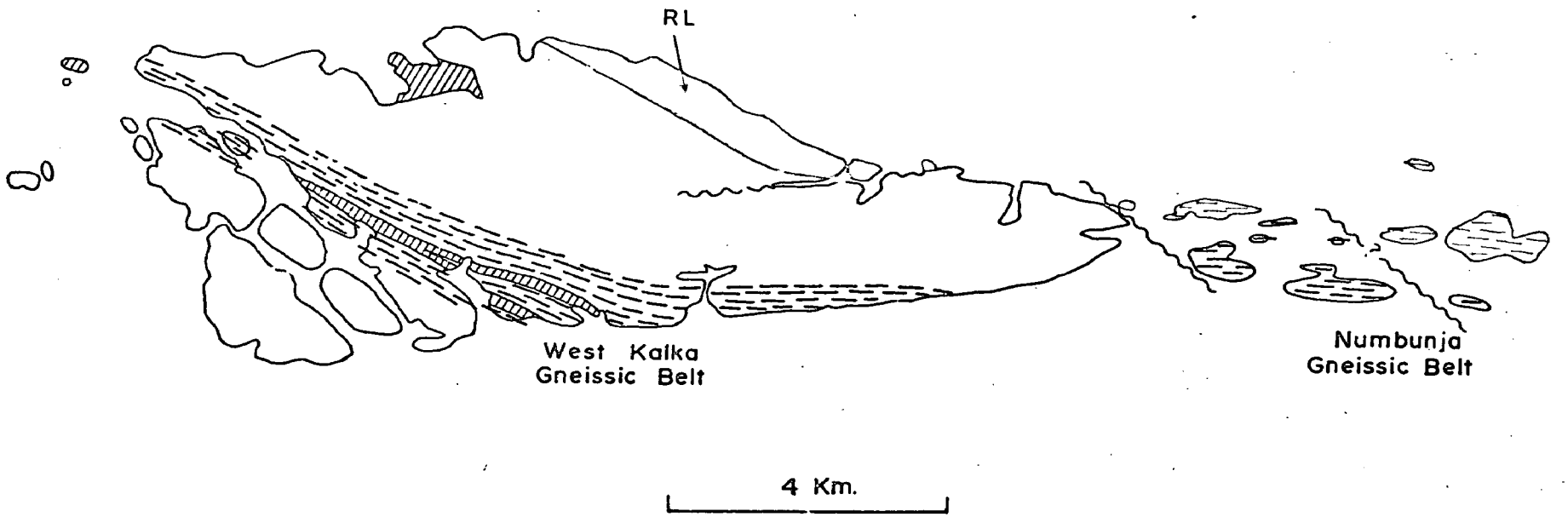
RL
West Kalka
Gneissic Belt
Numbunja
Gneissic Belt
4 Km.

FIGURE 34

Reconstruction of the Kalka - Gosse Pile protobody (dashed outline) after removal of folding and cross-faulting. Shown as an east-west cross-section. Present generalised outcrop patterns taken from this thesis and Moore, 1970a (granulite as vertical unbroken lines, Pyroxenite Zone as stipple, Norite Zone as blank, Olivine Gabbro Zone as cross-hatching, Anorthosite Zone as circles, fault contact to Gosse Pile as F). Numbunja and West Kalka Gneissic Belts shown as heavy dashed lines. Average orientation of L_1^9 at Kalka would be at 55^0 to the page towards the left.

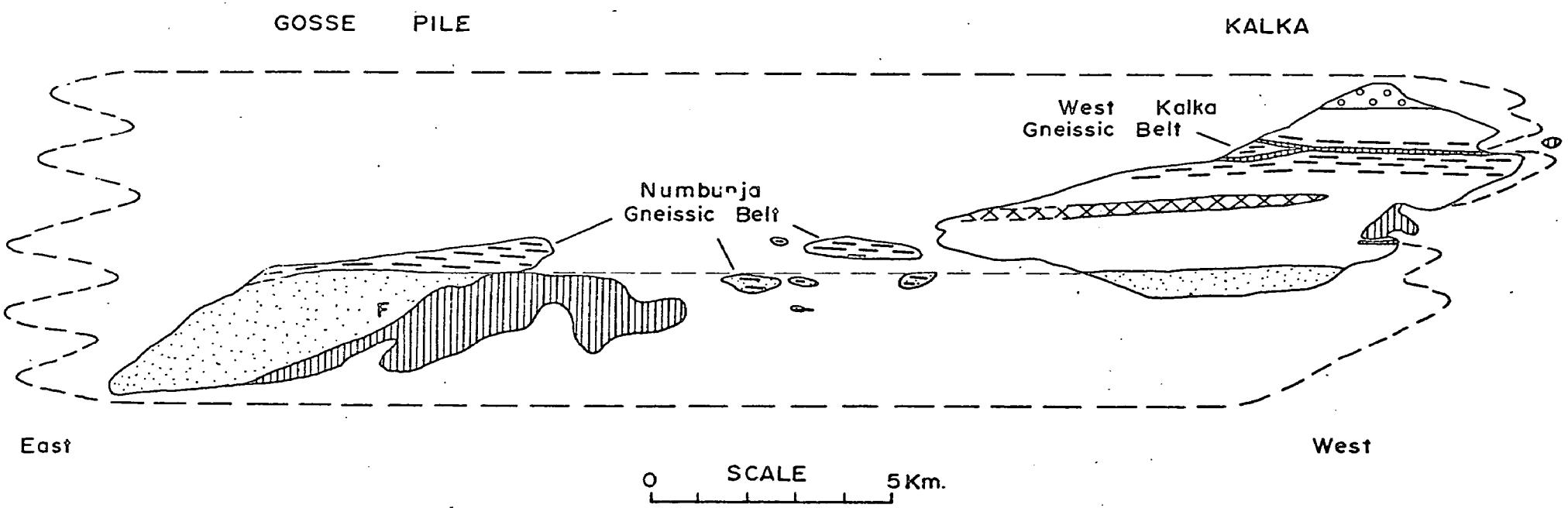
GOSSE PILE
KALKA
West Kalka Gneissic Belt
Numbunja Gneissic Belt
F
East
West
0 SCALE 5 Km.

FIGURE 35

A. Orientation of 130 poles to igneous layering, S_o^g, in the Kalka Intrusion (stereographic projection on the lower hemisphere of an equal area net; contoured by method of Strand, 1944, modified by A.W. Kleeman). Contour interval 1%, 2% and 4%. Slight tendency to secondary girdle formation in A, B and C (shown approximately as dashed line with pole to girdle shown as closed triangle).

B. Orientation of 112 poles to gneissic foliation, S_1^g, in the Kalka Intrusion. Contour intervals at 1%, 2%, 4% and 8%.

C. Orientation of 44 lineations, L_1^g, in the Kalka Intrusion. Contour intervals at 1%, 4%, 8% and 16%.

D. Orientation of 49 poles to granulite layering, S_o^m, near Ewarara (some data from Goode and Krieg, 1965) with associated girdle shown as dashed line. Mesoscopic F_2 fold axis shown as solid square, L_2^m lineations as open circles, pole to girdle as solid triangle.

E. Orientation of 28 poles to igneous layering, S_o^g, in the Ewarara Intrusion ("horizontal" layering as dots, "vertical" layering as crosses). Some data from Goode and Krieg, 1965.

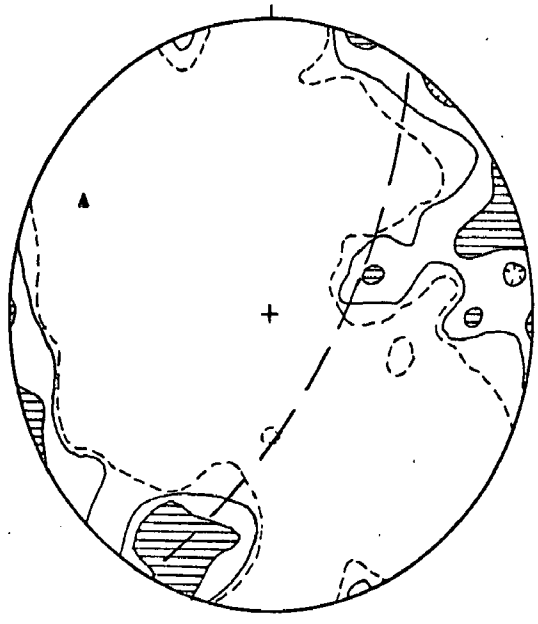

A

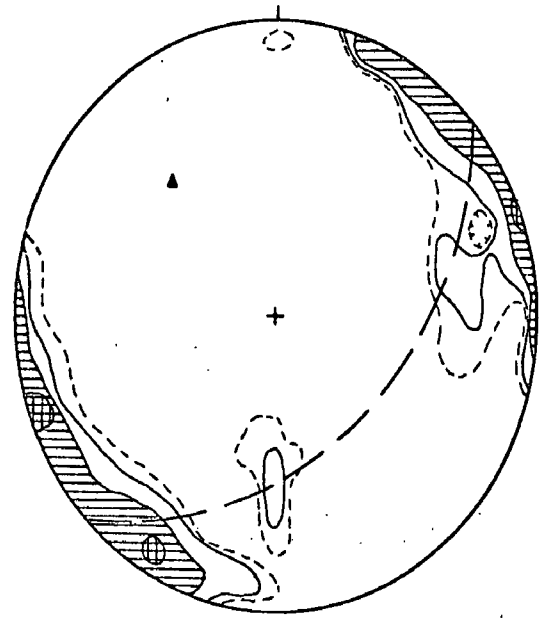

B

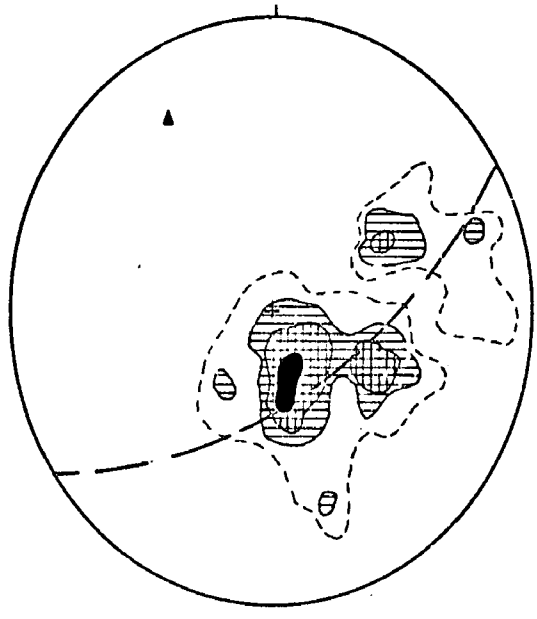

C

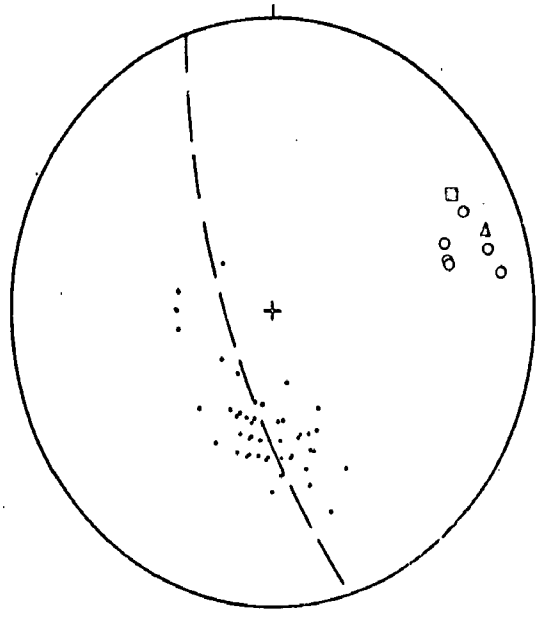

D

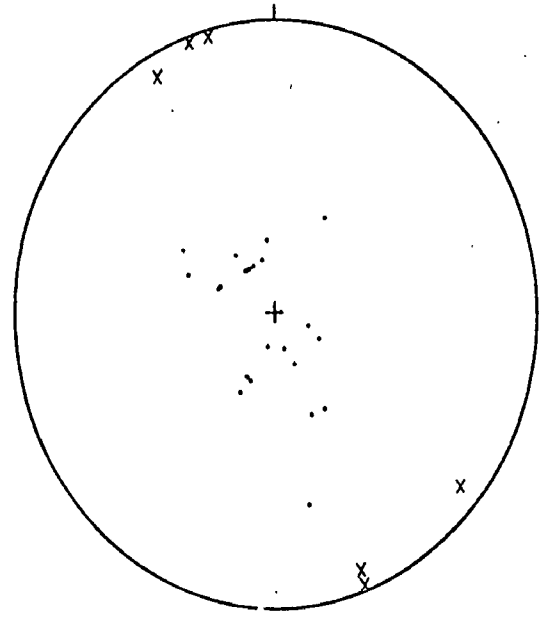

E

FIGURE 36

A. Distribution of Precambrian basement and cover terrains in Australia, showing the location of the Musgrave Block (after Parkin, 1969). Archaean rocks as fine stipple, Proterozoic basements (or undifferentiated Precambrian) as cross-hatching, Proterozoic cover rocks as heavy stipple.

B. Regional Bouger gravity anomalies in northwestern and central Australia, showing the position of the Anketell gravity ridge. Contoured at 20 milligal intervals (black: greater than 40 milligals, stippled: greater than -20 milligals). After Flavelle and Goodspeed, 1962; Lonsdale and Flavelle, 1963; Rowan, 1967.

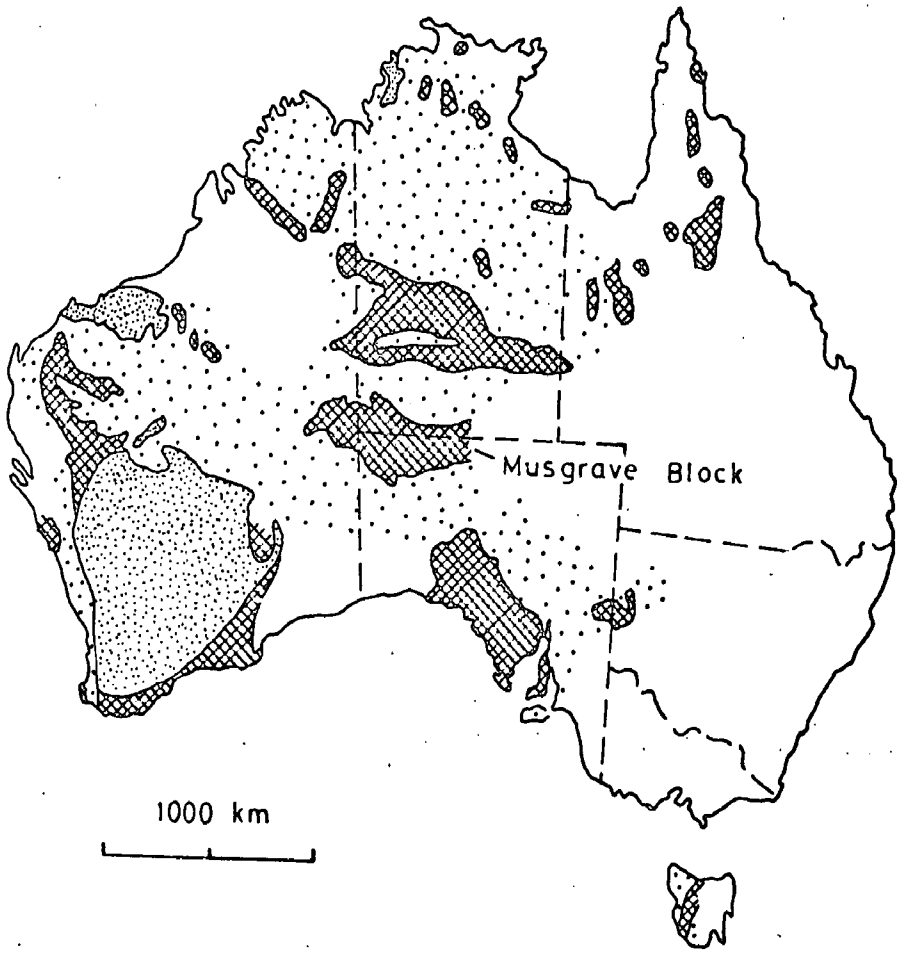

A

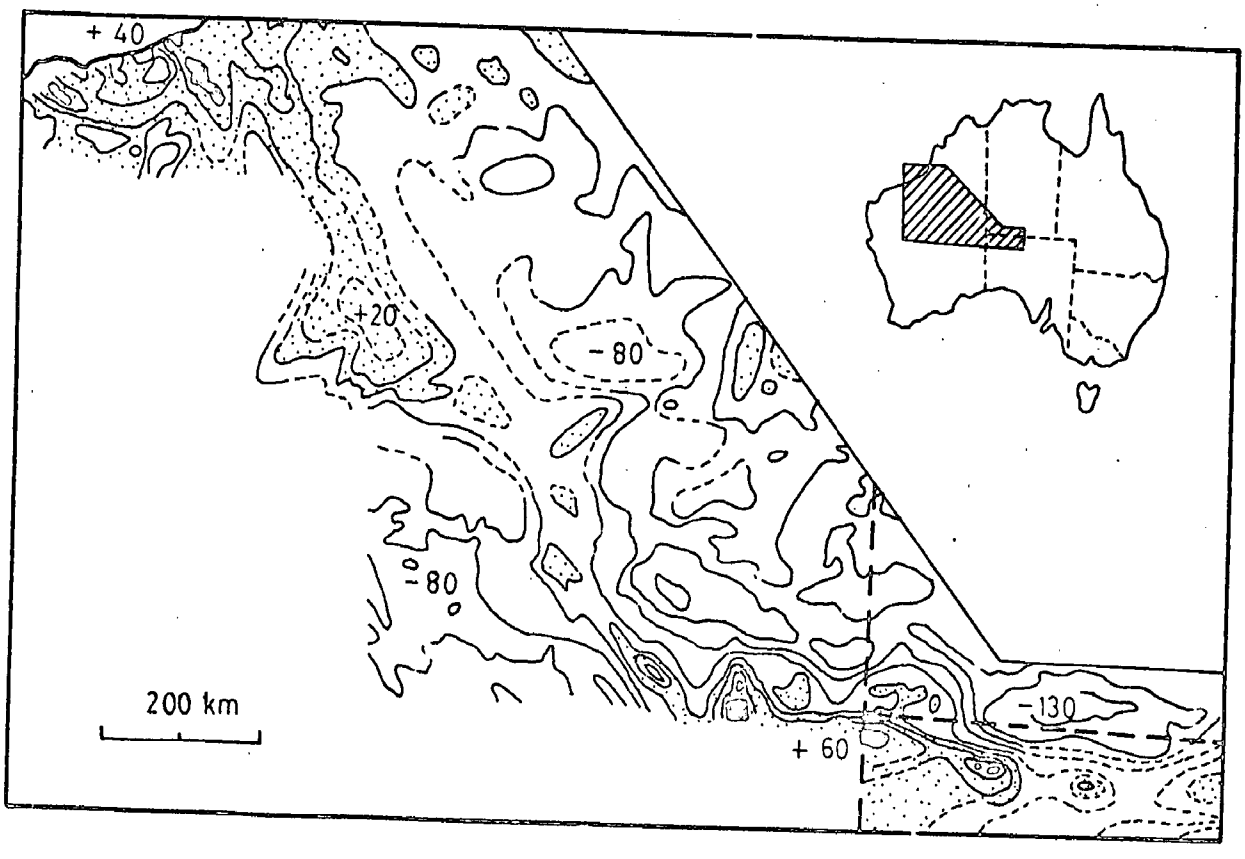

B

FIGURE 37

Structural and petrological terrains in the Musgrave Block (data only from Tomkinson and Musgrave Ranges). Granulite and amphibolite facies metasediments shown as stipple, Giles Complex intrusions in blue, Proterozoic sediments as horizontal lines, Tollu Volcanics as v symbols, lineaments as dashed lines. Crosses represent high pressure features recognised in Giles Complex intrusions; black circles - Type A dolerite dykes with pronounced foliation, red circles - undeformed Type A dolerites.

	Terrain	Lineament
Ia	Amphibolite facies gneisses with hornblende granites (Thomson, in Parkin, 1969).	
Ib	Granulite facies gneisses with Giles Complex intrusions.	
		Hinckley Fault
II	Granulite facies gneisses with Giles Complex intrusions (dominantly high pressure - see Chapter 11). IIa and IIb separated by Scarface Lineament (see Chapter 13.7).	
		Mann Fault
III	Retrograde granulite facies gneisses (Major et al., 1967; K.D. Collerson, pers. comm.).	
		Davenport Shear
IV	Granulite facies gneisses with Giles Complex intrusions (Major et al., 1967; K.D. Collerson, pers. comm.).	
		Woodroffe Thrust
V	Amphibolite facies gneisses (Major et al., 1967; K.D. Collerson, pers. comm.).	
		Ayliffe Thrust
VI	Granulite facies gneisses with Giles Complex intrusion.	

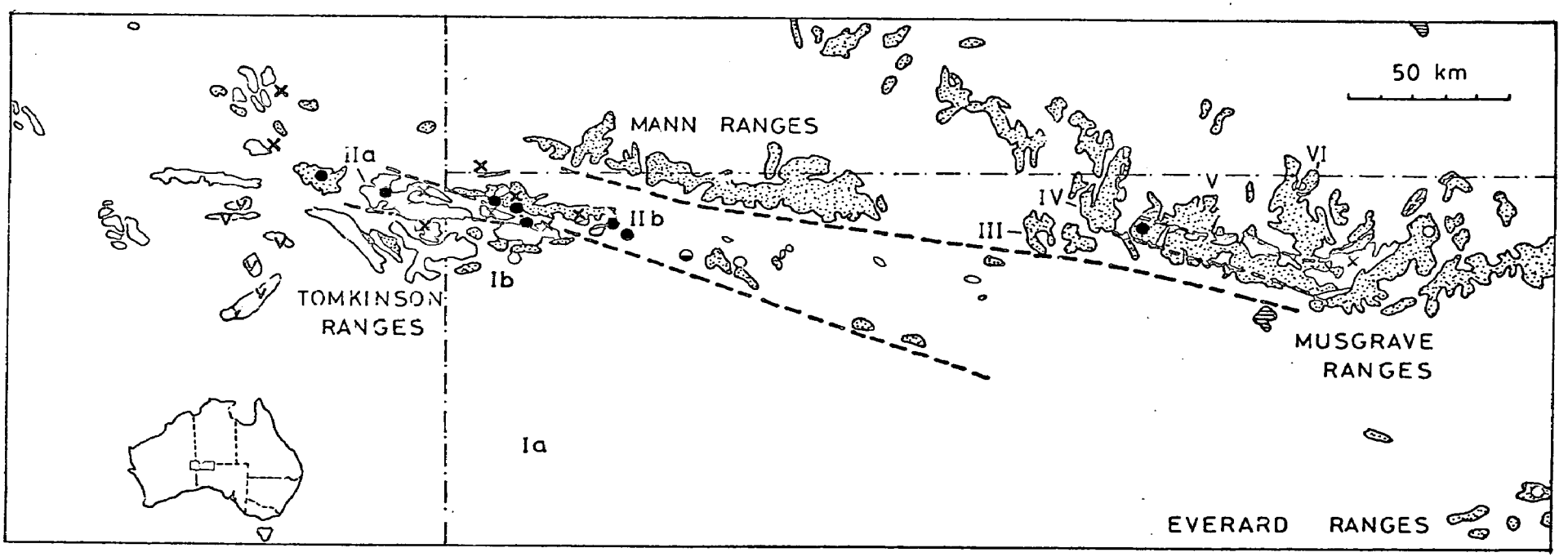
50 km
MANN RANGES
IIa
IIb
Ib
Ia
III
IV
V
VI
TOMKINSON
RANGES
MUSGRAVE
RANGES
EVERARD RANGES

FIGURE 38

Hypothetical packing textures.

A. Undisturbed packing of tabular crystals.

B. Packing of tabular crystals in agitated conditions (or post-depositional compaction).

C. Packing of equidimensional, equigranular crystals.

D. Packing of equidimensional, inequigranular crystals.

E. Packing of equidimensional and tabular crystals.

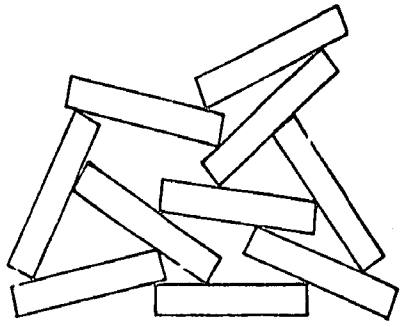

A

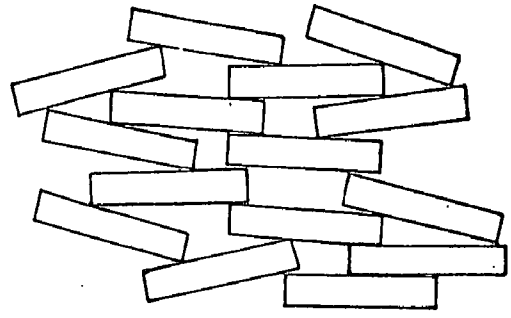

B

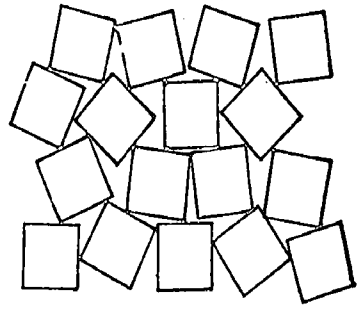

C

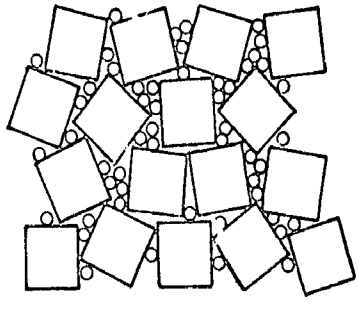

D

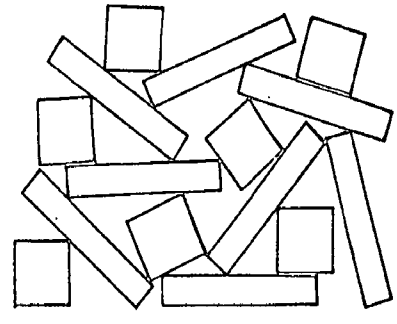

E

FIGURE 39

A. Differentiation trends for rocks with constant packing (olivine/liquid) ratios compared with liquid (L) and olivine (OL) trends - decreasing temperature. Data derived in Table 24.

1. olivine/liquid = 80/20
2. olivine/liquid = 70/30
3. olivine/liquid = 60/40
4. olivine/liquid = 50/50

B. Differentiation trends for rocks with variable packing ratios (compared with liquid and olivine trends) with decreasing temperature.

1. olivine/liquid packing ratio varies regularly from 80% at 1350°C to 50% at 1310°C.
2. olivine/liquid packing ratio varies regularly from 50% at 1350°C to 80% at 1310°C.
3. olivine/liquid packing ratio varies irregularly from 50% (1350°C) to 70% (1340°C) to 60% (1330°C) to 80% (1320°C) to 50% (1310°C)

C. Differentiation trend for rocks with variable olivine/liquid packing ratios (compared with liquid and olivine trends) at constant temperature.

D. Curves of rate of formation (c) of crystallization nuclei and the linear velocity of their growth (w) (after Zhdanov, 1965).

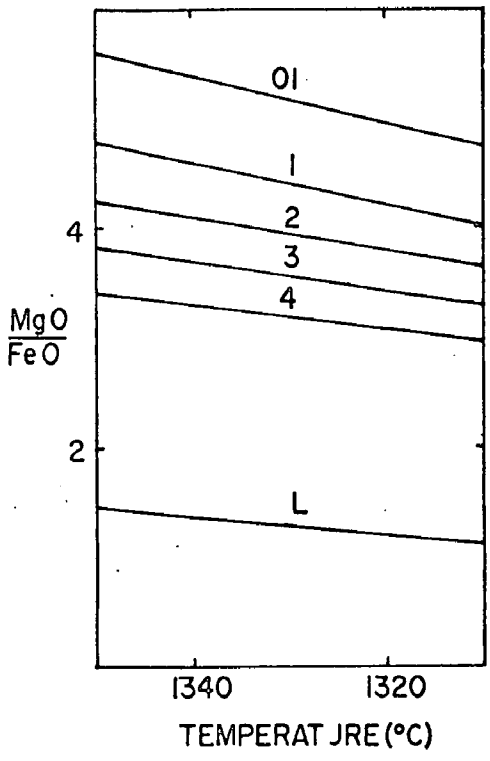
Ol
1
2
3
4
4
2
MgO
FeO
L
1340
1320
TEMPERATJRE (°C)

A

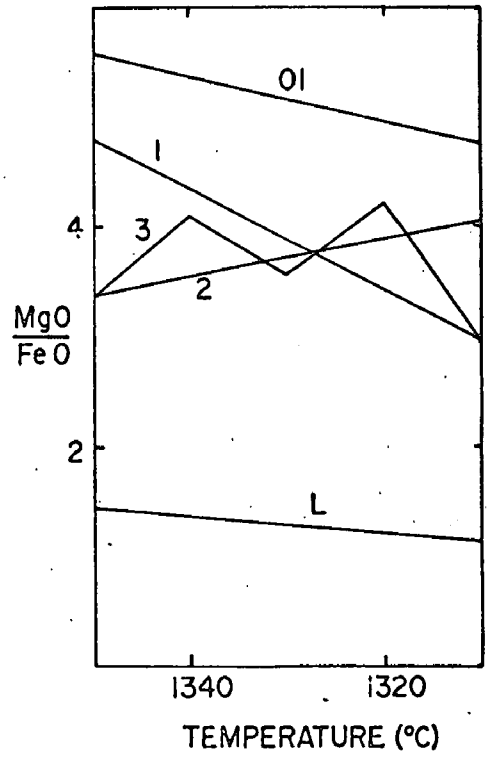
Ol
1
3
2
4
2
MgO
FeO
L
1340
1320
TEMPERATURE (°C)

B

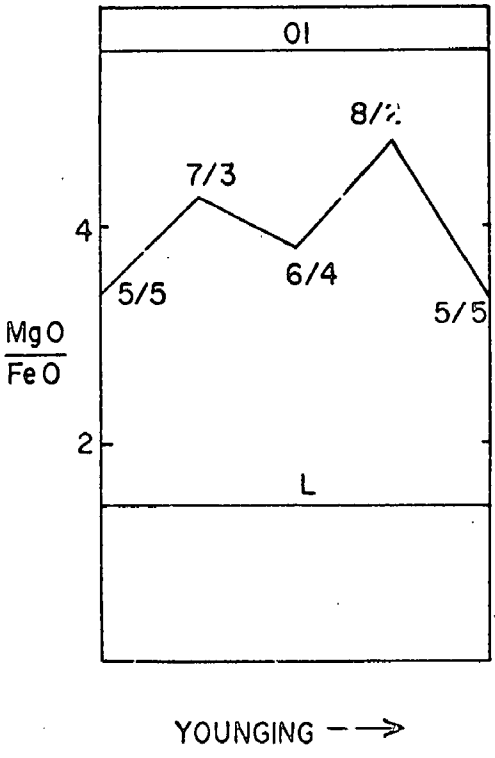
Ol
8/4
7/3
6/4
5/5
5/5
4
2
MgO
FeO
L
YOUNGING

C

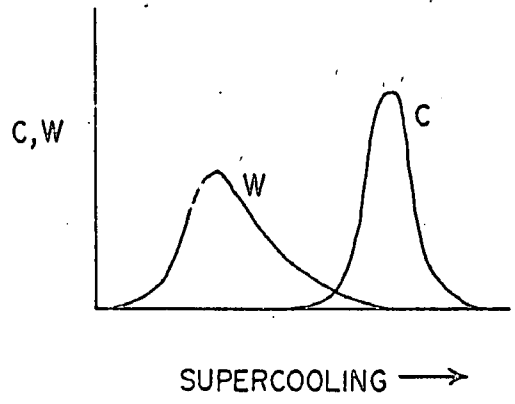
C,W
W
C
SUPERCOOLING

D

FIGURE 40

A. Variation of olivine (solid circles) and plagioclase (open circles) compositions in the Olivine Gabbro Zone of the Kalka Intrusion. Note displacement of the plagioclase curve towards the top of the sequence compared to the olivine curve.

B. Compositional variations for settled olivine - plagioclase pairs, Kalka Intrusion.

C. Compositional variations for co-crystallizing olivine - plagioclase pairs, Kalka Intrusion. Open circles from Olivine Gabbro Zone (OGZ), solid circles from Anorthosite Zone (AZ). Broken trend lines from South Mt Davies (SMD), Bell Rock (BR) and Blackstone (B) Intrusions (data from Nesbitt et al., 1970).

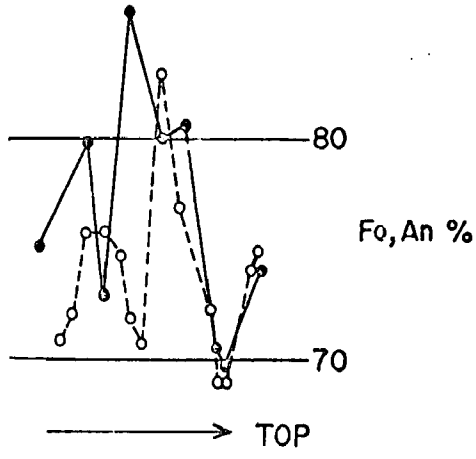

A

500m

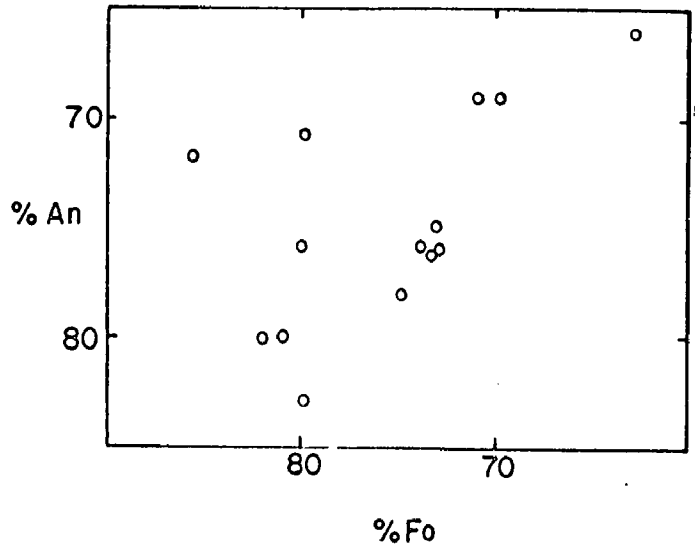

B

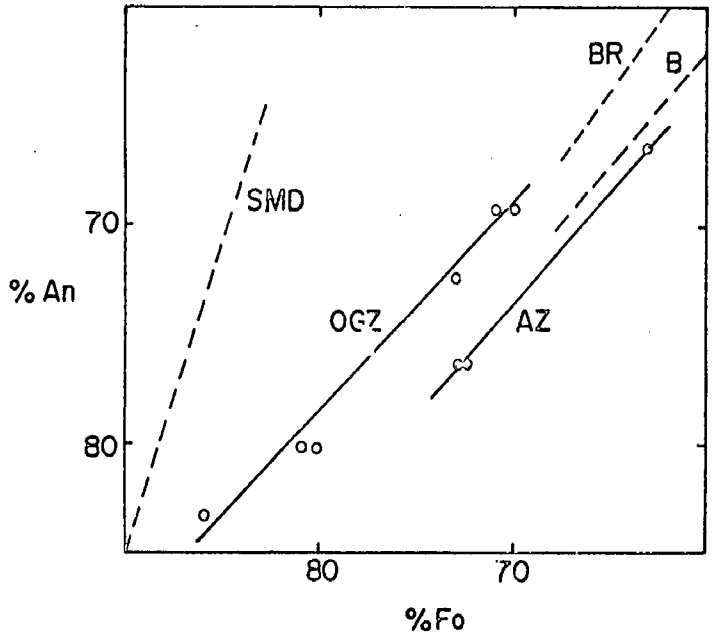

C

FIGURE 41

Operating conditions for X-ray fluorescence spectrography (compiled by A.R. Milnes).

E.M.	X-TUBE	kv.	ma.	line	2θ	beds	X'AL.	pcm.	COLL.	C.TUBE	soc.	ehr.	ATTN.	CHANNELS	counts	SAMPLE	%	GAS
A.	Cr.10 kw	44	20	kα	3506	·12/	PE.	2	coarse	fproportion	✓	390	2°	150	150	5000	fused button	10597	$Ar-IO/CH_2$
	Cr.27 kw	60	40	kα												10000			
Si.	Cr.10 kw	44	20	kα	7906	·24/	PE.	2	coarse	fproportion	✓	383	2°	150	150	8000	fused button	1357 3	$Ar-IO/CH_2$
	Cr.27 kw	60	40	kα												15500			
K	Cr.10 kw	44	20	kα	2046	·05/	PE.	2	coarse	fproportion	✓	382	2°	150	150	40000	fused button	13·43	$Ar-IO/CH_2$
	Cr.27 kw	60	40	kα												85000			
Fe	Cr.10 kw	44	20	kα	5745	·20/	LiF_{200}	1	coarse	fproportion	✓	376	2°	150	150	25000	fused button	3722	$Ar-IO/CH_2$
	Cr.27 kw	60	40	kα												45000			
Ti.	Cr.10 kw	44	20	kα	8607	·17/	LiF_{200}	1	coarse	fproportion	✓	374	2°	150	150	46000	fused button	7·04	$Ar-IO/CH_2$
	Cr.27 kw	60	40	kα												90000			
Ca	Cr.10 kw	44	20	kα	1301	·06/	LiF_{200}	1	coarse	fproportion	✓	379	2°	150	150	51000	fused button	11·17	$Ar-IO/CH_2$
	Cr.27 kw	60	40	kα												105000			
S.	Cr.10 kw	44	20	kα	8000	·08/	GE.	2	coarse	fproportion	✓	394	2°	150	150	1200	fused button	11·68	$Ar-IO/CH_2$
	Cr.27 kw	60	40	kα															
P.	Cr.10 kw	44	20	kα	11100	·06/	GE.	2	coarse	fproportion	✓	402	2°	150	150	1300	fused button	11·65	$Ar-IO/CH_2$
	Cr.27 kw	60	40	kα															
Mg.	Cr.10 kw	44	20	kα	10647	·40/	ADP.	2	coarse	fproportion	✓	389	2°	290	150	550	fused button	126 55	CH_2
	Cr.27 kw	60	40	kα												1600			
Na.	Cr.10 kw	44	20	kα	5312	·10/	KAP.	1	coarse	fproportion	✓		2°		150		pressed powder		CH_2
	Cr.27 kw	60	40	kα															
F.	Cr.10 kw	44	20	kα	8685		KAP.	1	coarse	fproportion	✓		2°		150		pressed powder		CH_2
	Cr.27 kw	60	40	kα															
Mn.	Mo.10 kw	50	18	kα	6291	·16/	LiF_{200}	1	coarse	fproportion	✓	384	2°	150	150	10500	fused button	10·41	$Ar-IO/CH_2$
	Mo.27 kw	60	40	kα															
Sr.	Mo.10 kw	50	18	kα	3587	1° 2θ off line	LiF_{220}	1	coarse	scintillation			2°	150	300		pressed powder		
	Mo.27 kw	60	40	kα															
Rb	Mo.10 kw	50	18	kα	3799	1° 2θ off line	LiF_{220}	1	coarse	scintillation			2°	150	300		pressed powder		
	Mo.27 kw	60	40	kα															
Ba.	Cr.10 kw	44	20	Lβ	9815	100°	PE.	?	coarse	fproportion	✓		2°	150	150		pressed powder		$Ar-IO/CH_2$
	Cr.27 kw	60	40	Lβ															

Counter dead time

Scintillation — 1·667 × 10^{-6} seconds

Fproportional — 1·054 × 10^{-6} s...

FIGURE 42

Classification of igneous rocks containing orthopyroxene, clinopyroxene, olivine and plagioclase. Tetrahedron exploded at 10, 30, 70 and 90% plagioclase critical modes and 10, 50 and 90% olivine critical modes. Dotted divisions at 10% orthopyroxene and 10% clinopyroxene critical modes. Abbreviations within tetrahedron: O olivine, L leuco-, Ms meso-, Ml mela-, Op orthopyroxenite, Cp clinopyroxenite, A anorthosite, D dunite, N norite, G gabbro, Pic picrite, Per peridotite, H harzburgite, Lh lherzolite, T troctolite, W websterite.

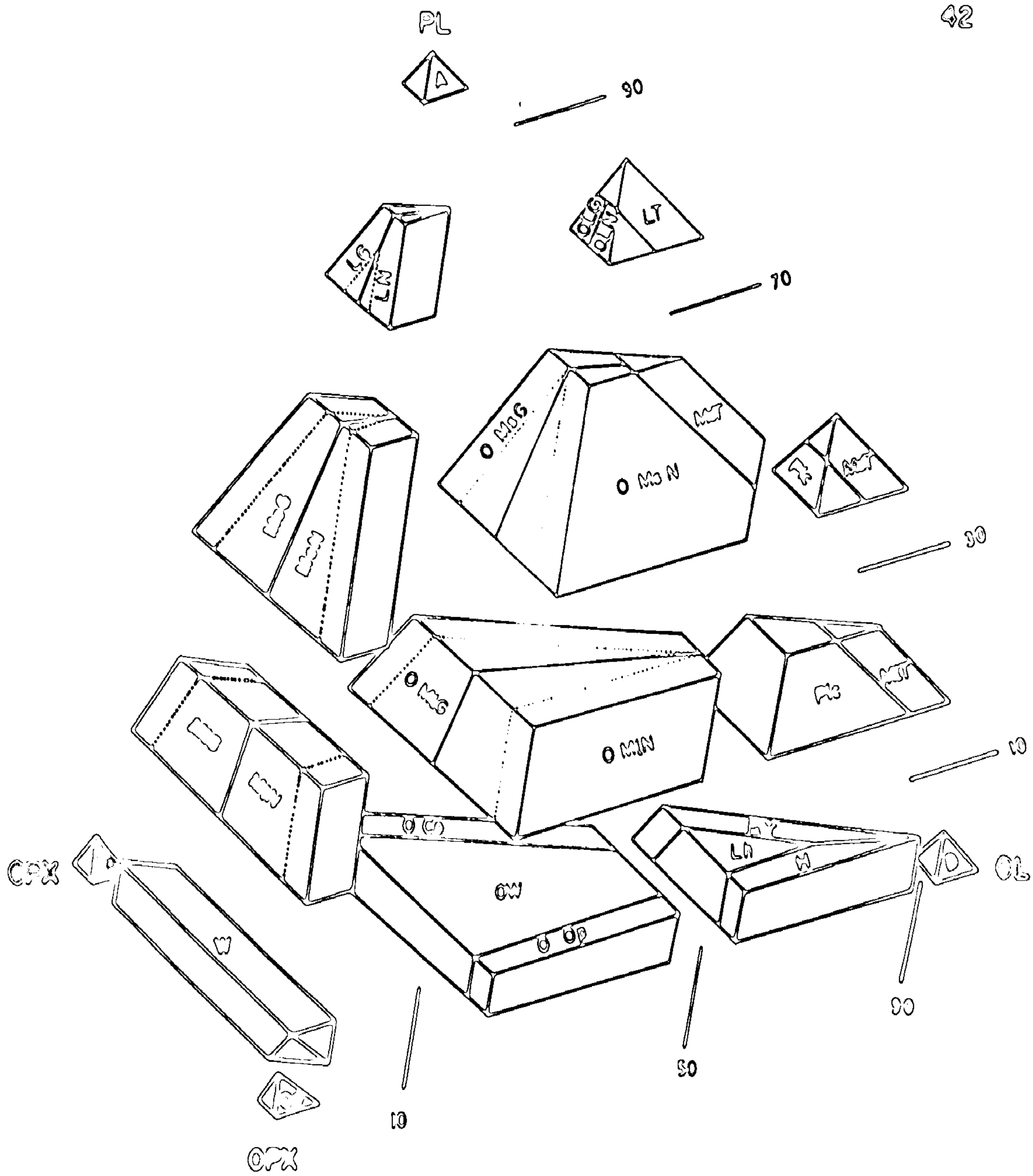
PL
90
LT
70
O MgG
MT
O Mg N
30
O MG
O MIN
Pk
MT
10
OW
W
CPX
OPX
CL
LA
10
50
90

FIGURE 43

A-D. Triangular diagrams showing classification of igneous rocks containing olivine, orthopyroxene, clinopyroxene and plagioclase. Symbols as in Figure 42.

E. Triangular diagram showing rock classification where ortho- and clino- pyroxenes cannot be differentiated. P pyroxenite; other symbols as in Figure 42.

F-H. Triangular diagrams showing partial classification for rocks consisting of:

F. magnetite (M) - pyroxene - plagioclase.

G. magnetite - olivine - pyroxene/plagioclase.

H. chromite (C) - olivine - pyroxene/plagioclase.

Mg magnetitite, Ch chromitite, other symbols as in Figure 42.

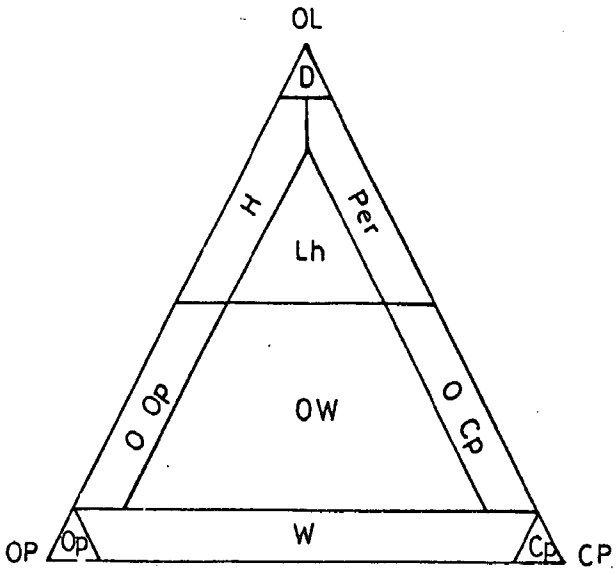
OL
D
H
Per
Lh
O Op
OW
O Cp
OP
Op
W
Cp
CP

A

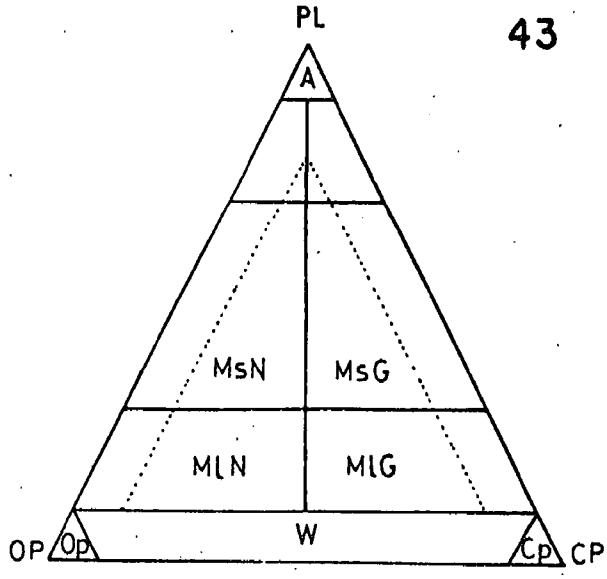
PL
A
MsN
MsG
MlN
MlG
OP
Op
W
Cp
CP

B

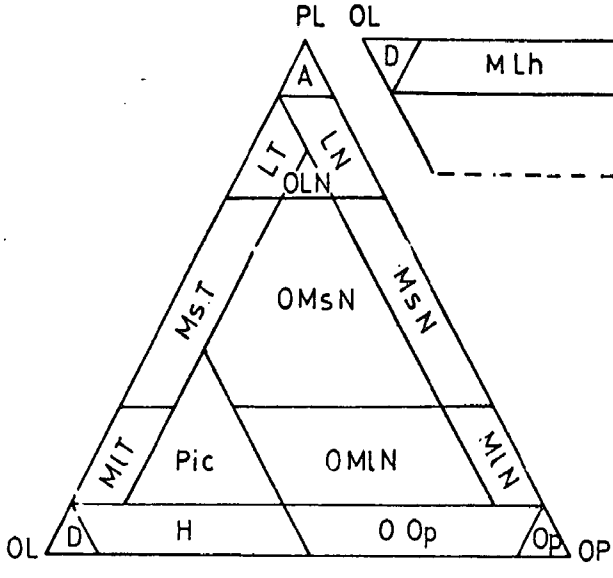
PL
A
LT
LN
OLN
MsT
OMsN
MsN
MlT
Pic
OMlN
MlN
OL
D
H
O Op
Op
OP

C

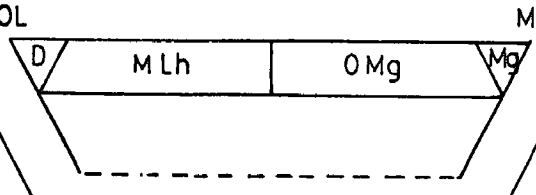
OL
M
D
M Lh
O Mg
Mg

G

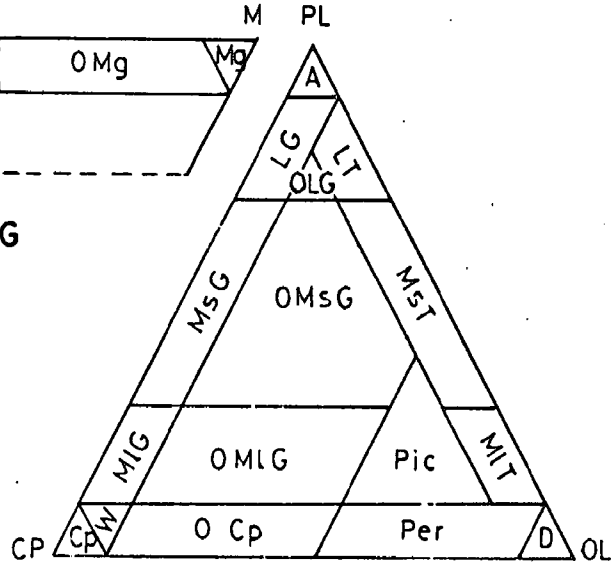
PL
A
LG
LT
OLG
MsG
OMsG
MsT
MlG
OMlG
Pic
MlT
CP
Cp
W
O Cp
Per
D
OL

D

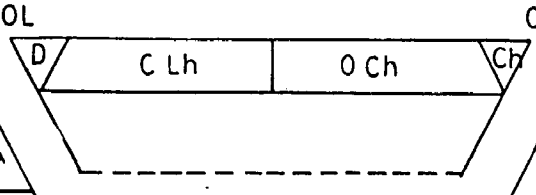
A
OL
C
M
D
C Lh
O Ch
Ch

H

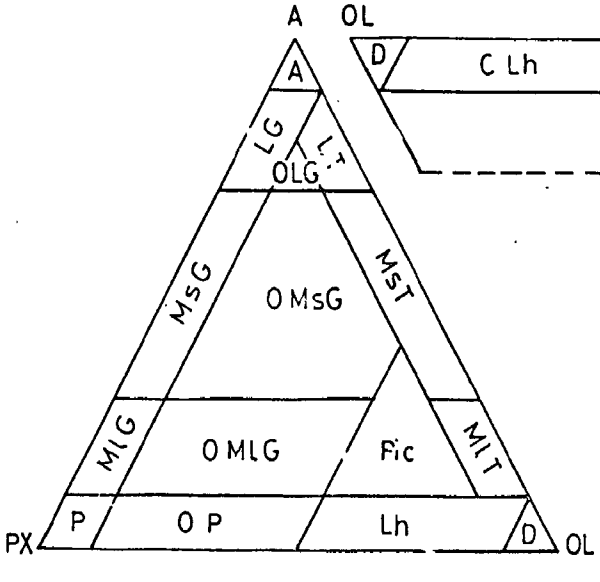
A
LG
LT
OLG
MsG
OMsG
MsT
MlG
OMlG
Pic
MlT
PX
P
O P
Lh
D
OL

E

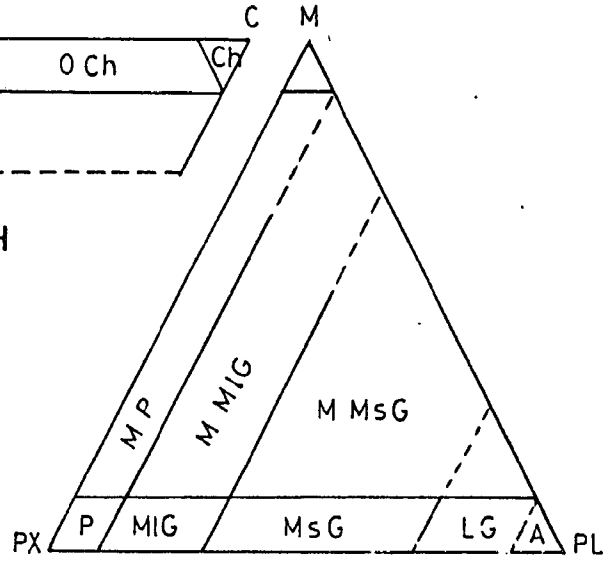
M
M P
M MlG
M MsG
PX
P
MlG
MsG
LG
A
PL

F

PLATES

PLATE 1 KALKA INTRUSION

Oblique aerial view of the Kalka Intrusion looking east towards the Gosse Pile (centre background) and Mt Davies (right background) Intrusions. Rocks in the foreground are from the N3 Subzone. Note the prominent igneous layering in the intrusion.

PLATE 2 EWARARA INTRUSION

Oblique aerial view of the Ewarara Intrusion looking to the west. The contact between ultramafics (dark) and layered acid granulites (light) can be seen in the foreground. Other features are shown on the overlay (including subhorizontal and vertical igneous layerings outlined by dashed and dotted lines respectively).

Photograph by R.W. Nesbitt.


GRANULITE
GRANULITE
OLIVINE
ENSTATITE
PICRITE
PLUG
84

PLATE 3 EWARARA INTRUSION

Oblique aerial view of the Ewarara Intrusion looking to the east. Distribution of rock types and structural features are shown on the overlay. The black "tip heaps" in the basal olivine orthopyroxenite unit at right foreground are weathering features. Dashed and dotted lines on the overlay represent subhorizontal and vertical layered horizons in the pyroxenite. Note the well developed layering in acid granulite (alternate dashed and dotted horizons on overlay).

Photograph by R.W. Nesbitt.

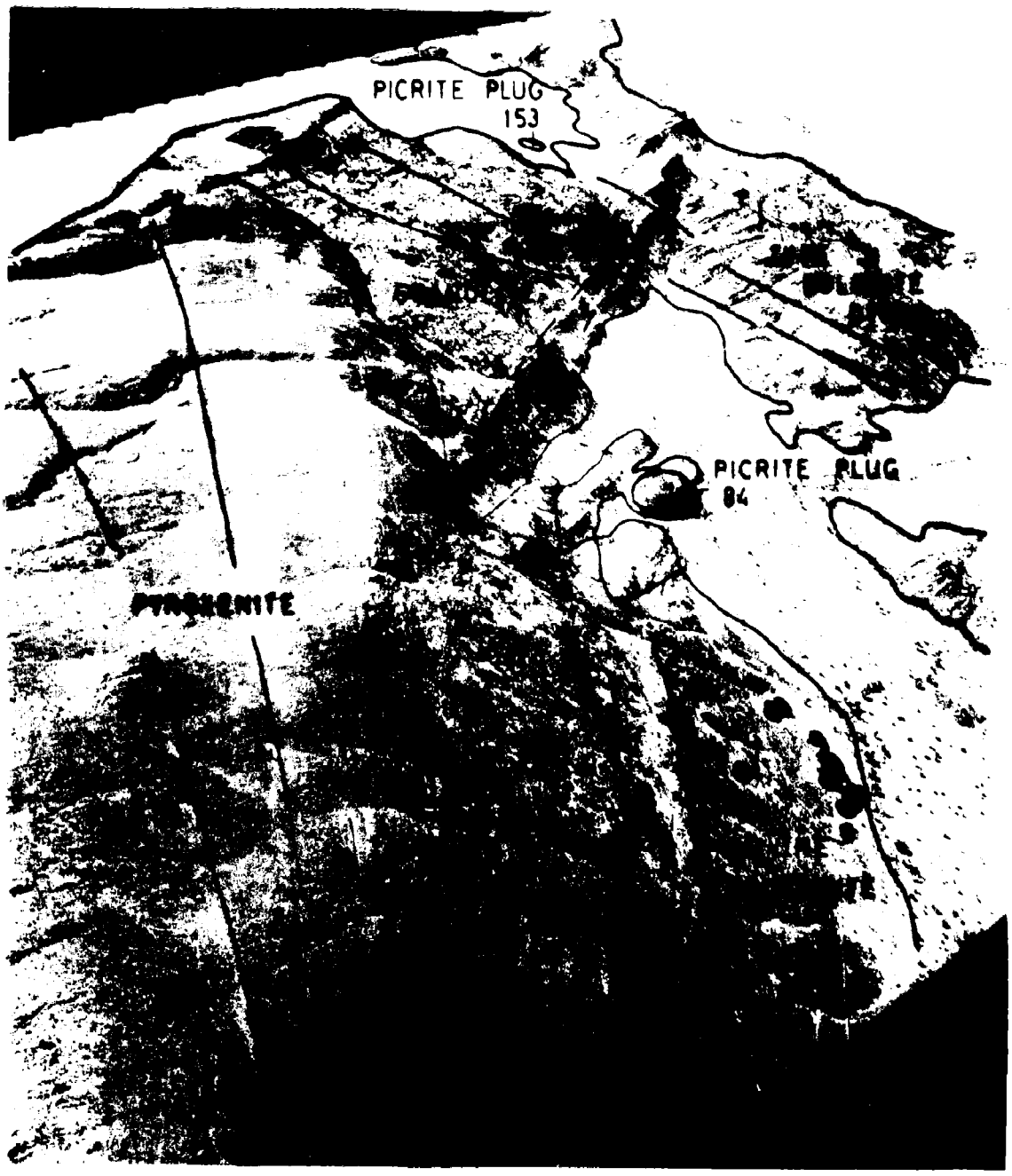
PICRITE PLUG
153
PICRITE PLUG
84
PYROXENITE

PLATE 4 EWARARA INTRUSION

View of Ewarara Intrusion from the southeast at picrite plug A300-710 showing the sub-horizontal basal contact and basal cumulates. The dashed horizon on the overlay marks a small scale layered horizon in the pyroxenites. Note the well developed banding in the acid granulites (dotted horizons on the overlay).

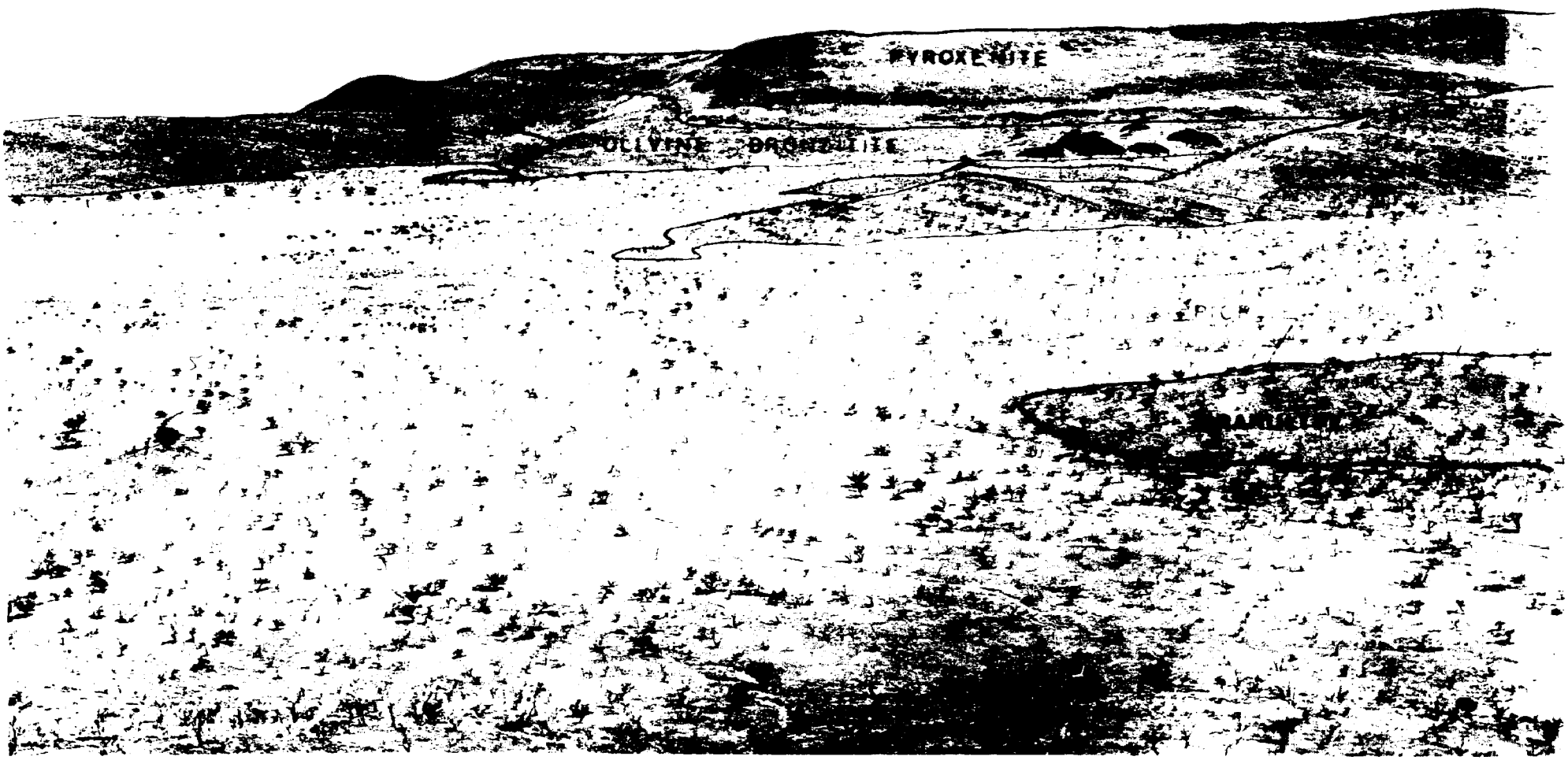
PYROXENITE
OLIVINE
GABBRO

PLATE 5 EWARARA INTRUSION

View of Ewarara Intrusion from the west, illustrating the sheet-like nature of the body. The contact between granulites (light) and ultramafics (dark) can be seen near the base of the slope. Ewarara Creek is in the middle distance.

PLATE 6

A. Granoblastic, inequigranular texture of quartz + feldspar + pyroxene $\pm$ garnet granulite. Note the common interlobate grain boundaries, and the slight grain elongation parallel to S_1^m.

A301-123a CP Width of field 5mm

B. Granoblastic, equigranular texture of plagioclase + orthopyroxene + clinopyroxene granulite. Grain boundaries are polygonal, and grain aggregates aligned to form S_1^m foliation.

A300-7 PPL Width of field 5mm

C,D Granoblastic, equigranular texture of garnet + clinopyroxene + plagioclase granulite.

A300-58 C. CP Width of field 5mm
D. PPL

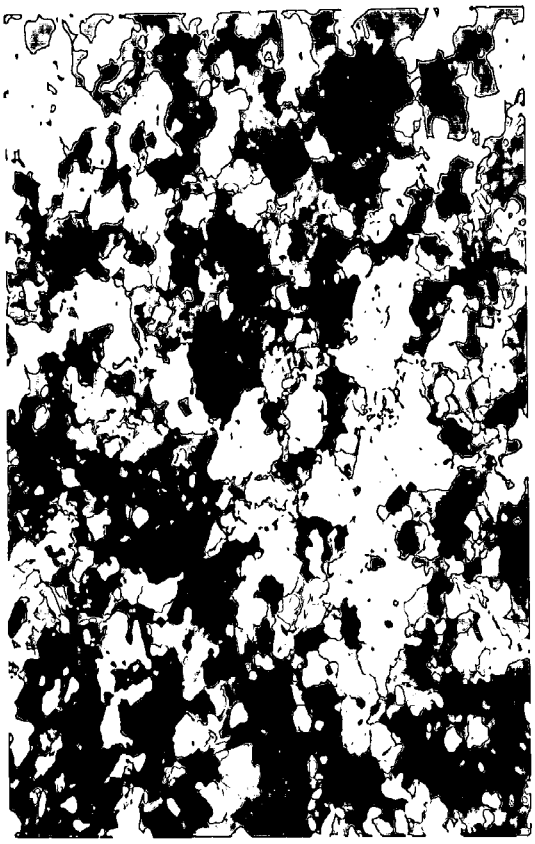

A

B

C

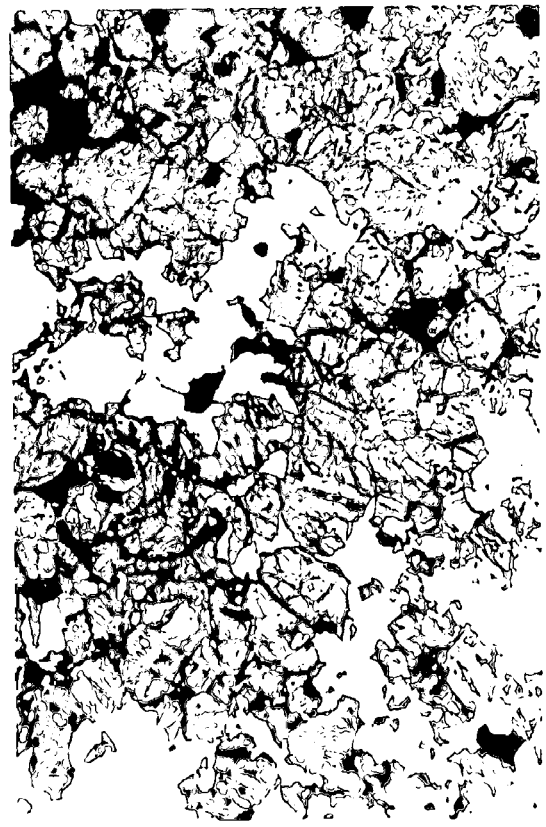

D

PLATE 7

A. Platy granoblastic quartz ribbons forming axial plane foliation, S_2^m, to open F_2 fold in quartz - feldspar - garnet granulite (fold outlined by bend in compositional layering, S_o^m e.g. thin garnet band (black) at left). Note overprinting of coarse-grained granoblastic texture by S_2^m.

A300-702 CP Width of field 22mm

B. Ribbon quartz grains bending around garnet porphyroblast (black, right centre), acid granulite.

A301-178 CP Width of field 1.4mm

C. Ribbon quartz grains wrapping around sillimanite porphryoblast, acid granulite. Note undulose extinction bands in sillimanite indicative of rotation.

A301-108 CP Width of field 1.4mm

D. Amoeboid grain boundaries in strained ribbon quartz, acid granulite.

A301-108 CP Width of field 0.2mm

A

B

C

D

PLATE 8

A. Quartz inclusions (white, rounded) in perthitic K-feldspar, producing "buckshot" texture, Ewarara. Note development of mesoperthite in feldspar. Microperthite is abundant in darker apparently barren areas.

A301-123a CP Width of field 1.4mm

B. "Myrmekitic" intergrowth associated with perthite feldspar boundaries, Ewarara.

A301-166 CP Width of field 0.9mm

C. "Myrmekitic" intergrowth between two feldspars(?) interpenetrant to perthite porphyroblasts, Minno.

A314-474 CP Width of field 1.4mm

D. Intergrowth between two feldspars or feldspar and quartz at perthite grain boundary, Ewarara.

A301-166 CP Width of field 1.4mm

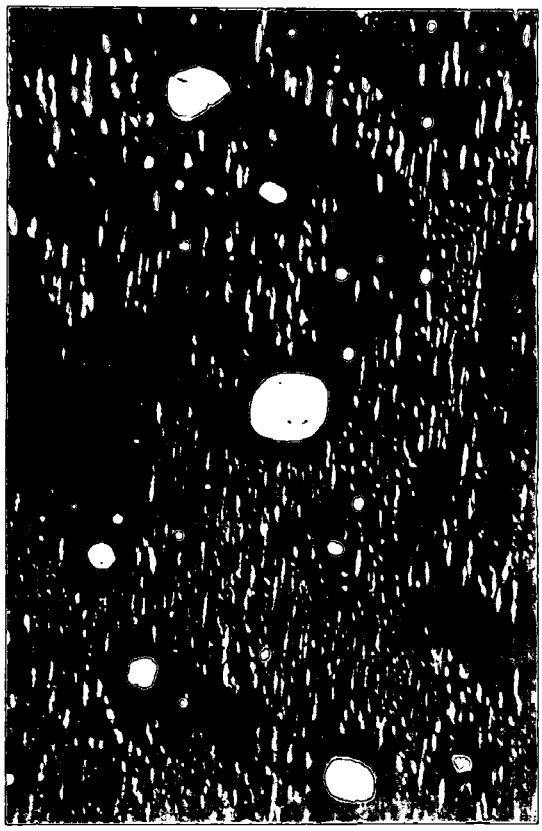

A

B

C

D

PLATE 9

A. Garnet - quartz intergrowths on opaques (probably ilmenite) in quartz + feldspar + pyroxene ± garnet granulites, Ewarara.

A301-72 PPL Width of field 0.9mm

B. Garnet - quartz intergrowths on opaques in quartz + feldspar + pyroxene ± garnet granulites, Ewarara. Note absence of quartz in garnet adjacent to opaques.

A301-72 PPL Width of field 0.9mm

C. Quartz inclusions in "spongy" garnet, acid granulite, Ewarara. Note straight boundaries between quartz grains within garnet and amoeboid quartz - quartz boundaries outside garnet.

A301-21 CP Width of field 0.9mm

D. Parallel corundum exsolution lamellae (centre) in ilmenite, garnet - clinopyroxene - plagioclase granulites, Ewarara.

A300-363 PPL Width of field 0.9mm

A

B

C

D

PLATE 10

A. Opaque exsolution rods in garnet from garnet - clinopyroxene - plagioclase granulite, Ewarara.

A300-58 PPL Width of field 0.2mm

B. Opaque exsolution plates in hornblende from basic granulite, Ewarara.

A300-58 PPL Width of field 0.9mm

C. Biotite associated with ragged orthopyroxene (arrowed) in acid granulite, Minno.

A314-474 PPL Width of field 0.9mm

D. Granular garnet surrounding biotite in acid granulite, Kalka.

A314-423 PPL Width of field 0.2mm

A

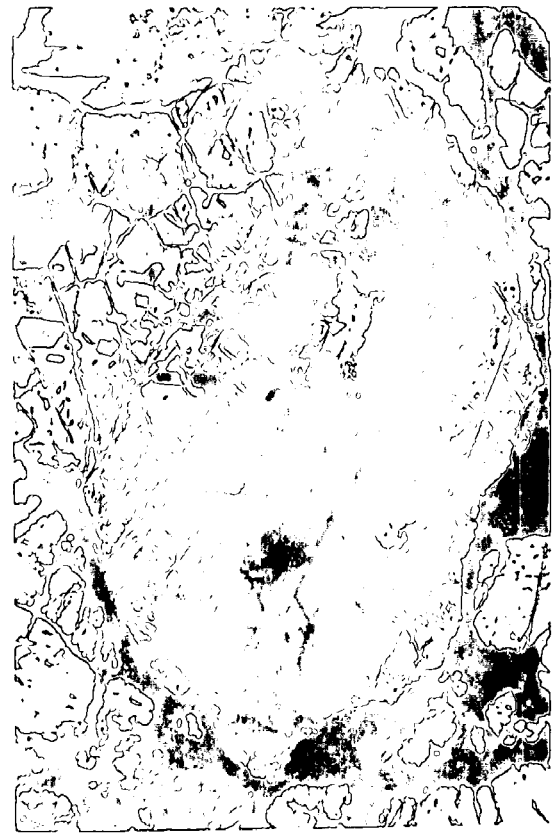

B

C

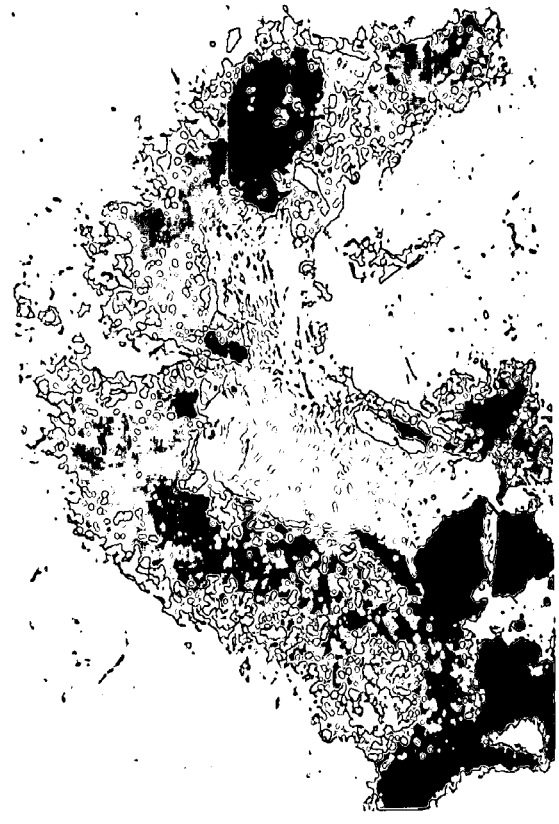

D

PLATE 11

A. Perthite rims (P, arrowed) around sillimanite (S) and garnet (G) in quartz + feldspar + garnet ± sillimanite granulites, Ewarara. Note separate distribution of sillimanite and garnet.

A301-15 PPL Width of field 1.4mm

B. Perthite rims around sillimanite (S) and garnet (G), Ewarara. Note partial rim of garnet on sillimanite.

A301-15 PPL Width of field 1.4mm

C. Perthite rim around garnet (G) partially enclosing sillimanite (S), Ewarara.

A301-15 PPL Width of field 1.4mm

D. Garnet (G) intergrown with biotite and quartz, Ewarara. Note the lack of a perthite rim.

PPL Width of field 0.9mm

A

B

C

D

PLATE 12

A. Sillimanite inclusions (dark grey) within garnet (black), acid granulite. Note absence of perthite rim on garnet.

A301-159 CP Width of field 0.9mm

B. Feldspar augen surrounded by finer grained quartz - feldspar - pyroxene groundmass, acid granulite. Note bending of S_1^m foliation, outlined by pyroxene aggregates, around augen.

A301-72 PPL Width of field 30mm

C. Magnetite (white) - hornblende (?) intergrowths at grain boundary of pyroxene, basic granulite.

A300-7 PPL (reflected light) Width of field 0.2mm

D. Fine-grained magnetite (white) - pyroxene (black) intergrowths in interstices in Type D dolerite, Kalka. Note rim of coarser grained magnetite around granular spinel (dark grey, centre).

A314-344 PPL (reflected light) Width of field 0.2mm

A

B

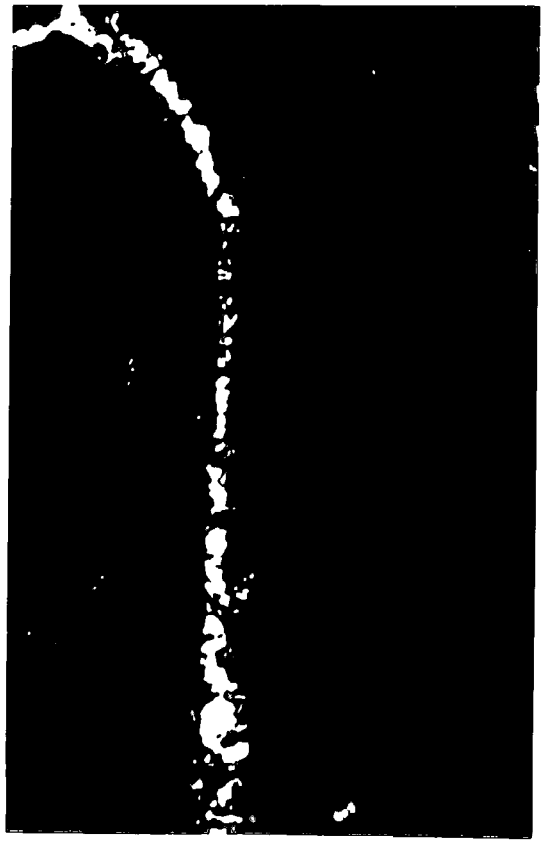

C

D

PLATE 13

A. Undeformed texture of Type A dolerite from south of Mt Davies. Note random orientation of plagioclase laths.

GM10 PPL Width of field 15mm

B. Localised development of plagioclase ribbons enclosing relic primary plagioclase lath, deformed Type A dolerite, Ewarara.

A314-440 CP Width of field 1.4mm

C. Deformed texture of Type A dolerite from north of Kalka. Note development of pronounced S_2^d foliation outlined by aligned plagioclase "laths".

A314-440 PPL Width of field 17mm

D. Recrystallized Type B dolerite, Ewarara. Note strong development of foliation outlined by monomineralic grain aggregates.

A300-93 PPL Width of field 12mm

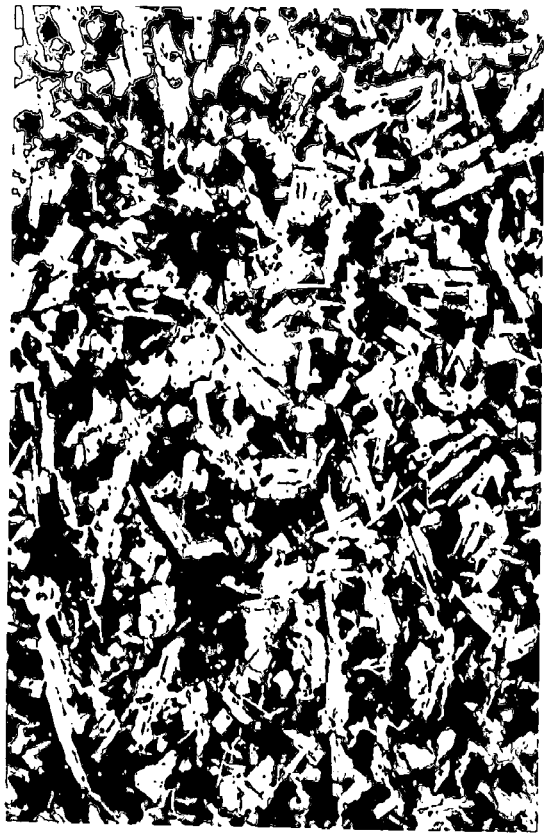

A

B

C

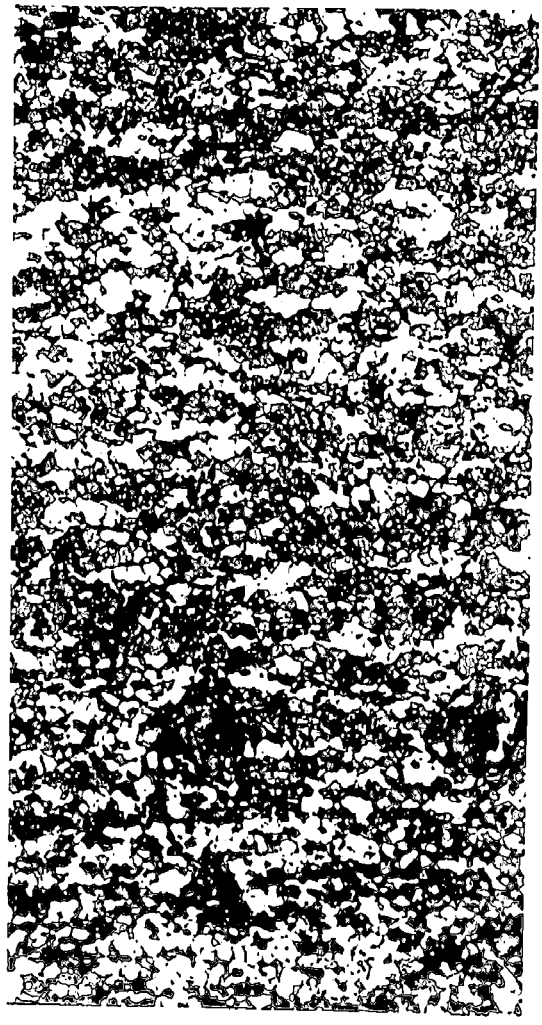

D

PLATE 14

A. Chill texture of fine-grained Type B dolerite, Ewarara. Note development of pyroxene-rich clumps.

A300-358 PPL Width of field 13mm

B. Aligned plagioclase microphenocrysts in marginal chill phase of Type C dolerite, Kalka. Note general increase in matrix grain size upwards.

A314-386 PPL Width of field 12mm

C. Texture of coarse-grained Type B dolerite, Ewarara. Note recrystallized pyroxenes, and pyroxene selvage in centre of unrecrystallized plagioclase laths.

A300-368 PPL Width of field 5mm

D. Random orientation of plagioclase laths in chilled Type C dolerite (without plagioclase phenocrysts), Kalka.

A314-382 PPL Width of field 5mm

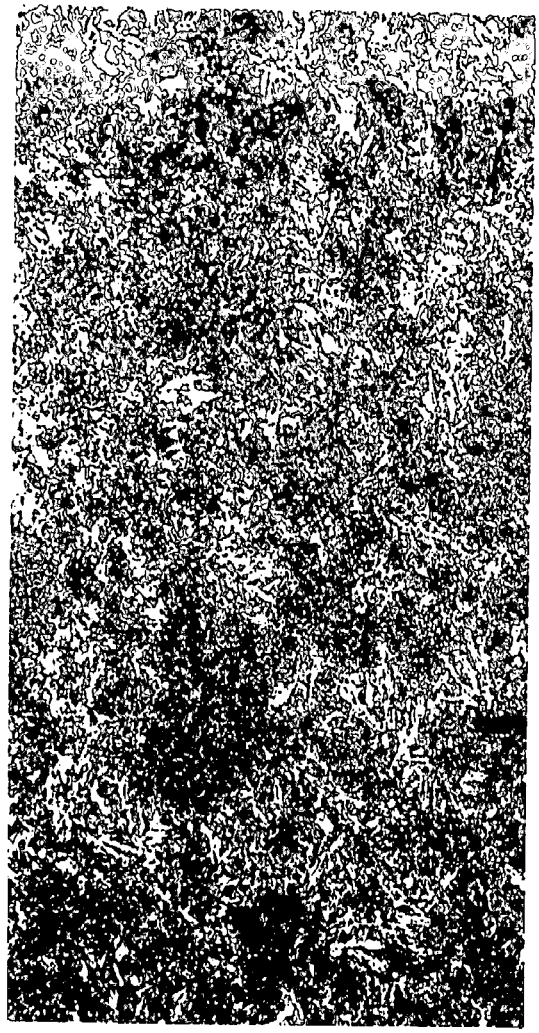

A

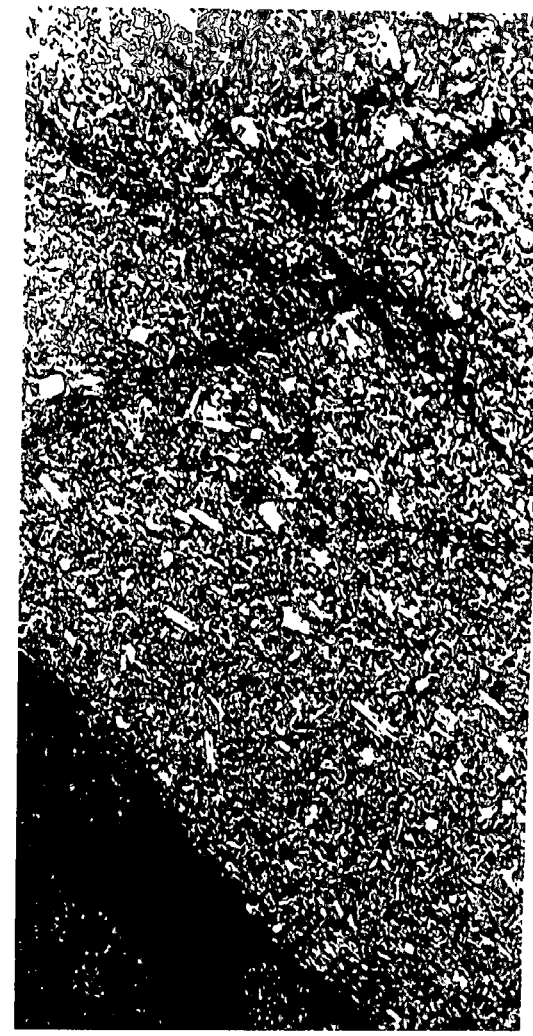

B

C

D

PLATE 15

A. Mantling of orthopyroxene by clinopyroxene, Type B dolerite.

A314-755 CP Width of field 1.6mm

B. Garnet rim (black) surrounding euhedral granular orthopyroxene/opaque aggregate (pseudomorph of olivine), Type D dolerite, Ewarara.

A300-10 CP Width of field 1.4mm

C. Annular zone of pyroxene inclusions in plagioclase phenocryst in Type D dolerite, Kalka.

A314-717 PPL Width of field 1.6mm

D. Sheaf-like clinopyroxene in Type D dolerite, Ewarara.

A300-10 PPL Width of field 0.9mm

A

B

C

D

PLATE 16

A. Olivine phenocrysts in Type D dolerite, Kalka. Note synneusis clumping of phenocrysts (lower left) and skeletal phenocryst (top centre).

A314-417 CP Width of field 5mm

B. Garnet patches in Type D dolerite, Ewarara.

A300-10 CP Width of field 5mm

C. Plagioclase phenocryst in medium-grained olivine dolerite matrix, Type C dolerite, Kalka.

Scale 4.3cm

D. Type D dolerite dyke, Kalka. Note sharp planar contacts and thin very fine-grained marginal zones.

Scale 12.5cm

A

B

C

D

PLATE 17

A. Intergrown boundary between two plagioclase phenocrysts with associated development of pyroxene and opaques. Note overgrowths of unclouded feldspar on clouded feldspar (especially) at left). Type C olivine dolerite dyke, Kalka.

A314-391 PPL

B. Planar grain boundary between plagioclase phenocrysts marked by pyroxene accumulations. Type C olivine dolerite dyke, Kalka.

A314-391 PPL

C. Internal zoning of fine opaque exsolution in olivine phenocrysts parallel to growth indentations. Type D porphyritic olivine dolerite dyke, Kalka.

A314-417 PPL

D. Intergrowth of plagioclase phenocryst with fine-grained matrix at end of lath. Type C olivine dolerite dyke, Kalka.

A314-391 PPL

A

B

C

D

PLATE 18

A. Rough alignment of plagioclase phenocrysts parallel to interface with phenocryst-free dolerite, Type C dolerite, Kalka.

A314-391 PPL Width of field 17mm

B. Brecciated Type D dolerite dyke margin, Ewarara, with development of pseudotachylite (black). Note disoriented rounded granulite blocks (right).

A301-144 PPL Width of field 13mm

C. Thin ferromagnesian-rich margin to olivine phenocryst, Type D dolerite, Kalka.

A314-417 PPL Width of field 0.5mm

D. Granular pyroxene margin to primary pyroxene crystal, Kalka.

A314-214 PPL Width of field 1.6mm

A

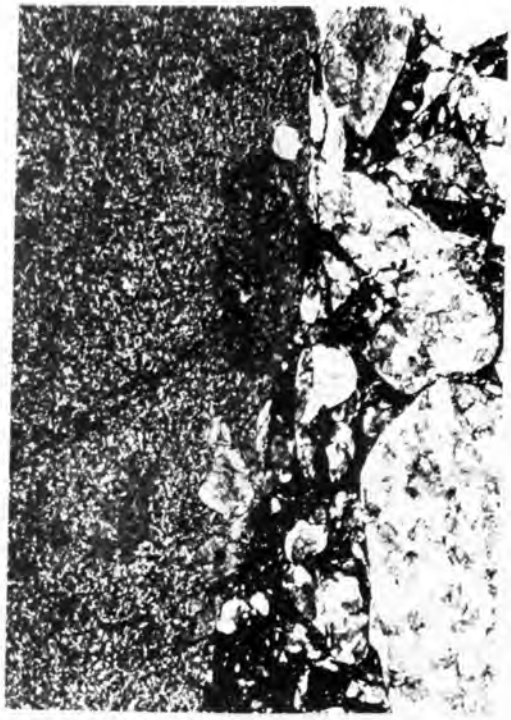

B

C

D

PLATE 19

A. Dunite texture, Ewarara.

A300-501a PPL Width of field 12mm

B. Picrite texture, Ewarara.

A300-84 PPL Width of field 18mm

C. Olivine leucogabbro texture, Ewarara. Note plagioclase lamination, and dark coronas (pyroxene/spinel) around orthopyroxene pseudomorphs after olivine.

A301-153 PPL Width of field 18mm

D. Quartz xenoliths in basaltic material, Ewarara.

A300-399a Scale 30mm

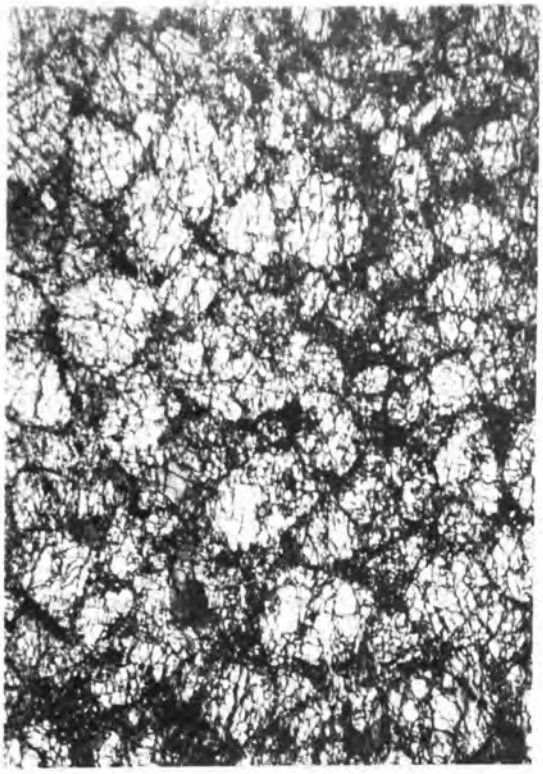

A

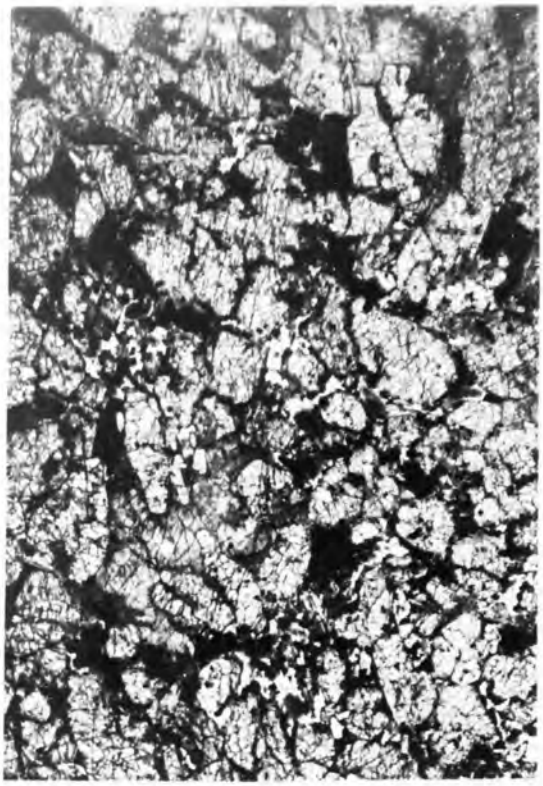

B

C

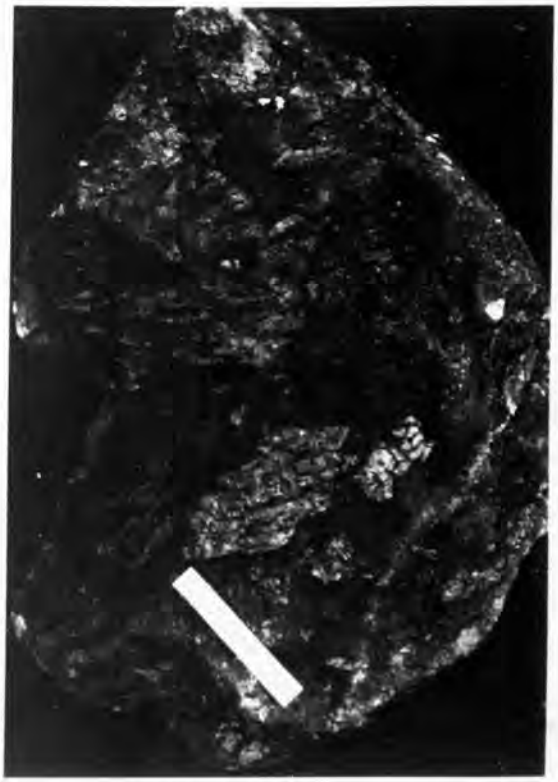

D

PLATE 20

A. Magnetite/ilmenite/spinel aggregates surrounded by rims of biotite (dark grey) and hornblende (h).

A300-712 PPL Width of field 1.4mm

B. Preferential development of opaque exsolution at edges of pyroxene grains adjacent to biotite (dark grey, centre) but not next to plagioclase or pyroxene (left, right).

A300-712 PPL Width of field 1.6mm

C. Radiating plagioclase laths, marginal dolerite. Note central trails of pyroxene inclusions in the laths.

A314-116a PPL Width of field 5mm

D. Contact between marginal dolerite and acid granulite (top right). Note thin pyroxene selvage at contact, with adjacent thin plagioclase selvage. Radiating plagioclase/pyroxene groups become coarser grained inwards from contact.

A300-83 PPL Width of field 14mm

A

B

C

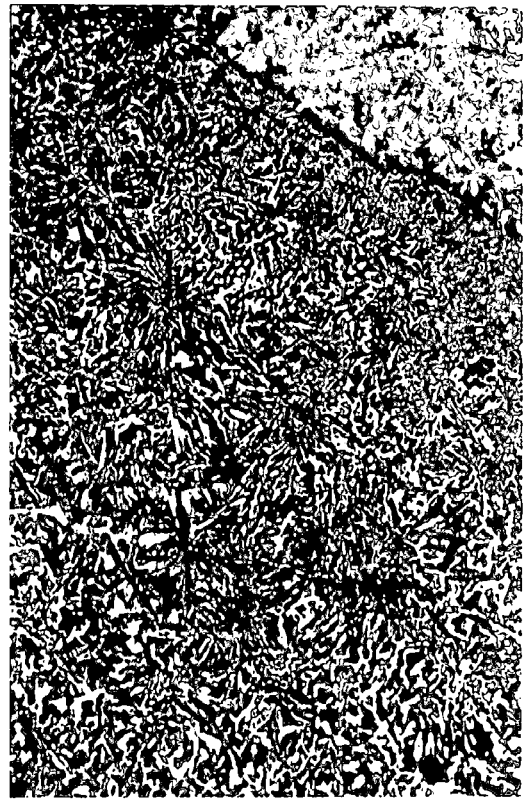

D

PLATE 21

A. Coarse-grained gabbroic xenoliths in medium-grained gabbro with plagioclase-rich margins, Kalka.

A314-385 Scale 4.3cm

B. Orthopyroxene phenocrysts in medium-grained gabbro, Kalka.

A314-360 PPL Width of field 18mm

C. Medium-grained gabbro texture, Kalka. Note plagioclase-rich schleiren.

A314-348 PPL Width of field 18mm

D. Opaques filling fractures in deformed plagioclase laths, gabbro, Kalka.

A314-190 PPL Width of field 7mm

A

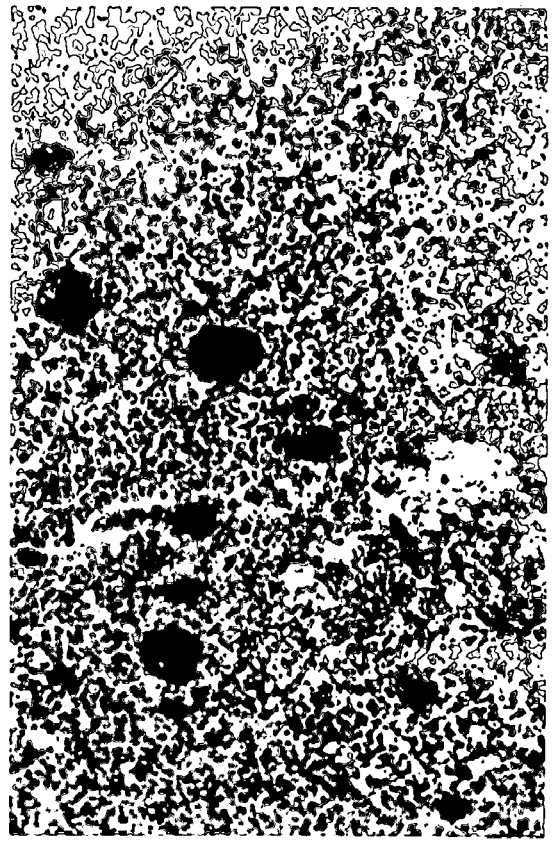

B

C

D

PLATE 22

A. Rounded clinopyroxene inclusions arranged in annular zone in orthopyroxene, transgressive norite, Ewarara.

A300-502a PPL Width of field 5mm

B. Wormy spinel aggregate, transgressive norite, Ewarara.

A300-502a PPL Width of field 0.9mm

C. Cross-section of skeletal apatite crystal, anorthosite, Ewarara. Note associated intergrowth of plagioclase and potassium feldspar (bottom).

A300-105b PPL Width of field 0.1mm

D. Plagioclase - potassium feldspar intergrowth adjacent to plagioclase phenocryst (right), anorthosite, Ewarara.

A300-105b PPL Width of field 0.9mm

A

B

C

D

PLATE 23

A. Relic primary pyroxene crystal (with opaque exsolution plates) surrounded by granular secondary pyroxene aggregates. Note small granular opaque grains in secondary assemblage indicating former extent of primary grain. Note development of S_4 fracture cleavage in both assemblages.

A300-368 PPL Width of field 1.4mm

B. Anorthosite texture, Ewarara. Plagioclase (white), plagioclase/K feldspar intergrowths (grey), pyroxene (black). Note bending of plagioclase laths.

A300-105b PPL Width of field 17mm

C. Fingerprint texture in clinopyroxene formed by spinel trails. Note granular spinel in associated recrystallized assemblage.

A300-502a PPL Width of field 0.9mm

D. Pyroxenite texture. Note interstitial nature of opaques.

A300-359 PPL Width of field 15mm

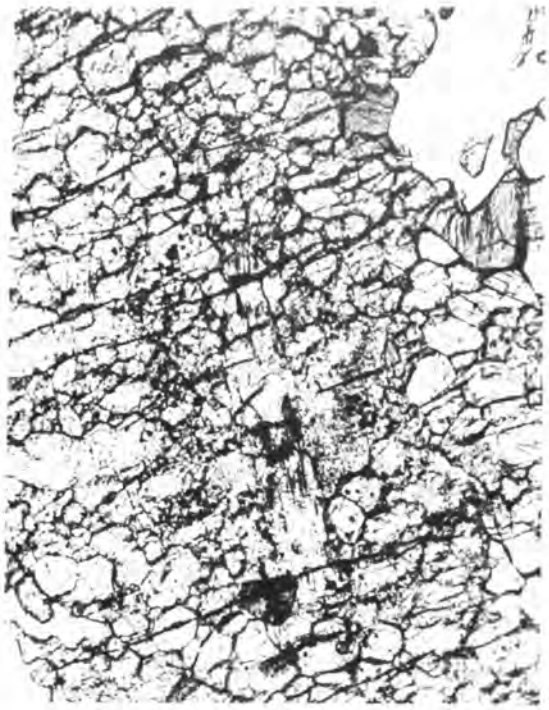

A

B

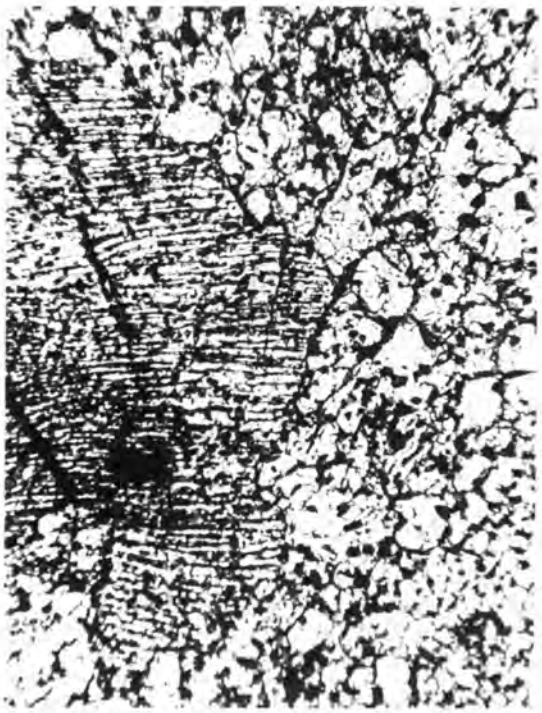

C

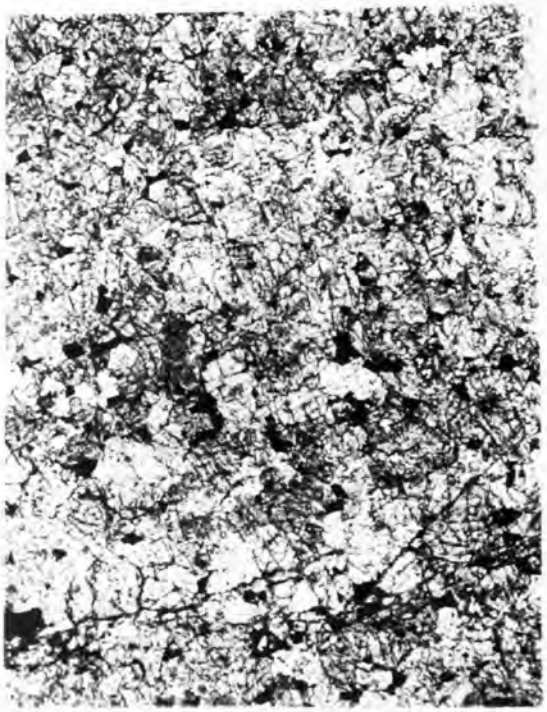

D

PLATE 24

A. Haematite lamellae in magnetite, acid pegmatite, Kalka.

A314-405d PPL (reflected light) Width of field 0.2mm

B. Ilmenite lamellae in haematite, acid pegmatite, Kalka. Note change of orientation of lamellae across twins, and presence of ilmenite rim at the edge of the haematite grains.

A314-405d PPL (reflected light) Width of field 0.2mm

C. Acid pegmatite in cores of F_2 folds, granulite xenolith, Johnson Creek, Kalka. Also note ovoidal potassium feldspar crystal near end of scale.

A314-96 Scale 4.3cm

D. Graphic intergrowth between quartz and orthoclase, acid pegmatite, Kalka.

A314-757 Scale 4.3cm

A

B

C

D

PLATE 25

A. Texture of pyroxenite band in garnet pyroxenite, Ewarara.

A300-713 CP Width of field 24mm

B. Plagioclase rims between spinel and pyroxene, garnet pyroxenite, Ewarara.

A300-713 PPL Width of field 0.9mm

C. Magnetite intergrowth in garnet porphyroblast, garnet pyroxenite, Ewarara.

A300-713 PPL Width of field 0.5mm

D. Garnet rims (g) between orthopyroxene (op) and plagioclase, garnet pyroxenite, Ewarara.

A300-713 PPL Width of field 0.5mm

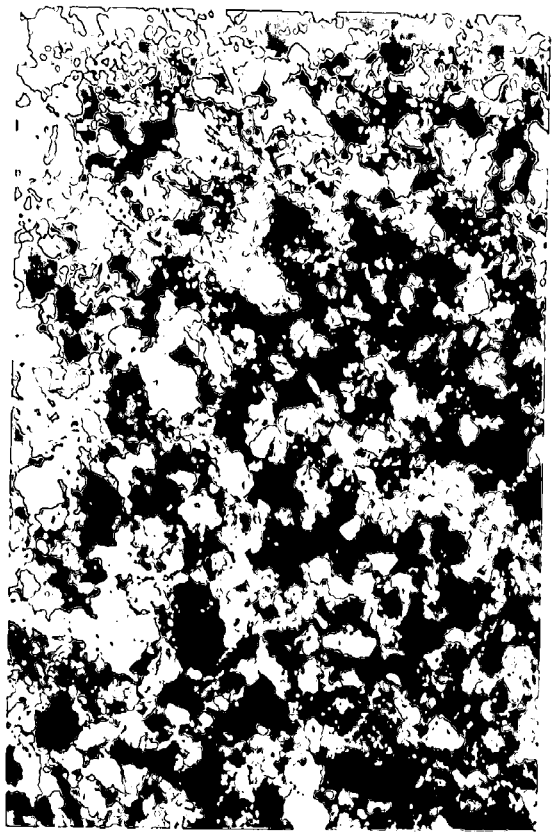

A

B

C

D

PLATE 26

A. Intergrowths between spinel (dark) and orthopyroxene (grey), and plagioclase (white) in garnet pyroxenite, near Ewarara.

A300-713 PPL Width of field 0.9mm

B. Garnet rim surrounding spinel (dark) in contact with orthopyroxene, garnet pyroxenite.

A300-713 PPL Width of field 0.5mm

C,D Garnet - orthopyroxene and plagioclase intergrowths adjacent and gradational to garnet porphyroblast, garnet pyroxenite. Note rare relic spinel grains (top of picture), one surrounded by garnet rim, the other with no associated garnet, suggesting a compositional control on the reaction spinel + orthopyroxene $\longrightarrow$ garnet.

A300-713 C. PPL Width of field 0.9mm
D. CP

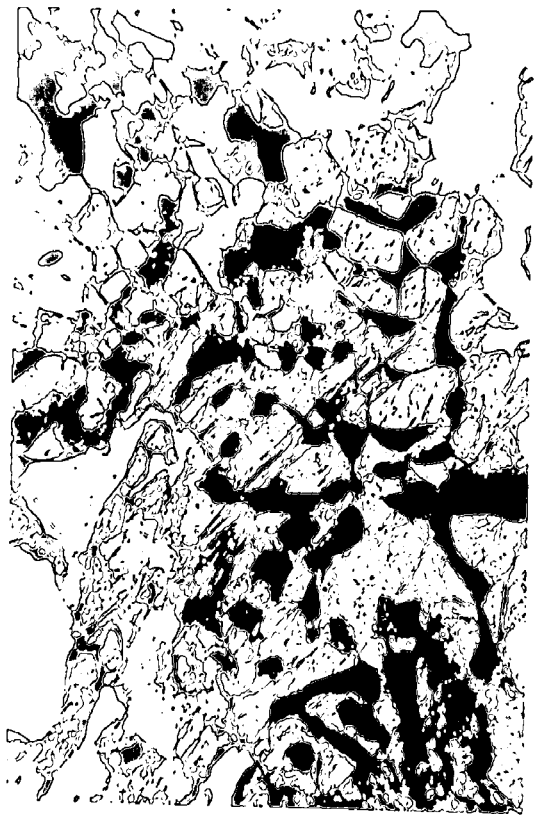

A

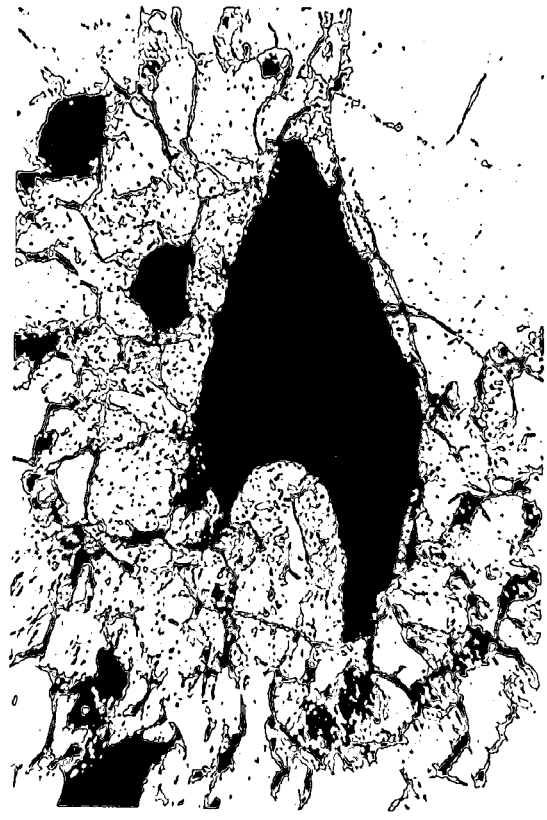

B

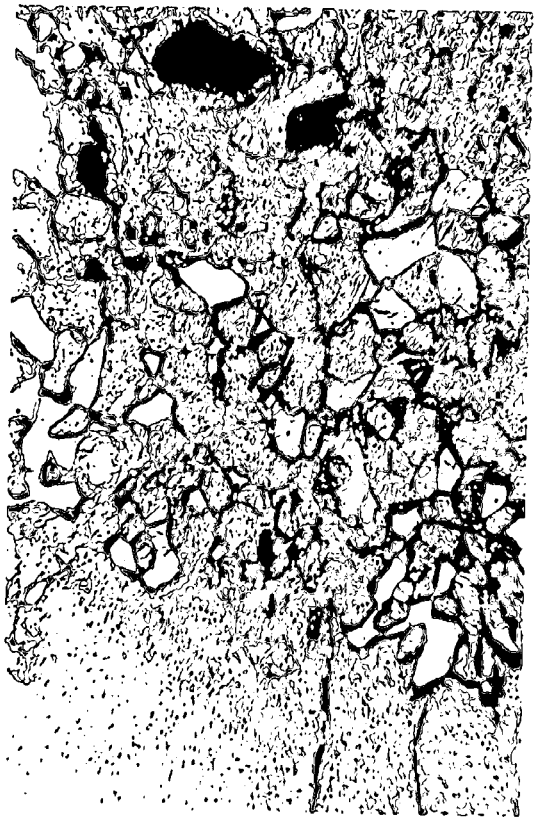

C

D

PLATE 27

A. Sharp contact between acid granulites and the chilled margin of the Ewarara Intrusion on the northwestern side of the body. Note the transgressive nature of the contact relative to the S_1^m foliation in the granulites.

B. Sub-horizontal fine scale igneous layering in the Pyroxenite Zone of the Ewarara Intrusion, northeastern Ewarara.

Photograph by G.W. Krieg. Scale 40cm

C. Small scale vertical igneous layering in Pyroxenite Zone of the Ewarara Intrusion, near the intertongued zone.

Scale 40cm

D. Flow alignment of potassium feldspar phenocrysts in the Taratap Adamellite, near Kingston, South-East of South Australia.

Scale 4.5cm

A

B

C

D

PLATE 28

A. Aligned elongate clinopyroxene plates in pyroxenite, Ewarara.

A300-700 Scale 4.3cm

B. Anhedral spinel crystal in centre of interstitial plagioclase grain, pyroxenite, Ewarara.

A300-132 PPL Width of field 0.9mm

C. Arrowhead structure outlined by massed spinel exsolution in elongate clinopyroxene, Ewarara. Note recrystallized matrix.

A300-700 PPL Width of field 5mm

D. Fabric delineated by variations in density of spinel exsolution in clinopyroxene and alignment of plagioclase aggregates in pyroxenite, Ewarara.

A300-700 PPL Width of field 5mm

A

B

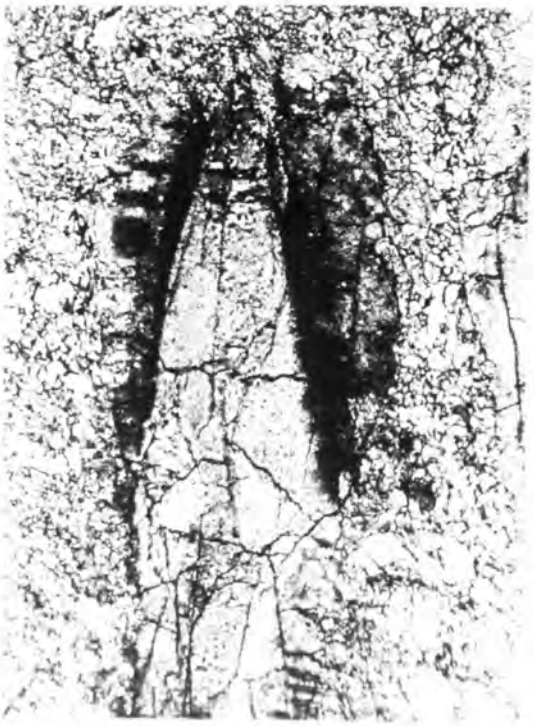

C

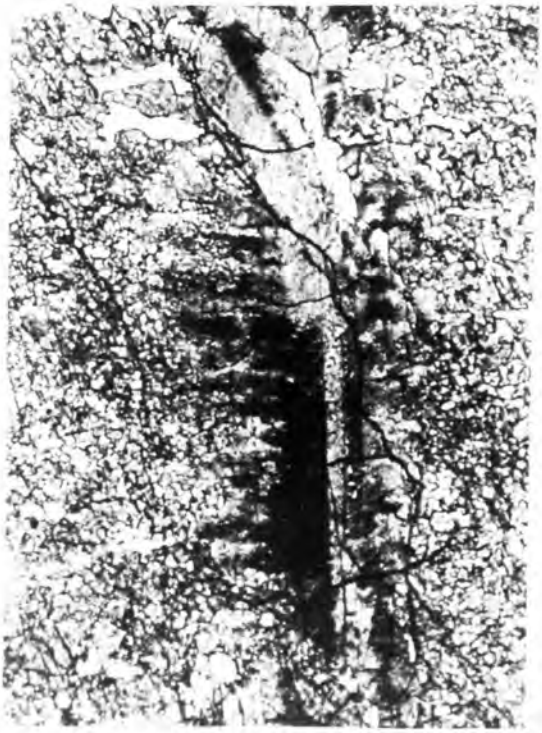

D

PLATE 29

A. Kalka Intrusion, looking south from the Ewarara Intrusion. Mt Kalka is the highest point of the ridge with Scarface forming the large cliff to its left, and Kalka Gorge the prominent ravine to its right. The other prominent gorge further to the right is Epipinja with Walter Hill forming the small peak to its right (both of these features are located on the photograph above the black "tip heap" in the middle foreground).

B. Mt Kalka from the southwest in the N2c Subzone in West Kalka. The granulite sliver occurs near the base of the slope. Note the prominent large scale layering near Mt Kalka summit.

C. Prominent large scale layering in the Norite Zone of the Kalka Intrusion taken from near the head of Kalka Gorge, looking east.

A

B

C

PLATE 30

A. Sharp boundary between quartz xenolith (right, white and black - note sutured internal boundaries) and dolerite, Kalka. Note "myrmekitic" intergrowths in dolerite (bottom left).

A314-472 CP Length of field 1.4mm

B. Plagioclase-rich doleritic rim (grey) between quartz - feldspar xenolith and normal dolerite, Kalka.

A314-472 PPL Length of field 11mm

C,D Acid lenses and blebs in recrystallized doleritic marginal phases, Kalka. Note prominent S_1^g foliation.

C. A314-451a Scale 4.3cm
D. A314-71

E. Acid vein cutting marginal basic rock, Kalka.

A314-451b Scale 5cm

F. "Myrmekitic" intergrowth at edge of acid vein in annealed basic rock, Kalka.

A314-451b PPL Length of field 2.0mm

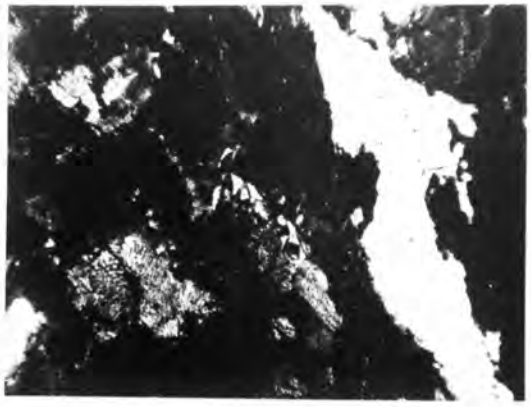

A

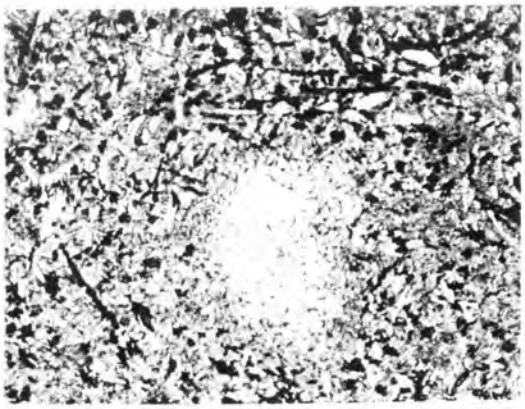

B

C

D

E

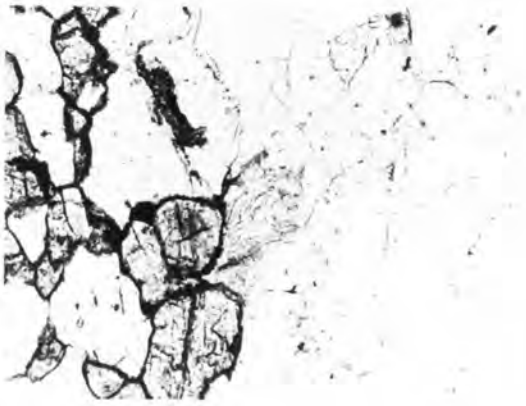

F

PLATE 31

A. Adcumulate texture in orthopyroxenite, Kalka. Note interlocking grain boundaries.

A314-92 CP Length of field 23mm

B. Orthocumulate texture in orthopyroxenite, Kalka. Note euhedral nature of cumulus orthopyroxene, and recrystallized groundmass.

A314-157 PPL Length of field 23mm

C. Orthocumulate texture in orthopyroxenite, Kalka. Note packing texture and lack of recrystallization.

A314-500 PPL Length of field 10mm

D. Interstitial plagioclase with development of antiperthite at grain edges, pyroxenite, Kalka.

A314-156 PPL Length of field 1.4mm

E. Planar igneous lamination outlined by cumulus plagioclase in leuconorite.

A314-148 CP Length of field 8mm

F. Cumulate texture, clinopyroxene leuconorite, Kalka. Note planar igneous lamination.

A314-146 PPL Length of field 23mm

G. Cumulate texture, magnetite gabbro, Kalka.

A314-234 PPL Length of field 24mm

H. Cumulate texture, dunite, Kalka.

A314-337 CP Length of field 24mm

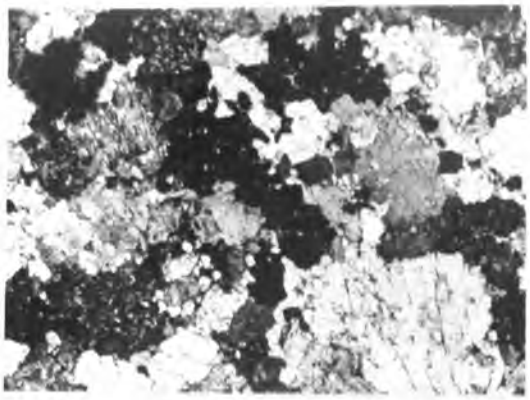

A

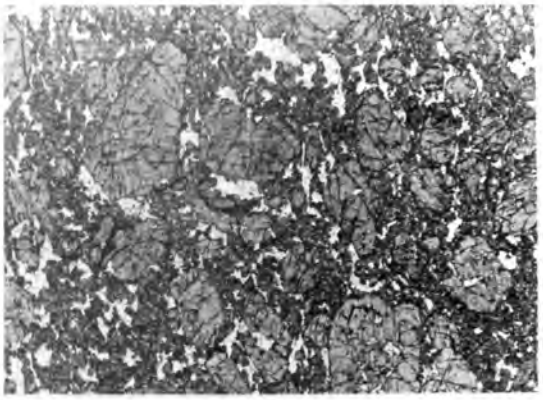

B

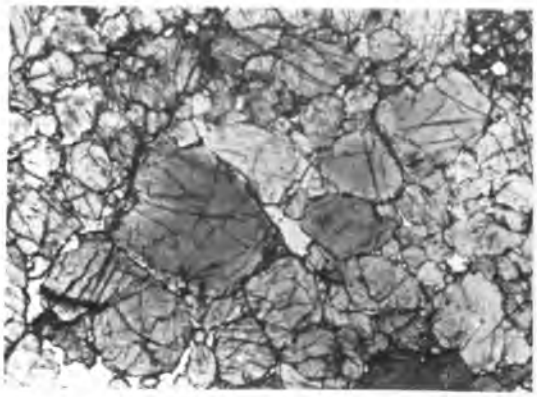

C

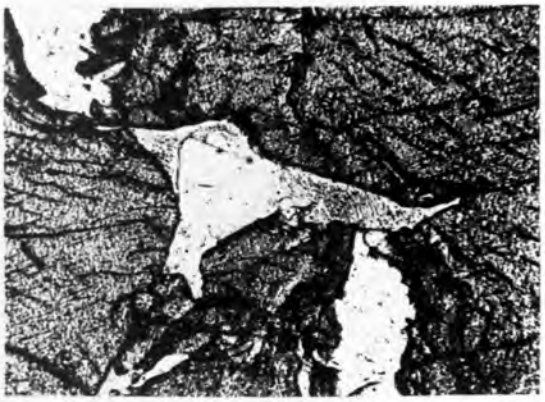

D

E

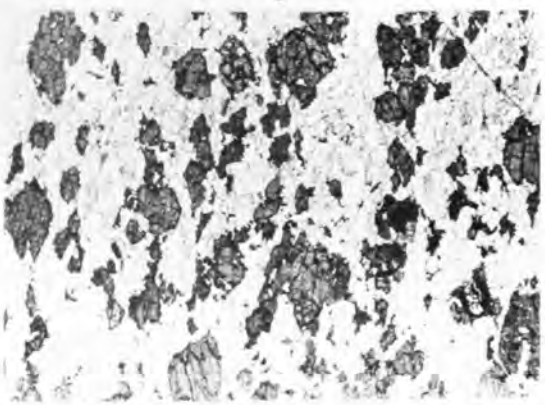

F

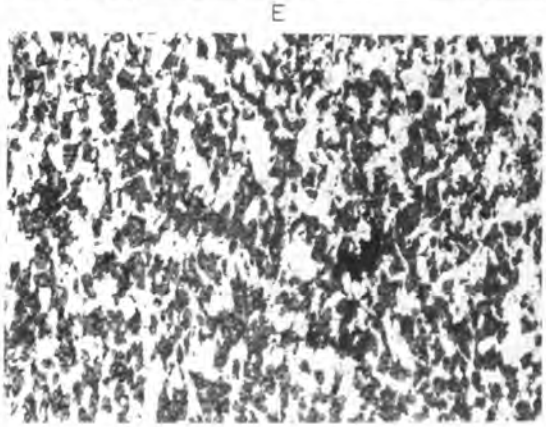

G

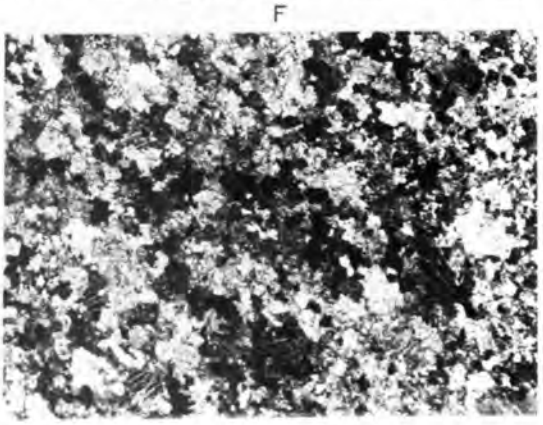

H

PLATE 32

A. Cumulate texture, troctolite, Kalka. Note plagioclase laths in olivine and local development of pyroxene/spinel symplectites (dark) at olivine - plagioclase boundaries.

A314-197 PPL Length of field 23mm

B. Orthopyroxene megacrysts in hybrid marginal phase, Ewarara.

Scale 4.3cm

C. Adcumulate texture, anorthosite, Kalka, showing development of minor interstitial pyroxene.

A314-198 PPL Length of field 23mm

D. Orthocumulate texture, leucogabbro, Kalka. Note major development of interstitial pyroxene (plagioclase is sole cumulus phase).

A314-388 PPL Length of field 8mm

E,F "Clump" textures in anorthosite, West Kalka.

Scale 12.5cm

G. Parallel arrangement of lenticular "clumps" in leucogabbro, West Kalka.

Scale 12.5cm

H. "Clump" texture, leucogabbro, West Kalka. Plagioclase is sole cumulus phase; pyroxene is interstitial phase in dark clumps (e.g. right), plagioclase in light clumps (centre).

A314-193 PPL Length of field 23mm

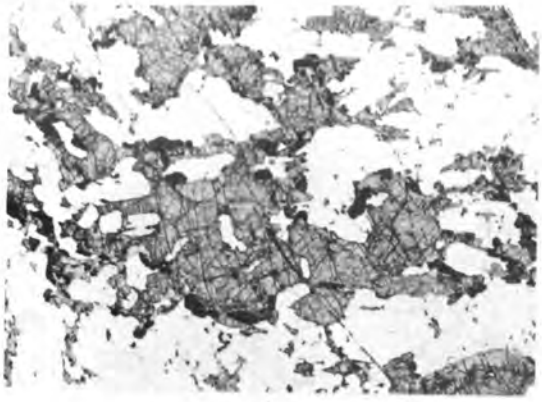

A

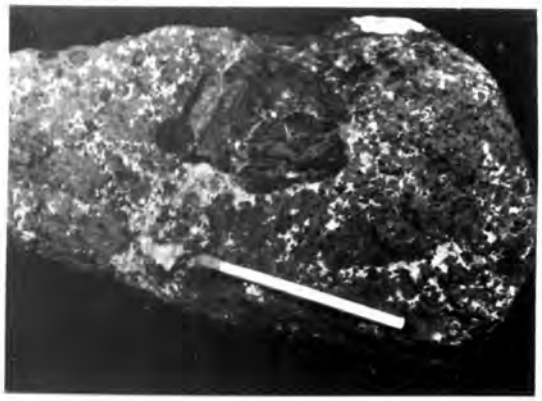

B

C

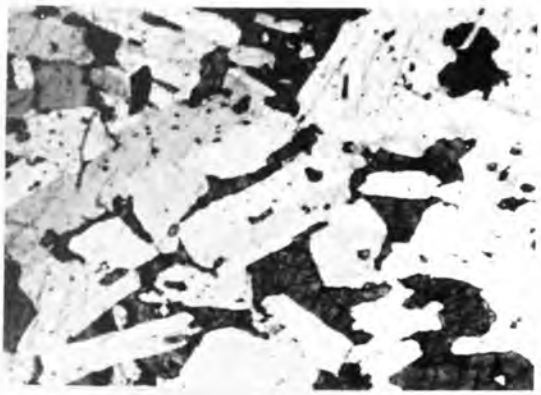

D

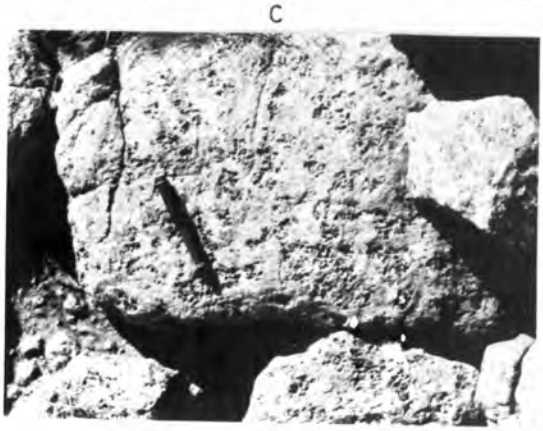

E

F

G

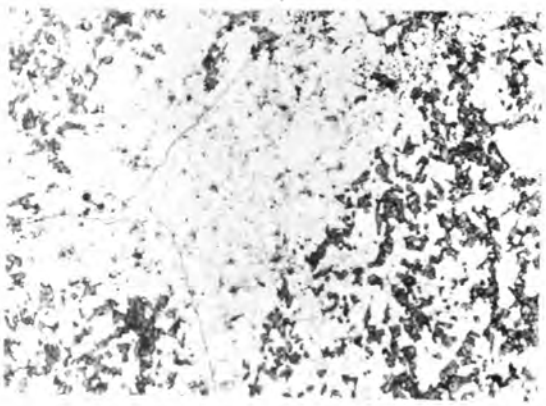

H

PLATE 33

A. Oblique aerial view of the southern part of the Kalka Intrusion, looking west towards Hinckley Range. Ninno Creek in left foreground, Ochre Creek right. Note presence of large scale igneous layering.

Photograph by R.W. Nesbitt.

B. Overturned small scale igneous layering formed by alternating pyroxene-rich and plagioclase-rich bands, Johnson Horizon, Waralkulpa. Note pyroxene-rich layer group (right) and plagioclase-rich layer group (left).

Scale 12.5cm
(pen, centre)

A

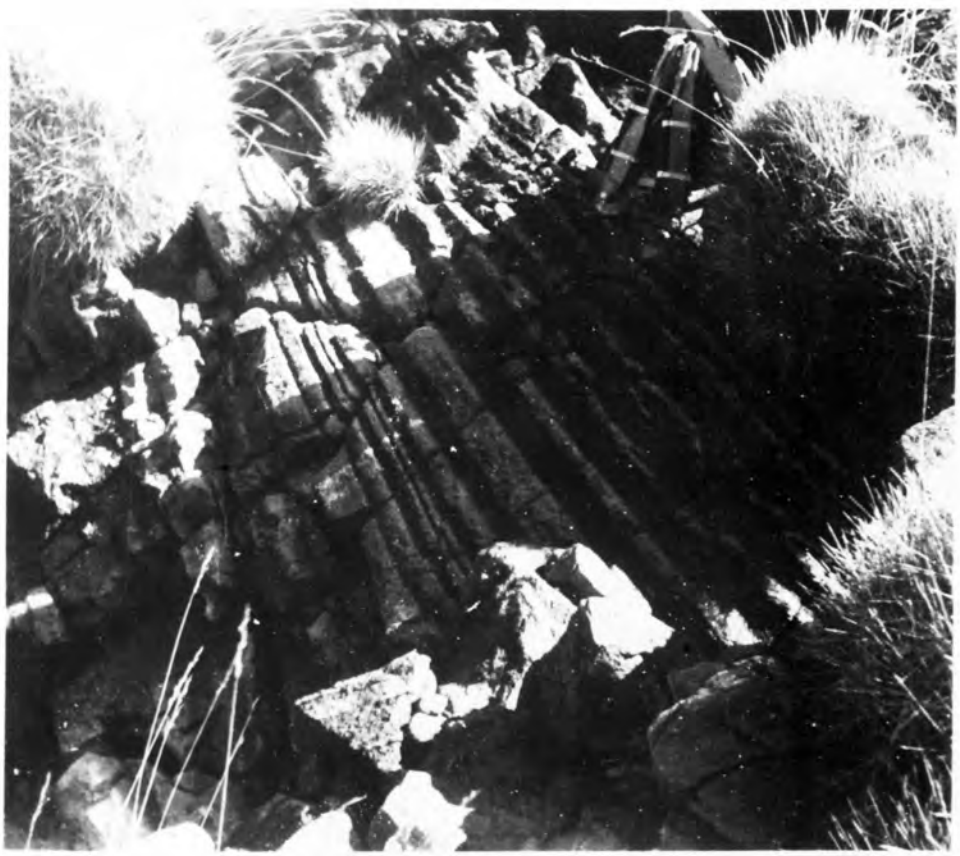

B

PLATE 34

A. Mineral graded layering (pyroxene-rich to plagioclase-rich), Johnson Horizon, Kalka.

Scale 12.5cm

B. Small scale isomodal layering, field station 509, Kalka.

Scale 12.5cm

C. Planar igneous lamination, orthopyroxenite, Kalka.

Scale 4.3cm

D. Continuous grading, small scale igneous layering, Rockhole Creek, Kalka.

Scale 12.5cm

E. Deformed banded quartzite "xenoliths" with associated "lacy network" veining of norites, Kalka.

Scale 12.5cm

A

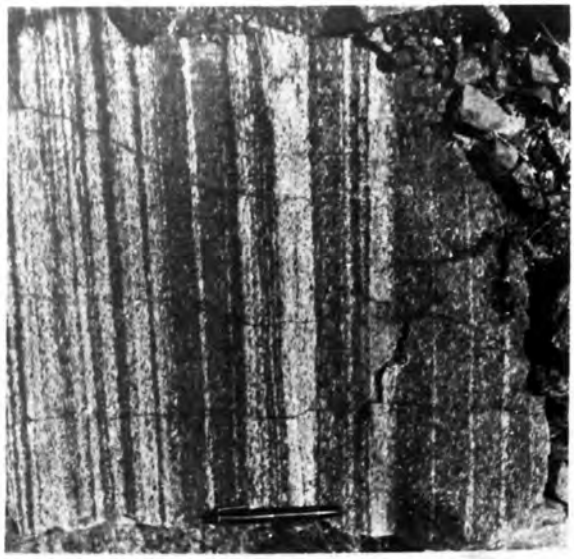

B

C

D

E

PLATE 35

A. Small scale igneous layering, Olivine Gabbro Zone, Kalka. Olivine-clinopyroxene layers (depressed) and clinopyroxene layers.

A314-400 Scale 4.3cm

B. Small scale igneous layering, N3 Subzone, Kalka. Olivine-rich layers (depressed), clinopyroxene-rich layers and rare plagioclase-rich layers.

A314-206 Scale 4.3cm

C. Part of scour channel, Kalka Gorge. Alternating mesonorite and anorthosite bands (bottom) cut-off by anorthosite band (below and parallel to hammer). Overlain by massive mesonorite.

Scale 90cm

D. Tectonic cross-stratification, Johnson Creek, Kalka. Both layering, S_0^9, and foliation, S_1^9, discordant between upper and lower parts.

Scale 4.3cm

E. Load cast by pyroxenitic band in mesonorite, Johnson Creek, Kalka. Foliation, S_1^9, parallel to scale throughout structure.

Scale 4.3cm

F. Small scale igneous layering, Kalka Intrusion. Alternation of isomodal pyroxenitic and mesonorite bands. Rare size graded mesonorite layers.

A314-235 Scale 4.3cm

A

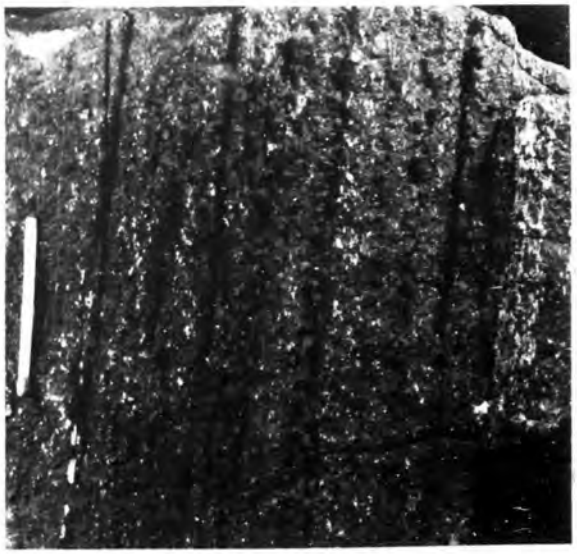

B

C

D

E

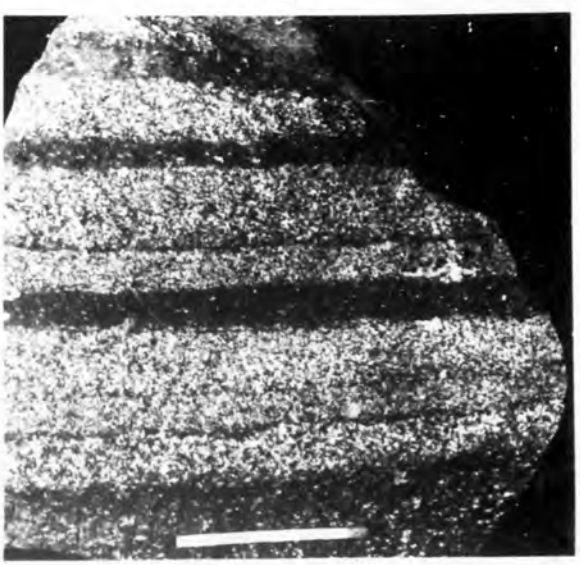

F

PLATE 36

A. Truncation of clinopyroxene band by younger clinopyroxenite band in anorthositic sequence, West Kalka.

Scale 2.5cm

B. Cross-stratification, West Kalka.

Scale 12.5cm

C. Small-scale igneous layering between pyroxenitic and leuco-gabbroic bands, West Kalka.

Scale 12.5cm

D. Lateral thickening of gabbroic band in anorthositic sequence, West Kalka.

Scale 12.5cm

E. Anorthositic lens, West Kalka. Note asymmetric structures developed on upper surface with associated thinning on crests in overlying gabbroic band.

Scale 90cm

A

B

C

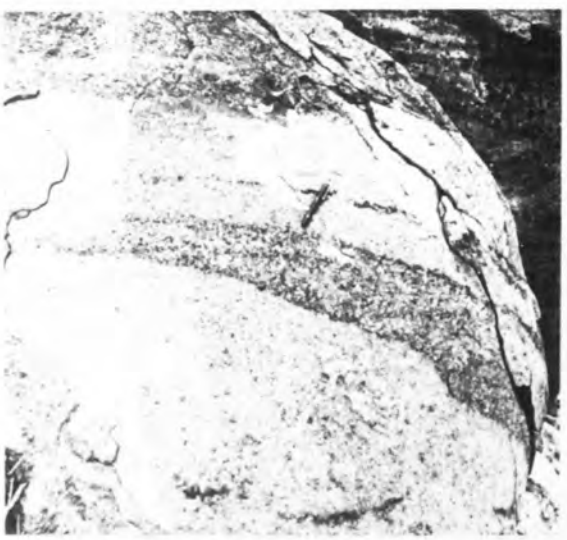

D

E

PLATE 37

A. Olivine - spinel intergrowth at olivine grain boundary, Kalka.

A314-182 PPL Length of field 1.4mm

B. Biotite - pyroxene(?) intergrowth, Kalka.

A314-196 PPL Length of field 0.3mm

C. Hornblende (dark grey) and clinopyroxene (medium grey) rims around opaques, Kalka.

A314-182 PPL Length of field 2.0mm

D. Clinopyroxene (grey) as optically continuous rims and lamellae in orthopyroxene (black), Kalka.

A314-450 CP Length of field 2.0mm

E. Hornblende forming irregular rims on clinopyroxene (exsolving opaques), Kalka.

A314-418 PPL Length of field 1.4mm

F. Magnetite exsolution plates in olivine.

A300-84 PPL Length of field 1.4mm

G. Pyroxene/spinel symplectite as discontinuous rim on cumulus clinopyroxene, Kalka.

A314-357 PPL Length of field 0.8mm

H. Double corona of orthopyroxene (lower rim) and clinopyroxene/spinel (upper rim) between olivine (bottom left) and plagioclase (top right). Plagioclase clouded to near opacity by small spinel rods.

A300-84 PPL Length of field 0.6mm

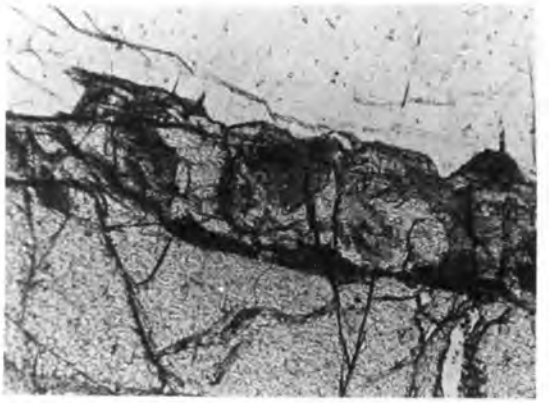

A

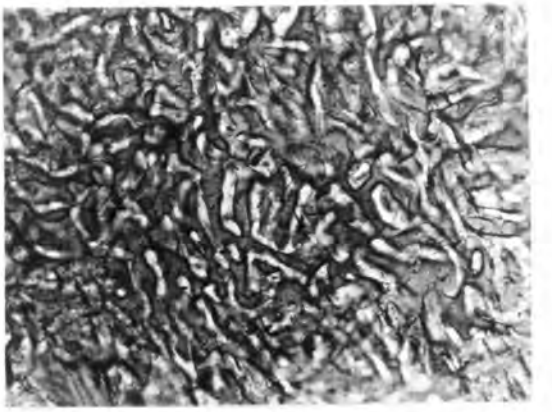

B

C

D

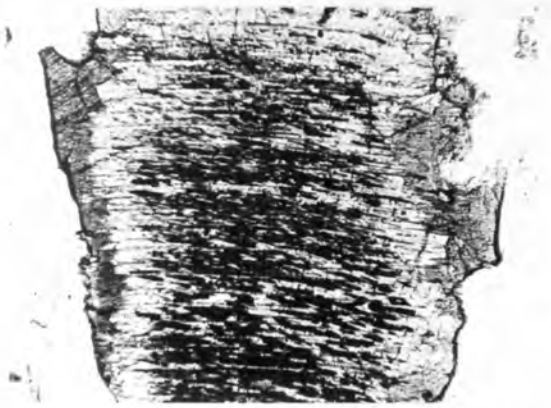

E

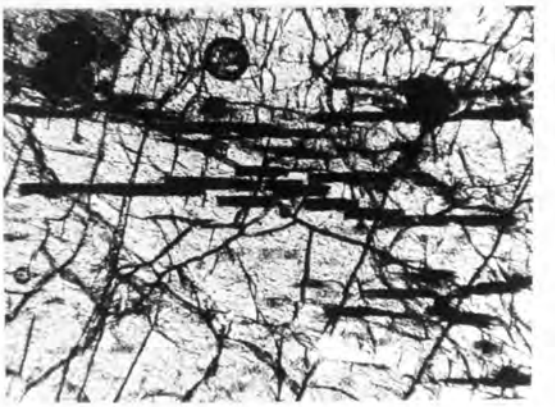

F

G

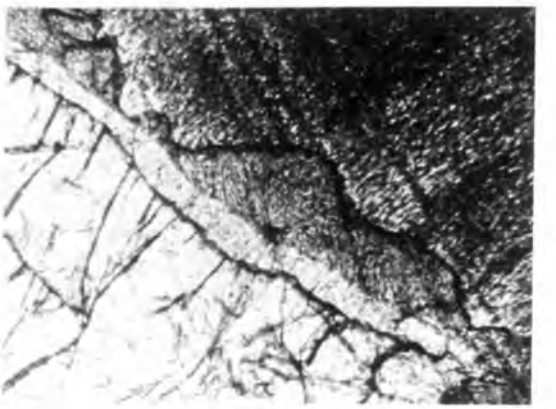

H

PLATE 38

A. Intergrowth between pyroxene (dark) and magnetite/ilmenite between cumulus olivine grains (large dark grains).

A314-233 PPL Length of field 0.6mm

B. Aggregate of pyrrhotite (top, white) and chalcopyrite (bottom, grey) in leucotroctolite, Kalka. Note twinning in chalcopyrite.

A314-357 PPL Length of field 0.3mm

C. Spinel exsolution lamellae in magnetite (light grey). Note decrease in lamellae grain size towards grain boundaries, intergrowth between magnetite and spinel(?) grains (centre left), intergrowth between spinel and ilmenite near ilmenite - magnetite grain boundary (centre right).

A314-357 PPL Length of field 0.3mm

D. Intergrowth between magnetite (bottom) and spinel (top) at grain boundary.

A300-359 PPL Length of field 0.3mm

E. Discontinuous spinel rim (black) between ilmenite (dark grey) and magnetite (light grey). Note decrease in grain size of spinel exsolution in magnetite towards grain boundary.

A314-362 PPL Length of field 0.3mm

F. Spinel (black) - haematite (white) exsolution lamellae in ilmenite.

A314-362 PPL Length of field 0.3mm

G. Oriented ilmenite inclusions (dark grey) with discontinuous spinel rims (black) in magnetite (light grey) containing spinel exsolution lamellae.

A314-201 PPL Length of field 0.3mm

H. Bireflectance variations in ilmenite, probably representing twinning.

A314-383 PPL Length of field 0.3mm

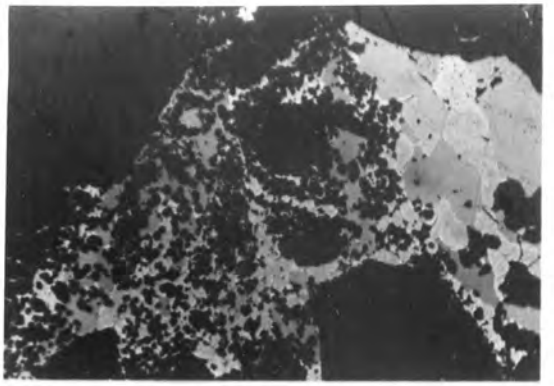

A

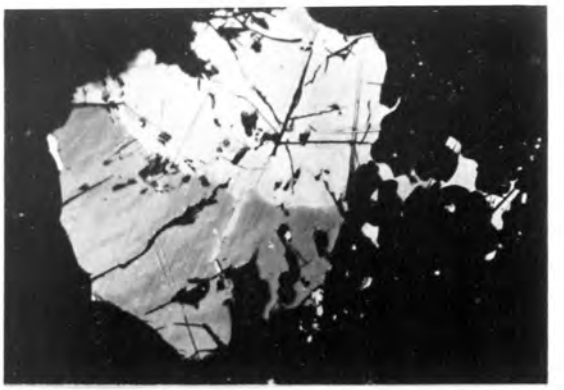

B

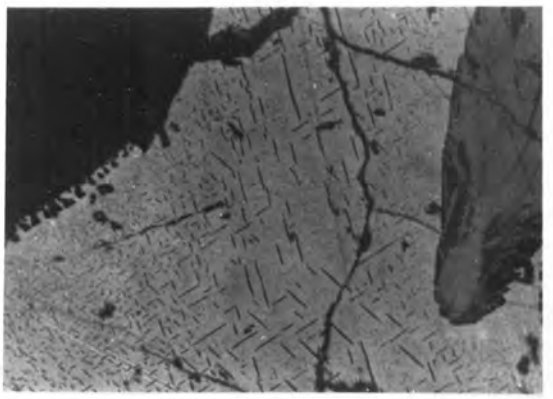

C

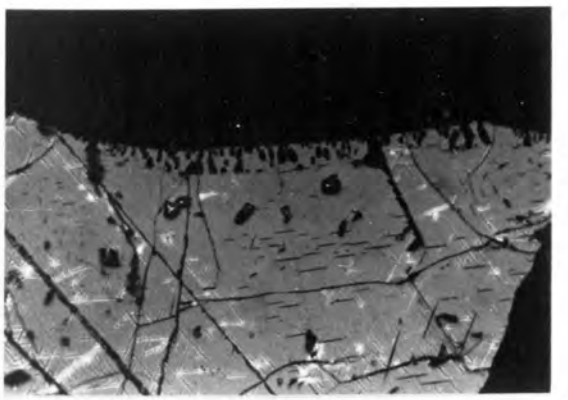

D

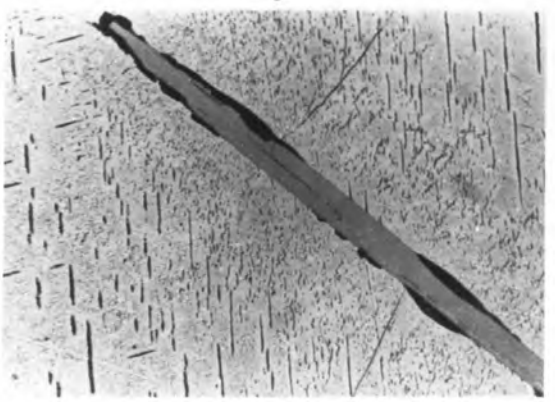

E

F

G

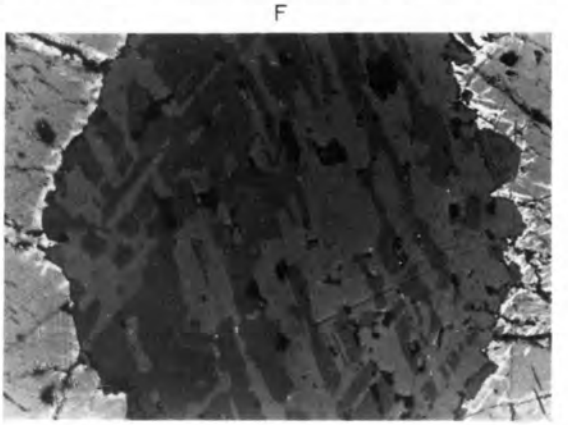

H

PLATE 39 ELECTRON MICROPROBE PHOTOMICROGRAPHS*

A,B. Orthopyroxene and chrome-bearing magnetite lamellae in clinopyroxene (A314-418). Width of field 50μ.

A. Ca K_α radiation (only orthopyroxene visible).
B. Fe K_α radiation

C. Clinopyroxene lamellae in orthopyroxene (A300-110).

Ca K_α radiation Width of field 100μ.

D,E. Spinel lamellae in clinopyroxene (A314-411).

D. Cr K_α radiation Width of field 50μ.
E. Fe K_α radiation

F. Rutile exsolution in clinopyroxene (A314-209).

Ti K_α radiation Width of field 100μ.

G-I. Orthopyroxene (op) and clinopyroxene/spinel (cs) reaction rims between olivine (ol) and plagioclase (pl). (A300-84). Note spinel exsolution in plagioclase.

G. Mg K_α radiation Width of field 100μ.
H. Ca K_α radiation
I. Fe K_α radiation

J-L. Chrome magnetite plates in orthopyroxene (A300-110).

J. Absorbed electron image Width of field 100μ.
K. Cr K_α radiation
L. Fe K_α radiation

* Photographs by Mr. P. Schultz of AMDEL, Adelaide.

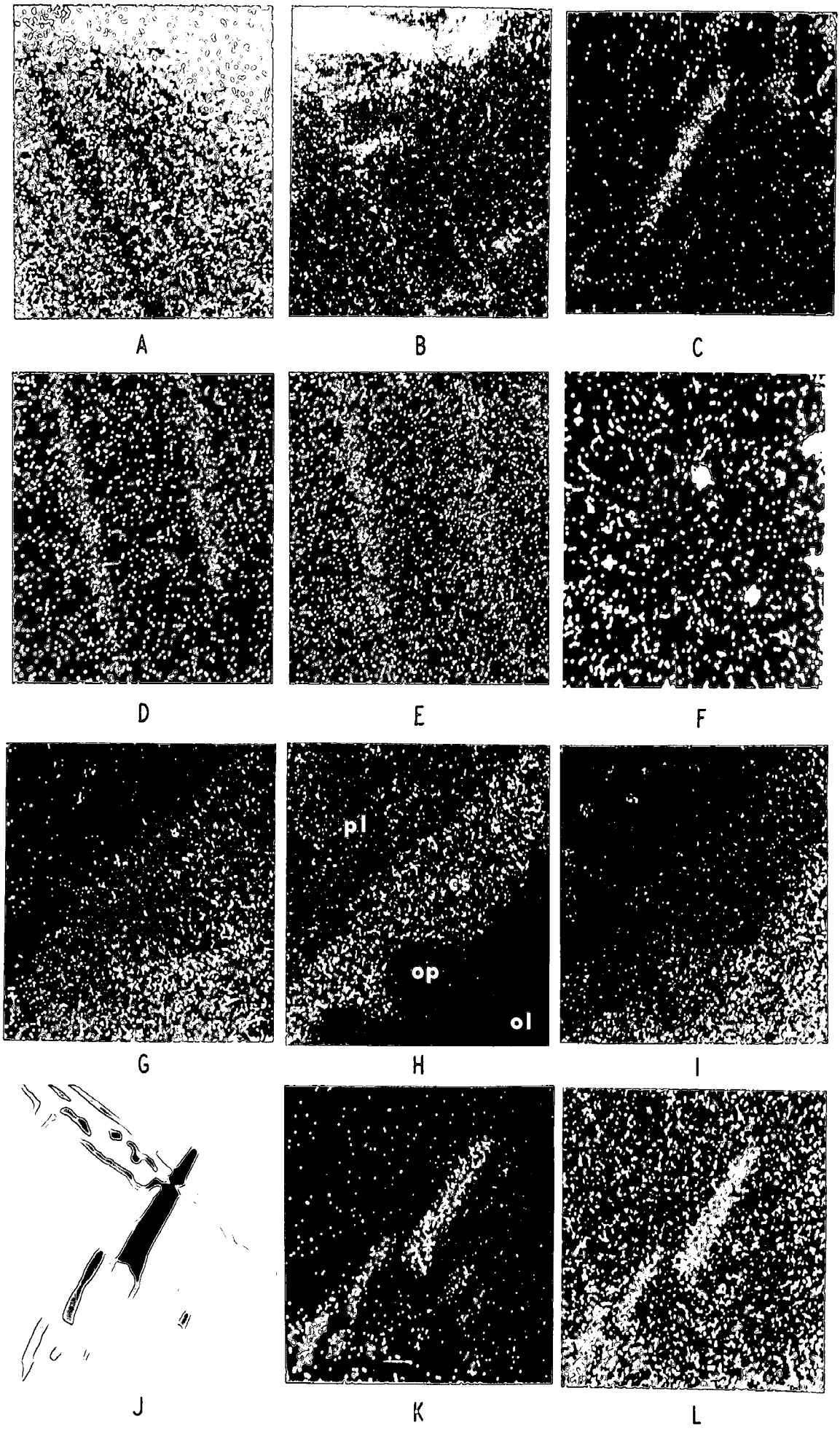
A
B
C
D
E
F
pl
cs
op
ol
G
H
I
J
K
L

PLATE 40 ELECTRON MICROPROBE PHOTOMICROGRAPHS*

A-C. Titaniferous magnetite exsolution in plagioclase (A314-418).

A. Absorbed electron image showing position of line scan. Width of field 50μ.
B. Ti K_α radiation (line scan)
C. Fe K_α radiation (line scan)

D-F. Spinel exsolution in plagioclase (A300-84).

D. Mg K_α radiation Width of field 50μ.
E. Si K_α radiation
F. Fe K_α radiation

G-J. Orthopyroxene - spinel intergrowths adjacent to spinel grain (sp) in olivine (A300-84).

G. Mg K_α radiation Width of field 100μ.
H. Al K_α radiation
I. Fe K_α radiation
J. Cr K_α radiation

K,L. Chrome-bearing magnetite lamellae in olivine (A300-84).

K. Cr K_α radiation Width of field 50μ.
L. Fe K_α radiation

* Photographs by Mr. P. Schultz of AMDEL, Adelaide.

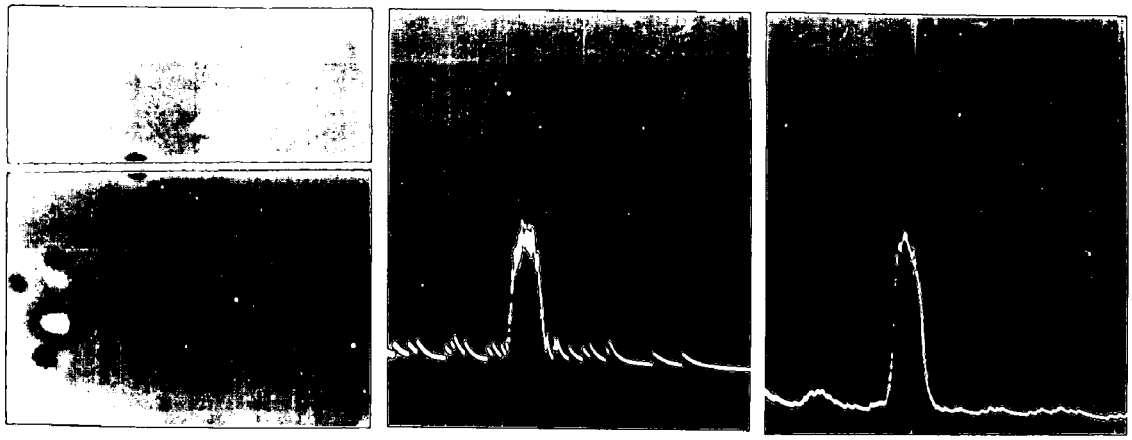

A B C

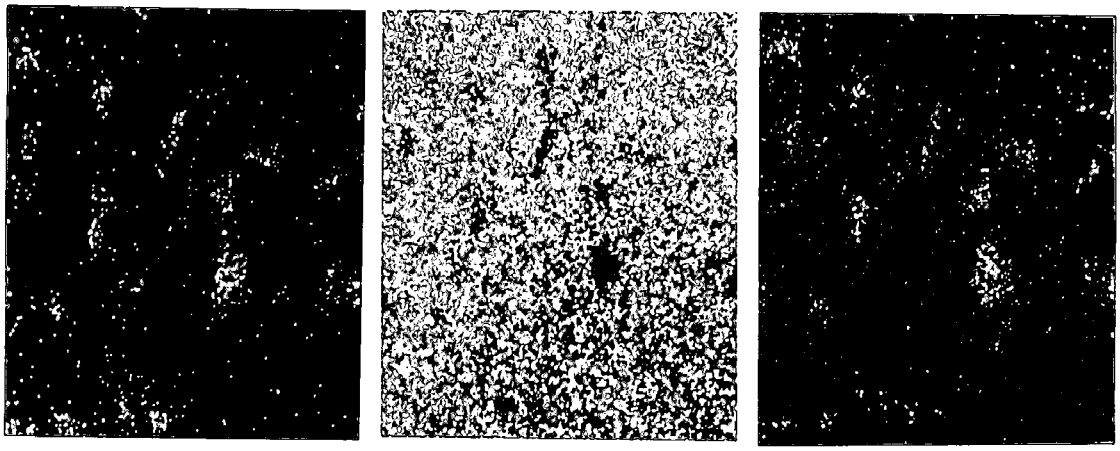

D E F

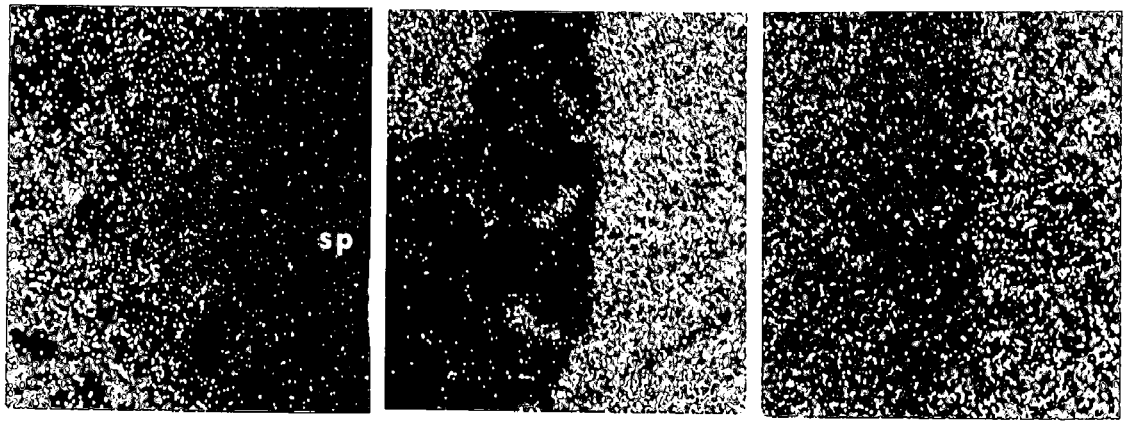

G H I

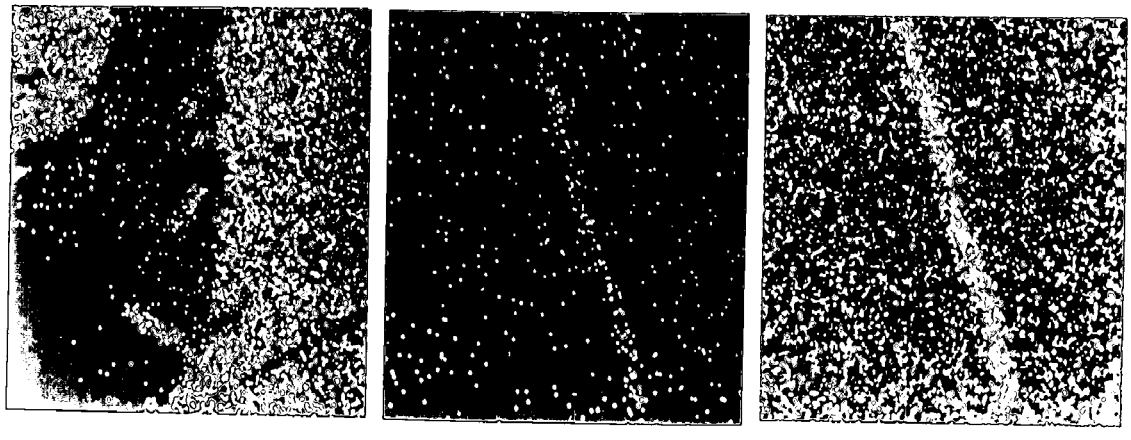

J K L

PLATE 41

A. Clinopyroxene lamellae in orthopyroxene. Note concentration of lamellae on plane of bending, and lack of lamellae adjacent to coarse irregular clinopyroxene patches.

A314-148 CP Length of field 2.0mm

B. Branching clinopyroxene lamellae in orthopyroxene.

A314-133 CP Length of field 2.0mm

C. Kinked orthopyroxene containing clinopyroxene lamellae.

A314-123 CP Length of field 2.0mm

D. Clinopyroxene exsolution lamellae in orthopyroxene (top half). Bushveld type lamellae (horizontal) and Stillwater type lamellae (upright).

A314-449 CP Length of field 0.8mm

E. Stillwater type (upright) and Bushveld type (oblique) clinopyroxene exsolution lamellae in orthopyroxene.

A314-449 CP Length of field 2.0mm

F. Orthopyroxene with opaque exsolution (rim) and spinel exsolution (core).

A300-710 PPL Length of field 1.4mm

G. Edge-parallel zoning in orthopyroxene outlined by concentration of clinopyroxene exsolution lamellae, Kalka.

A314-157 CP Length of field 2.4mm

H. Hourglass zoning in orthopyroxene outlined by massed clinopyroxene exsolution lamellae, Gosse Pile.

A313-245b CP Length of field 8mm

Photograph by A.C. Moore.

A

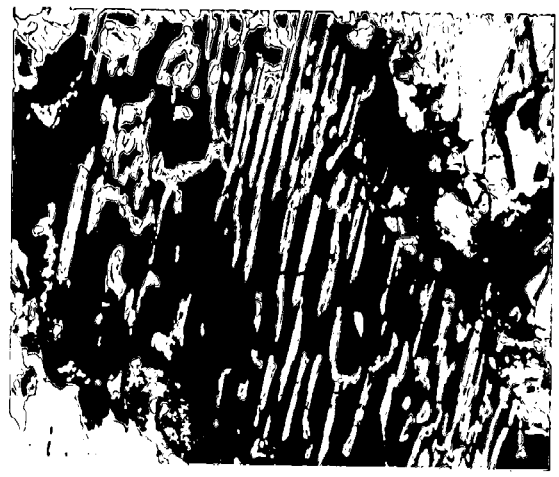

B

C

D

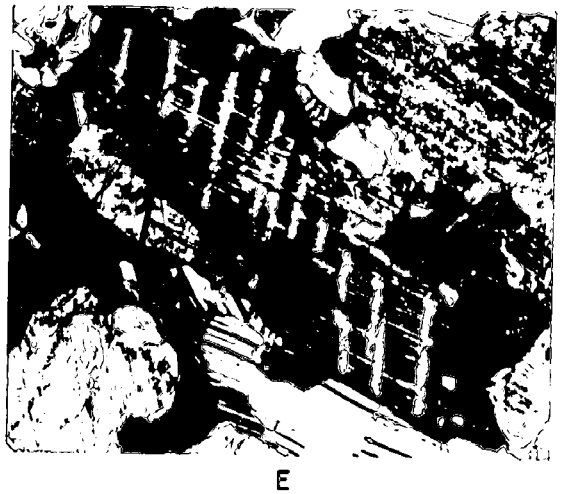

E

F

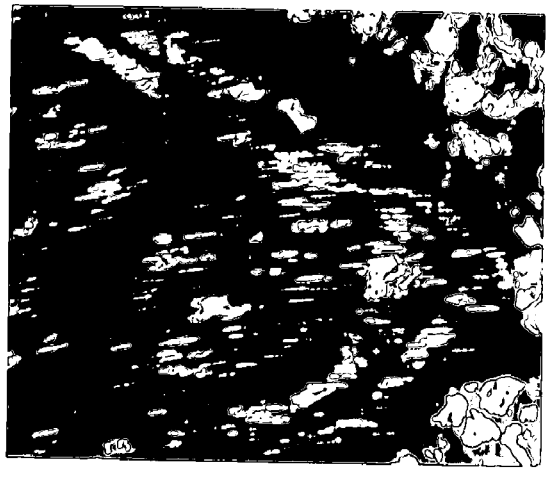

G

H

PLATE 42

A. Hourglass zoning in orthopyroxene, Ewarara. Dark coloured sector A contains massed spinel exsolution, light coloured sector B contains a few edge parallel zones relatively rich in spinel exsolution.

A300-113 PPL Width of field 1.6mm

B. Hourglass zoning in orthopyroxene, Ewarara. Note prominent edge parallel zones in sector B, olivine inclusion in sector A, and changes in slope of sector A - sector B interface.

A251-N248 PPL Width of field 1.6mm

C. Hourglass zoning in orthopyroxene, Ewarara. Note overgrowths rich in spinel exsolution on sector A and sector B.

A300-113 PPL Width of field 1.3mm

D. Hourglass zoning in orthopyroxene, Ewarara. Note edge parallel zoning in sector B and changes in slope of sector A - sector B interface.

A251-N248 PPL Width of field 1.6mm

A

B

C

D

PLATE 43

A. Spinel exsolution rods in orthopyroxene.

PPL Length of field 0.4mm

B. Rutile exsolution rods in orthopyroxene.

PPL Length of field 0.4mm

C. Magnetite exsolution plates in orthopyroxene.

A300-108 PPL Length of field 0.8mm

D. Irregular antiperthitic plagioclase inclusion (Type 2) in orthopyroxene, Kalka.

A314-413 PPL Length of field 1.4mm

E. Plagioclase inclusions in orthopyroxene, Hinckley Range. Type 1 inclusion (right) with lath-like shape and sharp boundaries, Type 2 inclusion (left) with rounded shape and intergrown boundary.

A307-2b PPL Length of field 1.4mm

F. Type 1 plagioclase inclusions aligned parallel to growth faces of orthopyroxene, Kalka.

A314-157 PPL Length of field 2.4mm

G. Irregular orthopyroxene lamellae and blebs in clinopyroxene.

A314-219 CP Length of field 2.4mm

H. Repeated epitaxial overgrowths between orthopyroxene (black) and clinopyroxene (white), Type B dolerite, Ewarara.

A301-23 CP Length of field 0.7mm

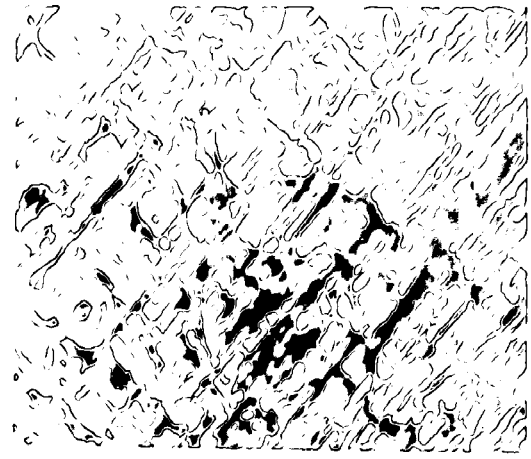

A

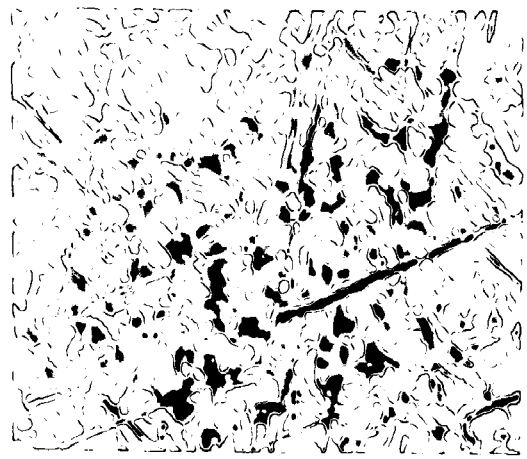

B

C

D

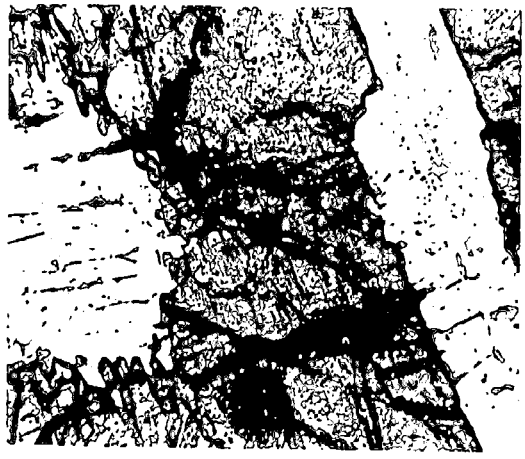

E

F

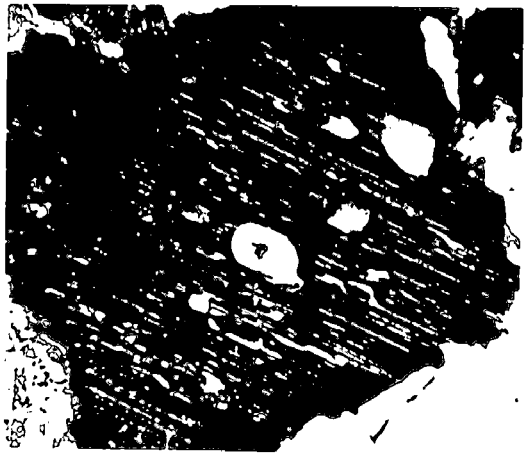

G

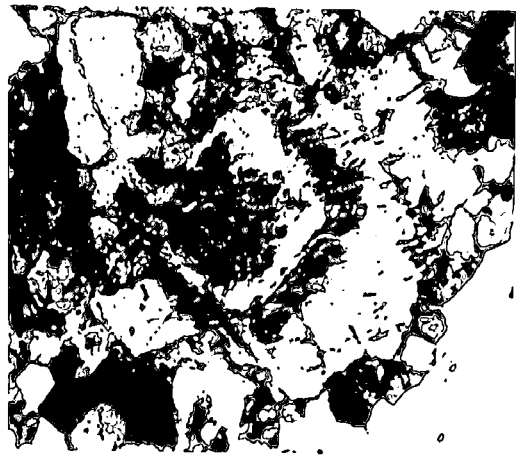

H

PLATE 44

A. Spinel exsolution plates in clinopyroxene. Note small aligned opaque rods in spinel plates.

A300-713 PPL Length of field 0.3mm

B. Rutile exsolution rods in clinopyroxene.

A314-219 PPL Length of field 0.3mm

C. Massed magnetite exsolution plates in clinopyroxene.

A314-418 PPL Length of field 0.9mm

D. Extinction variations in plagioclase, commonly associated with pyroxene inclusions.

A314-418 CP Length of field 2.4mm

E. Olivine phenocryst partially enclosed by plagioclase phenocryst in Type D dolerite. Olivine surrounded by thin fibrous orthopyroxene rim in both phenocryst and matrix.

A314-717 PPL Length of field 2.0mm

F. Fibrous orthopyroxene rim on olivine (top) in contact with plagioclase (bottom) and biotite (left centre).

A314-196 CP Length of field 0.3mm

G. Orthopyroxene/opaque intergrowth replacing olivine.

A300-67 PPL Length of field 1.0mm

H. Orthopyroxene/green spinel intergrowth within olivine.

A314-441a PPL Length of field 1.4mm

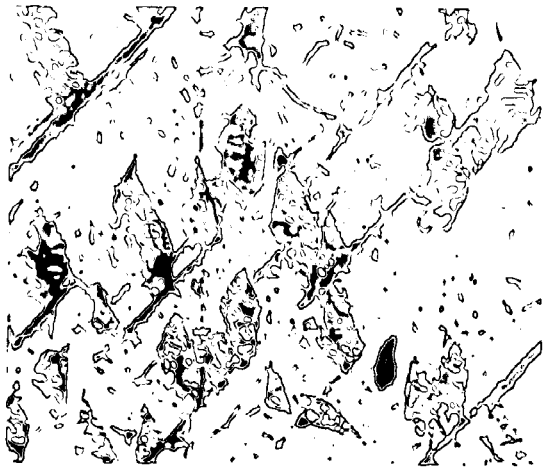

A

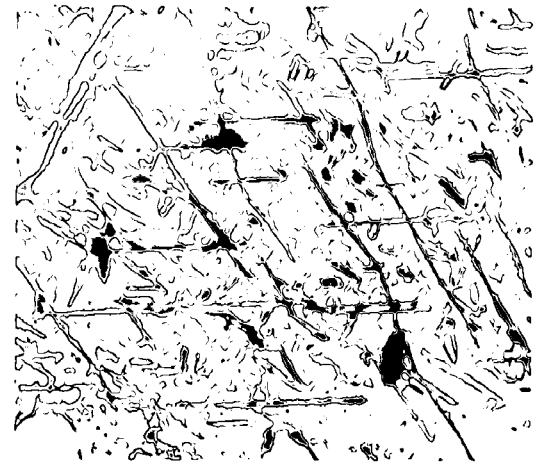

B

C

D

E

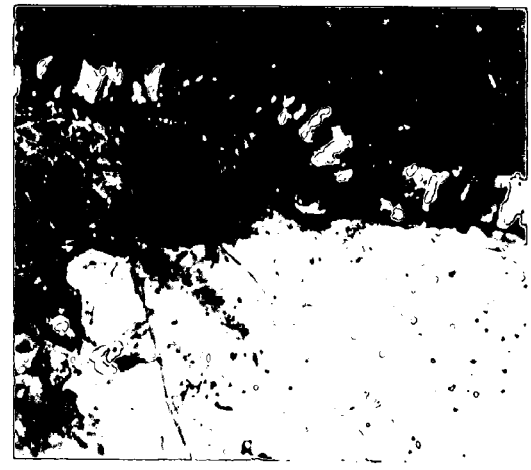

F

G

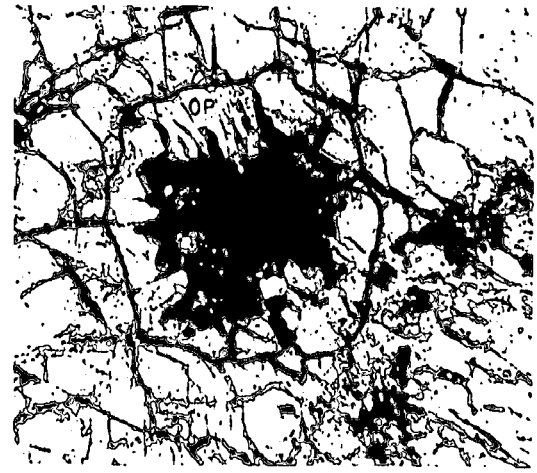

H

PLATE 45

A. Massed spinel rods in plagioclase. Note clear outer margin of laths.

A314-441a PPL Length of field 2.4mm

B. Crystallographic control on development of spinel exsolution (right) in plagioclase. Magnetite specks present in both areas. Note regular variations in particle density.

A300-501c PPL Length of field 1.4mm

C. Magnetite exsolution rods in plagioclase.

A314-418 PPL Length of field 0.3mm

D. Trains of magnetite in plagioclase.

A314-208 PPL Length of field 0.3mm

E. Coalescing of spinel particles in plagioclase. Note barren zone adjacent to coarse trail.

A314-755 PPL Length of field 0.3mm

F. Coalescing of spinel and magnetite particles in plagioclase with associated barren zone. Note variations in magnetite particle density and associated trails in host plagioclase.

A300-501c PPL Length of field 0.3mm

G. Unclouded plagioclase inclusion within plagioclase strongly clouded by fine magnetite particles.

A314-472 PPL Length of field 1mm

H. Concentrations of fine magnetite particles on twin planes in plagioclase.

A314-143 PPL Length of field 0.3mm

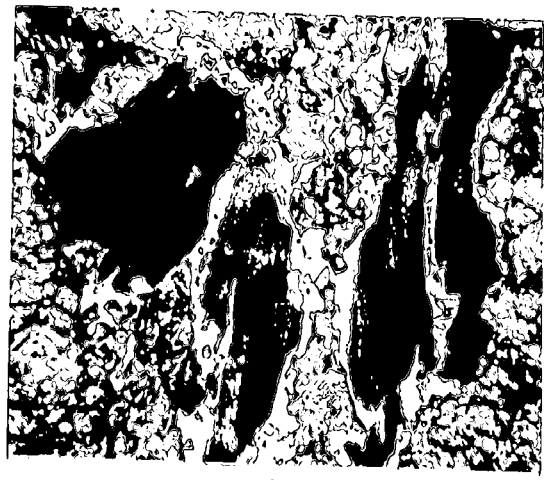

A

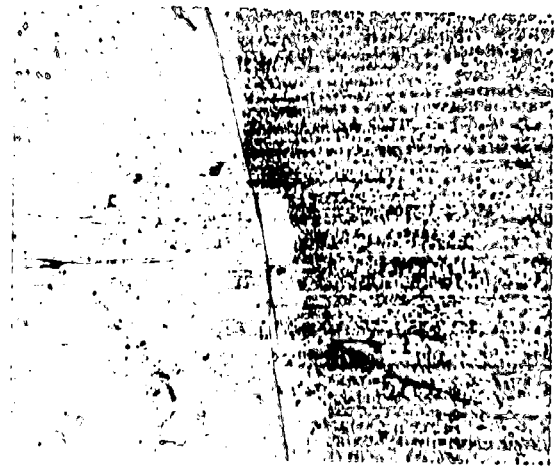

B

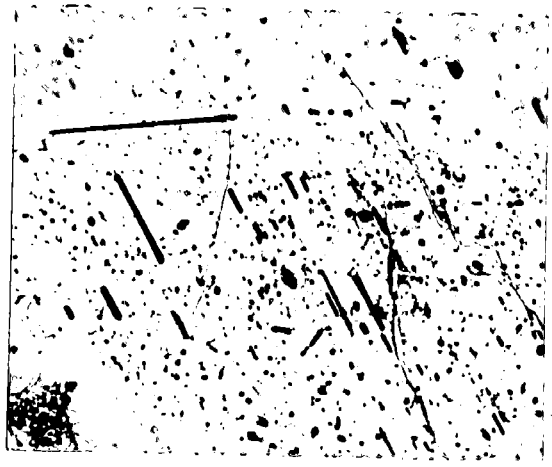

C

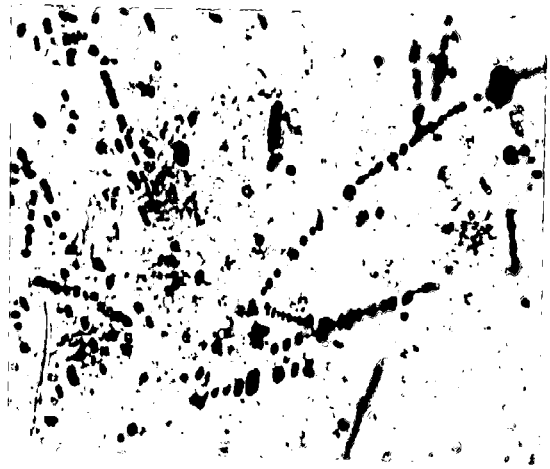

D

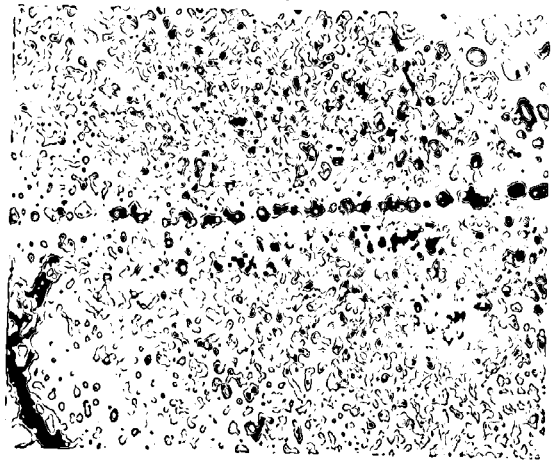

E

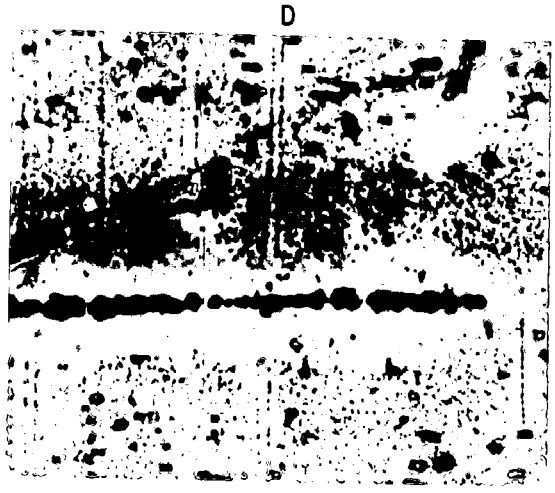

F

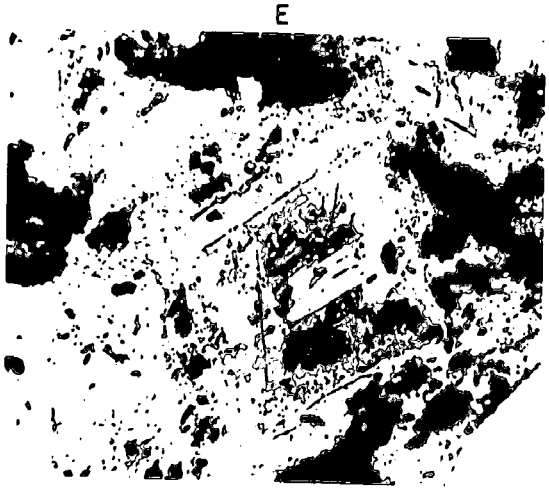

G

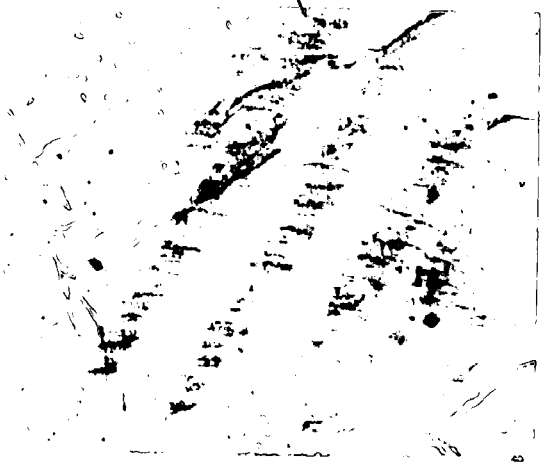

H

PLATE 46

A. Cumulus antiperthitic plagioclase.

A314-219 PPL Length of field 1.4mm

B. Development of antiperthite lamellae at grain boundaries of plagioclase clouded by magnetite.

A314-740 PPL Length of field 0.3mm

C,D. Pyroxene/hornblende plates in plagioclase. Note localised presence of fine spinel rods (top left, centre).

A300-502a C. PPL Length of field 0.8mm
D. CP

E. Pyroxene inclusion in untwinned plagioclase.

A314-418 PPL Length of field 0.8mm

F. Pyroxene inclusions on simple twin plane in plagioclase.

A314-418 CP Length of field 0.8mm

G. Albite/pericline glide twinning in plagioclase.

A314-357 CP Length of field 2.4mm

H. Albite glide twinning in plagioclase. Note lenticular nature of twins, and termination at plane of bending.

CP Length of field 0.7mm

A

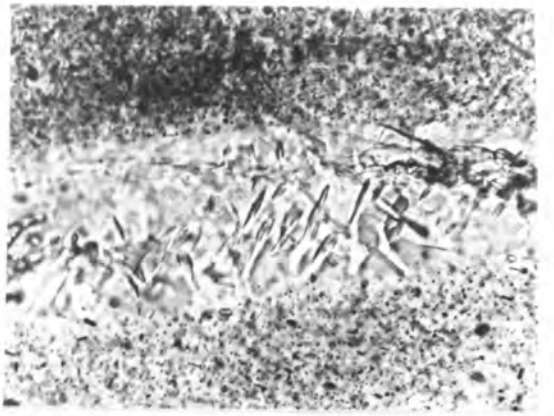

B

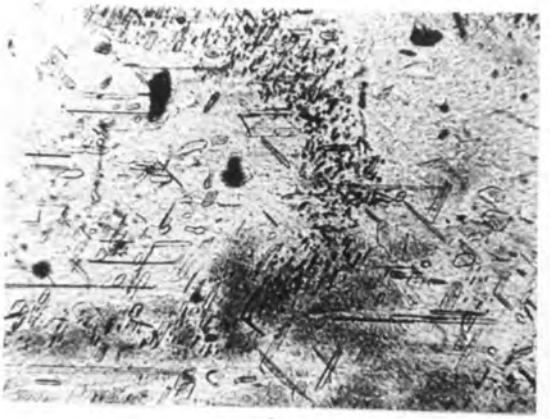

C

D

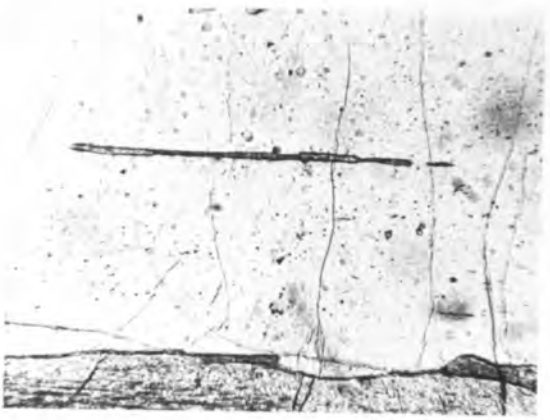

E

F

G

H

PLATE 47

A,B. Castellate texture. Intergrowth between oriented orthopyroxene projections and plagioclase at edge of clinopyroxene. Region of interpenetration associated with extinction zoning in plagioclase.

A307-17 A. PPL Length of field 1.4mm
B. CP

C,D. Castellate texture between orthopyroxene and plagioclase on maximum growth rate faces of clinopyroxene and in inclusion in clinopyroxene. Note orthopyroxene exsolution lamellae in clinopyroxene.

A314-219 C. PPL Length of field 2.0mm
D. CP

E. Globular intergrowth between pyroxene and plagioclase in interstitial area between major plagioclase laths. Note magnetite clouding of plagioclase.

A314-382 PPL Length of field 1mm

F. Wormy intergrowth between pyroxene and plagioclase in interstitial area between plagioclase laths and "massive" clinopyroxene.

A314-391 PPL Length of field 1.2mm

G. Development of pyroxene inclusions at end of plagioclase lath. Note recrystallized hornblende aggregates (top).

A300-368 PPL Length of field 2.0mm

H. Pyroxene inclusions in irregular plagioclase crystal.

A300-388 PPL Length of field 2.0mm

A

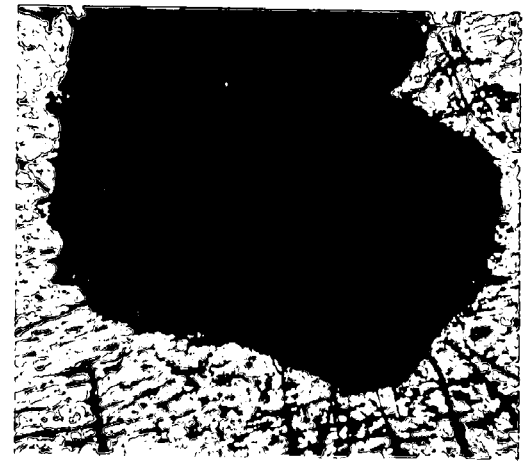

B

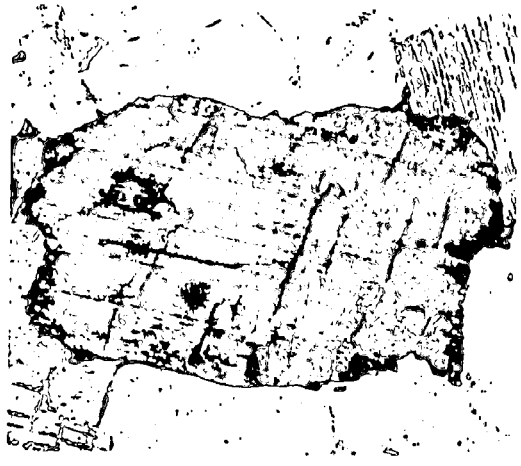

C

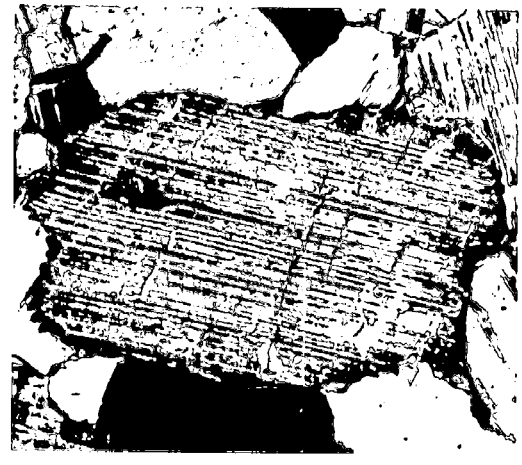

D

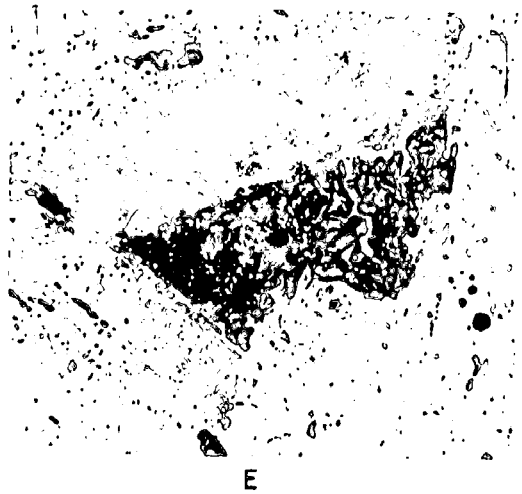

E

F

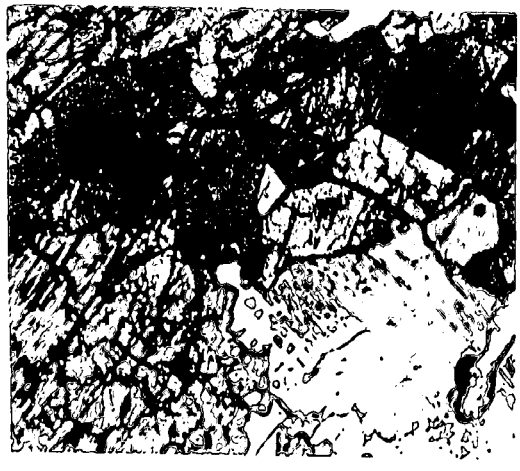

G

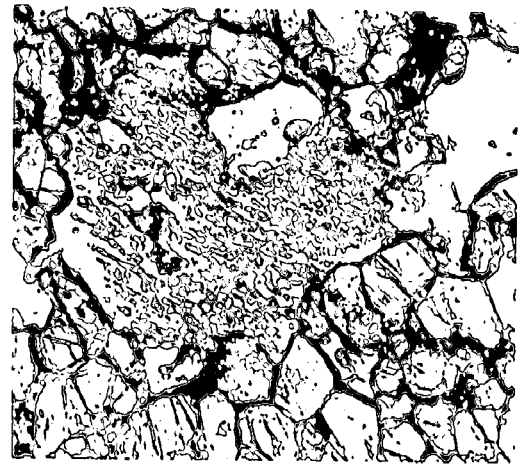

H

PLATE 48

A,B. Control of spinel particle concentration in plagioclase by multiple twinning. Note primary clear edges to plagioclase grain.

A301-153 A. PPL Width of field 1.6mm
B. CP

C,D. Lack of clouding of plagioclase by spinel particles associated with recrystallization - secondary clear edges.

A300-1 C. PPL Width of field 0.9mm
D. CP

A

B

C

D

PLATE 49

A. Norite augen gneiss showing the strong development of S_1^g foliation. Pyroxene augen are preserved in the foliation. From West Kalka Gneissic Belt, Kalka.

A251-172E Field of view 16.5cm wide

B. Development of S_1^g foliation (parallel to scale) oblique to primary small scale igneous layering S_o^g (vertical) in norite, Kalka.

A314-703 Scale 4.3cm

A

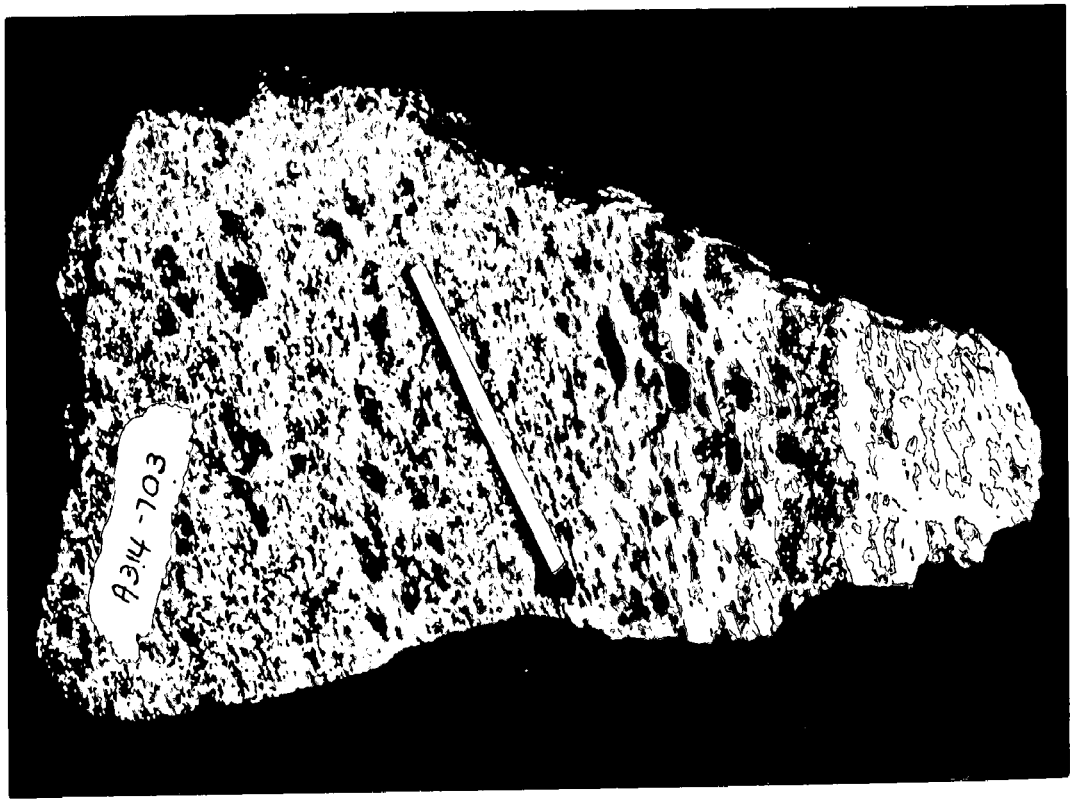

B

PLATE 50

A. Development of strong S_1^g layering and foliation in norite, Numbunja Gneissic Belt, Kalka.

A314-711 Scale 4.3cm

B. S_1^g layering and foliation in leucogabbro, Kalka.

A314-490 Scale 3cm

C. Annealed plagioclase and pyroxene S_1^g layers wrapping around an orthopyroxene porphyroblast, Kalka.

A314-711 PPL

D. Annealed plagioclase S_1^g layer enclosing plagioclase porphyroblasts to produce pseudofold in layering, Kalka.

A314-711 PPL

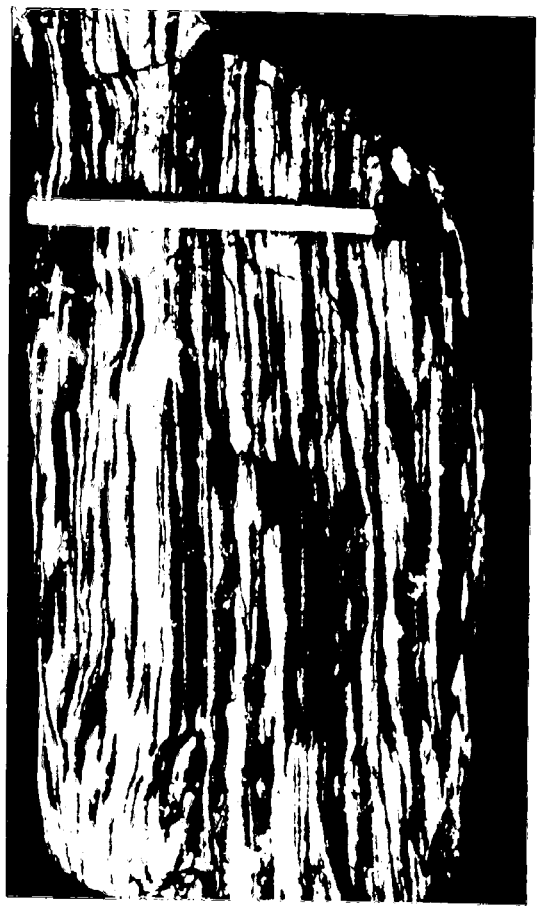

A

B

C

D

PLATE 51

A. Simple kinks in orthopyroxene from pyroxenite, Ewarara.

A300-124 CP Width of field 0.9mm

B. Conjugate kinks in orthopyroxene from pyroxenite, Kalka. Note development of recrystallized matrix.

A314-724 CP Width of field 5mm

C. Development of recrystallized grains along kink planes in orthopyroxene, Kalka. Note north-south kink with no evidence of recrystallization.

A314-724 CP Width of field 0.9mm

D. Recrystallization along kink planes and kink bands to form parallel series of elongate discrete but optically continuous crystals, Kalka. Cleavage indicates [001].

A314-724 CP Width of field 5mm

A

B

C

D

PLATE 52

A. Simple kinks in clinopyroxene, Kalka. Note light coloured orthopyroxene exsolution lamellae.

A314-743 CP Width of field 0.9mm

B. Kink bands in olivine, Kalka.

A314-411 CP Width of field 0.9mm

C. Kink bands perpendicular to albite glide twins in plagioclase, Ewarara. Note the changes in density of the twin planes over the kink planes.

A300-501c CP Width of field 1.6mm

D. Recrystallization train in plagioclase perpendicular to albite glide twins, Ewarara.

A300-501c CP Width of field 0.9mm

A

B

C

D

PLATE 53

A. "Flow" orthopyroxene surrounded by recrystallized matrix. Note thin elongate plagioclase inclusion (white) within porphyroblast. Line parallel to (100). S_4 fracture cleavage trending approximately "northeast" in porphyroblasts (note refraction between crystals).

A314-302c PPL Length of field 8mm

B. "Flow" orthopyroxene in recrystallized pyroxene matrix. Note clinopyroxene exsolution lamellae parallel to (100) and oblique to elongation direction.

A314-302c CP Length of field 8mm

C. Ribbon foliation, olivine melagabbro, Kalka.

A314-131 CP Length of field 4mm

D. Alignment of kink planes in pyroxenite, Kalka.

A314-726 CP Length of field 22mm

E. Concentration of clinopyroxene exsolution lamellae on kink plane in orthopyroxene, Kalka.

A314-212 CP Length of field 1.4mm

F. Secondary plagioclase assemblage surrounding primary plagioclase crystal.

A314-490 CP Length of field 1.4mm

G. Primary plagioclase lath with simple twinning surrounded by secondary pyroxene assemblage.

A301-23 CP Length of field 2.0mm

H. Orthopyroxene aggregate. Note straight grain boundaries and triple point junctions.

A314-756 CP Length of field 0.8mm

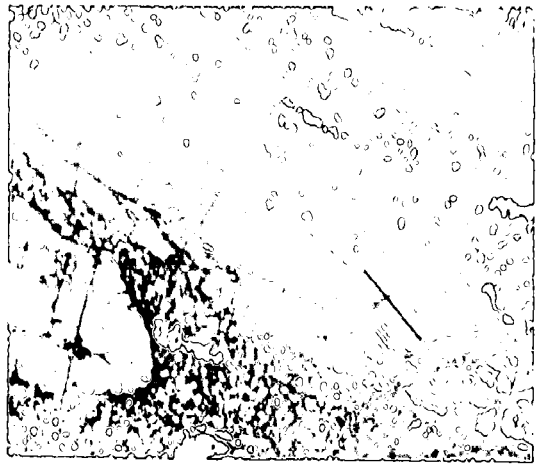

A

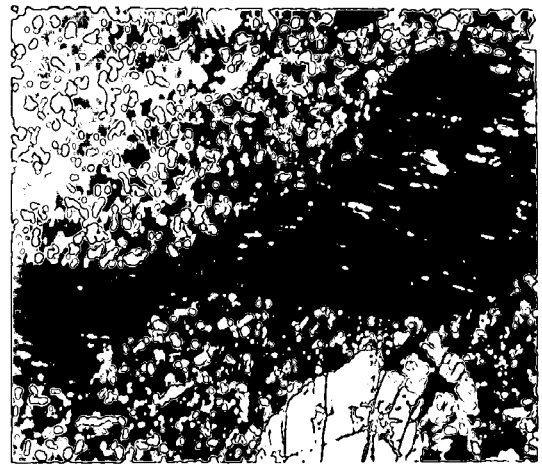

B

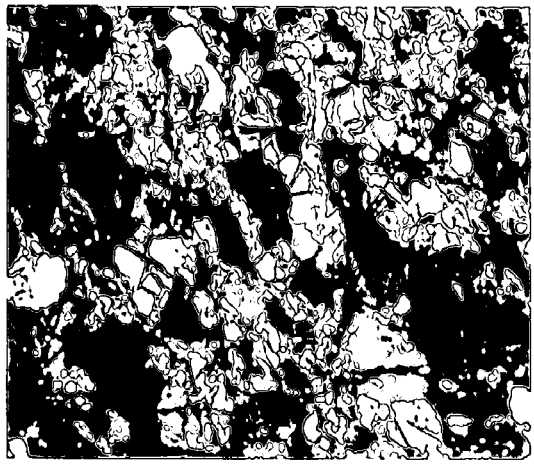

C

D

E

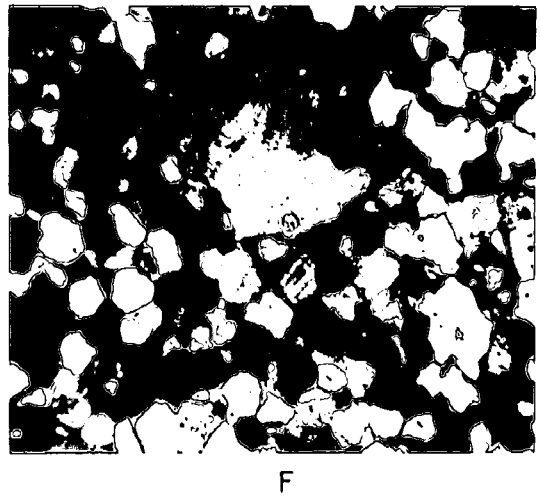

F

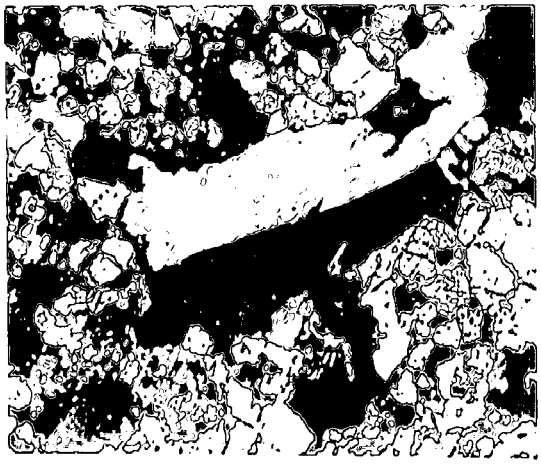

G

H

PLATE 54

A. F_2 folding of S_1^g foliation in norite, Kalka. Note crenulations in fold hinge.

A314-705 Scale 4.3cm

B. Development of S_2^m foliation outlined by quartz lenses (parallel to scale) oblique to S_o^m fine scale layering. Note presence of "hooks" in quartz.

A300-701 Scale 1.5cm

C. Mesoscopic F_2 folding of small scale igneous layering S_o^g in norite, Albitalbiti Creek, Kalka.

Scale 12.5cm (centre)

D. Rodding lineation L_2^m in quartz - feldspar - garnet granulite parallel to F_2 fold axis, in hinge zone of major F_2 antiform, Ewarara.

Scale 12.5cm

A

B

C

D

PLATE 55

A. F_2 fold in norite, Kalka. Note crenulations in fold hinge.

A314-730b Scale 4.3cm

B. Development of S_2^g foliation (parallel to scale) oblique to small scale igneous layering S_o^g and lenticular S_1^g layering - foliation (parallel to S_o^g) in norite, Teizi.

GM9 Scale 3cm

C. F_2 folding of small scale igneous layering, S_o^g, in norite, Kalka. Note slight development of lenticular grain aggregates parallel to axial plane in fold hinge.

A314-650 Scale 4.3cm

A

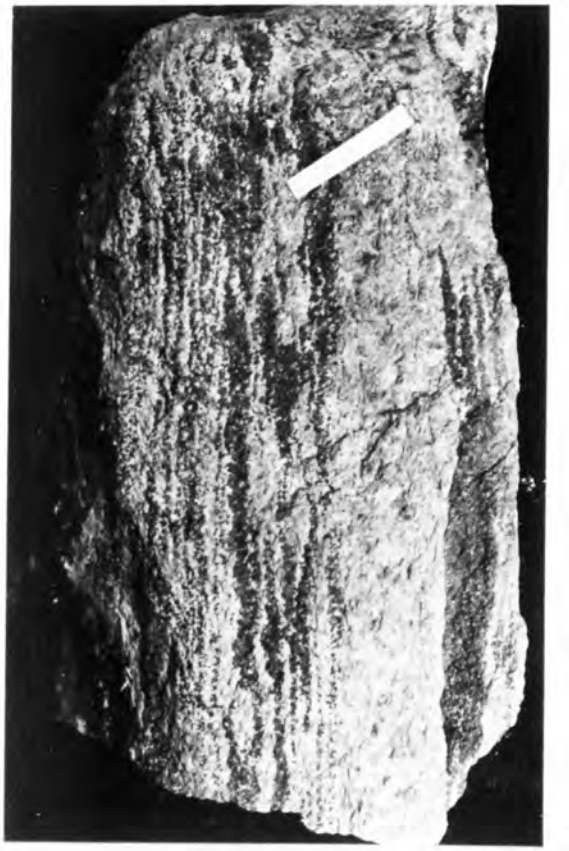

B

C

PLATE 56

A-C. Mylonitic rocks with complex internal structures, Kalka.

A. A314-71 Scale 4.3cm
B. A314-96
C. A314-71

D. Augen gneiss texture, olivine gabbro, Kalka.

A314-133 PPL Length of field 9mm

E. L_1^9 lineation, norite, Kalka.

A314-713a Scale 4.3cm

F. F_2 fold in acid granulite, Kalka. Note small F_3 warp (arrowed, bottom) in limb. Morphological preferred orientation of feldspar grains parallel to F_3 axial plane in thin section (direction marked on photograph as S_3).

A314-712c Scale 4.3cm

G. Variations in intensity of development of S_1^9 foliation, norite gneiss, Kalka.

A314-713a Scale 4.3cm

H. Layering produced by differential weathering, recrystallized pyroxenite, Kalka.

A314-310 Scale 4.3cm

A

B

C

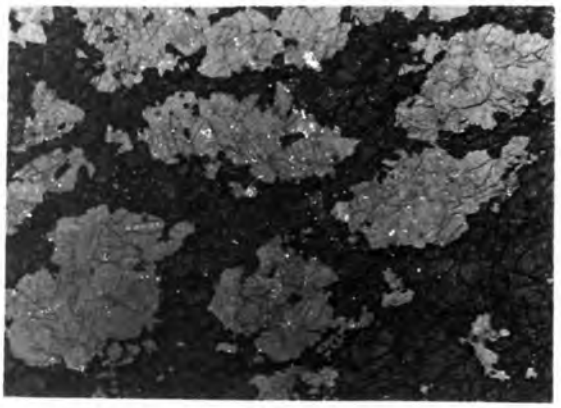

D

E

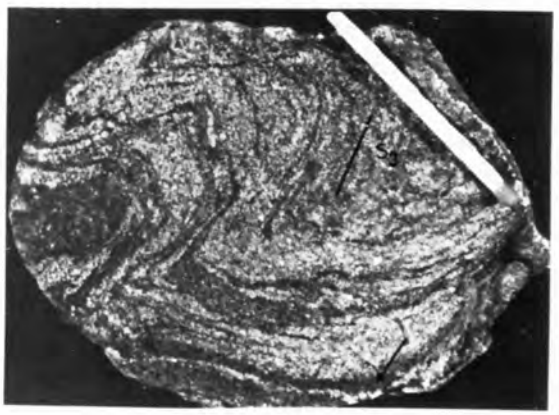

F

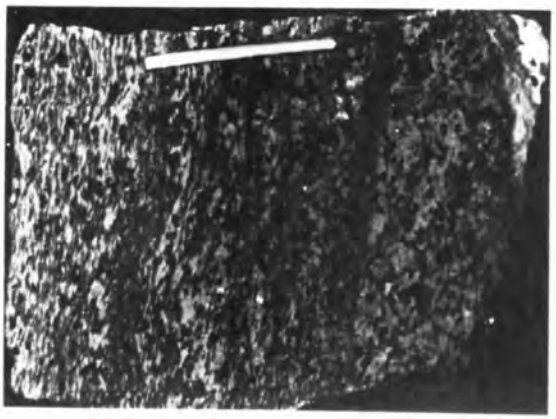

G

H

PLATE 57

A,B. Layering (horizontal) parallel to axial plane of F_2 fold and oblique to S_1^9 foliation, norite, Kalka. Note large grain size of central plagioclase crystal and flanking layers of finer grained pyroxene.

A314-705 A. PPL Length of field 8mm
B. CP

C. "Tails" of recrystallized grains on pyroxene porphyroblast, norite gneiss, Kalka.

A251-172E PPL Length of field 8mm

D. Gneissic norite texture, Kalka. Note "bridging" pyroxene trains oblique to general foliation.

A314-128 PPL Length of field 24mm

E. Compositional layering in mylonite, Hinckley Fault. Note granular garnets (dark).

A314-332 PPL Length of field 1.4mm

F. Plagioclase porphyroblasts in mylonitic layering, Hinckley Fault.

A314-332 PPL Length of field 1.4mm

G. Intrafolial folds in mylonite layering, Hinckley Fault.

A314-332 PPL Length of field 24mm

H. Pseudotachylite (black) separating brecciated pyroxenite fragments.

A301-86 PPL Length of field 24mm

A

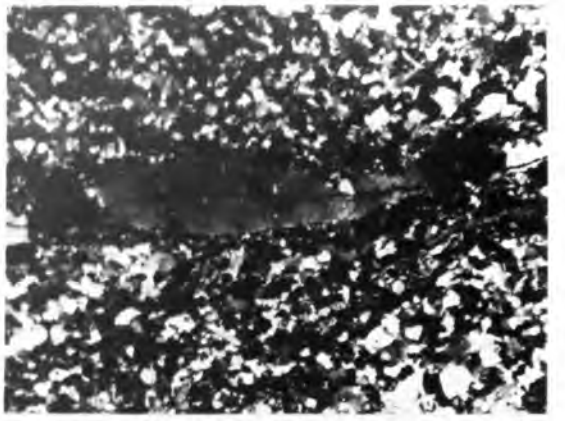

B

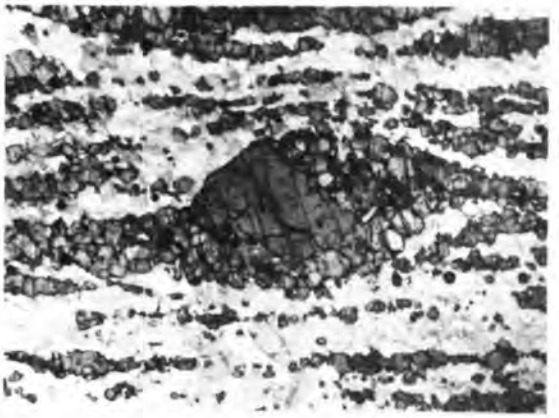

C

D

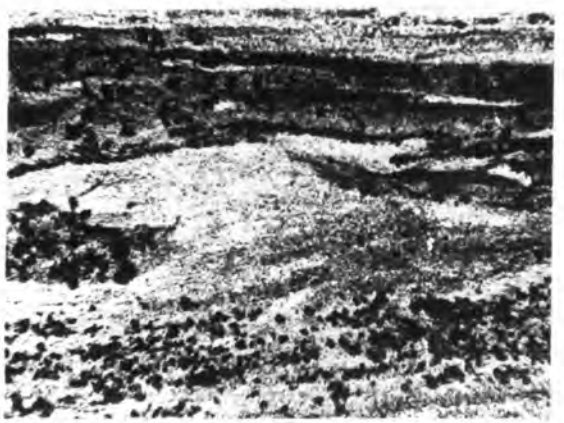

E

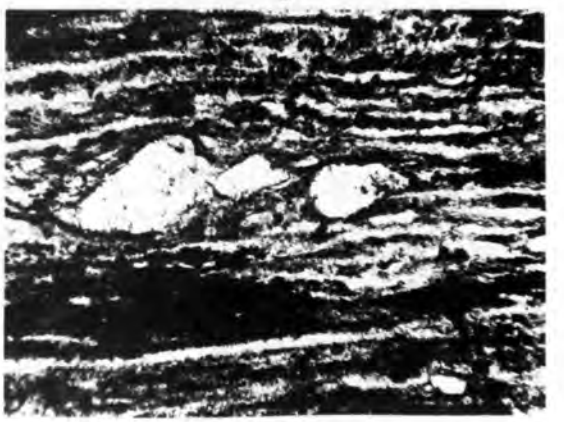

F

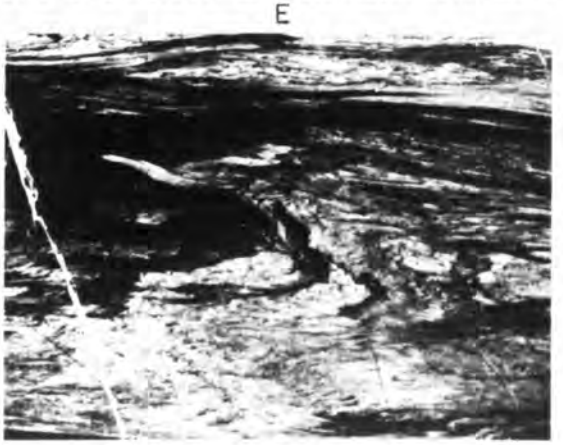

G

H

PLATE 58

A. Oblique aerial view of the southwest corner of the Kalka Intrusion (foreground) and the eastern parts of the Hinckley Intrusion (background), looking west. Note marked structural discontinuity in layering in the two bodies.

B. Oblique aerial view of southwest corner of Kalka, looking northeast. Note transgressive nature of Hinckley Fault (foreground) to layered gabbros.

C. Irregular "layering" in pyroxenite, Scarface Silcrete Zone.

Scale 12.5cm

D. Orthogonal "layerings" in pyroxenite outlined by preferential weathering, Scarface Silcrete Zone. One may represent S_4. Also note lineation of larger elongate pyroxenes parallel to line L.

Scale 4.3cm

A

B

C

D